DOCTOR OF PHILOSOPHY

An Analytical Field and Model Study of M-beam Bridge Decks

Kirkpatrick, James

Award date:
1982

Awarding institution:
Queen's University Belfast

AN ANALYTICAL FIELD AND MODEL STUDY

OF M-BEAM BRIDGE DECKS

Thesis submitted to

The Queen's University of Belfast

by

James Kirkpatrick, B.Sc., C.Eng., M.I.Struct.E., MRAeS, MIHE

for

The Degree of Doctor of Philosophy

in

The Faculty of Engineering

(Department of Civil Engineering)

April 1982

Opinions expressed in this thesis are not necessarily those of the Department of the Environment (N.I.) Roads Service.

SUMMARY

An analytical field and model study of M-beam bridge decks is presented. The field study involved testing four full size bridges during construction to establish the load distribution characteristics and included both tee beam and pseudo-box types of deck. After validating the grillage method of analysis using the results of these tests, simplified graphical methods of predicting the design bending moments in beams were developed analytically. These are applicable to beams at spacings varying from 1.0 m to 2.0 m with the latter being considered for economic reasons. When these design charts are combined with a series of interactive programs for the Hewlett Packard desk top computer they provide a streamlined design procedure which reduces design time to a minimum.

The strength of the standard 160 mm M-beam deck slab under the action of the abnormal vehicle wheel load was investigated in a series of tests on a $\frac{1}{3}$ scale model. The main variables were the percentage of steel reinforcement and the spacing of the beams. Twenty panels were tested and they all failed in a punching shear mode. A detailed analysis of results has shown that the ultimate capacity of bridge slabs is greatly enhanced by compressive membrane action and the failure load is virtually independent of the percentage of transverse reinforcement. A method of predicting the ultimate capacity, in which it is assumed that bridge slabs are fully restrained laterally, is presented. This is based on a modified punching shear equation with the enhancement due to compressive membrane action being accounted for by an equivalent percentage reinforcement parameter, the actual slab reinforcement being neglected. Excellent correlation is achieved with the model tests and with the results of relevant tests reported in the literature.

Finally, proposals are presented for the design of M-beam deck slabs using reduced levels of reinforcement which will provide an acceptable level of serviceability and further savings in the cost of M-beam decks over and above those achieved by increased spacing of the beams.

CONTENTS

NOTATION

The following notation covers the majority of symbols used in the text and any additional symbols are defined as they occur.

a'	distance from the compression face to the point at which the crack width is being calculated.
a_{cr}	distance perpendicular to the reinforcement from the point considered to the surface of the nearest reinforcing bar.
A_s	area of tension reinforcement perpendicular to the crack.
b_t	width of the section at the centroid of the tension steel.
c	column side length.
c_{min}	minimum cover to tensile reinforcement.
C_{min}	either the distance from the point at which the crack width is being considered to the surface of the nearest reinforcing bar running perpendicular to the crack or the distance from the point at which the crack width is being considered to the neutral axis whichever is the lesser.
C_c	force in compression zone of slab.
C_L	twisting inertia from longitudinal cross-section of pseudo-box deck.
d	effective depth of tension reinforcement.
E	Young's modulus.
f'_c	concrete cylinder compressive strength.
f_{cu}	concrete cube compressive strength.
f_t	concrete tensile strength.
f_y	characteristic yield strength of reinforcement.
G	shear modulus of elasticity.
h	overall slab depth.
i	bending inertia per unit width of deck.

i_o	torsional inertia per unit width of deck.
I	bending inertia of grillage beam.
j	bending inertia per unit length of deck.
j_o	torsional inertia per unit length of deck.
J	torsional inertia of grillage beam.
k	reduction coefficient.
K_m	coefficient for beam bending moment envelope.
L	span.
M	The midspan beam bending moment in an individual deck span.
M_A	bending moment at point A on bending moment envelope.
M_{ar}	maximum arching moment for an elastic/plastic material
$M_{ar(max)}$	maximum arching moment for a rigid/plastic material.
M_{av}	average midspan bending moment of all the beams in the deck.
M_B	bending moment at point B on bending moment envelope.
M_{max}	maximum M-beam bending moment due to live load
M_r	arching moment ratio.
$M_{(u)}$	arching moment
P	point load on slab
P_p	predicted slab capacity.
P_t	test load at failure.
q	proportioning factor for torsional inertia of pseudo-box deck.
R	arching parameter
R_b	beam reaction.
u	deflection parameter (Δ/h)
U_t	transfer cube strength.
U_w	28-day cube strength.
v_c	ultimate allowable shear stress.
w	uniformly distributed load.
(w)	theoretical crack width.
W	equivalent wheel load on beam.

x	lateral co-ordinate in x direction.
y	lateral co-ordinate in y direction.
$\bar{y}$	distance of centroid of HB vehicle from centre line of edge beam.
z	displacement perpendicular to elastic plate.
α	torsional parameter for load distribution.
Δ	deflection.
ε	strain.
ε_a	the apparent tensile strain in the concrete at the point under consideration in a direction perpendicular to the crack.
ε_c	plastic strain for an elastic/plastic material.
ε_m	the average strain, at the level where cracking is being considered, calculated allowing for the stiffening effect of the concrete in the tension zone.
ε_1	strain ignoring tension stiffening in the equation for ε_m
θ	flexural parameter for load distribution.
μ	Poisson's ratio
ρ	reinforcement ratio.
ρ_{av}	average reinforcement ratio.
ρ_e	equivalent reinforcement ratio.
ϕ	diameter of loading shoe.
σ	stress.

LIST OF PHOTOGRAPHS

ACKNOWLEDGEMENTS

I would like to thank the Department of the Environment (NI) Roads Service for sponsoring this research project and in particular the Director, Mr. T.A.N. Prescott for his continual support and encouragement.

I must also record my sincere thanks to Professor A.E. Long for giving so willing of his time supervising this work. His interest both practical and academic and his helpful advice have been an increasing source of support throughout the time of the project. I acknowledge too, the valuable assistance and advice given by Dr. W.M.C. Stevenson and Mr. D. Stewart of the Department of the Environment (NI) Roads Service.

I would like to thank Mr. W. McBride and the technical staff of the Department of Civil Engineering for their help and co-operation on many aspects of this project. In particular I would like to mention the following:-

Mr. A. Thompson and Mr. D. O'Loan for their advice and assistance with the instrumentation of both full scale and model bridges.

Mr. F. Crichton and Mr. A. Murray for their hard work and advice during the construction and testing of the model bridge.

Mr. G. Kirkham and Mr. R. Simpson for the construction and assembly of the formwork for the model.

Mr. J. Scott, Mr. R. Graham, Mr. N. Murray and other members of the metal workshop for the construction and assembly of the test rig and other equipment.

Mr. G.I.B. Rankin, colleague, for his much valuable advice and many interesting discussions.

Mrs. D. Brett for her care in typing the script.

I would also like to thank Miss H. Scott of the Department of the Environment (NI) Roads Service for her interest and patience in tracing the many

diagrams and also Mr. J. Woods for his skill in preparing the photographs.

Finally, to my wife Carol, I would like to record my appreciation for her continuous support and encouragement throughout the time of this research project.

CHAPTER ONE

INTRODUCTION

1.1 THE BACKGROUND TO THE RESEARCH

1.2 THE OBJECT AND SCOPE OF THE RESEARCH

1.1 THE BACKGROUND TO THE RESEARCH

Beam and slab construction has now become the most common type of bridge deck for simple spans up to about 30 m. It is a simple structural form which has the advantages of speed of erection with minimum disruption to existing traffic and as such it provides an economical solution to most problems.

The traditional gridwork of steel beams has now been refined with full advantage being taken of the considerable load distribution properties of this type of deck. However, over the last 20 years or so the development of high strength concrete and prestressing techniques coupled with a demand created by the expansion of the motorway network has resulted in the use of a variety of precast pretensioned beams which provide economic structures as well as advantages regarding long-term maintenance.

The use of bridge beams such as the M-beam, U-beam and Box-beam results in an orthotropic deck and research has been carried out to establish the stiffness parameters to be used for deck analysis which today generally means the use of a computer program. With the availability of so many bridge deck programs the analysis of simply supported structures has now become a routine procedure and considerable scope exists for standardisation of this type of deck.

Although the global analysis of bridge decks has reached a high level of refinement the same cannot be said of the analysis and design of the slab spanning between beams. The traditional elastic plate approach adopted by Westergaard in 1930 is still used today, whilst the structural advantages which arise from the inherent in-plane restraint

are largely ignored by bridge code authorities.

Recent research in this field has indicated that a more efficient slab is possible which will provide an acceptable level of safety and serviceability.

A recent trend, which is evident in most Codes of Practice, is towards more complicated requirements which has added considerably to the cost of design and checking. Therefore, any movement towards standardisation of bridge decks will, for the designer, ease some of the problems of interpretation of the current regulations. In this respect, the use of the desk top computer has now added a new dimension to design office practice with a potential for streamlining the complete design process.

Taking all these factors into account and in view of the economic restraints which have gradually increased over the last few years further development of the beam and slab bridge deck would seem to lie in the standardisation of the design procedure and an improvement in the structural efficiency of both beam and slab.

1.2 OBJECT AND SCOPE OF RESEARCH

In N. Ireland the demand for bridge beams is relatively small and market forces have, to a large extent, rationalised the range of beams available with the result that the MoT/C&CA M-beam has become a very common form of construction. Therefore, with the possibility of constructing a large number of M-beam bridges in the near future it was important that this type of deck should be developed to its full economic potential.

Therefore, the objectives of the research were to study:

1. the performance of M-beam bridge decks using full scale bridge tests to establish the load distribution characteristics. A

further aim was to integrate the findings of these tests into an analytical study in order to develop an improved design procedure which would be less restrictive in use than the Department of Transport's Standard Bridge.

2. deck slab design by means of tests on a full size bridge and a scale model. It was proposed that this would include a study of the punching shear strength of restrained bridge slabs resulting in improved recommendations for slab design.

Therefore, to provide a suitable background to the study of M-beam bridge decks the following chapter contains a brief review of the historical development of methods of analysis for beam and slab bridge decks.

CHAPTER TWO

BEAM AND SLAB BRIDGE DECKS - A HISTORICAL REVIEW

2.1 INTRODUCTION

With the introduction of steel and concrete to the field of structural engineering, a new era was opened up for bridge building and the use of a structural arrangement which provided lateral distribution of the rapidly increasing wheel loads became more important. In this respect the grid of beams built on an orthogonal network, intersecting at right angles and joined at the intersecting points, provide an efficient system for the distribution of wheel loads.

With the development of welding techniques and the facilities for the fabrication of large plate girders, this system quickly developed into a series of stiff longitudinal beams with relatively light transverse members and a reinforced concrete slab deck acting compositely with the beams. These were widely used for the longer spans but in the last 20 years or so the use of high strength concrete and prestressing wire has resulted in the development of the prestressed beam which now provides a very economic solution to many problems. As this type of construction marked an important milestone in the development of modern bridge decks it will now be considered in greater detail.

The Development of Prestressed Bridge Beams

The first non-proprietary standard bridge beams in the United Kingdom were proposed by Somerville and Tiller (1970), details of which are given in Fig. 2.1 and these were introduced in 1961. Their introduction by the Prestressed Concrete Design Group, now incorporated into the Concrete Society, was intended to exploit the economic advantages associated with the repetitive use of formwork and pretensioning facilities at the same time as retaining the advantages of competitive tendering. Although referred to as standard beams they are essentially a series of standard

shapes within which the prestressing tendons and secondary reinforcement are individually designed for each deck.

In 1971 as the result of co-operation between the Ministry of Transport and the Cement and Concrete Association the standard prestressed M-Beam was introduced by Manton and Wilson (1971) and is shown in Fig. 2.2. It covers the range of spans from 15 to 29 m and as a high proportion of highway bridge decks are within this category it is a popular choice. This type of beam offers an economic solution to most problems especially the railway/river or busy road crossing where interference with existing traffic must be kept to the absolute minimum.

During the early seventies, with the increase in the construction of motorways and elevated highways, beams that could span 30 m were developed. Typical of this type of beam was the "top hat" beam designed by G. Maunsell and Partners and first used for the Westway elevated section of the A40 (M) in London. The North West Road Construction Unit also designed a box-beam for use on the link roads of the Lancashire-Yorkshire motorway M62. Finally a U-beam was devised by Dow Mac Concrete Limited and G. Maunsell and Partners and independently by Dundee University. This particular group of beams all possess low transverse flexural rigidity in relation to high longitudinal rigidity. An investigation into the load distribution properties of these beams has been done by Cusens (1974) and the beams are shown in Fig. 2.3.

To exploit this structural arrangement to the full, methods of analysis and design were required that took full advantage of the considerable load distribution properties of this type of deck. As the spacing of the beams increased, the limiting factor became the strength

of the slab spanning between beams and distributing the wheel loads. Over the years researchers have approached the analysis of this type of deck from many different directions and these will be noted briefly:-

Methods of Analysis

The analysis of beam and slab bridge decks may be divided into 2 distinct categories:-

1. The overall analysis of the deck to provide forces for the design of the beams taking account of the lateral distribution of wheel loads.
2. The local analysis of the slab spanning between beams under the action of the wheel loads.

Therefore, this chapter gives a detailed description of the standard M-beam and reviews the historical development of the various methods of analysis for the overall deck and the local slab. Finally, conclusions are drawn which will form the basis of an analytical and experimental investigation of the M-beam bridge deck.

2.2 STANDARD M-BEAMS

2.2.1 Introduction

The MoT/C & CA standard M-beam has been designed as precast pre-tensioned units for use in composite voided slab (pseudo-box) and contiguous inverted T-beam and slab (tee beam) construction. In general these units require the use of deflected or debonded tendons. However, in Northern Ireland beams may only be manufactured with debonded tendons and all investigations have been restricted to this type of beam.

2.2.2 Beam Sections

Standard M-beams have a range of ten sections with dimensions as shown in Figure 2.4. Top flange width, web thickness and the whole

bottom flange are common to all sections. The bottom flange shape is such that the beams can be cast on the same pallet as the metricated standard box-beams proposed by Somerville and Tiller (1970).

The total depth changes in increments of 80 mm throughout the range. This is achieved with 3 web depths, each having the same 3 top flange depths (an extra top flange increment is provided for the largest beam).

Where transverse reinforcement is required through the bottom of the web, holes are provided at 600 mm centres. For decks without bottom in situ concrete the web holes are omitted except at the ends of the beam where an end hole may be used for transverse end diaphragms.

2.2.3 Types of Deck Construction

The beams are intended to be placed at 1 m centres which gives a 30 mm gap between the bottom flanges. Two forms of construction are possible, namely pseudo-box and tee beam.

Pseudo-Box

The "bottom flange" of the pseudo-box is formed by mild or high-tensile reinforcement placed through the performed holes in the webs of the beams and covered with a minimum of 50 mm of in situ concrete. A reinforced top slab is cast on permanent formwork (such as asbestos cement sheet) as shown in Figure 2.2(a).

Tee Beam

This is the simplest form of M-beam deck with a reinforced top slab cast on the permanent formwork as shown in Figure 2.2(b).

Slab

The top slab has been standardised at 160 mm. The 45 mm rebates in the top flange allow 15 mm for permanent formwork and a 30 mm projection of the flange into the in situ concrete, thus ensuring the

correct cover when the lowest reinforcement is laid on top of the pre-cast unit.

With the details of the M-beam decks now well defined, consideration will now be given to the methods used to analyse beam and slab bridge decks.

2.3 OVERALL ANALYSIS OF BEAM AND SLAB BRIDGE DECKS

2.3.1 Introduction

Early attempts to analyse the distribution of forces within the beam and slab grid framework were based on either end forces or end deformations of the beam members which also had zero torsional rigidity. These methods were developed using design tables but were very restrictive as they would only cover a limited range of structural systems and very simple loading. The work of the early researchers then followed two very distinct routes; namely plate theory and grid frameworks. Finally, and perhaps the most significant development in recent years, the use of computers allowed a much more sophisticated approach to the whole process of design. These various approaches will be considered in greater detail as well as the use of the computer orientated grillage analysis for M-beam decks and the latest proposals from the Department of Transport on the use of the proposed standard bridge deck.

2.3.2 The Plate Analogy

After World War II a major development occurred when a method was derived based on the analogy between a grid system and an orthotropic plate. The fundamentals of the new concept were established in the early twenties and from these a variety of procedures was derived although the most difficult problem at that time was finding a solution for the governing biharmonic equation. In 1946 a solution for orthotropic

plates of negligible torsional rigidity was given by Guyon (1946), who also showed that any combination of loading can be handled using coefficients of lateral distribution. Guyon (1949) also gave a solution for isotropic plates and, later on, Massonnet (1950) derived generally valid relations from the principles given by Guyon which also included the effect of torsion. Thus the advantages of the approach based on coefficients of lateral distribution were expeditiously combined with the correctness of solution relating to the orthotropic plate.

The load distribution theory of Guyon and Massonnet has been formulated into a design process by Morice and Little (1956) and Rowe (1962) and was also presented in the form of design charts by Morice, Little and Rowe (1956). The theory assumes that the bridge deck being analysed can be simulated by an equivalent orthotropic plate having the same average stiffness properties as the actual bridge. It is generally taken that this assumption is valid if the bridge consists of at least five longitudinal beams and has diaphragms at the supports. This method is still a popular choice for simple decks although the amount of arithmetic work can be considerable. Further developments by Cusens and Pama (1969) enabled a wider range of torsional and flexural stiffnesses to be considered. A review of the theory of Guyon and Massonnet applied to beam grids and orthotropic plates is given by Bareš and Massonnet (1968).

A slightly different application of plate theory applied to beam and slab bridges has been made by considering the reinforced concrete slab as a plate either resting on, or attached to, a number of elastic beams. This particular approach has been investigated by Newmark (1938), Siess (1949), Richart, Newmark and Siess (1949), and also by Thomas and

Short (1952). Most theoretical solutions assume that only the vertical loads are transferred from the plate to the beams ignoring the horizontal shear between the beam and slab. A theory due to Craemer (1954) however, assumes full connection between the two elements of the system and takes into account load distribution arising from forces in the plane of the plate, described by Craemer as disk effect.

The various theories of plate analysis have to a certain extent been generalised by their formulation into charts and tables, nevertheless, some of the methods require extensive calculations and this tends to make it difficult for the designer to obtain a clear understanding of the behaviour of the structure.

2.3.3 The Grillage Analogy

A simple method for the solution of a grid framework is the use of the deflection compatibility equations for the beam intersections and this has been done by Lazarides (1952). The number of equations can be quite large and if the torsional stiffness of the members are omitted there are about as many equations as there are beam intersection points. If torsion is taken into account this number may be multiplied by three. Unless the structure is very simple or has many lines of symmetry, solution by this method is most impractical.

Moment distribution or relaxation methods will provide a solution to almost any type of grid framework problem and can take into account bending and torsion of both longitudinal and transverse members. This approach has been investigated by Ewell, Okubo and Abrams (1952) who used an auxiliary force system for controlling the deflections at the intersections of the members and a moment and torque distribution process for transmission of the effects produced by the deflections. Although

moment distribution is of wide application the arithmetic work is extremely tedious and except in the simplest of cases, almost impossible.

The solution of the elastic grillage has always been of interest to engineers and several methods of analysis have developed based on various simplifying assumptions. Hetényi (1938) for example assumed that the grid deflects in such a manner that there is no rotation of individual members at their interconnections with other members. Other important methods are those of Pippard (1938, 1952) who assumed that transverse members could be replaced by a continuous transverse medium, and Leonhardt (1950) who replaced actual transversals by a single transversal of zero torsional rigidity. Hendry and Jaeger (1958) developed a method of solution using an harmonic analysis which was based on the assumption that the transverse members of a grid may be replaced by a uniformly spread medium.

At that time, all the various methods for the solution of grillages were severely limited in scope since hand methods had to be used for the solution of the simultaneous equations. Present day analysis of grillages is carried out using the stiffness method and computer programs are available for solving the large number of complex equations which are set up in the analysis.

The present day use of an equivalent grid for analysing reinforced concrete slab and pseudo-slab bridge decks may owe something to the successful application of the assumption made for the early methods of analysis of grid frame works. In effect the assumption made for the modern grillage analysis of slab type structures is quite the opposite to that made for the early grid frameworks and there is no reason to suppose that the analysis of a grid assuming a continuous medium should

not work in the opposite sense, namely, analysing a continuous medium assuming an equivalent grillage.

2.3.4 Computer Methods

In recent years, due to the necessity to analyse complex structures with confidence and accuracy, engineers have been faced with the problem of finding better methods of analysis for use in design and research. Fortunately the increased availability of digital computers coincided with this requirement and much of the hand calculation previously involved has been eliminated.

In general, computer methods fall into two categories. The first of these are the methods which analyse the structure as a whole. This involves formulating the governing differential equation for the structure, defining the boundary conditions, and solving the equations using a numerical technique, usually finite differences. The resulting simultaneous linear equations are then solved using matrix algebra or a relaxation technique. This method is quite satisfactory for a particular structure, but the generality is lost for other structures.

The second type of analysis involves dividing the structure into small elements. This group may be divided into:-

1. the finite element methods where the structure is divided into much smaller elements; and
2. finite strip or folded plate methods where the deck is assumed to have been formed into a number of parallel strips or plates spanning between supports and connected along their edges.

For finite element methods a large range of elements is now available, the most useful being the two-dimensional elastic plate bending elements and the beam element. In all these methods the stiffness method

of analysis is used as the basis for a solution. The selection of a computer program to analyse a particular bridge deck will depend on many variables such as the type of construction, skew, support system and continuity.

Obviously not every program will be suitable for every deck as all programs have their limitations which must be considered when the structure is being idealised into smaller plate or beam elements. Cusens and Pama (1975) have compared the various methods and from Table 2.1 it may be seen that the finite element and grillage methods can accommodate almost any type of deck, plan geometry and support conditions.

In general, finite element programs use both plate and beam elements and require a considerable amount of experience in the idealisation of the structure and interpretation of the output. Because of the complex nature of these programs they are expensive to operate in that they require a large amount of data preparation and computer time. However, the grillage analysis, which uses only the beam bending element, is an alternative which offers the versatility of the finite element program with a simplicity of approach which is preferred by engineers.

The approximate representation of bridge decks by a grillage of interconnected beam elements is a convenient way of analysing the behaviour of the bridge under load. The grillage analysis is probably the most popular computer method used for bridge decks. As can be seen from Table 2.1 it is suitable for almost all types of deck with the exception of the large cellular box beam, although Hambly (1974) has successfully applied a grillage analysis to this type of deck. A grillage analysis was chosen because it allowed a generalised support and loading condition to be considered.

Lightfoot and Sawko (1959) initiated the development of the computer orientated grillage analysis. This was continued by Sawko (1960, 1964, 1965) and at present the grillage analysis is available from various sources such as the Highway Engineering Branch of the Department of Transport (1975).

The main advantage of the grillage analysis is its complete generality, for at the joints any normal form of restraint to movement may be applied so that any support condition may be represented. Fixed supports, discrete columns and elastic foundations may all be represented without any difficulty. The plan form of the deck presents no real problem and skew, curved and irregular shapes may all be handled with comparative ease. A curved member is usually approximated by a series of short straight members although Sawko (1967) has produced a program for a grillage with curved beams.

The idealisation of the grillage mesh depends on the geometry of the deck and the support system. Beams should be placed coincident with lines of designed strength such as parallel to prestress, or diaphragms over supports. The choice between a skew or orthogonal grillage depends on the direction of the lines of strength and the designer's preference when detailing the transverse reinforcement steel in particular. As far as possible grillage support points should coincide with the prototype structure and in decks of high skew the correct bearing stiffness for these supports is important to give the correct distribution of shear at the ends of the beams.

An important aspect of any computer program is the time involved in the preparation of the input data and the cost of running the program on the computer. A comparison of costs for the suite of programs avail-

able from the Department of Transport's Highway Engineering Computing Branch is given in the user guide (1978) and from this the grillage analysis compares favourably with the alternative programs. It does show however that the time involved in the preparation of data for a skew deck with orthogonal members is high compared with skew members, as this type of mesh is not suitable for the computer's automatic mesh generation. This extra time is however offset by the ease in which the output may be applied directly by the engineer. This is not always the case in other programs such as finite elements, where a considerable degree of expertise is required for a correct interpretation. In the skew grillage the output is provided in the skew direction of the members and some correction is required before being used for design purposes.

2.3.5 Application of Grillage Analysis to M-Beam Bridge Decks

Mesh Configurations

Grillage analysis has been used extensively for the analysis of M-beam bridge decks in both the tee and pseudo-box forms of construction. West (1973) has made recommendations on the use of grillage analysis for slab and pseudo-slab bridge decks although he specifically excludes decks where transverse shear distortion of the box cells may influence the distribution.

In applying these recommendations to M-beam decks it is suggested that if there are many more than nine physical beams, these should be replaced by about nine (an odd number is preferred) equally spaced grillage beams positioned so that the centre-lines of the edge grillage beam coincides with the centre-lines of the edge physical beams. For a deck that is very wide, the number of longitudinal grillage beams should be increased so that, as a general rule, one grillage beam does not replace more than two physical beams.

Transverse beams should be placed at the abutments where diaphragms will normally be provided and at intermediate locations such that the ratio of spacing of transverse grillage beams to the spacing of longitudinal grillage beams is approximately 1.5:1 and that the total number of transverse members is odd. This ratio should also reflect the overall aspect ratio of the deck. The direction of the transverse beams should be parallel to the transverse reinforcement, as it has been found that for decks of small skew it is easier to detail the reinforcement in the skew direction. It is therefore accepted that a skew mesh should be used for analysis. As far as the pseudo-box type of construction is concerned the dilemma does not arise as steel must follow the direction of the web holes in the beams. This type of skew mesh also has the advantage of being suitable for automatic generation by computer.

Factors Influencing Section Properties

Existing design procedures based on grillage analysis use the recommendations of West (1973) which was based on an investigation by West (1973) of the use of grillage analysis for a wide range of bridge deck types and an unpublished report by the Cement and Concrete Association (1971).

Tee Beam

For the beam and slab construction the calculation of the longitudinal bending inertia is done by taking the value for one physical beam and its associated top slab and this is apportioned to all grillage beams as the inertia multiplied by the number of physical beams and divided by the number of grillage beams. The longitudinal torsional inertia is calculated by dividing the beam and slab into thin strips and the total

inertia is the sum of all the individual rectangles. The transverse grillage beams within the span are represented by plain rectangles of top slab only and inertias are calculated based on this.

Pseudo-box

For pseudo-box decks the longitudinal bending inertias are calculated and apportioned as for the beam and slab deck. The transverse bending inertia is based on the top slab acting with a quantity of bottom in situ concrete equivalent to an area 4D x 2.5D where D is the equivalent diameter of a single bar passing through the transverse hole. This recommendation by West (1973) is intended to include an allowance for tension stiffening by the bottom in situ concrete. The second moment of area for each grillage beam is calculated by factoring this value by the ratio of the spacing of the grillage beams/the spacing of the bottom steel.

The calculation of the torsional inertias for the pseudo-box deck is perhaps the most difficult to appreciate structurally. For the grillage analysis two twisting inertias are required, one longitudinal and one transverse. By calculating the torsional inertias in both the longitudinal and transverse direction and using them directly in the grillage analysis, an overestimation of the true torsional stiffness has been found to result for slab type structures. This is because the deck is a 2 dimensional continuous plate and a twist applied in one plane will produce a complementary twist in the orthogonal plane. Therefore, when analysing bridge decks of this type, it is normal practice to use only one half of the calculated torsional inertia in each direction. Thus for the pseudo-box system it is suggested by West (1973) that the torsional inertias be calculated as follows:-

$$\text{Longitudinal torsional inertia} = \frac{C_L}{1+q}$$

$$\text{Transverse torsional inertia} = \frac{qC_L}{1+q}$$

where C_L = the twisting inertia from the longitudinal cross-section

qC_L = the twisting inertia from the transverse cross-section

and q = a proportioning factor to be calculated.

A correction has to be applied to the above inertias if the width of the transverse and longitudinal beams is unequal. For the calculation of C_L, West (1973) recommends the use of the thin walled theory which is used extensively in aircraft structures. An alternative view has been expressed by Goodall (1971) who has stated that because the internal webs are ignored the above approach could underestimate the true inertia by up to 15%. In view of this he has developed a procedure for calculating the torsional inertia of a cellular section, based on membrane analogy, which takes into account the webs.

Clark (1975) has compared various methods of calculating the torsional inertia of voided slab bridges and suggests that for load distribution analysis the torsional inertia should be calculated by considering the flanges of the section to be a pair of coupled laminae.

Although an accurate estimate of both longitudinal and transverse torsional inertias is important, for a deck with constant bending inertias it is the sum of the two torsional inertias which control the deflections and hence the longitudinal bending moments in the deck. This applies to both grillage and load distribution methods of analysis and may be seen by considering the stiffness parameters used for load distribution where:-

$$\alpha = \frac{G(i_o + j_o)}{2E\sqrt{i_o + j_o}}$$

$$\theta = \frac{b}{2a}\sqrt[4]{\frac{i}{j}}$$

The coupling of the i_o and j_o terms in this manner means that it would be possible to have two decks with the same deflection profiles provided the sum of the two torsional inertias was the same. However, there would be an adjustment to the transverse bending moments, torsional moments and shear forces.

The calculation of the transverse torsional inertia is the subject of much debate and for this West (1973) suggests that the actual deck (Fig. 2.5) should be replaced by an internal grillage beam as shown in Fig. 2.6. For this type of section Kollbrunner (1969) has derived an expression for calculating the torsional inertia of this open sided box section. Essentially therefore, the short sections of longitudinal beams in Fig. 2.5 are replaced by side gussets of equal inertia.

A quarter scale model of a pseudo-box deck, tested at the Cement and Concrete Association (1971) was used by West to confirm his recommendation of the Kollbrunner (1969) method for calculating the transverse torsional inertia. The structure was formed of 18 precast prestressed PCDG inverted tee beams with transverse reinforcement threaded through the holes at the base of the web with in situ reinforced concrete placed to cover these bars. Asbestos cement shuttering was placed on preformed shoulders to span between the heads of the beams and an in situ reinforced concrete slab cast onto the beams. This slab was tied to the beams by stirrups left projecting from the upper surface of the beams. The loading was applied to the deck by a quarter scale representation of a vehicle similar to the HB vehicle.

Some doubt must be expressed as to the validity of applying the results of this test to an M-beam deck. The PCDG inverted tee beam has a bottom flange width of 493 mm whereas for the M-beam it is 970 mm. This means that for the same width of deck the model tested had twice as many cells as it would have had if quarter scale M-beams had been used. Also when bending in the transverse direction is considered, cracking would occur between each beam and hence twice as many cracks would be present which would adversely affect the distribution properties of the deck. Therefore, an M-beam deck should show much stiffer characteristics transversely thereby reducing the magnitude of the longitudinal bending moment and distributing it into beams that are remote from the application of the load.

Some doubt may also be expressed as to the effectiveness of the bottom transverse reinforcement. Because of the narrow width of the PCDG inverted tee beam, a complete bond of concrete and reinforcement would be essential within the hole in the web and generous entrant angles would be required to satisfy this condition.

2.3.6 Standard Bridges

The Department of Transport in 1971 set up a committee to investigate the possibility of producing a standard bridge for a given set of parameters. Deck types considered were U-beam for maximum span of 40 m, M-beam up to 29 m, reinforced concrete slab for continuous decks and short simply supported spans with the inverted tee beam (solid infill) for the under 14 m range. Steel beams with reinforced concrete composite slab were also considered. The work was shared between the Road Construction Units, Consultants and Constrado. The idea was to produce a completely detailed design as a series of completed drawings which would cover a broad range of situations and include provision for services, parapets and various footpath widths.

The recent publication from the Department of Transport (1978) is the result of this work and goes some way towards standardisation for certain highway intersections. It does however fall far short of the original concept of being able to provide an off-the-shelf deck for any given situation. The proposals take the form of 12 charts which cater for commonly occurring motorway and dual carriageway crossings in the United Kingdom. The procedure allows the design team to assess each new bridge site for the application of standard bridge designs before being presented to the appropriate authority for approval. For any given crossing there is no single choice that would be most economical in all circumstances, therefore a range of designs is offered for tender using various types of construction from which a final economic choice may be made. Superstructures are either simply supported or continuous, and a choice of spans up to 22 m is available, side road widths being 5.5 or 7.3 m with 2 m verges. The standard M-beam deck uses the M6 or M8 beams spaced at 1.5 m with the edge beam spacing reduced to cater for a service duct. The provision of services is obviously a problem as the edge beam becomes almost non-structural, being only supported by cross ties at the end diaphragms and at mid-span.

One of the first group of bridges constructed under a standard bridge tender is on the A604 Barhill to Godmanchester Road and the M-beam proved to be the most competitive for all four bridges concerned. However, in order to adopt the standard bridge procedure for this contract, it was found that the bridges were over-spanned and wider than necessary. Although M-beam construction was the most economic standard bridge, it has been found to be more expensive than M-beam bridges spec-

ifically designed for these sites, as this more conventional approach would have avoided the necessity of providing a bridge greater in span and width than required.

Applying the standard bridge approach to the particular case of Northern Ireland, the U-beam is not manufactured locally and steel beams tend to be expensive for the longest spans. This leaves the PCDG inverted tee beam and in situ concrete for the shorter spans, and the M-beam and voided in situ reinforced concrete slab for the longer spans above about 16 m. Therefore for the local situation much of the competitiveness of the Standard Bridge is lost.

2.3.7 Wider Applications of M-Beam Decks

The Department of Transport's Standard Bridge has been found to be unsuited for use in Northern Ireland but by increasing the spacing of the M-beams up to 2 m the range of spans accommodated could be increased from the present 15 to 29 m to 8 to 29 m.

A comparison of the costs of various types of bridge decks currently being constructed in Northern Ireland is presented in Appendix A and from Fig. A1 it may be seen that the M-beam deck could provide a very competitive design for spans from 8 to 29 m. It should also be noted that the M-beam deck will provide a lighter deck than other forms of concrete construction and in poor ground conditions this should be reflected in the cost of the substructure. This comparison of bridge types also takes into account the adjustments to beam size and slab reinforcement that are required when the beam spacing is increased. Although there are obvious economic advantages to be gained by spacing the beams, the limiting factor under the current design requirements is not one of beam capacity but the strength of the slab spanning be-

tween beams and distributing the wheel loads. Additional economies can be made by minimising the amount of reinforcing steel required in the standard 160 mm slab. With an optimum design in mind the development of methods of analysis for this type of deck slab will be reviewed.

2.4 LOCAL ANALYSIS OF BEAM AND SLAB BRIDGE DECKS

2.4.1 Introduction

The original concept of the M-beam deck was that the beams should be placed at 1 m intervals. Although increasing the spacing has considerable economic advantages (Appendix A) it does, however, introduce problems for the analysis and design of the slab. As the beam spacing increases, the slab between the beams can accommodate more wheels and this increases the stress levels experienced by the slab. An accurate analysis of the slab under this system of loading is a complex problem and must take into consideration the influence of such variables as the effect of surfacing on the distribution of wheel loads, boundary and support conditions provided by the beams, in-plane restraint and the effect of cracking on the serviceability and failure loads of the slab. Research into the load carrying characteristics of this type of slab has been underway for many years and historically may be divided into 3 distinct phases.

1. Classical elastic plate analysis including influence surfaces and current design code requirements.
2. Yield line analysis which will be permitted for use with the new limit state code BS 5400 (1978).
3. The most recent advances in slab analysis which takes into account the considerable enhancement due to in-plane restraint.

Therefore, this part of the chapter reviews the historical development of the various methods of analysis for slabs under the action of concentrated wheel loads. Although the main objective is to study reinforced concrete bridge slabs, reference has been made to other applications where this has been considered necessary to complete the review.

2.4.2 Elastic Plate Analysis

The behaviour of plates under loads acting perpendicular to their planes has interested the early researchers at the time of the industrial revolution and it was the French mathematician Lagrange who, in 1811, succeeded in describing flexural plate responses by a fourth order partial differential equation.

$$\frac{\partial^4 z}{\partial x^4} + \frac{2\partial^4 z}{\partial x^2 \partial y^2} + \frac{\partial^4 z}{\partial y^4} = \frac{12(1 - \mu^2)w}{Eh^3}$$

This equation, for all its precise symmetry and compactness, has a number of shortcomings in its use for analysing concrete bridge slabs. For example, it does not permit a closed format direct solution, has difficult boundary conditions, is not directly applicable to concentrated wheel loads and finally it does not consider cracks which occur in concrete bridge slabs.

Progress was slow in overcoming these difficulties although the combination of vertical shears and twisting moments permitted the expression of reactions in the theorem of Thomson and Tait (1867). A further improvement was the use of a Fourier series for load representation by Whittaker and Watson (1915) who proved that although the series describing concentrated loads are divergent, further successive integrations by which shears, moments, rotations and displacements are obtained produce usable, convergent series.

In due course a solution of the Lagrange equation in a finite form was derived by Nádai (1925) using a deductive process involving functions of a complex variable.

Proposals for computing the bending moments of bridge slabs under the influence of concentrated loads based on available test results was made by Kelley (1926) and finally, Westergaard (1930), having resolved the problem of an infinite bending moment under a point load by introducing a rigid disc under the load, published his article of historic importance.

Slab design requirements of not only the Department of Transport, but North America and most countries of the world are now based on Westergaard's equations which are from the analysis of an elastic plate. However, it is only in recent years that the effects of cracks, lateral restraint by beams and diaphragms and the continuity of the slab have been considered.

Westergaard's studies of reinforced concrete slab action under concentrated loads were directed towards the computation of maximum moments under a load concentrated over a small area. For a point load on a slab having a span of 10 to 20 times its thickness, he found the moment under the load to be about 0.3P. The value of the moment under the load varies only slightly with slab edge conditions and size of loaded area. For a load distributed over a circular area with a diameter equal to one tenth of the slab span, the maximum moment under the load was about 0.25P for a slab with edges fixed at the ends of the short span. The moment under the load in a direction normal to the maximum moment was 0.21P. Westergaard demonstrated that these moments

were nearly independent of the slab span. Westergaard's equations and application are given in Appendix D.

Westergaard's computational method was further developed by Newmark and Siess (1943) who recommended that slabs on I-beam bridges be proportioned for maximum slab moments of about 0.34P and 0.25P under similar conditions. They also recommended that over the beams provision be made for a negative moment of 2/3 or 3/4 of the maximum positive moment. Newmark (1949) recommended further simplification of the formula for moments under a wheel load. He stated that for ordinary proportions of I-beam bridges, the transverse slab moment under the wheel load varied from 0.2P to 0.28P and the longitudinal moment varied from 0.12P to 0.2P. He recommended that top transverse reinforcement over the beams should provide for a moment of resistance of 0.7 of the maximum slab moment, and that the top longitudinal reinforcement provide for 0.2 of the maximum slab moment.

A comprehensive work on influence surfaces of elastic plates has been published by Pucher (1964) in which 93 charts representing elastic plates of various shapes and support conditions are presented. The charts allow the rapid computation of plate and support forces. The Department of Transport recommend the use of these charts as an alternative to Westergaard. However, they are similar and are based on an elastic analysis with the usual assumptions which are:

1. The thickness of the plate is constant and small compared with other dimensions.
2. The material is homogeneous and isotropic and follows Hookes Law.

3. The deflections are small compared to the plate thickness.

While most of these assumptions may be valid for concrete slabs which are uncracked under a low level of loading, some doubt must be expressed as to their validity when the slab is extensively cracked and approaching its failure load.

A further development in the analysis of the elastic plate using influence surfaces was presented by Woodring and Siess (1968) for the moments in reinforced concrete floors continuous in 2 directions. These surfaces indicated maximum positive slab moments in the centre of the panel of about 0.2P for loads concentrated over a small area. Loads distributed over an area having a dia. of 0.1 span would result in smaller maximum moments. Woodring and Siess (1968) then determined equivalent load factors to convert concentrated loads to uniform loads which would produce the same moments as the concentrated loads. Their results clearly demonstrated that the equivalent load factor was not constant, but varied with location and moment.

As mentioned previously, the use of the analysis proposed by Westergaard (1930) has now become the established method in most countries for the estimation of the local moments in beam and slab bridge decks. The current standard of the Department of Transport also recommend the use of the influence surfaces by Pucher (1964). When the moments have been calculated the slab is designed in flexure using elastic methods. However, there are additional requirements to be met relating to crack control and punching shear and both these aspects of bridge slab design will now be considered.

Control of Cracking

The current standard specifies a permitted width of crack depending of whether the loading is type HA or HB whereas the new bridge code relates this to the degree of exposure.

The existing requirements are contained in the Department of Transport's Technical Memorandum (Bridges) BE1/73 and the crack width must be checked under the worst combination of dead and live loading. The crack width should not exceed 0.25 mm for HA loading and 0.30 mm for HB loading and is calculated from

$$(w) = K\, C_{min}\, \varepsilon_a$$

where K = 3.3 for deformed bars and 3.8 for plain bars.

For BS 5400 (1978) slab soffits are classified for exposure as "severe" and the crack width should not exceed 0.20 mm. Although there are deemed to satisfy clauses relating mainly to solid slab bridges, in general the crack width must be calculated from

$$(w) = \frac{3a_{cr}\,\varepsilon_m}{1 + \dfrac{2(a_{cr} - c_{min})}{h - x}}$$

where $$\varepsilon_m = \varepsilon_1 - \frac{1.2\, b_t h(a' - x)10^{-3}}{A_s(h - x)f_y}$$

and x = depth of the neutral axis

In the calculation of crack widths, strains are assumed to be proportional to their distance from the neutral axis, the position of which and the stresses in the steel reinforcement are calculated ignoring concrete in tension. The background to the control of cracking in design codes in general has been considered by Beeby (1979) and with particular ref-

erence to highway structures by Clark and Elliot (1981).

Although there is a difference in philosophy to the control of cracking between the existing standard and the new bridge code, these documents are similar in their approach to punching shear.

Punching Shear Requirements

Punching shear must be checked in solid slabs supported by columns and slabs supported by beams with loads applied by vehicle wheels.

In both the current United Kingdom standard of the Department of Transport Technical Memorandum (Bridges) BE1/73 (1973) and the proposed limit state code BS 5400 (1978) the critical section has been assumed to be at a distance of 1.5h from the perimeter of the loaded area, and the permissible shear stress is dependent upon the average of the tensile reinforcement in the transverse and longitudinal directions. This is based on work by Regan (1973) and although modified slightly in the code the permissible shear stress is given as

$$v_c = (\rho f_{cu})^{0.33}$$

In North America the AASHTO (1977) and CSA (1974) specifications state that punching shear resistance is deemed to be adequate when designed by the specified flexural methods. The recent Ontario Highway Bridge Design Code (OHBDC) (1979) is similar to the ACI 318 (1977) building code and specifies the critical section as d/2 from the loaded area with the permissible shear stress given as 0.33 f'_c for the OHBDC and 0.32 f'_c for the ACI-318 (1977) building code. In both these North American codes no allowance is made for the presence of steel reinforcement and the punching shear depends only on concrete strength.

The failure of bridge slabs in a punching shear mode has not been of interest to the early researchers possibly because wheel loads were much less than they are at present and flexural action was considered to be more important. However, it is recognised (Long (1975)) that flexural effects influence the capacity of a slab and for slender slabs failure can be considered to occur when a plastic hinge forms locally around the load.

Plastic methods will be permitted for bridge deck analysis when the new limit state code is introduced. There have been important developments in this field in the last forty years or so and although not entirely applicable to bridge decks the approach is worthy of further consideration.

2.4.3 Plastic Analysis of Slabs

Plastic methods of analysis for concrete structures was a natural development of the successful wartime application of plastic theory to steel frames and plates. Significant contributions were made in the United Kingdom by Hill (1950) and in North America by Prager and Hodge (1951). With the general trend of Codes of Practice towards limit state analysis, the yield line methods developed by Johansen (1962) have now become an accepted method for the analysis of reinforced concrete slabs. Yield line analysis is an upper bound plastic method where the designer must accurately predict the pattern of the collapse mechanism. It has been used extensively by researchers in the field of building slabs supported by beams or columns where the loading is of a uniformly distributed nature.

Yield line analysis of bridge slabs will be permitted by the Department of Transport when the new limit state code BS 5400 (1978)

is introduced. Heavy concentrated wheel loads will have to be considered and for this type of loading the yield line analysis still results in average moments spread over the full length of the yield line without the expected peak characteristic of the concentrated wheel. Because of this difficulty in analysing the point load, yield line methods are seldom used by bridge engineers, although Hogenstad (1953) presented a yield line analysis for a point load which recommended provisions for negative and positive reinforcement in 2 orthogonal directions such that the sum of the unit negative and positive moment of resistance was 0.16P. For a load distributed over a circle having a diameter 0.1 the span he found that the negative plus positive resistance should be 0.15P. A corresponding recommendation by Westergaard (1930) or Newmark and Siess (1943) would be about 0.3P.

Even though it is an upper bound plastic method, test results have shown it to give conservative results mainly due to the enhancement of the load carrying capacity by the considerable in-plane restraint provided by bridge deck slabs. It is now generally accepted that for an accurate estimate of the load capacity of reinforced concrete slabs, account must be taken of the in-plane restraint. The latest developments in research into the design of slabs including compressive membrane action will now be considered.

2.4.4 Compressive Membrane Action in Slab Design

The study of membrane action in slabs has increased in the last 10-15 years although the tremendous increase in the collapse load caused by this phenomenon has been known to researchers for many years. Westergaard and Slater (1921) observed this increase when a number of

full scale flat floor panels were tested to destruction early in the century. One of the earliest records of enhanced collapsed loads with horizontally restrained slabs occurs in the reports of pre-war tests by Thomas (1939). Probably the most well known tests on a complete building was done by Ockleston (1955) when the Old Dental Hospital, Johannesburg was tested to destruction. This showed that loads considerably greater than those predicted by yield line theory could be sustained by continuous concrete slab floors. About the same time Powell (1956) carried out a series of tests on encastré model slabs, and the collapse loads were extraordinarily large. The problem of compressive membrane action has been further researched by Wood (1961) Christiansen (1963) and Park (1964, 1965). Taylor and Hayes (1965) tested pairs of simply supported and restrained slabs and found that the restraint increased the capacity by up to 60%.

Most of this early research has been done on RC building slabs which were continuous over, and supported by, beams or in situ slab column structures. The loading required for this type of structure is uniformly distributed and a high proportion is permanent which introduces new problems relating to the long term nature of the compressive membrane forces and the time dependent creep and shrinkage effects.

When reinforced concrete bridge slabs are considered the loading is concentrated on relatively small areas and is very transient in nature. This type of slab would seem to be the ideal structure upon which to exploit the full benevolent effect of membrane forces in the slab. However, this has not been the case as at present almost all bridge codes adopt an elastic flexural design based on the work of Westergaard, and the tremendous economic advantages are not exploited.

As far as bridge design codes are concerned the notable exception is the Ontario Highway Bridge Design Code (1979) which is based on limit state principles and within certain limits takes full advantage of compressive membrane action.

In 1971 the American Concrete Institute annual convention held in Denver, Colorado, included a symposium regarding the cracking, deflection and ultimate load of concrete slab systems. A considerable number of papers presented involved the investigation and measurement of the compressive membrane forces and probably for the first time, an investigation relating to bridge slabs was presented by Tong and Batchelor (1971).

Their work was based on a 1/15 scale model of an 80 foot span, two lane, two girder bridge having two interior and two end diaphragms. Microconcrete was used for the model and it was loaded by a single elliptical pad representing the contact area of a pneumatic tyre. Tong and Batchelor stated that compressive membrane action exists in bridge slabs supported by conventional edge beams. This effect enhances both the flexural and shear capacity and ensured that all slabs failed at loads higher than those predicted by the yield line theory of Johansen (1962), regardless of actual mode of failure. If a very low reinforcement percentage is used punching failure would be eliminated altogether and the more desirable flexural mode would result.

An important paper was presented by Brotchie and Holley (1971) who reported the results of tests of 45 square slabs which spanned 38.1 cm. The slabs were unreinforced, or reinforced near the bottom only with smooth steel wire uniformly and equally distributed in each direction. Various boundary conditions were tested and a scaled concrete

mix was also used. An important feature of these tests was the measurement of the actual compressive membrane forces with the various types of support. However, as the loading was uniformly distributed the results are not directly applicable to concrete bridge decks. Brotchie and Holley did suggest however, that for slabs with a span to depth ratio of 20, the effect of arching was found to be significant and was equivalent in load capacity to approx 2% of conventional reinforcement. They suggested that even unreinforced slabs when laterally restrained are stronger than conventionally reinforced but unrestrained slabs with normal ratios of steel. The effect of arching action was even greater for thicker slabs, and for a span to depth ratio of 5 was found to be equivalent in load capacity to over 3% of conventional reinforcement. They concluded that external restraint and internal steel are basically similar in effect, and are only partially additive.

Further papers were also presented by Aoki and Seki (1971) who considered 14 square slabs ranging in size from 1.2 m to 1.6 m, with various constraints and concentrated central loads. Hopkins and Park (1971) also described tests carried out on a ¼ scale nine panel reinforced concrete slab and beam floor which was designed with allowance for membrane action. The test results showed that design allowing for membrane action is possible provided adequate safety margins are allowed. Park stated that "The doubt surrounding the long term behaviour of the floor and the requirement that design loads must be high before membrane action can be fully exploited limit the applicability of membrane action design to relatively thick heavily loaded slabs with reliable lateral restraint". Although Park was directing his comments to building slabs it would seem that the beam and slab bridge decks would meet these requirements as they combine reliable restraint,

heavy transient loads and for practical designs the span to depth ratio is usually low.

As mentioned previously, the Ontario Highway Bridge Design Code (1979) recommends the design of bridge slabs using a method which incorporates the effect of compressive membrane action. Although the research for this code was started initially by Tong and Batchelor (1971) important contributions were also made by Batchelor and Tissington (1976) who confirmed the absence of scale effects in the testing of small concrete bridge models, Batchelor, Hewitt, Csagoly and Holowka (1978) who investigated the strength of composite steel beam and concrete slab decks and Batchelor, Hewitt and Csagoly (1978) who verified that fatigue was not a problem in the performance of reinforced concrete bridge decks. The results of these various model studies were verified by an extensive series of field tests on existing bridge decks by Csagoly, Holowka and Dorton (1978). A total of thirty two bridges were chosen covering a wide range of types and parameters such as span, slab thickness, age, deterioration and reinforcement. A testing machine capable of providing a concentrated load of up to 445 kN, was specially designed and constructed for this purpose. The punching shear testing of existing bridge decks indicated that there was a very large reserve capacity against failure as no failure of restrained decks occurred. To complete the field testing two bridges were designed and constructed with extensive instrumentation to monitor the performance under test load. The first bridge was the Conestogo River Bridge which was reported by Dorton (1976) and was a three-span (34.77, 44.23, 34.77 m) steel girder composite slab deck with slab thicknesses of 177.8, 190.5 and 203.2 mm, reinforcement of 0.2, 0.3,

0.6 and 0.95 per cent and all the panels were successfully tested for a concentrated punching load of 43 tonnes. The stresses in the reinforcing bars were all found to be negligible. It was observed however, that the panels with 0.3 per cent reinforcement, regardless of other parameters involved, showed hairline cracking of limited extent that became invisible after the removal of the load.

The second major bridge tested was a composite prestressed concrete AASHTO girder bridge by Holowka and Csagoly (1980). It was four girders wide and extended over three spans, continuous for live load, with a composite concrete slab. The bridge was extensively instrumented and tested for both punching shear and overall vehicle weight effects. It was established that concrete slabs with 0.3 per cent reinforcement, supported by precast prestressed AASHTO girders do not require the assistance of intermediate diaphragms to develop the necessary membrane forces.

The final tests relating to the Ontario HBDC was carried out at the Ministry of Transportation and Communications by Holowka, Dorton and Csagoly (1979) and included a series of 27 circular slabs instrumented in order that the compressive membrane forces could be monitored. The slabs were 572 mm in diameter and the variables were slab thickness (31.75, 38.1 and 44.5 mm) and reinforcement percentage (0.2, 0.3 and 1.0). The concrete mix was scaled to give both compressive and tensile strengths similar to the prototype which had a cube strength of about 34 N/mm^2 at the time of test.

All specimens failed in a punching shear mode with 2 perpendicular cracks forming on the underside of the specimen, intersecting at the point of application of the load. Subsequently, an additional pattern

of radial cracking appeared and failure occurred when a large circular crack formed defining the boundary of the fustrum being pushed out. In addition to the measurement of the compressive membrane forces it was concluded that 0.3% isotropic reinforcement would provide a satisfactory deck slab. The background to slab design using the Ontario HBDC (1979) has been reviewed by Csagoly (1979).

An important series of tests was carried out at the Building Research Station by Snowdon (1973, unpublished) for the proposed floating airport at Maplin. Full scale slabs were used with a heavy concentrated load simulating a single aircraft wheel and were designed to utilise the effect of compressive membrane action.

The proposed construction consisted of a hollow raft one metre deep comprising top and bottom slabs separated by a series of orthogonally arranged concrete partitions which divided it into cells about 2 m square. The compartments were to be filled completely with polystyrene to provide permanent flotation.

Concrete cube strengths ranged from 44.8 to 78.5 N/mm^2 using quartz gravel, crushed limestone and Lytag lightweight aggregate. Slab thickness was limited to 100 and 125 mm with 2 and 3 different percentages of reinforcement respectively. The standard loading shoe was 200 mm diameter and a few tests were made using a 100 and 300 mm diameter shoe.

It was found that all the panels failed by punching, the failure was independent of type of aggregate and was directly proportional to the depth of the slab. It was also suggested that the greatly enhanced punching strength was proportional to the square root of the concrete strength.

In conclusion, it must be stated that compressive membrane forces are inherent in most beam and slab bridge decks and to minimise the cost of M-beam decks it is most important that account be taken of them for design purposes, therefore an improved understanding of these effects is required by bridge design engineers.

2.5 CONCLUSIONS

From the review of the literature and with particular reference to M-beam bridge decks, the following conclusions may be drawn.

1. Due to the reservations about the one quarter scale model used by West (1973) for his recommendations, a series of independent tests of both tee beam and pseudo-box decks will be required to establish their load distribution characteristics. With this in mind it was decided that four bridges which had been designed by and made available by the Department of the Environment for Northern Ireland Roads Service will be tested during construction. This will allow the load distribution properties of both types of deck to be monitored and other aspects of interest to be studied.
2. When the load distribution characteristics have been established they will form the basis of an analytical investigation to provide a simplified design procedure for the design of M-beam bridge decks.
3. Considerable economies may be made in the design of this type of deck by spacing the beams apart. To do this information will be required on the load distribution properties of the deck with the spaced beams and also on the serviceability and failure loads of

the slab spanning between beams and loaded with the HB vehicle. The Department of the Environment for Northern Ireland, Roads Service have agreed to make an additional bridge available for test purposes. It will be designed to suit the test program with two different beam spacings and four different percentages of steel reinforcement. The testing of the prototype slabs will allow a study to be made of the serviceability limit state but a model will be necessary for the ultimate condition. Due to the current financial restrictions it has not been possible to construct this bridge within the time scale of the project. However, it is hoped that it will be constructed and the tests completed in the near future.

4. To complement the prototype tests a model will be required to establish the ultimate load carrying capacity of the slabs with the various quantities of reinforcement. The model will have to reflect the boundary conditions and in-plane stiffness of the the prototype. This series of tests is required to complete the study of the M-beam deck. The only other tests of this type has been done in Ontario to meet a different design criteria and deck loading.

The programme of research is shown in Fig. 2.7 and indicates how the various investigations will be combined to achieve the objective of a simplified procedure with recommendations for the economic design of M-beam bridge decks. It will be seen from Fig. 2.7 that field testing of full scale bridges forms an important part of the programme and details of the bridges tested will now be presented.

A Type of Deck	Orthotropic Plate Theory	Orthotropic Plate Theory (Design Curves)	Folded Plate	Finite Element	Finite Strip	Grillage	Space Frame	Finite Differences
Slab	X	X		X	X	X		X
Pseudo-slab	X	X		X	X	X		X
Slab and beam				X	X	X		
Cellular			X	X	X	*	X	
Composite	X	X		X	X	X		X
Orthotropic	X	X		X	X	X		X
Box			X	X	X	*	X	
B Plan Geometry								
Right	X	X	X	X	X	X	X	X
Skew 20°				X		X	X	X
Curved	X			X	X	X	X	X
Arbitrary				X		X	X	X
C Support conditions								
Simply supported	X	X	X	X	X	X	X	X
Simply supported with intermediate supports	X		X	X	X	X	X	X
Arbitrary				X		X	X	X

*Very limited applicability

TABLE 2.1 - Comparison of Computer Methods (Cusens and Pama (1975))

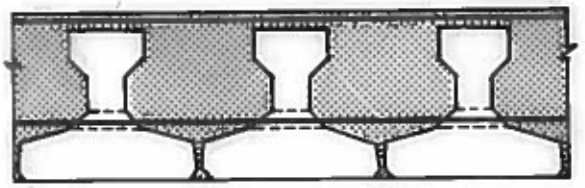

INVERTED T-BEAMS

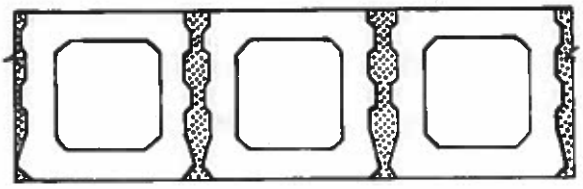

BOX-BEAMS

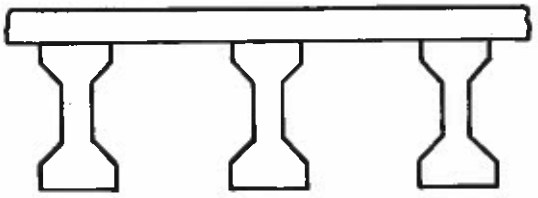

I-BEAMS

Fig. 2.1 PCDG standard precast pretensioned bridge beams

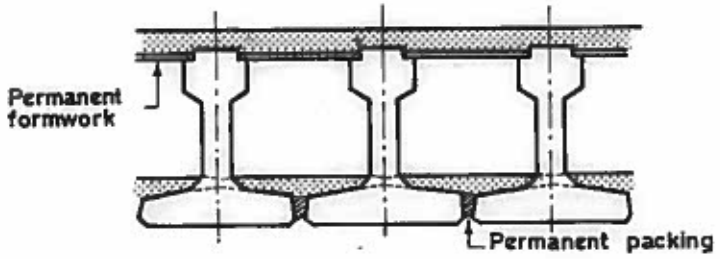

(a)

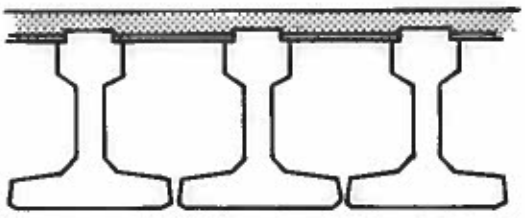

(b)

Fig. 2.2 The MoT / C&CA M-beam (a) Pseudo-box (b) T-beam

Fig. 2.1
Fig. 2.2

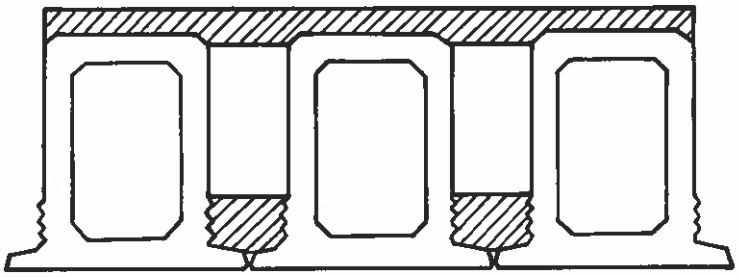

Top Hat Beam

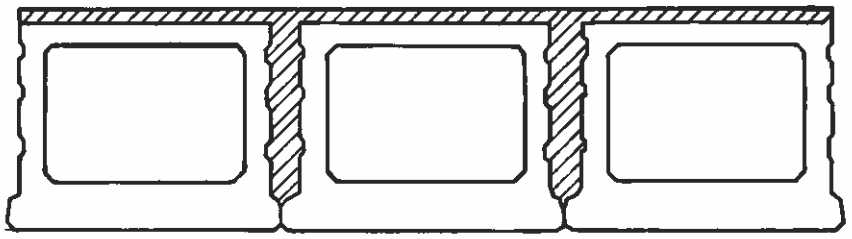

NWRCU Box-Beam

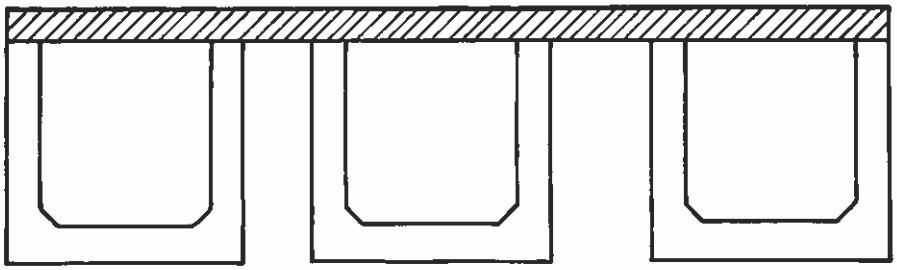

U-Beam

Fig. 2.3 Standard Box-Beams

Fig. 2.3

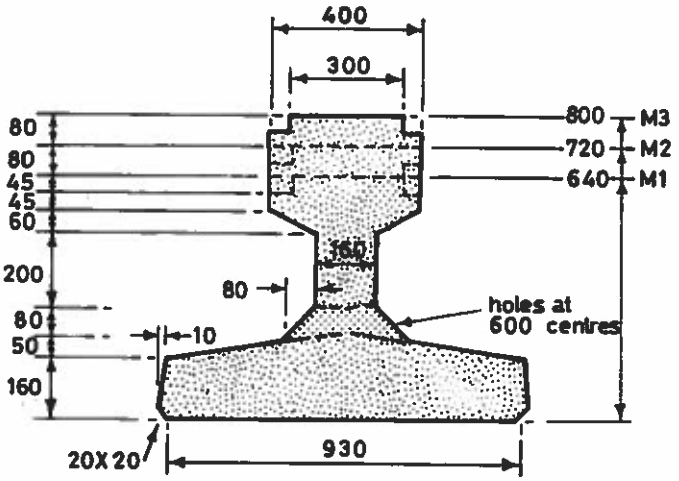

Beams positioned at one metre centres

Standard Sections M1 M2 & M3

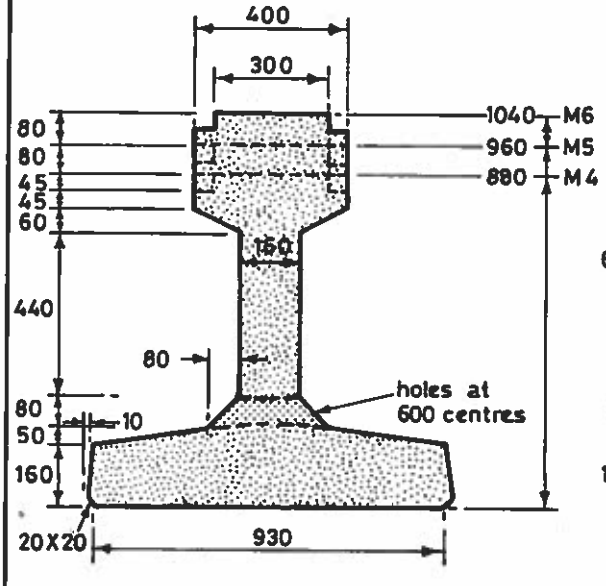

Beams positioned at one metre centres

Standard Sections M4 M5 & M6

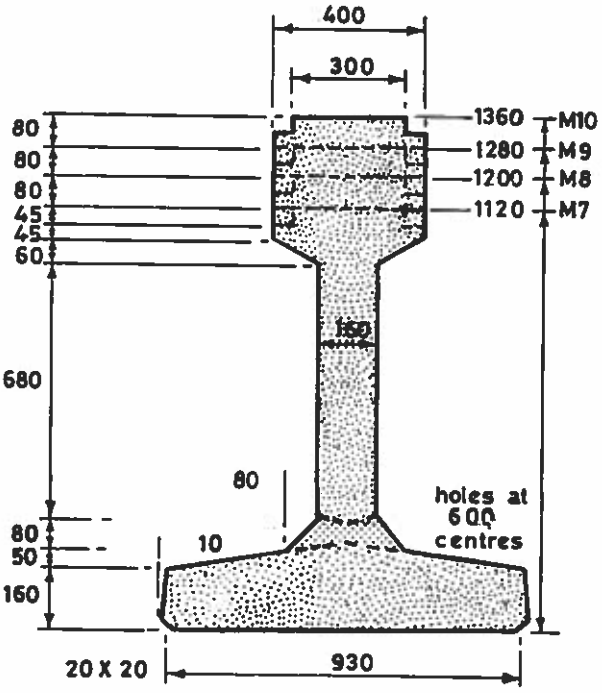

Beams positioned at one metre centres

Standard Sections M7 M8 M9 & M10

Fig.2.4 Standard M-Beam Sections

Fig.2.4

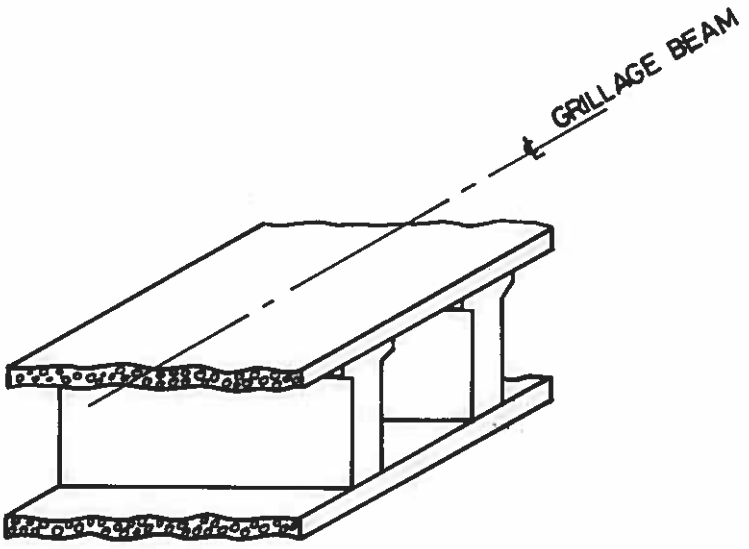

Fig 2.5 Actual Transverse Grillage Beam

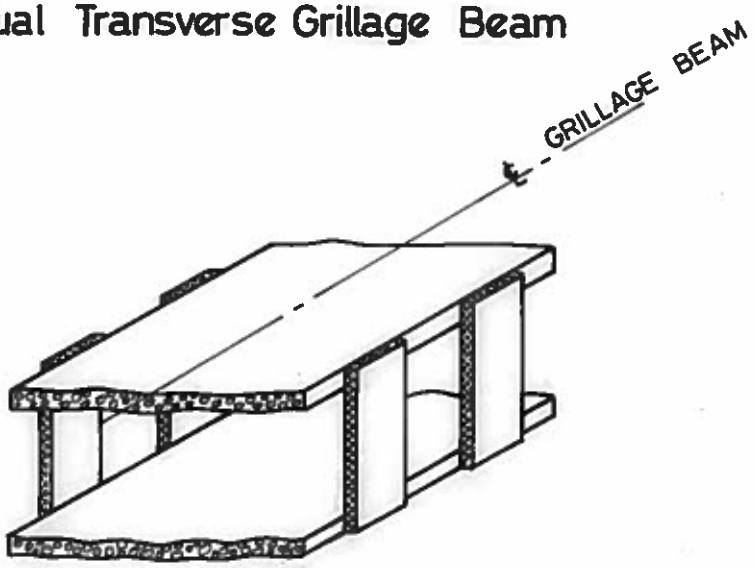

Fig 2.6 Idealised Transverse Grillage Beam

Fig.25
Fig.2.6

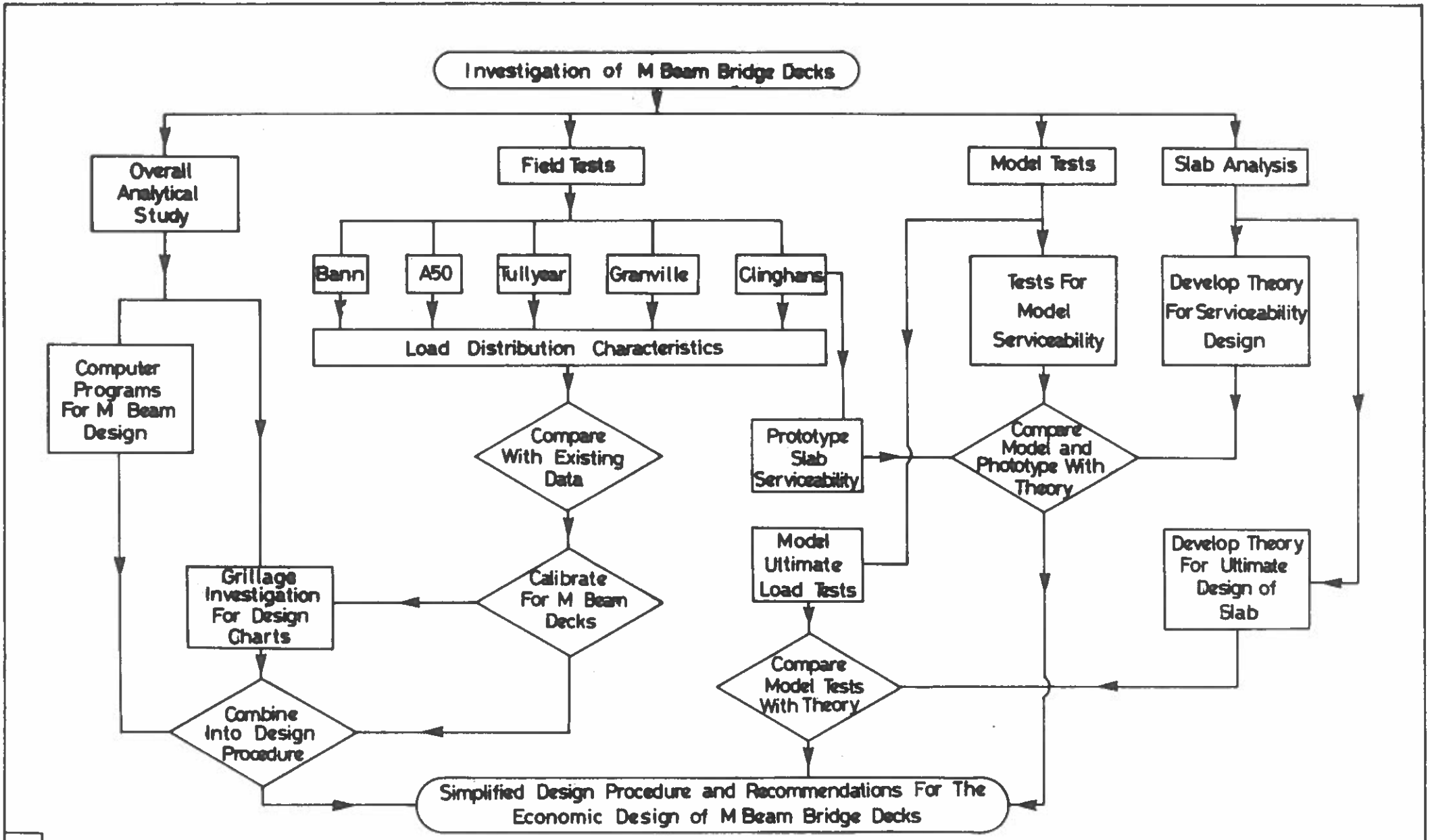

Fig. 2.7

Fig 2.7 Programme of Research

CHAPTER THREE

FULL SCALE LOADING TESTS

3.1 INTRODUCTION

In this country it is not normal practice to load test full scale bridge structures unless some doubt exists as to the capacity of the bridge to sustain the required load. This may be due to faulty workmanship or materials and is a more convenient way of proving the structural integrity of the bridge than removing the doubtful part and replacing it. During the late fifties a series of bridges were tested by Morice and Little (1954) and Rowe (1959) and the results of these tests were used to verify the method of load distribution that was being developed at that time. More recently a test by West (1970) was used for a theoretical comparison of strains in the cantilever slab of a 2 cell post-tensioned spine beam bridge with cantilevers.

The testing of full scale bridges may be arranged in a range of different ways depending on the main objectives. The design ultimate proof loading is the most difficult because of the problems of achieving the large concentrated load and the inherent danger of permanently damaging the structure. When the objective is to prove the serviceability of the bridge, and this is the most common type of test, the loading to be simulated is usually uniformly distributed and may be achieved by a large number of loaded commercial vehicles. A recent test of this type carried out locally is described by Cousins (1978). A further type of test, and possibly the most unusual, is to determine the distribution of load in the deck using commercial vehicles and accurate strain monitoring equipment. It was this type of test that was considered

necessary to validate the grillage analysis for M-beam bridge decks.

Although a considerable amount of work has been published on the use of the grillage analysis, very little is directly applicable to M-beam bridge decks and in particular those constructed in the form of the pseudo-box. As some doubt exists about the validity of the one quarter scale model tested at the C and CA (1971) and used by West (1973) for his recommendations, an independent series of tests would have considerable justification. Consequently, as a group of M-beam bridges was being constructed for the Department of the Environment for Northern Ireland, this represented an ideal opportunity for carrying out a series of carefully controlled tests on full size bridges.

The testing of a full scale bridge deck has the advantage that it will include all the usual variations in material and construction imperfections which are difficult, if not impossible, to simulate in the controlled laboratory environment. The full scale bridge will also have the correct support conditions which are extremely difficult to model in the laboratory.

An obvious disadvantage is of course the low level of concentrated load that can be applied as this is dependent upon the maximum size of lorry available. However, as it is the distribution of load rather than the magnitude of load that is being measured, this aspect is not so important provided the instrumentation can record accurately the strains induced in the concrete. Problems associated with time dependent effects such as creep and

shrinkage can be eliminated by applying the loading for only a short time and temperature variations can be monitored during the tests. During the course of these particular tests the opportunity was taken to investigate another aspect of M-beam bridge deck design which is of current interest. This is the effect of the edge stiffening due to the parapet upstand and the deck was tested before and after the upstand was cast.

Therefore, this chapter provides details of the preparation required for the testing of full scale bridge decks and gives details of the instrumentation and loading procedure used to complete this series of tests.

3.2 DETAILS OF BRIDGES

General

The bridge decks used for the tests were in the process of construction having previously been designed by the Department of the Environment for Northern Ireland. Four bridges were tested covering both tee and pseudo-box construction, each type having one right and one skew deck. Three of the bridges form part of the Banbridge By-Pass which is on the major north-south trunk road T4. The fourth bridge was on the Dungannon By-Pass which is a single carriageway continuation of the M1 motorway in Co. Tyrone. The locations of the bridge are shown in Fig. 3.1 and full details are given in Table 3.1. Three of the bridges are shown in Plates 3.1, 3.2 and 3.3.

Concrete Control Data

All the beams used in the construction of the test bridges were supplied by Macrete Limited, the concrete and three test cubes

for each beam being steam cured. One beam on each bridge was nominated for testing and from the measured beam deflection the value of the modulus of elasticity was calculated. There was considerable variation in the modulus, ranging from 37 to 49 kN/mm^2, although these values are well above the recommended value from the Department of Transport design standard, Technical Memorandum (Bridges) No BE2/73 (1973).

Load tests on the bridge decks were not carried out until the in situ deck slab had achieved its specified 28-day cube strength and this normally took from 10 to 12 days as the actual cube strength after 28 days was well above the specified strength. Details of all in situ concrete strengths and ages at the time of test are given in Table 3.2. The average 28-day cube strength for all beams are given in Table 3.3.

3.3 INSTRUMENTATION

3.3.1 Strain Monitoring Equipment

General

In planning this series of tests careful consideration was given to the measurement of the beam soffit strains and in view of the relatively low level of loading to be applied to the deck an accurate method for recording strains was of paramount importance. It was therefore decided that vibrating wire gauges would be the most suitable for this purpose as considerable expertise already existed within the Department of Civil Engineering in the use of this type of gauge on concrete structures. This was also verified by the results of the tests on the Ballymacross Railway Bridge (Kirkpatrick (1977)). Some details of the equipment, calibration

and installation will now be considered.

Strain Gauges and Calibration

To monitor the distribution of longitudinal strain across the deck, Tyler surface mounting recoverable acoustic strain gauges were located on the beam soffits. The gauges used had a 5.5" gauge length and prior to installation each one was subjected to a preliminary calibration check whilst mounted on its saddle plate. A plucking voltage of 24 volts was applied and the vibration period monitored on the strain measuring unit. Where initial tension adjustment was required this was effected on site. In these instances it was found that readings to within 2 or 3 digits on successive plucks of the wire were easily achieved.

Installation

The beam soffits were prepared by degreasing and wire brushing to remove any loose surface mortar. The gauges were then attached to the beam soffit using "Plastic Padding" which is a 2 mix compound proprietary product with a curing time of 15 to 30 minutes depending on the prevailing environmental conditions. Using this mounting technique the adjuster was left in contact with the end blocks throughout the adhesive setting period. When the adhesive had set, the gauge was then released and tested. The installation of the strain gauges is shown in Plate 3.4.

Usually every beam in one half of the deck was gauged and every alternate beam in the other half. Gauge positions on all 4 test decks are shown in Fig. 3.2 to 3.5. For the second test on each deck additional gauges were located on and in the vicinity of the parapet upstand to monitor strains in this area.

3.3.2 Measurement of Lorry Loads

Static loading was applied to the deck by 2 six-wheel lorries loaded with crushed stone and supplied by the site contractor. The total weight of each lorry was known from the quarry weighbridge docket but for the theoretical grillage analysis individual wheel loads were required. These were measured using a Digital Portable Weighbridge as used by Snaith (1978) which has been developed by the Civil Engineering Department of the Queen's University.

This portable unit is based on the TRRL system and the electronic peripheral equipment was completely redesigned to provide everything for operating the weighpad in one portable box. A digital output was incorporated which enabled the loads to be measured to higher level of accuracy than could be obtained with an analogue indicator. This weighpad had been used extensively for axle surveys by the Department of the Environment for Northern Ireland, Roads Service.

In this particular instance the weighpad was used in a specially constructed pit at a layby convenient to the test site. The lorries were taken to the layby and individual wheels weighed before being driven to the bridge for the load test. The use of the weighpad is shown in Plate 3.5.

3.4 BRIDGE DECK TEST LOADS

The loading applied to all decks consisted of 2 lorries each weighing approximately 30 tonnes and they were accurately located for each of the four loading positions. For the Bann and Granville bridges the lorries at midspan were placed transversely 1m on each side of the midspan with the rear axles on beam No. 2. They were

then moved forward until the rear axles were above beams 4, 6 and 10. For the A50 Road Bridge, where the skew was 26 degrees, the rear axles of the lorries were placed 1m on either side of the centre line of the beam on which they rested. For the Tullyear Road Bridge the first 2 positions were the same as for the Bann and Granville Bridges but as this deck was only 11m wide the remaining positions had to be adjusted to suit. For Case 3 the lorries were placed back to back on the longitudinal centre line at midspan. Case 4 was symmetrical to Case 1 with the lorries at the opposite side of the deck.

Loading positions for all decks are shown in Figs. 3.6 to 3.9. Lorry wheel loads are shown in Table 3.4 and as can be seen these gave excellent agreement with the docket weight issued at the quarry weighbridge.

3.5 TEST PROCEDURE

The positions of lorries were carefully marked out on the deck to ensure an accurate positioning of wheel loads. Immediately before the lorries were driven onto the deck a set of zero readings were taken on the strain recorder. The lorries were then driven onto the deck and positioned as required (Plate 3.6). Strain recordings and temperature readings on the thermocouples were then recorded before moving the lorries to the next load position. This procedure was repeated until all loading positions had been completed. The lorries were then removed and a set of zero readings taken. After about 30 minutes a further set of no load readings were taken.

At an early stage in the project the removal of the lorries from

the deck between each loading position was considered, this would have allowed the gauges to return to the zero readings before continuing with the next position. In general it took about 30 minutes for this to occur and as all tests were carried out at the discretion of the contractor the time involved made this procedure prohibitive. Whilst this may have been beneficial it was fortunate that there was only a small variation in temperature during the period of each test and subsequently only a nominal adjustment to readings from the vibrating wire strain gauges was required. The lorries, scaffolding and the interruption to the work programme were all paid for on a day works basis.

Parapet Upstand

After the parapet had been cast, additional gauges were added to the top of the parapet and also the deck slab above the 2 edge beams. The loading procedure was then repeated, the 2 lorries being loaded as near as possible to the same total load as was used for the first test.

Co-ordination of Load Tests

In conclusion, it must be stated that the successful completion of this series of load tests required a considerable amount of organisation of staff all representing different interests. Representatives from the Resident Engineer, Contractors, University, Quarry owners and the Royal Ulster Constabulary were all involved at various times and the timing and participation of each group was carefully planned. At a late stage in the construction of Ballymacoss Railway Bridge it was decided to try out the procedure and equipment planned for

the main series of tests. This was a most useful exercise, verifying the proposed test procedures and also produced worthwhile results as shown by Kirkpatrick (1977). That all the tests were carried out in an efficient manner is a tribute to all concerned. This is confirmed by the consistency of the results obtained which will be considered in detail in the next chapter.

Detail \ Bridge	Bann River	Granville Road	A50 Road Bridge	Tullyear Road Bridge
Construction	Tee	Tee	Pseudo-box	Pseudo-box
Effective span-m	24	23.03	18.6	16.6
Beam Size	M8	M7	M5	M2
No. of Beams	17	20	21	11
Skew^{o}	0	14	26	0

TABLE 3.1 - Details of Test Bridges

Bridge	Bann River	Granville Road	A50 Road	Tullyear Road
Beams				
Design 28-day strength N/mm^2	52.5	52.5	52.5	52.5
Actual 28-day strength N/mm^2	60.5	57.0	56.0	62.5
Age at time of beam test days	28	30	48	64
E at time of beam test kN/mm^2	37.2	40.4	39.0	49.2
Age at time of deck test No. 1	362	276	294	209
No. 2	405	326	348	314
Slab				
Design 28-day strength N/mm^2	37.5	30.0	37.5	37.5
Actual 28-day strength N/mm^2	45.0	43.2	47.3	53.3
Age at time of deck test:				
No. 1 - days	19	12	16	11
No. 2 - days	62	62	70	116

TABLE 3.2 - Concrete Details

Beam No.	Bann River Bridge	Granville Road Bridge	A50 Road Bridge	Tullyear Road Bridge
1	57.5	58.7	55.7	57.5
2	58.5	56.3	55.7	57.0
3	58.5	56.3	55.7	57.0
4	60.5	57.8	59.2	61.0
5	60.5	57.8	59.2	63.0
6	57.3	58.0	59.2	62.5
7	57.3	58.0	59.3	59.5
8	60.5	57.0	59.3	58.5
9	60.5	57.0	59.3	64.0
10	57.0	57.5	57.8	60.5
11	57.0	57.5	57.8	58.5
12	56.6	62.1	57.8	
13	56.6	62.1	55.2	
14	59.5	59.8	55.2	
15	59.5	59.8	55.2	
16	57.5	57.8	55.0	
17		57.8	55.0	
18		60.5	55.0	
19		60.5	58.2	
20		58.7	58.2	
21			58.2	
Test Load - kN	233.5	178.0	180.5	135.0
Deflection - mm	47.2	39.6	29.5	25.0
Elastic Mod. kN/mm^2	37.2	40.4	39.0	49.2

TABLE 3.3 - 28-Day Cube Strengths of all Beams

Bridge	Lorry A - kN			Total Weigh Pad	Total Quarry Docket
	Front	Centre	Rear		
BANN					
Test No. 1	72.0	116.0	109	297.0	298.0
Test No. 2	70.4	117.2	125.6	313.2	311.0
GRANVILLE					
Test No. 1	81.0	126.8	119	326.8	307.9
Test No. 2	76.0	129.8	121.8	327.6	312.4
A50					
Test No. 1	66.7	122.3	120.8	309.8	302.6
Test No. 2	70.1	120.1	115.1	305.2	309.6
TULLYEAR					
Test No. 1	70.3	108.0	119.4	297.7	296.7
Test No. 2	68.4	111.2	114.1	293.7	298.2
Bridge	Lorry B - kN			Total Weigh Pad	Total Quarry Docket
	Front	Centre	Rear		
BANN					
Test No. 1	65.4	120.0	117.0	302.4	302.0
Test No. 2	65.1	119.1	117.6	301.8	304.0
GRANVILLE					
Test No. 1	77.8	121	120	318.8	310.3
Test No. 2	60.2	140.8	119.6	320.6	313.4
A50					
Test No. 1	71.1	120.7	123.7	315.5	309.0
Test No. 2	68.2	115.3	121.1	304.6	304.4
TULLYEAR					
Test No. 1	67.3	126.3	106.0	299.6	306.8
Test No. 2	66.0	119.6	117.1	302.7	303.4

TABLE 3.4 - Lorry Axle Loads

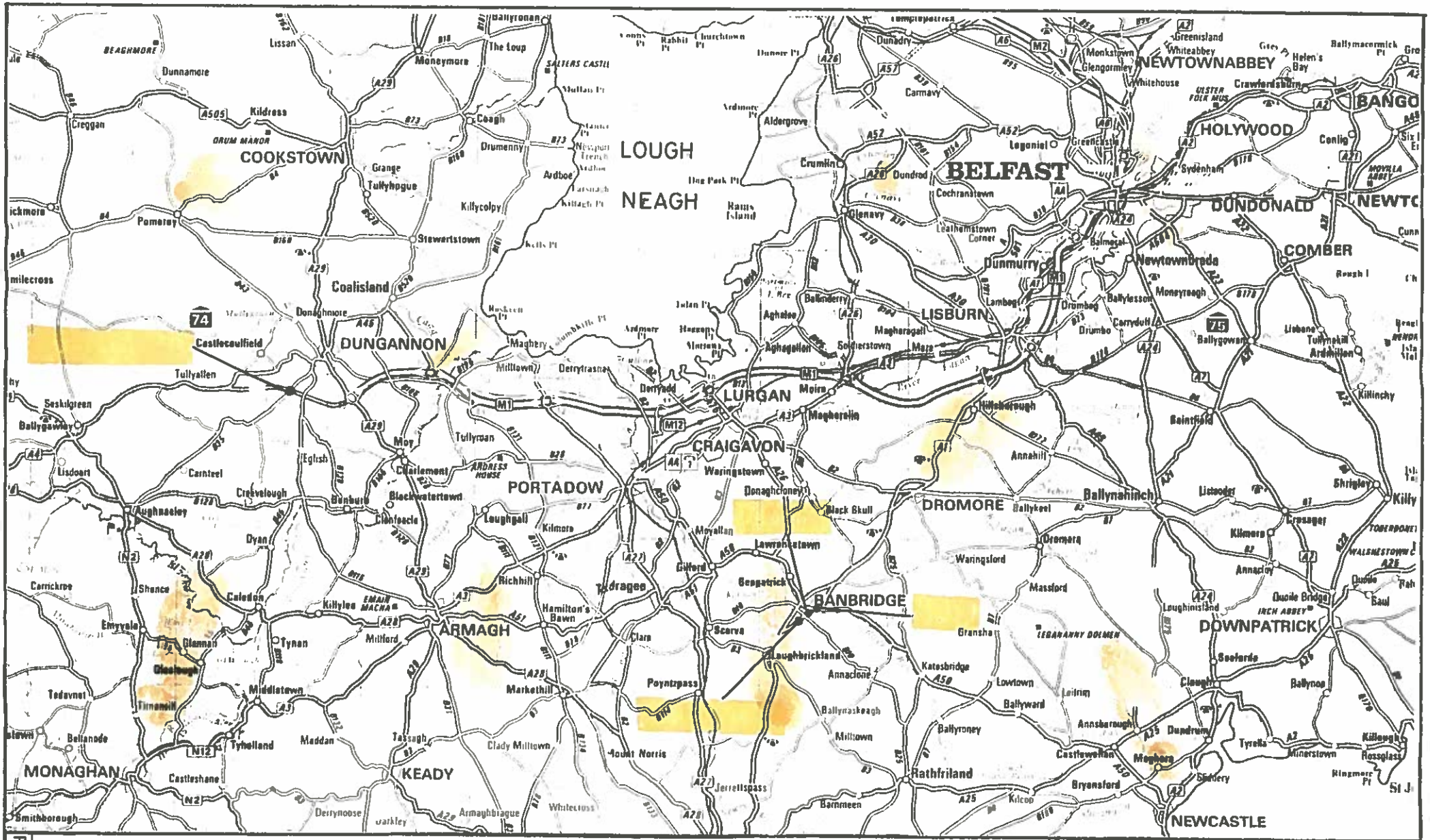

Fig.31 Fig. 3.1 Location of Test Bridges

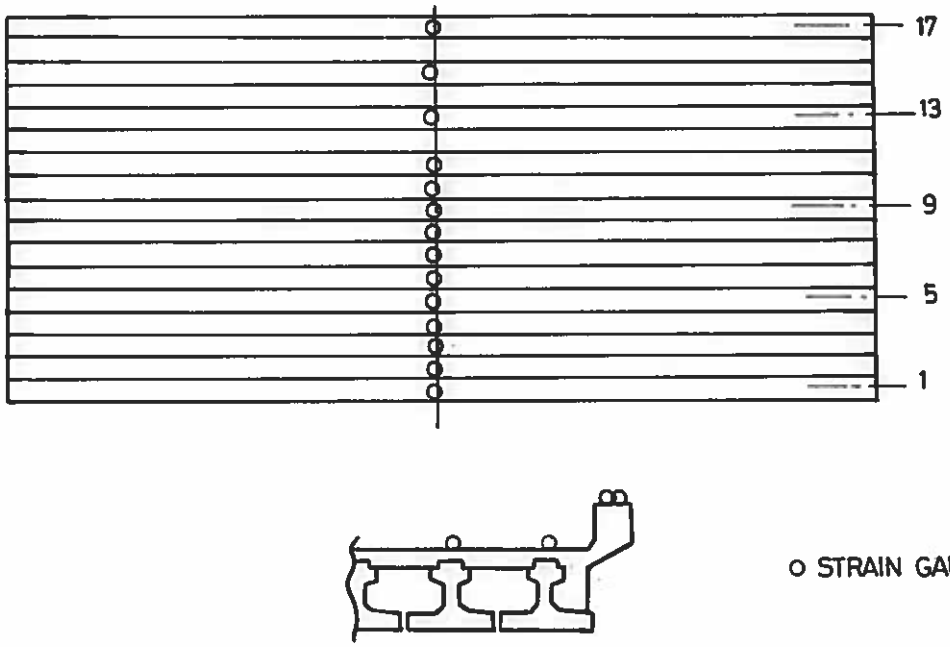

Bann River Bridge

Fig. 3.2 Position of Strain Gauges

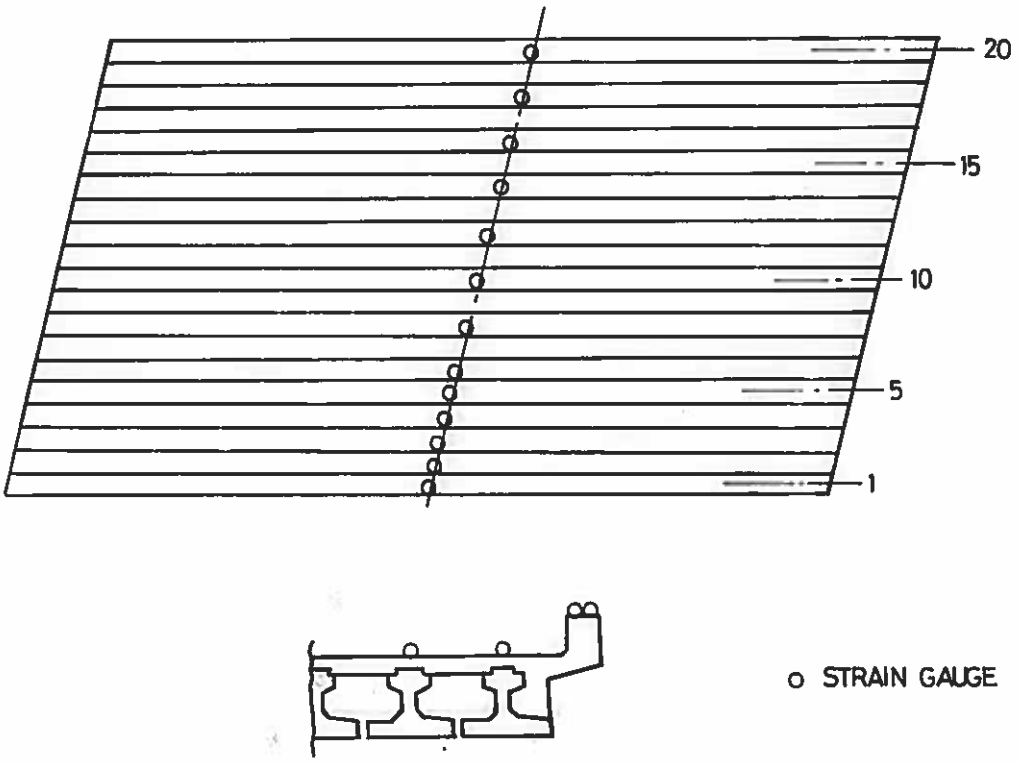

Granville Road Bridge

Fig 3.3 Position of Strain Gauges

Fig. 3.2
Fig. 3.3

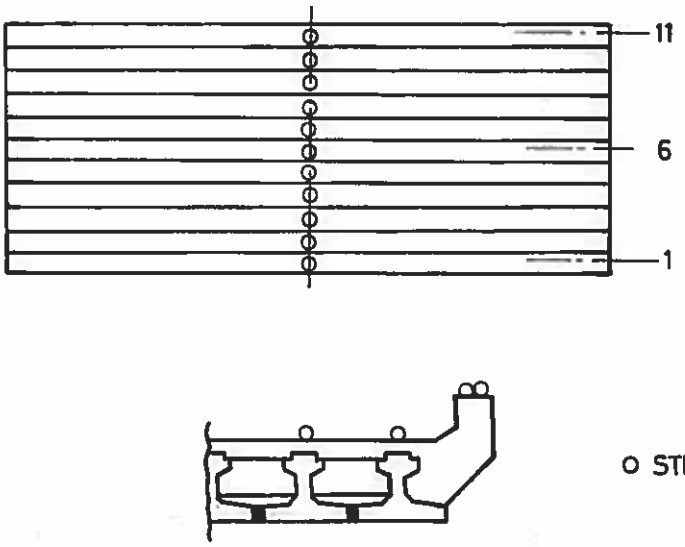

Tullyear Road Bridge

Fig. 3.4 Position of Strain Gauges

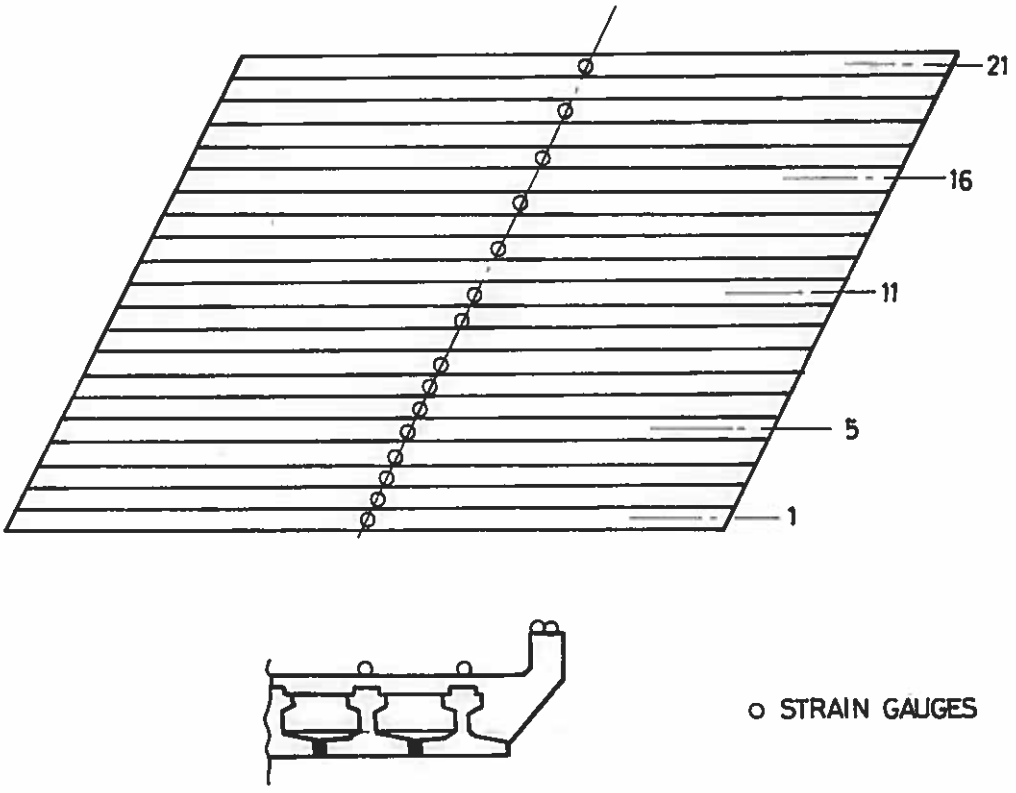

A50 Road Bridge

Fig. 3.5 Position of Strain Gauges

Fig3.4
Fig3.5

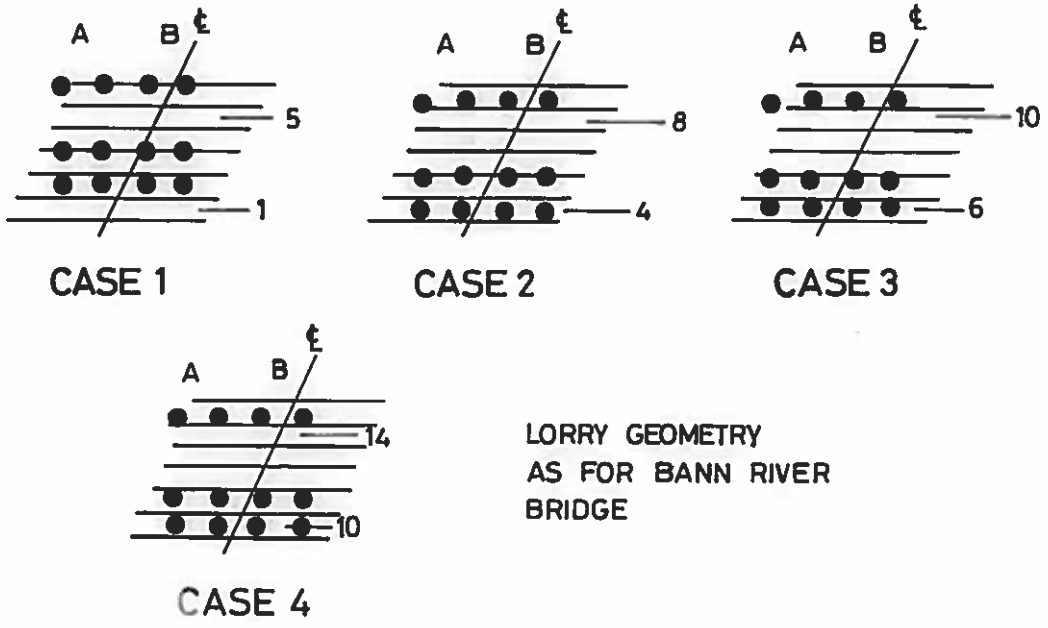

Fig 3.6 A 50 Road Bridge
Positions of Lorries

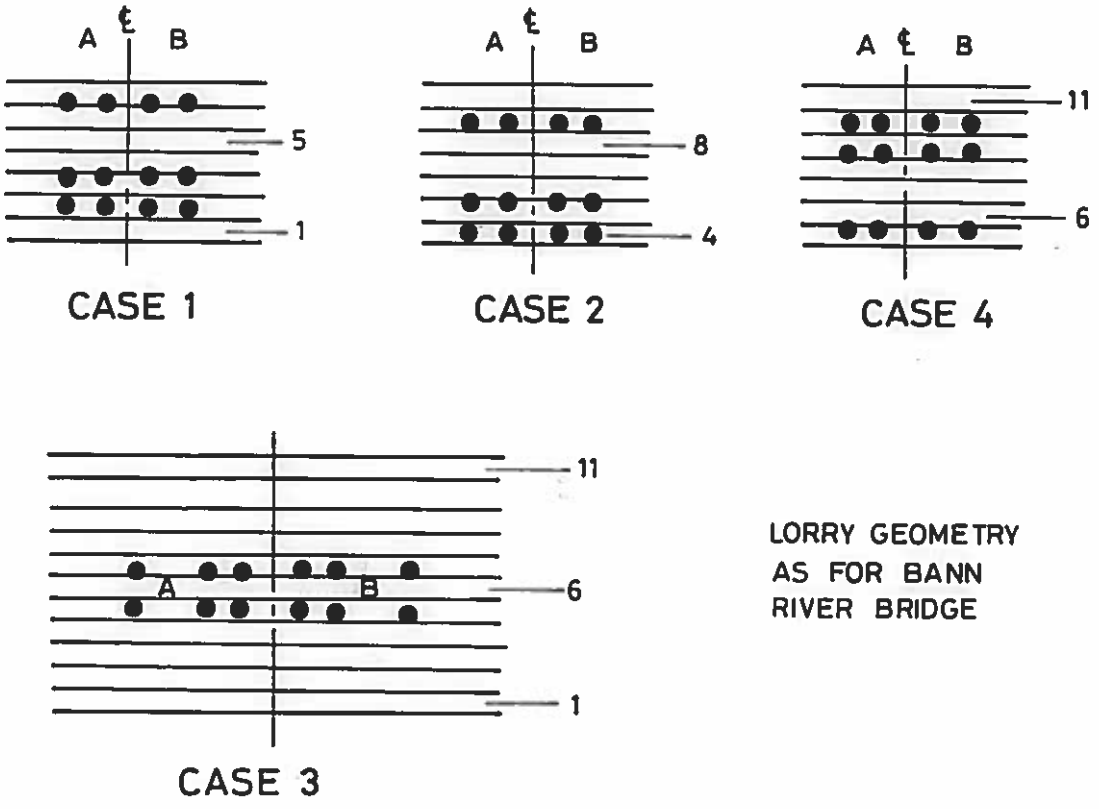

Fig 3.7 Tullyear Road Bridge
Positions of Lorries

Fig.3.6
Fig.3.7

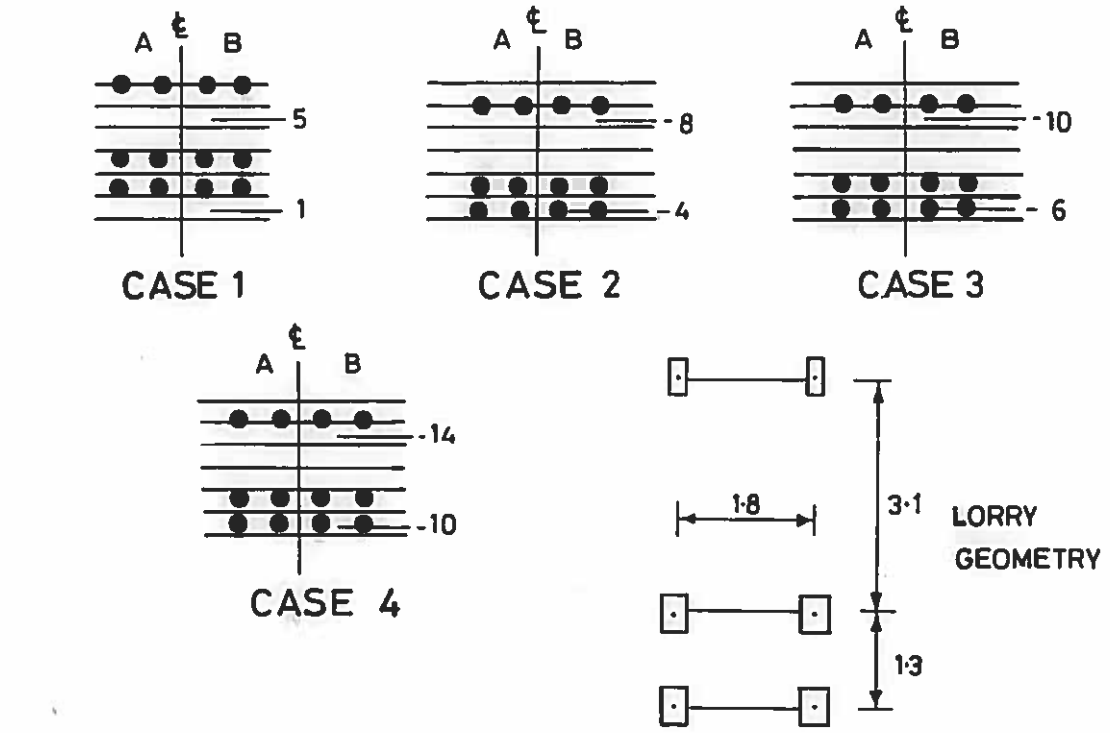

Fig 3.8 Bann River Bridge
Positions of Lorries

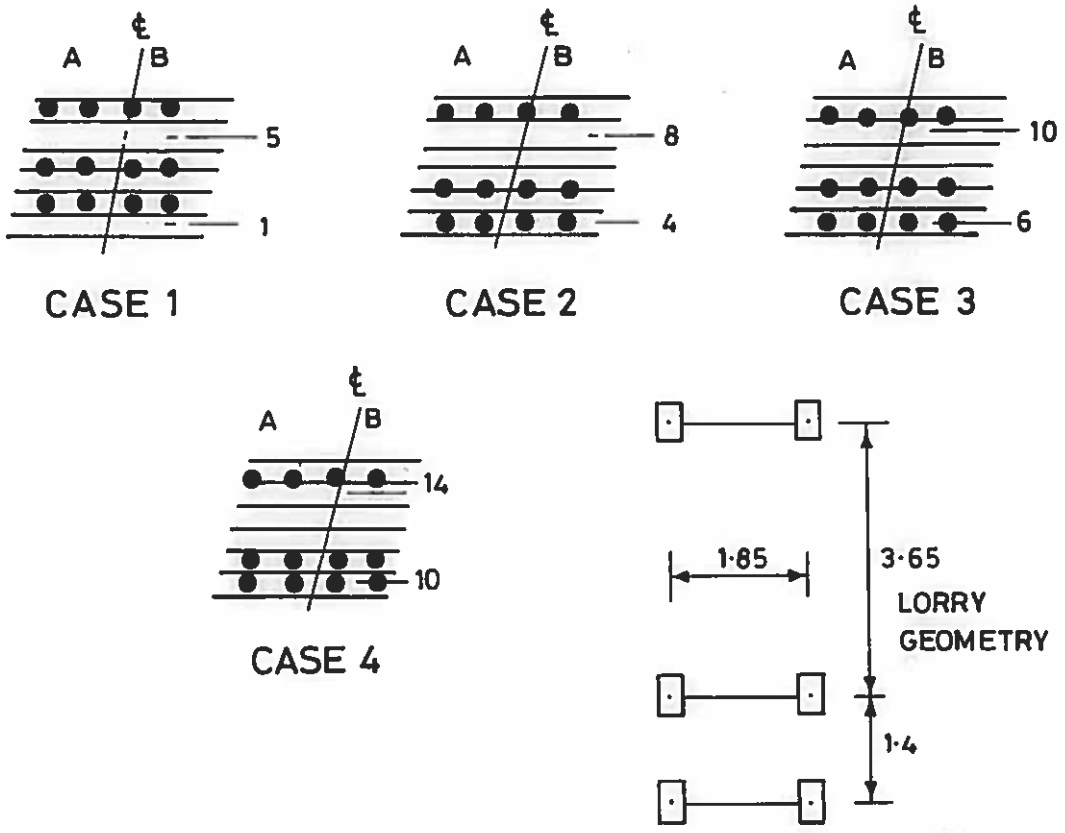

Fig 3.9 Granville Road Bridge
Positions of Lorries

Fig.3.8
Fig3.9

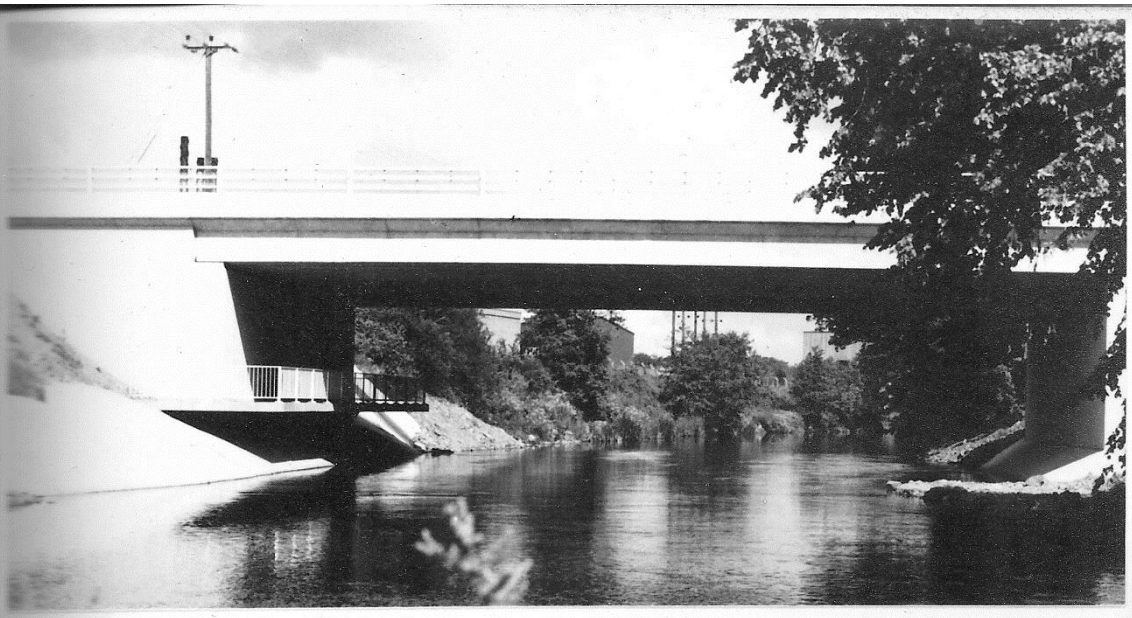

PLATE 3.1 THE BANN RIVER BRIDGE

PLATE 3.2 THE TULLYEAR ROAD BRIDGE

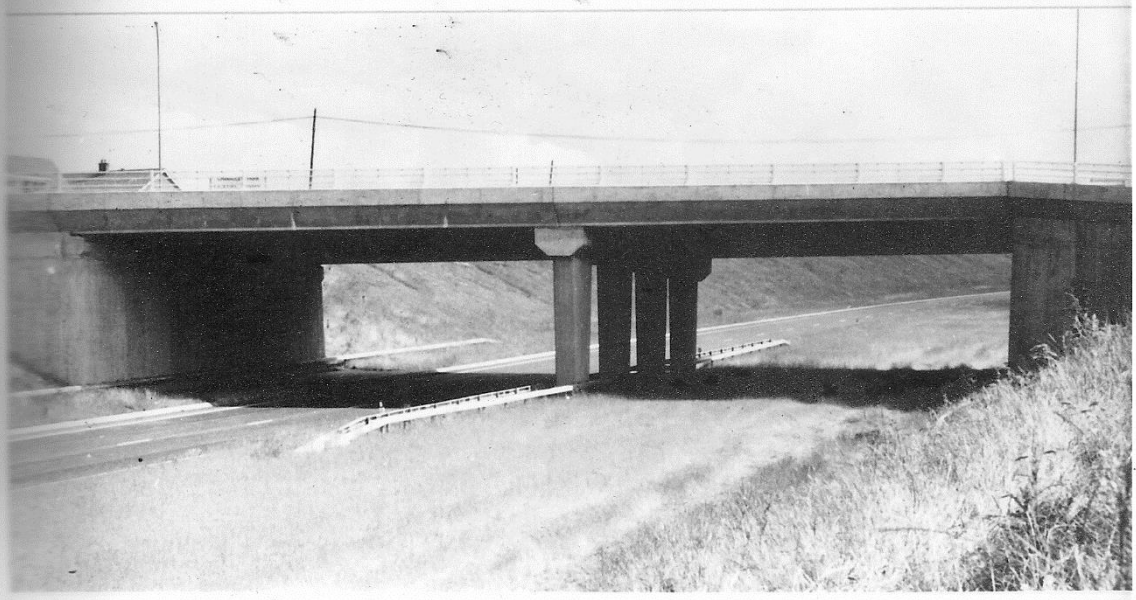

PLATE 3.3 THE A50 ROAD BRIDGE

PLATE 3.4
STRAIN GAUGES BEING ATTACHED TO THE BANN RIVER BRIDGE

PLATE 3.5 THE DIGITAL PORTABLE WEIGHPAD

PLATE 3.6 TEST LORRIES ON THE A50 ROAD BRIDGE

CHAPTER FOUR

PRESENTATION AND DISCUSSION OF RESULTS

4.1 INTRODUCTION

The results of nine loading tests on M-beam bridge decks which were carried out during the period August 1977 and March 1979 are presented. The main objectives were to establish the load distribution characteristics of both tee and pseudo-box types of deck and the influence of the parapet upstand on the distribution of load.

All tests were carried out during construction with the exception of the second test on the A50 road bridge. As this bridge was important to the transportation network in the area it was opened, unsurfaced, to local traffic and as a consequence the second test required a road closure order under Police supervision. It should also be pointed out that loading case No. 4 was omitted because kerbs had been laid on one side at the deck and thus prevented the correct positioning of the lorries for this test.

The test results were compared with theoretical grillage analysis and whilst, in general, agreement was very good it was found that for the pseudo-box construction there was a difference in the shape of the load distribution curve. As this was apparently due to inadequate methods for estimating the torsional inertia of this type of deck, a parallel investigation was carried out which involved the testing of a series of polystyrene models covering the range of beam sizes and representing a transverse grillage beam. Full details of this parallel investigation are given in Appendix B.

4.2 EXPERIMENTAL PROCEDURE

All period readings from the strain meter were converted into strains and the corresponding concrete stresses calculated. Although

a value for the elastic modulus was calculated at the time of the individual beam test for each bridge a considerable period of time had elapsed before the deck loading test was carried out. The bridge deck was then composite with the addition of the in situ concrete slab which was of a variable nature in both quality and slab depth and because of this the use of straight conversion of strain to stress by the elastic modulus was considered unsatisfactory. The method adopted was to use the calculated elastic modulus to convert strains to stresses and then to use the nominal composite beam section modulus to convert this to individual beam moments. These moments were then summed across the deck and the result compared with the total applied bending moment.

The final individual beam bending moment was then calculated as follows:

$$\text{Final beam BM} = \frac{M_t}{M_m} \times \text{(original nominal moment in each beam)}$$

where M_t = total applied bending moment from lorry wheel loads

M_m = sum of the beam moments based on a nominal elastic modulus.

This combined adjustment therefore took into account variations in the modulus of elasticity and also the irregularities due to modular ratio and construction tolerances.

4.3 TEE BEAM CONSTRUCTION

4.3.1 Analytical Idealisation

A theoretical analysis of the test decks was carried out using the grillage analysis. The bridge decks were idealised and section properties calculated in accordance with the recommendations for tee

beam decks by West (1973) for comparison with both series of tests with and without the parapet upstand. The idealised grillages are shown in Figs. 4.1 and 4.2 and the section properties are given in Table 4.1.

4.3.2 Details of Moments

The Bann River Bridge and Granville Road Bridge were both of tee beam construction and the midspan distribution of beam soffit stresses are given in Figs. 4.3 and 4.4. Tests with and without the parapet upstand are shown and these are compared with the theoretical results using a grillage analysis. Excellent correlation has been achieved for this type of deck which indicates that the basic assumptions and idealisation is reasonably correct as the mathematical model performs in a similar manner to the full scale bridge deck. However, under the wheel loads the test results showed a more localised effect than the grillage analysis which was based on 1.8 physical beams to 1.0 grillage beam . This may be seen on the distribution of beam soffit stresses as high stresses on the beams on which the axle loading occurred.

When a more refined grillage of one physical beam to one grillage beam is used, as can be seen in Figs. 4.3 and 4.4 it shows a much better prediction of these peak stresses. However, in practice the use of a fine mesh will increase both data preparation and computer time considerably and if storage is a problem only a limited number of loading cases may be run at any one time. For design purposes the coarse mesh as suggested by West (1973) will give a reasonably accurate estimate of the distribution of load.

In Figs. 4.3 and 4.4 Loading Case 1, it can be seen that the effect of edge stiffening by the parapet upstand is to reduce the beam soffit stresses in the beams near the edge. It is of interest to note that for this loading case the soffit stresses from the grillage analysis, without the upstand, are of the same order as those obtained from the test with the upstand included. This would suggest that this relatively simple analysis is adequate and would have the advantage that it avoids the complexity of assigning appropriate section properties for the upstand in the alternative grillage analysis. On this basis it is recommended that the deck analysis should be based on the properties of the composite beams alone. Another factor favouring this approach is that it provides conservative estimates of beam moments. This particular loading case can be seen to be the most critical and indeed will in almost all circumstances be utilised for the selection of the beam size and for that matter the levels of prestress of all the beams in a deck.

The results of the strain gauge readings on top of the parapet and deck slab are given in Figs. 4.5 and 4.6. When compared with the results of the grillage analysis they show good agreement on the beam soffit but tend to be less consistent on the deck slab and the top of the parapet.

The theoretical analysis takes into account the stiffening effect of the edge feature which was simulated in the grillage analysis. The effect of the edge stiffening is to reduce the stresses in the beams near the edge. This was to be expected but it is a local

effect and is only of importance when the deck can experience live load close to the parapet. For traffic remote from the parapet the edge beams carry little load and the edge stiffening is not important.

The stiffening effect of the upstand may be seen in Figs. 4.7 and 4.8 which show the distribution of bending moment in the beams near the edge of the deck. The edge beam with the upstand attracts more moment with a subsequent reduction in the moment carried by the inner beams.

After the first test and before the second a set of zero readings were taken for both the strain gauges and the thermocouples. For the Granville Road Bridge the difference in the measured mean temperature during the 2 tests was only $0.15^{o}C$, based on the temperature of the 2 edge beam soffits local to the strain gauges and the air temperature.

As the temperature was virtually constant, the difference in the beam soffit strain gauge readings were compared and they indicated that a certain amount of creep due to prestress was still taking place even though the beams were 276 days old at the time of the first test. During the 50 days between the tests the average creep measured was 35 microstrain which was consistent over all the beams, except the two edge beams on either side of the deck where the change in strain was zero on the edge beam and very small on the second beam. This may be accounted for by the addition of the parapet in situ concrete which is carried on the edge beams, thereby cancelling the effect of the compressive creep strain. This effect was also apparent in the other 3 bridges tested, but as the temperature

was different during the first and second test in each case a direct comparison was not possible.

From the individual beam tests the value of the elastic modulus measured ranged from 37 to 49 kN/mm^2. The current design criteria gives a value of 34.5 ± 6 kN/mm^2 for concrete with a 28-day cube strength of 52.5 kN/mm^2. As all the cube strengths for beam concrete were comfortably above 52.5 kN/mm^2 it would seem that the aggregate used for concrete in Northern Ireland is of a high standard and it would be reasonable to use the 34.5 ± 6 kN/mm^2 value for design purposes.

4.4 PSEUDO-BOX CONSTRUCTION

4.4.1 Analytical Idealisation

A theoretical analysis of these decks was carried out using a grillage analysis in a similar manner to that described in paragraph 4.3.1 for the tee beam construction. The idealised grillages are shown in Figs. 4.9 and 4.10 and the section properties are given in Table 4.2.

4.4.2 Details of Moments

The Tullyear and A50 Road Bridges were both of pseudo-box construction and the midspan distribution of beam soffit stresses are given in Figs. 4.11 to 4.14. Tests with and without the parapet upstand are shown and these are compared with the theoretical results from the grillage analysis.

Considering the tests without the parapet for these 2 decks it may be seen that for loading case No. 1, which is the most critical,

the measured soffit stresses on beam No. 1 were 20% less than the theoretical stresses based on the grillage analysis and the recommended method of calculating the section properties of the members by West (1973). This difference in maximum stresses is also evident in the other loading cases and for the test carried out after the parapet upstand had been cast. At an early stage of the project a preliminary test was carried out by Kirkpatrick (1977) on Ballymacoss Railway Bridge and the results are shown in Figure 4.15. This follows the consistent pattern of results achieved for all the pseudo-box decks.

As discussed in Chapter 2 the distribution of longitudinal bending moments and deflections are dependent on the sum of the torsional inertias in the longitudinal and transverse directions. This may be illustrated for the pseudo-box deck by considering the influence of the torsional and bending inertias of a transverse grillage beam on the longitudinal beam soffit stresses. Referring to Figures 4.16 and 4.17 the original distribution of beam soffit stresses for load case No. 1 is shown with the torsional and bending inertias having a factor of unity. When the bending inertia is increased by a factor of 7 there is virtually no change in the level of the maximum stress. However, when the torsional inertia is increased by a factor of 7 there is a significant reduction in the stress level. By increasing the bending inertia as well as the torsional inertia there is again no worthwhile difference in the stress level from when only the torsional inertia was increased.

A comparison of test and theoretical results would seem to indicate that the recommended method underestimates the torsional

stiffness of the pseudo-box deck. The longitudinal torsional inertia is usually calculated by considering each beam width as a single cell and proportioning this to each grillage beam. If the complete transverse section of the deck was considered as a single cell an increase of up to 100% could be achieved for the wider decks of at least 20 beams. However, this is not a significant increase in terms of the total torsional inertia of the deck. The use of the single cell theory for the calculation of the torsional inertia of a multi-cell bridge deck is a well tried and generally accepted method, as such it is not open to much doubt about its accuracy. In view of this it would seem that most of the underestimation of torsional inertia is due to the the method of calculating the transverse torsional inertia which is based on a publication by Kollbrunner (1969). Assuming then that it is the transverse torsional inertia which is underestimated, and in order to accurately model the test results, the transverse torsional inertia would require to be increased by a factor of about 7 and the distribution of beam soffit stresses with this factor included in the grillage analysis is shown in Figures 4.11 to 4.15. This shows a much better correlation with the test results and it is significant that the shape of the distribution curve is now modelled much more accurately, especially load case No. 1 which is the most critical simulating the HB vehicle in the most eccentric position.

In order to investigate further the problem of the torsional inertia of the pseudo-box deck a short series of tests was planned using polystyrene models. The basis of these tests was to compare the torsional stiffness of a solid transverse grillage beam, the tor-

sional inertia of which may be calculated by the method of St. Venant, with the pseudo-box grillage beam, for which the calculation of the torsional inertia is in doubt. However, the results of the tests on the polystyrene models did not give the increase in the torsional inertia that would have been required to model the test results, but indicated a marginal increase in the values calculated by the recommended method. Details of this series of tests are given in Appendix B.

As mentioned in Chapter 2 the recommendations for this type of deck were based on a one quarter scale model using the standard inverted tee beams by Somerville and Tiller (1970) which are approximately half the width of the standard M-beam. This means that for the same width of deck the model tested had twice as many cells as it would have had if quarter scale M-beams had been used.

Also, if cracking occurs between each beam due to tranvserse bending, more cracks would be present which would adversely effect the distribution properties of the deck. Therefore, it is not unreasonable that the deck with broader beams should show considerably stiffer transverse distribution properties which result in a reduction in the magnitude of the longitudinal bending moment and superior load distribution characteristics. However, it is worthy of note that the two 30 tonne trucks used to load the test bridges may not have been sufficient to cause cracking of the in situ concrete between the beams and a high estimate of the transverse deck stiffness may have been obtained relative to its long-term performance. In contrast, in the one quarter scale model tested at the C & CA (1971) extensive cracking had developed due to the application of a test

load equivalent to an abnormal vehicle of 180 tonnes. These results have also been analysed by Loo and Cusens (1978) using a finite strip method and this shows a good correlation with the model test results when all the bottom joints are considered cracked. However, when the joints are assumed to be uncracked a distribution similar to the tests on the full size bridges is achieved. While the cracking of the concrete forming the bottom longitudinal joints is an important aspect, the main question is one of modelling accuracy in the use of PCDG inverted tee beams to represent an M-beam deck and as a consequence it is proposed that after a period of service these bridges will be tested again to establish if any change in the transverse deck stiffness has occurred due to cracking between the beams.

The problem of the transverse stiffness of the pseudo-box deck has not been fully resolved. The full scale tests have highlighted an aspect of M-beam deck analysis which requires further investigation and research in the near future.

The measured stresses for the tests with and without the parapet upstand show very little difference and it would seem that the edge stiffening does not have a very significant effect on the beam soffit stresses local to the edge. This is probably not unexpected as the pseudo-box deck behaves in a manner similar to a reinforced concrete slab with a very flat distribution of load and the addition of an area of slab at the edge would not make any appreciable difference to the distribution of stress in the edge beams.

The Tullyear Road Bridge had only 11 beams, and strain gauges were attached to all of them which allowed a check on the symmetry

of the results. Loading case 3 was symmetric and loading cases 1 and 4 were anti-symmetric and all these cases gave good agreement as regards the symmetry of results which was a good check on the performance of the strain gauges and monitoring equipment.

The results of the strain gauge readings on top of the parapet and on the deck slab are given in Figures 4.18 and 4.19. They are compared with the grillage analysis which includes a factor of 7 on the torsional inertia of the transverse grillage beam. There is a reasonable comparison with the beam soffit readings but, in general, the comparison of strains for these tests was poor.

The effect of the edge stiffening on the distribution of beam bending moment is shown in Figures 4.20 and 4.21. There is good correlation between the test results and the grillage analysis which includes a factor of 7 on the torsional inertia of the transverse grillage beams.

4.5 CONCLUSIONS

From the series of tests on both tee beam and pseudo-box types of deck the following conclusions may be drawn:-

Tee Beam Construction

1. The grillage analysis used with the idealisation and recommendations by West (1973) provides a good basis for the analysis of this type of deck.
2. Edge stiffening provides some relief to the edge beam soffit stresses. This was more significant in load case No. 1 and, in particular, the test on Granville Road Bridge. Load cases

2 and 3 show a slight increase in beam soffit stresses but the difference was small and the level of stress for these cases was low.

3. For design purposes the effect of the edge stiffening associated with the standard edge feature need not be considered and the analysis can be based on the stiffness of the composite beams alone. This will provide a conservative estimate of beam moments in beams close to the edge of the deck.

Pseudo-Box Construction

1. Measured beam soffit stresses for these decks were about 20% less than those predicted by the grillage analysis based on the recommendations of West (1973).
2. A good correlation of beam soffit stresses was obtained when the torsional inertia of the transverse grillage beams was increased by a factor of 7.
3. The addition of edge stiffening to this type of deck showed only a very nominal change in edge beam soffit stress.

General

For the design of M-beam bridge decks the following recommendations may be made:-

1. Grillage analysis provides a good basis for deck analysis.
2. Existing methods of idealisation are satisfactory for tee beam construction.
3. For both forms of deck the influence of edge stiffening should be ignored and the analysis based on the stiffness of the composite beams only, which will provide a safe design in the region of the edge beam.

4. For the pseudo-box construction the calculation of the torsional inertia of the transverse grillage beam has not been resolved in a satisfactory manner and there is a need for further investigation into this aspect of M-beam deck analysis. However, until this problem is fully explained a simple empirical approach may be adopted and a good correlation of all pseudo-box test results has been achieved by increasing the torsional inertia of the transverse grillage beams by a factor of 7.

Finally, it must be stated that the testing of full scale bridge decks using commercial vehicles and suitable monitoring equipment has proved to be a practical and inexpensive approach to the establishment of the load distribution characteristics. In order that the information provided by the tests can be of use and possibly incorporated into future designs it must be presented to designers in a form that can be easily understood and used. With this in mind, the results of the tests and the above recommendations will be incorporated into a simplified design procedure aimed at improving the economics of M-beam decks. Details of this will be considered in the next Chapter.

Member	Bann River Bridge		Granville Road Bridge	
	I 10^9 mm^4	J 10^9 mm^4	I 10^9 mm^4	J 10^9 mm^4
1 no U/S	235	7.4	189	6.3
1 with U/S	415	7.4	385	6.3
2	235	7.4	189	6.3
3	1.09	2.7	0.76	1.8
4	133	37.1	99	33.6
Phy/grill beam	1.889		1.818	

TABLE 4.1 Section Properties of Tee Beam Decks

Member	Tullyear Road Bridge		A50 Road Bridge	
	I 10^9 mm^4	J 10^9 mm^4	I 10^9 mm^4	J 10^9 mm^4
1 no U/S	49.68	28.03	139.23	48.72
1 with U/S	119.50	28.03	243.7	48.72
2	49.68	28.03	139.23	48.72
3	3.75	47.32	6.26	81.95
4	32.88	44.24	61.22	70.96
Phy/grill beam	1.222		1.75	

TABLE 4.2 Section Properties of Pseudo-Box Bridge Decks

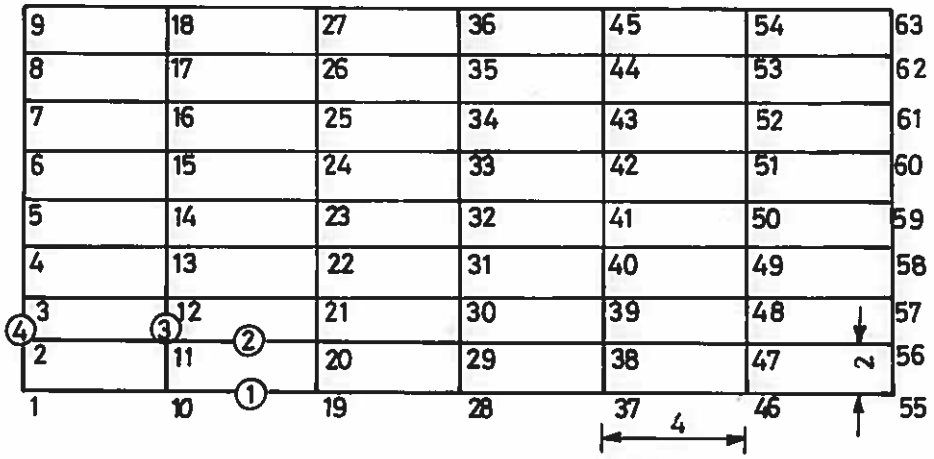

Bann River Bridge

Fig. 4.1 Idealised Grillages & Section Properties for Test Bridges

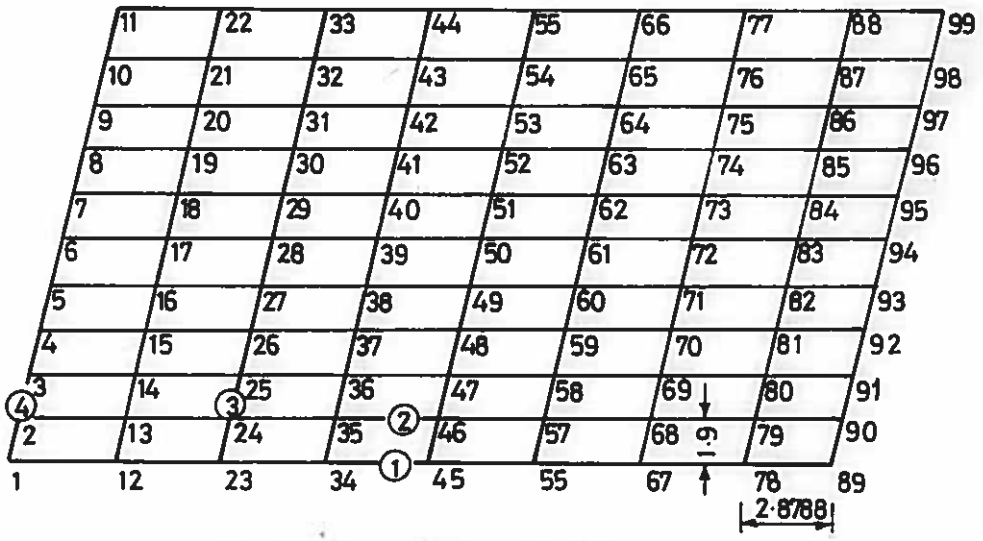

Granville Road Bridge

Fig 4.2 Idealised Grillages & Section Properties for Test Bridges

Fig.4.1
Fig.4.2

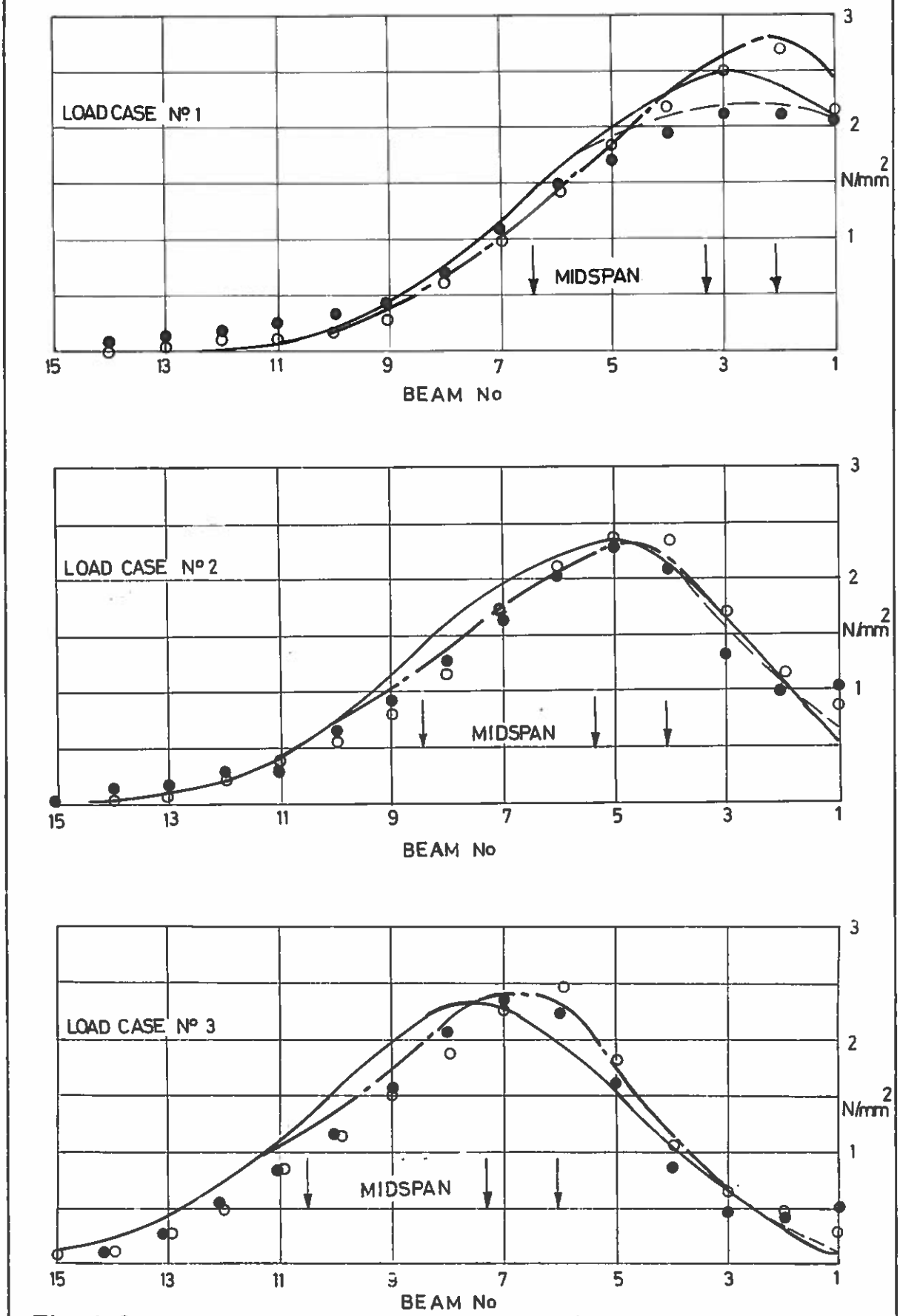

Fig 4.3 Bann River Bridge (Tee Beam)
Beam Soffit Stresses

—— Grillage No Upstand
– – – Grillage With Upstand
—·— Grillage Fine Mesh No Upstand
o Experimental No Upstand
• Experimental With Upstand

Fig.4.3

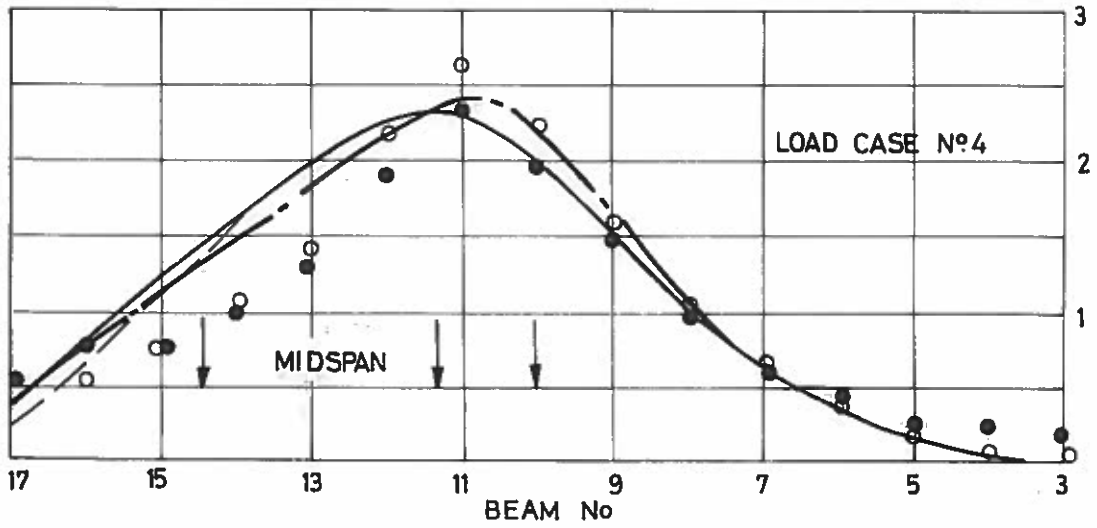

Fig 4.3 contd

Bann River Bridge (Tee Beam)
Beam Soffit Stresses

—— Grillage No Upstand ○ Experimental No Upstand
– – – Grillage With Upstand ● Experimental With Upstand
—·— Grillage Fine Mesh No Upstand

Fig 4.3

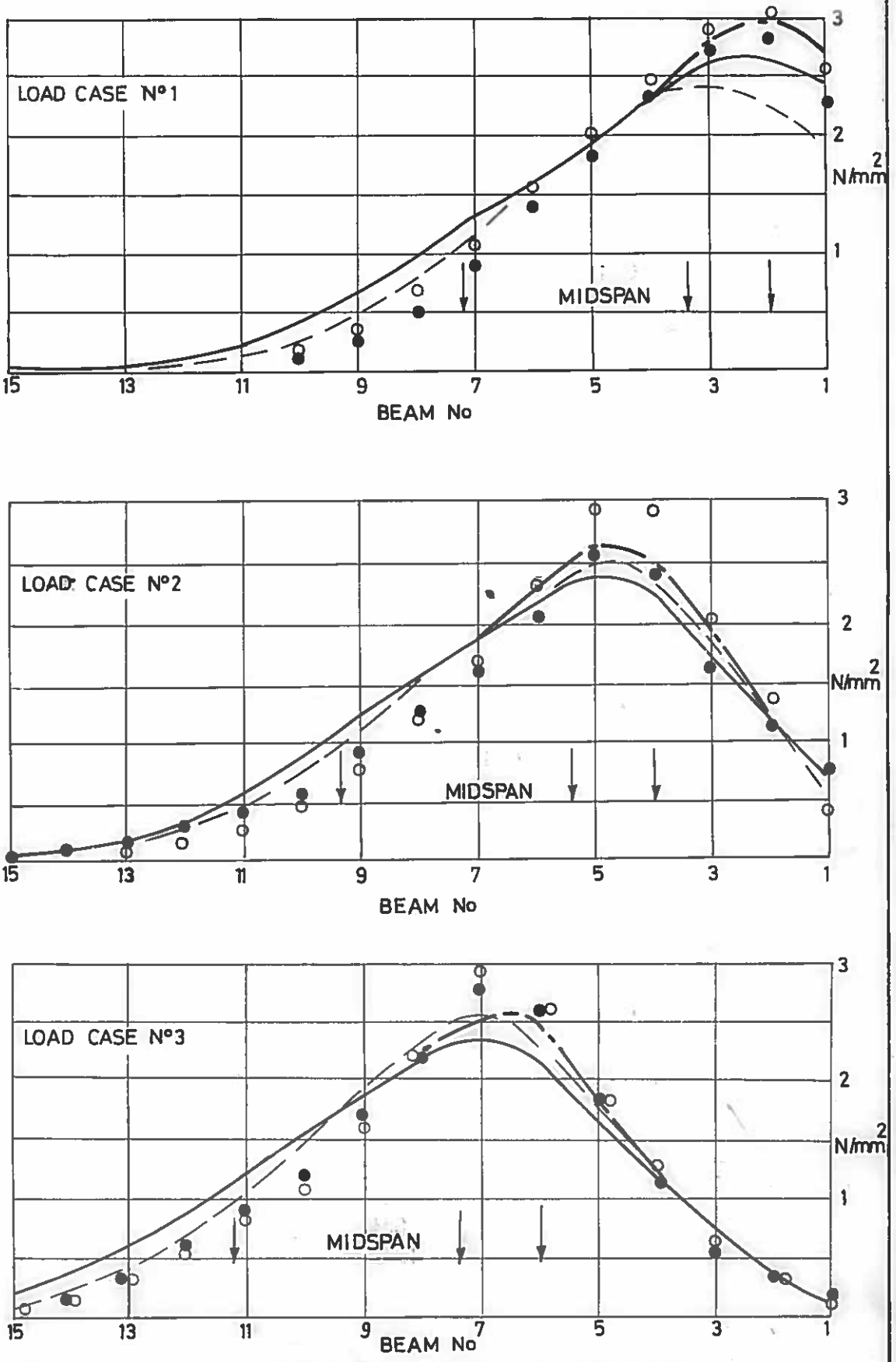

Fig 4.4 Granville Road Bridge (Tee Beam)
Beam Soffit Stresses

——— Grillage No Upstand ○ Experimental No Upstand
– – – – Grillage With Upstand ● Experimental With Upstand
—·— Grillage Fine Mesh No Upstand

Fig.4.4

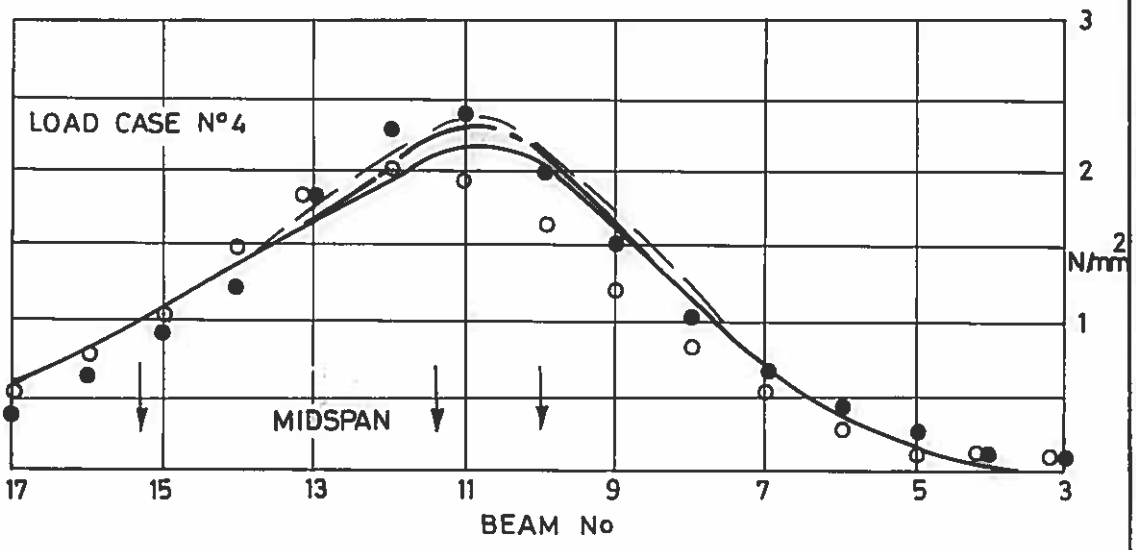

Fig. 4.4 contd. Granville Road Bridge (Tee Beam)
Beam Soffit Stresses

—— Grillage No Upstand ○ Experimental No Upstand
– – – Grillage With Upstand ● Experimental With Upstand
—·— Grillage Fine Mesh No Upstand

Fig.4.4.contd

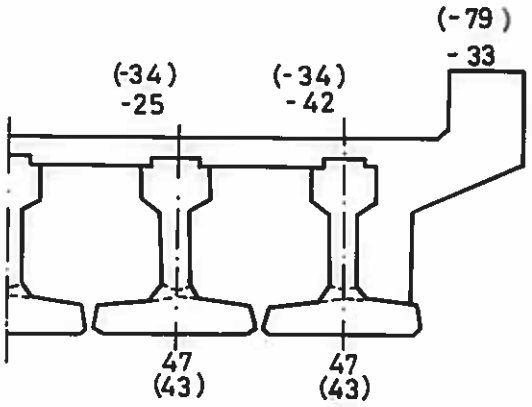

STRAINS IN BRACKETS ARE BASED ON GRILLAGE ANALYSIS

Fig. 4.5 Bann River Bridge
Edge Feature Strain Distribution (με)
Load Case Nº1

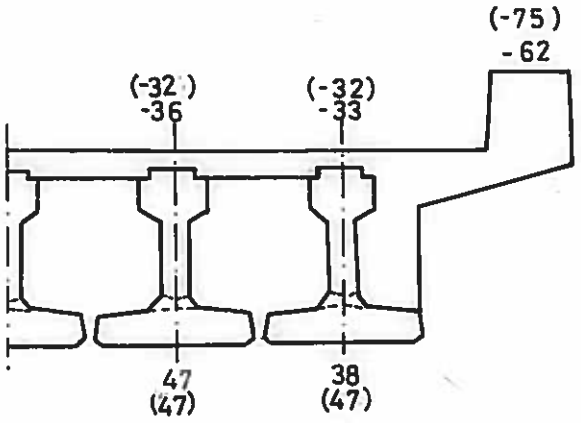

STRAINS IN BRACKETS ARE BASED ON GRILLAGE ANALYSIS

Fig 4.6 Granville Road Bridge
Edge Feature Strain Distribution (με)
Load Case Nº1

Fig 4.5
Fig.4.6

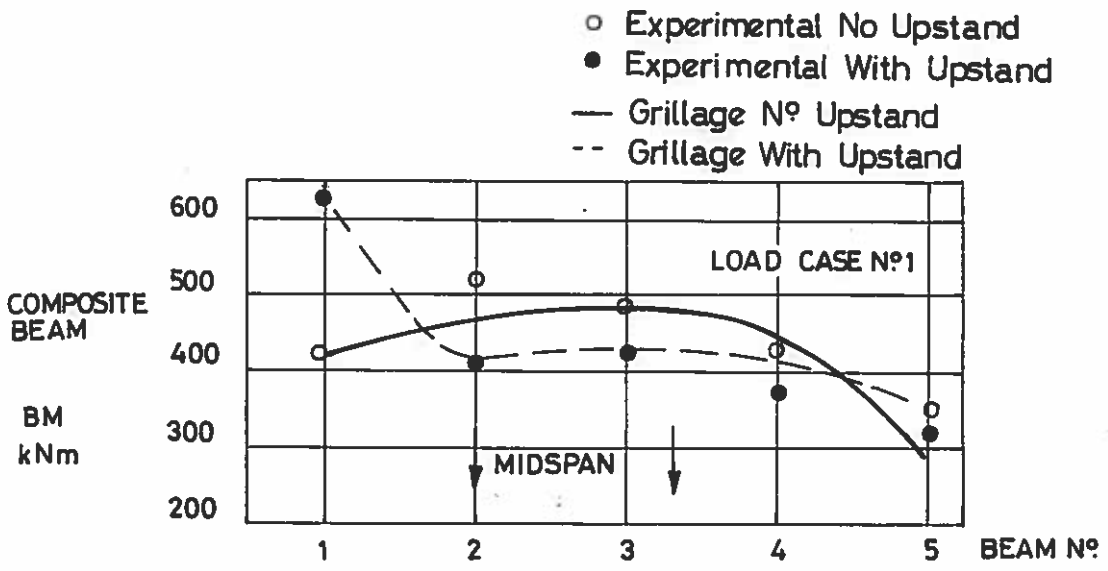

Fig. 4.7

Bann River Bridge
Beam Bending Moments Load Case Nº1

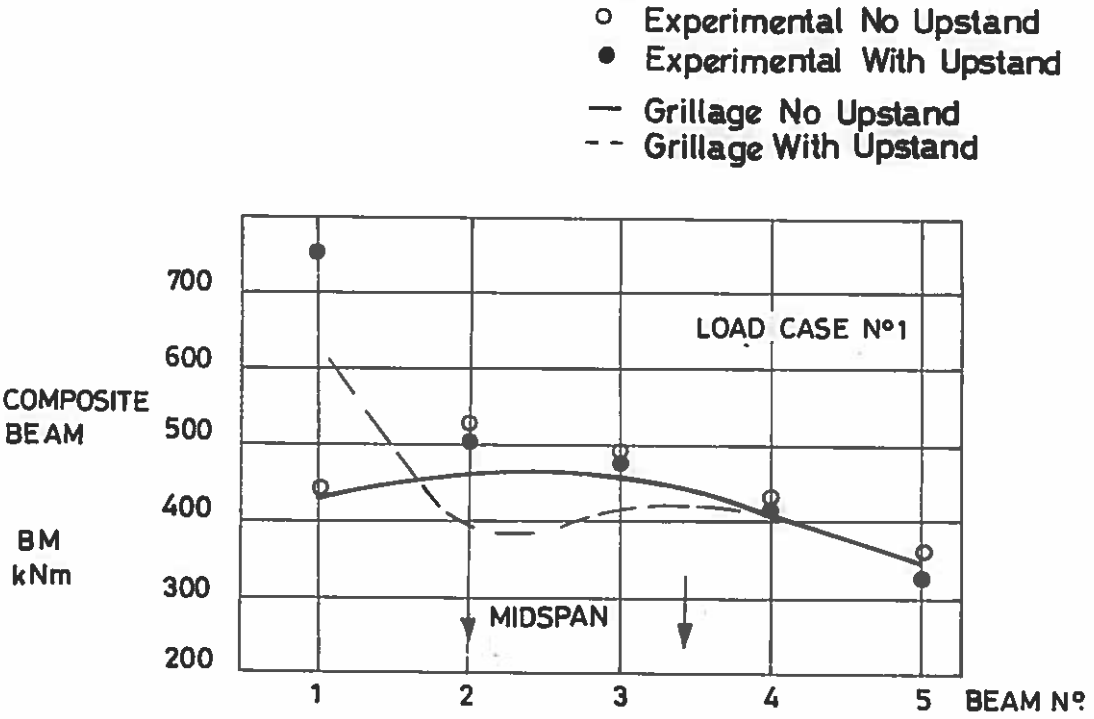

Fig. 4.8

Granville Road Bridge
Beam Bending Moments Load Case Nº1

Fig. 4.7
Fig. 4.8

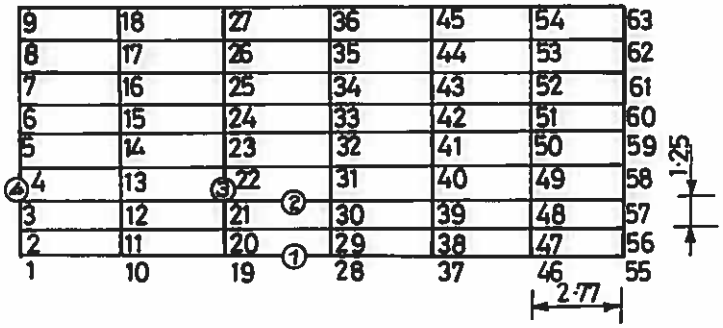

Tullyear Road Bridge

Fig 4.9 Idealised Grillages & Section Properties For Test Bridges

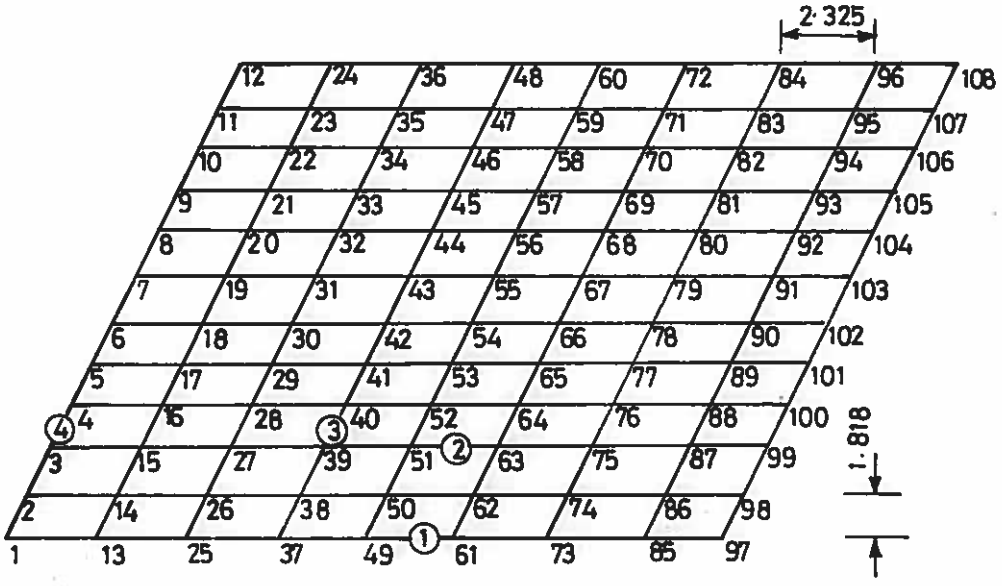

A5 Road Bridge

Fig 4.10 Idealised Grillages & Section Properties for Test Bridges

Fig.4.9
Fig.4.10

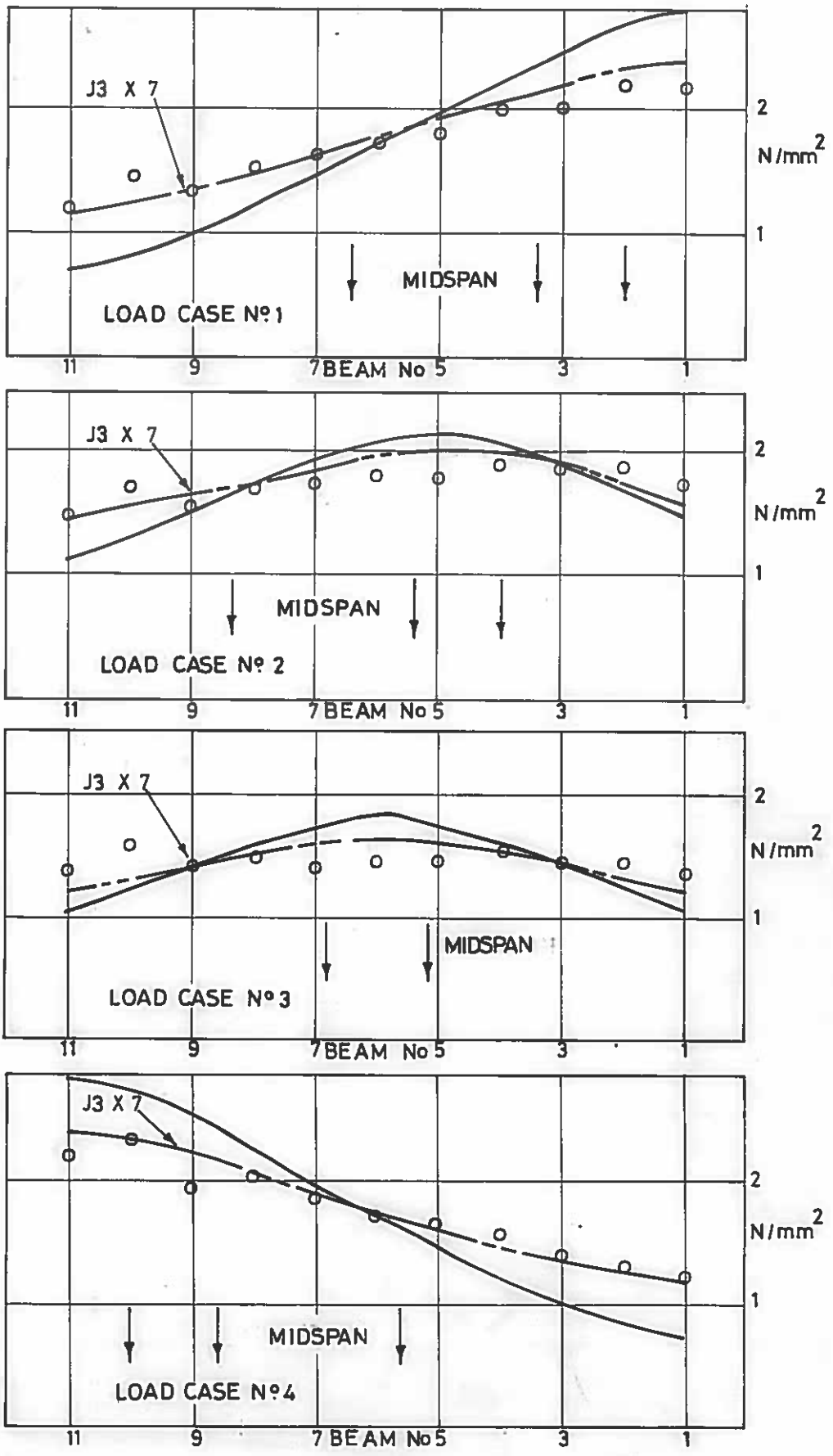

Fig 4.11 Tullyear Road Bridge (Pseudo-Box)
Beam Soffit Stresses

—— Grillage No Upstand o Experiment No Upstand

Fig4.11

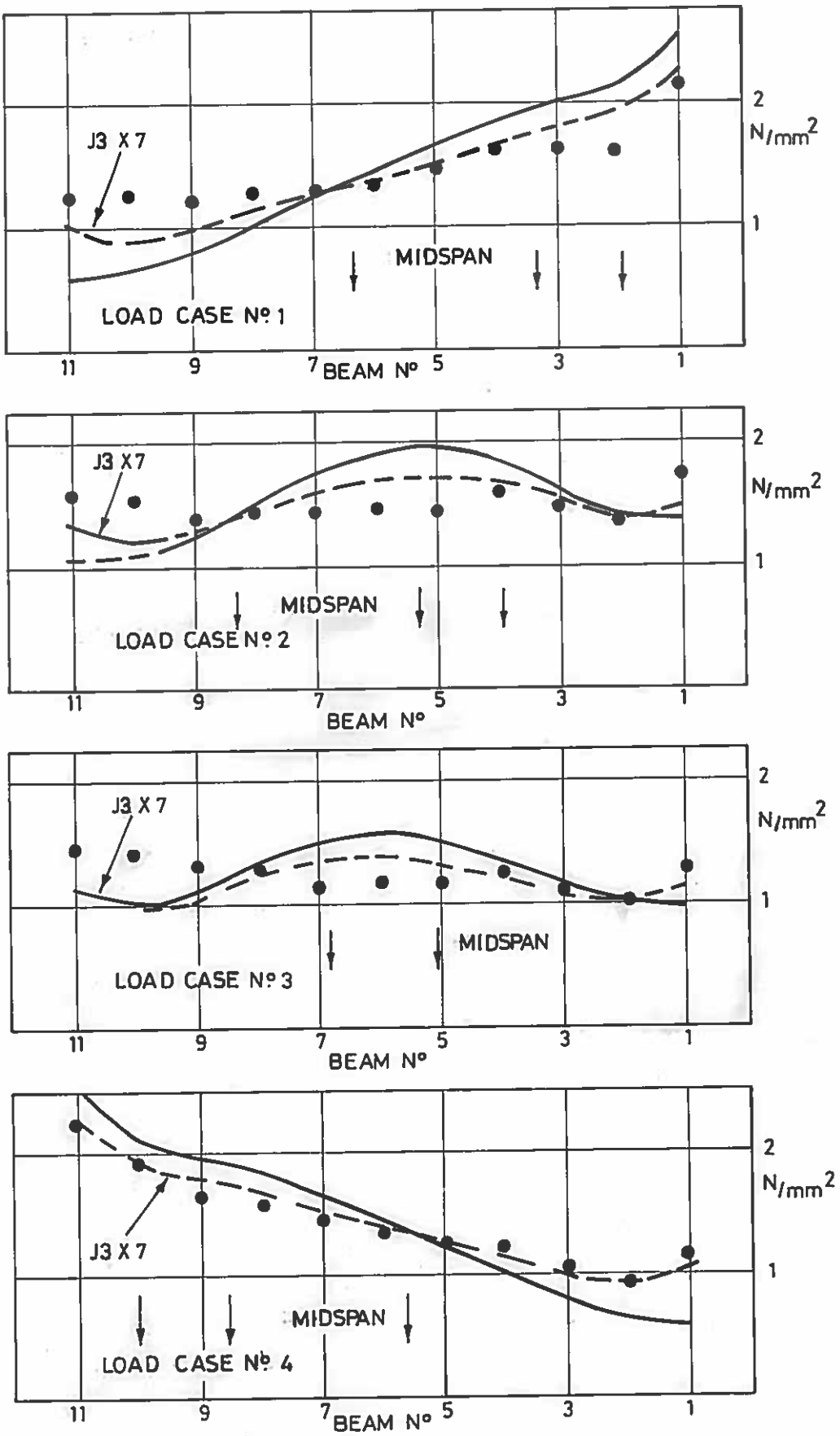

Fig 4.12 Tullyear Road Bridge (Pseudo-Box)
Beam Soffit Stresses
—— Grillage With Upstand ● Experimental with Upstand

Fig.4.12

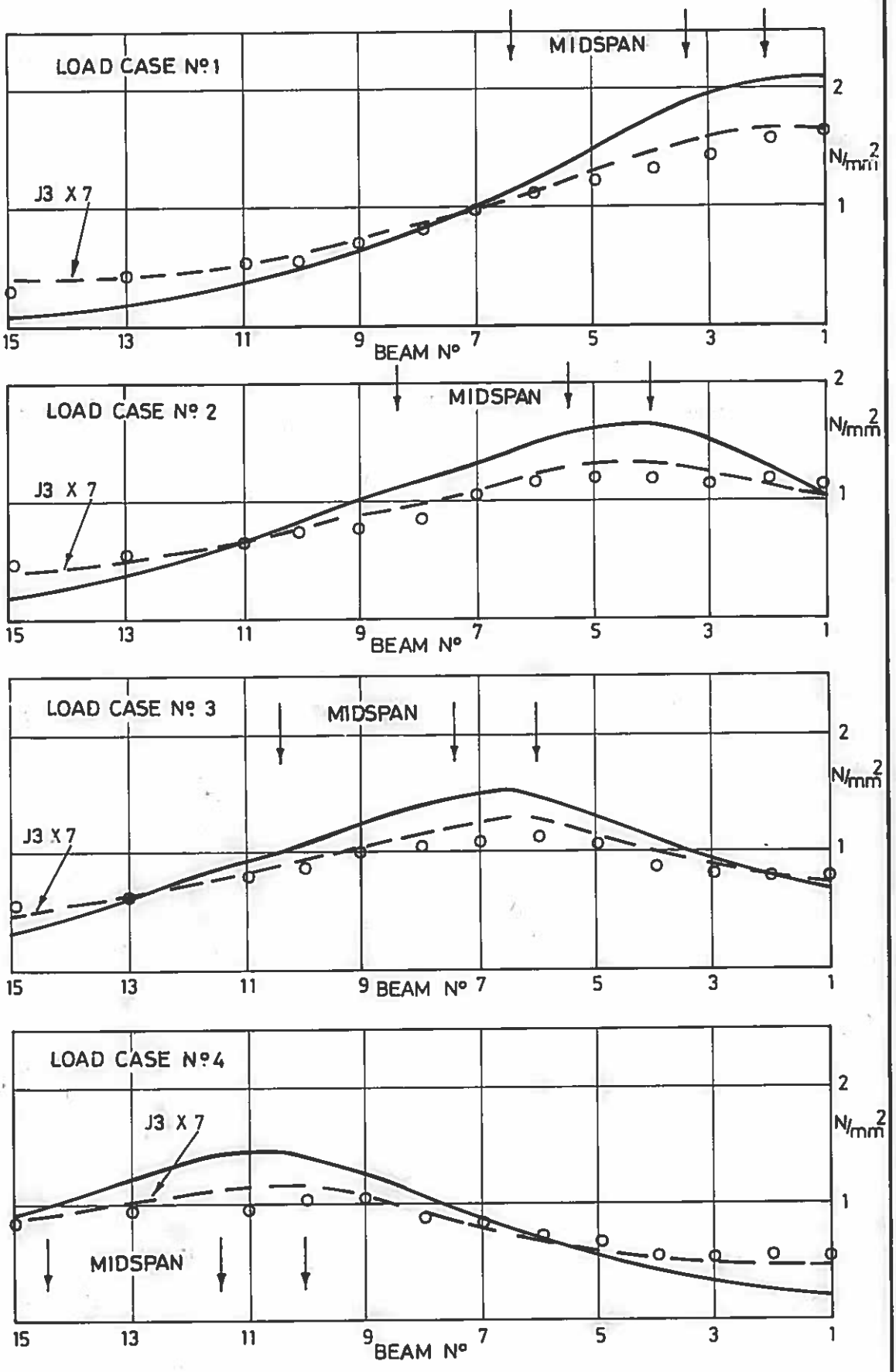

Fig 4.13 A50 Road Bridge (Pseudo-Box)
Beam Soffit Stresses

—— Grillage No Upstand o Experimental No Upstand

Fig.4.13

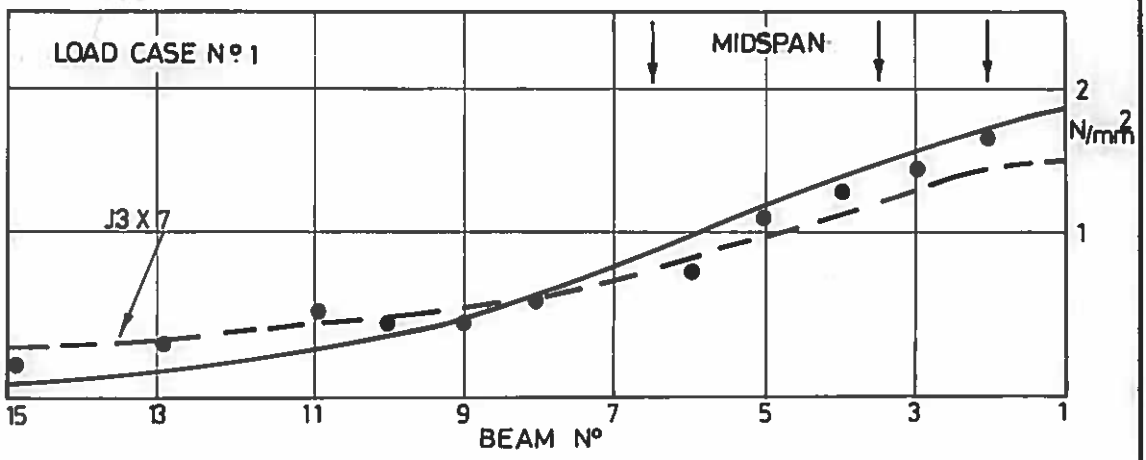

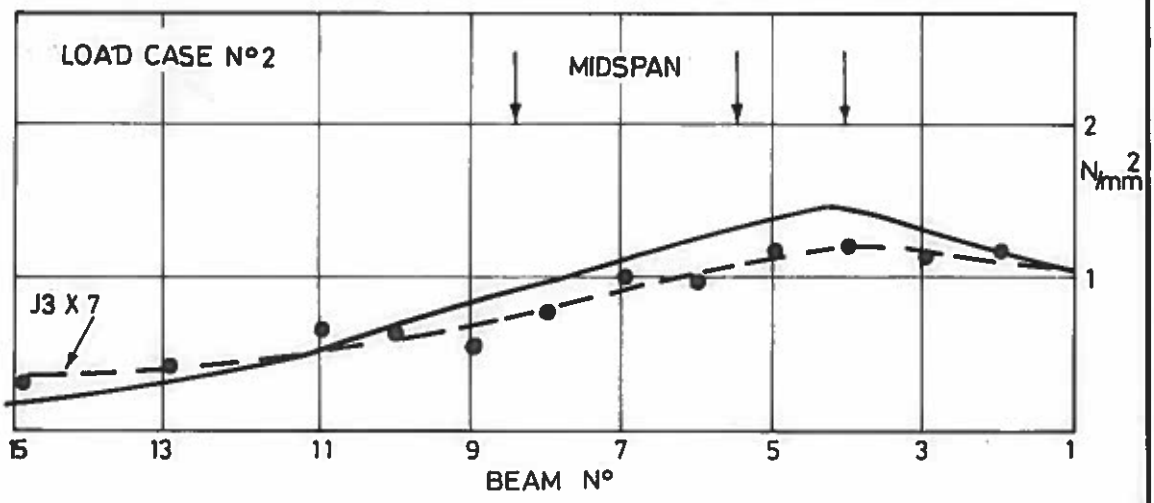

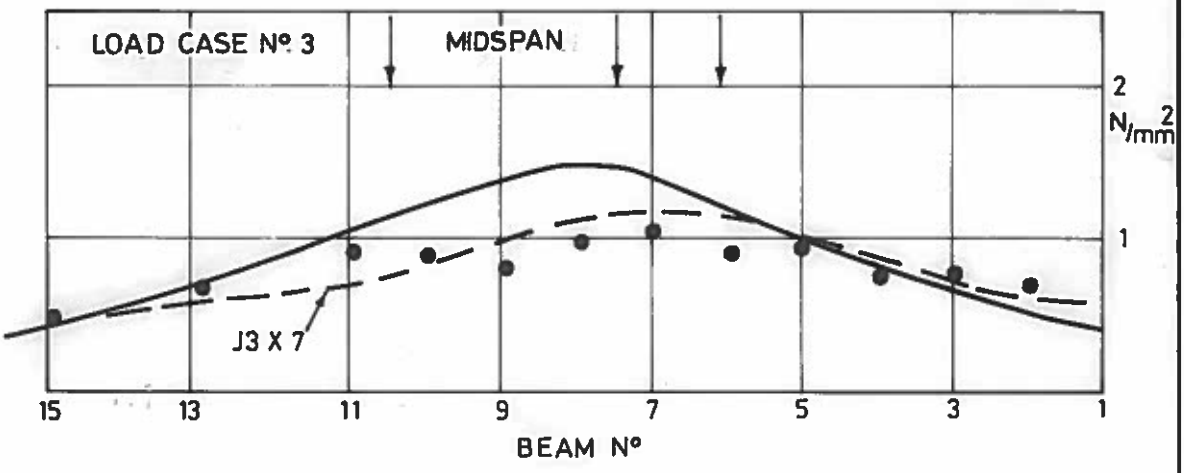

Fig 4.14 A50 Road Bridge (Pseudo-Box)
Beam Soffit Stresses

—— Grillage With Upstand • Experimental With Upstand

NOTE: GAUGE N° 1 DAMAGED

Fig.4.14

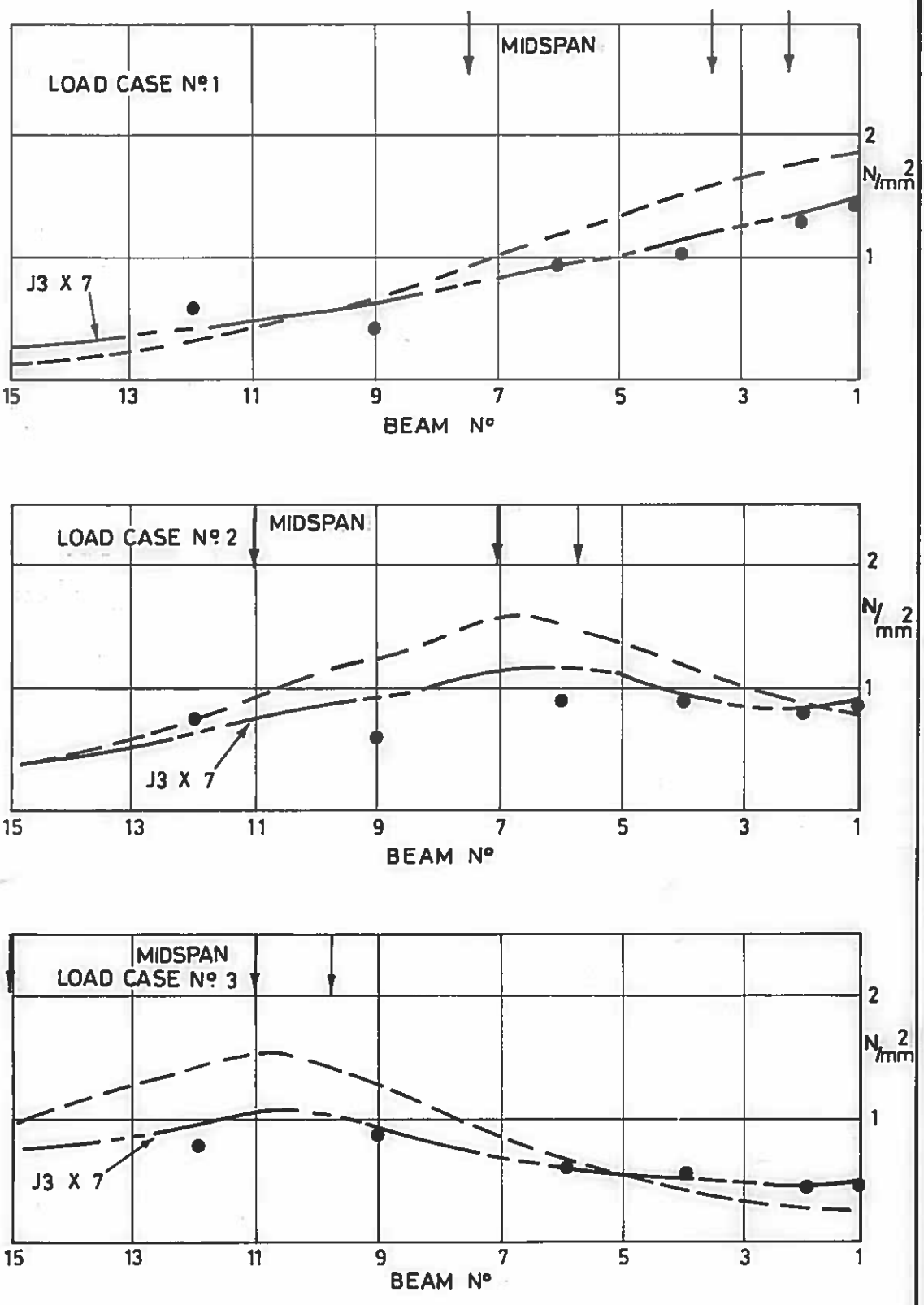

Fig 4.15 Ballymacoss Railway Bridge (Pseudo-Box)

Beam Soffit Stresses

– – – Grillage With Upstand • Experimental With Upstand

Fig. 4.15

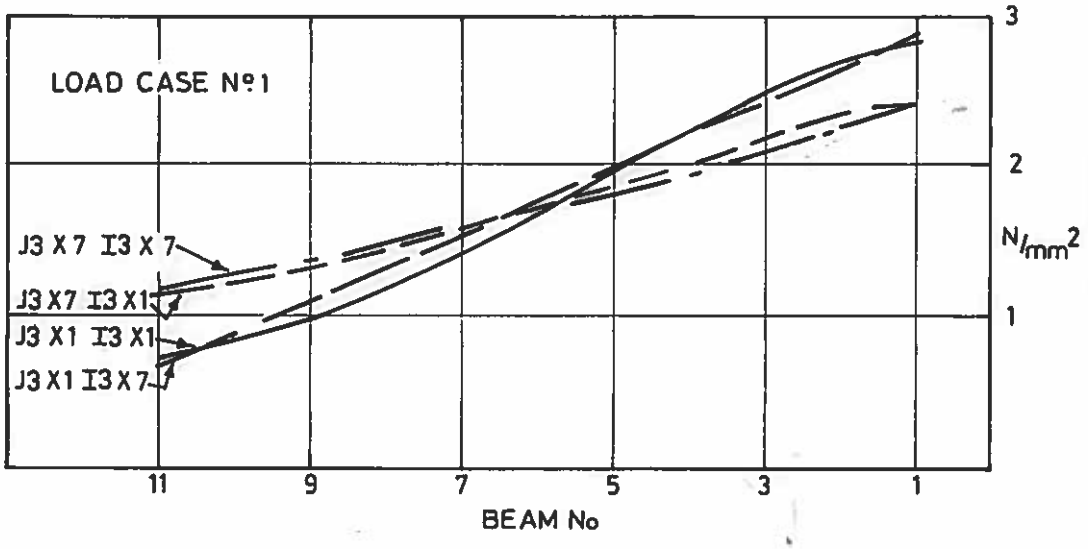

Fig 4.16 Tullyear Road Bridge (Pseudo-Box)

Beam Soffit Stresses from Grillage Analysis and variation in section properties of Idealised transverse grillage beams.

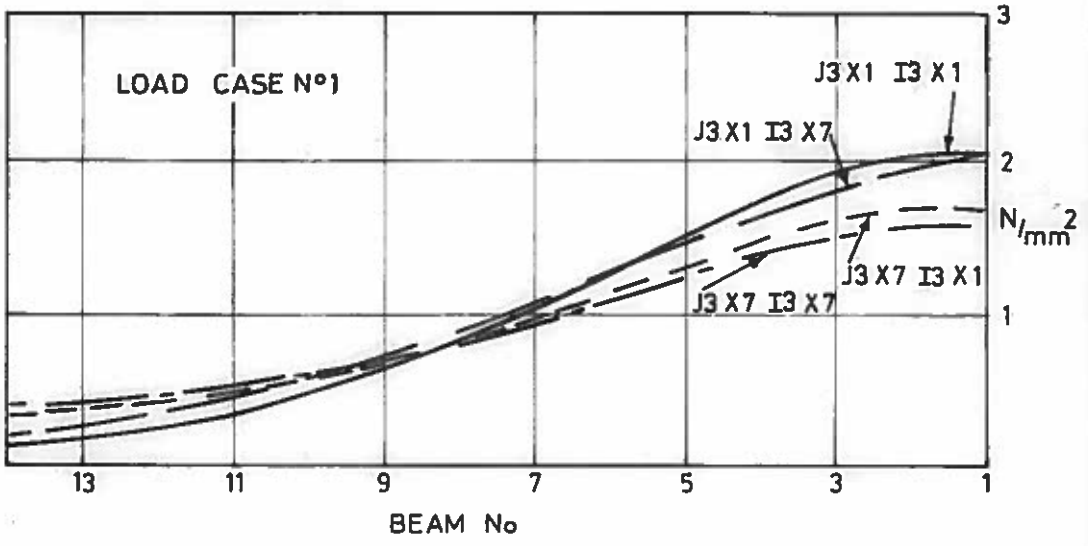

Fig 4.17 A50 Road Bridge (Pseudo-Box)

Beam Soffit Stresses from Grillage Analysis and variation in section properties of Idealised transverse grillage beams

Fig.4.16
Fig.4.17

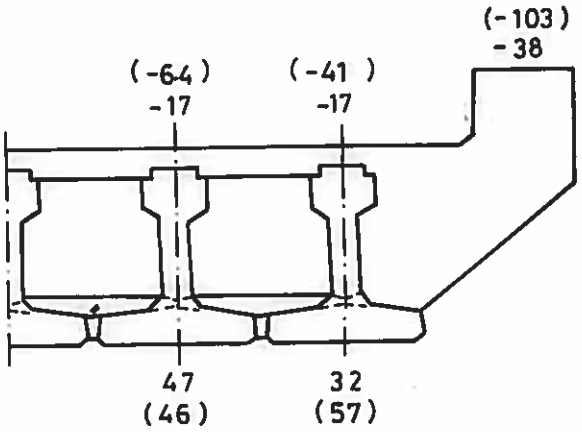

STRAINS IN BRACKETS ARE BASED ON GRILLAGE ANALYSIS WITH J3 x 7

Fig. 4.18 Tullyear Road Bridge
Edge Feature Strain Distribution (με)
Load Case Nº 1

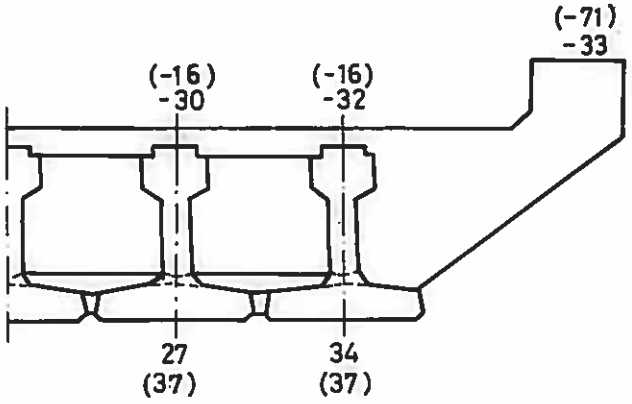

STRAINS IN BRACKETS ARE BASED ON GRILLAGE ANALYSIS WITH J3 x 7

Fig 4.19 A50 Road Bridge
Edge Feature Strain Distribution (με)
Load Case Nº 1

Fig.4.18
Fig.4.19

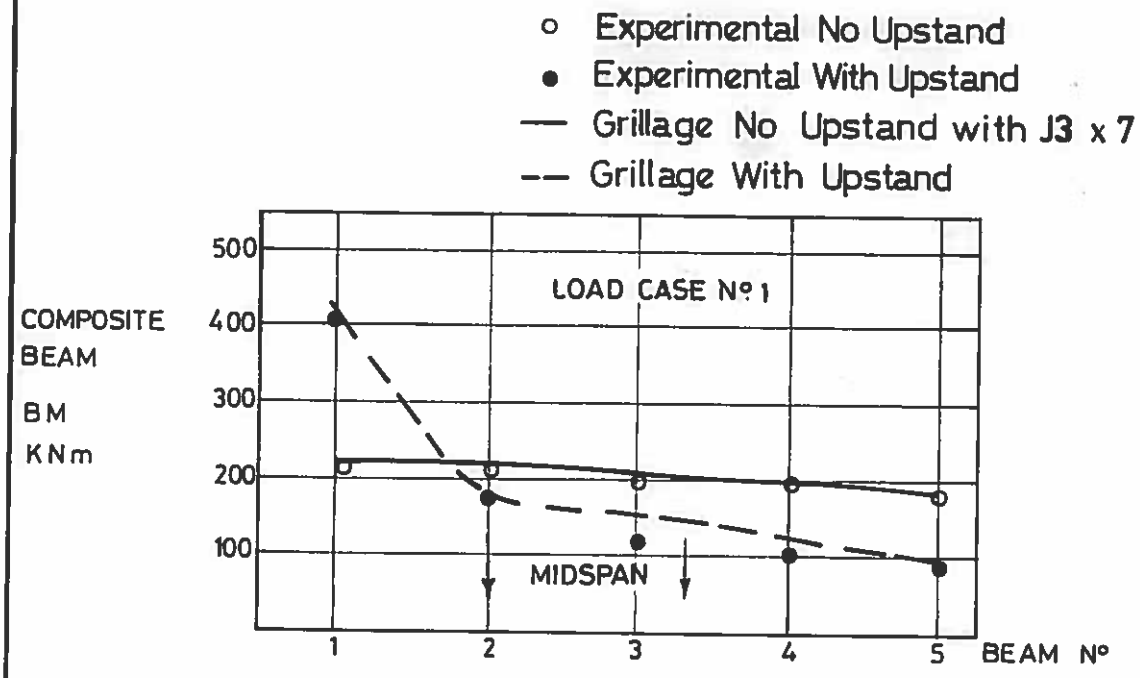

Fig 4.20 Tullyear Road Bridge
Beam Bending Moments Case Nº1

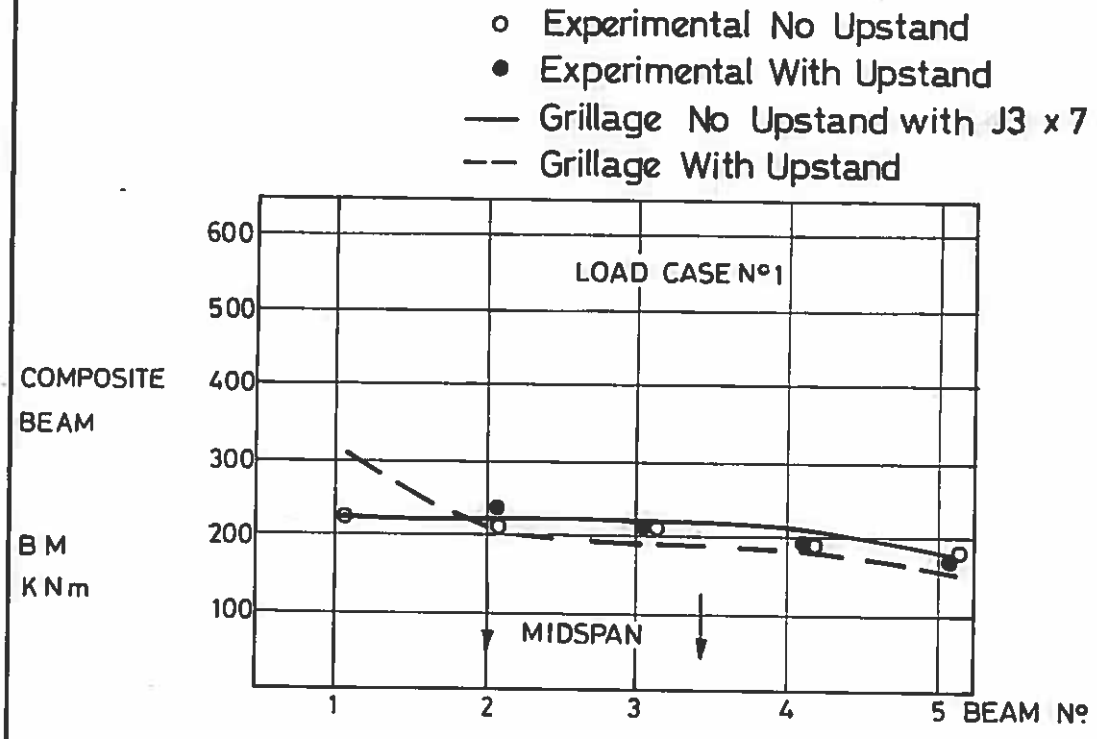

Fig 4.21 A50 Road Bridge
Beam Bending Moments Case Nº1

NOTE: GAUGE Nº1 DAMAGED

Fig.4.20
Fig.4.21

CHAPTER FIVE

DESIGN METHODS FOR M-BEAM BRIDGE DECKS

5.1 INTRODUCTION

One of the main objectives of this project is to consider those parameters that influence the economics of M-beam bridge decks with a view to improving the cost effectiveness of design and construction. It is extremely difficult to quantify the cost of the design process as compared with construction which can be evaluated to a large extent by the quantity of materials required to build the structure. However, certain aspects of design which are of a repetitive or complex nature may be assessed in detail on the basis of the time required in relation to other activities such as the preparation of contract documents and drawings which can be readily quantified.

One such aspect, and an important one in any bridge design, is the initial idealisation and analysis of the proposed structure. This process takes a considerable amount of time as decisions have to be made on such things as traffic lane and verge widths, critical combinations of loading cases, idealisation of the structure and the calculation of the stiffness properties, all of which have to be prepared for input to the computer. However, most M-beam bridge decks have considerable similarities and as such, scope must exist for some degree of standardisation which would avoid the preparation of a new grillage analysis for every proposed bridge.

An important aspect, especially when contract dates are being considered, is the requirement that all designs must be checked by a competent engineer. This mandatory requirement also adds to the design time and it is usually accepted that the engineer responsible for checking should adopt an alternative method for checking the

analysis from that used by the designer. Therefore, if some degree of standardisation could be achieved for M-beam decks it would also reduce and simplify the work involved in checking.

A further consideration is that there has been a general trend over the last few years towards more complex design requirements. This has created a problem of interpretation and hence an increase in the time required for design. In particular, the eventual adoption by the Department of Transport of the new limit state design code BS5400 (1978) with its increase in load combinations and variable length abnormal vehicle will add considerably to design time and ultimately the design costs.

Economies of construction may be achieved in a number of different ways, the most important being the reduction in the number of beams used in the deck. In Northern Ireland, M-beams are normally used at 1m spacing as recommended, however a major saving can be made by increasing the spacing and using fewer beams. An additional advantage of this approach is a lighter deck and this should be reflected in reduced costs for the sub-structure. There is another advantage that may be derived from spacing the beams in that they may be used for spans less than the 15m which is recommended for the standard 1m spacing. This means that they are in direct competition with other forms of construction usually adopted for spans of 8 to 15m and it will be shown in Appendix A that M-beam construction when used for spans of this order and at spacings of up to 2m is very competitive.

Spacing the beams does, however, introduce other constraints

relating to the strength of the reinforced concrete slab spanning between the beams. When this type of slab is designed using current methods it usually produces a steel requirement of about 2%. However, recent research has shown that this could be reduced by a considerable amount and if this could be justified it would be an additional economy. This particular aspect of M-beam deck design is of major importance and will be considered in detail in the next chapter.

The need for standardisation of M-beam decks and the ever increasing complexity of design requirements has occurred at a time when great advances have been made in large main frame computers and the smaller more versatile desk top models. In this chapter, both these computers are used to their best advantage to develop a simplified design procedure which will provide a high degree of standardisation and eliminate most of the problems of the complex design requirements. The main frame computer was used with a grillage analysis program to deduce the required bending moments which were then presented graphically for the extended range of spans and typical deck widths. In this analytical study the results of the load tests from the previous chapter were incorporated and hence accurate estimates of the beam bending moments can be deduced without the necessity for a separate grillage analysis for each bridge deck considered.

The requisite information can then be transferred to a desk top computer and with the use of a set of interactive programs the design can be completed in a very short time. Additional guidance

is provided for secondary reinforcement in the beam and the estimation of bending moments in the slab. This streamlined procedure is more flexible than the Department of Transport Standard Bridges (1978) even though it applies only to M-beam decks.

However, before considering the details of the proposed procedure and to allow a comparison to be made with it, the existing design requirements and procedure will be reviewed.

5.2 EXISTING DESIGN PROCEDURE

5.2.1 General

Before the detail design of an M-beam can be considered the complete bridge deck must be idealised into a form suitable for analysis by hand or computer methods. The analysis will then provide the bending moments and shear forces required for detail beam design. The overall procedure for the analysis and design of an M-beam bridge deck is illustrated in the flow chart shown in Fig. 5.1.

This simplified flow chart contains all the necessary procedures which must be carried out to the standards laid down in the design requirements which will now be reviewed.

5.2.2 Design Requirements

Existing requirements for the design of reinforced concrete are given in DTp Technical Memorandum (Bridges) BE1/73 (1973) and for prestressed concrete bridges are given in DTp Technical Memorandum (Bridges) BE2/73 (1973). Design must also be in accord with the appropriate Codes of Practice such as the British Standards Institution CP115 (1969) and CP116 (1969). The more important permissible stresses and recommended concrete cube strengths are given below.

Precast Concrete

	compression	
28-day cube strength (Uw)	52.5 N/mm^2	
Transfer cube strength (Ut)	40.0 N/mm^2	
Maximum Permissible Stresses	compression	tension
at transfer of prestress	Ut/2	-1.0 N/mm^2
under working load	Uw/3	0 N/mm^2

In situ Concrete

	compression	
28-day cube strength (Uw)	30 N/mm^2	
	or 37.5 N/mm^2	
Maximum permissible stresses	compression	tension
under working load	Uw/3	3.6 N/mm^2
		or 4.2 N/mm^2

Prestressing Strand

A wide choice of prestressing strand is now available. The initial prestressing force should not exceed 70% of the ultimate strength and if possible low relaxation strand should be used in order to keep losses to a minimum.

5.2.3 Factors Influencing Beam Selection

Initial beam selection can have an important influence on the final construction cost of the deck. Current tender prices indicate that the tee beam construction is considerably more economic than a similar pseudo-box deck which is one beam size smaller. In general it is only when clearance is absolutely critical that a pseudo-box construction is preferred. The main problem with the pseudo-

box construction is the fixing of the bottom transverse steel to provide the slab which is a time-consuming job and an obvious cost penalty. A choice of a suitable beam size may be made from Fig. 5.2 which is from the publication by Manton and Wilson (1971) and is based on a span to depth ratio of between 19 and 20.

5.2.4 Detail Flexural Design

For the detail design of the M-Beam, bending moments and shear forces are best presented in the form of envelopes and should be divided into components due to:-

1. Beam self-weight
2. In situ concrete
3. Superimposed dead load
4. Live load

Additional stresses from the following must also be considered:-

5. Differential Shrinkage and Creep
6. Temperature
7. Wind

It should be noted that for an individual beam an envelope of maximum bending moment is all that is required to design the beam for bending, but to provide shear reinforcement for the beam various configurations of bending moment and shear force should be considered. Therefore alternative live load cases, in addition to those producing maximum values, should be investigated.

With the beam size and design bending moments now defined, an acceptable arrangement of tendons and debonding may now be achieved for the midspan section. Transfer and final losses are assumed and

a prestressing force and eccentricity calculated and translated into a practical arrangement with reference to the manufacturer's standard end plate. Losses are checked and the process repeated until convergence is achieved. Moving towards the support, alternative sections of beams are checked under the same prestress and a new set of bending moments. This is repeated until the permissible stress allowed under prestress at transfer and self-weight is reached. At this point a debonding calculation must be carried out by adjusting the number of tendons and associated eccentricity until a suitable strand pattern giving acceptable stresses is achieved. This process is repeated along the beam until the support is reached. Tendons should be debonded as evenly as possible along the beam and excessive debonding should be avoided close to the end block. Where the section under consideration is within the transmission zone, stresses due to prestress should be adjusted to suit the transmission length based on the size and type of tendon being used.

5.2.5 Shear Reinforcement

With the beam now designed in flexure and with envelopes of various cases of bending moments and shear forces, the shear reinforcement may now be detailed. Various sections of the beam must be considered in accordance with the flow chart of DTp Technical Memorandum (Bridges) No BE 2/73 (1973). This is a two-part procedure with both cracked and uncracked sections being checked. The interpretation and application of this flow chart is both tedious and complicated and as a consequence is likely to give rise to errors. If the beam is being works tested a check should also be made to

ensure that the reinforcement is adequate when the test loads are applied to the beam section without the composite action of the slab.

5.2.6 Ultimate Moment of Resistance

An iterative process is used to find the line of zero stress, and for concrete a rectangular stress block of 0.4 x the 28-day characteristic cube strength is assumed in conjunction with the tendon data taken from the manufacturer's load extension curves. A worthwhile increase in the moment of resistance may be achieved by the addition of high yield reinforcing bars longitudinally in the top slab and where an increase is required at a later stage in the design this addition is preferred to an increase in concrete strength or the redesign of tendons.

5.2.7 Beam Test Loads

Test loading of prestressed beams is at the discretion of the design engineer and in general the requirements of the test should be specified on the drawings and contract documents. A test can give a good indication of the load capacity of the beam and is particularly useful if there is some doubt about the quality of material or workmanship. The calculation of test loads is based on the Department of Transport Technical Memorandum (Bridges) No. BE 2/73 (1973) and the Department of Transport, Specification for Road and Bridge Works (1976), where the load if possible should induce a tensile bending stress appropriate to the cube strength of the concrete at the time of test. Where, however, under a lesser loading the compressive stress in bending at any point exceeds 0.5 x

the cube strength of the concrete (after allowing for losses appropriate to the age of the beam when tested) or the bending moment at any section exceeds the ultimate moment of resistance divided by a factor of 1.2, this loading should not be exceeded. At the design stage the possibility of having to test the beams should be considered and adequate shear reinforcement provided.

5.2.8 Deck Slab

The transverse reinforcement in the deck slab should be in the same direction as the idealised grillage members. For modest skew this may be parallel to the abutments although a loss in efficiency of deck steel results as the skew increases. The grillage analysis will provide global bending moments to which the effects of the local wheel loads must be added using the method of Westergaard (1930) or Pucher (1964).

Finally, it must be emphasised that although the requirements for the detail design of M-beams are well defined in the various Technical Memoranda and Codes of Practice, the routine detailing process just described can take a considerable period of time and involve a vast amount of numerical calculations. In an attempt to streamline this existing procedure the use of both main frame and desk top computers will be investigated and the simplified design procedure proposed will now be discussed.

5.3 SIMPLIFIED DESIGN PROCEDURE

5.3.1 General

When considering the flow chart of Fig. 5.1 which shows the existing design requirements it may be seen that the design process

has 2 distinct phases. The first of these is the idealisation of the structure and the analysis which produces the member forces. In the second phase the member forces are used for the detail design of the structural elements. For a beam and slab bridge deck the structural parameters are usually well defined, although for the M-beam type of deck it was considered necessary to establish these by load tests, and the idealisation and analysis can be achieved in a single operation using a standard program and a main frame computer. In contrast, the second phase involving the detail design often requires an iterative process of refinement to achieve an economic structure.

With these 2 phases firmly established the whole design process may be streamlined by using the main frame computer to provide the large amount of data required to form the basis of generalised design charts which would avoid the repetitive and expensive use of the computer for every bridge considered. The desk top computer would then be used to do the detail design, a task for which it is ideally suited as it provides an interactive facility which gives the engineer complete control of the design process.

By incorporating these improvements into the flow chart in Fig. 5.1 the design procedure may now be streamlined to that shown in Fig. 5.3. This approach will produce a considerable saving in time and some details of these improvements will now be considered.

5.3.2 Idealisation and Analysis

As stated previously the structural shapes and stiffness parameters of beam and slab bridge decks are well defined from the point

of view of initial idealisation. Therefore, the main problem is one of repetitive analysis and how to provide the required information in an alternative form that is convenient and simple to use. M-beam bridge decks are usually analysed using a grillage analysis such as the Department of Transport HECB GRIDS Program (1975) and it was envisaged that this program would form the basis of an analytical investigation aimed specifically at generating graphs of live load bending moments due to standard HA and HB loading for a range of spans and widths of decks. This would avoid the necessity of running a new analysis for every deck considered. This standardisation of analysis would require to have sufficient accuracy for initial design with a more rigorous analysis, if necessary, carried out for checking purposes. This type of graphical presentation also has the advantage that it avoids the possibility of the occasional or unfamiliar computer user accepting results in isolation and in error. The graphical presentation of this type of information would provide considerable savings in the man hours and computer time required for this phase of the design process.

5.3.3 Detail Design

To complete the detail design the various design steps in the flow chart in Fig. 5.1 have, with the exception of the idealisation and computer analysis, been programmed to suit the Hewlett Packard 9830A desk top computer. Details of the individual programs are given in the flow charts in Appendix C.

The use of the desk top computer allows the detail design of an M-beam to be completed in a few hours and as detail drawings of

beams and deck tend to follow the same pattern the production of contract drawings has now been reduced to a matter of filling in a few tendon details and numbers of reinforcing bars required in the beam and slab.

An alternative program called PREBEM is now available from the Department of Transport Highway Engineering Computing Branch (1977) for use on an ICL 1900 or a computer of similar capacity. It provides a detail design for most of the precast pre-stressed beams currently available. However, it has the disadvantage that for a given envelope of bending moment and shear forces it produces a unique design which cannot be amended by the designer. It is also unsuitable for checking an existing design where the tendon arrangement has already been specified.

These problems do not arise when using the beam design program for the Hewlett Packard desk top computer. This is an interactive program and for a given set of bending moments the required number of tendons and the associated eccentricity is recommended. The designer may accept or amend this recommendation as required, giving him complete control of the tendon arrangement and tendon debonding. Because of this flexibility of data input this program is ideal for checking existing designs where all the detail has already been specified.

The use of the desk top computer programs in this manner provides a streamlined facility for completing the second phase of the design process. Therefore, the outstanding part of the design process which is the provision, in a graphical form, of charts of live load bending moments will now be considered in detail.

5.4 DESIGN CHARTS

5.4.1 Introduction

With the load distribution characteristics of M-beam bridge decks now established the findings of the previous chapter have been used to formulate a standard procedure for this type of deck. The grillage analysis, incorporating the necessary information, was used to generate design moments which have been presented in a graphical form. Throughout it was assumed that the self-weight and superimposed dead load moments can be calculated on a strip basis.

The economic advantages of spacing the beams has already been discussed even though in their original conception M-beam decks were intended to be used at 1m spacing and in Northern Ireland this has been the practice to date. However, in this particular project considerable emphasis has been placed on economy of design and with this in mind an obvious saving is to place the beams at a spacing greater than the standard 1m, even though this will mean an increase in the depth of the beam by one or two sizes. This of course has been done in certain areas of England with an appropriate adjustment to the strength of the slab. For the standard placing of the beams at 1m spacing the usual range of spans covered is from 15 to 29m. However, when the spacing is increased the spans that may be accommodated by each beam is reduced. For beam spacing of 1.5m the range of spans is 10 to 24m and for 2m spacing it is 8 to 20m. The use of the M-beams for spans less than 15m means that they are now in direct competition with other forms of construction

such as the solid reinforced concrete slab and the standard pre-tensioned concrete inverted tee beam with a solid infill. On investigation it has been found that the M-beam is very competitive (Appendix A) at spans from 8 to 15m and in the situation where ground conditions are poor, the relatively light weight of the M-beam deck, as compared with the other forms of concrete construction, should show additional economy in the design of the sub-structure. A chart has been derived with the recommended beam size for the new range of spans using beam spacings at 1.0, 1.5 and 2.0m and is given in Fig. 5.4. A comparison of deck costs for the smaller beams and shorter spans is given in Appendix A.

In the provision of charts of this type it is important that the scope and limitations of the charts should be well established and defined. Other aspects which are equally important such as the generalised grillages and loading, the basis of the non-dimensional moment distribution curves and the application and use of the charts will all be described in detail.

5.4.2 Specification for Design Charts

It was important that the specification for the design charts was based on a realistic assessment of the most important requirements for M-beam deck design and should be of sufficient accuracy to allow the design to proceed to the contract stage. With this in mind the following requirements were specified for the design charts.

1. Cover all spans between 8 and 29m i.e. the expanded range of application of the M-beam.
2. Provide a transverse distribution of longitudinal bending moment so that the most heavily loaded beam may be identified

when the live load is combined with the dead load and superimposed dead load.

3. Applicable to widths of deck which are typical for the application of a generalised form of the Standard Highway Loading Type HA and HB.

4. Suitable for application to decks having up to 30^{o} skew.

5. Provide an acceptable level of accuracy.

With the main requirements of the design charts now specified a generalised approach to the use of the grillage analysis will now be considered in detail.

5.4.3 Generalised Grillages

As the basis for investigating the load distribution in M-beam bridge decks and to comply with the requirements of span width and skew as defined in the preceding paragraph, an extensive series of grillage analyses were carried out from which all the relevant information could be extracted. For all spans, skews of 0, 10, 20 and 30 degrees were considered and for the 1m spacing spans of 15, 20 and 26m and widths of 9, 13, 17 and 21 beams were investigated in both tee and pseudo-box construction. For the 1.5m spacing spans of 12, 18 and 24m and widths of 7, 9, 11, 13 and 15 beams were considered. For the 2.0m spacing spans of 10, 15 and 20m and widths of 5, 7, 9 and 11 beams were required.

To facilitate the generation of so many grillages a program was written for the Hewlett Packard desk top computer which provided an automatic mesh generation system with the section properties required from very basic input data. The output from this program was in a

convenient form for input to the main frame grillage analysis program. For tee beam construction the grillages were based on the recommendations of West (1973) as discussed in Chapter 4. However, for pseudo-box construction the recommendations based on the load distribution tests as discussed in Chapter 4 have been used. For both tee and pseudo-box construction the stiffening effect of the edge feature has not been considered as this has been shown to produce a safe and conservative design.

Although an orthogonal mesh is ideal for use with the grillage analysis it is generally accepted that for skews up to 30^{o} a high degree of accuracy will be achieved with a parallelogram mesh and this type of mesh has been used in the grillage investigation for the design charts. It also has the advantage that it is suitable for the automatic mesh generation system of the grillage program which is an important facility as it saves a large amount of time required for data preparation and reduces the quantity of input cards for the computer. Idealised grillages are shown in Figs. 5.5 to 5.7 and section properties are shown in Tables 5.1 to 5.4.

5.4.4 Generalised Loading

It was most important that the loading to be used in the calculation of live load bending moments should be of a sufficiently general nature to cover all the critical design cases likely to be considered in any design situation. The various loadings finally adopted were the result of a wide-ranging review of existing bridge deck designs and full details of these will be given in the following sections under the separate classifications of Standard Highway Loading Type HA and HB.

Standard Highway Loading Type HA

In Northern Ireland the Department of the Environment Roads Service is responsible for specifying the intensity of loading that a bridge should be designed to carry. The latest amendment to the current DTp bridge loading document Technical Memorandum (Bridges) BE 1/77 (1977) recommends that all bridges should be designed to carry at least 30 units of HB loading. However each new bridge is considered in its own environment and for accommodation roads, bridleways and byways, the HB requirement may be relaxed and the loading adopted is then a uniformly distributed load plus a knife-edge load.

With this in mind and although possibly of secondary importance, design charts for a limited width of decks have been included and it is envisaged that in practice they will be used mainly for comparative purposes as $wL^2/8$ for the UDL and WL/4 for KEL will give satisfactory results.

The standard highway loading as defined in the DTp Technical Memorandum (Bridges) BEl/77 (1977) requires that 2 lanes be loaded with full HA loading and the remainder with $^1/_3$ HA. For the narrow decks the central 6m has been assumed to constitute two 3m lanes and has been loaded with full HA of 10.5 kN/m^2. The remainder on each side has been considered to be a pedestrian footway but for simplicity has been loaded with $^1/_3$ HA rather than a footpath loading of 4.0 kN/m^2. This slight deficiency was more than compensated for by the inclusion of the $^1/_3$ HA knife-edge load, but was also more convenient when expanding the loading for the wider decks where an additional lane is required as the additional beams are all loaded

with $^1/_3$ HA loading. It should be noted that as full HA loading of 10.5 kN/m^2 and a midspan knife-edge load of 40 kN/m has been used throughout and no allowance has been made for reduced loading due to loaded lengths over 23m or the possibility of actual traffic lanes being greater than 3m. The resulting bending moments are therefore conservative and an adjustment based on a more accurate assessment of the actual loading may be made as suggested in paragraph 5.4.6. Use of Charts. Generalised HA loading is shown in Fig. 5.8 to 5.10.

Standard Highway Loading Type HB

The abnormal vehicle used for Type HB loading is defined by weight and geometry in the current Standard, DTp Technical Memorandum (Bridges) BE1/77 (1977) and for the generalised situation required for the design charts it had to be positioned in the most eccentric position transversely. This will produce a concentration of load in the beams near the edge of the deck as the lateral distribution of this load will be in one direction, i.e. towards the centre of the deck. For the vehicle positioned towards the centre of the deck more beams will be effective and hence a better distribution of load will result with a corresponding reduction in individual beam bending moment. Defining the various positions of the HB vehicle transversely also means catering for a range of footpath widths as the HB vehicle may be positioned 200mm from the raised kerb. The first kerb position considered was approximately at the centre line of the second beam from the edge. This assumed a 1.5m footpath plus a parapet cantilever and this was considered the minimum width possible. This meant the centroid of the HB vehicle was 2.35m from the centre line of the edge

beam which was used as the datum. The alternative kerb positions considered gave HB vehicle centroids of 3.35 and 4.35m from the centre line of the edge beam with footpath widths of 2.5 and 3.5m plus the parapet cantilever. This range of vehicle positions applied to the range of deck widths considered will cover almost all the current motorway and trunk road requirements.

Associated with the standard highway loading Type HB is $^1/_3$ of the Type HA loading and this has been applied to those traffic lanes not occupied by the HB vehicle. The magnitude of this loading was 3.5 kN/m^2 UDL and 13.3 kN/m knife-edge and again no reduction has been made for loaded lengths over 23m or traffic lane widths greater than 3m. Generalised Standard Highway loading Type HB and HB + $^1/_3$ HA is shown in Figs. 5.11 and 5.12 and is for the beams at 1.0m spacing. For the 1.5 and 2.0m spacing the loading is identical with the appropriate adjustment to the beam layout.

With the idealised grillages and loading now standardised the theoretical basis of the design charts will now be developed.

5.4.5 Basis of Charts

For design purposes the maximum longitudinal bending moment in each physical beam due to dead and live load is required and this usually means considering at least the six beams near the edge, each of which will have a different combination of dead and live load. To accommodate this type of investigation charts of maximum longitudinal bending moment have been drawn for the range of spans appropriate to the beam spacing and the various width of decks considered. These are based on the generalised grillages and loading defined in

paragraph 5.4.4. The variation in maximum longitudinal bending moment with span is almost linear and in general shows maximum values occurring when the HB vehicle is in the most eccentric position transversely. The values of maximum bending moment shown in the charts do not always occur at midspan but tend to concentrate under the centre two axles of the HB vehicles which are 6.1m apart. This tendency is more pronounced for the shortest spans under 20m and for the longer spans the midspan usually shows a maximum. This is due to the finer mesh used for the shortest spans relative to the axle spacing of the HB vehicle and may be compared in Fig. 5.5 and Table 5.1. This small difference is not important as the envelope of maximum live load bending moment used for design has an almost constant value between the centre axles of the HB vehicle thereby defining the shape of the envelope for any given maximum bending moment. In the design of an M-beam deck it is usual practice to detail the beam to carry the maximum loads that may be applied to it and then to make all the other beams in the deck identical thereby providing a considerable reserve of strength should the maximum loading combination ever occur.

With the maximum longitudinal live load bending moment now established it is therefore necessary to consider the transverse distribution of longitudinal bending moment across the deck which when added to the dead and superimposed dead load will give the maximum bending moment that can occur and the position of the particular beam in the deck.

The transverse distribution of longitudinal bending moment has been defined using the non-dimensional parameter M/M_{av}

Where M = The midspan bending moment in an individual deck beam

M_{av} = The average midspan bending moment of all the beams in the deck

This non-dimensional parameter M/M_{av} has been found to be effectively independent of span and varies only with width of deck and loading arrangement applied to it. The transverse distribution of M/M_{av} for the cases which include the HB vehicle show a maximum for the 21 beam deck, as the wider the deck the smaller will be M_{av} and hence for a given value of M the ratio M/M_{av} will be large.

The use of the charts for the estimation of the transverse distribution of longitudinal bending moment will provide a quick conservative solution with an acceptable level of accuracy. The scatter of results from the analysis of the HA loading was 4%, from the HB loading 6% and from the HB + $^1/_3$ HA loading 6%. The most conservative values of M/M_{av} have been plotted in all cases. Although an acceptable level of accuracy is required from the design charts overall the accuracy of the transverse distribution of longitudinal bending moment is not so critical provided the position of the maximum bending moment is correct and the shape of the curve is a reasonable approximation as defined by the parameter M/M_{av}. There is also a reserve of strength in the adjacent beams especially in the tee beam construction which shows a greater variation of longitudinal bending moment in the transverse direction than the pseudo-box construction which has a much flatter distribution similar to a reinforced concrete slab.

For M-beam decks live load represents only 30 to 50% of the total design bending moments so that an error of 6% in the estimation of the live load bending moment is reduced to 1.8 to 3% when dead and superimposed dead load is added for design purposes.

The design charts are therefore based on the assumption that:

1. The maximum longitudinal bending moment occurs at midspan
2. For design purposes this maximum bending moment may be combined with a transverse distribution of longitudinal bending moment based on the midspan values of the non-dimensional parameter M/M_{av}.

Charts of maximum bending moment and M/M_{av} for various loading arrangements and deck construction are given in Figs. 5.13 to 5.36.

It should be noted that for the 1m spacing the charts of maximum bending moment per beam have a separate graph for each width of deck considered. However, as the spacing of the beams increased, the capacity of the deck to distribute the wheel loads laterally was decreased and the maximum bending moments depended upon the local wheel loads only and were effectively independent of the number of beams in the deck, hence only a single graph is shown for 1.5 and 2.0m spacing. With the basis of the charts firmly established consideration will now be given to the use of the charts for the design of an M-beam bridge deck.

5.4.6 Use of Charts

Procedure for Design and Checking

With the design charts available for estimating the live load bending moments the procedure to be adopted would be that for init-

ial design they would be used for a very quick calculation of bending moment. The design would proceed using the various programs available for the Hewlett Packard desk-top computer and could be completed in a few hours. Under the technical approval of structures checking system, the engineer responsible for checking would use a grillage analysis or a suitable method to do a more accurate investigation. This would allow particular aspects of deck loading such as loaded length, traffic lanes and footpath widths to be investigated including a more refined analysis of the overall bridge deck which could not be generalised. Therefore if the slightly more comprehensive analysis carried out using the grillage analysis during the checking should indicate that an increase in live load bending moment is required, the small adjustment can be made before the contract is awarded or manufacture begins.

Application of Charts

In order to estimate the live load bending moment using the charts the following bridge deck parameters must be defined - effective span, number of beams and skew. For deck loading the transverse position and number of units of the HB vehicle is also required. For the maximum bending moments the charts of the HB loading plus $^1/_3$ HA and the correct number of beams should be used and for the given span and position of HB vehicle the maximum bending moment may be read. Deck width and vehicle position may be interpolated when they do not coincide with the given data.

After reading M_{max}, the transverse distribution may now be considered. By using the chart with the correct vehicle position,

the maximum value of M/M_{av} for the given deck width is read. This is in fact M_{max}/M_{av} and as M_{max} has been established from the bending moment chart the value of M_{av} may now be calculated. The non-dimensional parameter M/M_{av} may now be read from the curve at each beam in the deck and knowing M_{av} the bending moment at each beam may be calculated. A typical example is considered in Fig. 5.37.

For the Standard Highway loading type HA with a lane width greater than 3 m and a loaded length greater than 23 m the intensity of loading may be reduced. The transverse distribution should be calculated using the design charts which are based on the loading as shown in Figs 5.8 to 5.10. The actual reduced loading should be calculated and compared with the loading of Figs. 5.8 to 5.10. Reduction factors based on the reduced loading divided by 10.5 or 3.5 may be calculated and the original distribution of bending moments reduced to give a more accurate estimate.

For the HB + $\frac{1}{3}$ HA loading, the $\frac{1}{3}$ HA is based on 3.5 kN/m^2 and a reduction similar to the HA loading may be made. The effect of the $\frac{1}{3}$ HA loading may be estimated by calculating the difference between HB + $\frac{1}{3}$ HA and HB. The $\frac{1}{3}$ HA part may be reduced in proportion to the actual intensity of the $\frac{1}{3}$ HA to the 3.5 kN/m^2 on which the charts are based. The moments from the original HB loading are then added to the reduced $\frac{1}{3}$ HA moments to complete the design.

Reduced HB Loading

Two sets of charts have been prepared for each beam spacing using 45 units of Standard Highway Loading Type HB. The first set uses the HB vehicle on its own and the second has the additional $\frac{1}{3}$ Type HA loading. Maximum design bending moments will occur when

the deck is loaded with the HB vehicle plus $^1/_3$ HA but for some roads a reduced standard of loading is acceptable and an HB vehicle of 37½ or 30 units may be required. The set of charts of 45 units of HB vehicle only may be used to deduce the design bending moments for this reduced standard.

The procedure to be adopted is as follows:-

For the given deck parameters the individual beam bending moments should be calculated as described for both 45 units of HB loading and also 45 units of HB plus $^1/_3$ HA. By subtracting these the beam bending moments due to $^1/_3$ HA only may be calculated. The bending moments for 45 units of HB only may then be reduced to the required loading, such as 37½ or 30 units, and these values are then added to the bending moments for $^1/_3$ HA. This will then give the design bending moments for the reduced HB loading plus $^1/_3$ HA loading.

5.4.7 Skew Decks

In the specification for design charts it was considered desirable that up to 30 degrees of skew should be accommodated and in this respect it has been investigated for both tee and pseudo-box construction.

The generalised arrangement of grillage and loading that was used for the right decks was extended for angles of skew of 10, 20 and 30 degrees. The effective span was kept constant with a subsequent reduction in square span. However, this showed that only a very small reduction of about 3% maximum occurred, with most of the grillages showing negligible reduction in longitudinal bending moments.

It is therefore recommended that no reduction in longitudinal bending moment should be made for decks with an angle of skew less than 30 degrees. The order of the reduction that could be considered is well within the accuracy required from the design charts.

The previous paragraphs have described how the design charts may be used to provide a transverse distribution of longitudinal bending moment which when combined with the dead load and superimposed dead load will allow the critical beam to be isolated for design purposes. However, having established the critical beam, the distribution of bending moment in the longitudinal direction is then required and in paragraph 5.2.4 it was suggested that this is best presented in the form of an envelope as this allows the longitudinal beam sections to be considered. Therefore to expand the simplified presentation of data for beam design, envelopes of longitudinal bending moments for both type HA and HB loading will now be considered.

5.5 ENVELOPES OF BENDING MOMENTS

5.5.1 Introduction

For a complete design of an M-beam, bending moments are best presented in the form of an evenlope. As it is not known initially where the prestressing strand is to be debonded after the midspan tendon arrangement has been decided, the envelope provides all the information required for the design to proceed at any beam section. The midspan section will be designed to the full live load moment but as sections away from midspan are considered and as the dead load compensation reduces, the condition at transfer becomes the critical design parameter. Therefore for bending design a live load

envelope is only of importance around the middle third of the span as this is the part of the beam which is affected by the HB vehicle as it moves across the deck. If a rigorous design of shear reinforcement is to be carried out, a range of individual bending moment cases and associated shear forces are required. Envelopes of Standard Highway Loading Type HA and HB each have their own particular shape and characteristics, both of which will be considered.

5.5.2 Standard Highway Loading Type HA

The envelope of this type of loading is the parabolic distribution of bending moment from the uniformly distributed part of the loading with the bending moment due to the knife-edge load, which may occur at any point on the span, superimposed. By adding the two bending moment equations the bending moment of the envelope M may be equated to:-

$$M = (L - x)(\frac{w}{2} + \frac{40}{L})$$

The midspan bending moment may be established from the design charts and with x = L/2 the value of w may be calculated from the above equation. Knowing w, the bending moment at any point x may now be calculated and the envelope completed.

5.5.3 Standard Highway Loading Type HB

The idealised envelope for this type of loading is based on the geometry of the abnormal vehicle and is shown in Fig. 5.38. As maximum bending moments occur under the centre 2 axles the envelope of bending moment is constant between these axles which are 6.1m apart. This part of the envelope will allow the initial detailing of the ten-

don pattern and an estimation must now be made of the bending moment at point B (Fig. 5.38) which will depend on the bending moment at A and the span of the deck. As the bending moment at A may be calculated from the design charts then for any given span the bending moment at B may be calculated as follows with reference to Fig. 5.38.

$$M_A = R_b(L/2 - 3.05) - 1.8W$$

$$R_b = 2W$$

$$W = R_b/2$$

$$M_A = R_b(L/2 - 3.05) - 0.9R_b$$

$$= R_b(L/2 - 3.05 - 0.9)$$

$$= R_b(L/2 - 3.95)$$

$$R_b = M_A/(L/2 - 3.95)$$

$$M_B = M_A(L/2 - 4.85)/(L/2 - 3.95)$$

$$= Km.M_A$$

where $K_m = (L/2 - 4.85)/(L/2 - 3.95)$

Values of the coefficient K_m have been plotted for spans of 9.7 to 29m and are given in Fig. 5.39. At a span of 9.7m point B coincides with the support point. For spans of 8 to 9.7m point A should be taken as 0.15L from the support to avoid having tendons debonded inside the transmission zone. Having established the bending moment at B a straight line distribution has been assumed from B to the support. This part of the envelope is unimportant as design is always to the critical transfer condition although the inspection of a series of design envelopes has shown that only very occasionally on the longer spans would a straight line distribution be exceeded in this area.

Although this analysis is based on the geometry of the HB vehicle, when the additional $^1/_3$ HA loading is added it increases the bending moment by about 10%. As the loading is still predominately HB this approach is still valid for both the HB and HB + $^1/_3$ HA types of loading.

The use of this type of envelope for live load bending moments should give a reasonably accurate debonding pattern for the prestressing strand near the centre third of the beam as the transfer condition will govern design over the remaining end thirds of the beam.

To complete the design of an M-beam bridge deck 2 other aspects of the requirements must be considered. These are the provision of secondary reinforcement in the beams and the estimation of the transverse bending moments in the deck slab from the overall analysis. Both these requirements will now be considered with a view to providing a completely flexible design procedure.

5.6 SECONDARY REINFORCEMENT FOR BEAMS

The design of secondary reinforcement for composite prestressed beams is based on the provisions of the Department of Transport Technical Memorandum (Bridges) BE 2/73. For a rigorous analysis a range of both HA and HB loading cases should be considered and the critical case occurs when $(Q - 0.8\ Q_{cm})$ is a maximum, where

Q = The shear force due to the dead and live load with ultimate factors applied according to Clause 7 of BE2/73 (1973).

Q_{cm} = The shear capacity of the plain concrete section cracked in flexure.

This calculation is long and complicated and has to be repeated at various sections along the beam. For initial design an empirical layout of steel is proposed which is based on a study of existing designs and will apply to the full range of M-beams used in either pseudo-box or tee beam at up to 2m spacing. The proposed steel arrangement is shown in Fig. 5.40 and should be satisfactory when the beam is composite with the deck slab and subjected to live loads. Although the use of beams at up to 2m spacing has considerable economic advantages, it was thought that difficulties could arise regarding the shear strength. However a series of typical designs using beams at 2m spacing has been completed indicating that the shear strength is satisfactory and the empirical arrangement shown in Fig. 5.40 will provide an acceptable level of safety.

When provision is made at the design stage to test a beam then the secondary reinforcement proposed in Fig. 5.40 should be checked by applying the test loads to the monolithic beam. A program is available for the desk top computer to carry out this check as it is possible that test loads on the monolithic beam will be more critical than live loads applied to the composite beam.

5.7 TRANSVERSE BENDING MOMENTS FROM OVERALL ANALYSIS

The deck slab which spans between the precast beams is required to resist forces from two distinct sources which may be defined as follows:-

1. Global effects due to the overall deflection of the beams relative to each other; and
2. Local effects due to individual wheel loads applied to the slab spanning between beams.

Bending moments due to local wheel loads are usually estimated by the methods of Westergaard (1930) or Pucher (1964) and are dependent upon the thickness of surfacing on top of the slab.

Maximum global bending moments due to 45 units of the abnormal vehicle have been calculated for a range of decks and these bending moments which are given in Table 5.5 may be used for design purposes and should be added to the bending moments from the local wheel loads.

5.8 COMPARISON OF CHARTS WITH EXISTING DESIGNS

This chapter has been concerned with the design of M-beam bridge decks and in particular the development and use of the charts to simplify the design procedure. It will be of interest to compare the accuracy of the charts with some existing designs which have been prepared using more rigorous analyses. This comparison will now be made with some recent designs by the DOE (NI), Roads Service. These are typical examples and many more have been compared by the DOE (NI) and have been found to be satisfactory. Both tee and pseudo-box construction at 1m spacing have been considered.

5.8.1 Tee Beam Construction

Two bridge decks have been compared and details of the Mourne River Bridge and Ballymacoss Railway Bridge are given in Table 5.6.

The comparison of bending moment distributions for these 2 bridge decks are given in Figs 5.41 and 5.42. For the HB vehicle only case there is excellent agreement for both these bridges and for the HB + $^1/_3$HA case the design charts show an overestimation of 6% for the Mourne River Bridge and 4% for the Ballymacoss Railway Bridge.

For design purposes these values are quite satisfactory although

it should be noted that when these moments are added to the dead loads the amount of overestimate is negligible. No correction has been made for the reduced $\frac{1}{3}$HA loading due to lane width or loaded length.

5.8.2 Pseudo-Box Construction

Again two bridges have been compared and details are given in Table 5.6. It will be seen from Figs 5.43 and 5.44 that the design charts give bending moments which are considerably less than the original design and this is due to the increased torsional inertia of the idealised transverse grillage beam which has been incorporated into the design charts. This comparison therefore shows the amount of overdesign which occurs from the use of the existng design recommendations and with the test results incorporated into the design charts it should be possible to use a smaller beam for the pseudo-box construction than would normally be used.

In this chapter the many aspects of M-beam bridge deck design have been considered and the proposed simplified procedure will provide a streamlined alternative to the standard approach. This will reduce the design time to a few days with a subsequent saving in man hours and the additional economies that may be achieved by spacing the beams will also have a significant effect on the contract price of the bridge. The design charts and detailed running instructions for the desk top computer programs have been published by Kirkpatrick (1979) and are currently being used by the DOE (NI) Roads Service.

The increased spacing of the beams does however, when the slab is analysed by the recommended method, produce bending moments which requires bottom transverse reinforcement of at least 2%. Recent research has however indicated that when the in-plane restraint which

is inherent in this type of bridge slab is taken into account reinforcement may be reduced considerably. If this reduction in steel reinforcement could be achieved for the standard 160mm M-beam slab it would represent an additional saving both in steel content and in the time required for fabrication. However, to justify such a reduction in steel content the load capacity of the slab would require to be established by test and a more appropriate method of analysis developed which would allow for the in-plane restraint inherent in this type of slab.

Therefore, an experimental programme to establish the serviceability and ultimate capacities of the standard M-beam slab with the beams spaced at up to 2m will now be planned and details will be discussed in the next Chapter.

Span m	Grillage Property	9 Beam Deck	13 Beam Deck	17 Beam Deck	21 Beam Deck
15	L-m	2.5	2.5	2.5	1.875
	B-m	1.0	1.5	2.0	1.8182
	Phy/Grill beam	1.0	1.444	1.888	1.75
	I1 x $10^9 mm^4$	39.05	56.41	73.76	68.34
	J1 "	3.17	4.65	6.12	5.65
	I2 "	0.68	0.68	0.68	0.51
	J2 "	1.64	1.64	1.64	1.21
	I3 "	31.81	31.81	31.81	28.98
	J3 "	16.88	16.88	16.88	16.67
20	L-m	3.333	3.333	3.333	2.5
	B-m	1.0	1.5	2.0	1.8182
	Phy/Grill beam	1.0	1.444	1.888	1.75
	I1 x $10^9 mm^4$	74.95	108.26	141.57	131.16
	J1 "	3.49	5.12	6.74	6.22
	I2 "	0.91	0.91	0.91	0.68
	J2 "	2.21	2.21	2.21	1.64
	I3 "	71.25	71.25	71.25	64.84
	J3 "	26.96	26.96	26.96	26.67
26	L-m	4.333	4.333	4.333	3.25
	B-m	1.0	1.5	2.0	1.8182
	Phy/Grill beam	1.0	1.444	1.888	1.75
	I1 x $10^9 mm^4$	146.72	211.93	277.14	256.76
	J1 "	4.61	6.73	8.85	8.17
	I2 "	1.18	1.18	1.18	0.89
	J2 "	2.89	2.89	2.89	2.15
	I3 "	160.75	160.75	160.75	146.22
	J3 "	40.57	40.57	40.57	40.20

TABLE 5.1 - Section Properties of Standard Grillages

Tee Beam Construction Beams spaced at 1.0 m centres

Span m	Grillage Property	9 Beam Deck	13 Beam Deck	17 Beam Deck	21 Beam Deck
15	L-m	2.5	2.5	2.5	1.875
	B-m	1.0	1.5	2.0	1.8182
	Phy/Grill beam	1.0	1.444	1.888	1.75
	I1 x 10^9 mm^4	40.65	58.71	76.78	71.13
	J1 "	21.89	32.17	42.43	33.89
	I2 "	3.38	3.38	3.38	2.54
	J2 "	324.73	306.04	296.94	266.07
	I3 "	31.81	31.81	31.81	28.98
	J3 "	42.97	40.49	39.26	34.50
20	L-m	3.333	3.333	3.333	2.5
	B-m	1.0	1.5	2.0	1.8182
	Phy/Grill beam	1.0	1.444	1.888	1.75
	I1 x 10^9 mm^4	79.56	114.92	150.28	139.23
	J1 "	37.37	54.91	72.42	56.19
	I2 "	9.98	9.98	9.98	7.49
	J2 "	728.28	686.91	666.47	614.39
	I3 "	71.25	71.25	71.25	64.84
	J3 "	91.90	86.51	83.85	75.95
26	L-m	4.333	4.333	4.333	3.25
	B-m	1.0	1.5	2.0	1.8182
	Phy/Grill beam	1.0	1.444	1.888	1.75
	I1 x 10^9 mm^4	158.55	229.02	299.49	277.47
	J1 "	59.26	87.02	114.74	87.46
	I2 "	27.49	27.49	27.49	20.61
	J2 "	1414.07	1332.94	1292.90	1224.09
	I3 "	160.75	160.75	160.75	146.21
	J3 "	170.37	160.18	155.16	145.15

TABLE 5.2 - Section Properties of Standard Grillages

Pseudo-box Construction

Span m	Grillage Property	7 Beam Deck	9 Beam Deck	11 Beam Deck	13 Beam Deck	15 Beam Deck
12	L-m	2.0	2.0	2.0	2.0	2.0
	B-m	1.5	1.5	1.5	1.5	1.5
	Phy/Grill Beam	1.0	1.0	1.0	1.0	1.0
	I1 x 10^9 mm^4	33.622	33.622	33.622	33.622	33.622
	J1 "	2.944	2.944	2.944	2.944	2.944
	I2 "	36.432	36.432	36.432	36.432	36.432
	J2 "	3.115	3.115	3.115	3.115	3.115
	I3 "	0.683	0.683	0.683	0.683	0.683
	J3 "	1.364	1.364	1.364	1.364	1.364
	I4 "	27.790	27.790	27.790	27.790	27.790
	J4 "	19.690	19.690	19.690	19.690	19.690
18	L-m	3.0	3.0	3.0	3.0	3.0
	B-m	1.5	1.5	1.5	1.5	1.5
	Phy/Grill Beam	1.0	1.0	1.0	1.0	1.0
	I1 x 10^9 mm^4	100.99	100.99	100.99	100.99	100.99
	J1 "	4.457	4.457	4.457	4.457	4.457
	I2 "	108.19	108.19	108.19	108.19	108.19
	J2 "	4.628	4.628	4.628	4.628	4.628
	I3 "	1.024	1.024	1.024	1.024	1.024
	J3 "	2.046	2.046	2.046	2.046	2.046
	I4 "	105.17	105.17	105.17	105.17	105.17
	J4 "	37.252	37.252	37.252	37.252	37.252
24	L-m	4.0	4.0	4.0	4.0	4.0
	B-m	1.5	1.5	1.5	1.5	1.5
	Phy/Grill Beam	1.0	1.0	1.0	1.0	1.0
	I1 x 10^9 mm^4	187.15	187.15	187.15	187.15	187.15
	J1 "	6.063	6.063	6.063	6.063	6.063
	I2 "	199.25	199.25	199.25	199.25	199.25
	J2 "	6.234	6.234	6.234	6.234	6.234
	I3 "	1.366	1.366	1.366	1.366	1.366
	J3 "	2.728	2.728	2.728	2.728	2.728
	I4 "	228.42	228.43	228.43	228.43	228.43
	J4 "	51.22	51.22	51.22	51.22	51.22

TABLE 5.3 - Section Properties of Standard Grillages

Beams Spaced at 1.5m Centres

Span m	Grillage Property	5 Beam Deck	7 Beam Deck	9 Beam Deck	11 Beam Deck
10	L-m	1.667	1.667	1.667	1.667
	B-m	2.0	2.0	2.0	2.0
	Phy/Grill Beam	1.0	1.0	1.0	1.0
	I1 x 10^9 mm^4	36.432	36.432	36.432	36.432
	J1 "	3.115	3.115	3.115	3.115
	I2 "	41.071	41.071	41.071	41.071
	J2 "	3.456	3.456	3.456	3.456
	I3 "	0.569	0.569	0.569	0.569
	J3 "	1.137	1.137	1.137	1.137
	I4 "	26.216	26.216	26.216	26.216
	J4 "	19.483	19.483	19.483	19.483
15	L-m	2.50	2.50	2.50	2.50
	B-m	2.0	2.0	2.0	2.0
	Phy/Grill Beam	1.0	1.0	1.0	1.0
	I1 x 10^9 mm^4	108.19	108.19	108.19	108.19
	J1 "	4.628	4.628	4.628	4.628
	I2 "	120.45	120.45	120.45	120.45
	J2 "	4.969	4.969	4.969	4.969
	I3 "	0.853	0.853	0.853	0.853
	J3 "	1.704	1.704	1.704	1.704
	I4 "	99.116	99.116	99.116	99.116
	J4 "	36.149	36.149	36.149	36.149
20	L-m	3.333	3.333	3.333	3.333
	B-m	2.0	2.0	2.0	2.0
	Phy/Grill Beam	1.0	1.0	1.0	1.0
	I1 x 10^9 mm^4	199.25	199.25	199.25	199.25
	J1 "	6.234	6.234	6.234	6.234
	I2 "	220.21	220.21	220.21	220.21
	J2 "	6.575	6.575	6.575	6.575
	I3 "	1.138	1.138	1.138	1.138
	J3 "	2.273	2.273	2.273	2.273
	I4 "	215.141	215.141	215.141	215.141
	J4 "	49.694	49.694	49.694	49.694

TABLE 5.4 - Section Properties of Standard Grillages

Beams Spaced at 2 m Centres

Bending Moment	Pseudo-Box	Tee Beam		
		1.0m	1.5m	2.0m
Hogging	40	15	10	10
Sagging	80	40	30	25

TABLE 5.5 - Transverse Global Bending Moments - kNm/m

Detail \ Bridge	Mourne River Bridge	Ballymacoss Railway Bridge	A50 Road Bridge
Span - m	25.75	21.5	18.6
Beam size	M8	M6	M5
No. of beams	12	24	21
Skew - ^{o}	0	0	26

TABLE 5.6 - Bridges Used for Comparison of Charts with Existing Design

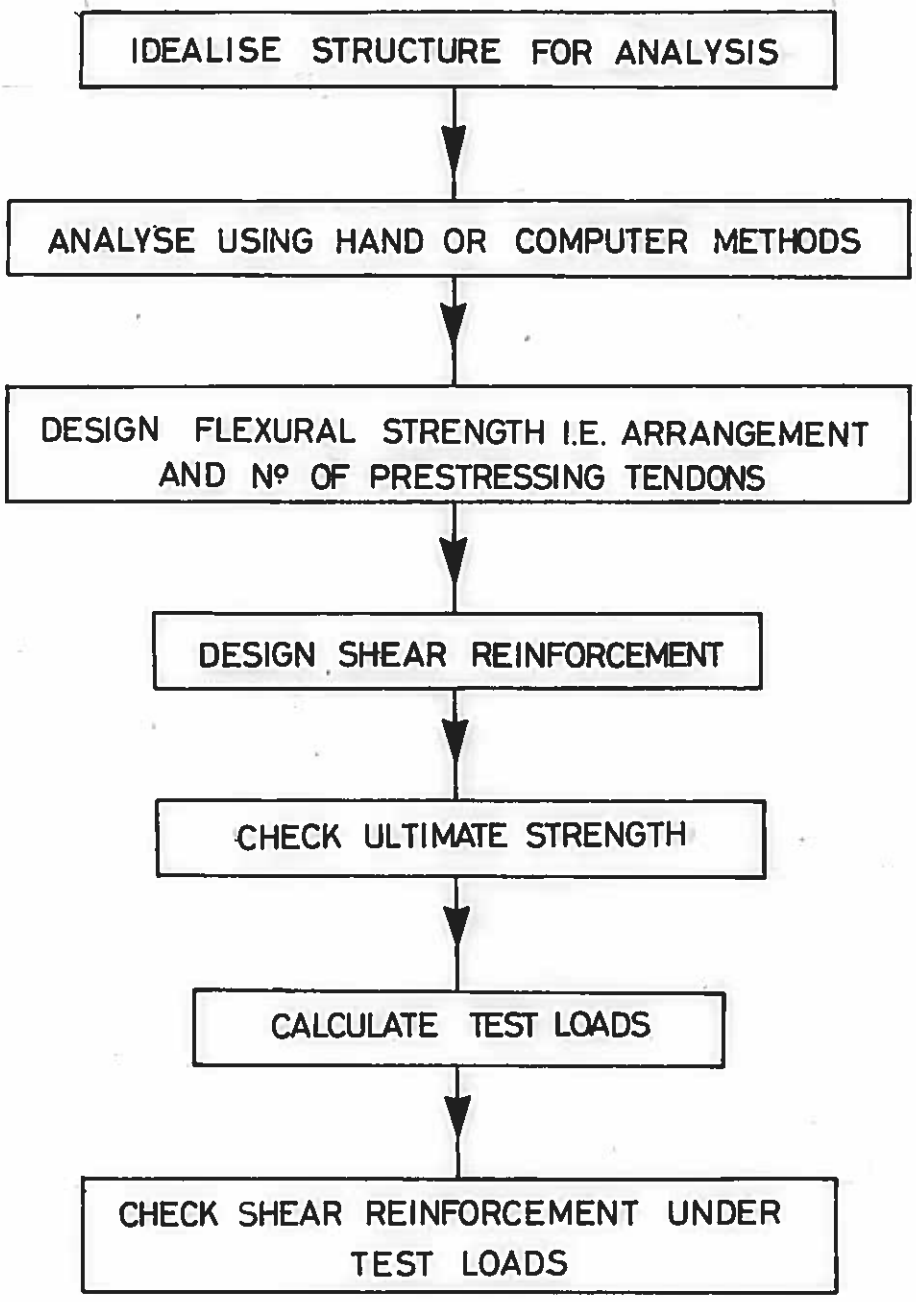

Fig. 5.1 Flow Chart for the Design of M-Beam Bridge Decks

Fig. 5.1

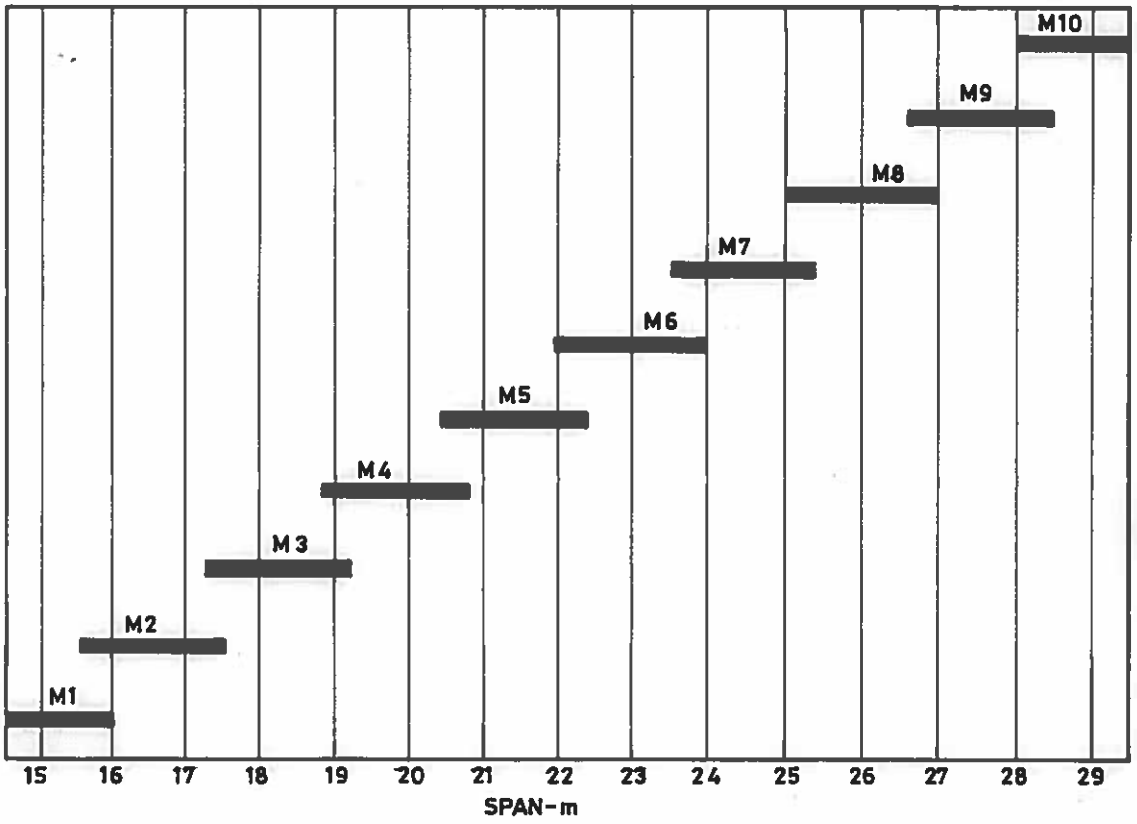

Fig 5.2. Choice of Section for Preliminary Design by Manton & Wilson (1971)

Fig.5.2

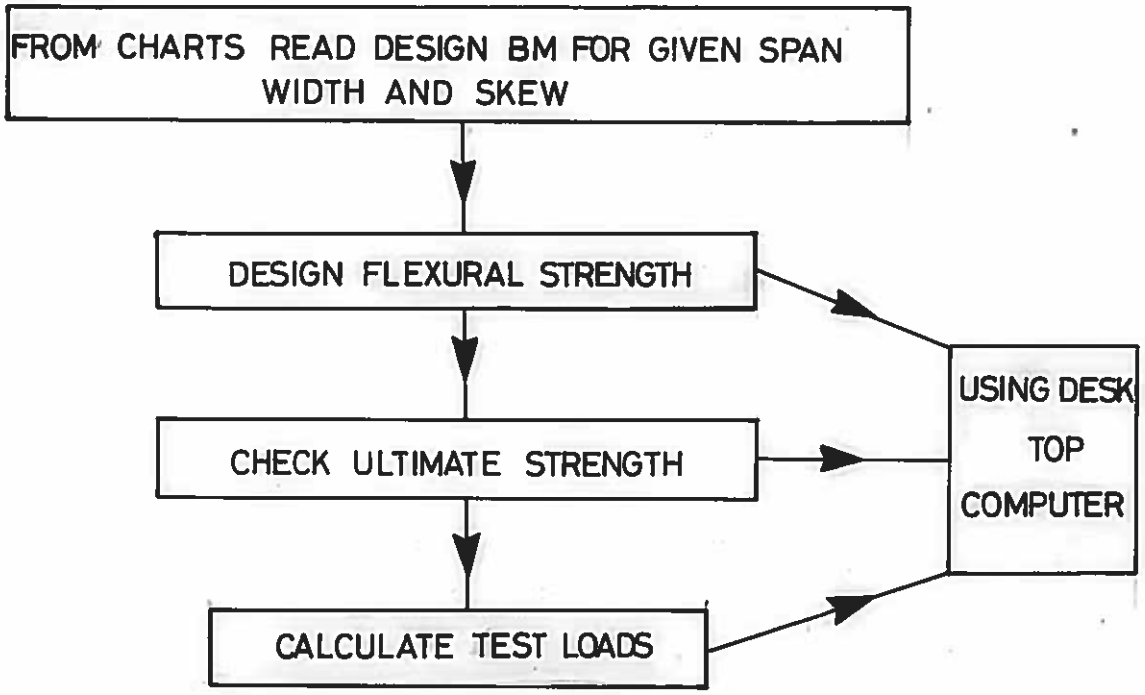

Fig. 5.3 Flow Chart for the Design of M-Beam Bridge Decks Using Design Charts and Desk Top Computer

Fig. 5.3

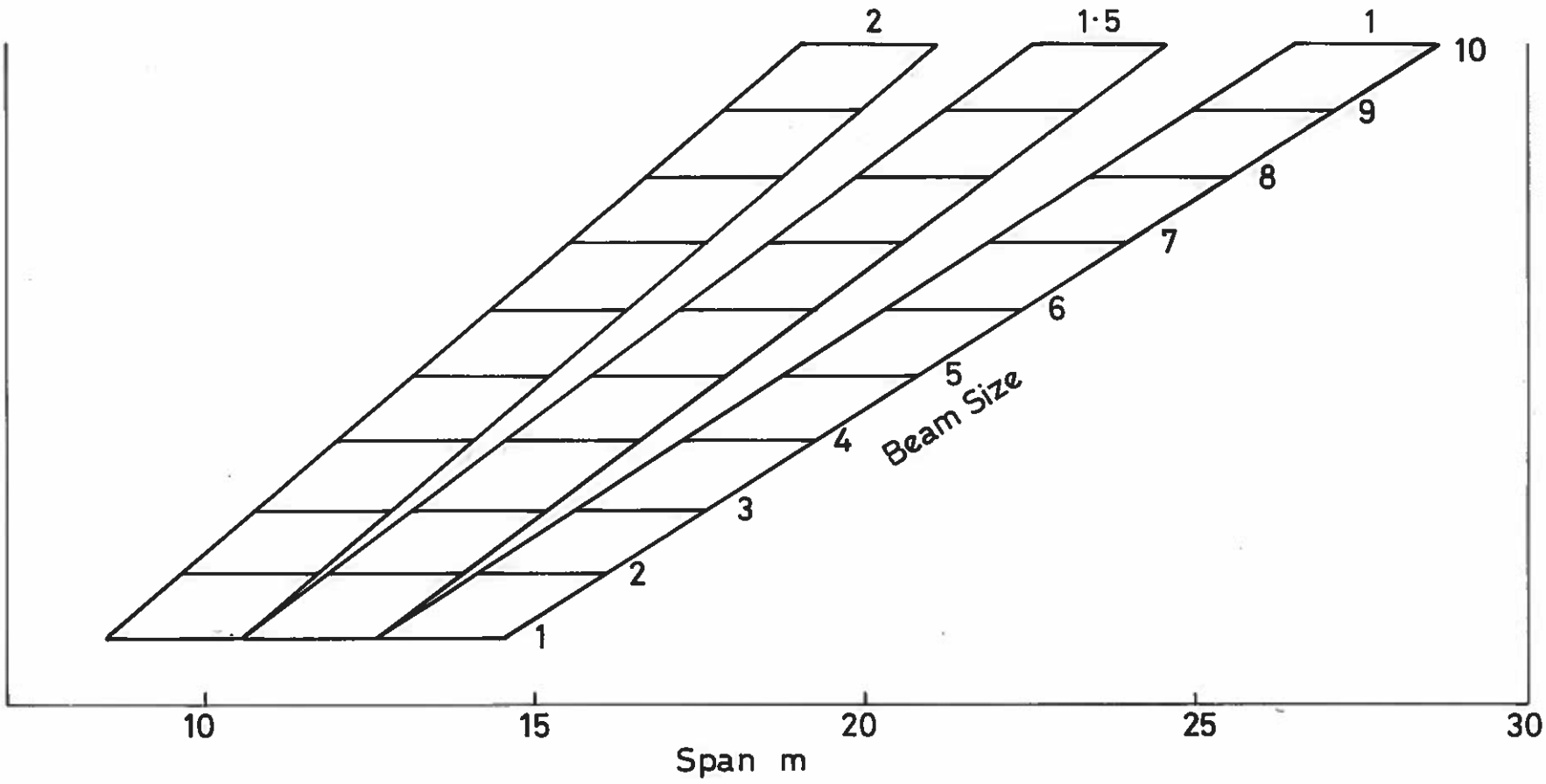

Fig.5.4 Choice of Section for Preliminary Design - Spaced Beams

Fig.5.4

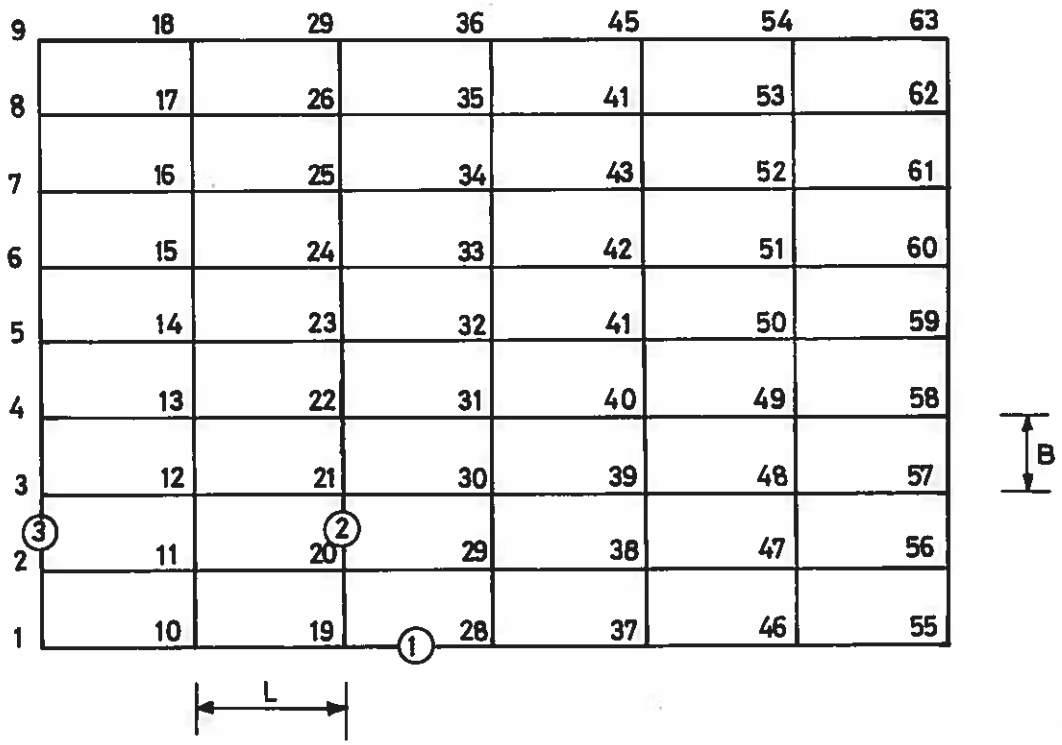

FIG. 5.5 Idealised Grillage for all 9 13 and 17 Beam Decks (For details see tables 5.1 and 5.2)

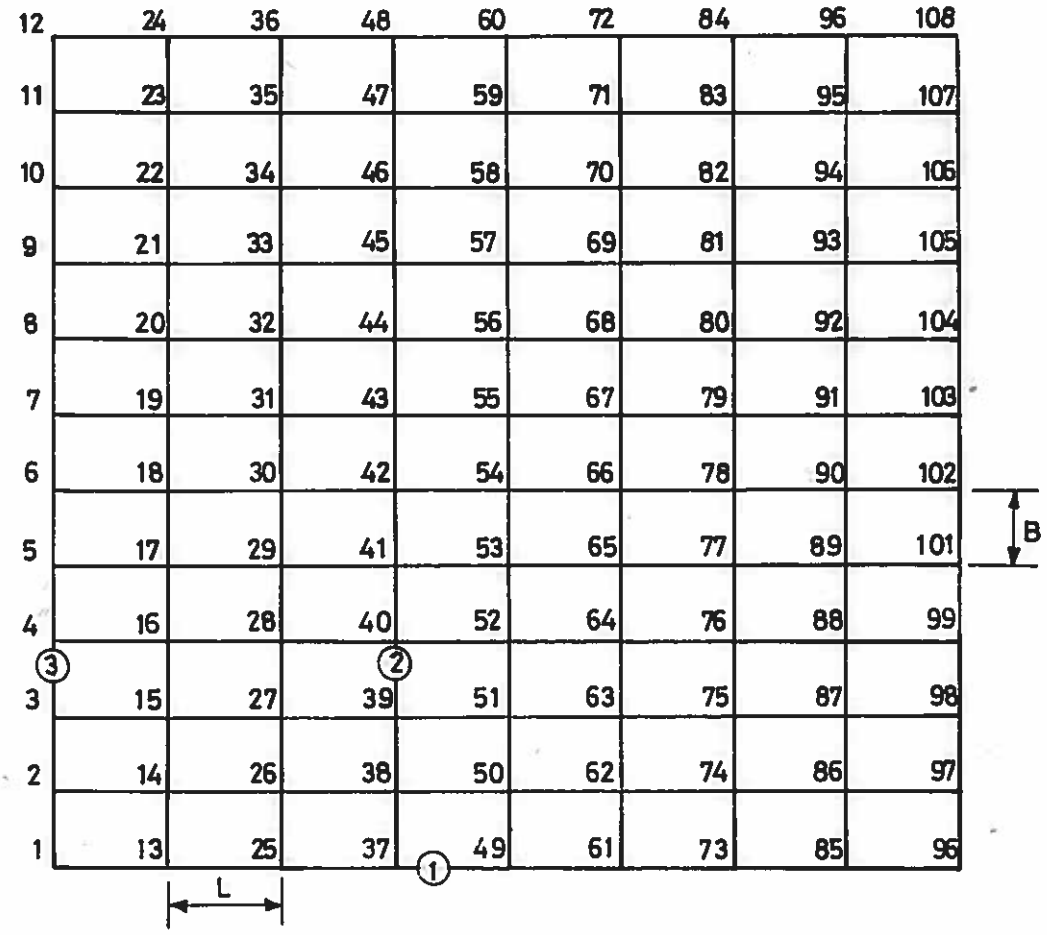

FIG. 5.6 Idealised Grillage for all 21 Beam Decks (For details see tables 5.1 and 5.2)

Fig.5.5
Fig.5.6

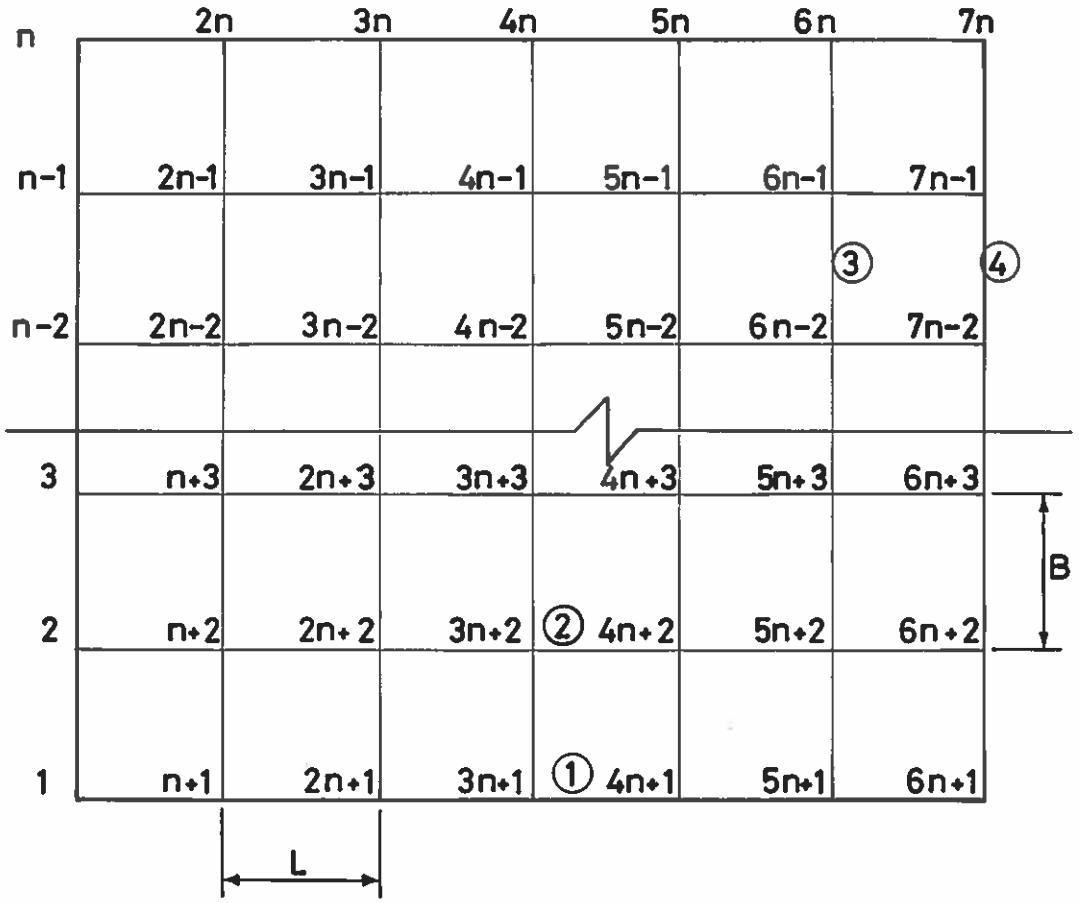

2 m Spacing

5 Beam decks; n = 5

7 Beam decks; n = 7

9 Beam decks; n = 9

11 Beam decks; n = 11

1·5m Spacing

7 Beam decks; n = 7

9 Beam decks; n = 9

11 Beam decks; n = 11

13 Beam decks; n = 13

15 Beam decks; n = 15

Fig 5.7 Idealised Grillage for All Decks with Beams Spaced at 1·5m & 2·0m Centres

(For details see tables 5.3 & 5.4)

Fig 5.7

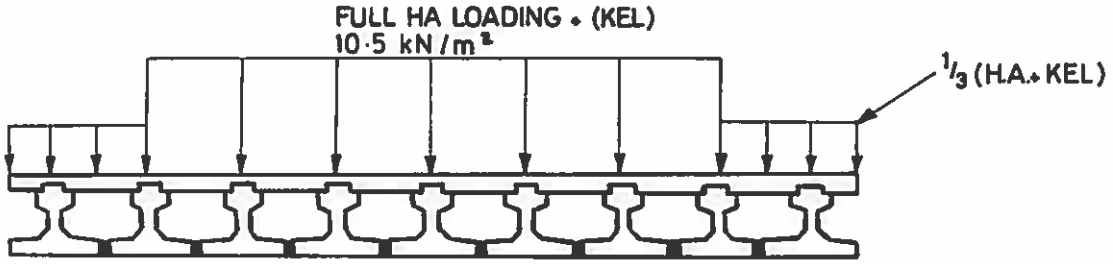

(a) 9 Beam Deck

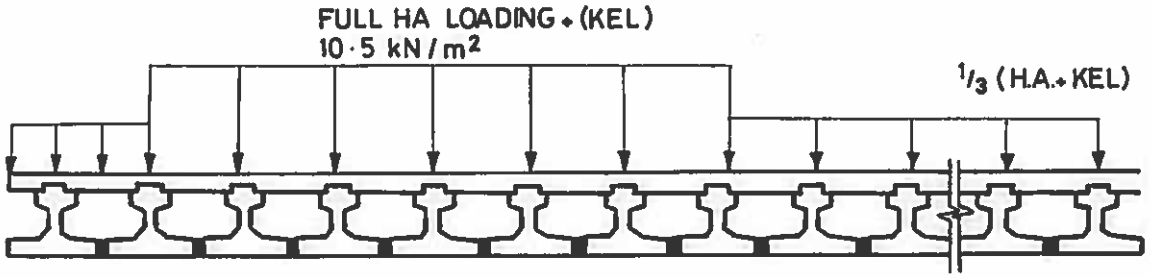

(b) 13 Beam Deck

Fig. 5.8 H.A. Loading for 9 & 13 Beam Decks
1m Spacing

Fig.5.8

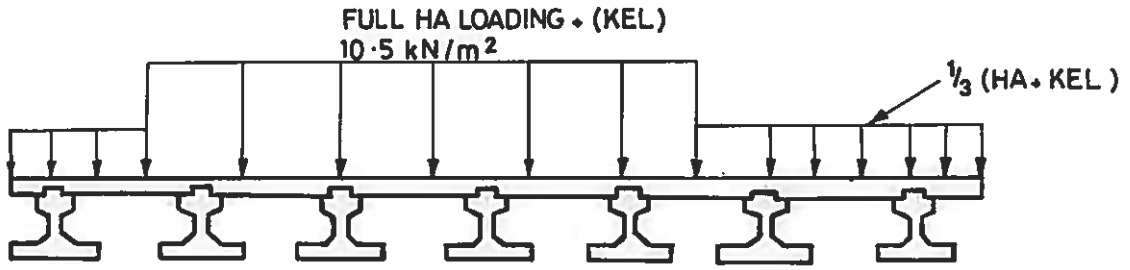

(a) 7 Beam Deck

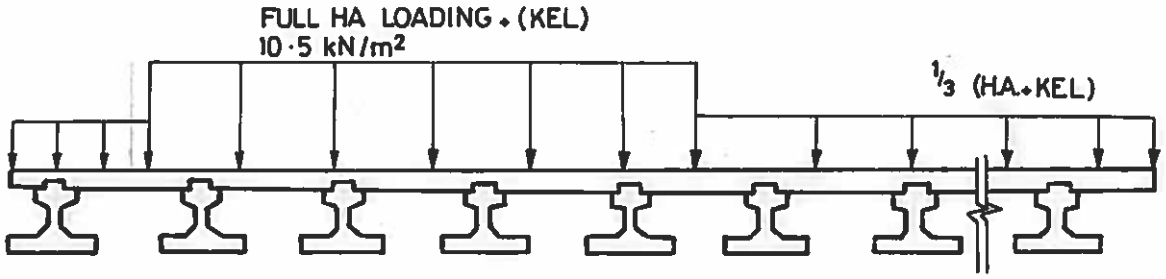

(b) 9 Beam Deck

Fig. 5.9 H.A. Loading for 7 & 9 Beam Decks
1·5 m Spacing

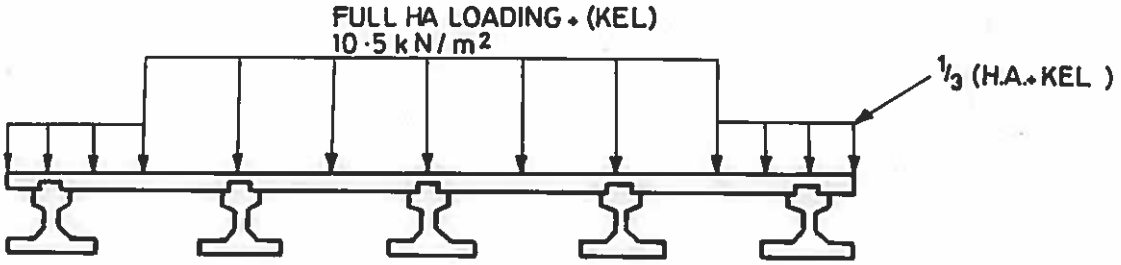

(a) 5 Beam Deck

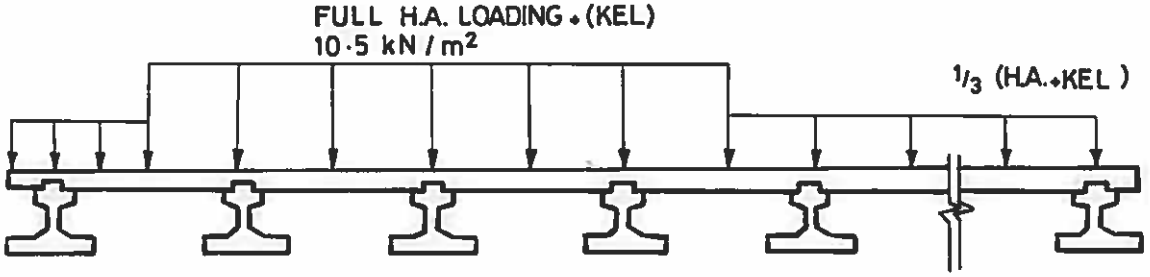

(b) 7 Beam Deck

Fig. 5.10 H.A. Loading for 5 & 7 Beam Decks
2 m Spacing

Fig.5.9
Fig.5.10

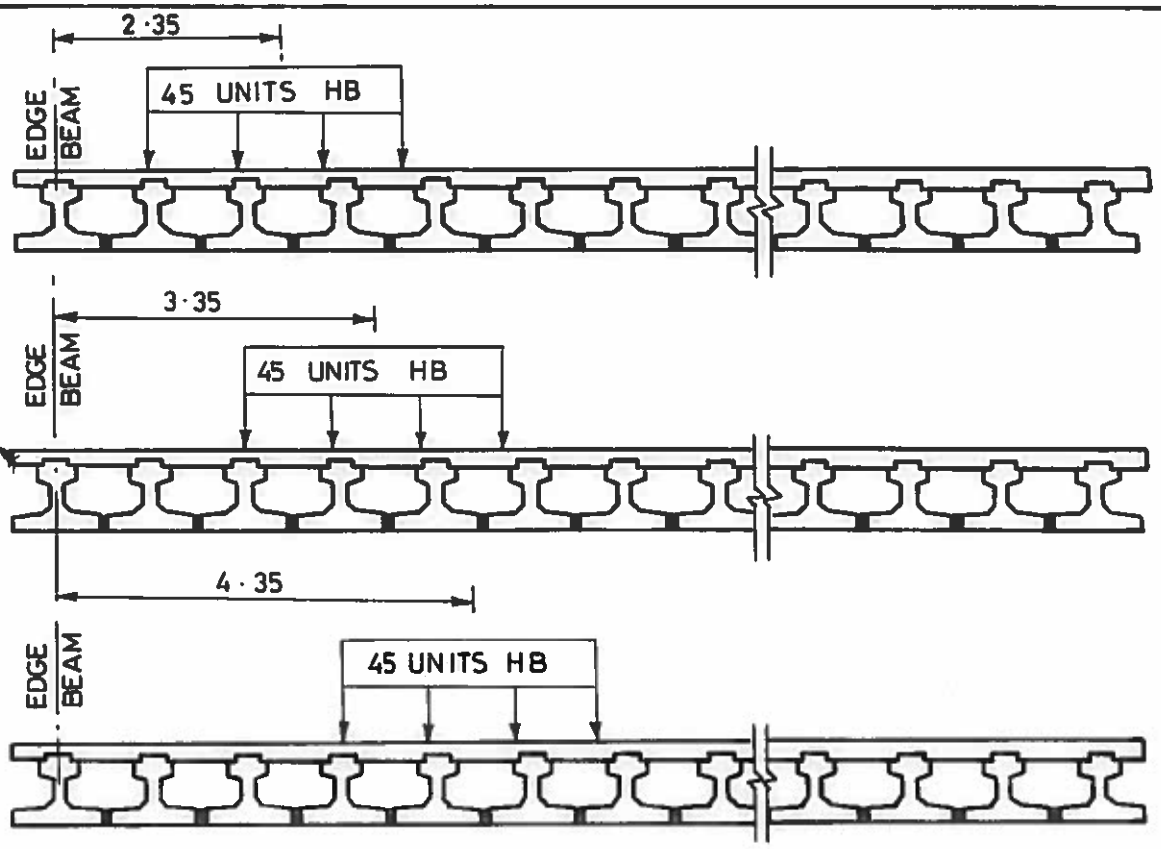

Fig 5.11 Cases for 45 Units Type HB Loading

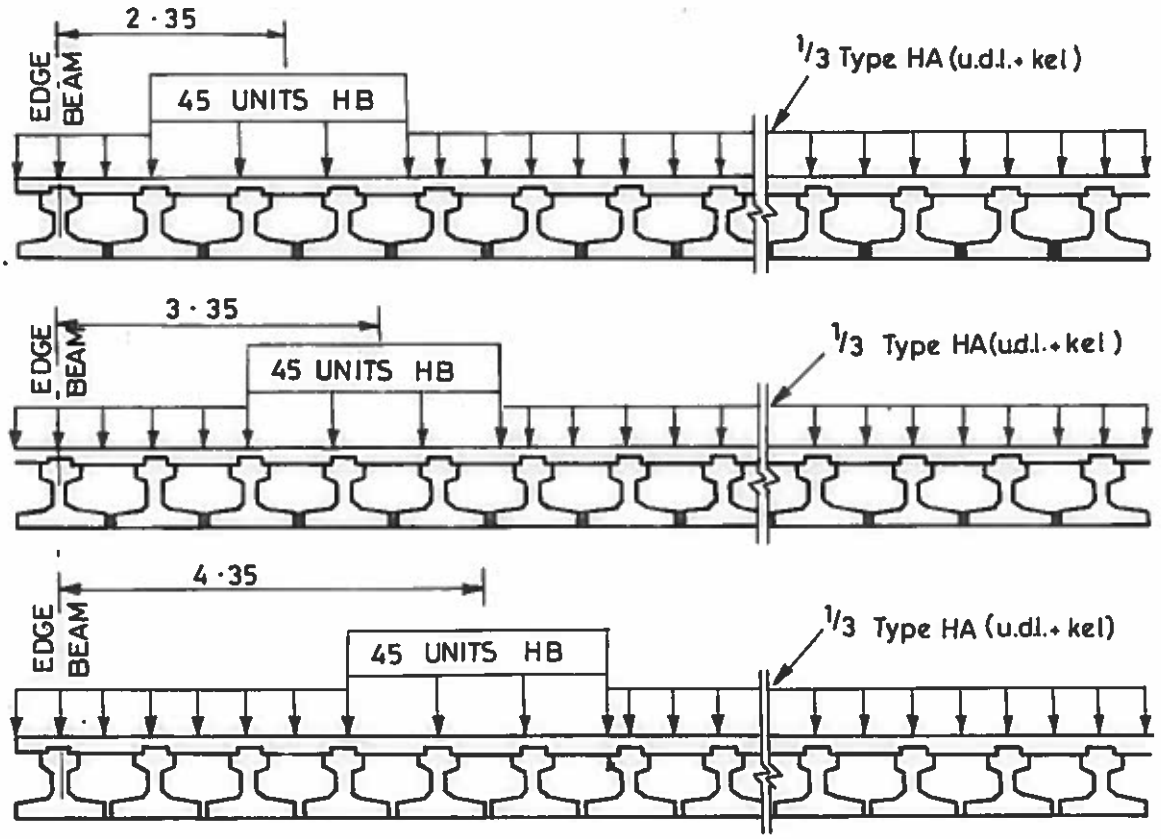

Fig 5.12 Cases for 45 Units Type HB Loading and 1/3 Type HA (u.d.l. + k.e.l.)

Fig 5.11
Fig 5.12

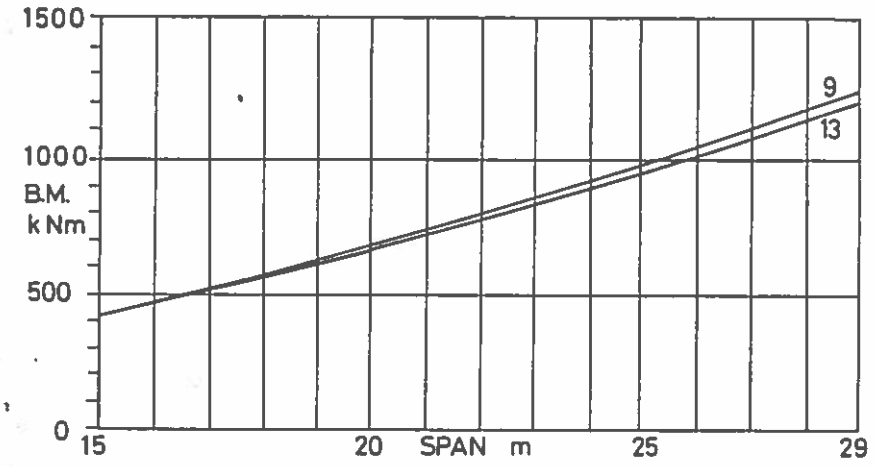

Fig. 5.13 Tee Beam Construction 1·0m Spacing

Maximum Bending Moment Per Beam

Type HA Loading

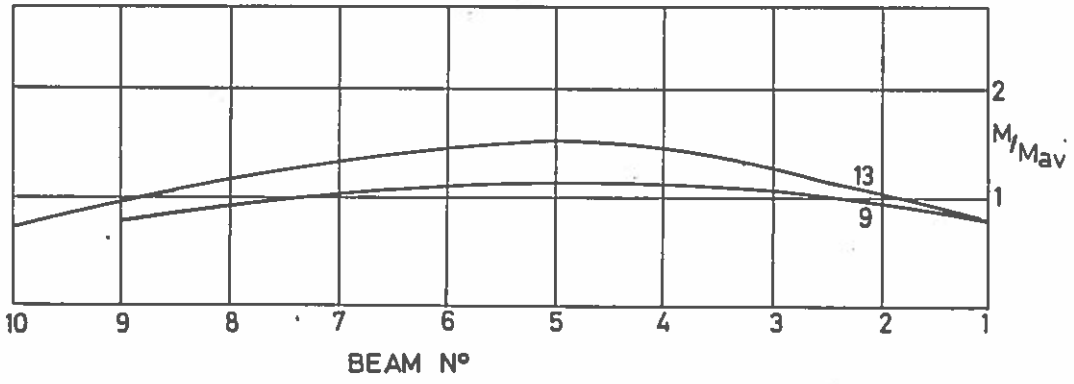

Fig. 5.14 Tee Beam Construction 1·0m Spacing

Transverse Distribution of Bending Moments

Type HA Loading

Fig.5.13
Fig.5.14

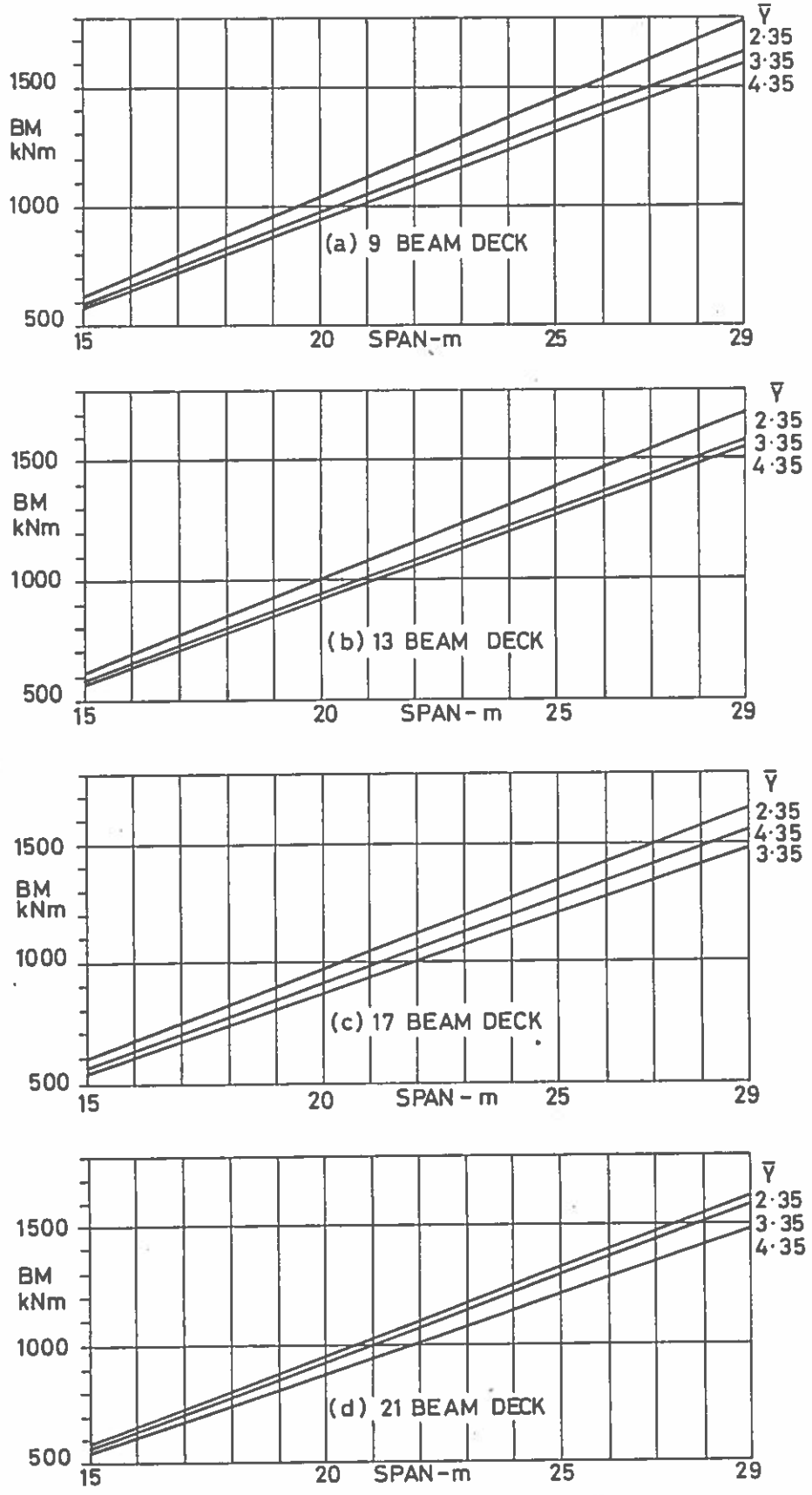

Fig. 5.15 Tee Beam Construction 1·0m Spacing

Maximum Bending Moment Per Beam

45 Units Type HB Loading

Fig.5.15

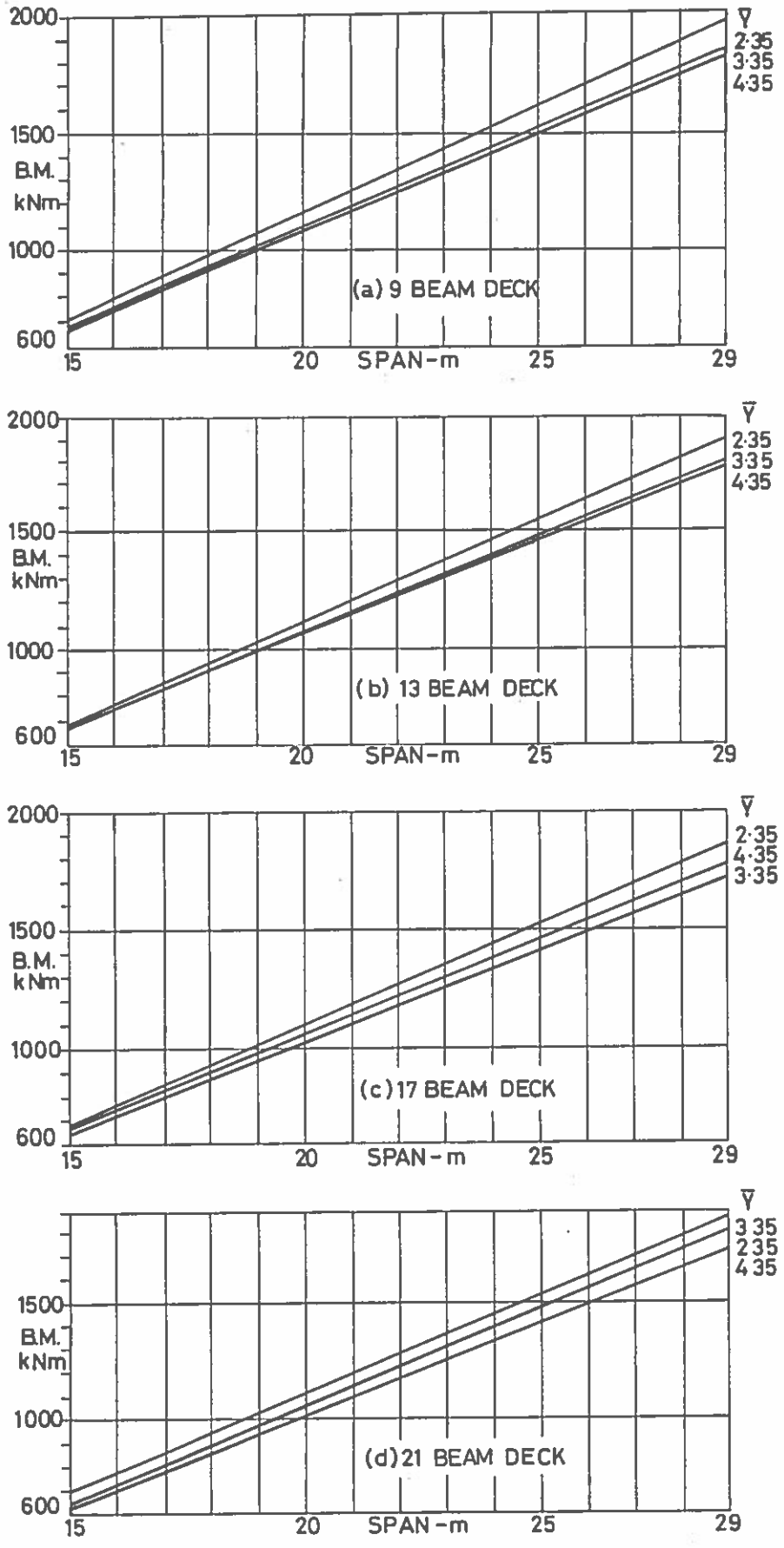

Fig. 5.16 Tee Beam Construction 1·0m Spacing

Maximum Bending Moment Per Beam

45 Units Type HB Loading + 1/3 HA

Fig.5.16

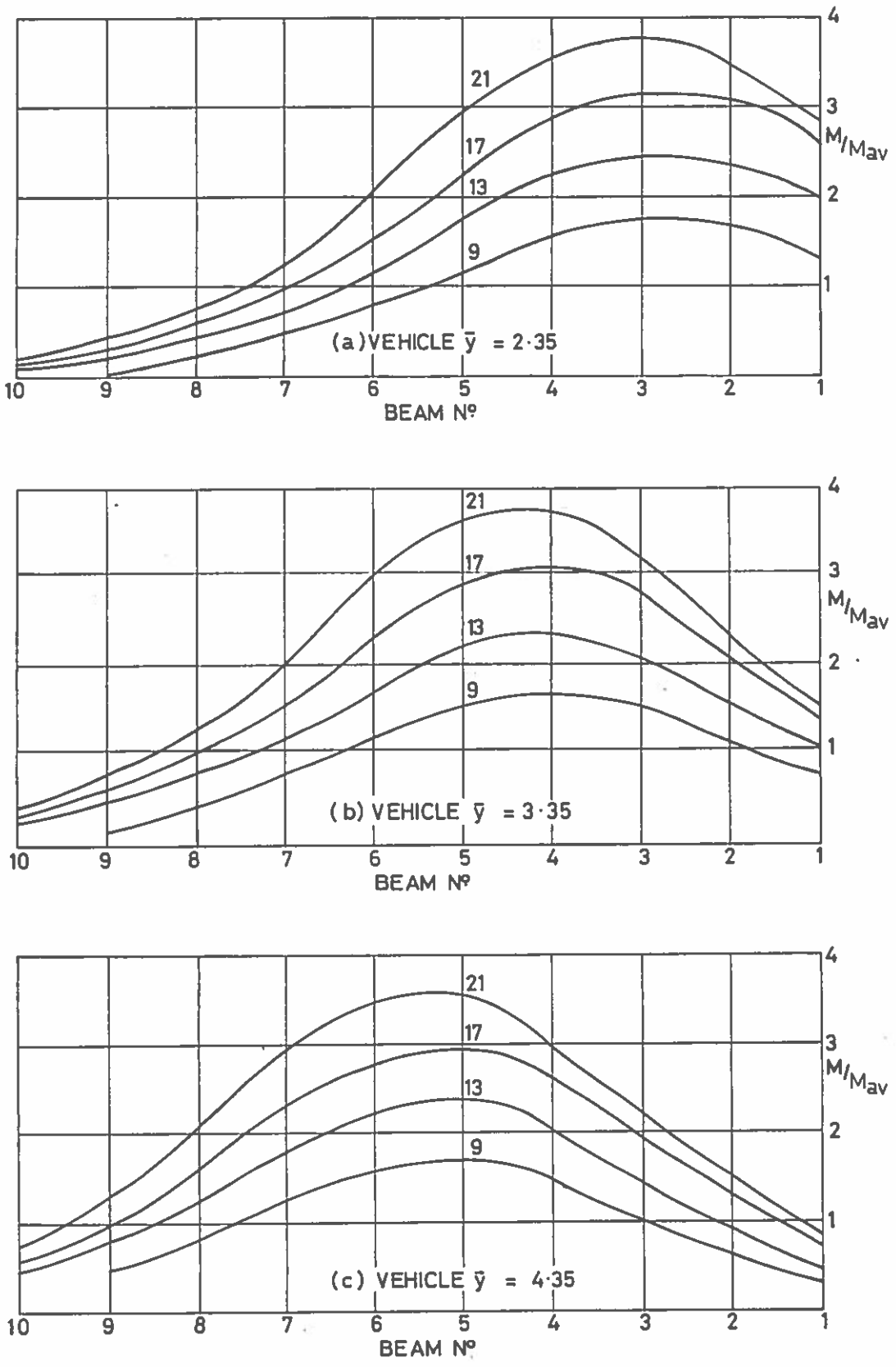

Fig. 5.17 **Tee Beam Construction 1·0m Spacing**

Transverse Distribution of Bending Moment

45 Units Type HB Loading

Fig.5.17

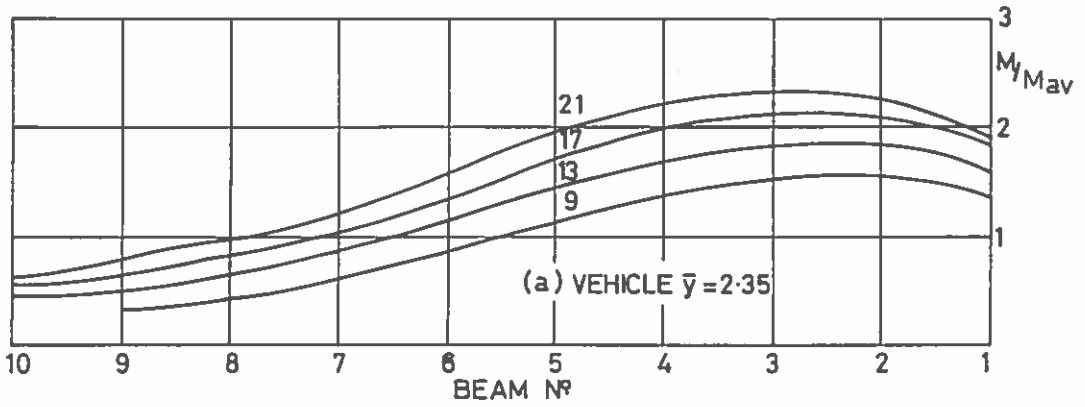

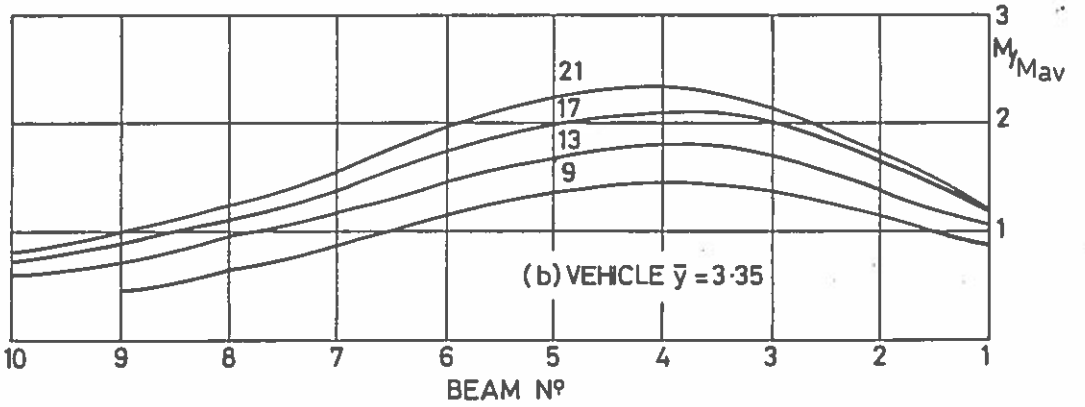

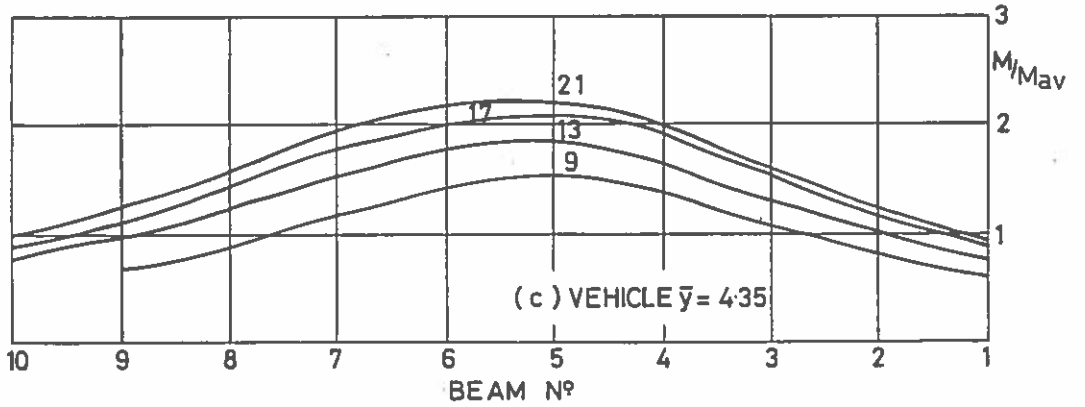

Fig. 5.18 Tee Beam Construction 1·0m Spacing

Transverse Distribution of Bending Moment

45 Units Type HB. Loading + 1/3 H.A.

Fig.5.18

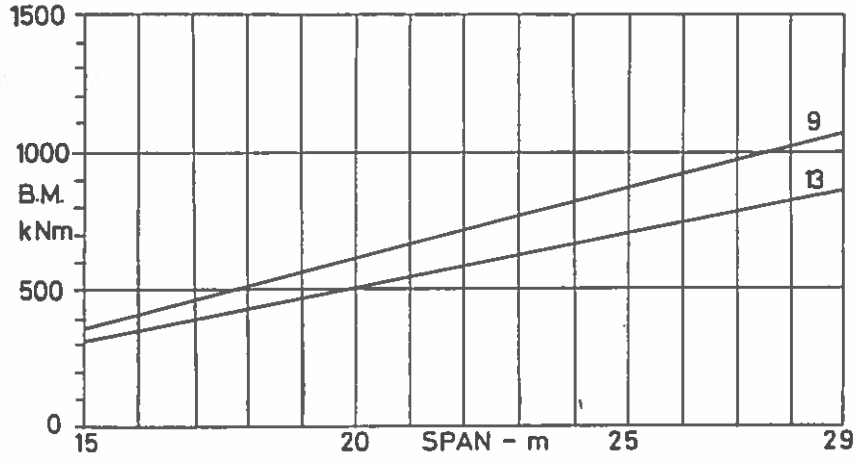

Fig. 5.19 Pseudo-Box Construction 1·0m Spacing

Maximum Bending Moment Per Beam

Type HA Loading

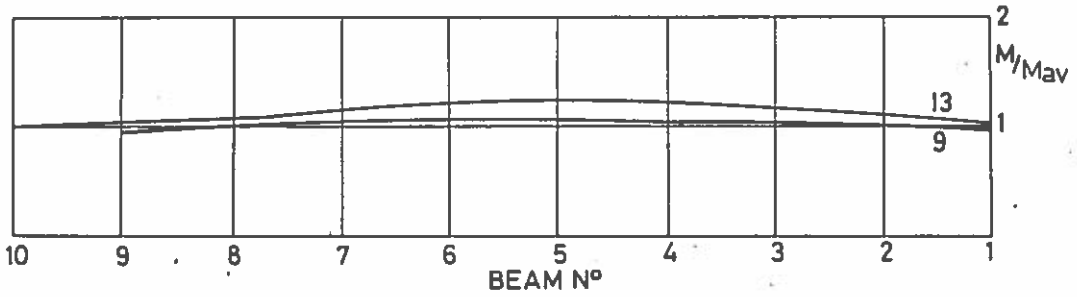

Fig. 5.20 Pseudo-Box Construction 1·0m Spacing

Transverse Distribution of Bending Moments

Type HA Loading

Fig.5.19

Fig.5.20

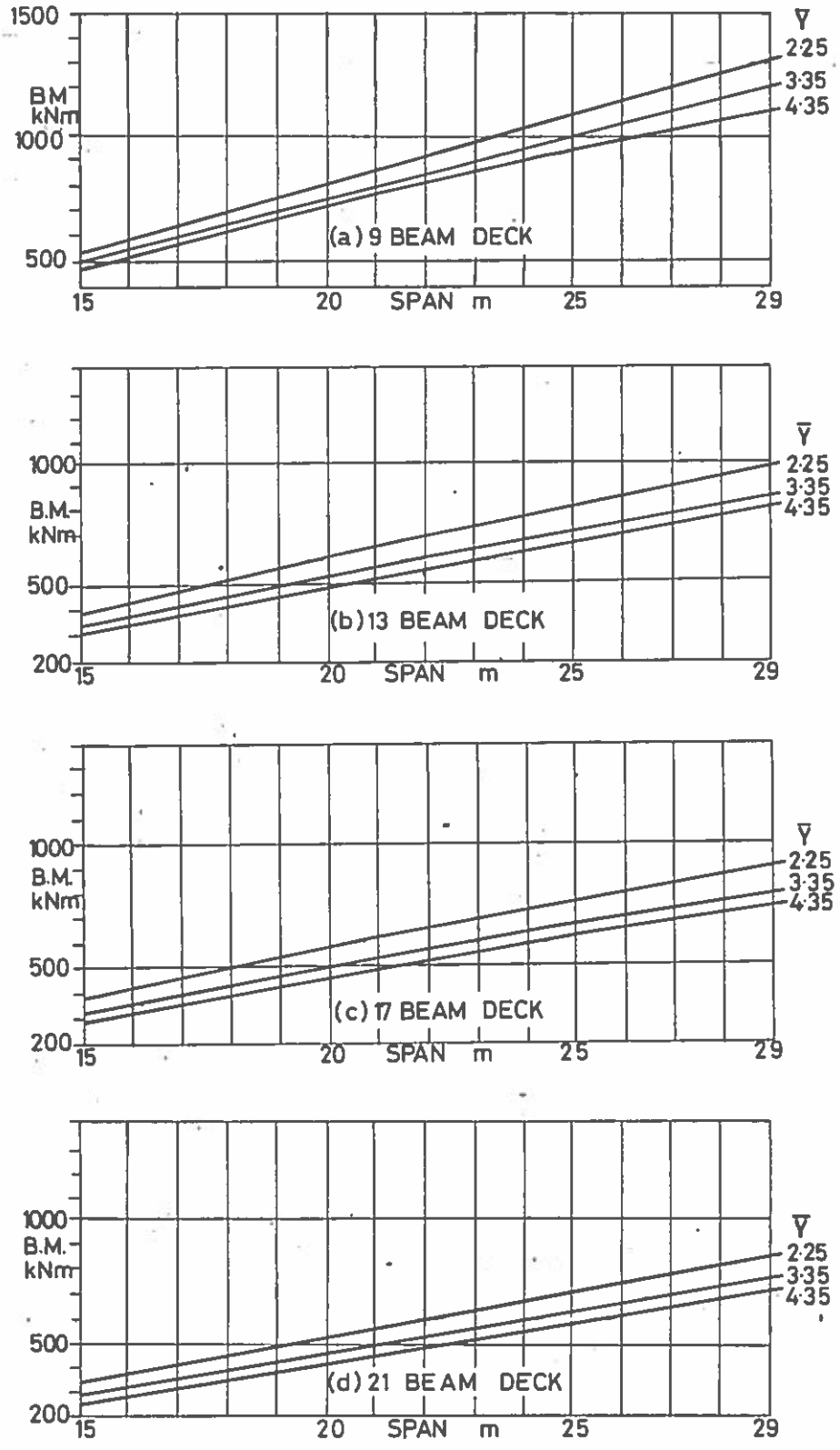

Fig. 5.21 Pseudo-Box Construction 1·0m Spacing

Maximum Bending Moment Per Beam

45 Units Type HB Loading

Fig.5.21

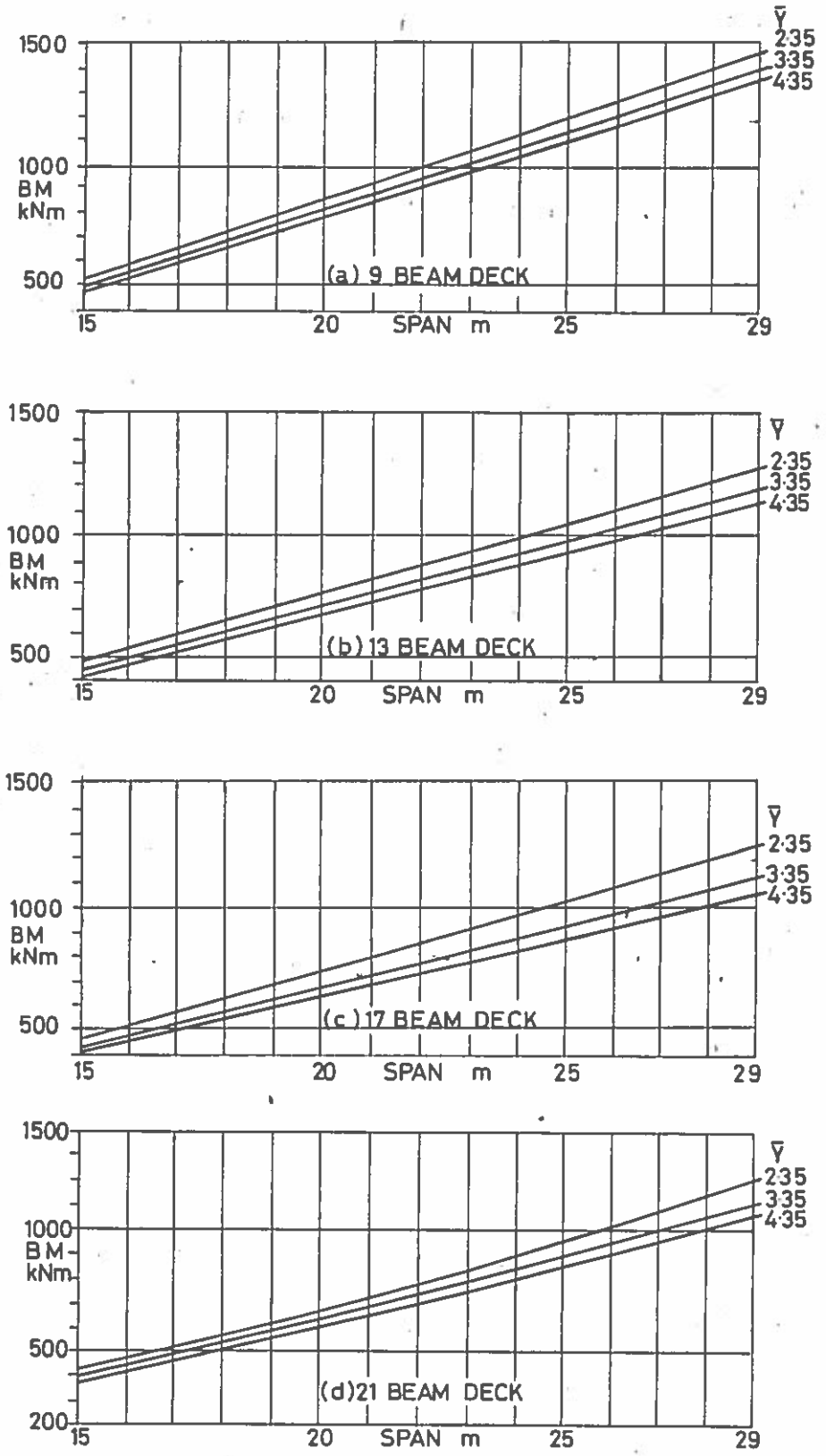

Fig. 5.22 Pseudo-Box Construction 1·0m Spacing

Maximum Bending Moment Per Beam

45 Units Type HB Loading + 1/3 HA

Fig.5.22

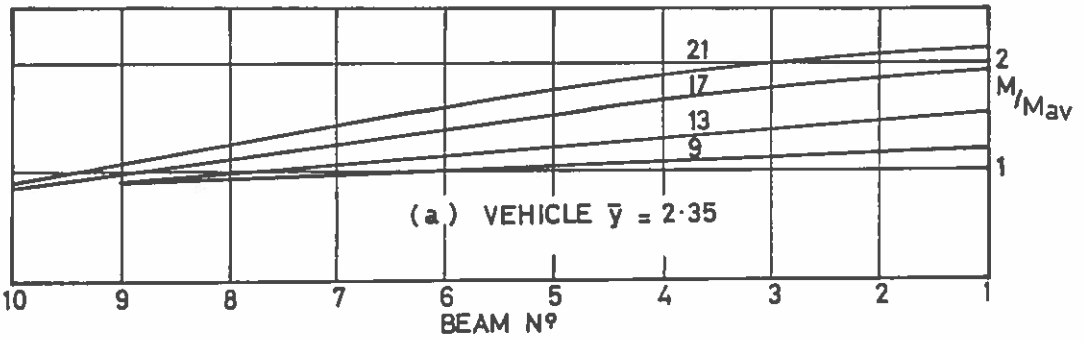

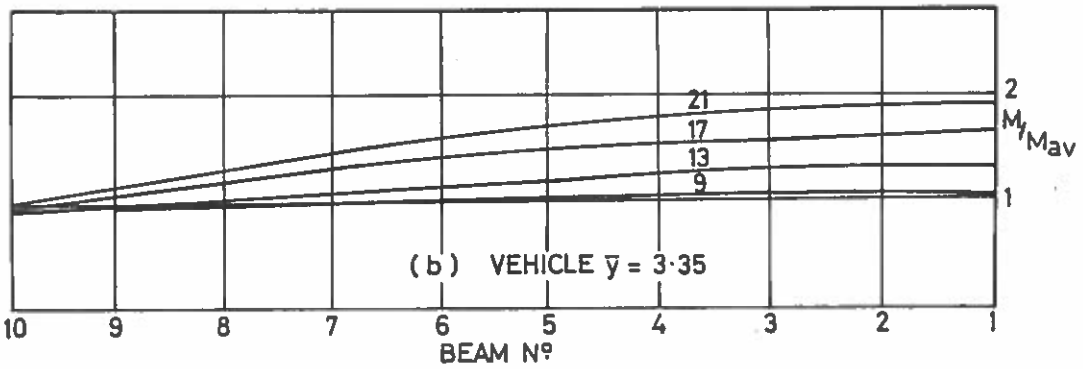

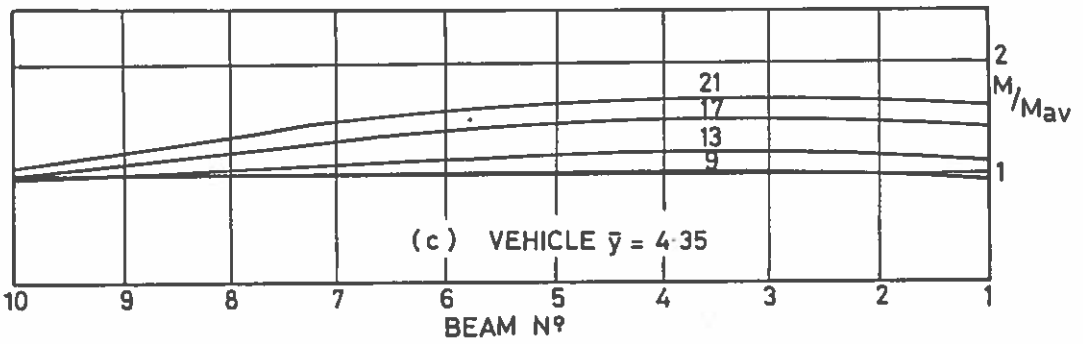

Fig. 5.23 Pseudo-Box Construction 1·0m Spacing

Transverse Distribution of Bending Moment

45 Units Type HB Loading

Fig.5.23

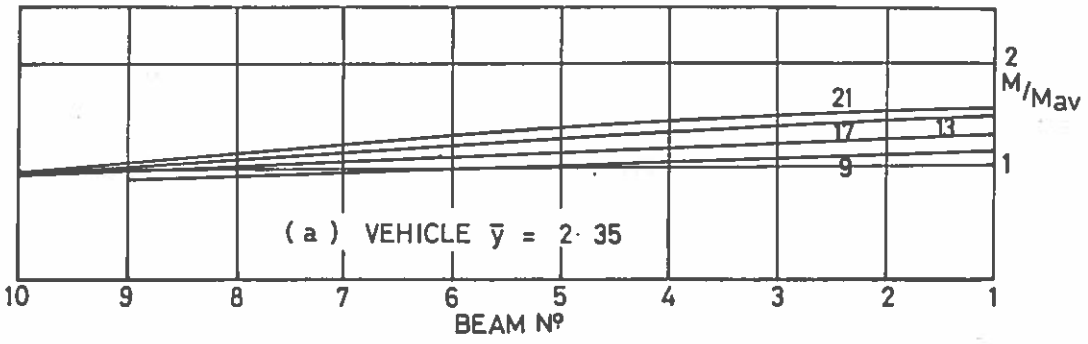

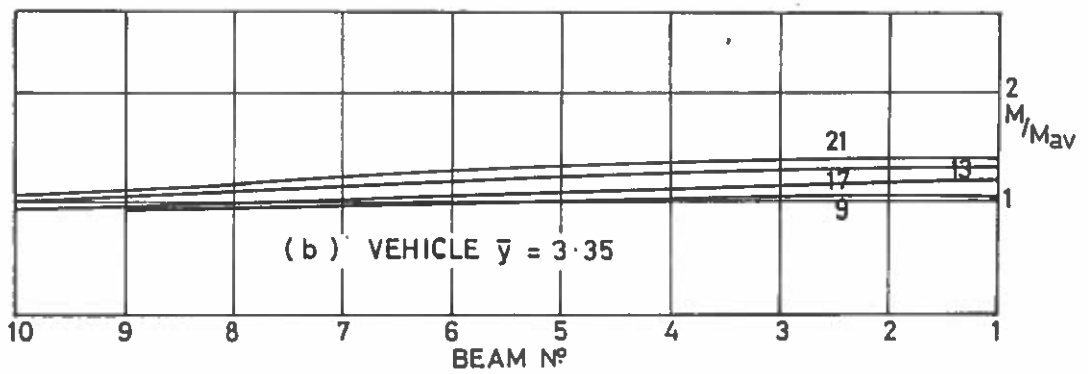

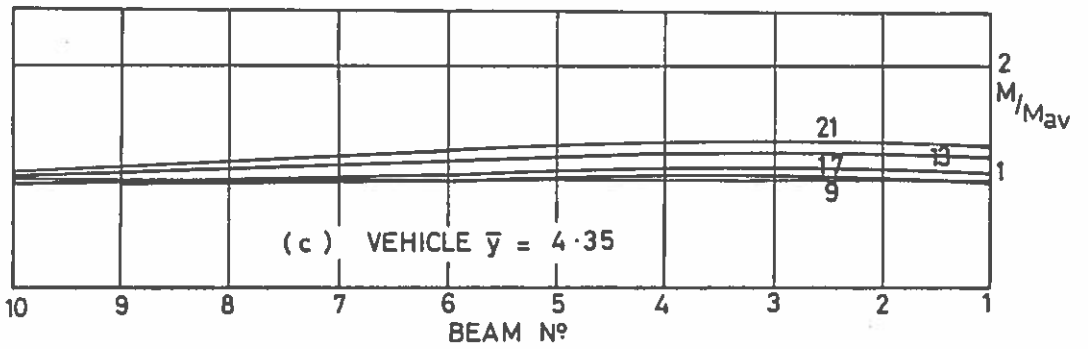

Fig. 5.24

Pseudo-Box Construction 1·0m Spacing

Transverse Distribution of Bending Moment

45 Units Type HB Loading + 1/3 H.A.

Fig.5.24

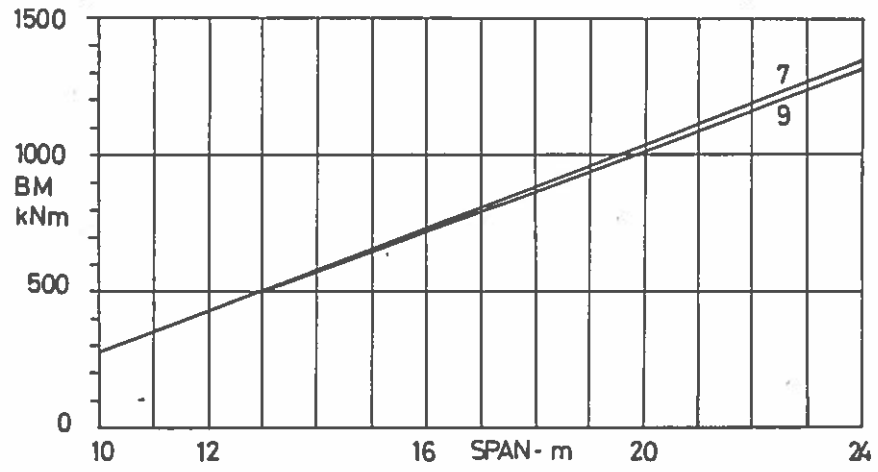

Fig. 5.25 Tee Beam Construction 1·5m Spacing

Maximum Bending Moment Per Beam

Type H A Loading

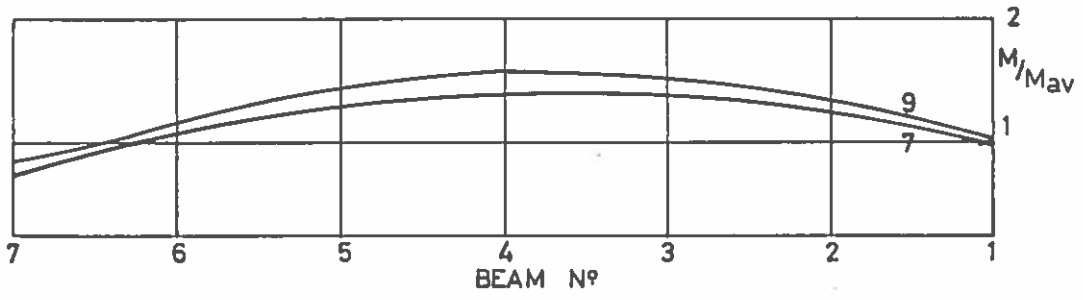

Fig. 5.26 Tee Beam Construction 1·5m Spacing

Transverse Distribution of Bending Moments

Type HA Loading

Fig.5.25
Fig.5.26

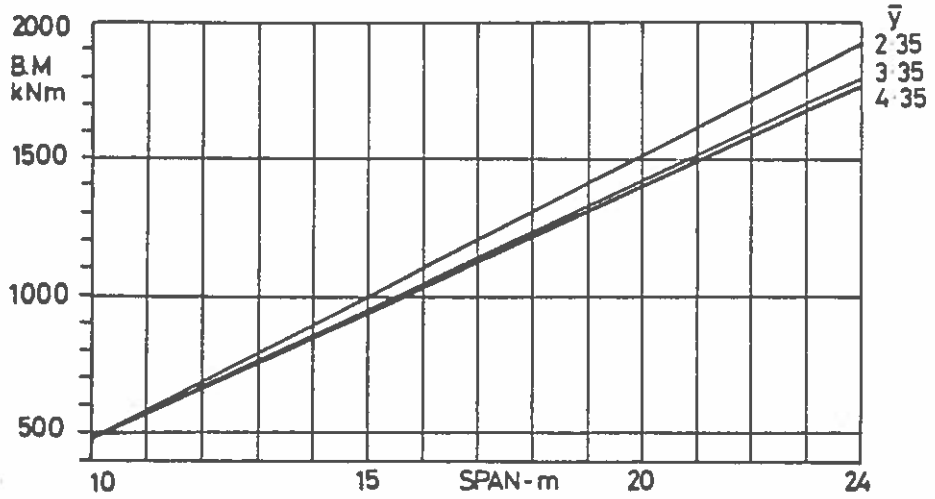

Fig. 5.27 Tee Beam Construction 1·5m Spacing
45 Units Type HB Loading
Maximum Bending Moment Per Beam

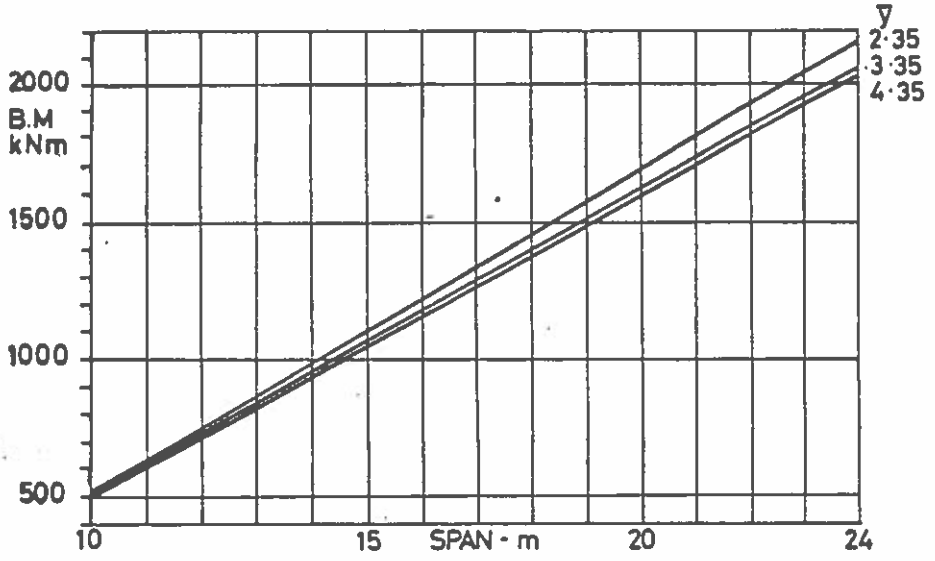

Fig. 5.28 Tee Beam Construction 1·5m Spacing
45 Units Type HB Loading + 1/3 HA
Maximum Bending Moment Per Beam

Fig.5.27
Fig.5.28

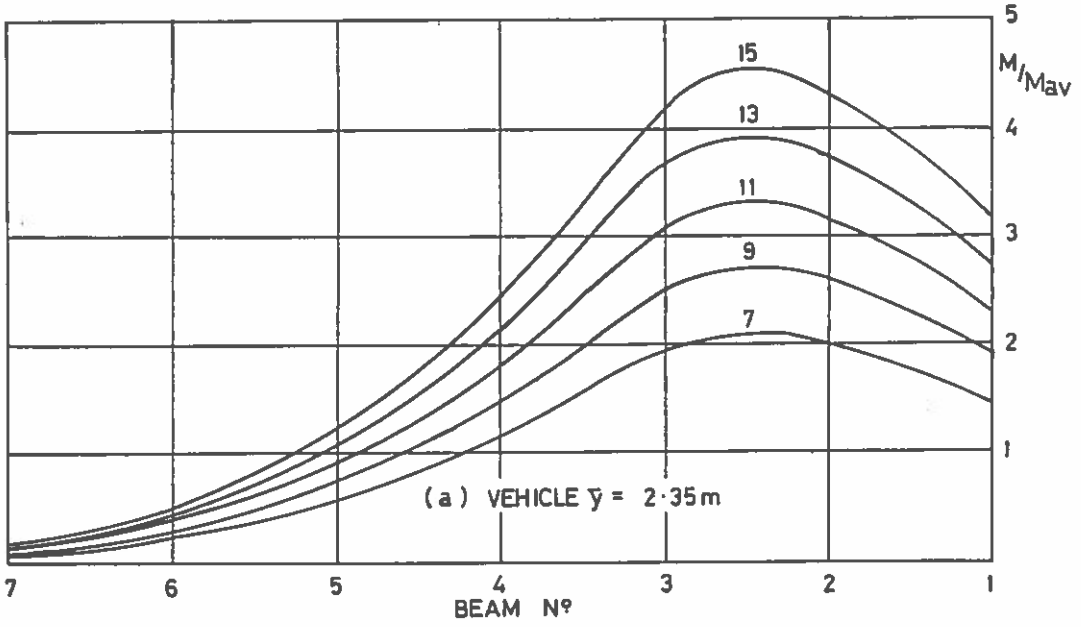

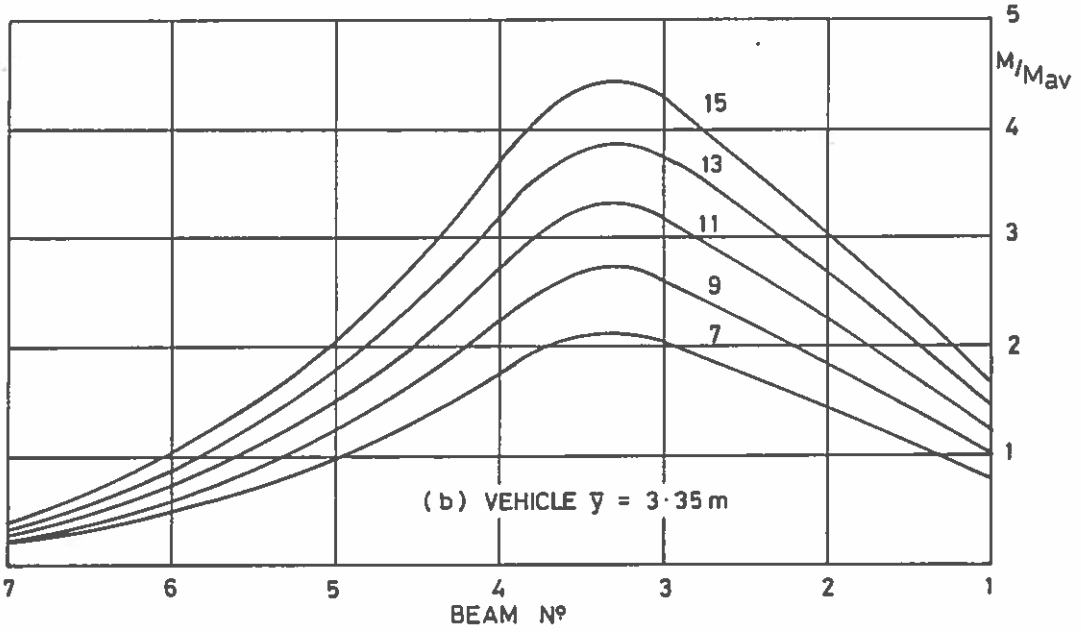

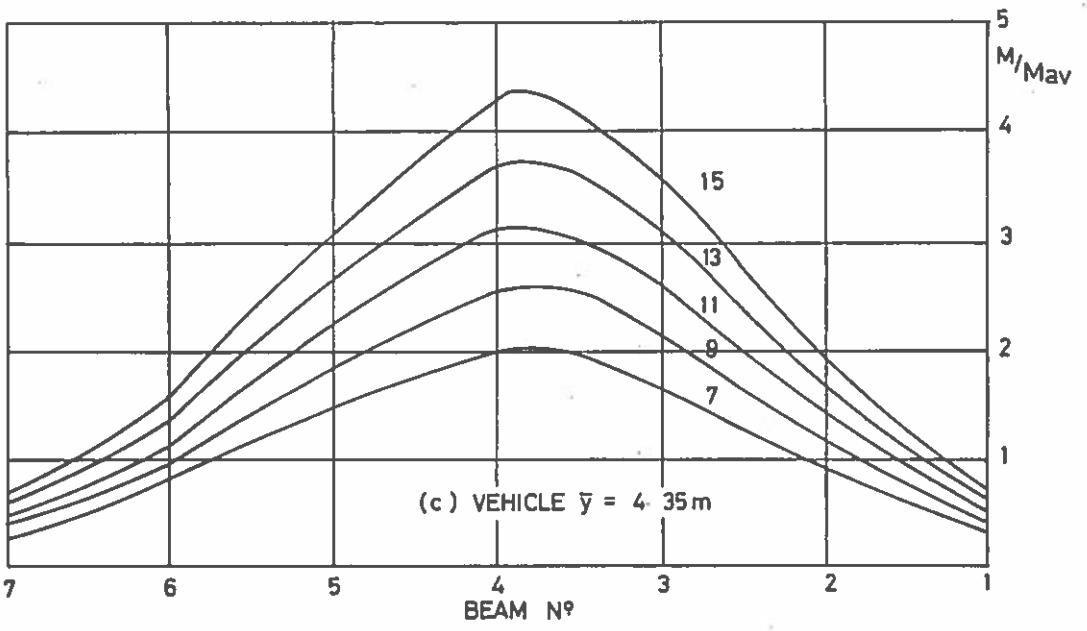

Fig. 5.29 Tee Beam Construction 1·5m Spacing
Transverse Distribution of Bending Moments
45 Units Type HB Loading

Fig.5.29

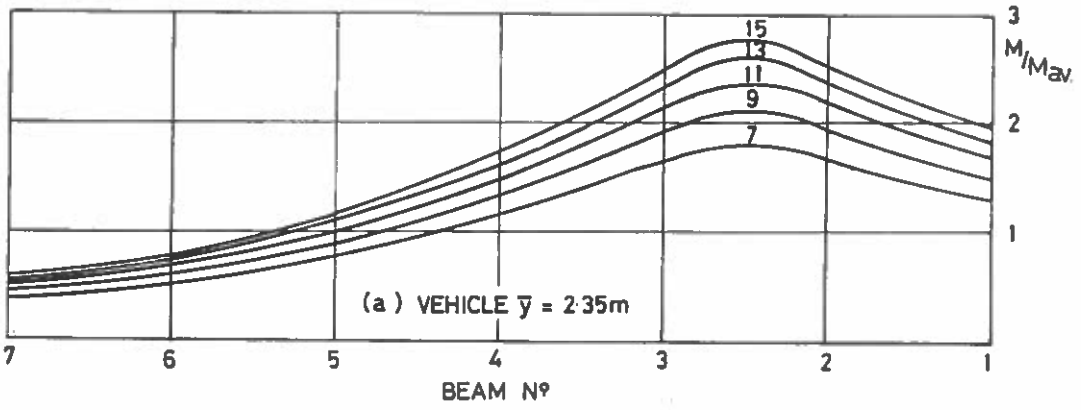

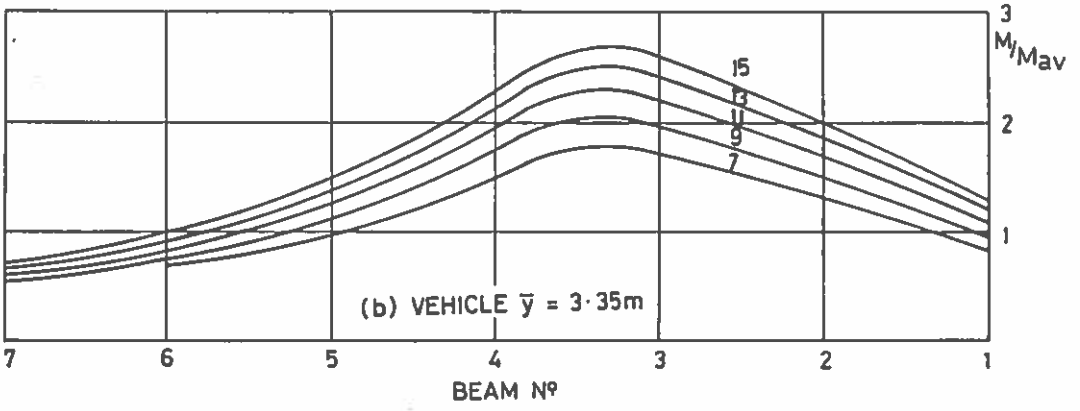

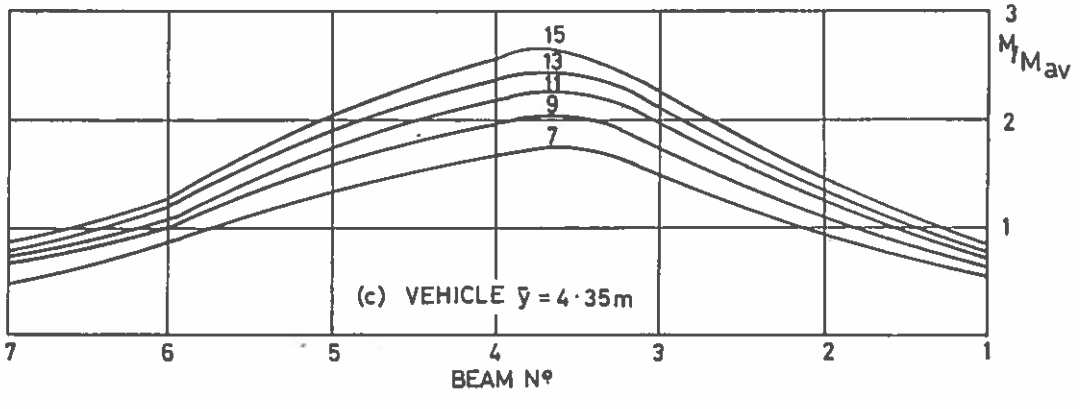

Fig. 5.30 Tee Beam Construction 1·5 Spacing

Transverse Distribution of Bending Moments

45 Units Type HB Loading + ⅓HA

Fig.5.30

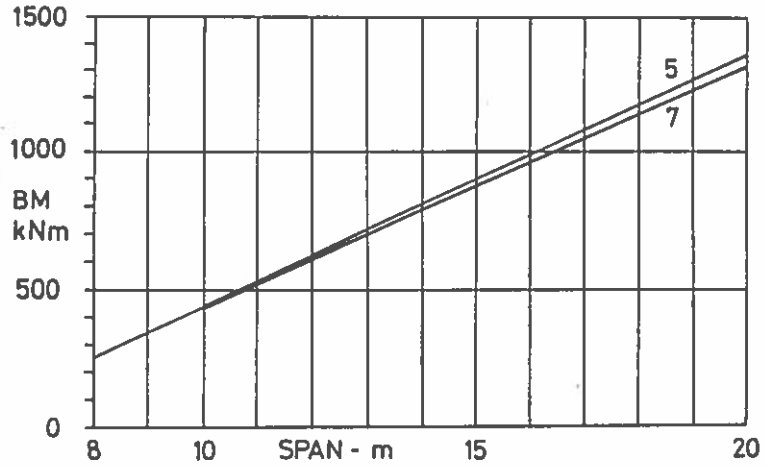

Fig. 5.31 **Tee Beam Construction 2·0m Spacing**

Maximum Bending Moment Per Beam

Type HA Loading

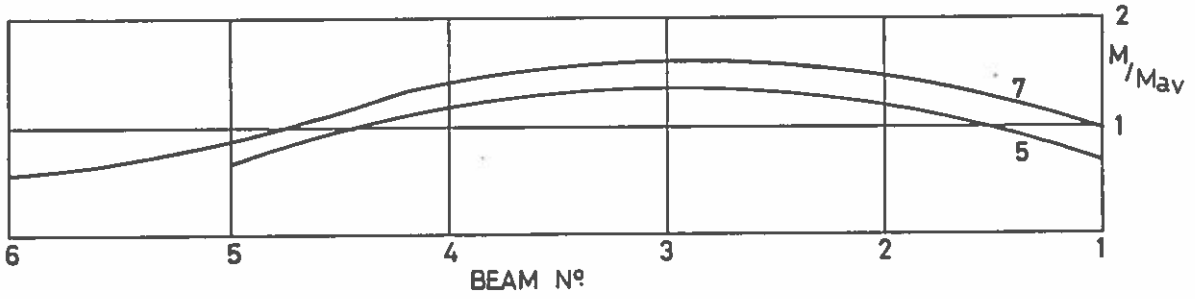

Fig. 5.32 **Tee Beam Construction 2·0m Spacing**

Transverse Distribution of Bending Moments

Type HA Loading

Fig.5.31
Fig.5.32

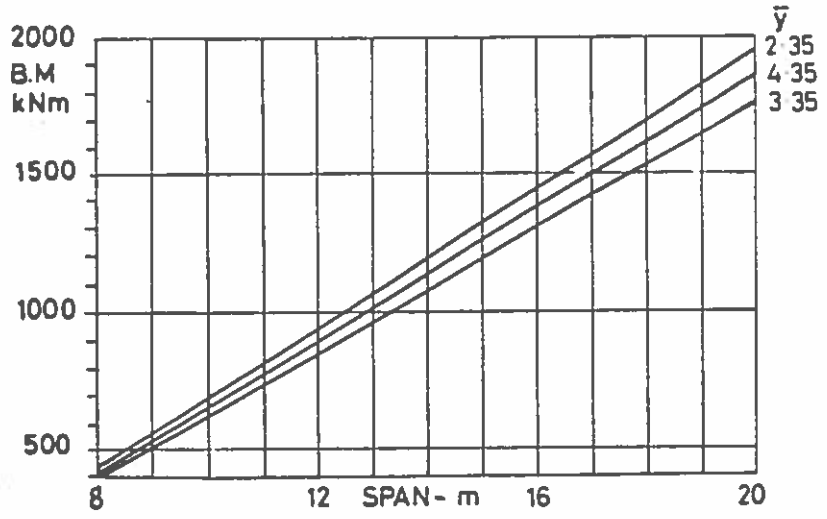

Fig. 5.33 Tee Beam Construction 2·0m Spacing
45 Units Type HB Loading
Maximum Bending Moment Per Beam

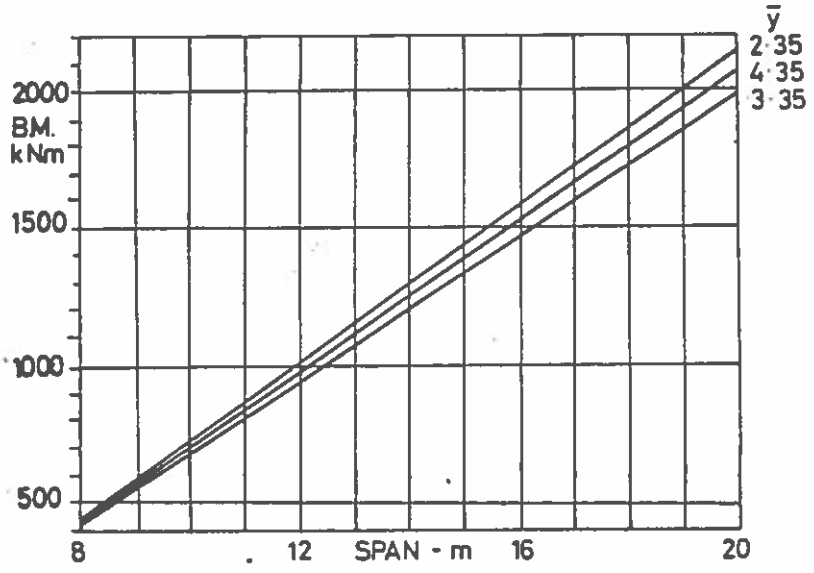

Fig. 5.34 Tee Beam Construction 2·0m Spacing
45 Units Type HB Loading + ⅓ HA
Maximum Bending Moment Per Beam

Fig. 5.33
Fig. 5.34

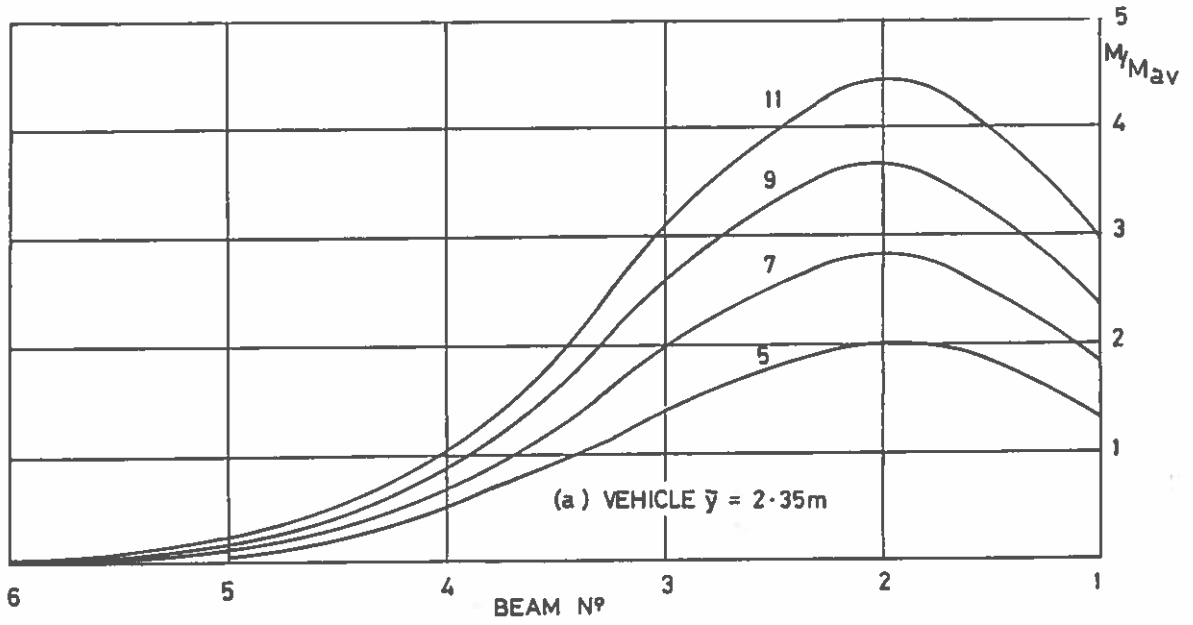

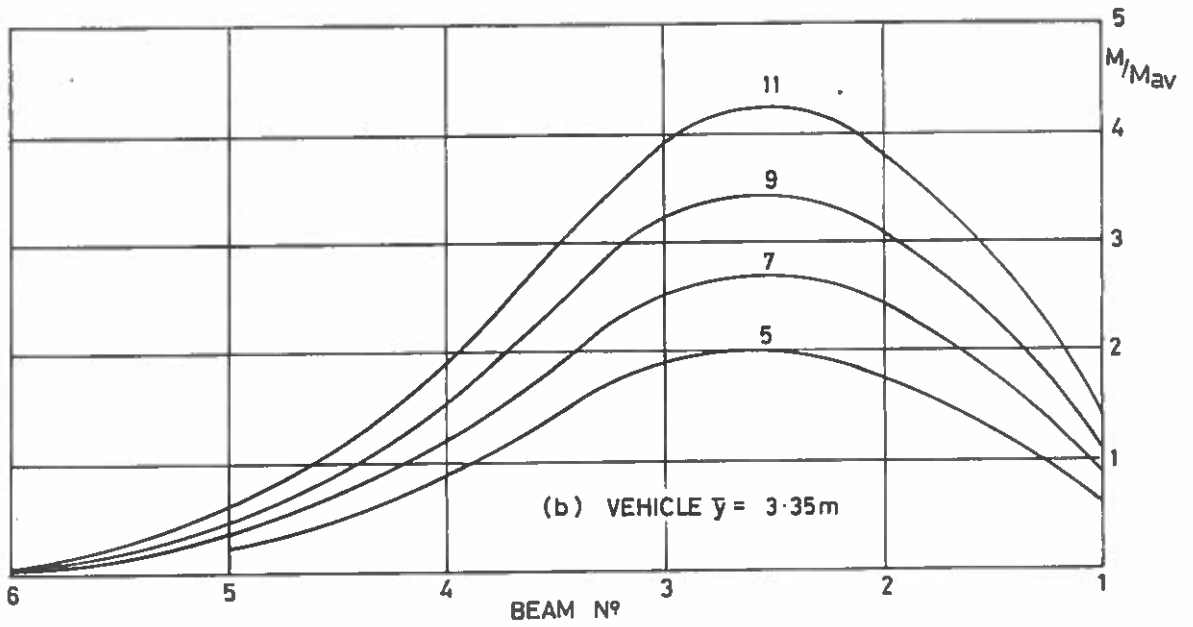

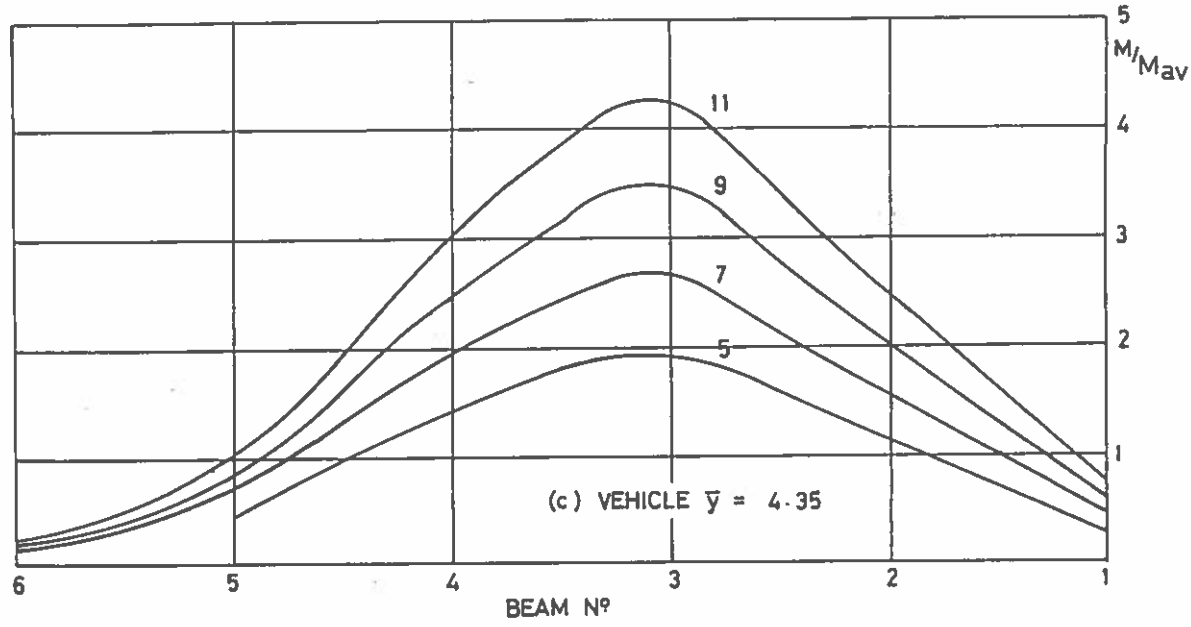

Fig. 5.35 Tee Beam Construction 2·0m Spacing
Transverse Distribution of Bending Moments
45 Units Type HB Loading

Fig.535

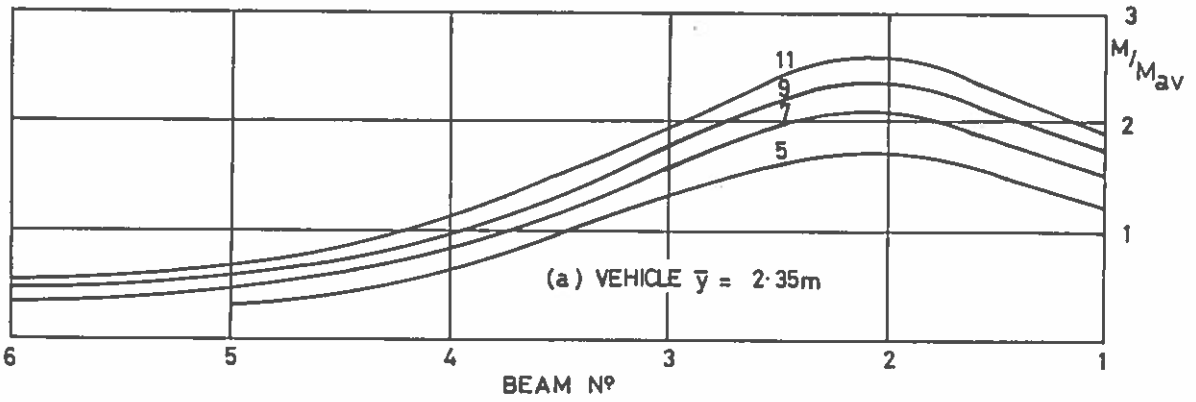

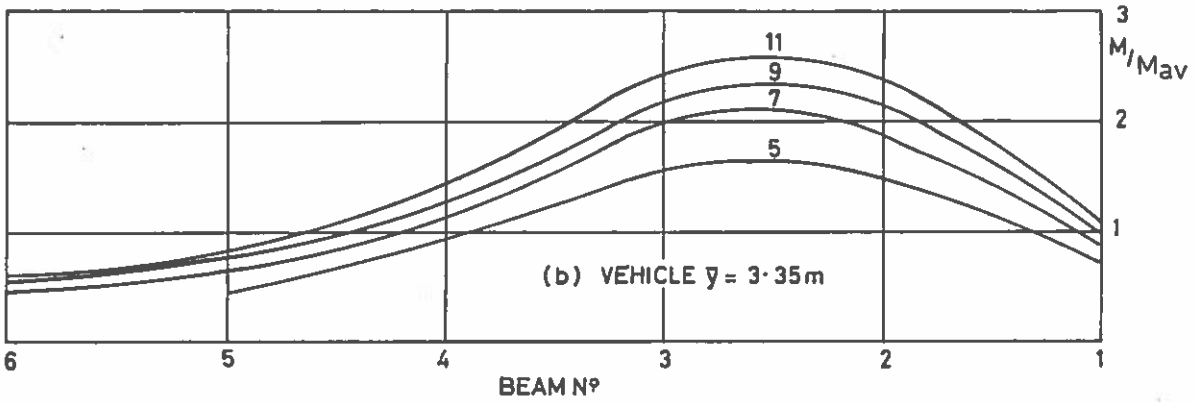

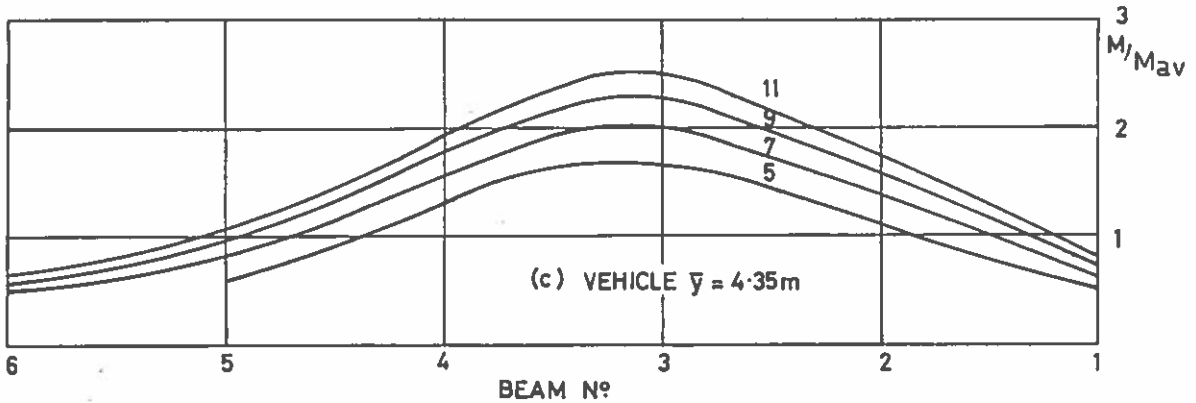

Fig. 5.36 Tee Beam Construction 2·0 Spacing

Transverse Distribution of Bending Moments

45 Units Type HB Loading + 1/3 HA

Fig.5.36

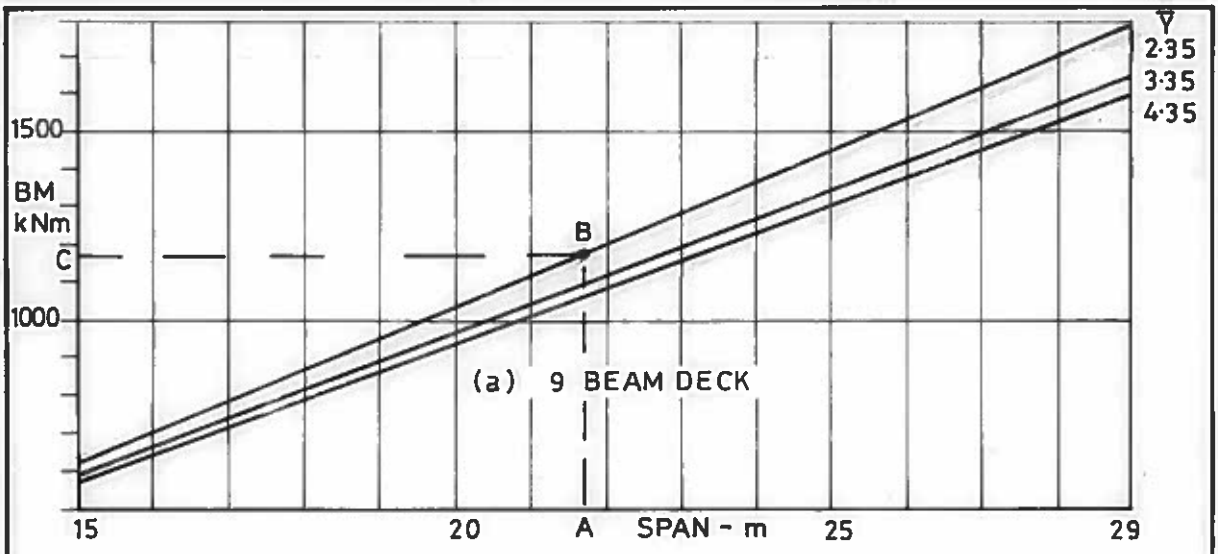

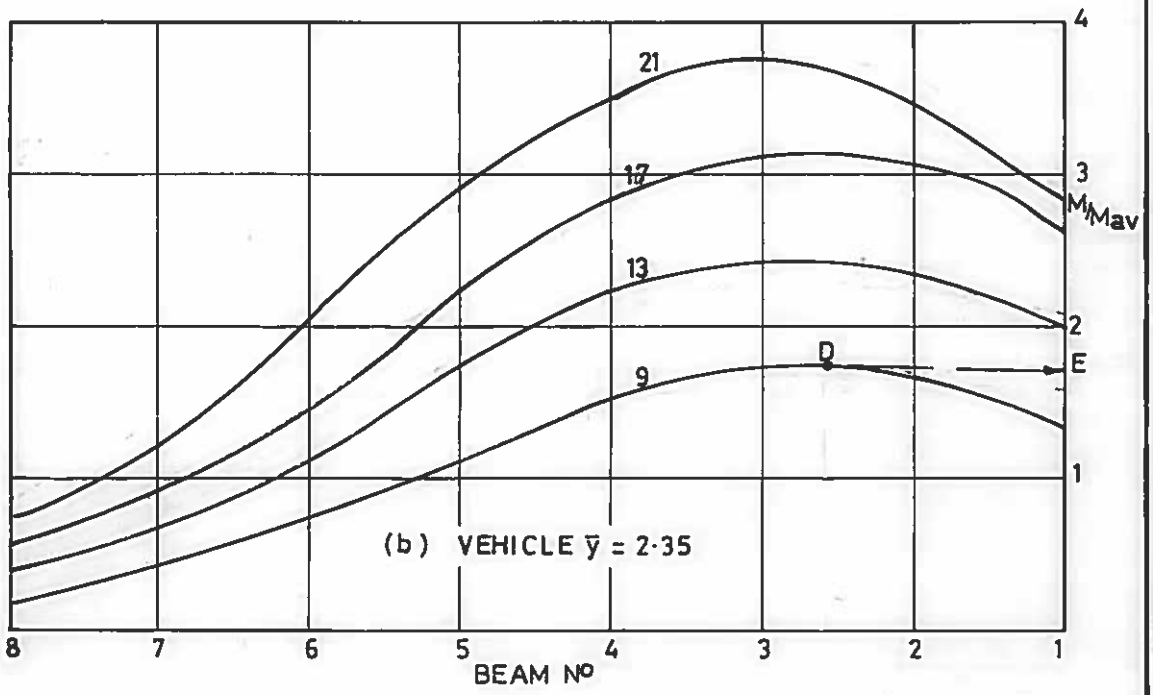

1. FOR BRIDGE DECK SPAN= 21·75m, 9 BEAMS WIDE AND HB VEHICLE $\bar{y}$ = 2·35
2. FROM BM CURVE SPAN=21·75m (A) READ Mmax (B)=1170 kNm (C)
3. FROM TRANSVERSE DISTRIBUTION CURVE FOR 9 BEAM DECK READ M_{max}/M_{av} (D) = 1·75 (E)
4. WITH Mmax = 1170 AND M_{max}/M_{av} =1·75 $\therefore M_{av} = {}^{1170}/_{1·75} = 668·6$ kNm
5. FROM 9 BEAM CURVE READ M/M_{av} AT EACH BEAM AND CALCULATE M BEAM

BEAM Nº	7	6	5	4	3	2	1
M/Mav	·4	·75	1·15	1·5	1·75	1·70	1·35
with Mav 668·6 M BEAM	267	501	769	1003	1170	1136	902

Fig 5.37 Example In The Use Of Design Charts

Fig5.37

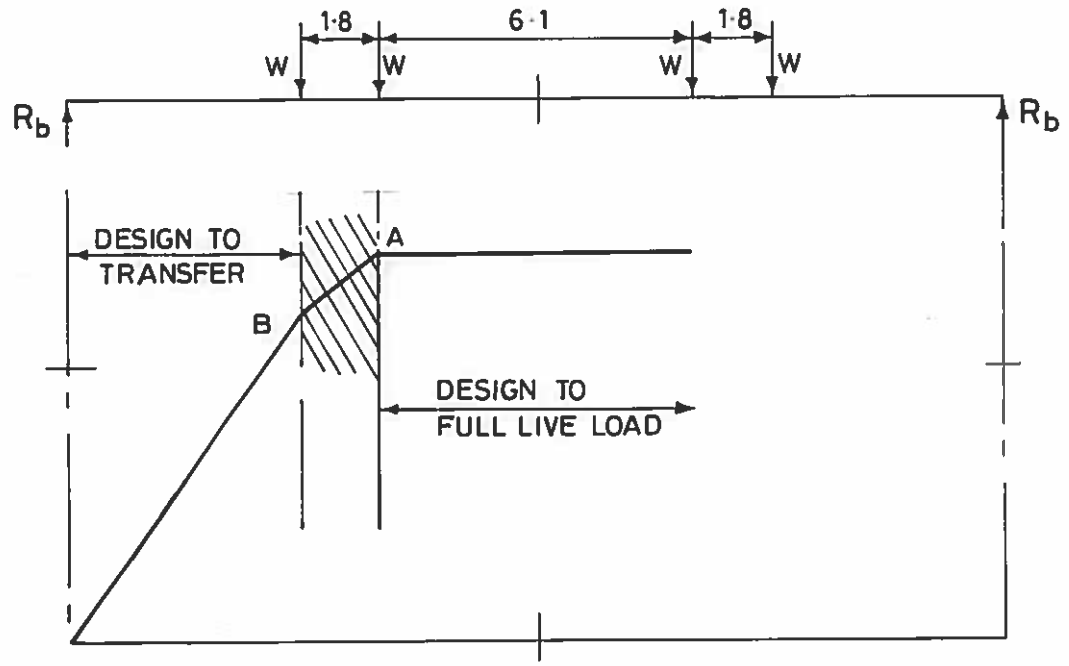

Fig. 5.38 Idealised Envelope of Bending Moment For Standard Highway Loading Type HB and HB + 1/3 HA

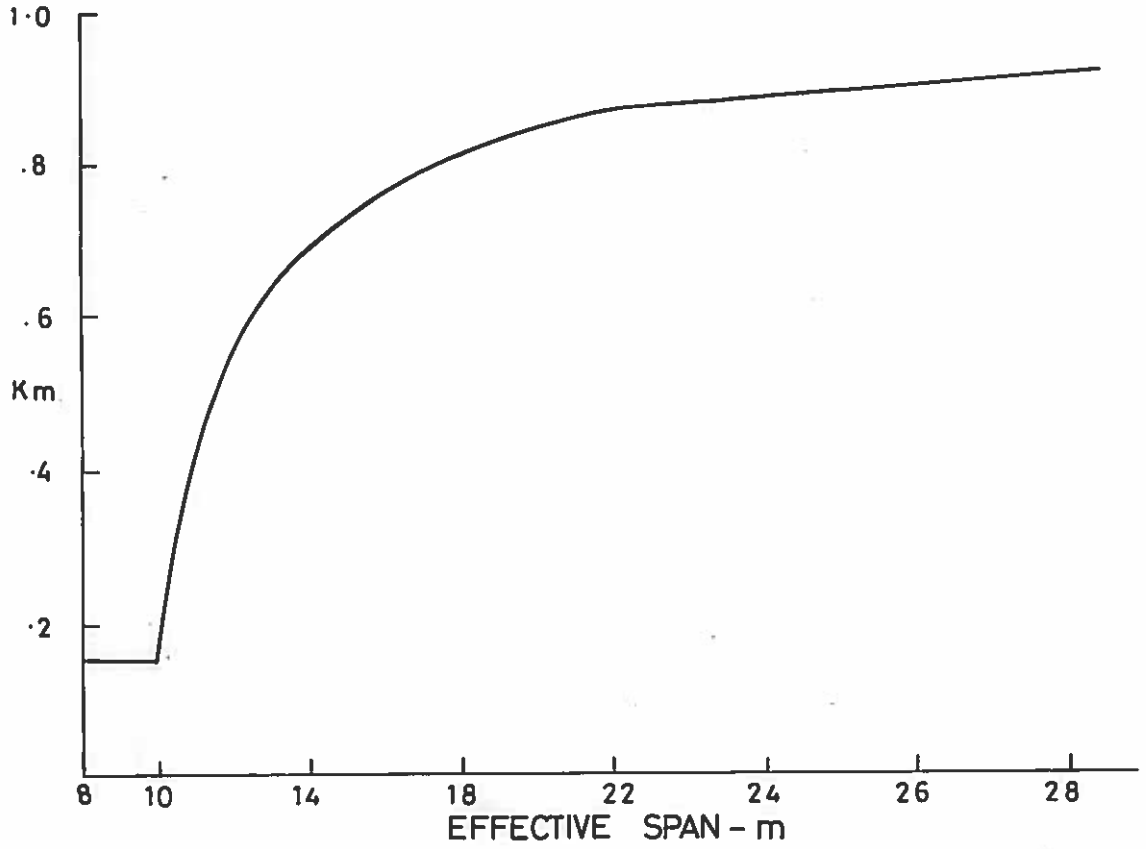

Fig. 5.39 Bending Moment Coefficent Km

Fig.5.38
Fig.5.39

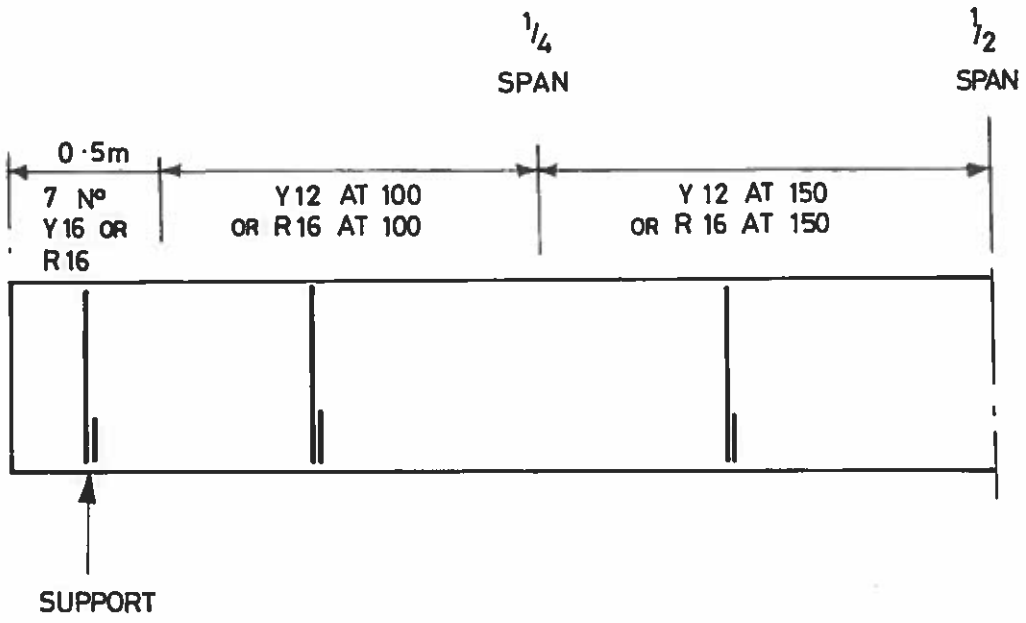

Fig . 5.40 Standard Secondary Reinforcement

Fig.540

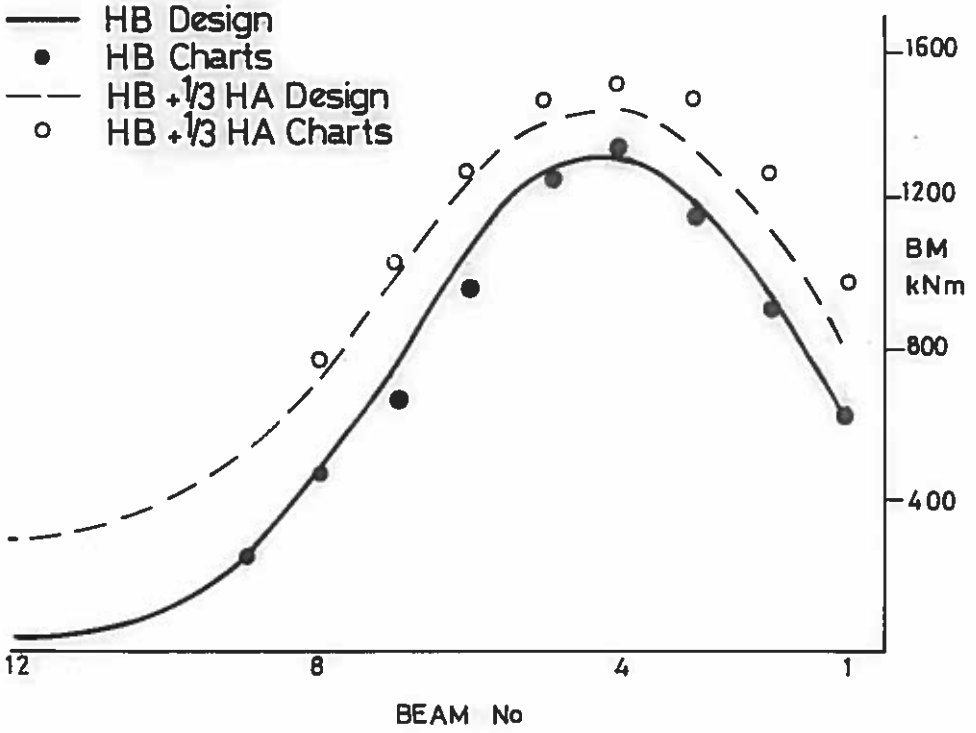

(a) Transverse Distribution

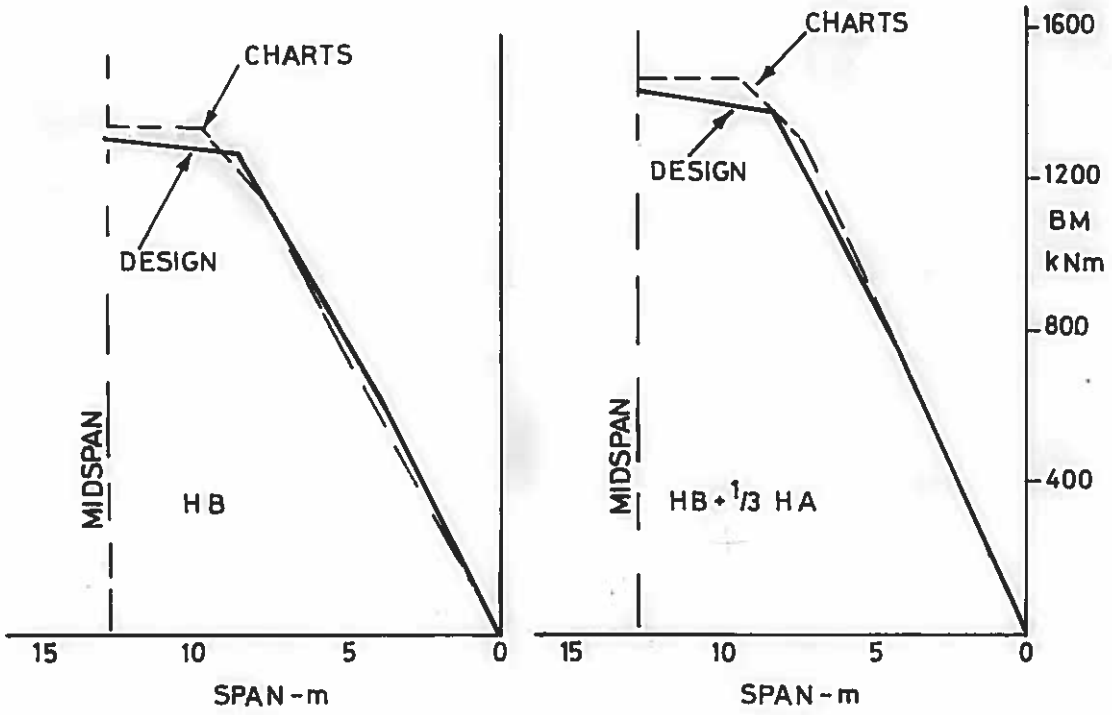

(b) Longitudinal Distribution

Fig 5.41 Mourne River Bridge
Tee Beam Construction
Comparison Of Bending Moments From Charts And Original Design

Fig.5.41

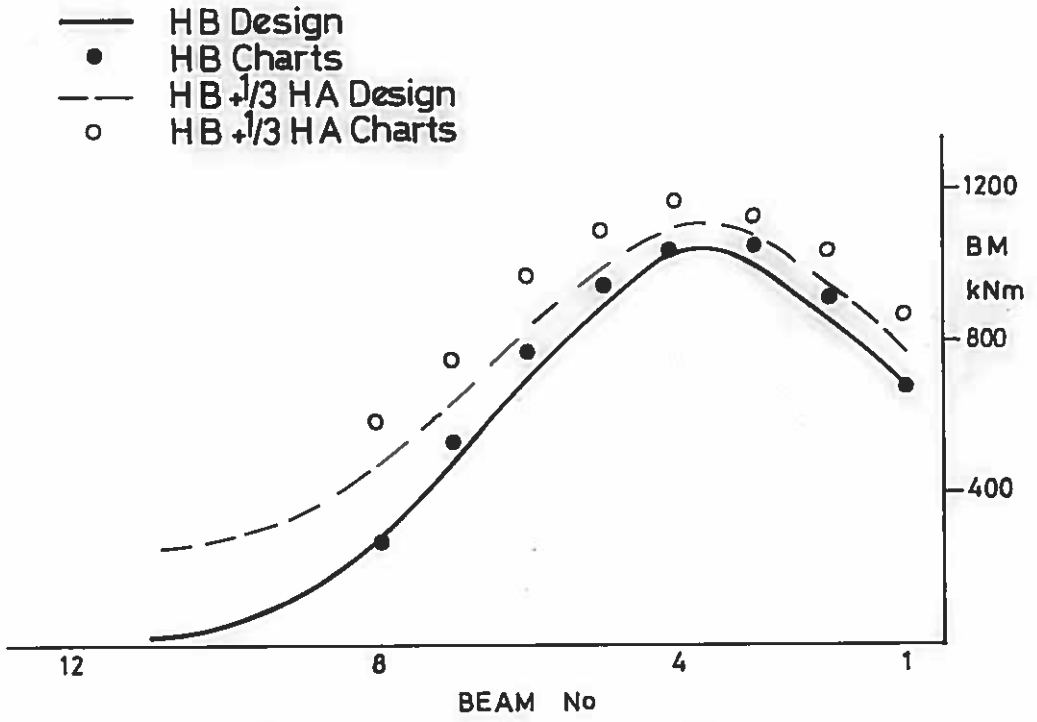

(a) Transverse Distribution

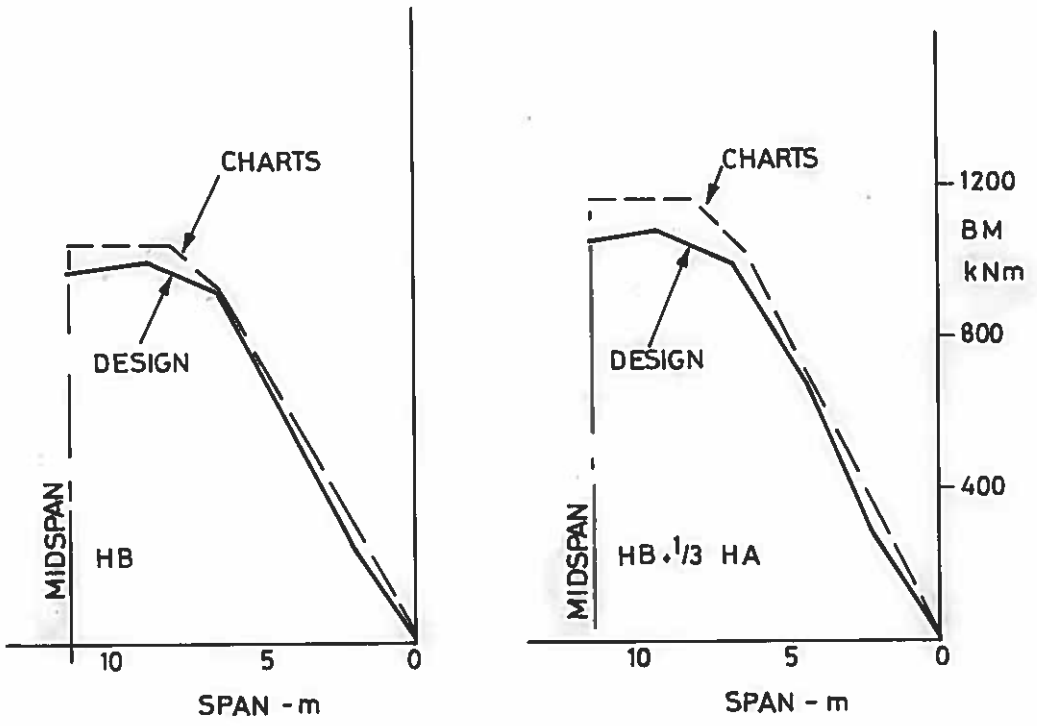

(b) Longitudinal Distribution

Fig 5.42 Ballymacoss Railway Bridge

Tee Beam Construction

Comparison Of Design Bending Moments

From Charts and Original Design

Fig542

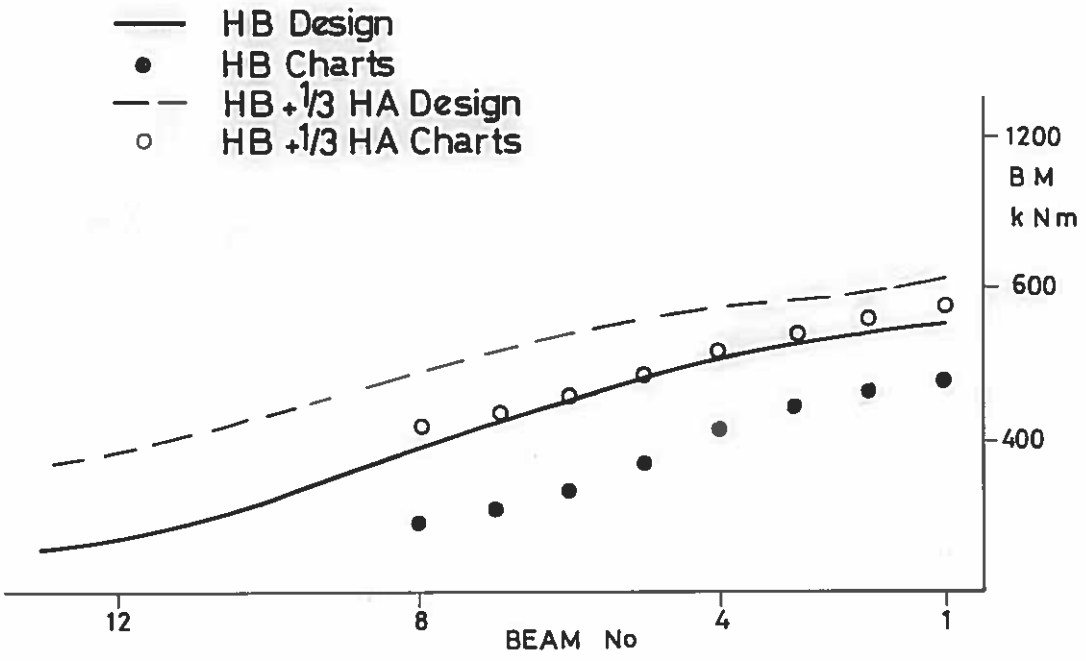

(a) Transverse Distribution

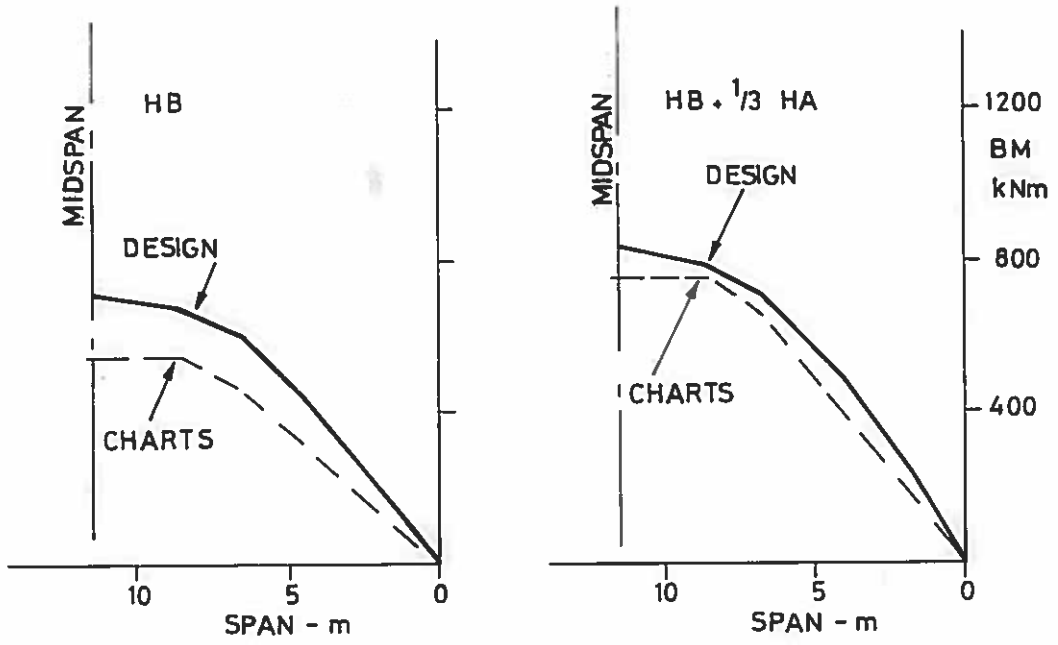

(b) Longitudinal Distribution

Fig 5.43 Ballymacoss Railway Bridge

Pseudo-Box Construction

Comparison Of Bending Moments

From Charts And Original Design

Fig.5.43

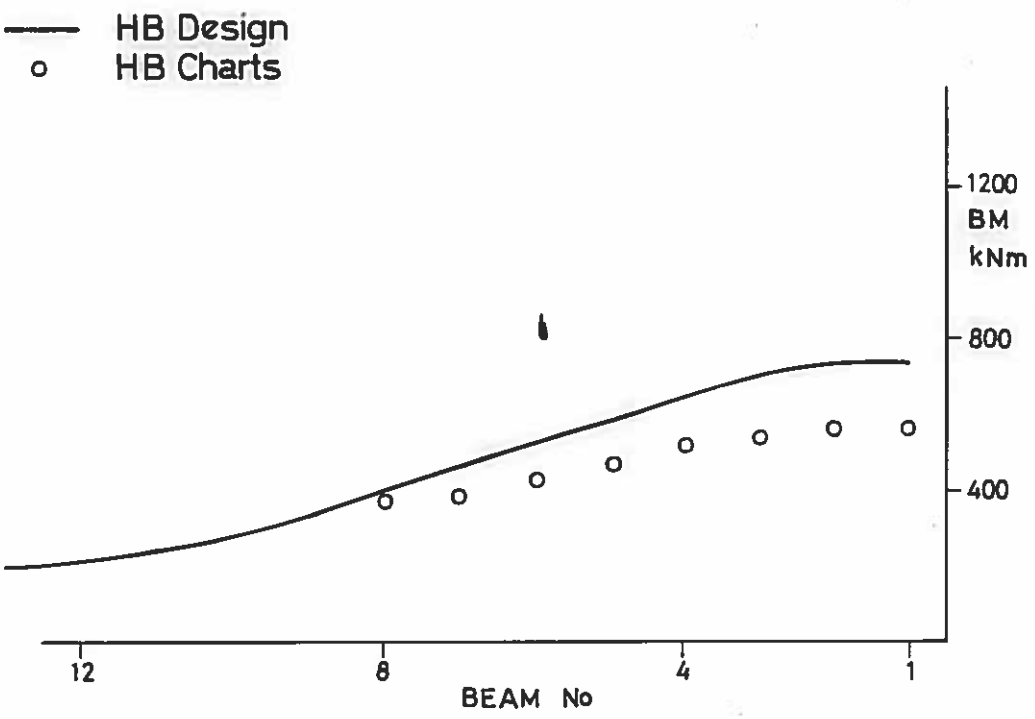

(a) Transverse Distribution

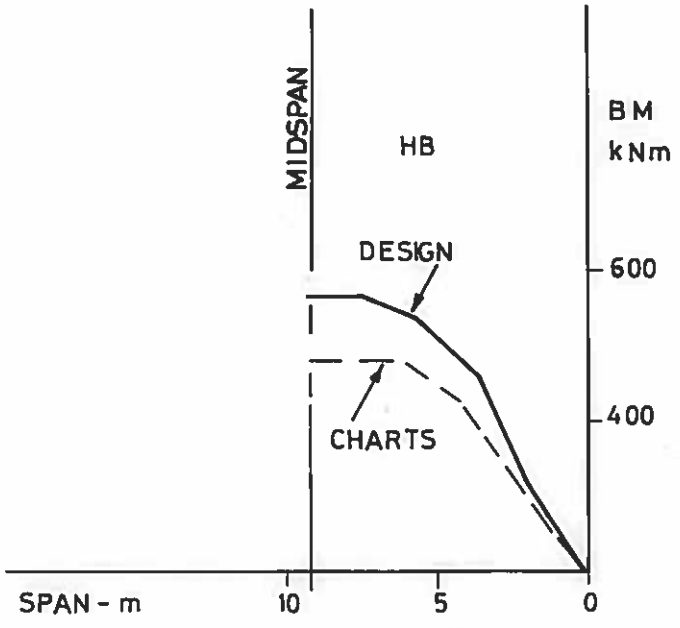

(b) Longitudinal Distribution

Fig 5.44 A50 Road Bridge
Pseudo-Box Construction
Comparison Of Bending Moments
From Charts And Original Design

Fig.5.44

CHAPTER SIX

STRUCTURES FOR ASSESSING THE STRENGTH OF DECK SLABS

6.1 INTRODUCTION

The considerable economic advantages of using the standard M-beams spaced at up to 2m has already been established, however, in the design of beam and slab bridge decks it is usual practice to seek an optimum solution based on beam size, spacing and slab thickness. As standardisation was an important aspect of this project the slab thickness must remain at 160mm and hence a solution must be based on beam size and spacing although the steel reinforcement in the slab may be varied.

The Department of Transport has recommended that the slab should be designed flexurally using elastic methods with the usual restrictions in bar spacing for crack control and the transverse moments calculated from the overall analysis of the deck are added to the local moments which are estimated by the methods of Westergaard (1930) or Pucher (1964). However, when the slab is designed to these moments a requirement for steel reinforcement in excess of 2% can occur. It is also recommended that the slab should be checked for punching shear under the concentrated wheel load and this is done on a critical perimeter and permissible stress basis. The apparent high level of slab reinforcement that is required from the existing methods of analysis may result in an overdesign of the deck slab as recent research has indicated the presence of an enhancement in the load capacity of the slab due to compressive membrane action from the considerable in-plane restraint which is inherent in a bridge slab of this type.

Therefore, to provide a minimum cost deck it was of the utmost importance that this enhancement be utilised to the full and the

strength of the slab established by suitable tests and in due course a more appropriate theoretical basis developed which would accurately predict the strength of the slab for any given set of variables.

In planning a programme of tests consideration was given to the possibility of utilising both full size structures and scale models. As some experience in the instrumentation and testing of full size bridge decks had already been gained during the load distribution tests discussed in Chapters 3 and 4, serious consideration was given to the use of the full size deck for slab tests. There were obvious difficulties regarding the magnitude of the load to be applied for the ultimate condition, however, there were distinct advantages in using a full size structure to investigate the performance of the slab for serviceability at working load. As far as the ultimate capacity of the slab was concerned it was accepted that some form of scale model using microconcrete and a carefully controlled programme of construction, instrumentation and testing would be required.

Therefore, this chapter takes the form of an assessment of the use of full size and scale model bridge decks which would form the basis of an experimental programme planned to establish the serviceability and ultimate load capacities of the standard 160mm slab with variable beam spacing and steel reinforcement. First of all, however, some thought was given to the type of loading that would be appropriate for these structures.

6.2 SLAB LOADING FOR TEST STRUCTURES

The principal load that is applied to bridge decks in the United Kingdom is the abnormal vehicle and this is defined by weight and geo-

metry in the Department of Transport Technical Memorandum (Bridges) No. BE1/77 (1977). This is a hypothetical vehicle which has 2 bogies each with 2 axles 1.8m apart and 4 wheels on each axle 0.9m apart with the maximum load on any single wheel 112.5 kN. With the beams at 2m spacing the slab can accommodate a single wheel midway between the beams, and the adjacent wheels will then be virtually on top of the 2 supporting beams. A second wheel on the rear axle will also be at midspan but 1.8m to the rear. This arrangement would seem to constitute the most critical case as tests by Tong and Batchelor (1971) have shown that wheel loads applied to a panel bounded by beams will have no effect on adjacent panels. Therefore, the appropriate loading that was considered for test purposes was the single 112.5 kN wheel load spread over a contact area to give a tyre pressure of 1.4 N/mm^2. Consideration was also given to the application of a second wheel 1.8m behind the first and on the longitudinal centre line of the panel. It would seem that the second wheel is sufficiently remote from the first to avoid serious interaction, however, this possibility was to be verified by test.

The use of either the single or double wheel loading arrangement has the advantage that although it may be increased until it caused local failure of the slab it would still represent only a relatively small proportion of the total load capacity of the deck. This would allow the slab to be tested, if necessary, to a load considerably greater than the working load of 112.5 kN. It should be noted that if the complete HB vehicle was to be simulated then there would be a strong possibility of the beams failing before the slab capacity could be reached. With this in mind consideration will

now be given to the testing of full size bridge decks during construction to establish the strength of the standard M-beam slab.

6.3 SLAB TESTS USING FULL SCALE BRIDGE DECKS

The testing of full scale bridge structures was discussed in paragraph 3.1 and it was concluded that except for a few tests by Morice and Little (1954) and Rowe (1959) it was not the usual practice in the United Kingdom to use full scale bridges for test purposes. However, there would seem to be considerable merit in the use of an actual bridge structure to establish the strength of a particular element, in this case the strength of the slab under the action of a concentrated wheel load. An actual bridge deck would be ideal for this purpose as it would provide the correct support and slab restraints which are considered to be of the utmost importance in establishing the true strength of the slab.

In recent years an extensive programme of testing in-service bridges has been carried out at the Ministry of Transportation and Communications, Ontario by Csagoly, Holowka and Dorton (1978). The background to this particular series of tests was the increase in the permitted legal weight limit for vehicles which was increased to a maximum of 62 tonnes and an additional factor which was giving cause for concern at that particular time was the serious deterioration of many concrete decks due to regular use of de-icing salts which was accentuated by the policy of using totally unprotected concrete decks as the running surface. Thirty two decks covering a wide range of types and states of deterioration were selected and tested with a single concentrated wheel load of 445 kN which was

about 4 times the standard wheel load. This load was applied by an hydraulic ram on a specially constructed loading vehicle and only 2 badly deteriorated panels failed at less than the 445 kn.

This series of tests was also used to investigate some of the proposed provisions of the Ontario Highway Bridge Code (1979) and culminated in the building of the Conestogo River Bridge as reported by Dorton (1976) which was designed and constructed with extensive instrumentation and testing facilities built into the structure. The Conestogo River Bridge is a 3 span (34.77, 44.23, 34.77m) continuous steel plate girder bridge with a concrete deck slab that was longitudinally prestressed for full composite action and was selected as a development bridge to investigate a number of new research findings and design techniques. Details of the geometry and construction are given in Fig. 6.1.

The deck slab for the south half of the bridge was designed for transverse bending by the usual CSA (1974) and AASHTO (1973) working stress method which gave a reinforcing steel requirement of almost 1%. The north half of the deck contained 12 test panels each 2.64m by 2.75m long with 3 different slab thicknesses of 177.8, 190.5 and 203.2mm. For each slab thickness 4 different transverse steel percentages were selected - 0.95, 0.6, 0.3 and 0.2. The upper value being the AASHTO (1973) requirement and the lower value was the minimum for temperature and shrinkage requirements.

All 32 panels tested safely withstood the 43 tonne applied punching shear load. Under this load fine cracks were observed on the underside of the test slab but they virtually disappeared once the load had been removed. The crack patterns were similar in their extent whatever the reinforcing steel percentage.

This bridge was used to investigate many other aspects of design and construction such as the strength of shear connectors, impact and vibration and the distribution of load between the girders. It represented a major contribution to bridge research and illustrated the potential of testing a full size structure when the instrumentation and testing facilities had been planned at the design stage.

It was therefore concluded that a full size bridge deck would be ideal for establishing the serviceability capacity of the M-beam deck slab. The availability of such a bridge was discussed with the DOE (NI) Roads Service and it was agreed that a suitable bridge would be provided for test purposes and would include the necessary variations in beam spacings and slab reinforcement. Details of this bridge will be provided in the next chapter.

The use of the full scale bridge to investigate the ultimate capacity of the slab was not considered because of the difficulty in providing a large concentrated load and the possibility of causing structural damage to a new bridge about to be opened to traffic. Therefore, it was evident that this aspect of the tests would have to be pursued using scale models and the possible alternatives that were available will now be considered.

6.4 SLAB TESTS USING MODELS

6.4.1 General

Models have been used for many years to simulate the distribution of load in prototype bridge decks. Various materials have been tried but it is now accepted that a scaled microconcrete mix gives the best representation of a concrete prototype. In general,

models may be divided into 2 broad categories which may be defined as follows:-

1. Localised Structural Models
2. Complete Structural Models

Both these models will be assessed as to their suitability for establishing the serviceability and ultimate load capacity of the standard M-beam slab.

6.4.2 Localised Structural Models

This type of model has been used by many researchers to investigate the strength of building slab column structures. However, it has not enjoyed the same degree of popularity in the field of bridge research, nevertheless, 2 recent examples of bridge type slabs have been tested using this type of model and both have utilised the main advantage by testing a large number of specimens.

At the Building Research Station, Snowdon (1973) tested 65 slabs as part of a feasibility study for a floating runway at the proposed new airport at Maplin. The construction was to be double slab hollow boxes prestressed together and filled with polystyrene for permanent flotation. The test frame consisted of a nine cell area of runway section of top slabs only. The centre slab was omitted to accommodate the full size test specimen. The loading simulated the single wheel of an aircraft and details of the test frame are shown in Fig. 6.2. An important feature of the test frame was the use of a high strength plaster to bed the slab into the frame and this provided the in-plane restraint which was an important feature of these tests.

The other example of this type of model was a series of tests by Holowka, Dorton and Csagoly (1979) at the Ministry of Transportation and Communications, Ontario. This research was to assist in the development of the Ontario Highway Bridge Design Code (1979). An unusual aspect of this series of tests was the choice of a circular shaped specimen. The purpose of this was two-fold, the punching failure pattern of reinforced concrete slabs is usually circular or elliptical and the measurement of restraining forces was made easier by measuring the hoop strains in the restraining ring. Details of the test frame and the restraining ring are shown in Fig. 6.3 and 27 slabs were tested.

Although both these series of tests simulated the considerable in-plane restraint provided by the adjacent slab, they did, however, omit the moment restraint provided by the continuity of the slab over the beams and the flexibility of the beams which support the slab.

The main advantage of the localised structural model is the ease with which the specimen may be constructed and hence there is virtually no limit on the number of specimens that may be fabricated and tested. The disadvantage is the difficulty of simulating the true boundary conditions of the prototype and this usually means a detailed assessment of the prototype and careful design of the test rig. Boundary conditions can best be simulated with a model of the complete structure and this type of model will now be considered.

6.4.3 Complete Structural Models

The use of a model of the complete structure has been the most common approach adopted by bridge researchers. This type of model may

be used to investigate 2 different aspects of structural performance. These are the global distribution of loads within the deck and the local strength of a particular element of the structure. A review of experimental work on slab and pseudo-slab bridges has been published by Clark and West (1973) and some of the more notable models used to investigate both global and local effects will now be considered.

Global Effects.

The use of models to simulate the global distribution of forces and deformations in bridge decks requires the model to be scaled in every detail and particular attention should be paid to the quality control of the material and the simulation of support conditions that are appropriate to the prototype.

A major programme of tests was carried out at the University of Illinois Engineering Experiment Station and many aspects of steel I-beam and concrete slab decks were investigated using ¼ scale models. Tests on simple span right bridges were carried out by Newmark, Siess and Penman (1946), simple span skew bridges by Newmark, Siess and Peckham (1948) and two-span continuous right bridges by Siess and Viest (1953). Over this period twenty two models (Fig. 6.4) were tested and the main objective was to establish the distribution of load to the steel beams for the various types of decks. This was used to supplement earlier analytical studies by Newmark (1938), Jensen (1939) and Newmark and Siess (1942). These tests were also used to investigate the ultimate load capacity of the steel beams and they were loaded mainly by two wheels on a single axle straddling the beam.

Both composite and non-composite decks were tested and the effectiveness of shear connectors investigated. These results led to further research by Siess, Viest and Newmark (1952) on small scale tests of channel shear connectors and by Viest, Siess, Appleton and Newmark (1952) on full size tests on channel shear connectors.

This type of model is also suitable for the verification of theoretical methods of analysis such as load distribution and was used successfully by Little (1954, 1955), Rowe (1958) and Best and Rowe (1959). A series of ¼ scale precast prestressed concrete pseudo-slab model decks was tested by Cusens (1974) who showed that longitudinal stresses were adequately predicted by a 2 dimensional orthotropic plate analysis and the transverse stresses could be predicted by a 3 dimensional strip analysis.

Some of the recent models tested at the Cement and Concrete Association include a ¼ scale pseudo-box deck (1971) formed from precast prestressed concrete beams. This model is relevant to this particular project and some details are given in Figure 6.5. An important contribution to the use of voided slab decks has been made by Elliot, Clark and Symmons (1979) who have tested ¼ scale model. Although the main interest was the distribution of load within the model additional tests on the local punching strength of the voids was also carried out and details of this model are shown in Figure 6.6.

The loading on most of these models represented the scaled version of the standard abnormal vehicle, however, in the present investigation the main interest is in the strength of the individual

reinforced concrete slab under the action of only part of the HB vehicle's train of wheels and models that have been used for this type of loading will now be considered.

Local Effects

The use of a complete model bridge deck to investigate the strength of individual elements has been used successfully by researchers interested in establishing the failure loads of the slab of certain types of composite bridge decks. The important advantage of this type of model is that the slab under the action of the test load has the correct continuity of support over the beams and also provides the correct in-plane restraint. The global deformations of the beams and slab are also modelled correctly.

The series of tests, which were described previously at the University of Illinois Engineering Experiment Station using ¼ scale steel beam and concrete slab models by Newmark, Siess and Penman (1946), Newmark, Siess and Peckham (1948) and Siess and Viest (1953) were also used to investigate the local punching strength of the concrete slab. Each model slab was tested extensively using the double wheel straddling the steel beam and all the test panels failed by the simulated wheel load punching a hole through the slab. It is also of interest that the transverse bottom reinforcement in the slab yielded at about 40 to 60% of the punching failure load.

Tong and Batchelor (1971) used a 1/15 scale model to investigate the presence of in-plane forces under a single concentrated load and details of this model are given in Figure 6.7. Although described as complete models they were, in fact, single and multi-panelled specimens with edge beams to provide restraint. Nevertheless, they showed the importance of the edge restraint on the strength of bridge slabs.

This type of model was used by Batchelor and Tissington (1976) in their investigation of scale effects in reinforced concrete models. The basic models were similar to that shown in Figure 6.7 and scales of $1/15$, $1/12$, $1/10$, $1/8$ and $1/6$ were adopted and this series of tests confirmed the absence of scale effects in concrete models of this type.

A complete structural model was used by Batchelor, Hewitt, Csagoly and Holowka (1978) in their investigation of the punching strength of concrete slabs supported compositely by steel beams.

In this case the stiffness of the beams was more important with the correct support conditions to give exact modelling of the prototype. This particular model is shown in Figure 6.8.

As stated previously the main advantage of this type of model to test individual slab elements is the correct simulation of the slab boundary conditions as regards in-plane and moment restraint. However, there are disadvantages; in particular, the size of the model can be very large and depending on the prototype size this may be unavoidable unless a small scale is used which introduces difficulties in the scale of fabrication and construction. The construction of complete structure models are expensive in the amount of man hours involved. They also require extensive facilities for fabrication, material handling, storing and batching aggregate as well as mixing, transporting and placing concrete. A large area of laboratory space is utilized for a considerable period of time during construction, instrumentation and testing. Finally and perhaps the most important aspect is that all the tests

must be carried out on a single model because of the time and expense involved in the fabrication it is most unlikely that additional models can be used.

6.5 CONCLUSIONS

In considering the possible type of structures that could be used to establish the true strength of the standard M-beam deck slab it was decided that the full size bridge deck should be utilised to investigate the performance under service load and a $^1/_3$ scale model of this prototype would be the most appropriate to confirm the serviceability and establish the ultimate strength of the standard slab. The main reasons for these decisions were as follows:-

1. The complete structural model of a beam and slab bridge deck provides the correct boundary conditions for the testing of the slab element. This factor out-weighed the disadvantages of cost and time required for fabrication.
2. As a full size prototype bridge would be available for testing, the complete structural model could be a scaled version of the prototype which would allow a comparison of performance, for serviceability at least, between prototype and model.
3. The size of the model was not a problem as the testing laboratory could accommodate a $^1/_3$ scale model of the prototype structure and this was the size adopted.
4. The facilities for the storage, batching, mixing and placing of concrete could accommodate this size of model.

5. As the deck was of multi-beam construction and with bands of transverse reinforcement it would be possible to have 20 test panels which was an advantage usually associated with the localised structural model.

Due to the current financial restrictions it has not been possible to proceed with the construction of the prototype bridge within a timescale suitable for the completion of this thesis. However, the replacement bridge has been designed by the author who will supervise the construction and testing and as a temporary structure is currently being used it is hoped that construction will start in the near future. With this in mind details of the prototype and the design and construction of the model will be given in the next chapter.

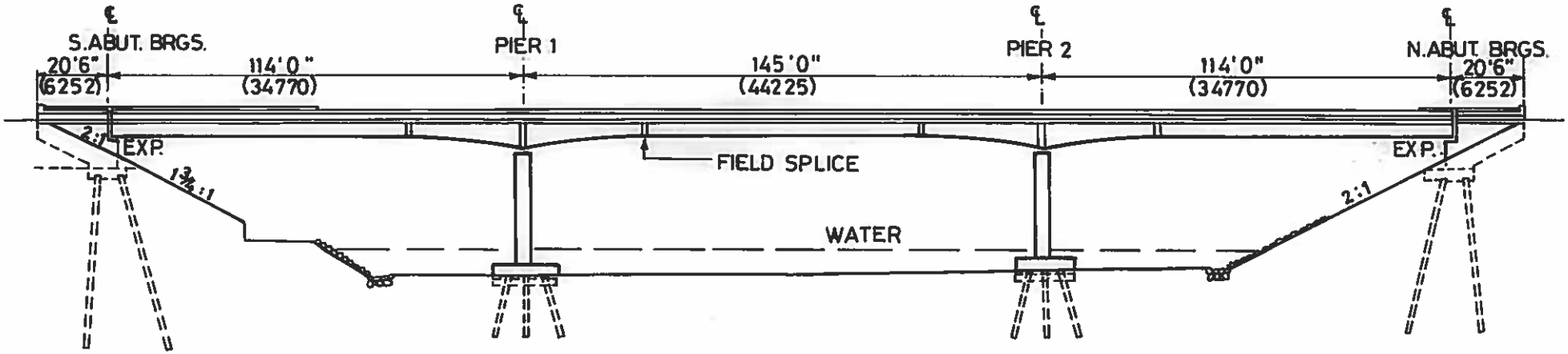

Elevation

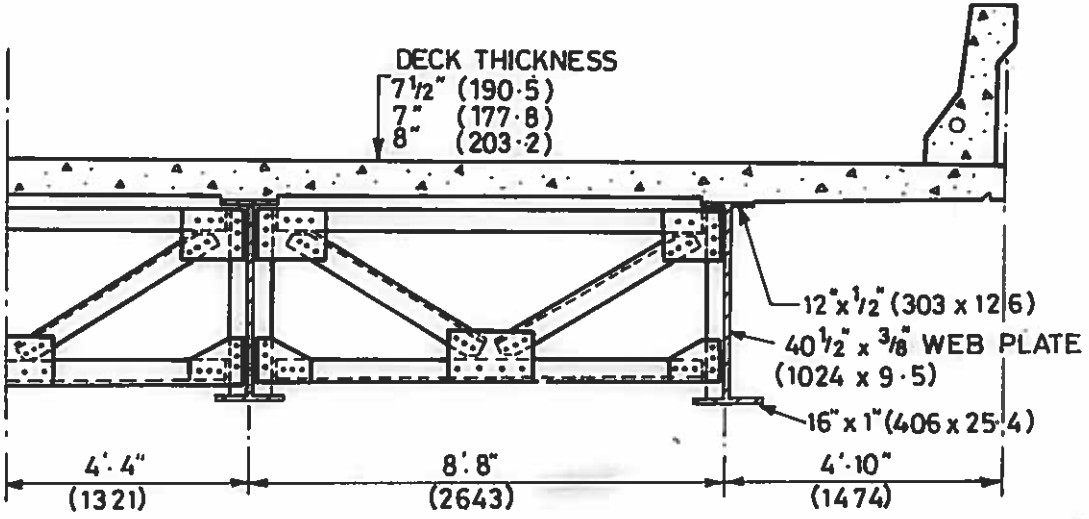

Half Cross-Section

FIG. 6.1 Details of Conestogo River Bridge

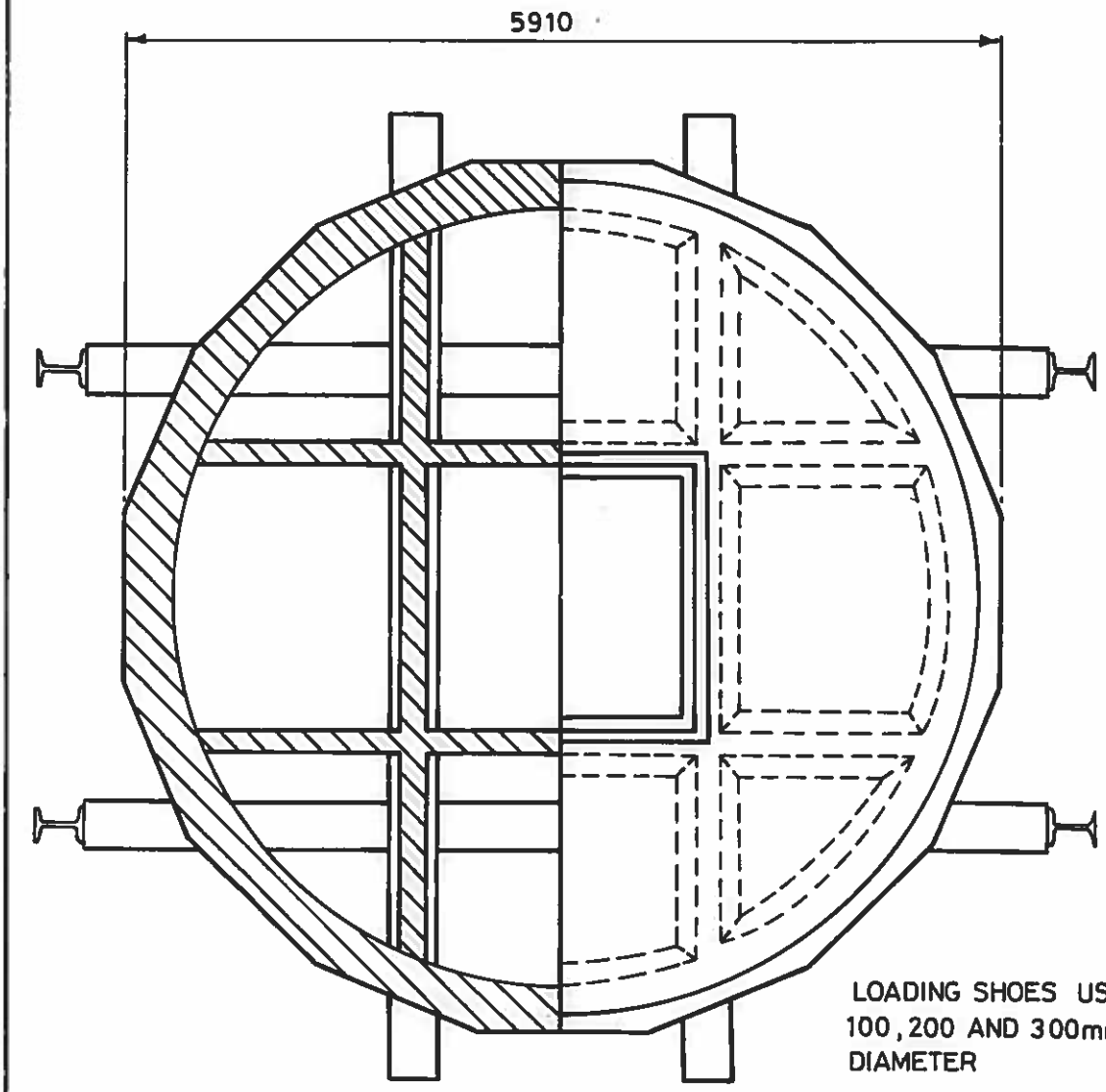

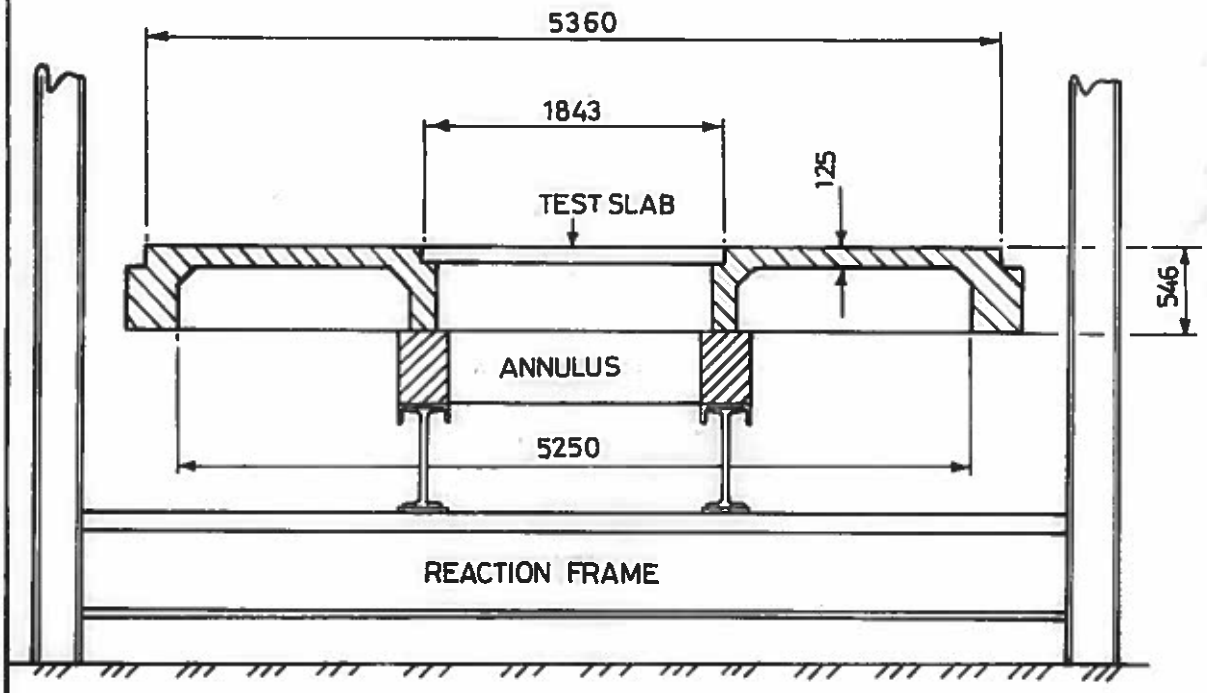

FIG. 6.2 Details of Test Rig and Reaction Frame For Maplin Tests

Fig. 6.2

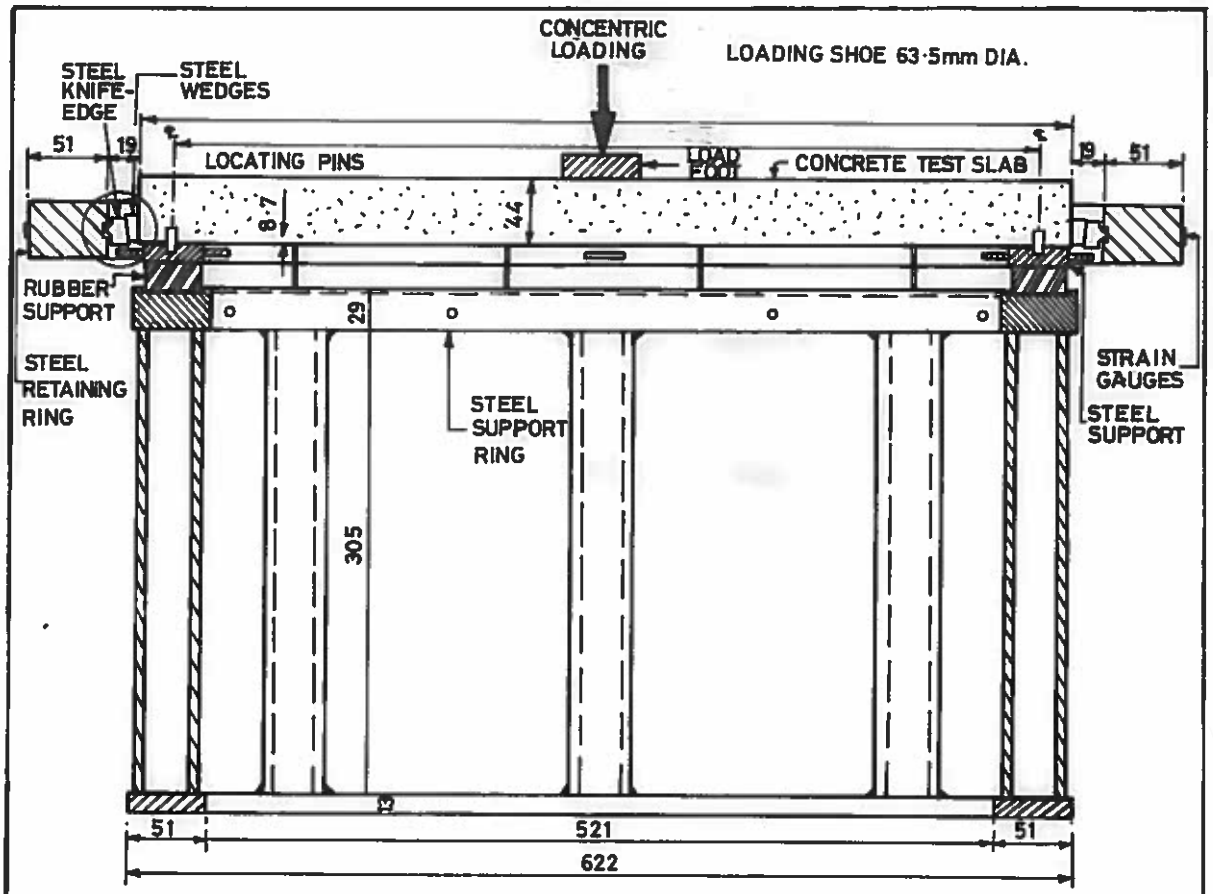

(a) Section Through Testing Aparatus

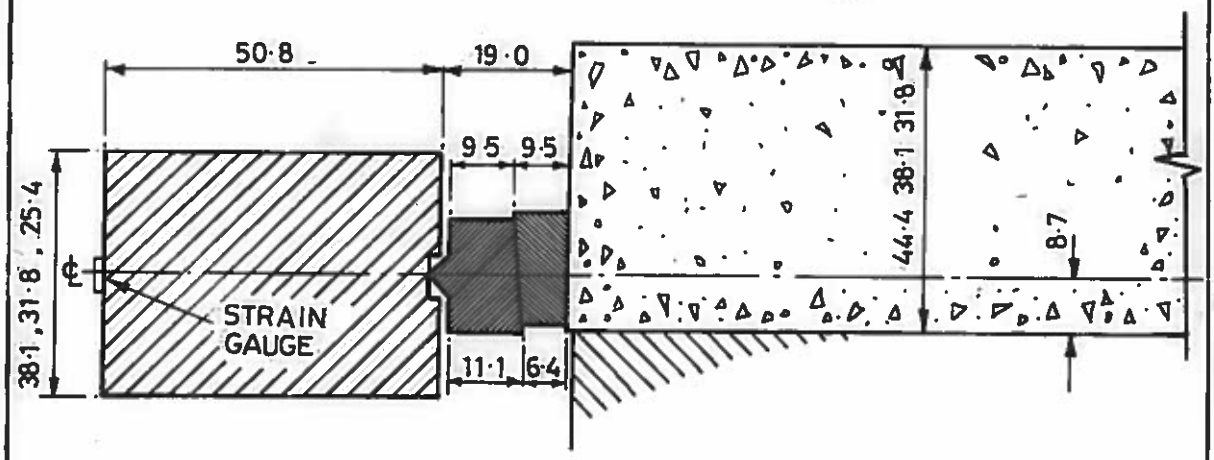

(b) Method of Providing an Axial Restraining Force

FIG. 6.3 Ontario Circular Slab Tests

Fig.6.3

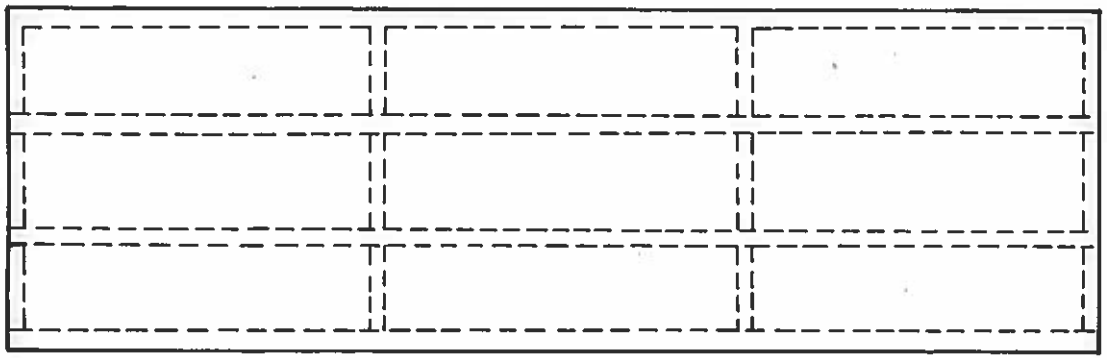

Plan

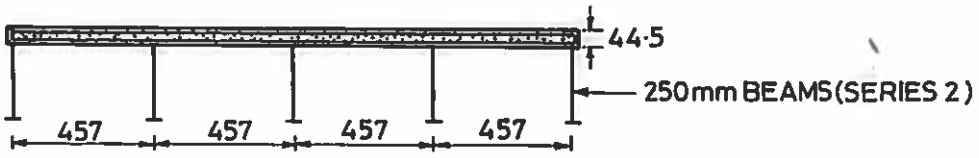

Transverse Section

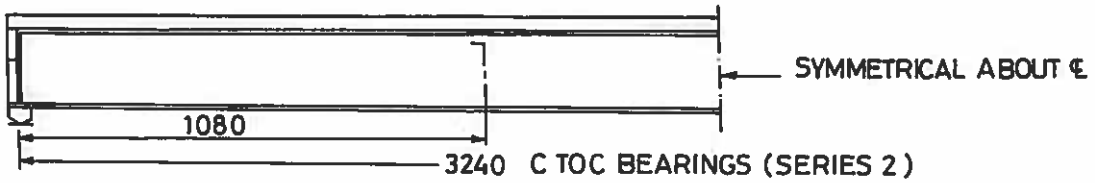

Longitudinal Section

LOADING SHOE 93·25mm DIAMETER

Fig. 6.4 Typical Beam and Slab Model Tested at The University of Illinois

Fig.6.4

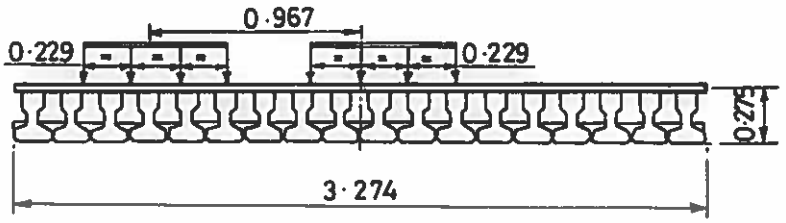

Cross Section

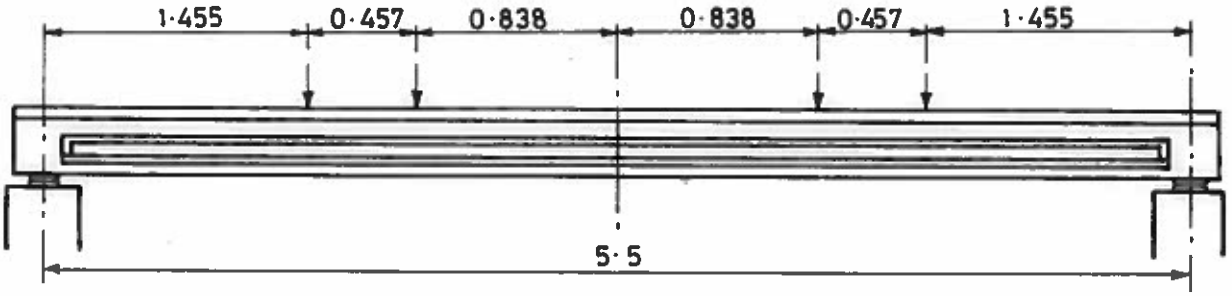

Elevation

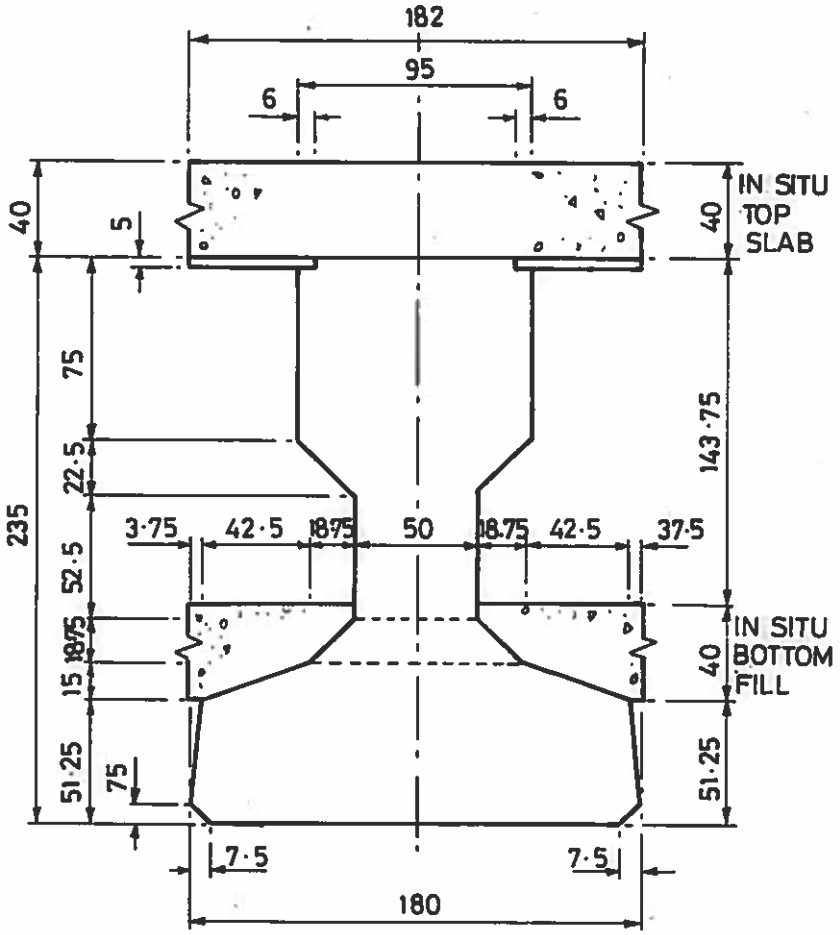

Details of Beams

FIG. 6.5 C&CA ¼ Scale Pseudo-Box Deck

Fig. 6.5

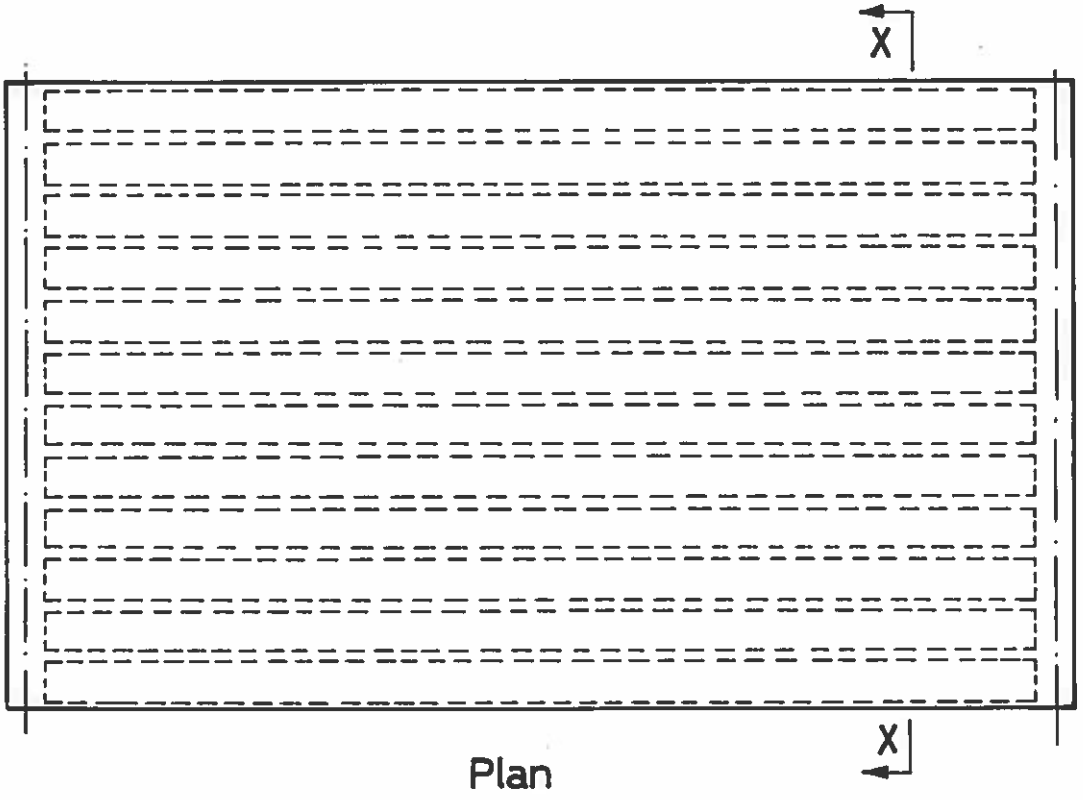

Plan

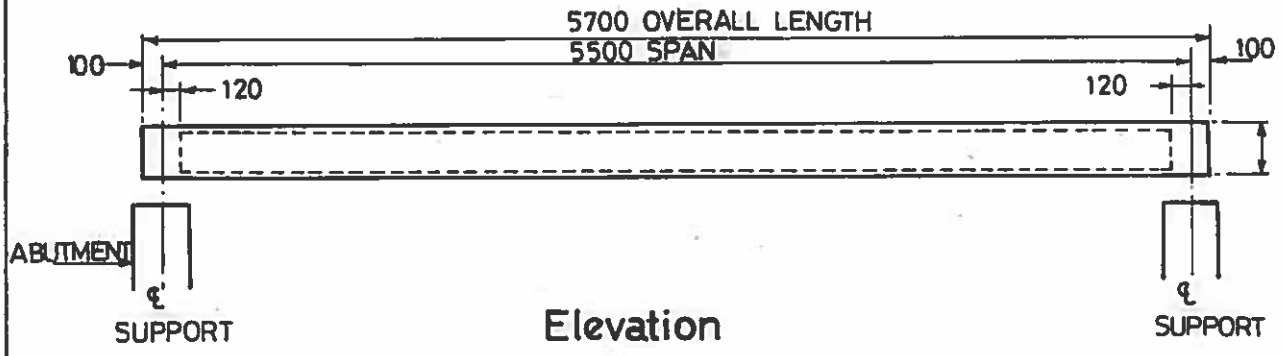

Elevation

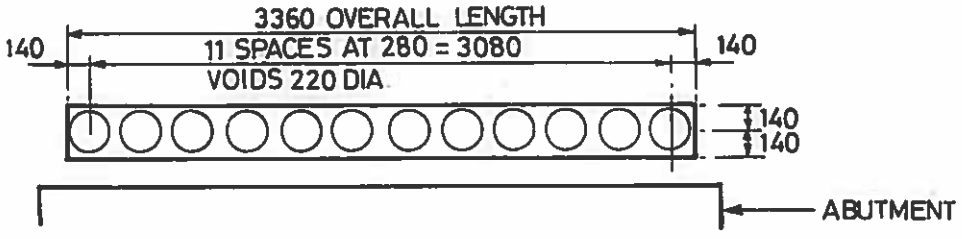

Section X-X

FIG. 6.6 C&CA 1/3 Scale Voided Slab Deck

Fig.6.6

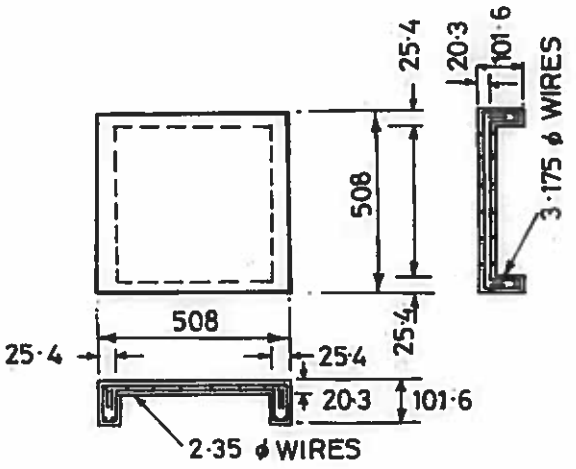

Single Panel Slab

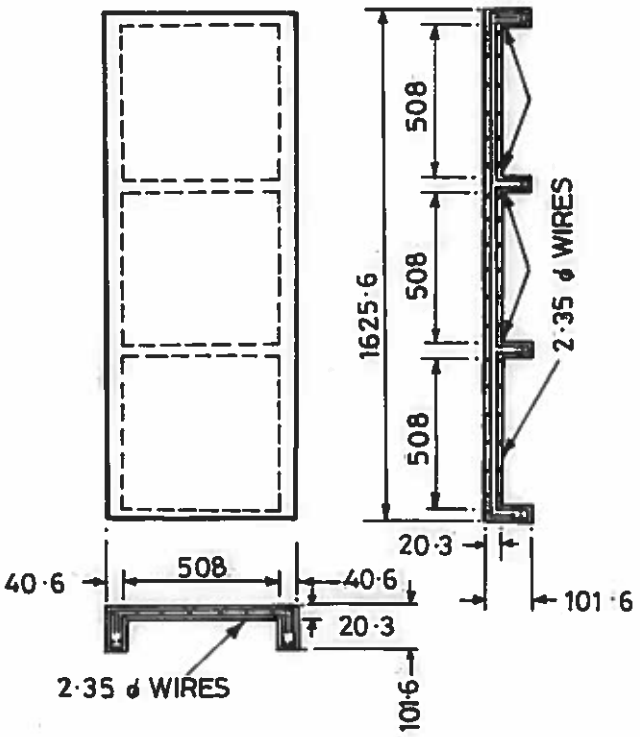

General Layout of Bridge Specimen

FIG. 6.7 Bridge Models Tested By Tong and Batchelor

Fig.6.7

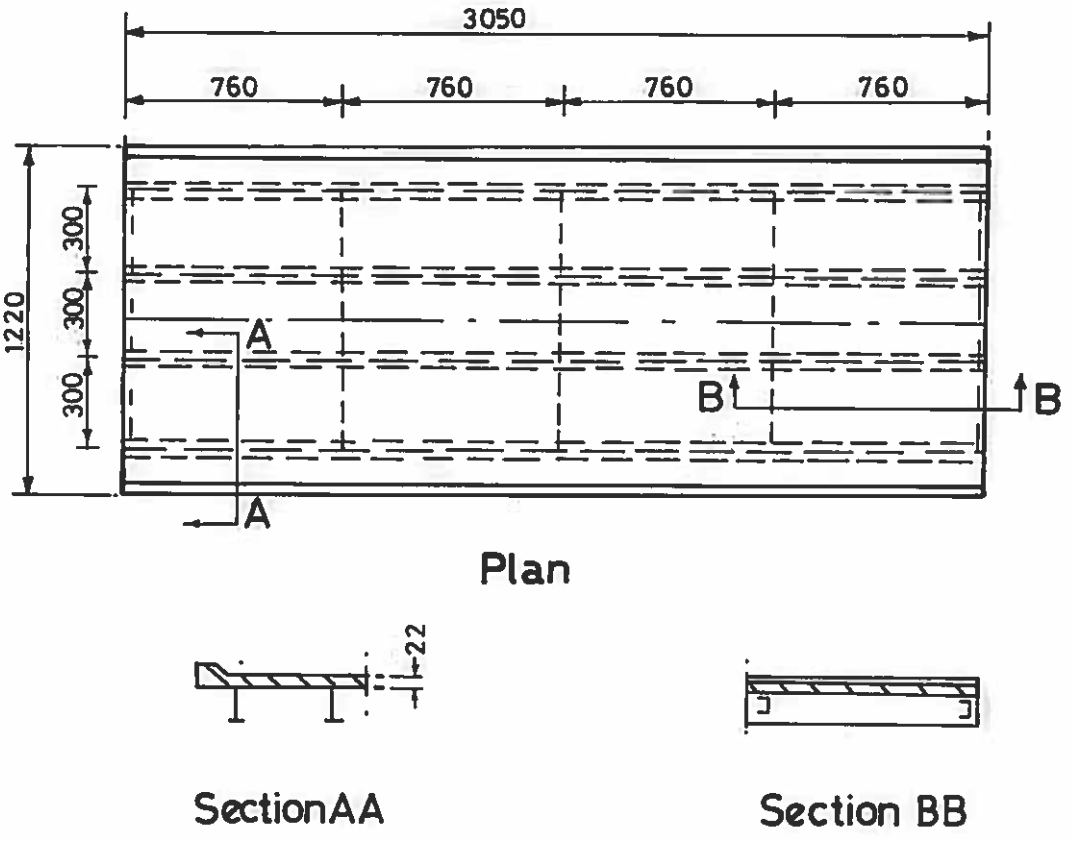

ELLIPTICAL LOADING SHOE WITH MAJOR AXIS OF 95·25mm AND MINOR AXIS OF 63·5

FIG. 6.8 Model of Four - Girder Bridge Tested by Batchelor, Hewitt, Csagoly & Holowka

Fig6.8

CHAPTER SEVEN

DESCRIPTION OF TEST STRUCTURES AND EXPERIMENTAL PROCEDURE

7.1 INTRODUCTION

It has been established that both prototype and model structures would be used to investigate the strength of the standard M-beam slab and when the construction and testing was being planned considerable thought was given to the difference in approach that was considered necessary for each structure.

The model was constructed in the ideal environment of the laboratory and this allowed careful control of the construction of formwork and bending and placing of the steel reinforcement to a high degree of accuracy. This was essential to provide the dimensional accuracy required in a model of this type. The laboratory environment was also ideal for the drying, storing, batching, mixing, placing and curing the microconcrete slab. The model was loaded with a lightweight jack and a data logger was used to monitor the various measurements taken during each test.

The advantages of the controlled laboratory environment may be contrasted with the experience gained in the testing of full size structures. The overall control of material quality and construction tolerances are the responsibility of the site supervision and this will result in a structure that is typical of the current system of reasonable compromise between contractor and client. From the testing aspect, the magnitude of the concentrated load required could not be achieved using a commercial vehicle and a loading frame with an hydraulic jack was adopted. With the magnitude of load in mind this frame had to be of sufficient strength and stiffness to provide the required loads with an appropriate factor of safety. It was also im-

portant that the loading frame was suitable for transporting to the site and moving around the bridge without special lifting facilities. Therefore, a safe working area in the form of scaffolding and platform for access to the complete bridge soffit was specified. Other important factors which must be planned during field testing are the problems of adverse weather conditions, the complete co-operation of the contractors representatives and the proper briefing of site staff if they are taking part in the test. Another aspect is the proper servicing, testing and the provision of spares for equipment to be used during the test.

Therefore, with this comparison of the construction and testing of both model and prototype structures in mind, this chapter considers the design of the test structures and the proposed test rig for the prototype. However, as the prototype tests have not as yet been completed a slightly greater emphasis has been placed on the design, construction and instrumentation of the model.

7.2 DETAILS OF PROTOTYPE DECK

7.2.1 General

The DOE (NI) Roads Service has agreed to provide an experimental bridge to complete the investigation into spaced M-beams and the strength of the slab to be used with this form of M-beam deck. The bridge to be used carries the C329 Banbridge to Dromara Road across the Tullinsky Cut River which is in the townland of Clinghans and the exact location is shown on the map of Fig. 7.1. The previous two-span masonary arch had collapsed in a flood situation in January

1980 and a temporary structure has been in service since then and this is shown in Plate 7.1. The detail design of this deck will now be considered.

7.2.2 Deck Design

As Clinghans Bridge was on a C class road the use of the abnormal vehicle was considered inappropriate and the bridge was designed to the standard highway loading type HA. This consisted of a UDL of 10.5 kN/m^2 and a KEL of 40 kN/m or the 2 No. 112.5 kN wheels 0.9 m apart and placed transversely across the carriageway. The accidental loading vehicle which as defined in paragraph 4.7 of DTp Memorandum (Bridges) BE1/77 (1977) was also considered but was found to be less critical than the 2 No. 112.5 kN wheels. The overal analysis was done on a strip basis and an assessment of the maximum transverse bending moments in the deck was made using Westergaard (1930), details of which is given in Appendix D.

The main design criterion for Clinghans Bridge, in addition to the standard highway loading, was the provision of a variation in beam spacing up to 2 m and various percentages of transverse reinforcement in the deck slab to allow the assessment of these variables on the strength of the slab. With this in mind the final design consisted of 6 No standard M3 beams spaced alternatively at 2 m and 1.5 m centres with a standard in situ concrete deck slab of 160 mm. The bridge deck had an effective span of 14 m, 8^{o} skew and a 5.5 m carriageway with a 2.0 m footway on each side.

For the transverse reinforcement in the deck slab the Westergaard method produced a requirement for 1.7% steel reinforcement under the highway pavement. This was based on a crack width of 0.25 mm with

bars at 150 mm spacing. For test purposes deck reinforcement ranging from 0.25% which was approximately the minimum for temperature and shrinkage, up to a maximum of 1.7% was provided, the intermediate values being 0.6% and 1.1% (appendix D). The minimum reinforcement would be placed under the pavement so that current standards would be maintained for the highway part of the deck and provision for the overslabbing of the pavement area would be included in the contract documents. A generalised sketch of the deck design is shown in Fig. 7.2.

7.2.3 Test Procedure

For testing the slab of Clinghans Bridge a concentrated load of at least twice the standard wheel load of 112.5 kN would be required with a provision for an additional load if necessary. As a commercial vehicle would be unsuitable it was decided to provide holes in the deck remote from the test area and to load the slab using a 50 tonne hydraulic jack through a framework of beams and tie rods as shown in Fig. 7.3. The rig has been designed to be easily moved and to allow excess for the visual inspection of the slab soffit during the test. Provision has also been made to monitor the slab deflections using transducers and if cracking occurs the width and development will be measured.

The opportunity will also be taken to carry out a series of load distribution tests using commercial vehicles as discussed in Chapter 3. These tests were considered necessary to validate the use of grillage analysis for tee beam decks with the beams spaced apart.

It was decided that the requirements for the load testing of Clinghans Bridge would be included in the contract documents and details of these additional clauses will now be considered.

7.2.4 Contract Details of Tests

To ensure the full co-operation of the contractor and to establish the actual cost of the test programme it was decided that all requirements relating to the testing of the bridge should be incorporated into the contract documents and these additional clauses are now listed.

Preamble

It is intended to carry out tests, for research purposes, by DOE (NI) Roads Service personnel prior to the laying of the deck waterproofing and kerbs.

(a) Close board scaffolding will be required under the entire soffit area of the deck to permit ready access to any part of the beams and slab soffits.

(b) Contractor to accommodate test presence at the steel fixing stage by allowing certain reinforcing bars to be taken off the site to have strain gauges fitted.

(c) 24 No. additional concrete cubes will require to be made at deck slab casting stage. Transport for testing will be provided by DOE (NI).

(d) Two six-wheel lorries (with drivers) with a total weight of approximately 30 tonnes each will be required for a period of 3 hours.

(e) There will be a period of 5 working consecutive days during which all the tests will be carried out and no contractual work

will be permitted on or under the structure. All debris will have to be removed from the deck prior to the start of tests.

(f) After the tests it may be required to cast a 50 mm thick concrete screed 1.75 m wide on top of the deck slab under the downstream verge, the surface affected being scabbled and have a bonding agent applied.

(g) The holes in the deck will require to be filled with 20/40 concrete on completion of testing.

(h) Deck slab to be a steel floated U1 finish with a tolerance of 1 mm per m.

Notes

The contractor will not be responsible for any damage caused to the structure by the special tests in this section.

These special tests will cause a certain amount of disruption to the contractor's pattern of work, the cost of which will be deemed to be included in the above items.

With arrangements now completed for the construction and testing of the prototype the remainder of this chapter will be devoted to the design and construction of the model and the provision of a suitable test rig and instrumentation.

7.3 DETAILS OF THE MODEL

7.3.1 Introduction

In order to simulate the behaviour of the prototype the model was designed as a true one third scale representation with one exception.

As the experimental work related only to the behaviour of the reinforced concrete slab the pretensioned M-beams were represented by reinforced concrete beams of equivalent stiffness having an identical width of top flange to the standard M-beam thus ensuring the correct support conditions for the individual panels. Details of the reinforced concrete beam is given in Fig. 7.4 and the calculations relating to strength and stiffness is given in Appendix E. In all other aspects the model is fully representative of the prototype and in particular the end diaphragms and parapet upstand were all included in the model to ensure the slab could develop its full potential of in-plane forces.

The deck was supported on concrete block walls with a steel plate and rubber bearing pad between the plate and beam. Details of the model deck are given in Fig. 7.5.

7.3.2 Details of Slab Reinforcement

The design of the prototype slab for the 2 No. 112.5 kN wheel loads using the equations of Westergaard indicated that steel reinforcement of the order of 1.7% was required (Appendix D) under the highway pavement. For test purposes additional areas of reinforcement equivalent to approximately 1.2%, 0.5% and 0.25% were provided in the model and are represented by 4 areas of slab approximately 1200 mm wide in the span-wise direction and the full width of the deck in the transverse direction. The reinforcement extends the full width of the deck without laps. Therefore with this banding of reinforcement, 3 panels equivalent to 2 m beam spacing and 2 panels equivalent to 1.5 m beam spacing are available providing a total of 20 panels the notation of which is given in Fig. 7.6. Both prototype and model

deck are reinforced using the same amount of steel top and bottom and longitudinally approximately 0.3% of high yield steel is provided.

7.4 FABRICATION OF MODEL

7.4.1 Beams

The beams were cast in 2 batches of 3 beams each. Standard steel shutters were used for the outer framework and 20 mm blockboard was used to divide the box into 3 troughs. The steel reinforcement was assembled and placed in each trough with a polystyrene former to provide a hole at each end of the beam for the diaphragm steel. The 2 sets of beams were then cast on a 20 mm plywood base. Ready mixed concrete was used having a specified 28-day cube strength of 40 N/mm^2. Details of the cube strengths are given in Table 7.1 and the beams are shown in Plate 7.2.

7.4.2 Slab Reinforcement

Three different types of steel were used to reinforce the slab in the transverse direction. In the bottom of the 1.7% and 1.2% panels a 6 mm dia. high yield bar of Swedish manufacture was used. This type of reinforcement was specially annealed to produce a consistent and distinct yield stress of 530 N/mm^2 and a long yield plateau as shown in the stress strain curve of Fig. 7.7. The reinforcement used in the top of these panels was also of 6 mm diameter but had a less distinct yield point and a yield stress of 488 N/mm^2 (Fig. 7.7). The reinforcement used in the top and bottom of the 0.5% and 0.25% panels was a plain 3 mm diameter bar with a distinct yield point of 338 N/mm^2 (Fig. 7.7). Typical deck reinforcement is shown in Plate 7.3 and the parapet steel in Plate 7.4. The complete deck steel is

shown in Plate 7.5.

7.4.3 Concrete

As it was most important that the deck slab should be cast using a properly scaled concrete, considerable care was taken in developing suitable mix proportions. Two important aspects of modelling the prototype concrete were considered:-

1. The maximum aggregate size should be consistent with that of the other model dimensions.
2. The ratios of tensile strength to compressive strength for the model mix should be close to that for the prototype concrete.

The first of these requirements was easily achieved by using a crushed basalt with a maximum particle size of 6 mm. The latter requirement was only fulfilled after experimenting with several trial mixes of differing proportions and compositions. The concrete mix chosen contained the 6 mm crushed basalt, a zone 2 sand (BS 882) and a sand (or grit) with a grading shown in Table 7.2. These were combined in certain proportions to give the total grading, as illustrated in Table 7.2 which has the characteristic of having a relatively low proportion of fine particles (i.e. those passing the 1.18 mm sieve).

To achieve a high workability and high strength an aggregate cement ratio of 4.0 and a water cement ratio of 0.58 were used. The proportions of each component for 1 m^3 of wet concrete are shown in Table 7.3.

The concrete compressive strength and split cylinder tensile strength were determined from control specimens (Section 7.4.4) on

the day of testing each panel. Designation of panels and batches are given in Fig. 7.8 and the results of the control specimens are summarised in Table 7.4.

7.4.4 Casting and Curing

The deck slab was cast in four transverse strips corresponding to the different areas of reinforcement. End stops were provided between each area of reinforcement and the deck was cast in alternate bays. The steel reinforcement with the end stops in place is shown in Plate 7.6. The concrete was mixed in a 0.1 m^3 capacity mixer situated in the laboratory adjacent to that in which the deck slab was to be cast and tested. The casting of each bay required approximately 3 batches of concrete and the location of each batch was recorded and shown in Fig. 7.8. The concrete was compacted using an internal poker vibrator and was later screeded to remove excess concrete. Several hours after testing the concrete was finished using a steel float. After a further five hours it was floated again to give a very smooth surface. Control specimens in the form of three cubes and one cylinder were taken from each batch. The slab was allowed to cure for ten days under damp hessian and a polythene sheet which covered the complete deck. The corresponding control specimens were cured in water.

7.5 TEST APPARATUS

7.5.1 Test Frame

The test frame which was purpose built for this model consisted of two beams spanning transversely below the deck and bolted to the strong floor at 0.6 m intervals. Two rigid portals were bolted to

these beams in the spanwise direction and finally a purpose built loading beam was hung from the top of the portals in the transverse direction. Full details of the test frame are shown in Fig. 7.9 and a three dimensional sketch of the test frame and model is shown in Fig. 7.10 and Plate 7.7.

7.5.2 Loading System

Hydraulic jacks were used to load the model. For the single wheel load a long stroke jack was attached to the beam with a chain pull plate, the main body of the jack resting between the two channels which made up the loading beam.

For the double wheel load a jack with a shorter stroke but larger diameter bore was used. This jack rested below the loading beam with a 25 mm thick circular plate to distribute the load to the bottom flanges of the channels.

Between the end of the ram of the jack and the loading shoe a spherical ball joint was used to ensure proper seating of the loading shoe in the event of a misalignment of the jack. The slab was therefore loaded by the jack to the loading beam and carried to the strong floor by the portals and floor beams. This is shown in Plate 7.7 and the loading shoes are shown in Plates 7.8 to 7.10.

7.6 INSTRUMENTATION

The construction of this model was expensive in terms of time and materials so that the maximum amount of instrumentation was incorporated into each panel. An electronic data acquisition unit was used and the various measurements are discussed under separate headings.

7.6.1 Measurement of Applied Load

The load was applied by a hand operated pump and the pressure reading monitored on a gauge in series with the system. Prior to testing the two jacks used had been compared with an accurate compression testing machine and accurate calibration graphs obtained.

7.6.2 Deflections

The deflection of each slab was monitored along the central longitudinal and transverse axes (Fig. 7.11) using displacement transducers with up to 25 mm travel. These electric resistance transducers resolve to 0.01 mm and were calibrated against a barrel micrometer. They were found to be well within the manufacturer's limits on linearity, 0.2% of full range. They were mounted beneath the slab to allow the measurement of the deflection directly below the applied load which would have been extremely difficult from the top. The displacement transducers were mounted on a frame of 62 mm x 62 mm square hollow steel section positioned below the slab. This frame was rigid and was supported by the reinforced concrete beams and giving deflections of slab relative to the beams. Because the deflection monitoring system was located below the slab it was possible that as deflections became large, the two may come into contact. This presented two problems:-

1. A displacement transducer could be seriously damaged by a slab bearing directly on it after it had reached the limit of its travel.
2. The support given to the slab through this mechanism would create unrealistic conditions of support.

To overcome these problems a bolt was fitted to the transducer bracket which would come into contact with the slab just before it would reach the limit of its travel. The bar holding the transducer was clamped to the frame and if the slab fouls the bolt it is designed so that the bar will slip when this load is applied. The deflection frames and transducers are shown in Plate 7.11.

7.6.3 Strains in the Reinforcement

The development of strains in the reinforcement in selected areas of each slab was recorded. Foil strain gauges, 3 mm long, were used with the 6 mm diameter bars and gauges 1 mm long were used with the 3 mm diameter bars. The strain gauges were attached to the side of the bar and positioned to measure the strains in what were considered to be the three most important areas defined as follows:-

1. The bottom transverse bar through the centre of the loading pad.
2. The bottom longitudinal bar through the centre of the loading pad.
3. The top transverse bar over the beam.

The positions of all strain gauges are shown in Fig. 7.12.

7.6.4 Crack Developments

In order to make visual observation of cracks as easy as possible care had been taken to ensure a good concrete surface finish and prior to testing one coat of white emulsion paint had been applied. At regular intervals during testing the surface was examined and any cracks present were highlighted with a black felt marker and the load at which they developed recorded. At the end of the test the panel

was photographed top and bottom and the crack development traced at various loads. The development of crack widths was also measured during the tests using an optical comparator.

7.7 TEST PROCEDURE

The load was applied to the slab in small increments and all deflections and strains recorded. At each load increment the load was held for a short time to allow the slab to creep and to inspect for cracks before the readings were recorded. On test panel D2 a 150 mm diameter loading shoe was used to simulate the extra distribution of load due to surfacing. The load was held at 50kN for 24 hours and the deflections due to creep recorded every hour.

As the prototype could not be built and tested within a suitable time scale only the tests of the model have been completed and the results are presented in the next chapter.

Cube	7 Day	28 Day
1	35	46.5
2	36	45.7
3	36	47.2
Av	35.6	46.4

Table 7.1 - Beam Cube Strengths N/mm^2

	Percentage of aggregate passing the following sieves					
	10 mm	5 mm	2.36 mm	1.18 mm	600 μm	300 μm
Grading of coarse sand or grit	100	99	71	23	11	3
Total aggregate grading	100	91	75	26	14	5

Table 7.2 - Sieve Analysis of Concrete Aggregate

Water	263 kg
Cement	455 kg
Sand (Zone 2)	407 kg
Sand (Coarse Grit)	876 kg
6 mm crushed basalt	555 kg

Table 7.3 - Proportions for 1 m^3 of Concrete

Test Panel	Batch	Average Cube Compressive Strength f_{cu} (N/mm^2)	Split Cylinder Tensile Strength f_t (N/mm^2)	f_t/f_{cu}
A	1	39.8	3.85	0.097
	2	40.4	3.41	0.084
	3	44.7	3.47	0.078
B	1	41.3	3.06	0.074
	2	43.5	3.18	0.073
	3	41.5	3.25	0.078
C	1	37.4	3.37	0.090
	2	38.9	3.28	0.084
	3	41.3	4.07	0.099
D	1	44.0	3.25	0.074
	2	45.6	3.47	0.076
	3	44.0	4.04	0.092
AVERAGE		41.9	3.48	0.083

Table 7.4 - Concrete Strengths at Day of Testing

Note: Cubes 100 mm, Cylinders 200 x 100 mm dia.

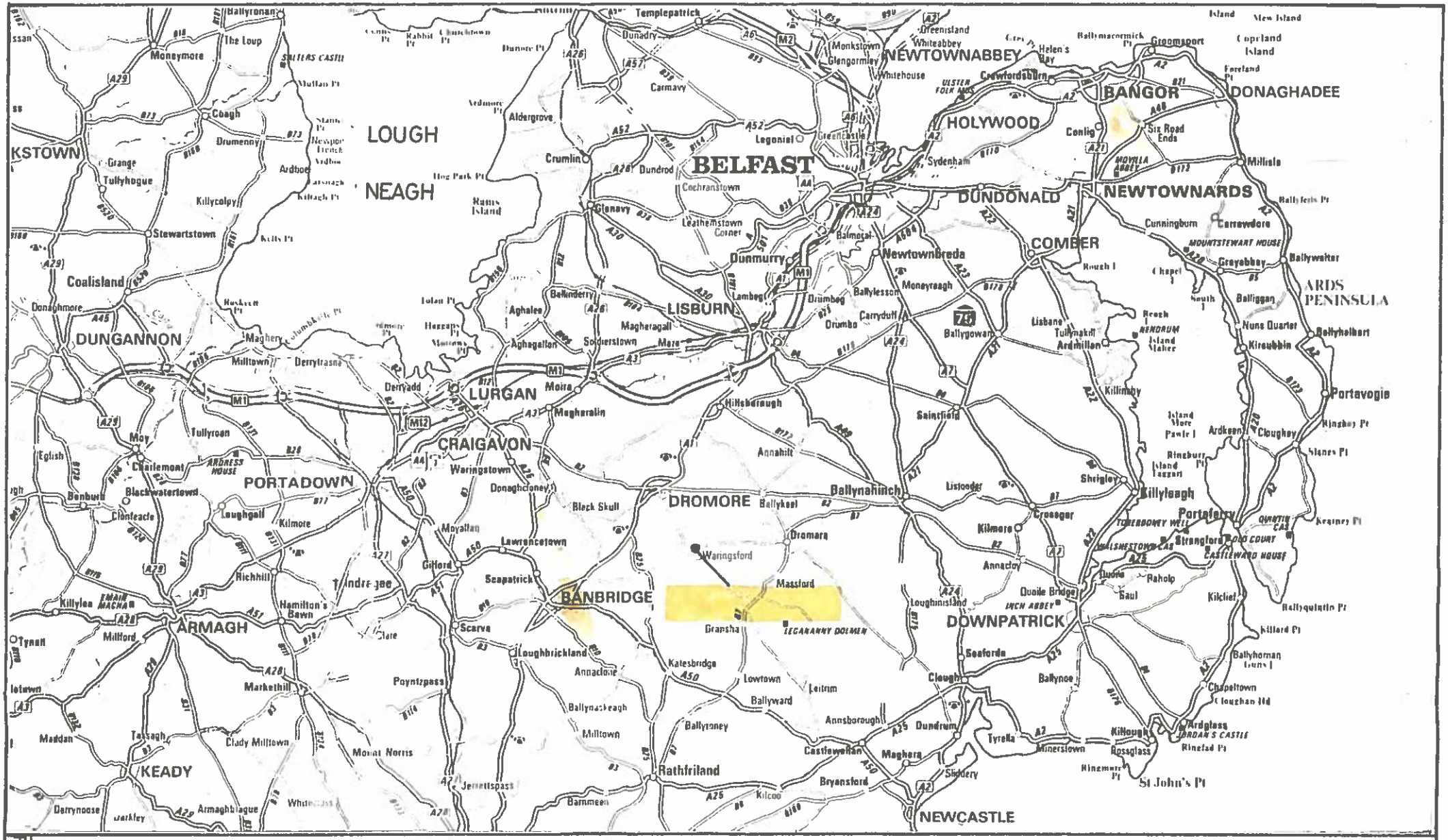
LOUGH NEAGH
BELFAST
NEWTOWNABBEY
BANGOR
DONAGHADEE
HOLYWOOD
NEWTOWNARDS
DUNDONALD
COMBER
Newtownbreda
Dunmurry
LISBURN
Moneymore
Coagh
Coalisland
DUNGANNON
Stewartstown
Killycolpy
Tullyhogue
Grange
Ballyronan
The Loup
Templepatrick
Dunadry
Carnavy
Monkstown
Glengormley
Whitehouse
Greenisland
Whiteabbey
Crawfordsburn
Helen's Bay
Groomsport
Conlig
Six Road Ends
Millisle
Cunningburn
Carrowdore
Greyabbey
Ballywalter
ARDS PENINSULA
Ballyhalbert
Portavogie
Nuns Quarter
Kircubbin
Ballyfeis Pt
Ballyquintin Pt
Killard Pt
Ballyhoman
Chapeltown
Ardglass
Killough
Rossglass
St John's Pt
Tyrella
Dundrum
Annsborough
Seaforde
Clough
Ballynoe
Ballyward
Lowtown
Leitrim
Katesbridge
Loughbrickland
Scarva
Banbridge
Waringsford
Massford
Dromara
Gransha
LEGARANNY DOLMEN
Loughinisland
Quoile Bridge
DOWNPATRICK
Saul
Raholp
Ardkeen
Cloughey
Portaferry
Strangford
Killyleagh
Shrigley
Ballynahinch
Dromore
Ballykeel
Annahilt
Hillsborough
Saintfield
Crossgar
Killinchy
Ballygowan
Carryduff
Drumbo
Ballylesson
Moneyreagh
Lambeg
Drumbeg
Belfast
Sydenham
Dundrod
Cochranstown
Leathemstown Corner
Balmoral
Cregagh
Ballyhanwood
Ballyhackamore
Knock
Belvoir
Finaghy
Malone
Stranmillis
Ormeau
Ballymacormick Pt
Copeland Island
Island Mew Island
Foreland Pt
Millisle
Ballyfeis Pt
Ballywalter
Ballyhalbert
Portavogie
Ringboy Pt
Slanes Pt
Kearney Pt
Ringhaddy Pt
Rinnamurry Pt
Rinefad Pt
Ringneill Pt
Island Taggart
Island More
Pawle I
Island Hendrum
Island Mahee
Chapel I
Rough I
Lisbane
Tullynakill
Ardmillan
Ballyalton
Ballyrainey
Ballyhenry
Ballyrenan
Ballyrolly
Ballyrogan
Ballyrush
Ballyskeagh
Ballyvester
Ballywalter
Ballywillwill
Ballywoodock
Ballyworkan
Ballyvarley
Ballyvarnet
Ballyvarra
Ballyvarrick
Ballyvarrigan
Ballyvarrin
Ballyvarrow
Ballyvarry
Ballyvarsh
Ballyvarshan
Ballyvarshin
Ballyvarshon
Ballyvarshun
Ballyvarshy
Ballyvarsk
Ballyvarskan
Ballyvarskin
Ballyvarskon
Ballyvarskun
Ballyvarsky
Ballyvarsl
Ballyvarslan
Ballyvarslin
Ballyvarslon
Ballyvarslun
Ballyvarsly
Ballyvarsm
Ballyvarsman
Ballyvarsmin
Ballyvarsmon
Ballyvarsmun
Ballyvarsmy
Ballyvarsn
Ballyvarsnan
Ballyvarsnin
Ballyvarsnon
Ballyvarsnun
Ballyvarsny
Ballyvarsp
Ballyvarspan
Ballyvarspin
Ballyvarspon
Ballyvarspun
Ballyvarspy
Ballyvarst
Ballyvarstan
Ballyvarstin
Ballyvarston
Ballyvarstun
Ballyvarsty
Ballyvarsw
Ballyvarswan
Ballyvarswin
Ballyvarswon
Ballyvarswun
Ballyvarswy
Ballyvary
Ballyvaryan
Ballyvaryin
Ballyvaryon
Ballyvaryun
Ballyvary
Ballyvarz
Ballyvarzan
Ballyvarzin
Ballyvarzon
Ballyvarzun
Ballyvarzy
Ballyvas
Ballyvasan
Ballyvasin
Ballyvason
Ballyvasun
Ballyvasy
Ballyvat
Ballyvatan
Ballyvatin
Ballyvaton
Ballyvatun
Ballyvaty
Ballyvaw
Ballyvawan
Ballyvawin
Ballyvawon
Ballyvawun
Ballyvawy
Ballyvax
Ballyvaxan
Ballyvaxin
Ballyvaxon
Ballyvaxun
Ballyvaxy
Ballyvay
Ballyvayan
Ballyvayin
Ballyvayon
Ballyvayun
Ballyvayy
Ballyvaz
Ballyvazan
Ballyvazin
Ballyvazon
Ballyvazun
Ballyvazy
Ballyvb
Ballyvban
Ballyvbin
Ballyvbon
Ballyvbun
Ballyvby
Ballyvc
Ballyvcan
Ballyvcin
Ballyvcon
Ballyvcun
Ballyvcy
Ballyvd
Ballyvdan
Ballyvdin
Ballyvdon
Ballyvdun
Ballyvdy
Ballyve
Ballyvean
Ballyvein
Ballyveon
Ballyveun
Ballyvey
Ballyvf
Ballyvfan
Ballyvfin
Ballyvfon
Ballyvfun
Ballyvfy
Ballyvg
Ballyvgan
Ballyvgin
Ballyvgon
Ballyvgun
Ballyvgy
Ballyvh
Ballyvhan
Ballyvhin
Ballyvhon
Ballyvhun
Ballyvhy
Ballyvi
Ballyvian
Ballyvin
Ballyvion
Ballyviun
Ballyviy
Ballyvj
Ballyvjan
Ballyvjin
Ballyvjon
Ballyvjun
Ballyvjy
Ballyvk
Ballyvkan
Ballyvkin
Ballyvkon
Ballyvkun
Ballyvky
Ballyvl
Ballyvlan
Ballyvlin
Ballyvlon
Ballyvlun
Ballyvly
Ballyvm
Ballyvman
Ballyvmin
Ballyvmon
Ballyvmun
Ballyvmy
Ballyvn
Ballyvnan
Ballyvnin
Ballyvnon
Ballyvnun
Ballyvny
Ballyvo
Ballyvoan
Ballyvoin
Ballyvoon
Ballyvoun
Ballyvoy
Ballyvp
Ballyvpan
Ballyvpin
Ballyvpon
Ballyvpun
Ballyvpy
Ballyvq
Ballyvqan
Ballyvqin
Ballyvqon
Ballyvqun
Ballyvqy
Ballyvr
Ballyvran
Ballyvrin
Ballyvron
Ballyvrun
Ballyvry
Ballyvs
Ballyvsan
Ballyvsin
Ballyvson
Ballyvsun
Ballyvsy
Ballyvt
Ballyvtan
Ballyvtin
Ballyvton
Ballyvtun
Ballyvty
Ballyvu
Ballyvuan
Ballyvuin
Ballyvuon
Ballyvuun
Ballyvuy
Ballyvv
Ballyvvan
Ballyvvin
Ballyvvon
Ballyvvun
Ballyvvy
Ballyvw
Ballyvwan
Ballyvwin
Ballyvwon
Ballyvwun
Ballyvwy
Ballyvx
Ballyvxan
Ballyvxin
Ballyvxon
Ballyvxun
Ballyvxy
Ballyvy
Ballyvyan
Ballyvyin
Ballyvyon
Ballyvyun
Ballyvyy
Ballyvz
Ballyvzan
Ballyvzin
Ballyvzon
Ballyvzun
Ballyvzy
Ballyw
Ballywan
Ballywin
Ballywon
Ballywun
Ballywy
Ballyx
Ballyxan
Ballyxin
Ballyxon
Ballyxun
Ballyxy
Ballyy
Ballyyan
Ballyyin
Ballyyon
Ballyyun
Ballyyy
Ballyz
Ballyzan
Ballyzin
Ballyzon
Ballyzun
Ballyzy
Ballz
Ballzan
Ballzin
Ballzon
Ballzun
Ballzy
Ballzz
Ballzzan
Ballzzin
Ballzzon
Ballzzun
Ballzzy
Ballzzz
Ballzzzan
Ballzzzin
Ballzzzon
Ballzzzun
Ballzzzy
Ballzzzz
Ballzzzzan
Ballzzzzin
Ballzzzzon
Ballzzzzun
Ballzzzzy
Ballzzzzz
Ballzzzzzan
Ballzzzzzin
Ballzzzzzon
Ballzzzzzun
Ballzzzzzy
Ballzzzzzz
Ballzzzzzzan
Ballzzzzzzin
Ballzzzzzzon
Ballzzzzzzun
Ballzzzzzzy
Ballzzzzzzz
Ballzzzzzzzan
Ballzzzzzzzin
Ballzzzzzzzon
Ballzzzzzzzun
Ballzzzzzzzy
Ballzzzzzzzz
Ballzzzzzzzzan
Ballzzzzzzzzin
Ballzzzzzzzzon
Ballzzzzzzzzun
Ballzzzzzzzzy
Ballzzzzzzzzz
Ballzzzzzzzzzan
Ballzzzzzzzzzin
Ballzzzzzzzzzon
Ballzzzzzzzzzun
Ballzzzzzzzzzy
Ballzzzzzzzzzz
Ballzzzzzzzzzzan
Ballzzzzzzzzzzin
Ballzzzzzzzzzzon
Ballzzzzzzzzzzun
Ballzzzzzzzzzzy
Ballzzzzzzzzzzz
Ballzzzzzzzzzzzan
Ballzzzzzzzzzzzin
Ballzzzzzzzzzzzon
Ballzzzzzzzzzzzun
Ballzzzzzzzzzzzy
Ballzzzzzzzzzzzz
Ballzzzzzzzzzzzzan
Ballzzzzzzzzzzzzin
Ballzzzzzzzzzzzzon
Ballzzzzzzzzzzzzun
Ballzzzzzzzzzzzzy
Ballzzzzzzzzzzzzz
Ballzzzzzzzzzzzzzan
Ballzzzzzzzzzzzzzin
Ballzzzzzzzzzzzzzon
Ballzzzzzzzzzzzzzun
Ballzzzzzzzzzzzzzy
Ballzzzzzzzzzzzzzz
Ballzzzzzzzzzzzzzzan
Ballzzzzzzzzzzzzzzin
Ballzzzzzzzzzzzzzzon
Ballzzzzzzzzzzzzzzun
Ballzzzzzzzzzzzzzzy
Ballzzzzzzzzzzzzzzz
Ballzzzzzzzzzzzzzzzan
Ballzzzzzzzzzzzzzzzin
Ballzzzzzzzzzzzzzzzon
Ballzzzzzzzzzzzzzzzun
Ballzzzzzzzzzzzzzzzy
Ballzzzzzzzzzzzzzzzz
Ballzzzzzzzzzzzzzzzzan
Ballzzzzzzzzzzzzzzzzin
Ballzzzzzzzzzzzzzzzzon
Ballzzzzzzzzzzzzzzzzun
Ballzzzzzzzzzzzzzzzzy
Ballzzzzzzzzzzzzzzzzz
Ballzzzzzzzzzzzzzzzzzan
Ballzzzzzzzzzzzzzzzzzin
Ballzzzzzzzzzzzzzzzzzon
Ballzzzzzzzzzzzzzzzzzun
Ballzzzzzzzzzzzzzzzzzy
Ballzzzzzzzzzzzzzzzzzz
Ballzzzzzzzzzzzzzzzzzzan
Ballzzzzzzzzzzzzzzzzzzin
Ballzzzzzzzzzzzzzzzzzzon
Ballzzzzzzzzzzzzzzzzzzun
Ballzzzzzzzzzzzzzzzzzzy
Ballzzzzzzzzzzzzzzzzzzz
Ballzzzzzzzzzzzzzzzzzzzan
Ballzzzzzzzzzzzzzzzzzzzin
Ballzzzzzzzzzzzzzzzzzzzon
Ballzzzzzzzzzzzzzzzzzzzun
Ballzzzzzzzzzzzzzzzzzzzy
Ballzzzzzzzzzzzzzzzzzzzz
Ballzzzzzzzzzzzzzzzzzzzzan
Ballzzzzzzzzzzzzzzzzzzzzin
Ballzzzzzzzzzzzzzzzzzzzzon
Ballzzzzzzzzzzzzzzzzzzzzun
Ballzzzzzzzzzzzzzzzzzzzzy
Ballzzzzzzzzzzzzzzzzzzzzz
Ballzzzzzzzzzzzzzzzzzzzzzan
Ballzzzzzzzzzzzzzzzzzzzzzin
Ballzzzzzzzzzzzzzzzzzzzzzon
Ballzzzzzzzzzzzzzzzzzzzzzun
Ballzzzzzzzzzzzzzzzzzzzzzy
Ballzzzzzzzzzzzzzzzzzzzzzz
Ballzzzzzzzzzzzzzzzzzzzzzzan
Ballzzzzzzzzzzzzzzzzzzzzzzin
Ballzzzzzzzzzzzzzzzzzzzzzzon
Ballzzzzzzzzzzzzzzzzzzzzzzun
Ballzzzzzzzzzzzzzzzzzzzzzzy
Ballzzzzzzzzzzzzzzzzzzzzzzz
Ballzzzzzzzzzzzzzzzzzzzzzzzan
Ballzzzzzzzzzzzzzzzzzzzzzzzin
Ballzzzzzzzzzzzzzzzzzzzzzzzon
Ballzzzzzzzzzzzzzzzzzzzzzzzun
Ballzzzzzzzzzzzzzzzzzzzzzzzy
Ballzzzzzzzzzzzzzzzzzzzzzzzz
Ballzzzzzzzzzzzzzzzzzzzzzzzzan
Ballzzzzzzzzzzzzzzzzzzzzzzzzin
Ballzzzzzzzzzzzzzzzzzzzzzzzzon
Ballzzzzzzzzzzzzzzzzzzzzzzzzun
Ballzzzzzzzzzzzzzzzzzzzzzzzzy
Ballzzzzzzzzzzzzzzzzzzzzzzzzz
Ballzzzzzzzzzzzzzzzzzzzzzzzzzan
Ballzzzzzzzzzzzzzzzzzzzzzzzzzin
Ballzzzzzzzzzzzzzzzzzzzzzzzzzon
Ballzzzzzzzzzzzzzzzzzzzzzzzzzun
Ballzzzzzzzzzzzzzzzzzzzzzzzzzy
Ballzzzzzzzzzzzzzzzzzzzzzzzzzz
Ballzzzzzzzzzzzzzzzzzzzzzzzzzzan
Ballzzzzzzzzzzzzzzzzzzzzzzzzzzin
Ballzzzzzzzzzzzzzzzzzzzzzzzzzzon
Ballzzzzzzzzzzzzzzzzzzzzzzzzzzun
Ballzzzzzzzzzzzzzzzzzzzzzzzzzzy
Ballzzzzzzzzzzzzzzzzzzzzzzzzzzz
Ballzzzzzzzzzzzzzzzzzzzzzzzzzzzan
Ballzzzzzzzzzzzzzzzzzzzzzzzzzzzin
Ballzzzzzzzzzzzzzzzzzzzzzzzzzzzon
Ballzzzzzzzzzzzzzzzzzzzzzzzzzzzun
Ballzzzzzzzzzzzzzzzzzzzzzzzzzzzy
Ballzzzzzzzzzzzzzzzzzzzzzzzzzzzz
Ballzzzzzzzzzzzzzzzzzzzzzzzzzzzzan
Ballzzzzzzzzzzzzzzzzzzzzzzzzzzzzin
Ballzzzzzzzzzzzzzzzzzzzzzzzzzzzzon
Ballzzzzzzzzzzzzzzzzzzzzzzzzzzzzun
Ballzzzzzzzzzzzzzzzzzzzzzzzzzzzzy
Ballzzzzzzzzzzzzzzzzzzzzzzzzzzzzz
Ballzzzzzzzzzzzzzzzzzzzzzzzzzzzzzan
Ballzzzzzzzzzzzzzzzzzzzzzzzzzzzzzin
Ballzzzzzzzzzzzzzzzzzzzzzzzzzzzzzon
Ballzzzzzzzzzzzzzzzzzzzzzzzzzzzzzun
Ballzzzzzzzzzzzzzzzzzzzzzzzzzzzzzy
Ballzzzzzzzzzzzzzzzzzzzzzzzzzzzzzz
Ballzzzzzzzzzzzzzzzzzzzzzzzzzzzzzzan
Ballzzzzzzzzzzzzzzzzzzzzzzzzzzzzzzin
Ballzzzzzzzzzzzzzzzzzzzzzzzzzzzzzzon
Ballzzzzzzzzzzzzzzzzzzzzzzzzzzzzzzun
Ballzzzzzzzzzzzzzzzzzzzzzzzzzzzzzzy
Ballzzzzzzzzzzzzzzzzzzzzzzzzzzzzzzz
Ballzzzzzzzzzzzzzzzzzzzzzzzzzzzzzzzan
Ballzzzzzzzzzzzzzzzzzzzzzzzzzzzzzzzin
Ballzzzzzzzzzzzzzzzzzzzzzzzzzzzzzzzon
Ballzzzzzzzzzzzzzzzzzzzzzzzzzzzzzzzun
Ballzzzzzzzzzzzzzzzzzzzzzzzzzzzzzzzy
Ballzzzzzzzzzzzzzzzzzzzzzzzzzzzzzzzz
Ballzzzzzzzzzzzzzzzzzzzzzzzzzzzzzzzzan
Ballzzzzzzzzzzzzzzzzzzzzzzzzzzzzzzzzin
Ballzzzzzzzzzzzzzzzzzzzzzzzzzzzzzzzzon
Ballzzzzzzzzzzzzzzzzzzzzzzzzzzzzzzzzun
Ballzzzzzzzzzzzzzzzzzzzzzzzzzzzzzzzzy
Ballzzzzzzzzzzzzzzzzzzzzzzzzzzzzzzzzz
Ballzzzzzzzzzzzzzzzzzzzzzzzzzzzzzzzzzan
Ballzzzzzzzzzzzzzzzzzzzzzzzzzzzzzzzzzin
Ballzzzzzzzzzzzzzzzzzzzzzzzzzzzzzzzzzon
Ballzzzzzzzzzzzzzzzzzzzzzzzzzzzzzzzzzun
Ballzzzzzzzzzzzzzzzzzzzzzzzzzzzzzzzzzy
Ballzzzzzzzzzzzzzzzzzzzzzzzzzzzzzzzzzz
Ballzzzzzzzzzzzzzzzzzzzzzzzzzzzzzzzzzzan
Ballzzzzzzzzzzzzzzzzzzzzzzzzzzzzzzzzzzin
Ballzzzzzzzzzzzzzzzzzzzzzzzzzzzzzzzzzzon
Ballzzzzzzzzzzzzzzzzzzzzzzzzzzzzzzzzzzun
Ballzzzzzzzzzzzzzzzzzzzzzzzzzzzzzzzzzzy
Ballzzzzzzzzzzzzzzzzzzzzzzzzzzzzzzzzzzz
Ballzzzzzzzzzzzzzzzzzzzzzzzzzzzzzzzzzzzan
Ballzzzzzzzzzzzzzzzzzzzzzzzzzzzzzzzzzzzin
Ballzzzzzzzzzzzzzzzzzzzzzzzzzzzzzzzzzzzon
Ballzzzzzzzzzzzzzzzzzzzzzzzzzzzzzzzzzzzun
Ballzzzzzzzzzzzzzzzzzzzzzzzzzzzzzzzzzzzy
Ballzzzzzzzzzzzzzzzzzzzzzzzzzzzzzzzzzzzz
Ballzzzzzzzzzzzzzzzzzzzzzzzzzzzzzzzzzzzzan
Ballzzzzzzzzzzzzzzzzzzzzzzzzzzzzzzzzzzzzin
Ballzzzzzzzzzzzzzzzzzzzzzzzzzzzzzzzzzzzzon
Ballzzzzzzzzzzzzzzzzzzzzzzzzzzzzzzzzzzzzun
Ballzzzzzzzzzzzzzzzzzzzzzzzzzzzzzzzzzzzzy
Ballzzzzzzzzzzzzzzzzzzzzzzzzzzzzzzzzzzzzz
Ballzzzzzzzzzzzzzzzzzzzzzzzzzzzzzzzzzzzzzan
Ballzzzzzzzzzzzzzzzzzzzzzzzzzzzzzzzzzzzzzin
Ballzzzzzzzzzzzzzzzzzzzzzzzzzzzzzzzzzzzzzon
Ballzzzzzzzzzzzzzzzzzzzzzzzzzzzzzzzzzzzzzun
Ballzzzzzzzzzzzzzzzzzzzzzzzzzzzzzzzzzzzzzy
Ballzzzzzzzzzzzzzzzzzzzzzzzzzzzzzzzzzzzzzz
Ballzzzzzzzzzzzzzzzzzzzzzzzzzzzzzzzzzzzzzzan
Ballzzzzzzzzzzzzzzzzzzzzzzzzzzzzzzzzzzzzzzin
Ballzzzzzzzzzzzzzzzzzzzzzzzzzzzzzzzzzzzzzzon
Ballzzzzzzzzzzzzzzzzzzzzzzzzzzzzzzzzzzzzzzun
Ballzzzzzzzzzzzzzzzzzzzzzzzzzzzzzzzzzzzzzzy
Ballzzzzzzzzzzzzzzzzzzzzzzzzzzzzzzzzzzzzzzz
Ballzzzzzzzzzzzzzzzzzzzzzzzzzzzzzzzzzzzzzzzan
Ballzzzzzzzzzzzzzzzzzzzzzzzzzzzzzzzzzzzzzzzin
Ballzzzzzzzzzzzzzzzzzzzzzzzzzzzzzzzzzzzzzzzon
Ballzzzzzzzzzzzzzzzzzzzzzzzzzzzzzzzzzzzzzzzun
Ballzzzzzzzzzzzzzzzzzzzzzzzzzzzzzzzzzzzzzzzy
Ballzzzzzzzzzzzzzzzzzzzzzzzzzzzzzzzzzzzzzzzz
Ballzzzzzzzzzzzzzzzzzzzzzzzzzzzzzzzzzzzzzzzzan
Ballzzzzzzzzzzzzzzzzzzzzzzzzzzzzzzzzzzzzzzzzin
Ballzzzzzzzzzzzzzzzzzzzzzzzzzzzzzzzzzzzzzzzzon
Ballzzzzzzzzzzzzzzzzzzzzzzzzzzzzzzzzzzzzzzzzun
Ballzzzzzzzzzzzzzzzzzzzzzzzzzzzzzzzzzzzzzzzzy
Ballzzzzzzzzzzzzzzzzzzzzzzzzzzzzzzzzzzzzzzzzz
Ballzzzzzzzzzzzzzzzzzzzzzzzzzzzzzzzzzzzzzzzzzan
Ballzzzzzzzzzzzzzzzzzzzzzzzzzzzzzzzzzzzzzzzzzin
Ballzzzzzzzzzzzzzzzzzzzzzzzzzzzzzzzzzzzzzzzzzon
Ballzzzzzzzzzzzzzzzzzzzzzzzzzzzzzzzzzzzzzzzzzun
Ballzzzzzzzzzzzzzzzzzzzzzzzzzzzzzzzzzzzzzzzzzy
Ballzzzzzzzzzzzzzzzzzzzzzzzzzzzzzzzzzzzzzzzzzz
Ballzzzzzzzzzzzzzzzzzzzzzzzzzzzzzzzzzzzzzzzzzzan
Ballzzzzzzzzzzzzzzzzzzzzzzzzzzzzzzzzzzzzzzzzzzin
Ballzzzzzzzzzzzzzzzzzzzzzzzzzzzzzzzzzzzzzzzzzzon
Ballzzzzzzzzzzzzzzzzzzzzzzzzzzzzzzzzzzzzzzzzzzun
Ballzzzzzzzzzzzzzzzzzzzzzzzzzzzzzzzzzzzzzzzzzzy
Ballzzzzzzzzzzzzzzzzzzzzzzzzzzzzzzzzzzzzzzzzzzz
Ballzzzzzzzzzzzzzzzzzzzzzzzzzzzzzzzzzzzzzzzzzzzan
Ballzzzzzzzzzzzzzzzzzzzzzzzzzzzzzzzzzzzzzzzzzzzin
Ballzzzzzzzzzzzzzzzzzzzzzzzzzzzzzzzzzzzzzzzzzzzon
Ballzzzzzzzzzzzzzzzzzzzzzzzzzzzzzzzzzzzzzzzzzzzun
Ballzzzzzzzzzzzzzzzzzzzzzzzzzzzzzzzzzzzzzzzzzzzy
Ballzzzzzzzzzzzzzzzzzzzzzzzzzzzzzzzzzzzzzzzzzzzz
Ballzzzzzzzzzzzzzzzzzzzzzzzzzzzzzzzzzzzzzzzzzzzzan
Ballzzzzzzzzzzzzzzzzzzzzzzzzzzzzzzzzzzzzzzzzzzzzin
Ballzzzzzzzzzzzzzzzzzzzzzzzzzzzzzzzzzzzzzzzzzzzzon
Ballzzzzzzzzzzzzzzzzzzzzzzzzzzzzzzzzzzzzzzzzzzzzun
Ballzzzzzzzzzzzzzzzzzzzzzzzzzzzzzzzzzzzzzzzzzzzzy
Ballzzzzzzzzzzzzzzzzzzzzzzzzzzzzzzzzzzzzzzzzzzzzz
Ballzzzzzzzzzzzzzzzzzzzzzzzzzzzzzzzzzzzzzzzzzzzzzan
Ballzzzzzzzzzzzzzzzzzzzzzzzzzzzzzzzzzzzzzzzzzzzzzin
Ballzzzzzzzzzzzzzzzzzzzzzzzzzzzzzzzzzzzzzzzzzzzzzon
Ballzzzzzzzzzzzzzzzzzzzzzzzzzzzzzzzzzzzzzzzzzzzzzun
Ballzzzzzzzzzzzzzzzzzzzzzzzzzzzzzzzzzzzzzzzzzzzzzy
Ballzzzzzzzzzzzzzzzzzzzzzzzzzzzzzzzzzzzzzzzzzzzzzz
Ballzzzzzzzzzzzzzzzzzzzzzzzzzzzzzzzzzzzzzzzzzzzzzzan
Ballzzzzzzzzzzzzzzzzzzzzzzzzzzzzzzzzzzzzzzzzzzzzzzin
Ballzzzzzzzzzzzzzzzzzzzzzzzzzzzzzzzzzzzzzzzzzzzzzzon
Ballzzzzzzzzzzzzzzzzzzzzzzzzzzzzzzzzzzzzzzzzzzzzzzun
Ballzzzzzzzzzzzzzzzzzzzzzzzzzzzzzzzzzzzzzzzzzzzzzzy
Ballzzzzzzzzzzzzzzzzzzzzzzzzzzzzzzzzzzzzzzzzzzzzzzz
Ballzzzzzzzzzzzzzzzzzzzzzzzzzzzzzzzzzzzzzzzzzzzzzzzan
Ballzzzzzzzzzzzzzzzzzzzzzzzzzzzzzzzzzzzzzzzzzzzzzzzin
Ballzzzzzzzzzzzzzzzzzzzzzzzzzzzzzzzzzzzzzzzzzzzzzzzon
Ballzzzzzzzzzzzzzzzzzzzzzzzzzzzzzzzzzzzzzzzzzzzzzzzun
Ballzzzzzzzzzzzzzzzzzzzzzzzzzzzzzzzzzzzzzzzzzzzzzzzy
Ballzzzzzzzzzzzzzzzzzzzzzzzzzzzzzzzzzzzzzzzzzzzzzzzz
Ballzzzzzzzzzzzzzzzzzzzzzzzzzzzzzzzzzzzzzzzzzzzzzzzzan
Ballzzzzzzzzzzzzzzzzzzzzzzzzzzzzzzzzzzzzzzzzzzzzzzzzin
Ballzzzzzzzzzzzzzzzzzzzzzzzzzzzzzzzzzzzzzzzzzzzzzzzzon
Ballzzzzzzzzzzzzzzzzzzzzzzzzzzzzzzzzzzzzzzzzzzzzzzzzun
Ballzzzzzzzzzzzzzzzzzzzzzzzzzzzzzzzzzzzzzzzzzzzzzzzzy
Ballzzzzzzzzzzzzzzzzzzzzzzzzzzzzzzzzzzzzzzzzzzzzzzzzz
Ballzzzzzzzzzzzzzzzzzzzzzzzzzzzzzzzzzzzzzzzzzzzzzzzzzan
Ballzzzzzzzzzzzzzzzzzzzzzzzzzzzzzzzzzzzzzzzzzzzzzzzzzin
Ballzzzzzzzzzzzzzzzzzzzzzzzzzzzzzzzzzzzzzzzzzzzzzzzzzon
Ballzzzzzzzzzzzzzzzzzzzzzzzzzzzzzzzzzzzzzzzzzzzzzzzzzun
Ballzzzzzzzzzzzzzzzzzzzzzzzzzzzzzzzzzzzzzzzzzzzzzzzzzy
Ballzzzzzzzzzzzzzzzzzzzzzzzzzzzzzzzzzzzzzzzzzzzzzzzzzz
Ballzzzzzzzzzzzzzzzzzzzzzzzzzzzzzzzzzzzzzzzzzzzzzzzzzzan
Ballzzzzzzzzzzzzzzzzzzzzzzzzzzzzzzzzzzzzzzzzzzzzzzzzzzin
Ballzzzzzzzzzzzzzzzzzzzzzzzzzzzzzzzzzzzzzzzzzzzzzzzzzzon
Ballzzzzzzzzzzzzzzzzzzzzzzzzzzzzzzzzzzzzzzzzzzzzzzzzzzun
Ballzzzzzzzzzzzzzzzzzzzzzzzzzzzzzzzzzzzzzzzzzzzzzzzzzzy
Ballzzzzzzzzzzzzzzzzzzzzzzzzzzzzzzzzzzzzzzzzzzzzzzzzzzz
Ballzzzzzzzzzzzzzzzzzzzzzzzzzzzzzzzzzzzzzzzzzzzzzzzzzzzan
Ballzzzzzzzzzzzzzzzzzzzzzzzzzzzzzzzzzzzzzzzzzzzzzzzzzzzin
Ballzzzzzzzzzzzzzzzzzzzzzzzzzzzzzzzzzzzzzzzzzzzzzzzzzzzon
Ballzzzzzzzzzzzzzzzzzzzzzzzzzzzzzzzzzzzzzzzzzzzzzzzzzzzun
Ballzzzzzzzzzzzzzzzzzzzzzzzzzzzzzzzzzzzzzzzzzzzzzzzzzzzy
Ballzzzzzzzzzzzzzzzzzzzzzzzzzzzzzzzzzzzzzzzzzzzzzzzzzzzz
Ballzzzzzzzzzzzzzzzzzzzzzzzzzzzzzzzzzzzzzzzzzzzzzzzzzzzzan
Ballzzzzzzzzzzzzzzzzzzzzzzzzzzzzzzzzzzzzzzzzzzzzzzzzzzzzin
Ballzzzzzzzzzzzzzzzzzzzzzzzzzzzzzzzzzzzzzzzzzzzzzzzzzzzzon
Ballzzzzzzzzzzzzzzzzzzzzzzzzzzzzzzzzzzzzzzzzzzzzzzzzzzzzun
Ballzzzzzzzzzzzzzzzzzzzzzzzzzzzzzzzzzzzzzzzzzzzzzzzzzzzzy
Ballzzzzzzzzzzzzzzzzzzzzzzzzzzzzzzzzzzzzzzzzzzzzzzzzzzzzz
Ballzzzzzzzzzzzzzzzzzzzzzzzzzzzzzzzzzzzzzzzzzzzzzzzzzzzzzan
Ballzzzzzzzzzzzzzzzzzzzzzzzzzzzzzzzzzzzzzzzzzzzzzzzzzzzzzin
Ballzzzzzzzzzzzzzzzzzzzzzzzzzzzzzzzzzzzzzzzzzzzzzzzzzzzzzon
Ballzzzzzzzzzzzzzzzzzzzzzzzzzzzzzzzzzzzzzzzzzzzzzzzzzzzzzun
Ballzzzzzzzzzzzzzzzzzzzzzzzzzzzzzzzzzzzzzzzzzzzzzzzzzzzzzy
Ballzzzzzzzzzzzzzzzzzzzzzzzzzzzzzzzzzzzzzzzzzzzzzzzzzzzzzz
Ballzzzzzzzzzzzzzzzzzzzzzzzzzzzzzzzzzzzzzzzzzzzzzzzzzzzzzzan
Ballzzzzzzzzzzzzzzzzzzzzzzzzzzzzzzzzzzzzzzzzzzzzzzzzzzzzzzin
Ballzzzzzzzzzzzzzzzzzzzzzzzzzzzzzzzzzzzzzzzzzzzzzzzzzzzzzzon
Ballzzzzzzzzzzzzzzzzzzzzzzzzzzzzzzzzzzzzzzzzzzzzzzzzzzzzzzun
Ballzzzzzzzzzzzzzzzzzzzzzzzzzzzzzzzzzzzzzzzzzzzzzzzzzzzzzzy
Ballzzzzzzzzzzzzzzzzzzzzzzzzzzzzzzzzzzzzzzzzzzzzzzzzzzzzzzz
Ballzzzzzzzzzzzzzzzzzzzzzzzzzzzzzzzzzzzzzzzzzzzzzzzzzzzzzzzan
Ballzzzzzzzzzzzzzzzzzzzzzzzzzzzzzzzzzzzzzzzzzzzzzzzzzzzzzzzin
Ballzzzzzzzzzzzzzzzzzzzzzzzzzzzzzzzzzzzzzzzzzzzzzzzzzzzzzzzon
Ballzzzzzzzzzzzzzzzzzzzzzzzzzzzzzzzzzzzzzzzzzzzzzzzzzzzzzzzun
Ballzzzzzzzzzzzzzzzzzzzzzzzzzzzzzzzzzzzzzzzzzzzzzzzzzzzzzzzy
Ballzzzzzzzzzzzzzzzzzzzzzzzzzzzzzzzzzzzzzzzzzzzzzzzzzzzzzzzz
Ballzzzzzzzzzzzzzzzzzzzzzzzzzzzzzzzzzzzzzzzzzzzzzzzzzzzzzzzzan
Ballzzzzzzzzzzzzzzzzzzzzzzzzzzzzzzzzzzzzzzzzzzzzzzzzzzzzzzzzin
Ballzzzzzzzzzzzzzzzzzzzzzzzzzzzzzzzzzzzzzzzzzzzzzzzzzzzzzzzzon
Ballzzzzzzzzzzzzzzzzzzzzzzzzzzzzzzzzzzzzzzzzzzzzzzzzzzzzzzzzun
Ballzzzzzzzzzzzzzzzzzzzzzzzzzzzzzzzzzzzzzzzzzzzzzzzzzzzzzzzzy
Ballzzzzzzzzzzzzzzzzzzzzzzzzzzzzzzzzzzzzzzzzzzzzzzzzzzzzzzzzz
Ballzzzzzzzzzzzzzzzzzzzzzzzzzzzzzzzzzzzzzzzzzzzzzzzzzzzzzzzzzan
Ballzzzzzzzzzzzzzzzzzzzzzzzzzzzzzzzzzzzzzzzzzzzzzzzzzzzzzzzzzin
Ballzzzzzzzzzzzzzzzzzzzzzzzzzzzzzzzzzzzzzzzzzzzzzzzzzzzzzzzzzon
Ballzzzzzzzzzzzzzzzzzzzzzzzzzzzzzzzzzzzzzzzzzzzzzzzzzzzzzzzzzun
Ballzzzzzzzzzzzzzzzzzzzzzzzzzzzzzzzzzzzzzzzzzzzzzzzzzzzzzzzzzy
Ballz

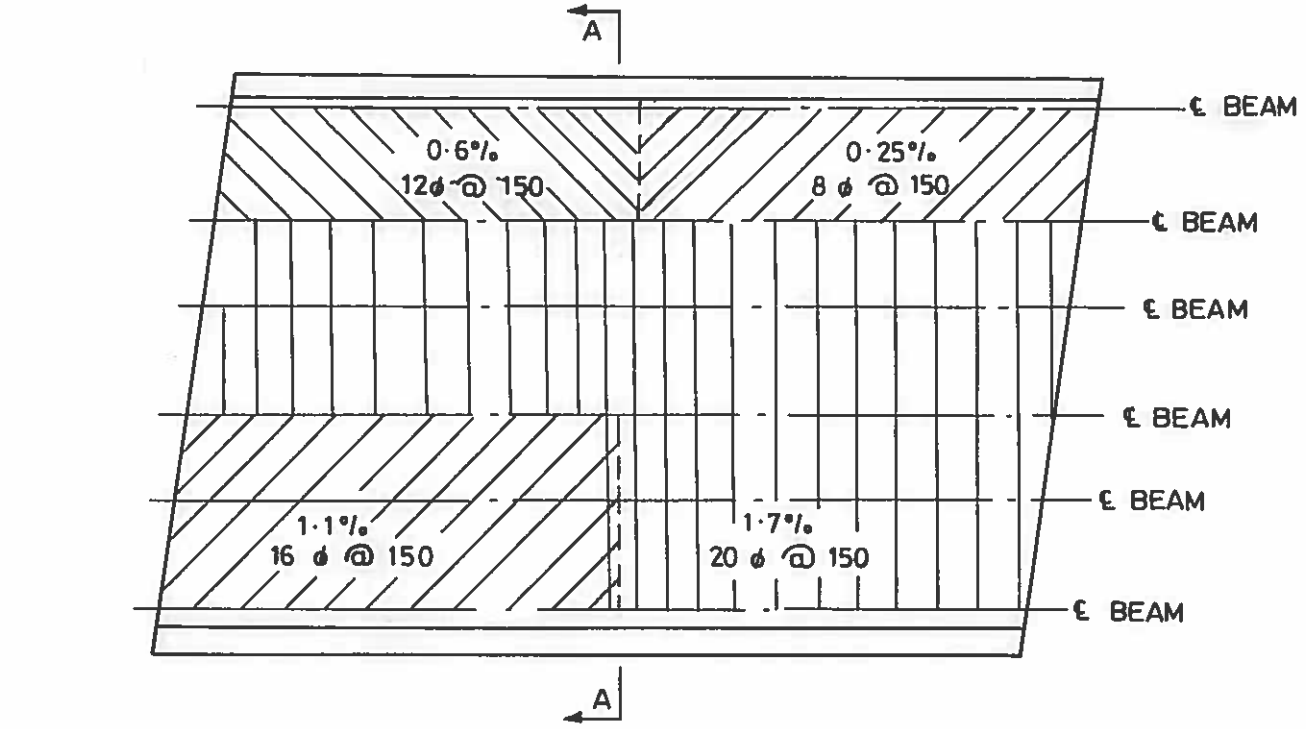

PLAN

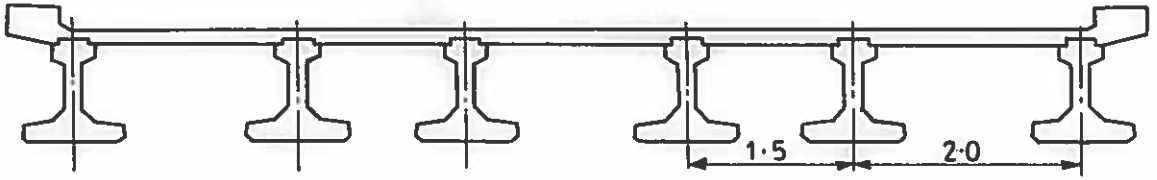

EFFECTIVE SPAN 14 m
SKEW 8°

SECTION A-A

Fig. 7.2. Reinforcement Details For Clinghans Bridge

Fig.7.2

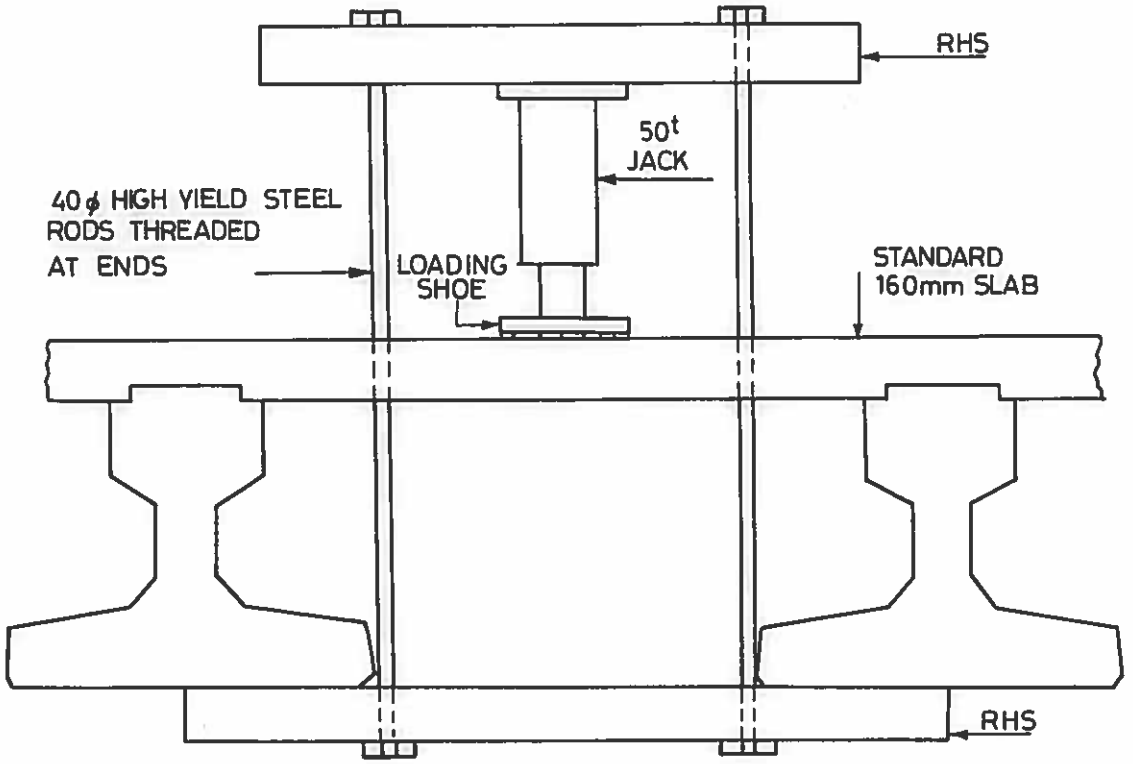

Section Through Deck

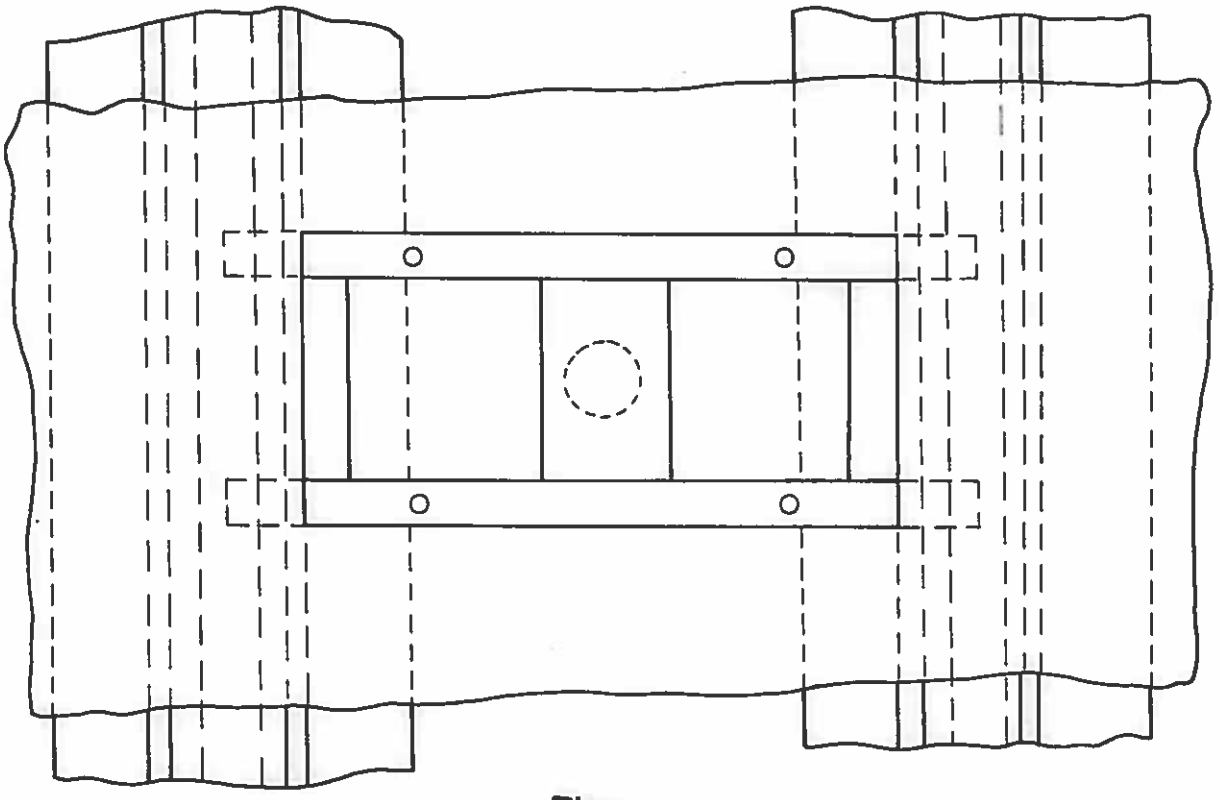

Plan

Fig. 7.3 Diagrammatic Sketch of Proposed Test Rig For Clinghans Bridge

Fig-7.3

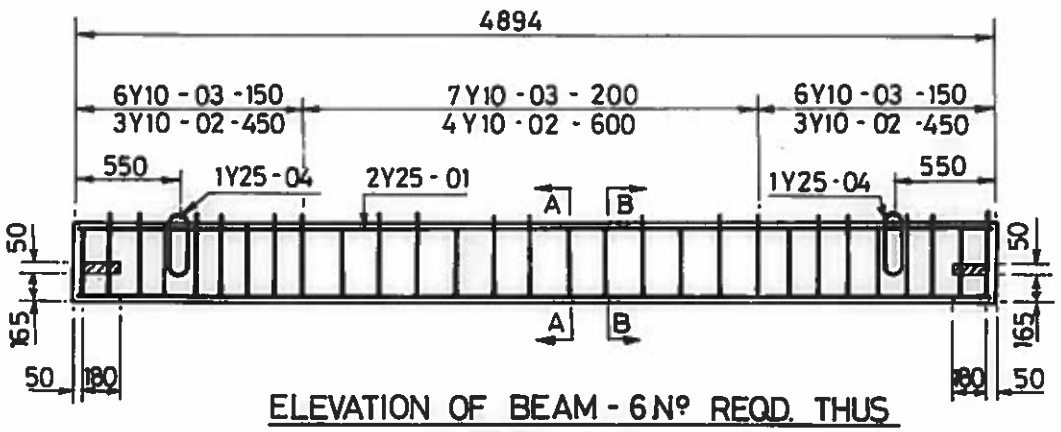

ELEVATION OF BEAM - 6 Nº REQD. THUS
Scale 1:40

PLAN OF BEAM
Scale 1:40

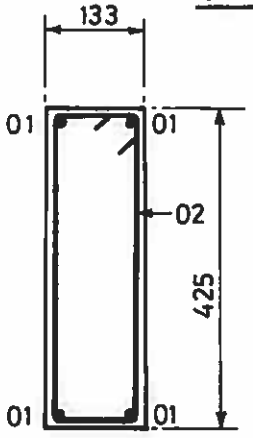

SECTION AA
Scale 1:10

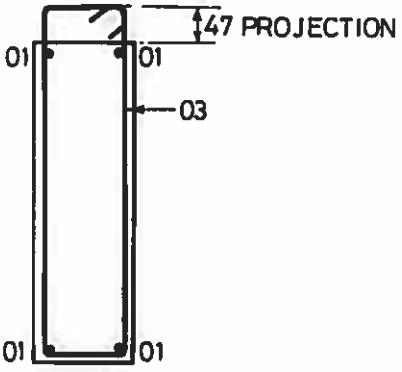

SECTION BB
Scale 1:10

BAR BENDING SCHEDULE

MEMBER	BAR MARK	TYPE & SIZE	Nº OF MEMBER	Nº IN EACH	TOTAL Nº	LENGTH OF BAR	SHAPE CODE	A	B
BEAM	01	Y 25	6	4	24	4855	20	STRAIGHT	
	02	Y10	6	10	60	1080	60	365	75
	03	Y10	6	19	114	1210	60	430	75
	04	Y25	6	2	12	1550	81	350	100

Fig. 7.4 Detail of Reinforced Concrete Beam

Fig. 7.4

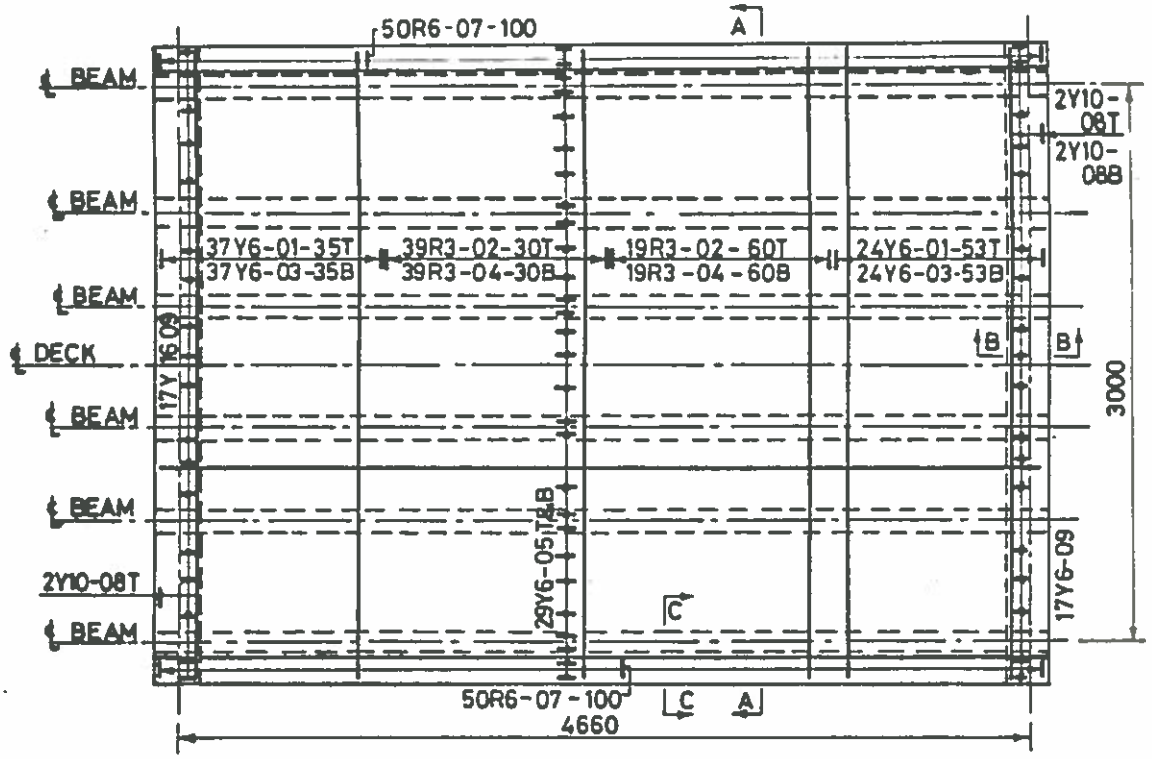

PLAN OF BRIDGE DECK

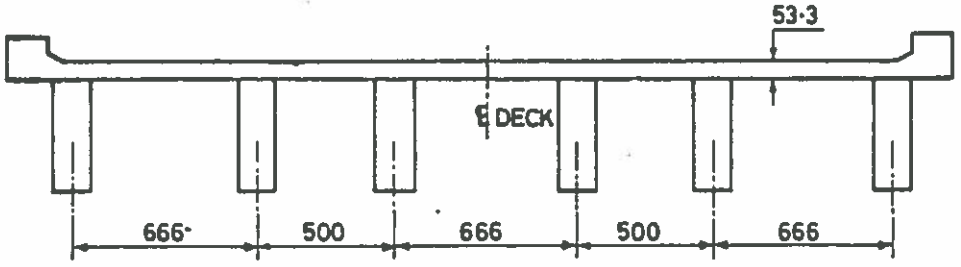

SECTION A A

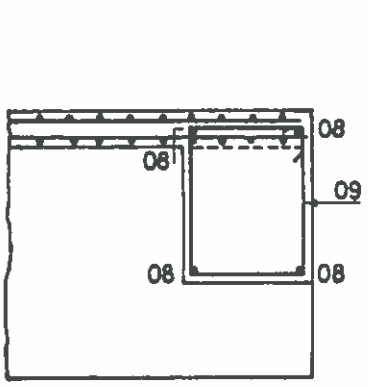

SECTION B B

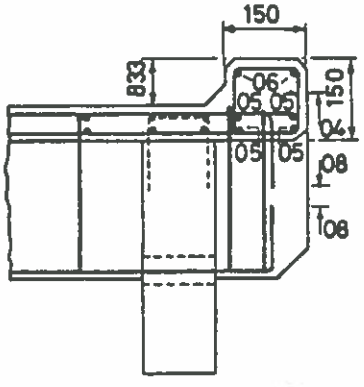

SECTION C C

Fig. 7.5 (Sheet 1) Details Of 1/3 Scale Model

Fig. 7.5

Member	Bar Mark	Type & Size	N° of Member	N° in Each	Total N°	Length Each bar	Shape Code	A	B
Slab	01	Y6	1	61	61	3460	20		
	02	R3	1	58	58	3460	20		
	03	Y6	1	61	61	3670	35	3468	
	04	R3	1	58	58	3670	35	3468	
	05	Y6	1	58	58	4880	20		
Parapet	06	Y6	2	2	4	5080	35	4880	
	07	Y6	2	50	100	625	60	126	126
Diaphragm	08	Y10	2	4	8	3460	38	120	3450
	09	Y6	2	17	34	1140	60	290	222

Fig. 7.5 (Sheet 2) Bar Bending Schedule

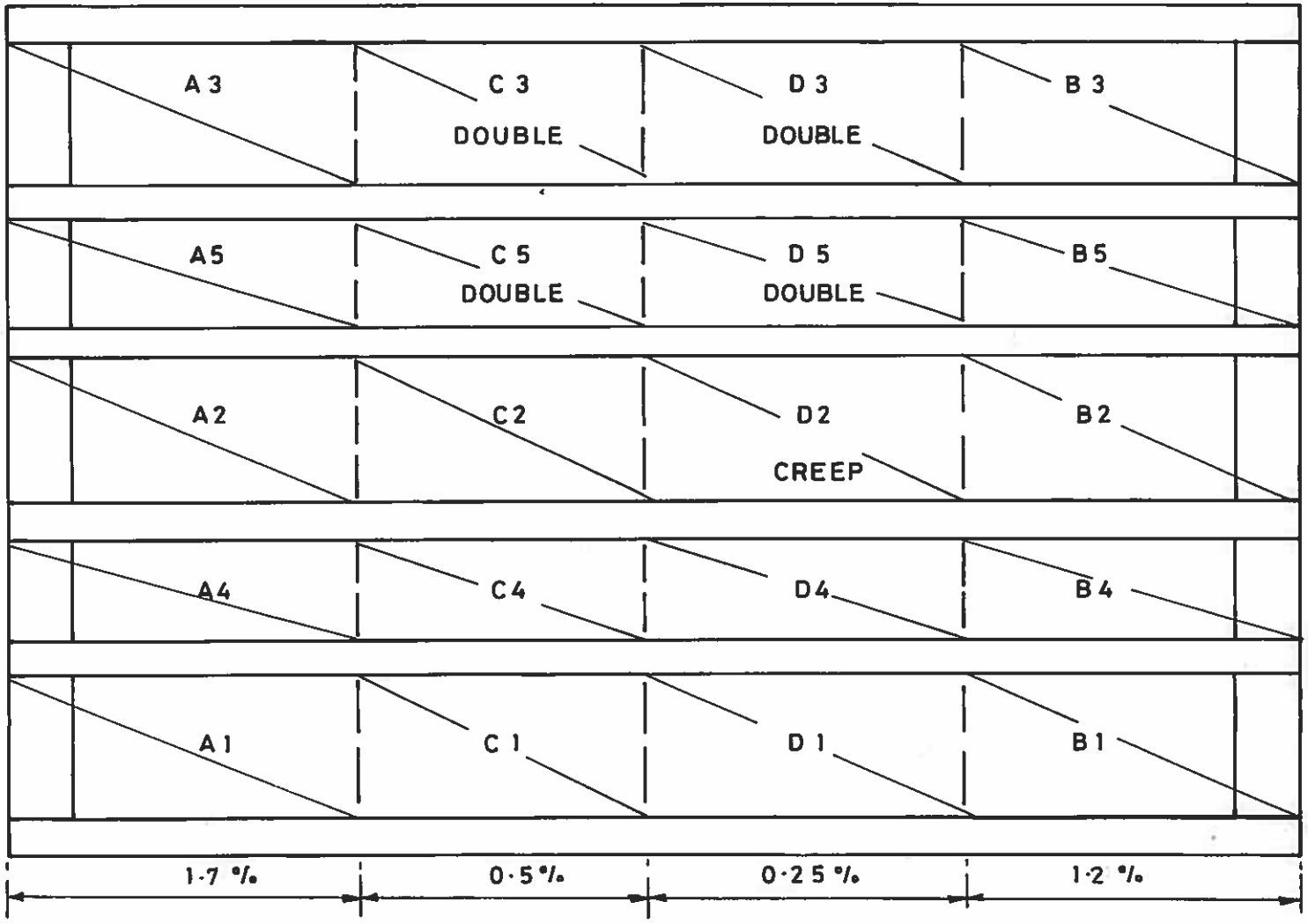

Fig. 7.6 Notation For Test Panels

Fig.7.6

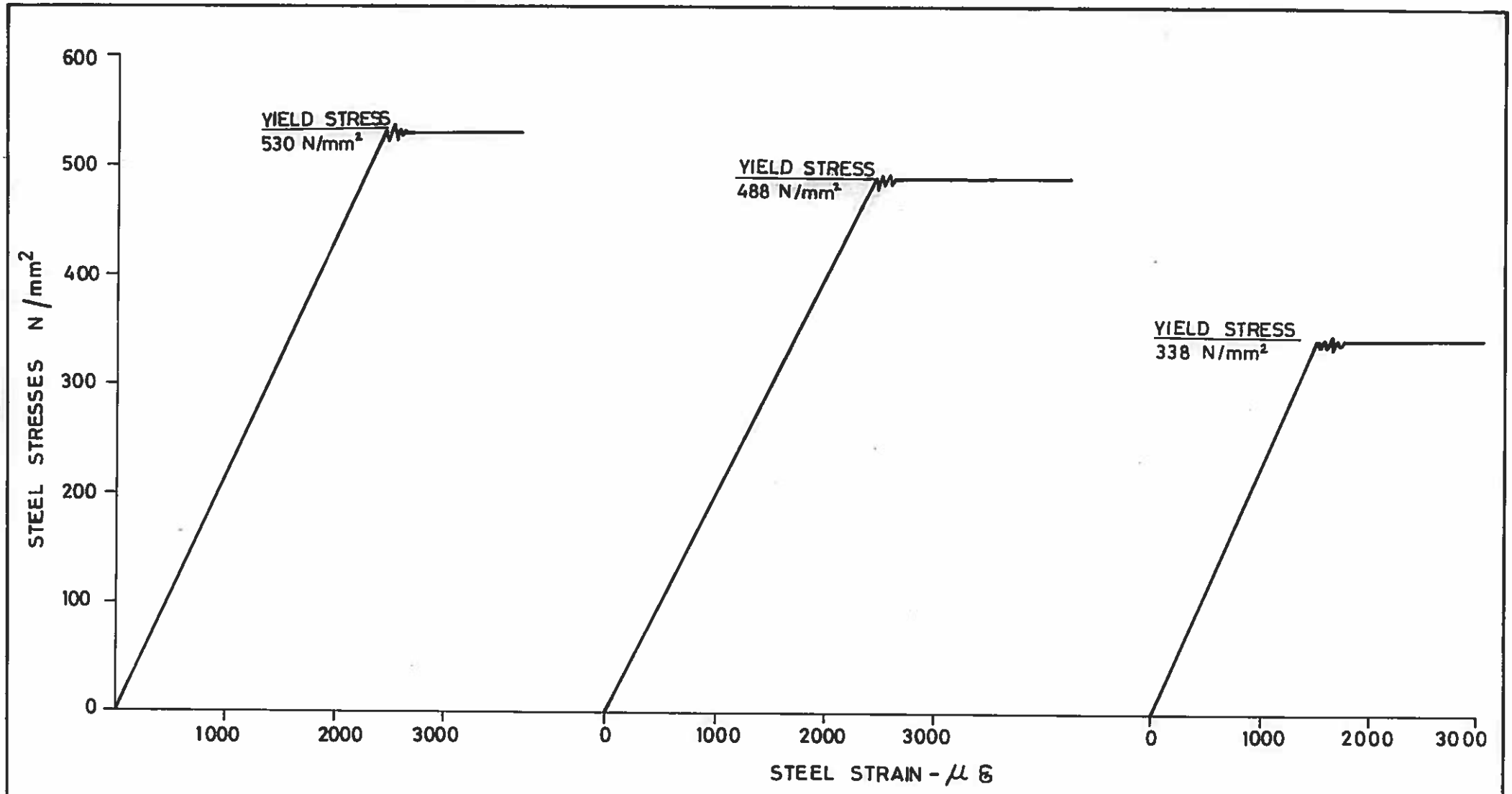

Fig. 7.7 Stress Strain Graphs For Slab Reinforcement

Fig.7.7

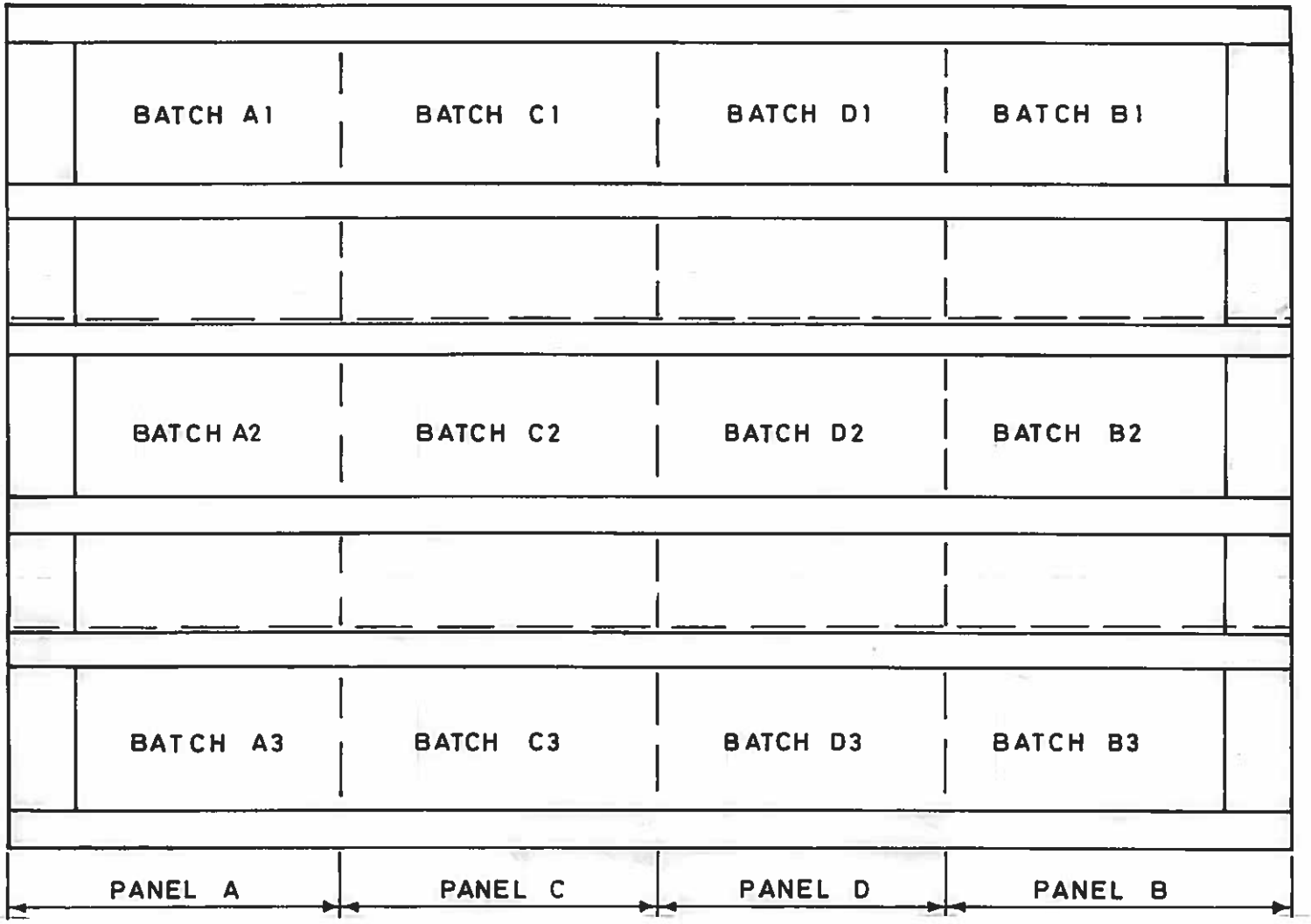

Fig. 7.8 Positions Of Concrete Batches

Fig. 7.8

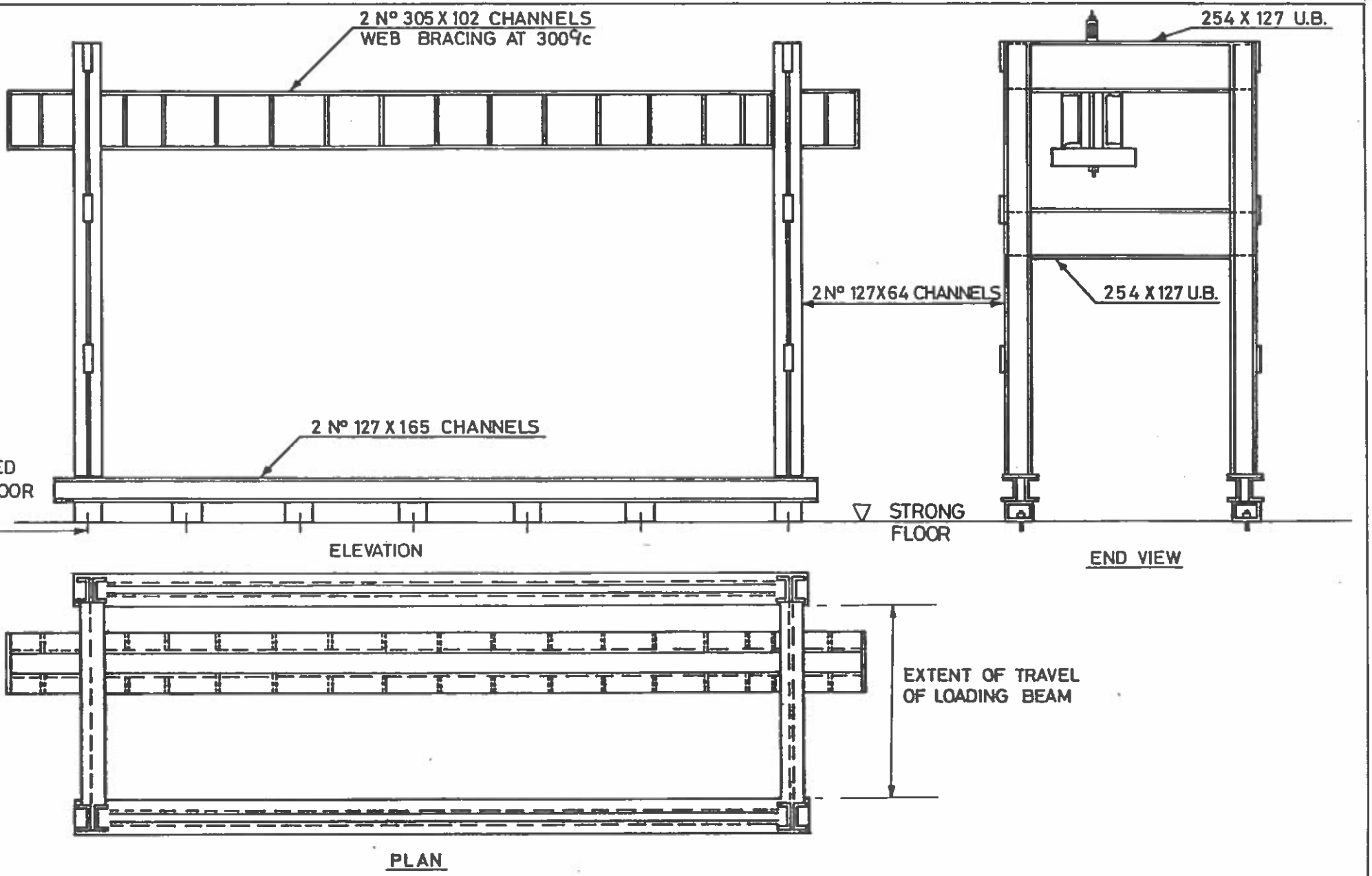

Fig. 7.9

Fig. 7.9 Details Of Test Frame

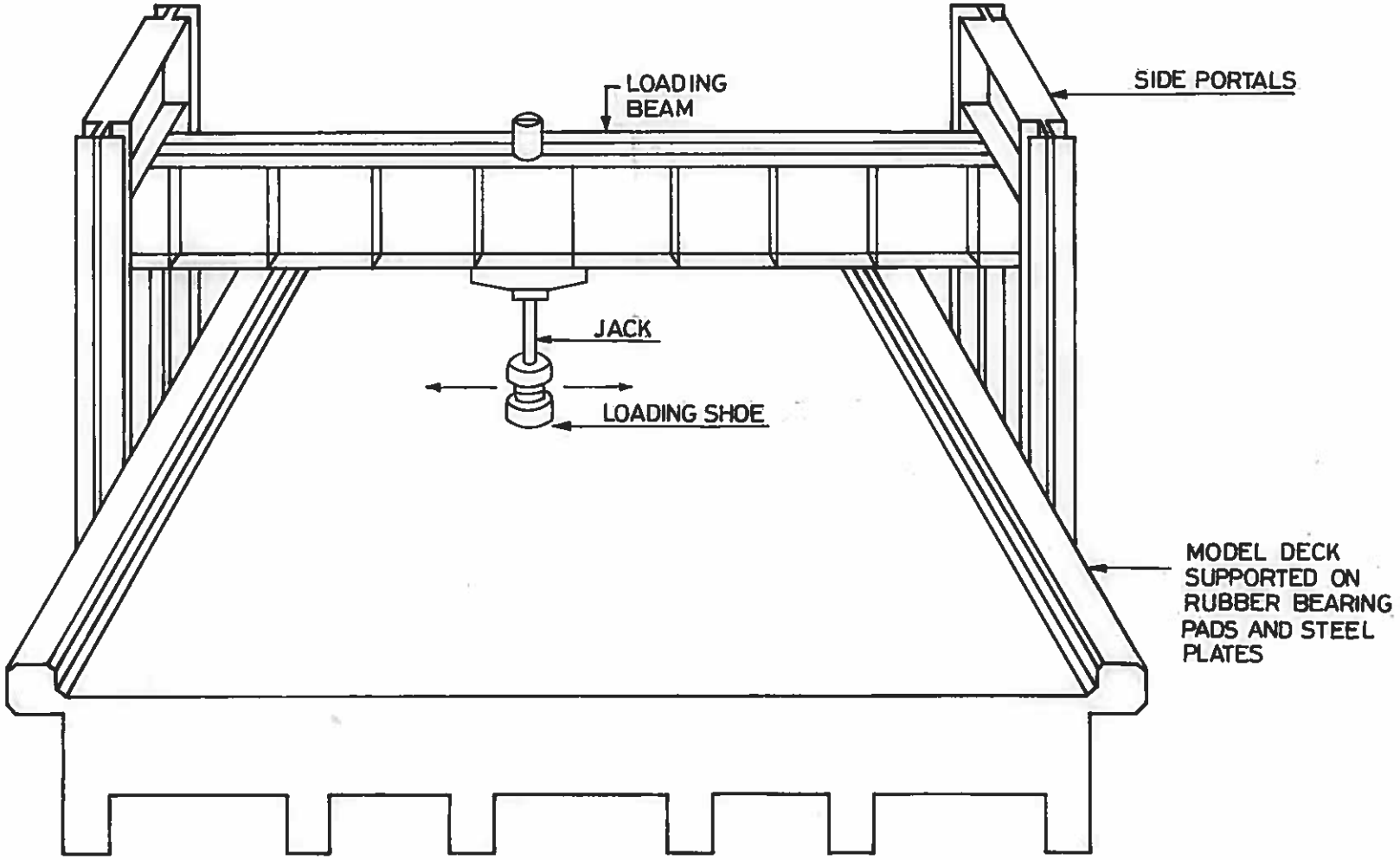

Fig. 7.10 View of Test Frame and Model

Fig. 7.10

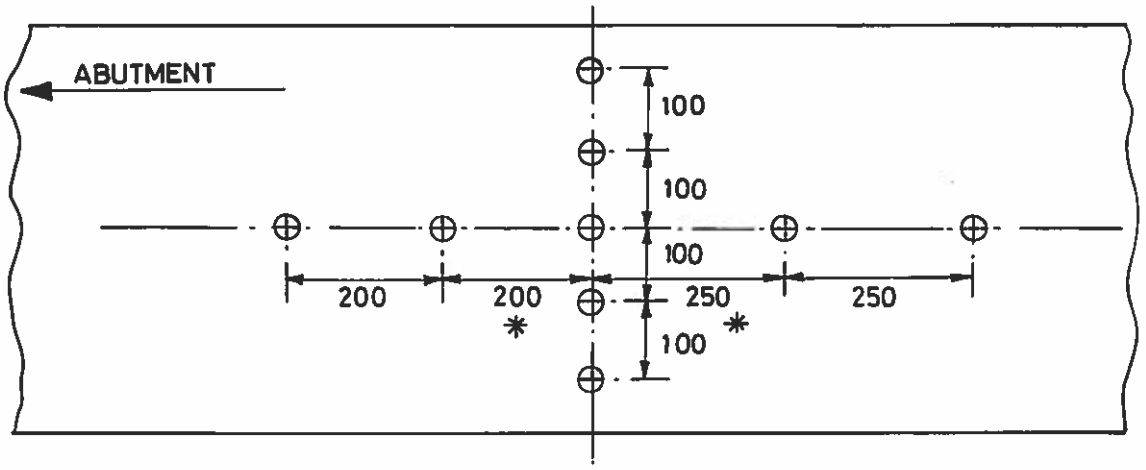

(a) Large Panels

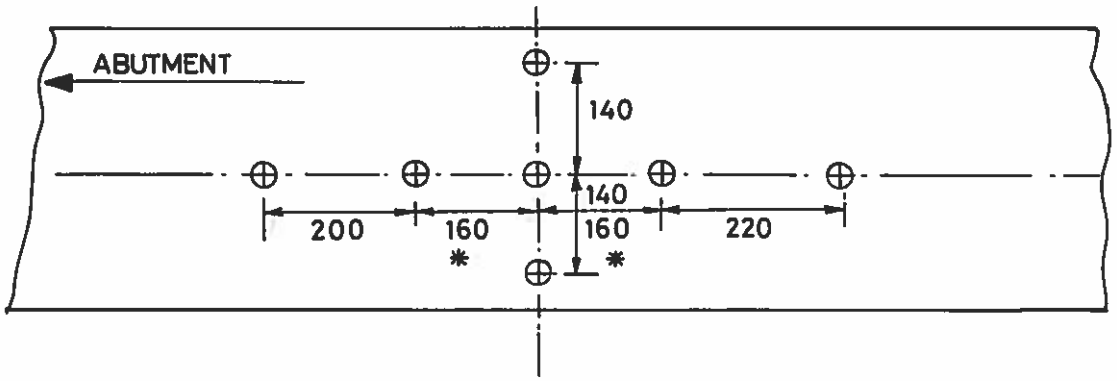

(b) Small Panels

For double wheel load, dimensions marked * were increased to 300 mm

Fig.7.11 Typical Position of Deflection Transducers

Fig.7.11

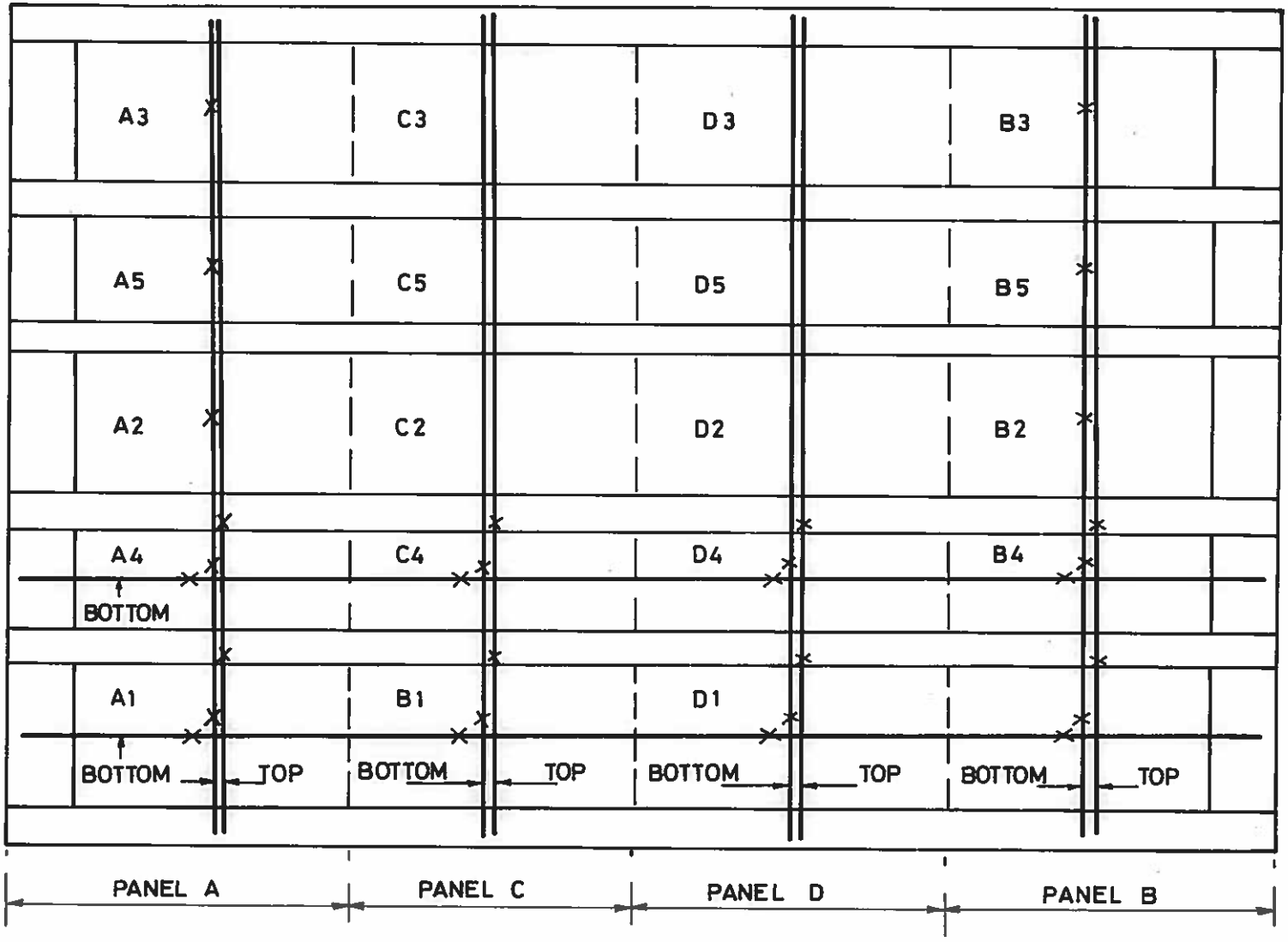

Fig. 7.12 Position of Reinforcement Strain Guages

Fig.7.12

Plate 7.1 Clinghans Bridge Site

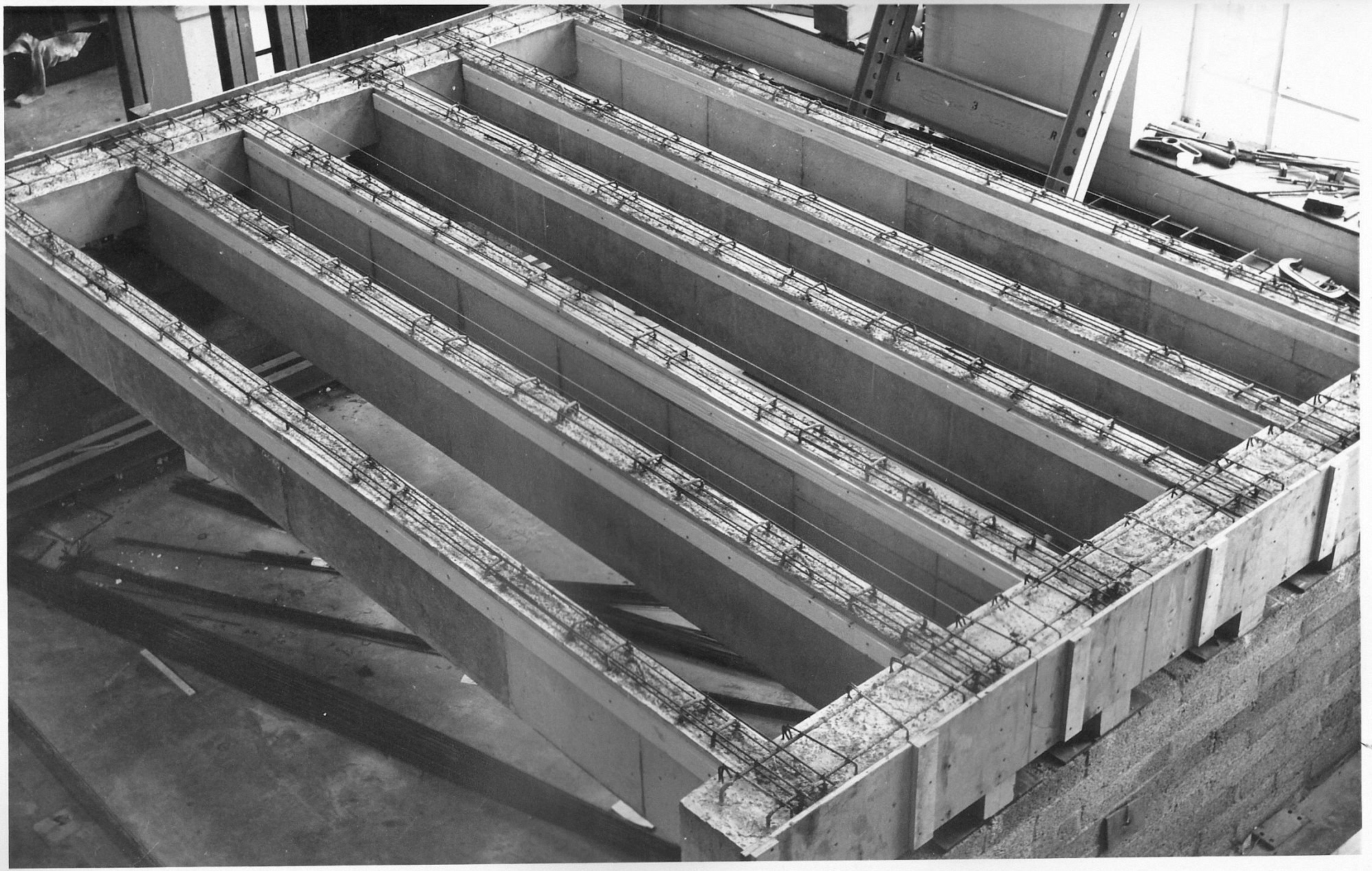

Plate 7.2 Model Beams and Diaphragms

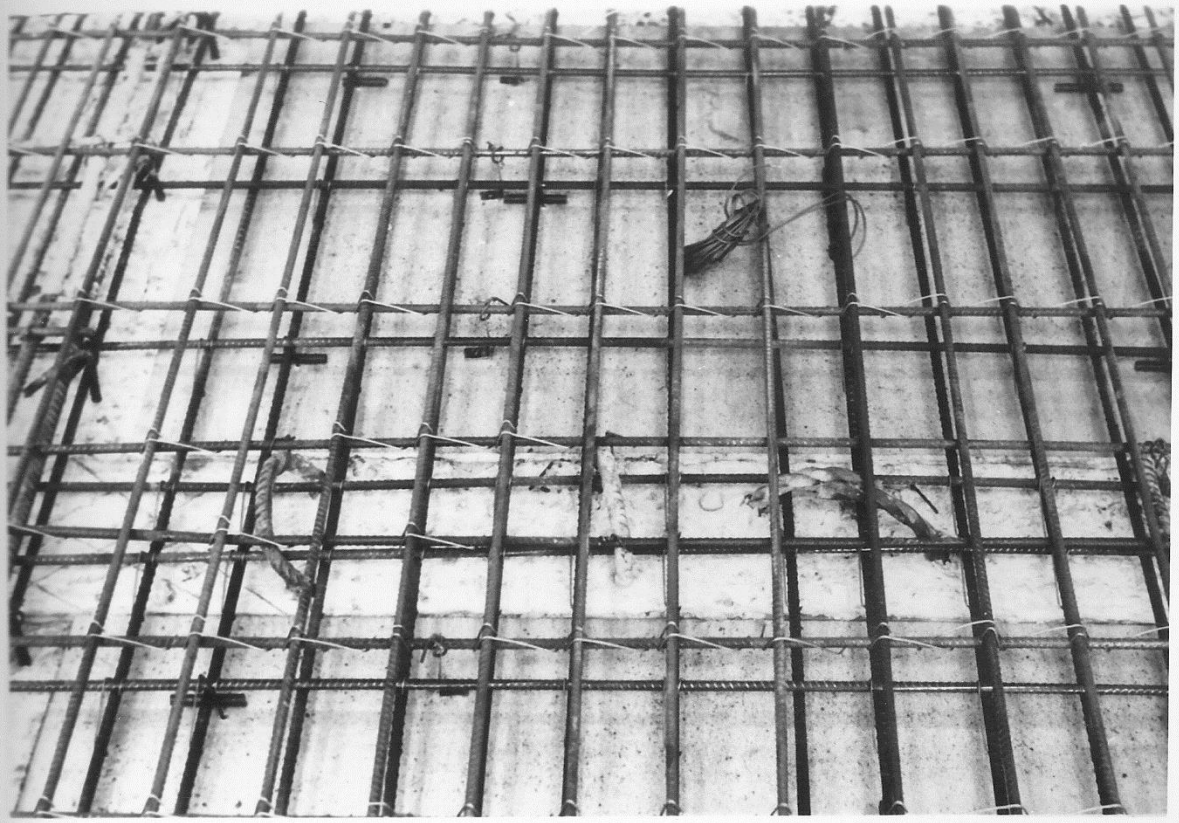

Plate 7.3 Typical Deck Reinforcement

Plate 7.4 Parapet Upstand Reinforcement

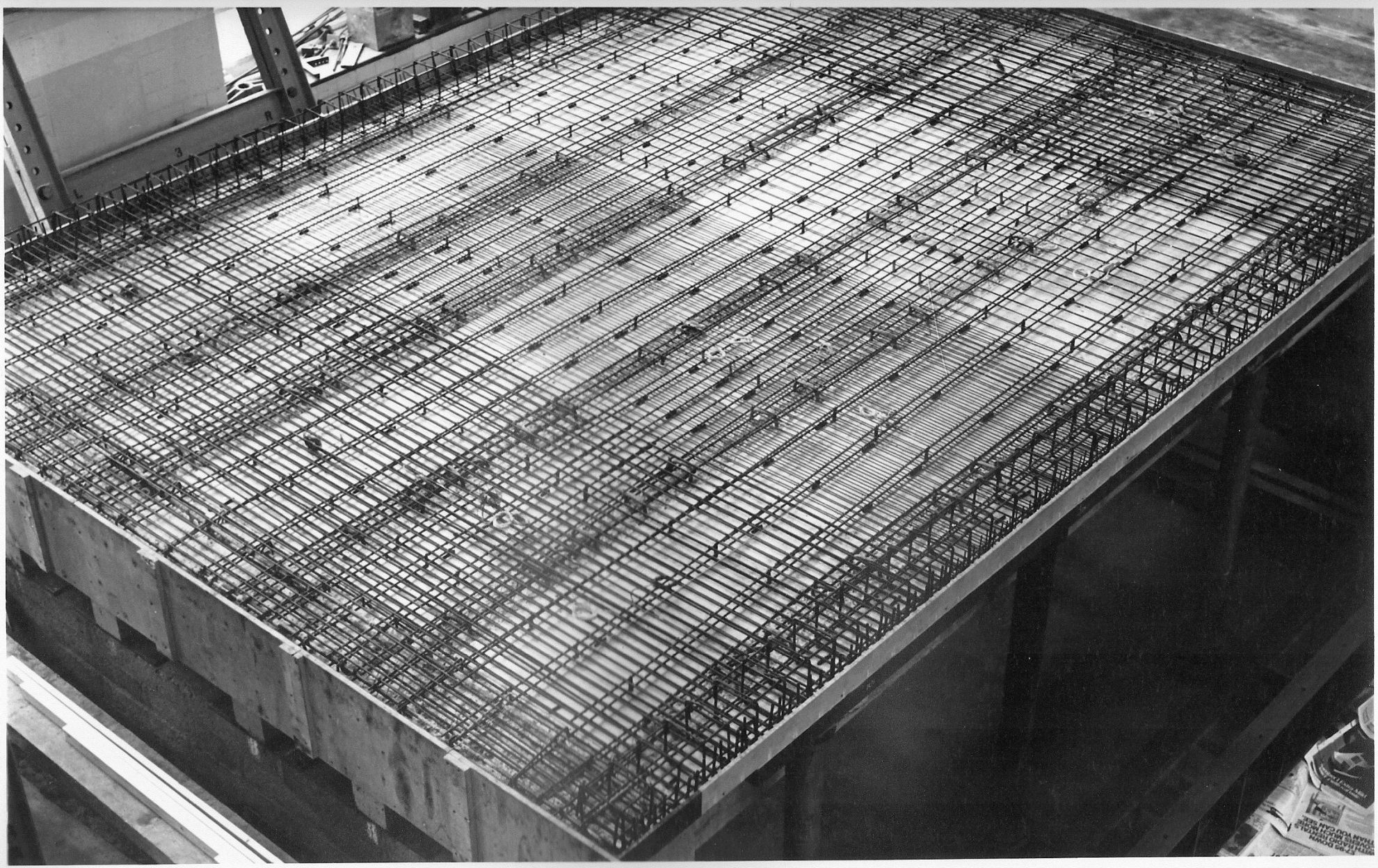

Plate 7.5 Completed Deck Reinforcement

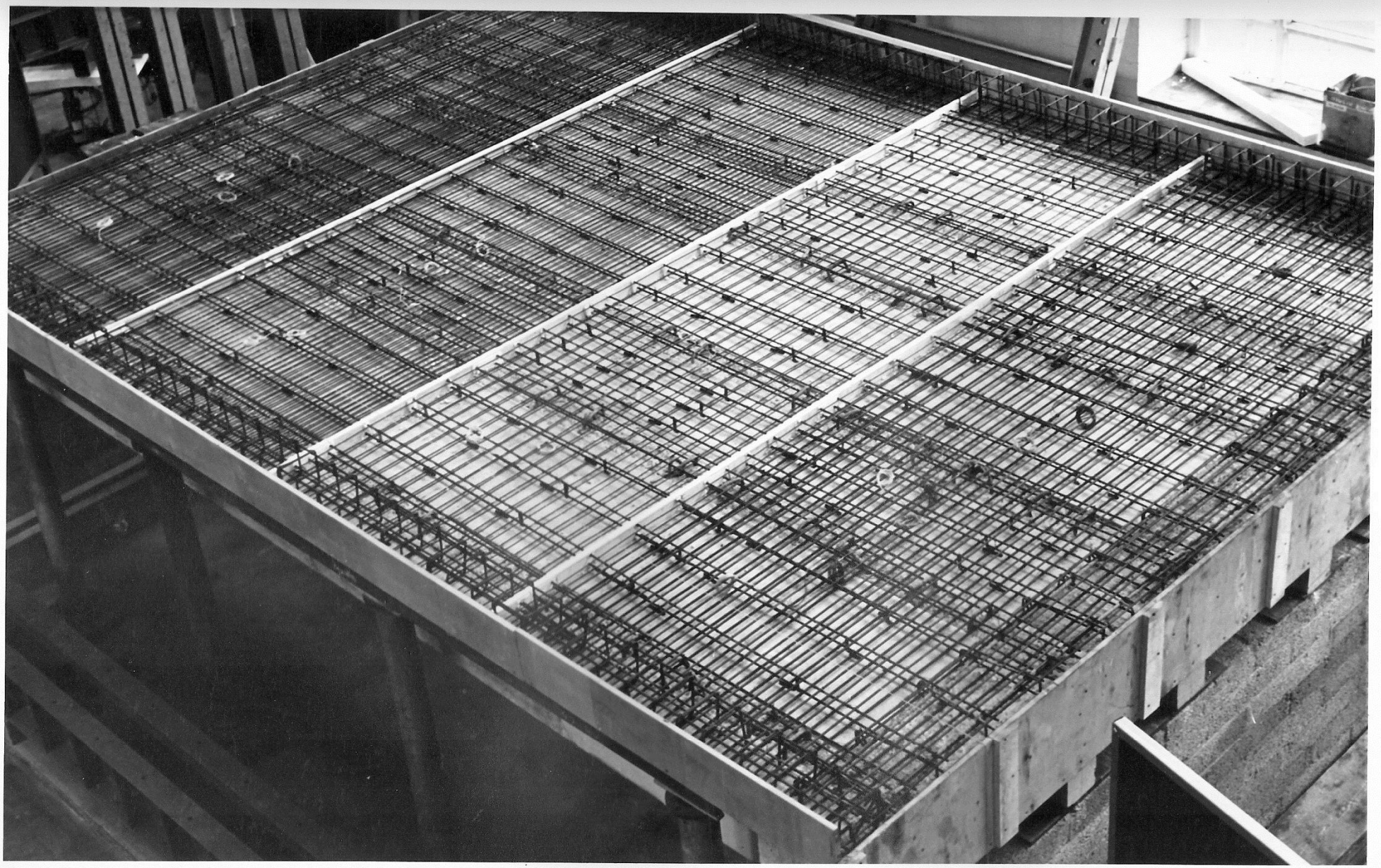

Plate 7.6 Completed Deck Reinforcement with End Stops for Casting

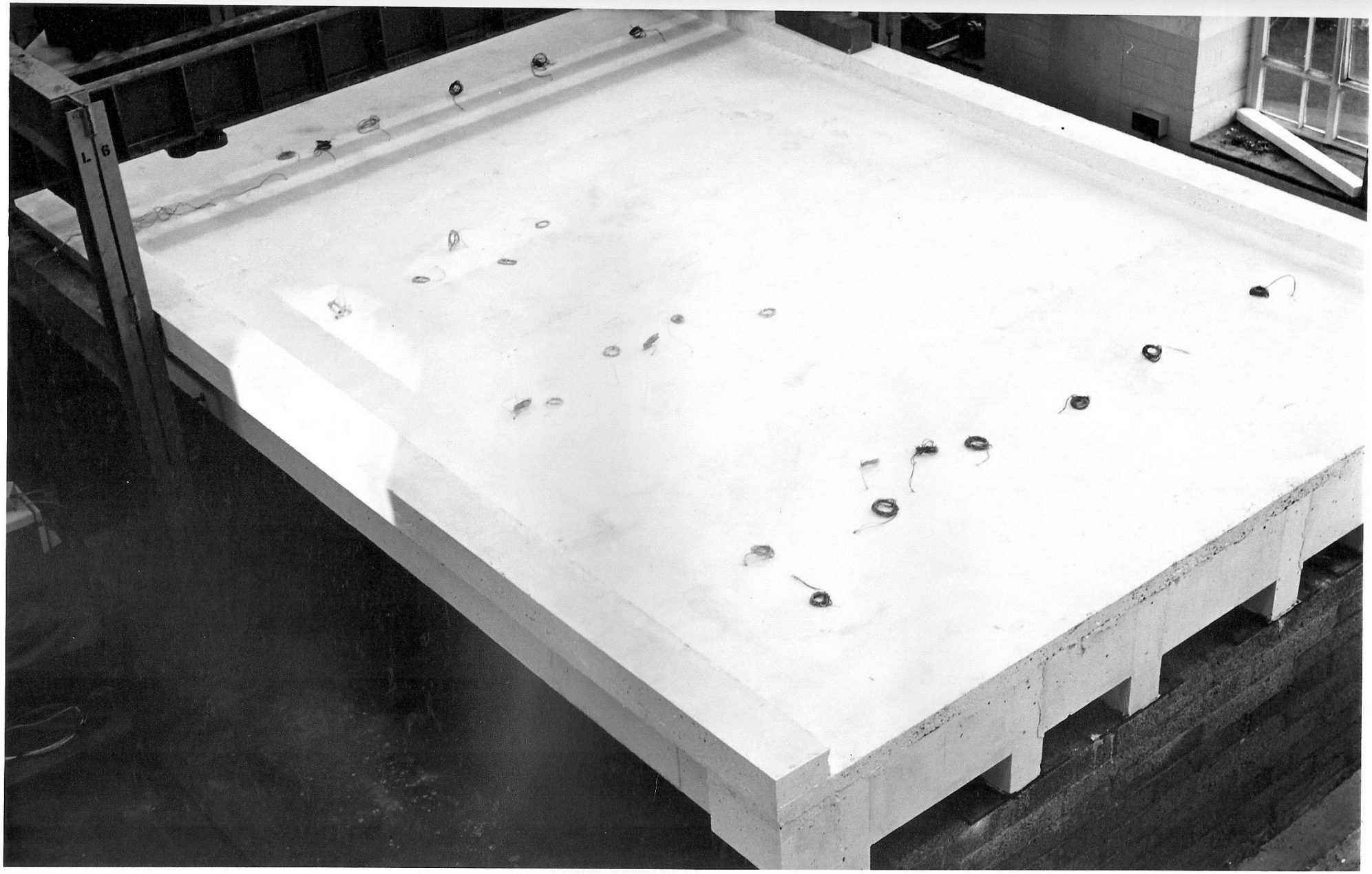

Plate 7.7 Model Deck and Test Frame

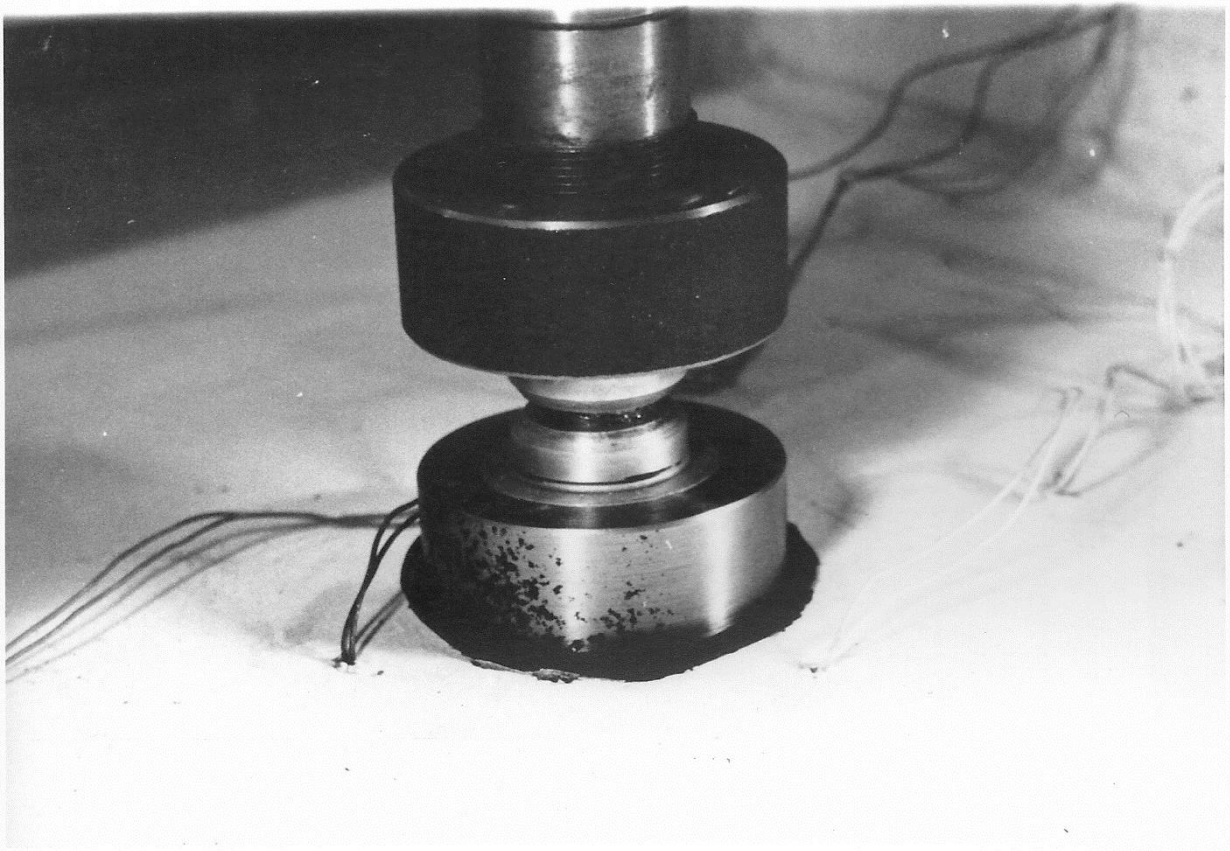

Plate 7.8 Single Wheel Loading Shoe

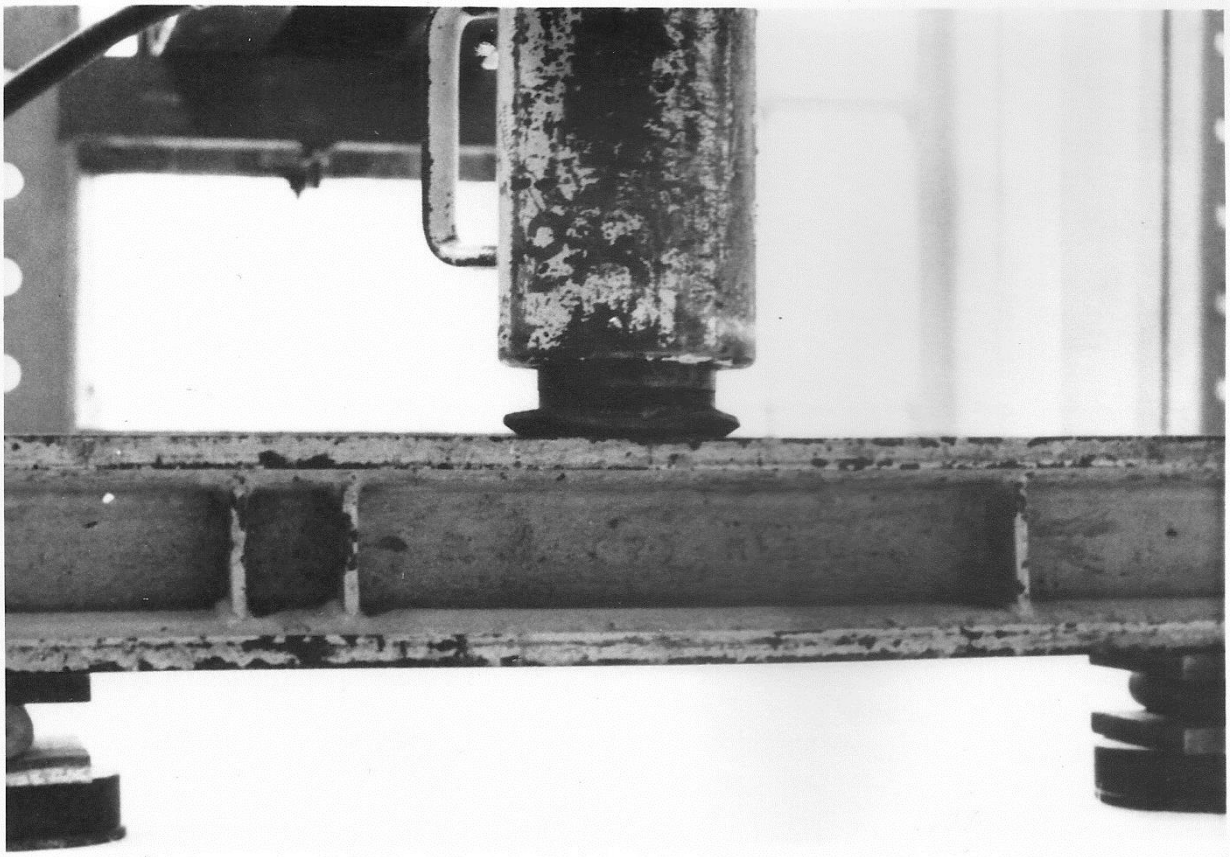

Plate 7.9 Double Wheel Loading Shoe

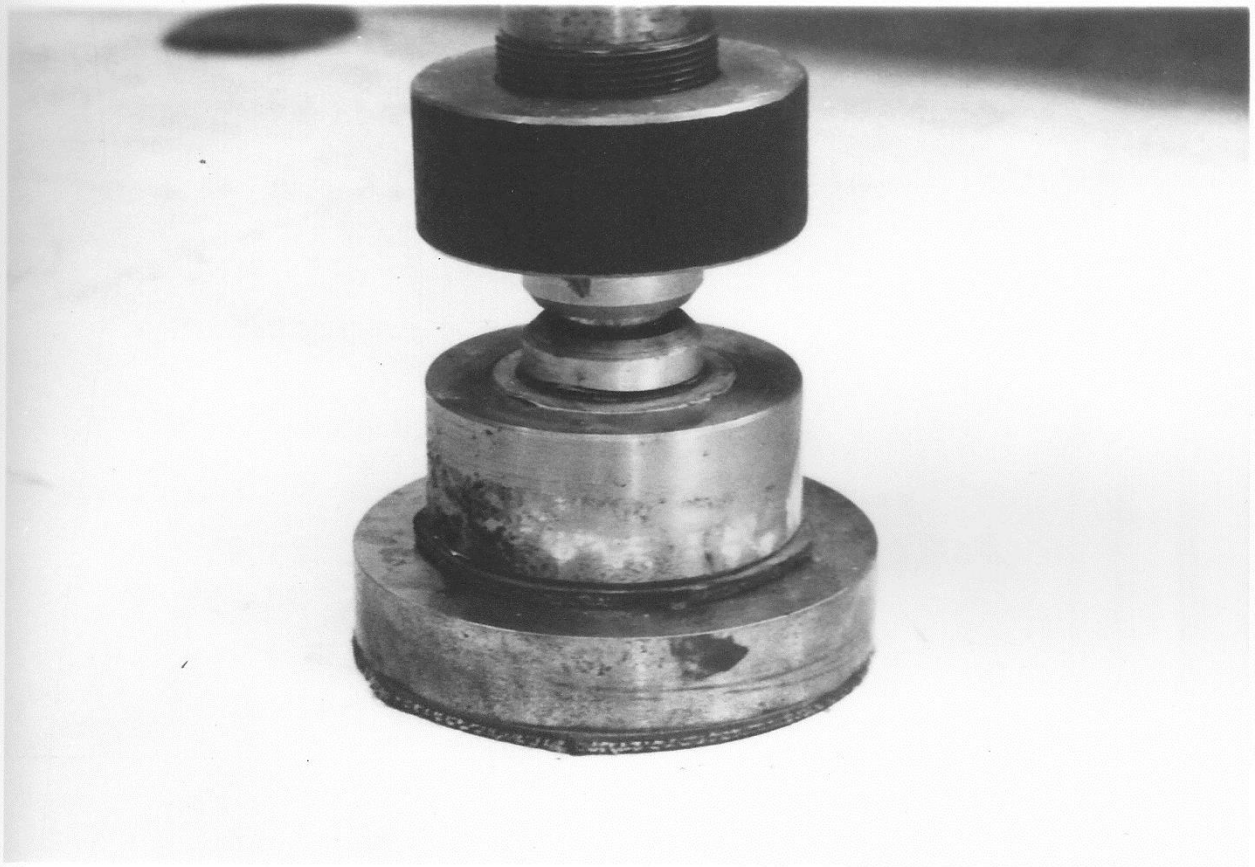

Plate 7.10 Single Wheel Loading Shoe for Creep Test

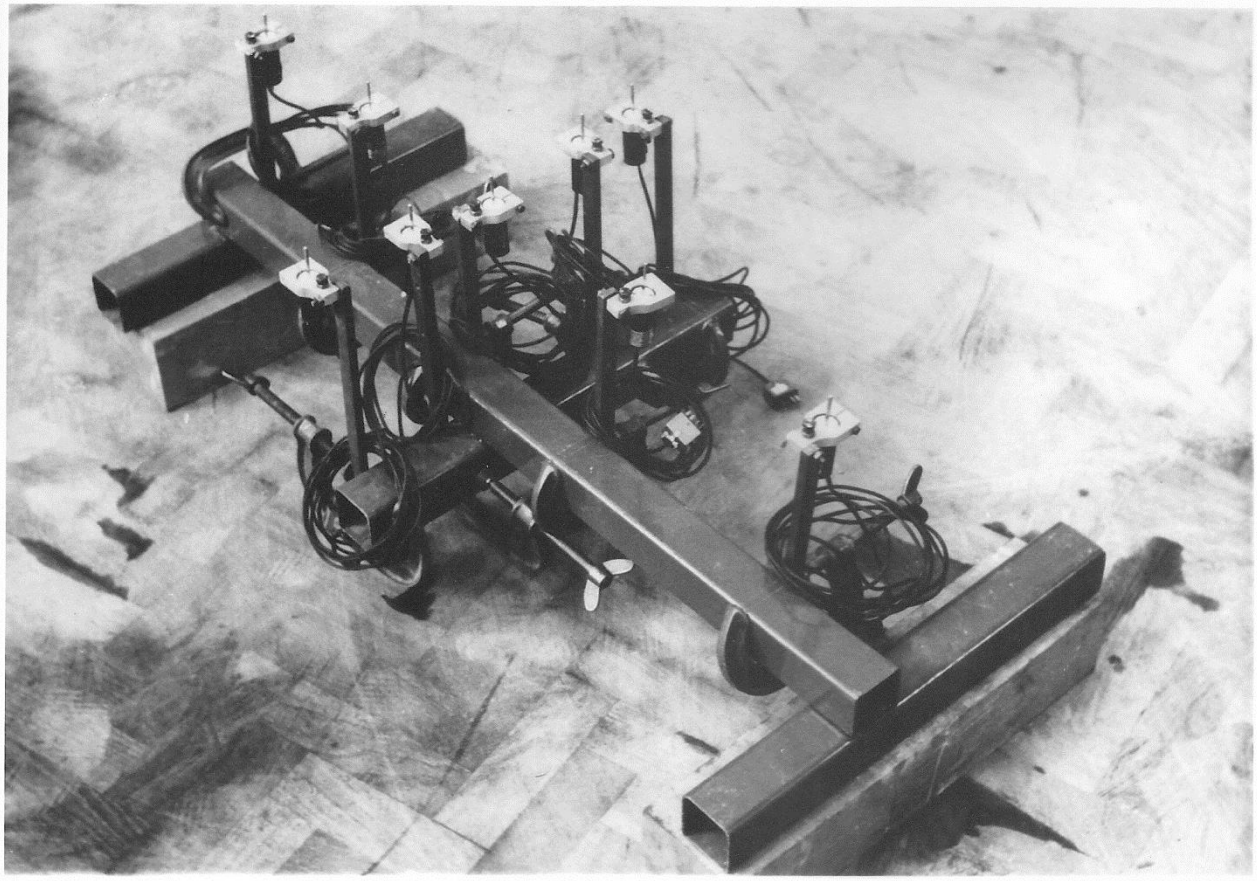

Plate 7.11 Deflection Transducers

CHAPTER EIGHT

PRESENTATION AND DISCUSSION OF RESULTS OF MODEL TEST

8.1 INTRODUCTION

The results of 20 tests on the reinforced concrete panels which formed the slab of the onethird scale model are presented. The tests were all carried out at the Queen's University of Belfast during November 1980.

As only a single model was being tested it was important that the maximum amount of information be recorded during the testing of each individual panel and this would then form the basis of a complete loading history for the panel. A test on a single panel usually took about 3 hours to complete and at working load and near failure, particular attention was paid to making an accurate record of observations and measurements. The importance of these particular points of the test was stressed because the design standards lay down certain criteria for serviceability and ultimate conditions and it was considered important that an accurate comparison be made.

Crack development was monitored at each load increment by marking the crack and numbering its extent with a felt tip pen. After failure both top and bottom surfaces of the slab were photographed and printed to the same scale to provide an accurate record of the progress of cracking. Crack widths were also monitored for comparison with the serviceability restrictions laid down in the design criteria.

Slab deflections were recorded at each load increment and the profiles showed the effect the various levels of reinforcement had on the deflection of the slab and also the local nature of the slab deflection under the wheels.

An attempt was made to record the strains in the transverse reinforcing bars in the bottom of the slab and as doubt has been expressed as to the validity of the current flexural analysis and elastic design of the slab, it was hoped that the recording of the steel strain at working load would give some indication of the distribution of forces within the slab.

When all the load tests had been completed the removal and disposal of the model was carefully planned to allow the maximum information to be recorded. In particular an accurate measurement of the thickness of each of the test panels was made as this dimension was considered to be critical in assessing the strength of a reinforced concrete slab. By careful cutting of the slab it was also possible to record the angle and extent of the failure zone for each slab.

The results now presented are typical for the 20 panels and a complete record of all the test results has been compiled by Kirkpatrick (1982). It is hoped that in due course it will be possible to compare these results with those of the prototype.

8.2 BEHAVIOUR AND CRACK PATTERNS OF MODEL

8.2.1 Behaviour of Model at Initial Stages

In all 20 tests a load of 12.5 kN which was equivalent to the 112.5 kN prototype service load was applied and then removed. For panels A, B and C no cracking of the slab occurred and the slab behaved elastically returning to almost exactly the same position on unloading. For panel D which had the minimum average reinforcement of 0.25% initial cracking was observed at about 10.5 kN which is equivalent to a service load of 94.5 kN or 38 units of HB loading.

When the load was re-applied cracking of the bottom surface of the slab was noted as the load was increased and the crack development was recorded. Details of the load causing initial cracking and the direction of the crack are given in Table 8.1. The development of typical crack patterns in panels A1, A4, D1 and D4 are shown in Figures 8.1 to 8.4. As the load was increased more cracks occurred in the bottom of the heavily reinforced panels, whereas in those panels that were lightly reinforced the initial cracks increased in width. Cracking of the top surface of the slab over the edge of the beam occurred much later and the load which caused the initial development and the direction of these cracks is recorded in Table 8.1.

Panels C3, C5, D3 and D5 were all tested using a double wheel which represented a single wheel on each of the axles of a bogie of the abnormal HB vehicle as defined in the current DTp standard. The initial cracking of the bottom surface of these panels was in the form of a typical yield line pattern with a single longitudinal crack extending from centre to centre of the loaded areas. Radial cracks then extended from the loaded areas away from the initial longitudinal crack. The development of cracks in these panels are shown Figs 8.5 to 8.8.

8.2.2 Behaviour of Model Near and at Ultimate

As the loading increased, the progress of crack development varied according to the size of the panel and the amount and spacing of reinforcement. For the large heavily reinforced panels - A1, A2 and A3, the number of cracks on the bottom surface increased radiating from the loading point although the actual width of these cracks appeared at a

spacing approximately equal to the pitch of the transverse reinforcement. On the top surface the cracking which had occurred along the line of the beams now followed a circular path at a radius of approximately 300 mm from the centre of the load. For the lightly reinforced panels these cracks tended to remain parallel to the beams.

Failure was always explosive and generated additional circumferential cracks on the bottom surface. The primary failure zone was always about 300 mm diameter on the bottom surface and the diameter of the loading shoe on the top surface. Secondary cracking occurred occasionally on the bottom surface with some concrete spalling.

The failure zone for the large panels did not extend to the edge of the beams. The failed section of concrete was always of the form of a truncated cone with a side slope at the top of about 45 degrees and an average side slope of about 25 degrees.

Typical failure patterns are shown in Plates 8.1 and 8.2 and sections of failure cones are shown in Plate 8.3.

For the heavily reinforced small panels initial cracking was similar to the large panels but as the load increased fewer radial cracks developed and the overall crack pattern extended over a smaller area. The final failure zone appeared to be restricted because of the close proximity of the beams, the failed area in all cases running along the intersection of the beam and slab. Although this corner of the slab was in compression at failure no crushing of the concrete was observed.

For the panels with reduced levels of reinforcement fewer cracks developed but the width of these cracks was greater. Where the pitch

of the transverse reinforcement was greater there was a tendency for the concrete to spall.

As the loading was gradually increased to about 70 kN some cracking of the reinforced concrete beams occurred. In general these cracks were vertical although when the panels next to the diaphragms were being tested some of these cracks tended towards a diagonal direction. This type of cracking increased as the panel being tested approached failure. The cracking of the beams in this manner was expected as each beam was only designed to carry a 50 kN point load in addition to the self-weight of the structure.

It was also observed that when the panels next to the parapet upstand were being tested vertical cracks occurred on the outside face of the upstand,the load at this stage of the test being a high proportion of ultimate. In some cases these cracks extended to the top and bottom horizontal faces of the parapet upstand which would appear to confirm that this section is making a positive contribution to the resistance of the compressive membrane forces. The area of concrete immediately below the loading shoe was being forced out radially and these forces were resisted by the unstressed slab remote from the load. For the edge panel these forces were resisted by tensile hoop stresses in the parapet edge beam which were a maximum at the outer face and hence caused the vertical cracks.

For the panels tested with the double wheel load the predictable yield line crack pattern between the loaded areas and extending radially from the loaded areas continued with additional radial cracking until failure occurred under a single loading shoe. As mentioned previously the reinforced concrete beams had been designed to carry a single point

load of 50 kN which was approximately half the expected capacity of each slab. However, for the double wheel test where the load capacity of the slab could be twice the single load, it was thought that the reinforced concrete beams may need some additional support. The first double wheel test was carried out on panel C3 and props were placed below the adjacent beams and midway between the loaded points. This produced a very rigid structure which caused the longitudinal cracks on the top surface in line with the edge of the beams to extend into panel D5 which has transverse reinforcement of the order 0.25%. These cracks did not extend in the opposite direction to panel A3 which had reinforcement of about 1.76% and had already been tested. The heavy reinforcement in this panel had obviously restricted the development of cracking in this direction. It should be noted that this test was the only one that produced any significant carry-over of cracking to adjacent panels and this has been attributed to propping of the beams. After failure of one of the double loading points the props were removed and the unfailed area loaded again. Further development of cracks occurred and this panel eventually failed at 102 kN which was comparable to a single wheel load for this type of panel. After this test it was decided that propping was unnecessary and the remaining double wheel tests were successfully completed without any obvious distress to the beams and with very little carry-over of cracks to adjacent panels. The development of crack patterns for typical panels are shown in Figures 8.1 to 8.8 and failure patterns are shown in Plates 8.1 and 8.2.

8.2.3 Crack Widths

The current bridge design standard restricts the width of crack permitted to 0.25 mm for HA loading and 0.3 mm for HB loading. However, the new code BS 5400 (1978) does not limit cracking in this manner but controls the width of crack by the degree of exposure expected and for soffits this is classed as severe and the width of crack is limited to 0.2 mm. During the tests on the model an attempt was made to monitor the development of crack widths using an optical comparator. The measurement of cracks on the bottom surface was extremely difficult because of the deflection measuring frame but the top surface was easily accessible and a regular measurement was made as the cracks developed. It was considered that the testing of the prototype bridge would provide a better opportunity to make an accurate assessment of the serviceability due to cracking, nevertheless the model tests do provide relevant information on crack widths which is now presented.

Measured cracks widths are shown, where applicable, on the crack patterns of Figures 8.1 to 8.8 and an estimate of the load which caused a crack width of 0.1 mm on the top and bottom of the slab is given in Table 8.2. It should be noted that the loads given for cracks on the bottom of the slab are approximate estimates owing to the difficulty of gaining access.

8.3 SLAB DEFLECTIONS

8.3.1 Deflection Profiles

The deflection profiles for typical panels tested are shown in Figures 8.9 to 8.16. These show the deflections of the slab relative to the beams along both the longitudinal and transverse centre line

axes for various increments of load. For the heavily reinforced panels the profiles in the longitudinal direction show a predictable zero slope under the wheel load with a very gradual reduction in deflection to zero at the edge of the panel. However, in the transverse direction where the panel spans between beams there is evidence of some rotation of the slab close to the beam.

As the steel reinforcement is reduced the deflection profiles change in character to much greater deflections under the wheel load and in the longitudinal direction an increase in the length of the slab deflected. The transverse profiles show much greater slope and a considerable rotation at the interface with the beam. (Figs 8.11 and 8.12).

The profiles for the panels loaded with the double wheel load show almost constant deflection between the loading points and outside this area the deflections of the slab fall off very quickly. (Figs 8.13-16).

In general the profiles show that the application of a wheel load corresponding to the standard HB vehicle to this type of slab produces only very localised deflections even though in certain cases the adjacent panel had already been loaded to failure with the subsequent loss of local slab stiffness. These local deflections confirm that the initial selection of the widths of the various bands of reinforcement which constituted each loading panel was realistic.

8.3.2 Load Deflection Curves

The variation of slab deflection with applied load at a point directly under the load for typical large and small panels are shown in Figure 8.17. These show the deflections of the two panels with various quantities of transverse reinforcement. The amount of reinforce-

ment in the slab is the most important factor affecting the deflection as this controls the degree of cracking that occurs. For the large panels the slab deflections increased more rapidly due to cracking as the load increased. This was not so apparent for the small panels which exhibited much straighter curves and smaller deflections at failure. A table of deflections prior to failure is shown in Table 8.3. This shows a remarkable consistency in the deflection experienced by similar panels immediately before failure occurred, the panels loaded with the double wheel showing twice the deflection of the single wheel. The load deflection curves for the panels with the double wheel loads are shown separately on Figure 8.18. For the small panels these are similar in shape and magnitude as the single wheel load indicating that the double wheel load applied to the small panel is no more critical than a single wheel load. However, for the large panel the deflections were much more pronounced as cracking increased rapidly with load. In particular panel D3 experienced very large deflections and a relatively low failure load. This particular panel was considered to be unrepresentative of the large panels with the double wheel loads as there was some initial cracking of this panel from the test on panel C3. In particular, the longitudinal crack down the centre of the panel must have reduced its initial stiffness although this should not have had a major influence on the ultimate capacity. Close to failure some crushing of the concrete occurred along this crack.

8.3.3 Service Load Deflections

The specified Department of Transport service load for bridge decks is a prototype load of 112.5 kN which is equivalent to a model load of

12.5 kN. The deflection at this load increment was recorded for all panels and is shown in Table 8.4.

Allowing for a linear scale factor of 3 the maximum prototype deflection under service load would be 1.65 mm which is due to the double wheel load on panel D5. Some cracking was observed at this level of loading but this was considered to be well within the limits permitted by the standard.

8.3.4 Deflection During Creep Test

During the testing of the model the effect of the running surface which would provide additional distribution of the wheel load to the concrete slab has not been considered. Therefore, to provide a more realistic loading area for the measurement of creep deflections a larger loading shoe of 150 mm diameter was used and the deflections recorded over a period of 24 hours with a constant load of 50 kN which is 4 times the service load and represents a tyre pressure of 2.83 N/mm^2. The 150 mm diameter loading shoe is shown in Plate 7.9. The deflections recorded during the 24-hour period are shown in Figure 8.19. This shows an initial increase in deflection of 0.32 mm over the first 8 hours but a considerable levelling out over the next 16 hours with only a 0.25 mm increase in deflection indicating that this type of slab is a very stable load-carrying structure.

The factor of 4 used during this test is extremely high as live loads applied to bridge decks are transient in nature and it is considered unlikely that it would experience even a service load of 112.5 kN for more than 24 hours.

8.4 STEEL STRAINS

Foil strain gauges were adhered to selected reinforcing bars in areas considered to be critical and the position of these are shown in Figure 7.12. The steel strains measured during the tests are shown in Figures 8.20 to 8.23. These strains are due to the application of the test load only, strains due to self-weight were considered to be negligible.

For the A and B series of tests 3 mm gauges were used with the 6 mm diameter high yield steel deformed bars and a high proportion of these gauges gave consistent results. For panels C and D series 1 mm gauges were used with the 3 mm diameter plain bars and only 2 of these gauges worked satisfactorily, both of these being in panel C.

It should be noted that these foil strain gauges are very fragile and have to survive in a very hostile environment during the casting and curing of the deck slab. Another important aspect of using foil strain gauges on reinforcing bars is that when cracking occurs near a gauge any tendency for bond slip to occur will damage the gauge. This was more noticeable on the plain 3 mm bars where the resistance to bond slip is much lower than with the deformed bars.

For the heavily reinforced panels A1, A2 and A3 the average strain measured just before failure on the bottom transverse reinforcement was about 1,000 $\mu\varepsilon$ (Figure 8.20). This is equivalent to a steel stress of about 200 N/mm^2. For panels B1, B2 and B3 the equivalent strains were about 1,200 $\mu\varepsilon$(Figure 8.21) and for the small panels B4 and B5 700 $\mu\varepsilon$ (Figure 8.21). Even though these strains should be considered in a qualitative rather than a quantitive manner they do

indicate relatively low stress levels in the transverse reinforcement prior to failure occurring. Figure 8.22 shows the strain in the top reinforcement over the edge of the beams for panels B1 and B4. For the large panel B1 this was about 1,000 με and for the small panel B4 about 600 με. These are of the same order as for the reinforcement in the bottom of the slab under the load.

Figure 8.23 shows the strains in the bottom transverse reinforcement for large panel C1 and the small panel C4. These had average transverse reinforcement of 0.49% and 3 mm diameter plain bars. For the large panel C1 the measured strain was almost 2,000 με and for the small panel C4 about 1,300 με. These values of strains would seem to indicate that the reinforcement had reached its yield stress of 338 N/mm^2 as the estimated yield strain was about 1,400 με.

The current Department of Transport requirements for slab design state that the slab should be designed in flexure under the effect of the 112.5 kN wheel loads of the HB vehicle; this vehicle will produce bending of the slab from both global and local effects. For this type of M-beam, slab reinforcement of the order of 1.7% will be required similar to the test slabs of panel A. As may be seen from Figure 8.20, at an equivalent model load of 12.5 kN, the steel strains were at a very low level. Even with average steel reinforcement of 0.49% (figure 8.23) the steel strains at a load of 12.5 kN were also very small. As no cracking was observed in any of these test panels at this level of loading this would indicate serious shortcomings in the current method of slab design which uses a simple flexural method and ignores other effects such as compressive membrane action which provides con-

siderable enhancement to the load carrying capacity.

8.5 FAILURE LOADS

8.5.1 Single Wheel Loads

The ultimate load capacity of each test panel was the load which caused the loading shoe simulating the wheel load to punch through the slab in the characteristic manner. These loads are presented in Table 8.5 and also in Figure 8.24.

From Table 8.5 and Figure 8.24 it may be seen that there is very little variation in the ultimate load capacity of all the panels loaded with the single wheel load even though the steel reinforcement varied from approximately 0.25% to 1.68%. It would therefore appear that the load capacity was almost independent of the quantity and quality of the steel reinforcement. The other important parameters measured during the test were the concrete cube strength at the time of test and the actual thickness of the slab and these are also given in Table 8.5.

8.5.2 Double Wheel Loads

The small panels C5 and D5 when loaded with the double wheel failed at loads which were approximately twice the failure load of panels C4 and D4 loaded with the single wheel load. These small panels represent the slab with the prototype M-beams spaced at 1.5 m and the double wheel load is obviously no worse than the single wheel load.

However the large panels C3 and D3 did show a reduction in load carrying capacity when the double wheel load was applied. This may have been due to the unnecessary propping of the beams for the panel C3 and a reduction of the stiffness of the surrounding slab highlighted by the cracking of the parapet upstand. Both the tests on the large panels were on the edge of the deck where the edge beam and parapet

have an important part to play in maintaining the in-plane stiffness of the slab.

Even though the large panels did show a reduction in capacity under the double load the failure load of 140 kN for D3 does give a factor of safety of 5.6 which is quite satisfactory.

8.5.3 Creep Test

Panel D2 had been loaded using a shoe of 150 mm diameter and the deflections that took place were measured over a 24-hour period. The load was then removed and the normal 106 mm diameter shoe substituted and the panel loaded until failure took place at 108 kN. As this failure load was of the same order as the other large panels it is obvious that the extended loading period did not adversely affect the ultimate load capacity of the panel.

8.6 REMOVAL OF MODEL

On the completion of the test programme careful consideration was given to the removal of the model which weighed approximately 8 tonnes. It was finally decided to cut the model into 6 longitudinal strips by sawing through the end diaphragms and along the centre line of the test panels leaving the beams intact. The main advantage of this method, was that it reduced the structure to the 6 beams and the associated slab and diaphragms which were both individually stable and of a weight suitable for moving by the existing overhead crane. However, the most important aspect of this approach was that it allowed the exact measurement of the thickness of the individual test panels. As well, the failure zones were photographed which allowed the angle of punching and the extent of failure of the slab to be assessed. The

measurement of the actual slab thickness was considered to be of paramount importance in predicting the punching capacity of the slab and these are given in Table 8.5. This allowed the actual percentage of steel reinforcement to be calculated for each test panel (Table 8.5). Sections through some typical failure cones are shown in Plate 8.3 and the diaphragm and slab sections are shown in Plate 8.4. Typical soffit failure areas and cones are shown in Plates 8.5 and 8.6.

8.7 CONCLUSIONS

From the tests on the one third scale model the following are the main conclusions that may be drawn.

1. The quantity of steel reinforcement has very little effect on the ultimate load capacity of the slab. It does however, influence the serviceability limits of cracking and deflection.
2. No cracking was observed at service load for the panels with average reinforcement levels of 0.49% and above, however, for the panels with the average of 0.25% reinforcement some cracking was observed although this was well within the current permitted crack widths. However, it should be noted that the plain 3 mm diameter bars have poor bond characteristics compared with the deformed bars used in the prototype.
3. Creep effects due to long-term loading, bearing in mind the transient nature of bridge live loads, does not have any adverse effect on the ultimate load carrying capacity of this type of bridge deck.
4. The results of these load tests are conservative as no allowance has been made for the additional load distribution effect of the road surfacing.

5. The strains measured in the bottom transverse reinforcement with the equivalent of the 112.5 kN service load must cast some doubt on the current method of analysis even at this relatively low level of live load as compared with the ultimate capacity.

6. The failure load of 140 kN for test panel D3 was for two 12.5 kN model wheel loads applied to the longitudinal centre line of the slab and represents the minimum factor of safety of 5.6. It should be noted that panels C3 and D3 were considered to be unrepresentative due to the additional cracking that occurred as a result of propping the beams. Therefore, if these results are ignored the next smallest factor of safety was for panel B4 which had a failure load for a single wheel of 90 kN which was equivalent to a factor of safety of 7.2.

7. All the test panels failed by punching shear even though the design was based on a flexural analysis. The panels with the 0.25% reinforcement, which should have had a greater tendency for flexural failure, also failured in a punching shear mode.

From the review of the test results for the model M-beam bridge deck it is apparent that the current methods of analysis are inadequate for the accurate prediction of the serviceability and ultimate load capacity of an M-beam deck. It can also be seen that relatively light transverse reinforcement in the deck slab is adequate and if this was incorporated into an actual design it would result in a considerable saving in the cost of both steel and fixing. Therefore, the next chapter will consider these problems with the development of a more appropriate method for the prediction of the ultimate load capacity of the M-beam

slab and will also consider the steel requirement for a satisfactory serviceability condition.

Test Panel		Bottom		Top	
		load kN	direction	load kN	direction
A	1	45	transverse	85	
	2	37	transverse	82	parallel
	3	22	transverse	67	to
ρ_{av} = 1.68%	4	37	trans/long	51	beams
	5	28	longitudinal	51	
B	1	16	transverse	40	
	2	16	longitudinal	40	parallel
	3	16	transverse	40	to
ρ_{av} = 1.19%	4	28	trans/long	51	beams
	5	28	trans/long	57	
C	1	22	trans/long	45	
	2	18	trans/long	40	parallel
double	3	40	longitudinal	69	to
ρ_{av} = 0.49%	4	18	transverse	52	beams
double	5	40	transverse	97	
D	1	10.5	longitudinal	28	
	2	10.5	longitudinal	28	parallel
double	3	22	longitudinal	48	to
ρ_{av} = 0.25%	4	10.5	longitudinal	40	beams
double	5	22	longitudinal	60	

TABLE 8.1 Load and Direction of Initial Cracking

Panel		Bottom	Top
A ρ_{av} = 1.68%	1	-	-
	2	45	86
	3	-	-
	4	45	74
	5	37	63
B ρ_{av} = 1.19%	1	32	63
	2	28	63
	3	32	50
	4	32	74
	5	34	80
C double ρ_{av} = 0.49% double	1	34	57
	2	28	57
	3	57	78
	4	28	69
	5	-	135
D double ρ_{av} = 0.25% double	1	19	33
	2	22	45
	3	-	-
	4	22	80
	5	-	110

TABLE 8.2 - Load to Cause a Crack Width of 0.1 mm - kN

Panel		A	B	C	D
large panels	1	2.2	3.0	6.6	6.1
	2	2.3	2.8	4.5	6.2
	3	2.2	3.0	10.0	13.6
small panels	4	1.2	1.1	2.2	2.5
	5	1.0	1.4	3.7	5.2

TABLE 8.3 - Deflection of Panel Prior to Failure - mm

Panel		A	B	C	D
large panels	1	0.08	0.11	0.13	0.28
	2	0.11	0.15	0.15	0.22
	3	0.12	0.17	0.29	0.55
small panels	4	0.09	0.06	0.11	0.07
	5	0.08	0.06	0.17	0.25

TABLE 8.4 - Service Load Deflections - mm

Panel		Load Type	Failure Load kN	Cube Strength at Time of Test N/mm^2	Slab Depth mm	Effect-ive Depth mm	$\rho\%$	$\rho_{av}\%$
A	1	single	102.5	39.8	57.3	48.3	1.67	1.68
	2	single	114.0	40.4	59.6	50.6	1.59	
	3	single	102.5	44.7	54.8	45.8	1.76	
	4	single	108.0	40.4	57.2	48.2	1.67	
	5	single	96.0	44.7	56.1	47.1	1.72	
B	1	single	108.0	41.3	55.5	46.5	1.14	1.19
	2	single	96.0	43.5	53.3	44.3	1.21	
	3	single	100.0	41.5	53.3	44.3	1.20	
	4	single	90.0	43.5	54.9	45.9	1.16	
	5	single	91.0	41.5	52.1	43.1	1.23	
C	1	single	106.0	37.4	57.1	49.6	0.48	0.49
	2	single	100.0	38.9	54.4	46.9	0.50	
	3	double	152.0	41.3	52.7	45.2	0.47	
	4	single	110.0	38.9	57.0	49.2	0.48	
	5	double	210.0	41.3	56.3	48.8	0.52	
D	1	single	96.0	44.0	53.6	46.1	0.24	0.25
	2	single	108.0	45.6	55.1	47.6	0.25	
	3	double	140.0	44.0	54.0	46.5	0.25	
	4	single	118.0	45.6	58.6	51.1	0.23	
	5	double	215.0	44.0	54.7	47.2	0.25	

TABLE 8.5 - Failure Loads and Details of Test Panels

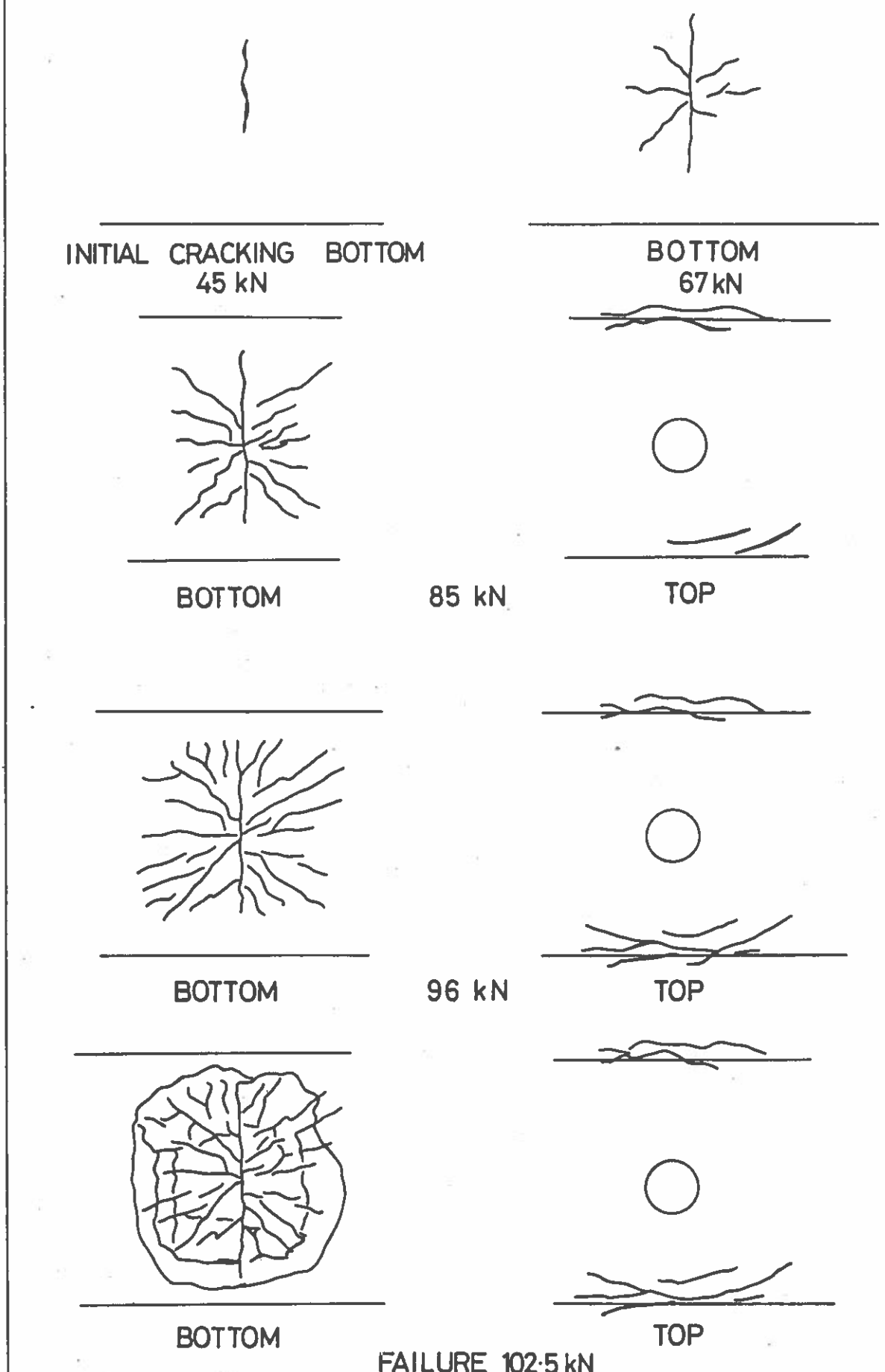

Fig. 8.1 Development of Crack Patterns Panel A1

Fig.8.1

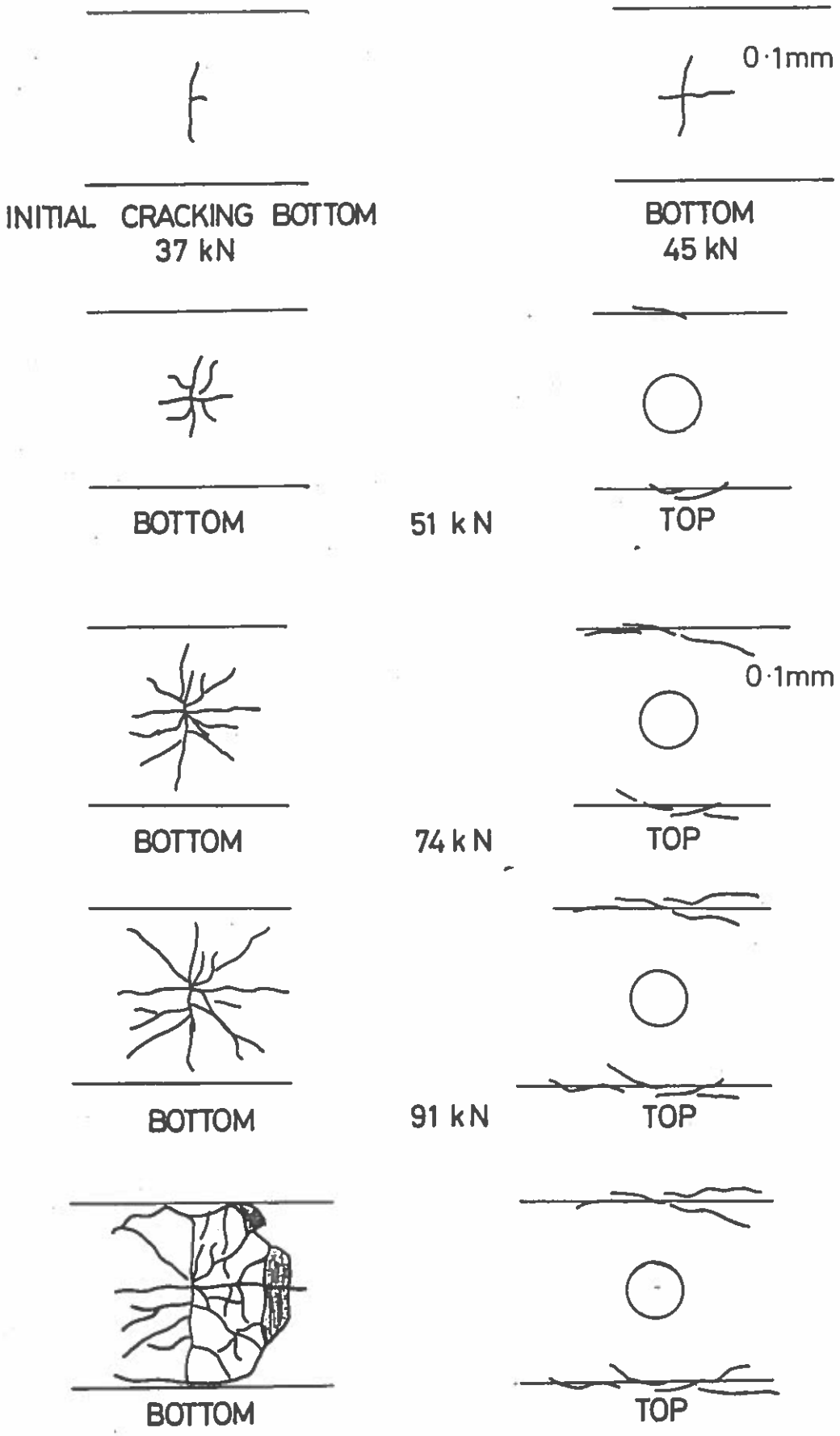

Fig. 8.2 Development of Crack Patterns Panel A4

Fig.8.2

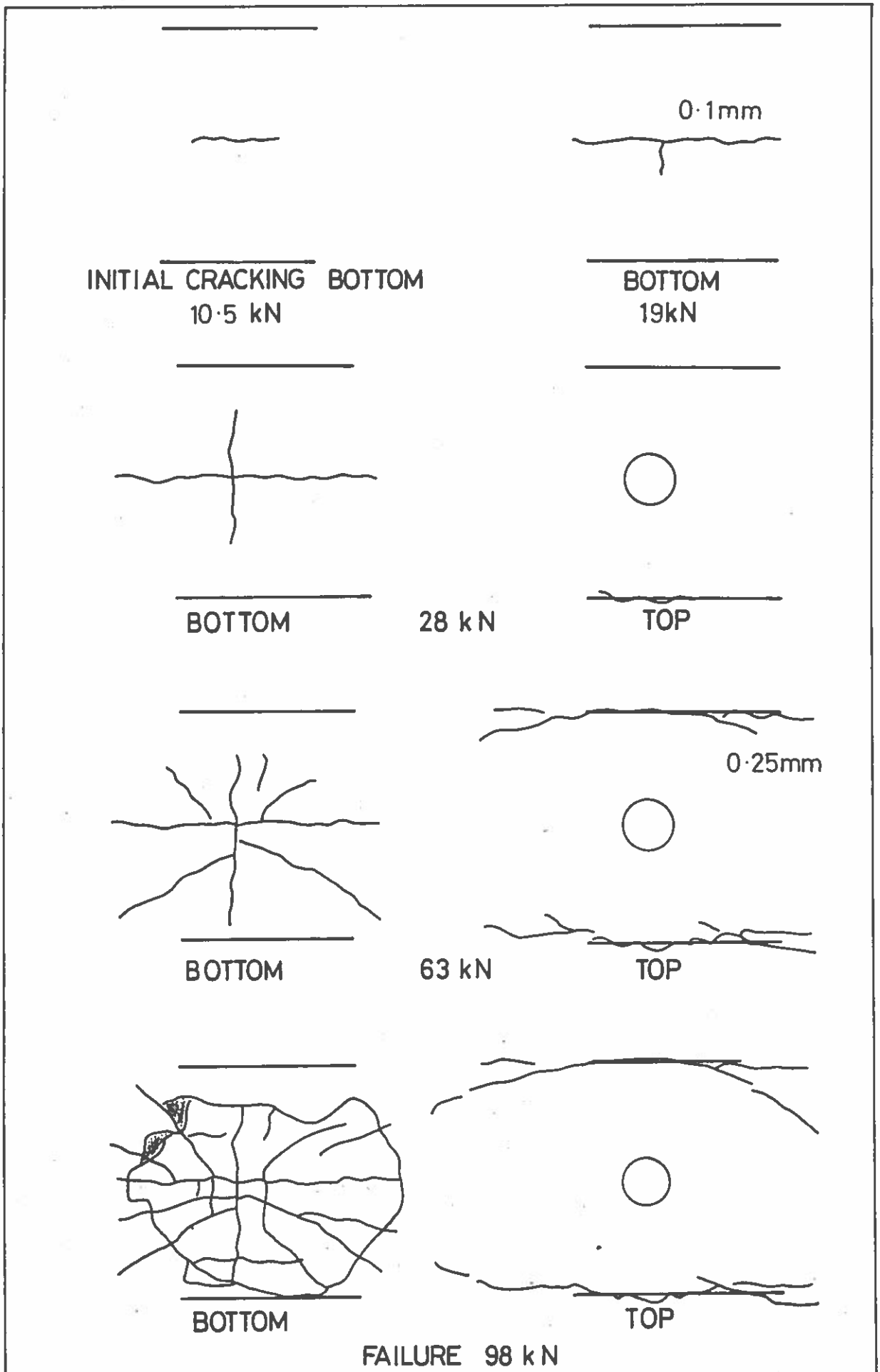

Fig. 8.3 Development of Crack Patterns Panel D1

Fig. 8.3

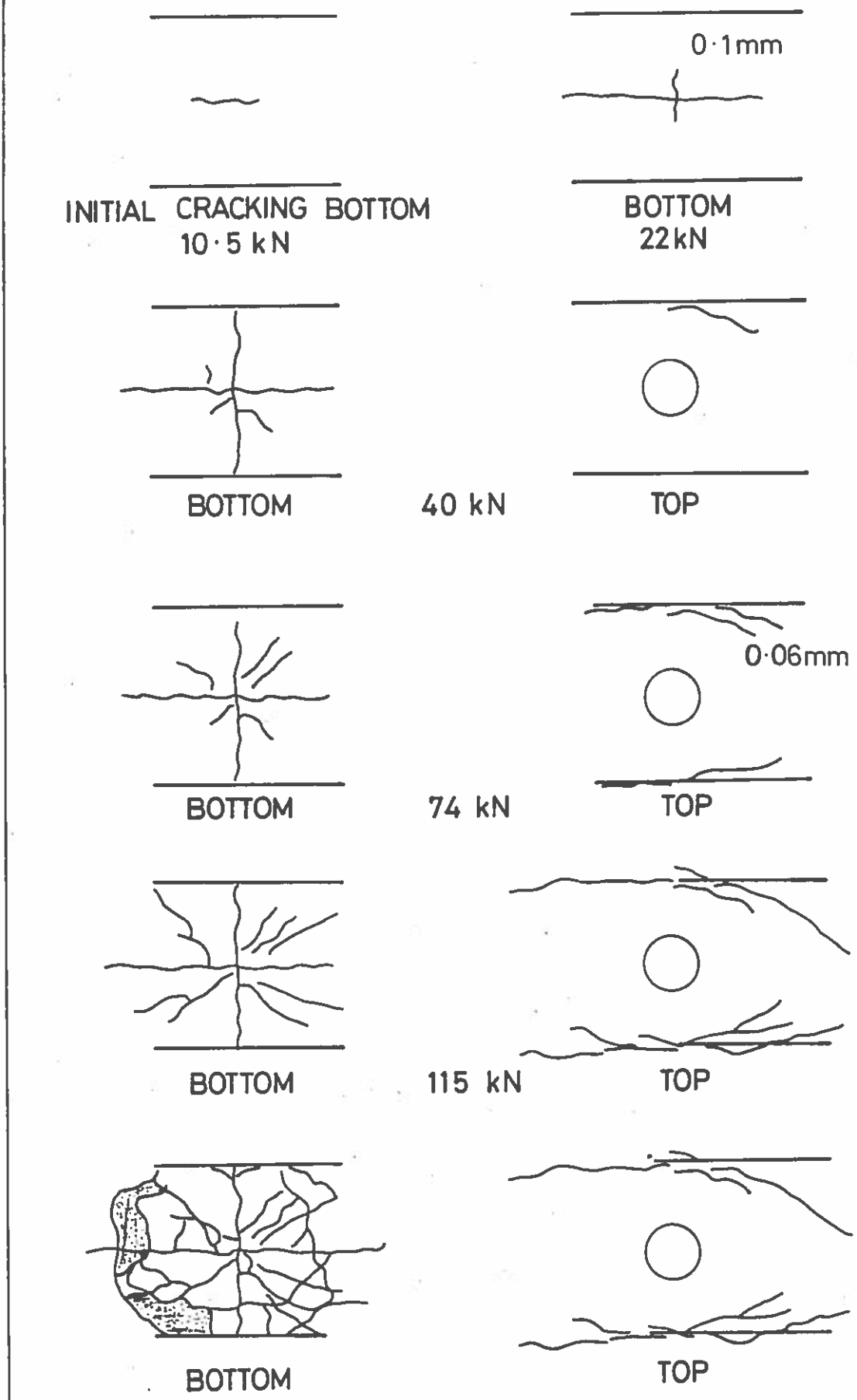

Fig. 8.4 Development of Crack Patterns Panel D4

Fig.8.4

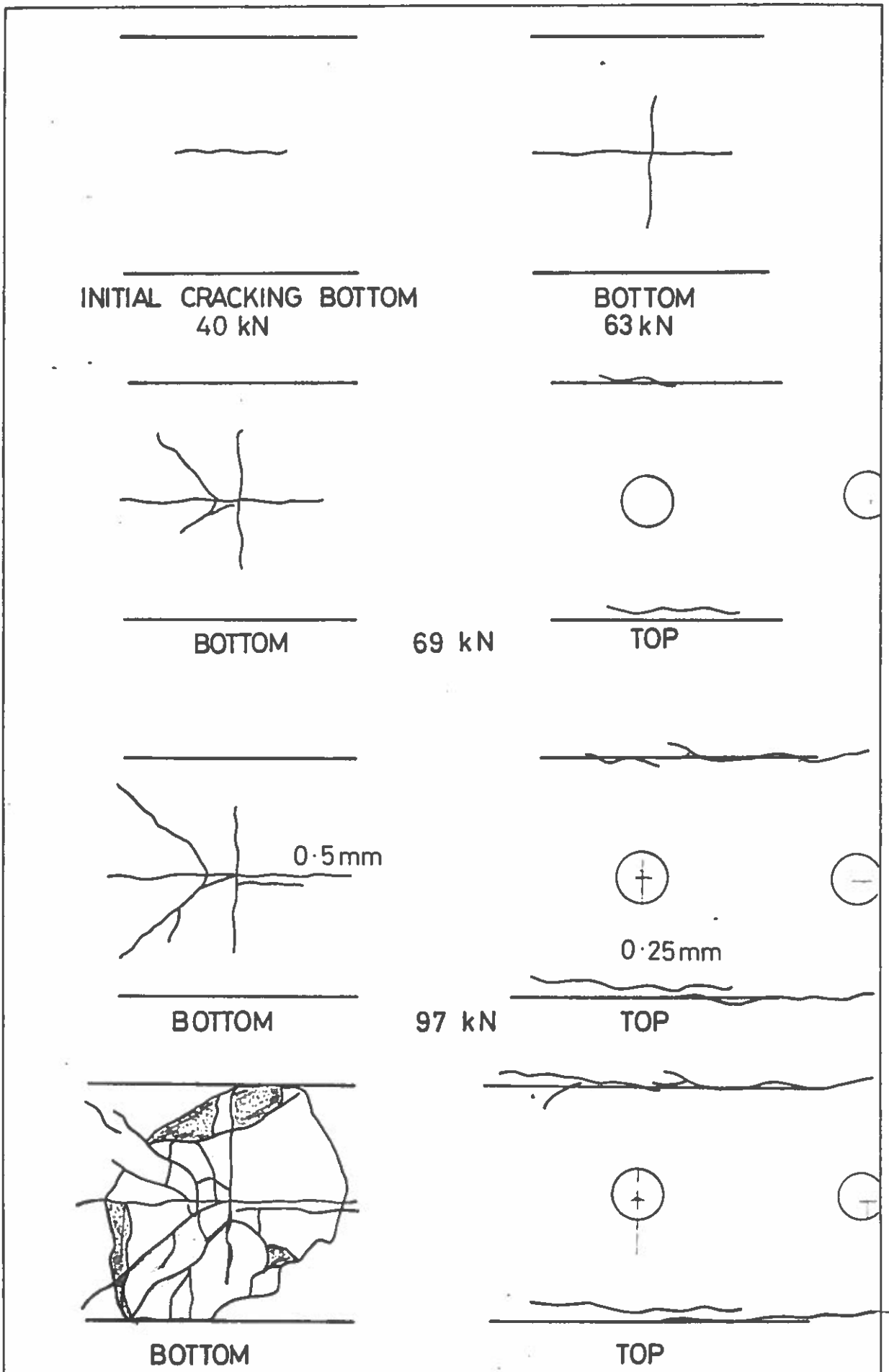

Fig. 8.5 Development of Crack Patterns Panel C3

Fig. 8.5

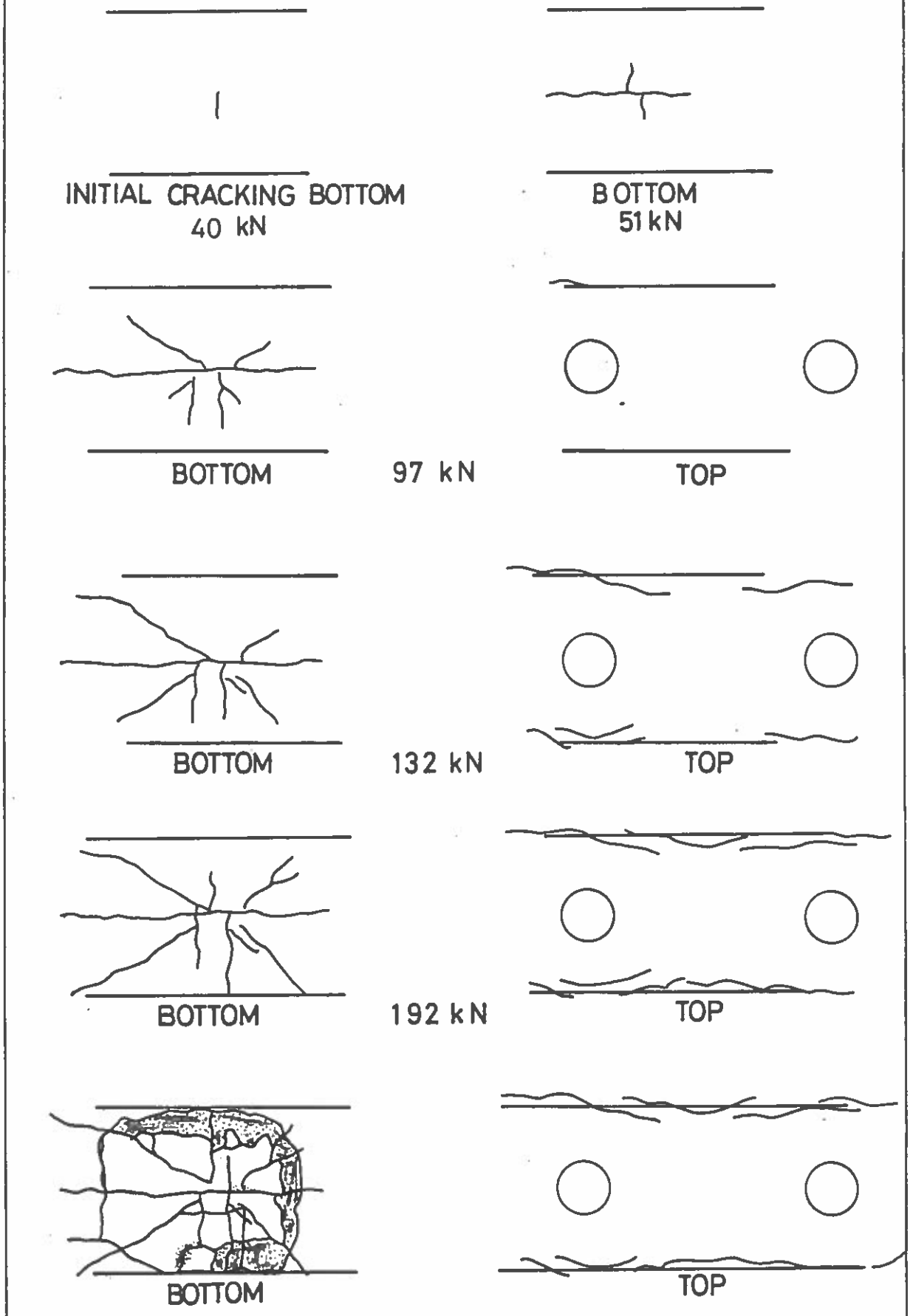

Fig.8.6 Development of Crack Patterns Panel C5

Fig. 8.6

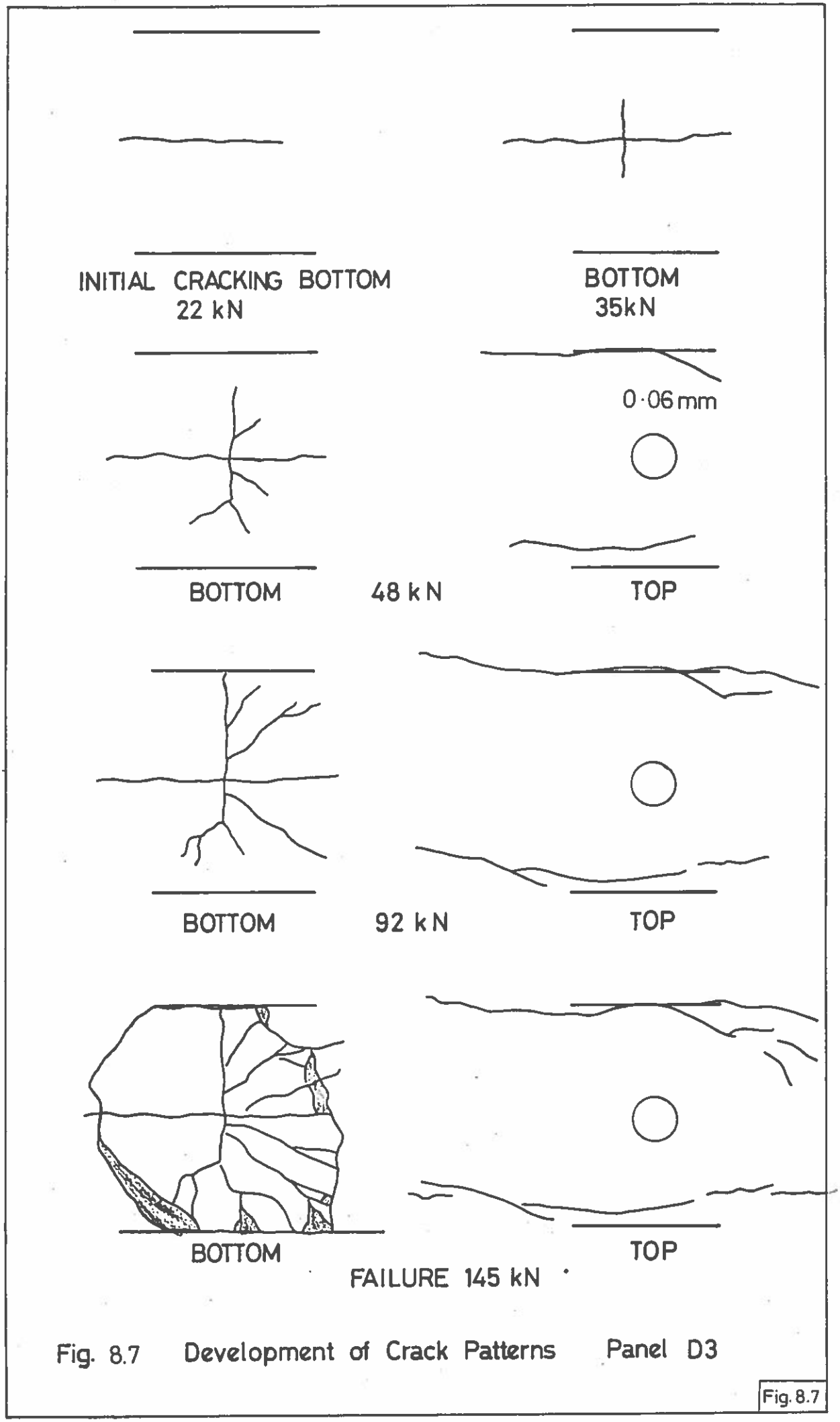

Fig. 8.7 Development of Crack Patterns Panel D3

Fig. 8.7

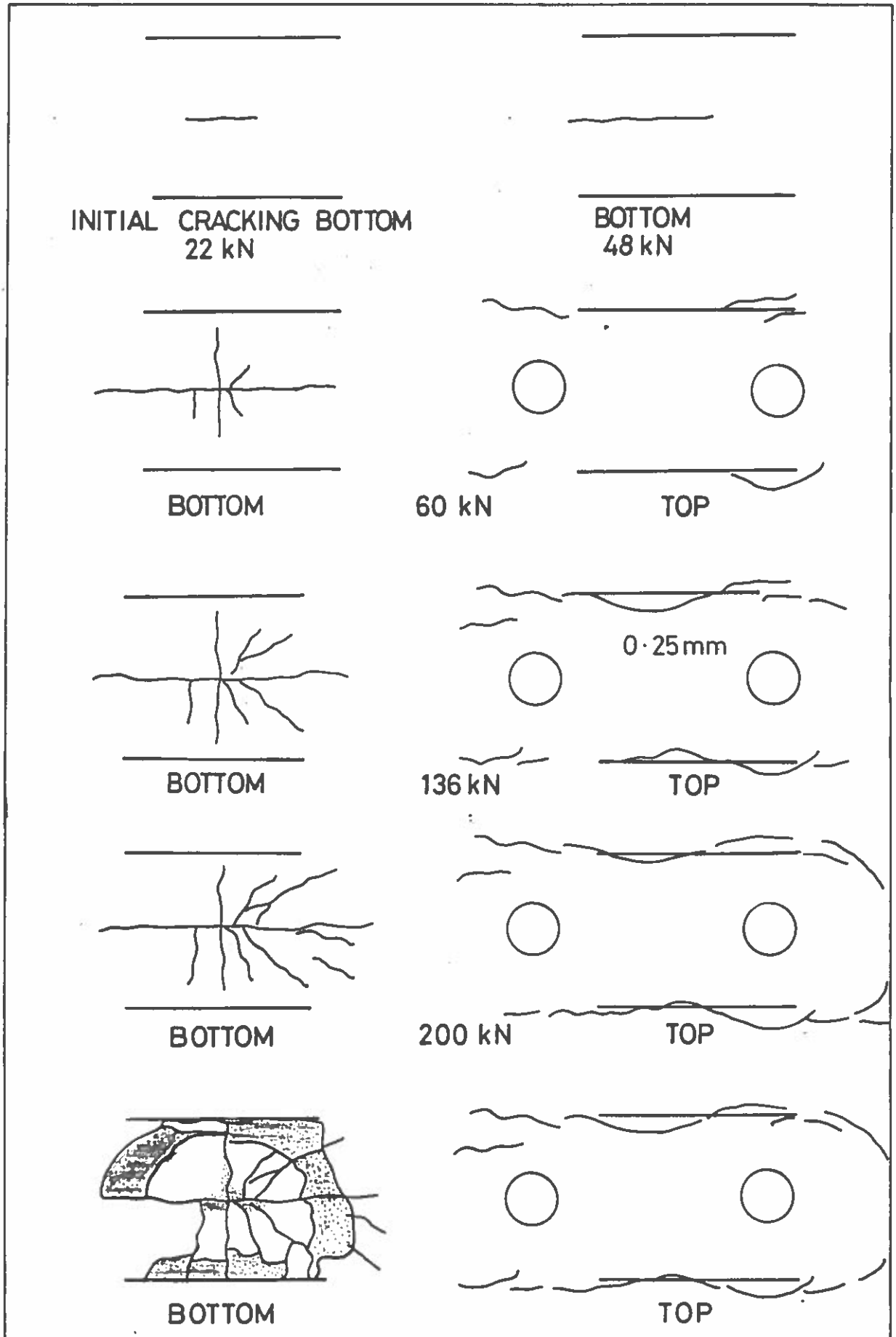

Fig. 8.8 Development of Crack Patterns Panel D5

Fig. 8.8

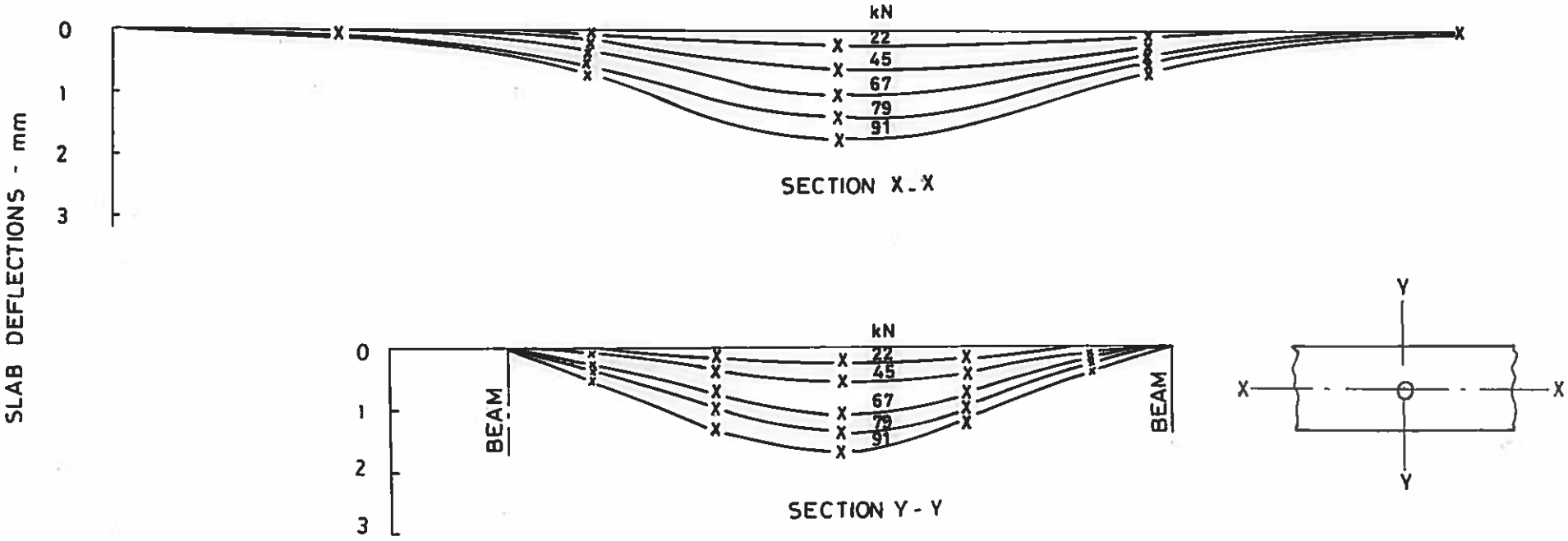

Fig 8.9 Deflection Profiles Panel A1

Fig 8.9

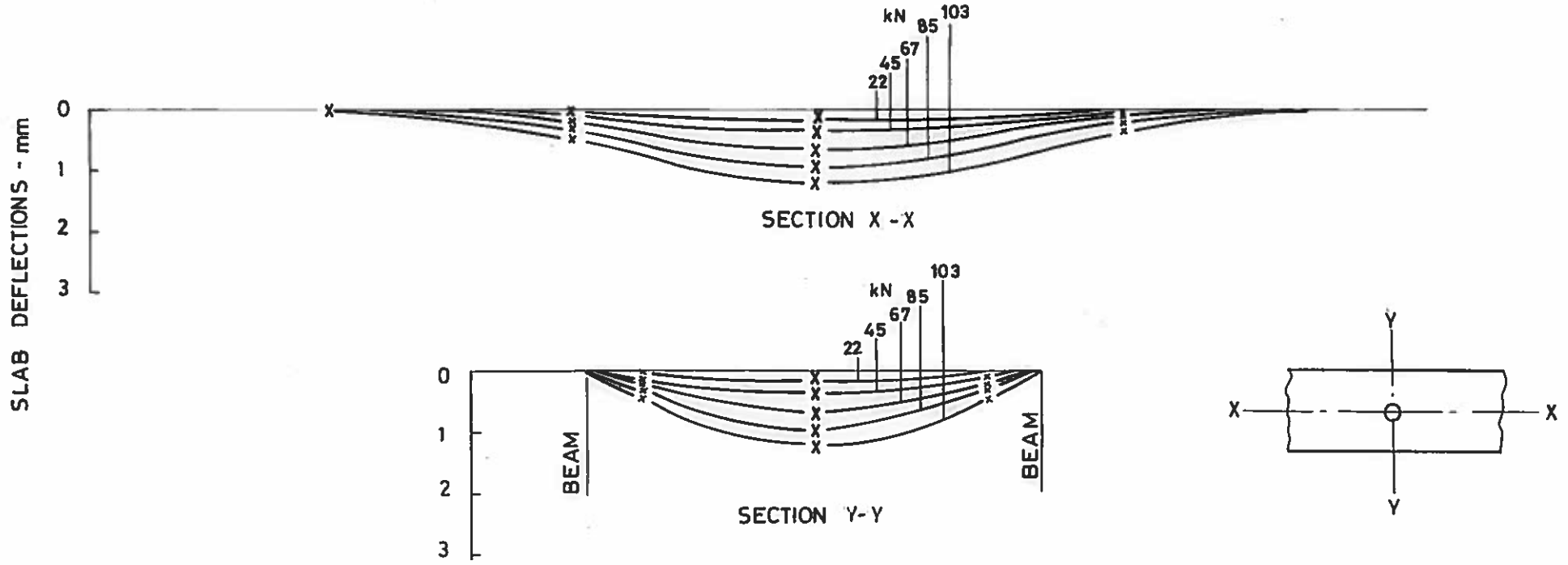

Fig. 8.10 Deflection Profiles Panel A4

Fig. 8.10

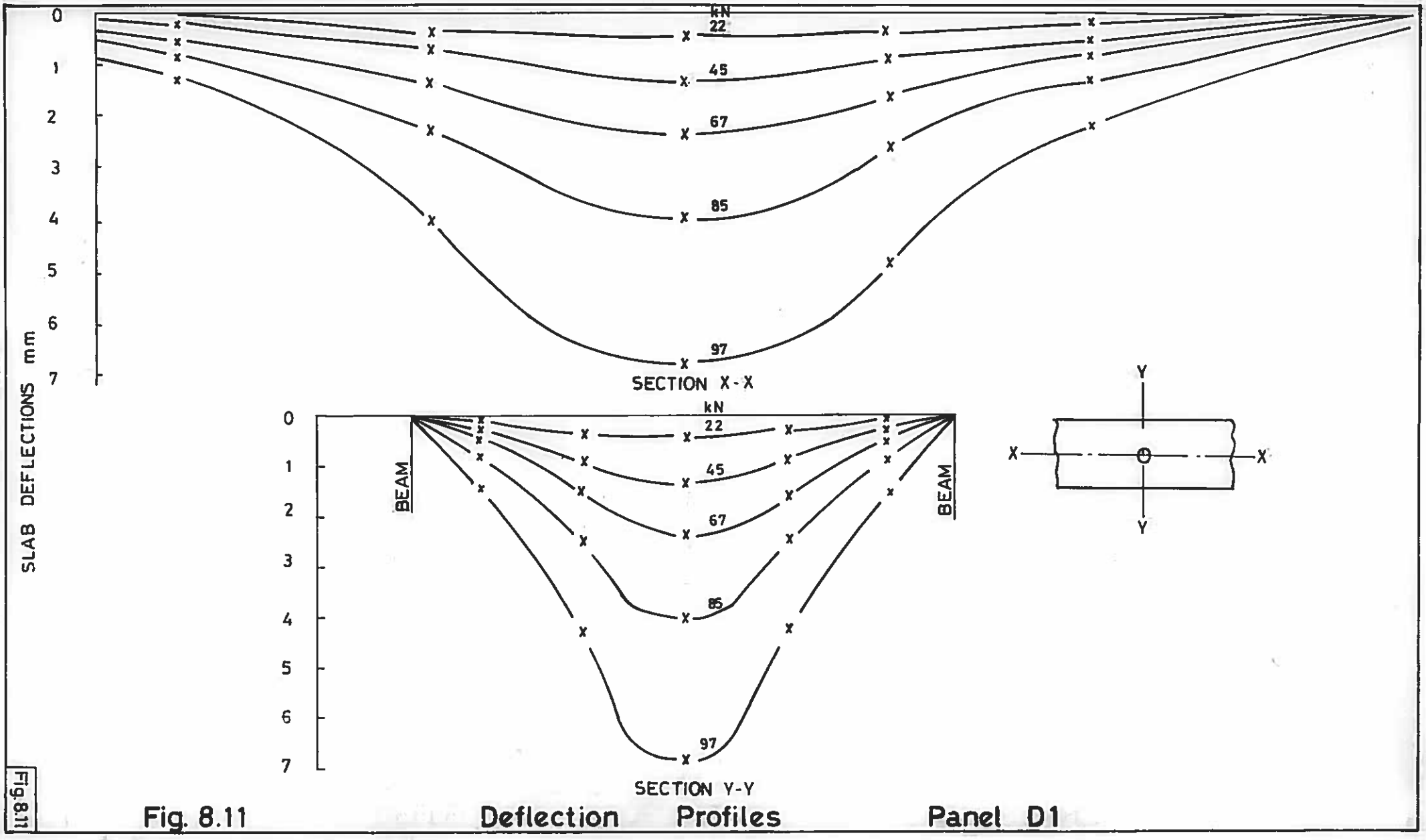

Fig. 8.11 Deflection Profiles Panel D1

Fig.8.11

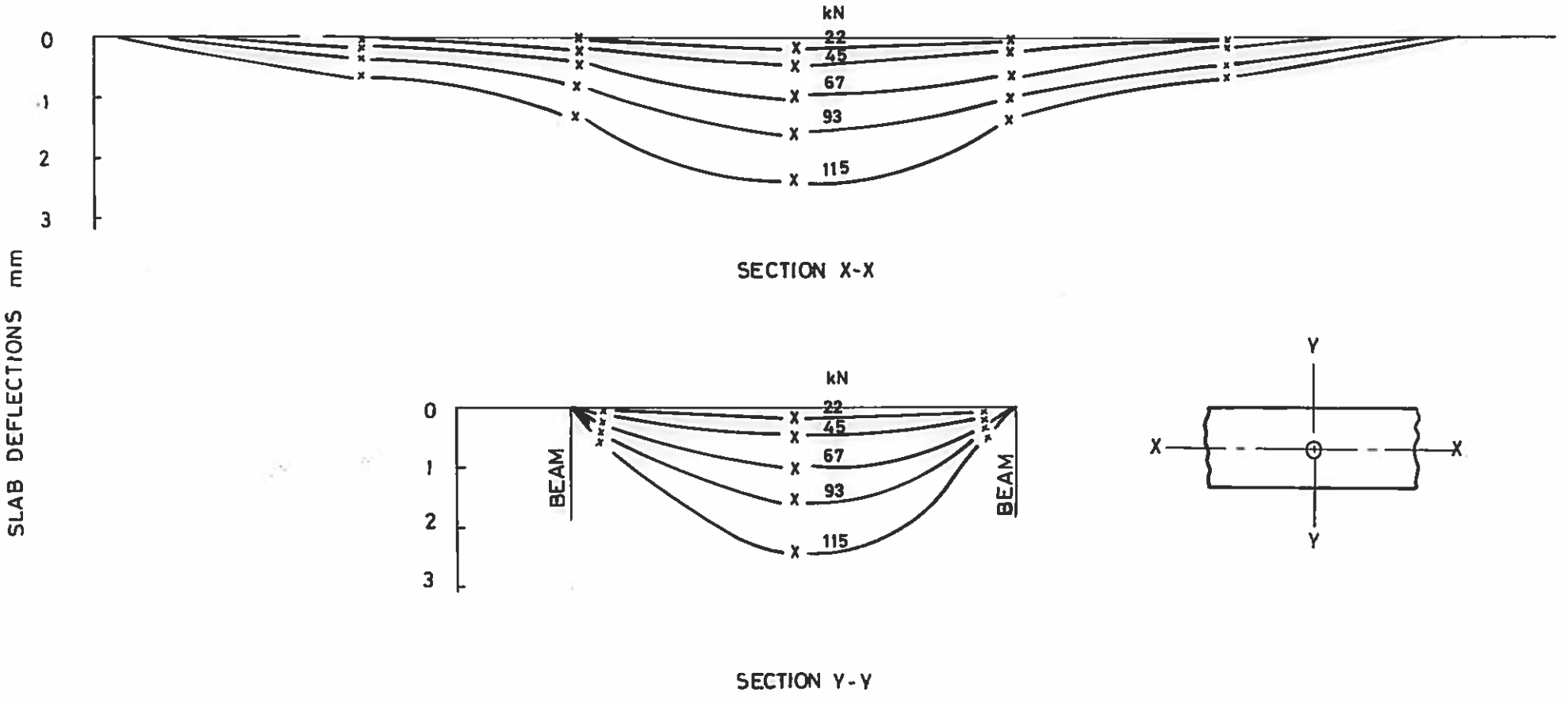

Fig. 8.12 Deflection Profiles Panel D4

Fig. 8.12

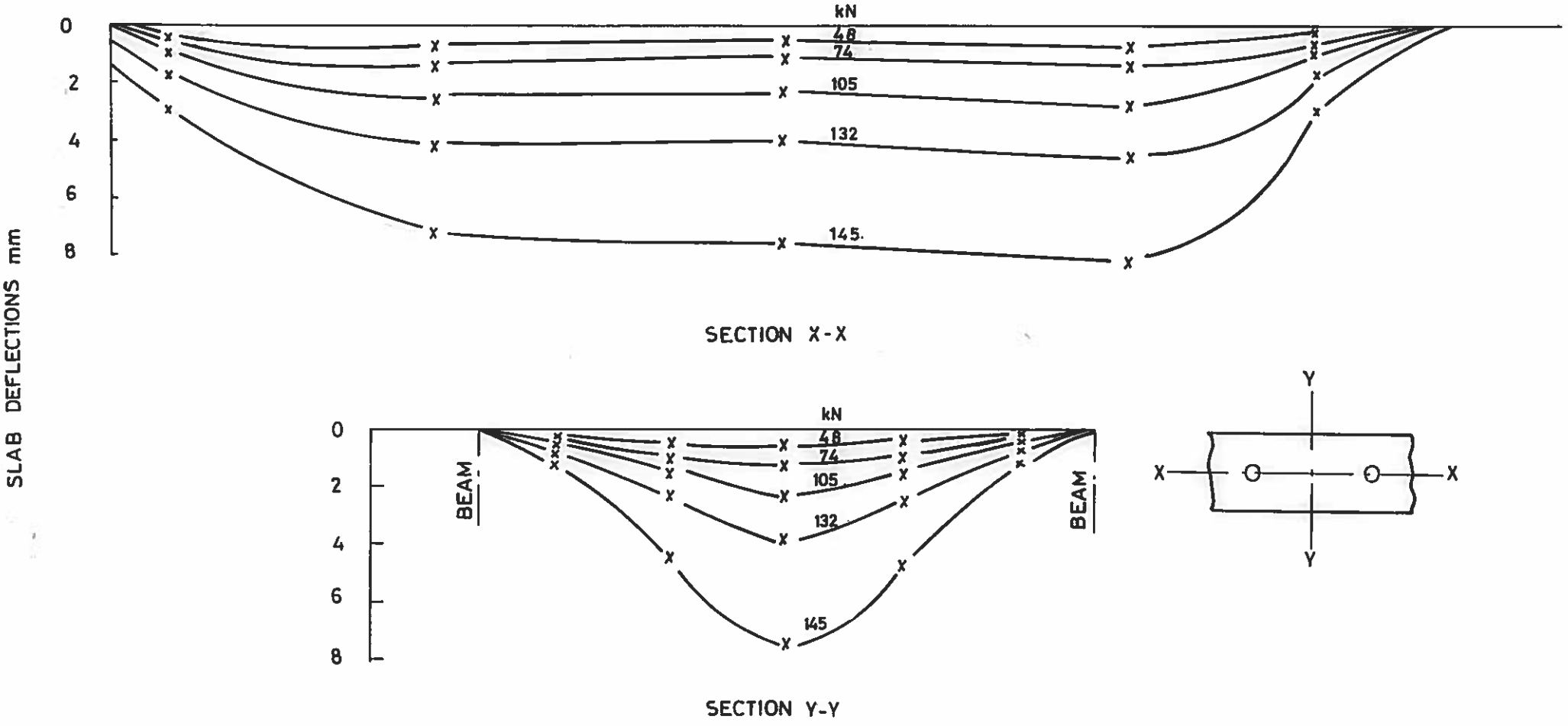

Fig. 8.13 Deflection Profiles Panel C3

Fig. 8.13

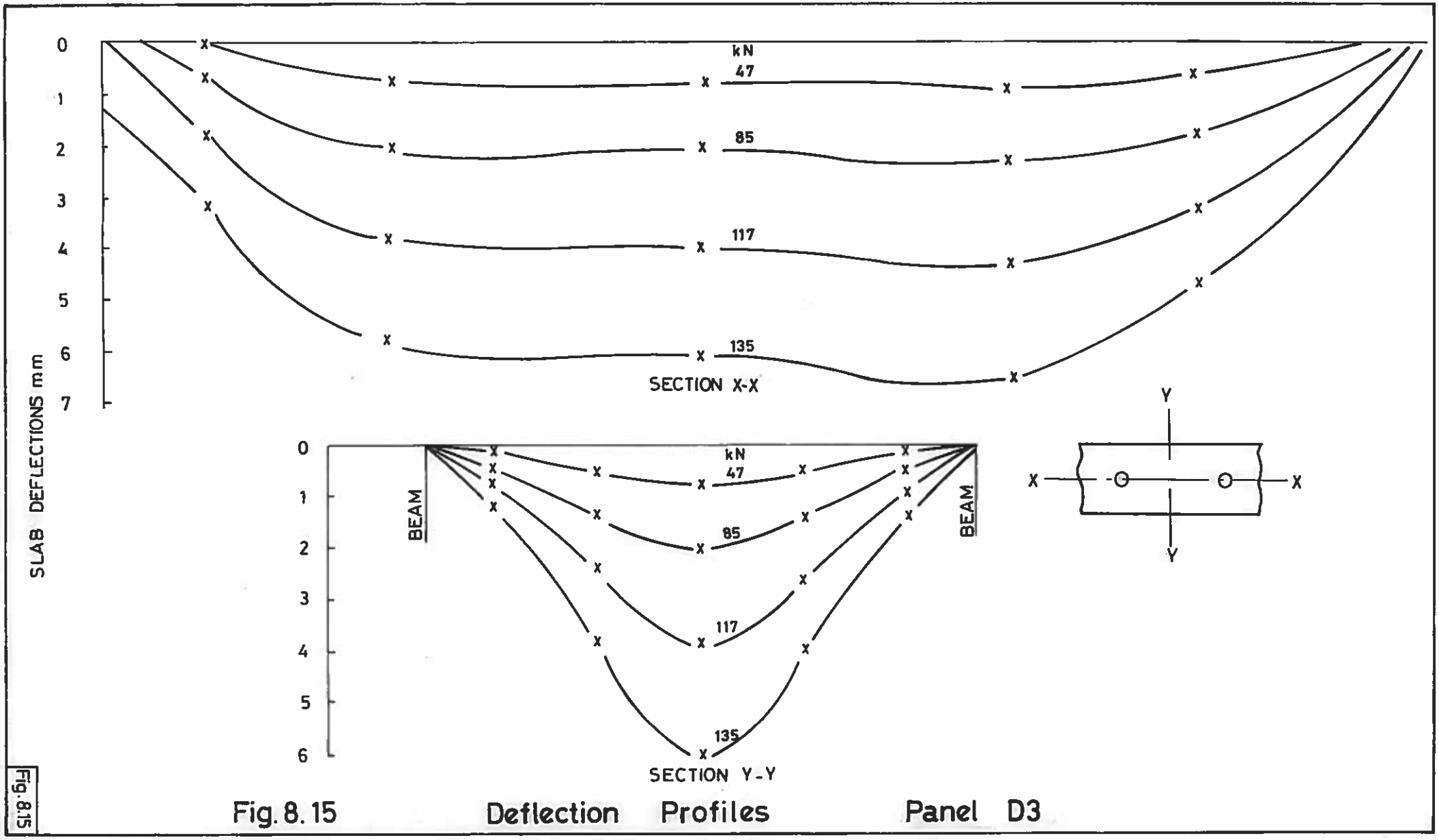

Fig. 8.15 Deflection Profiles Panel D3

Fig. 8.15

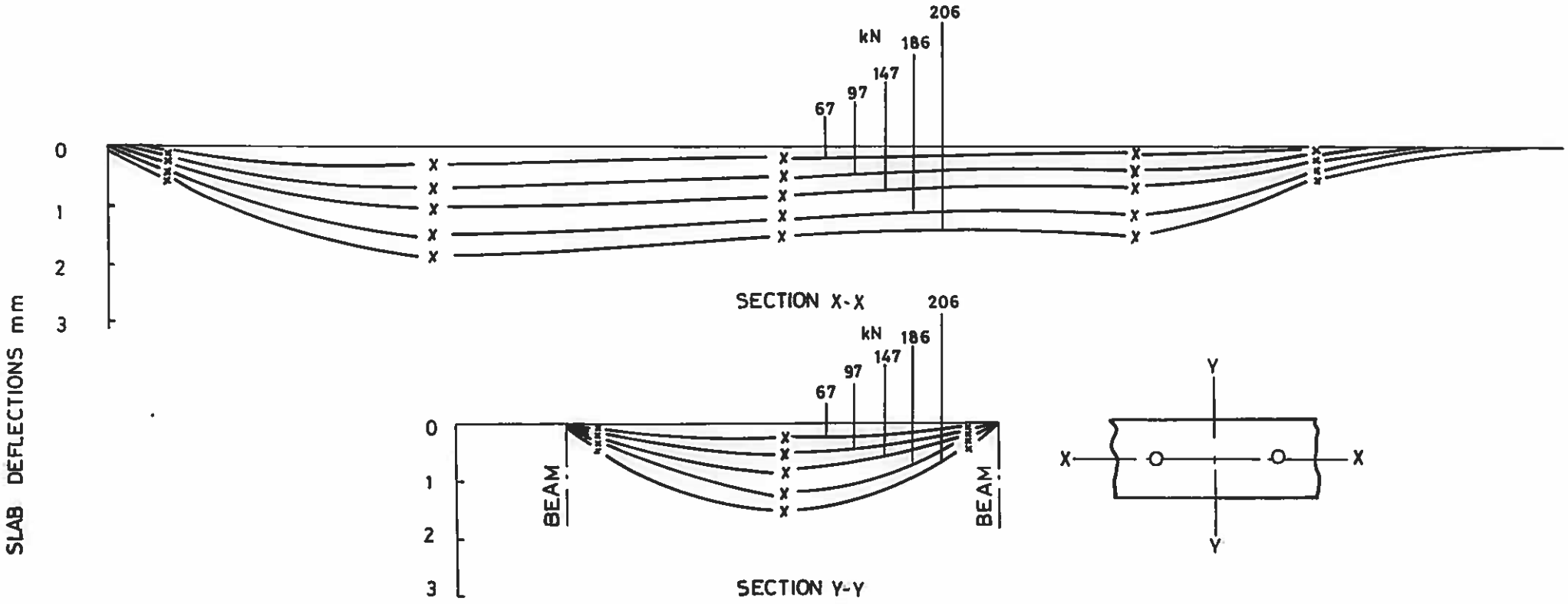

Fig. 8.14 Deflection Profiles Panel C5

Fig. 8.14

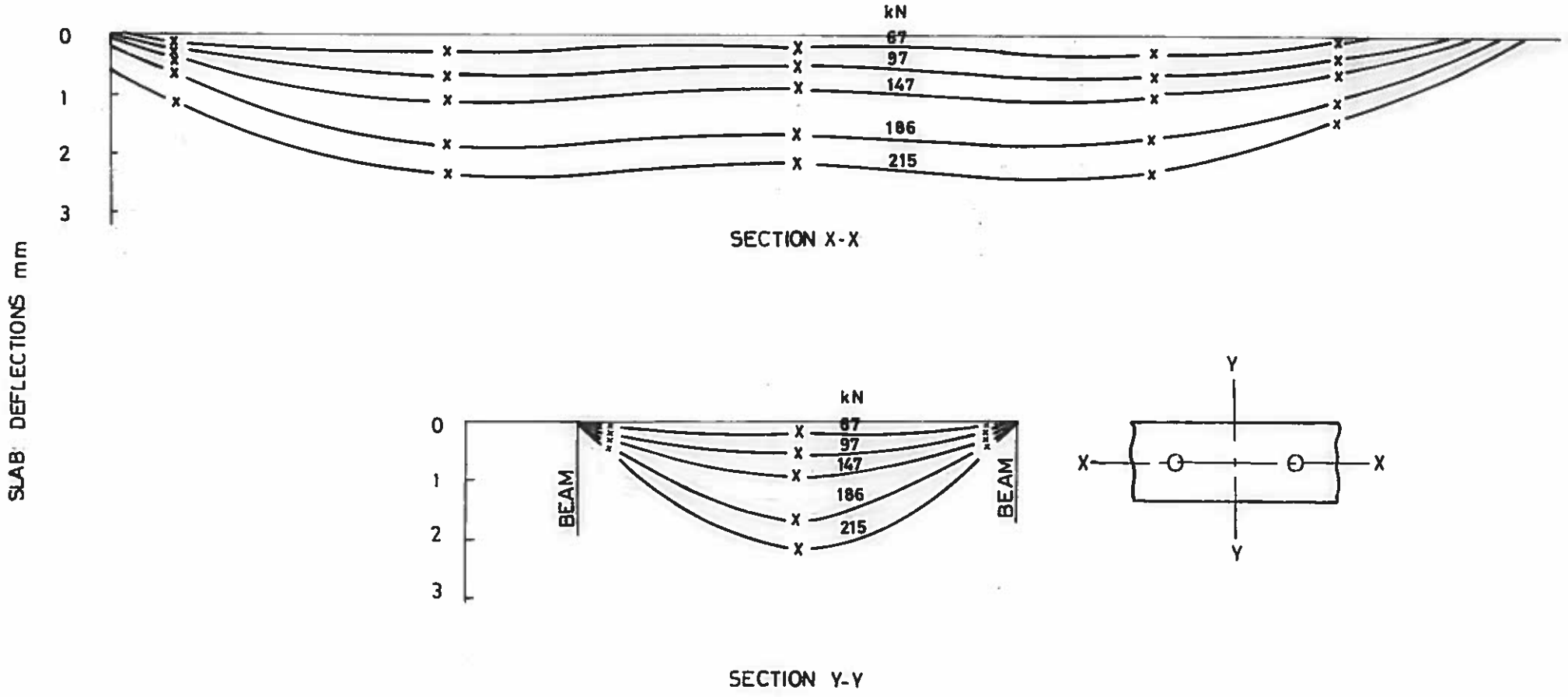

Fig. 8.16 Deflection Profiles Panel D5

Fig 8.16

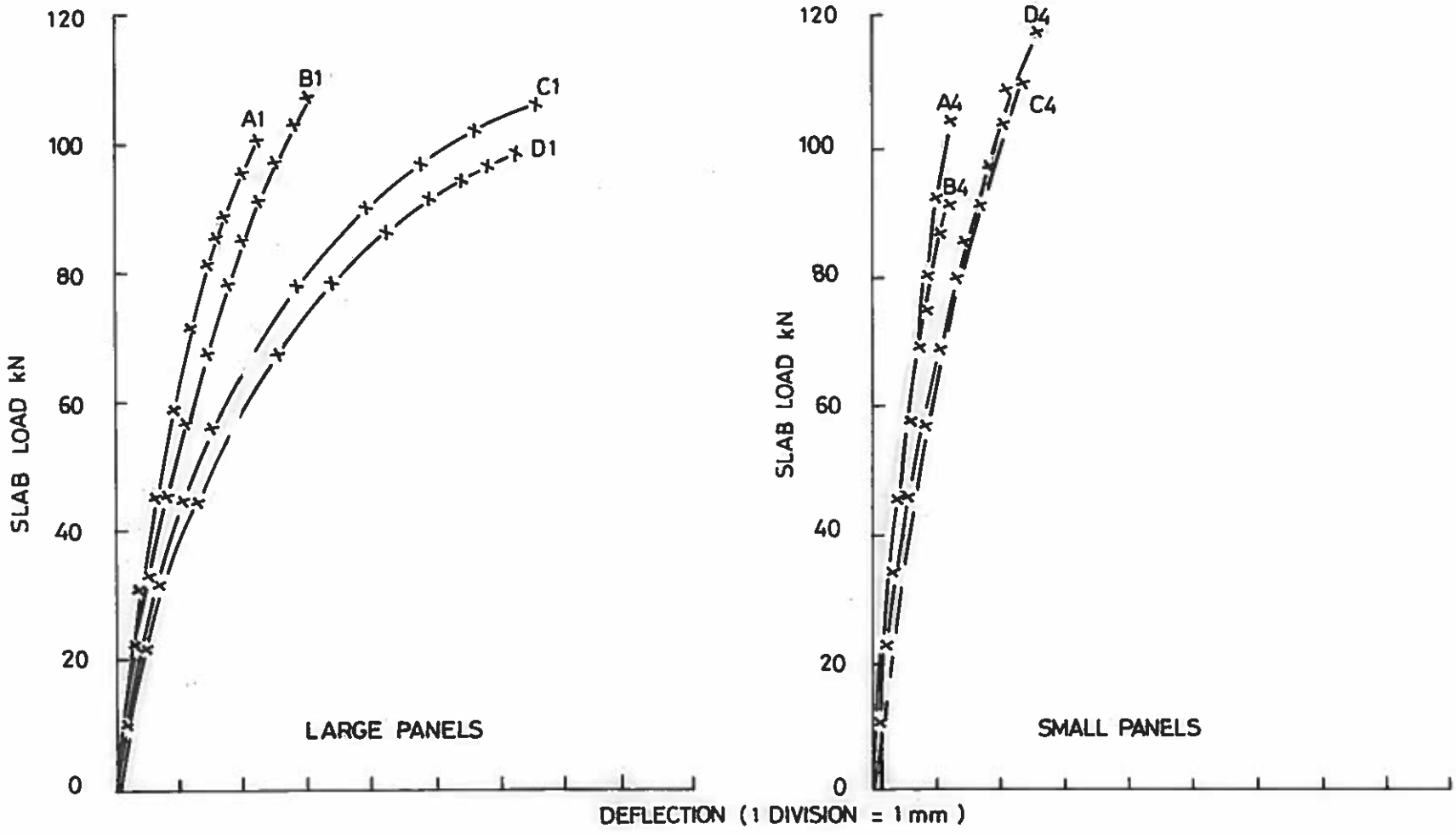

Fig. 8.17 Typical Load Deflection Graphs for Large and Small Slabs Under Single Wheel

Fig. 8.17

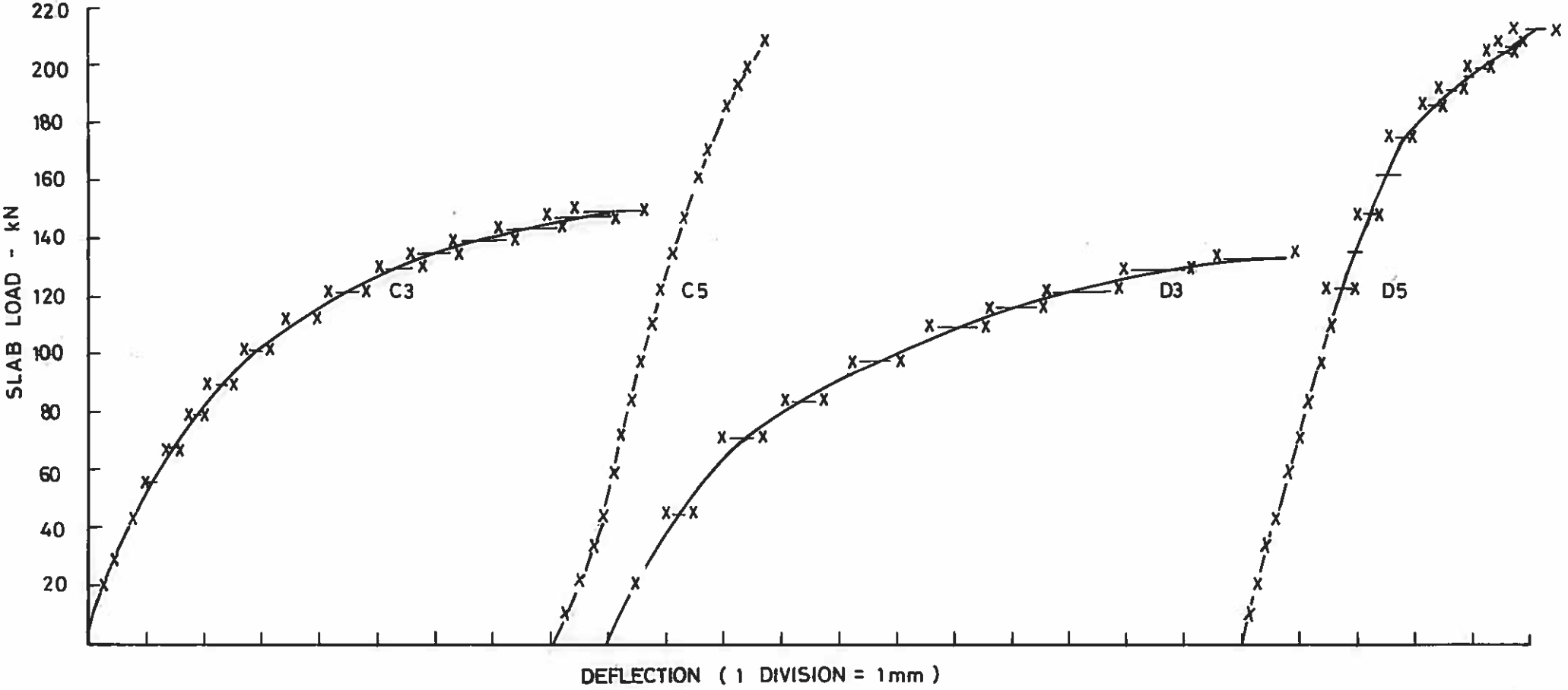

Fig. 8.18 Load Deflection Graph For Slabs C and D Deflections Under Double Wheels

Fig. 8.18

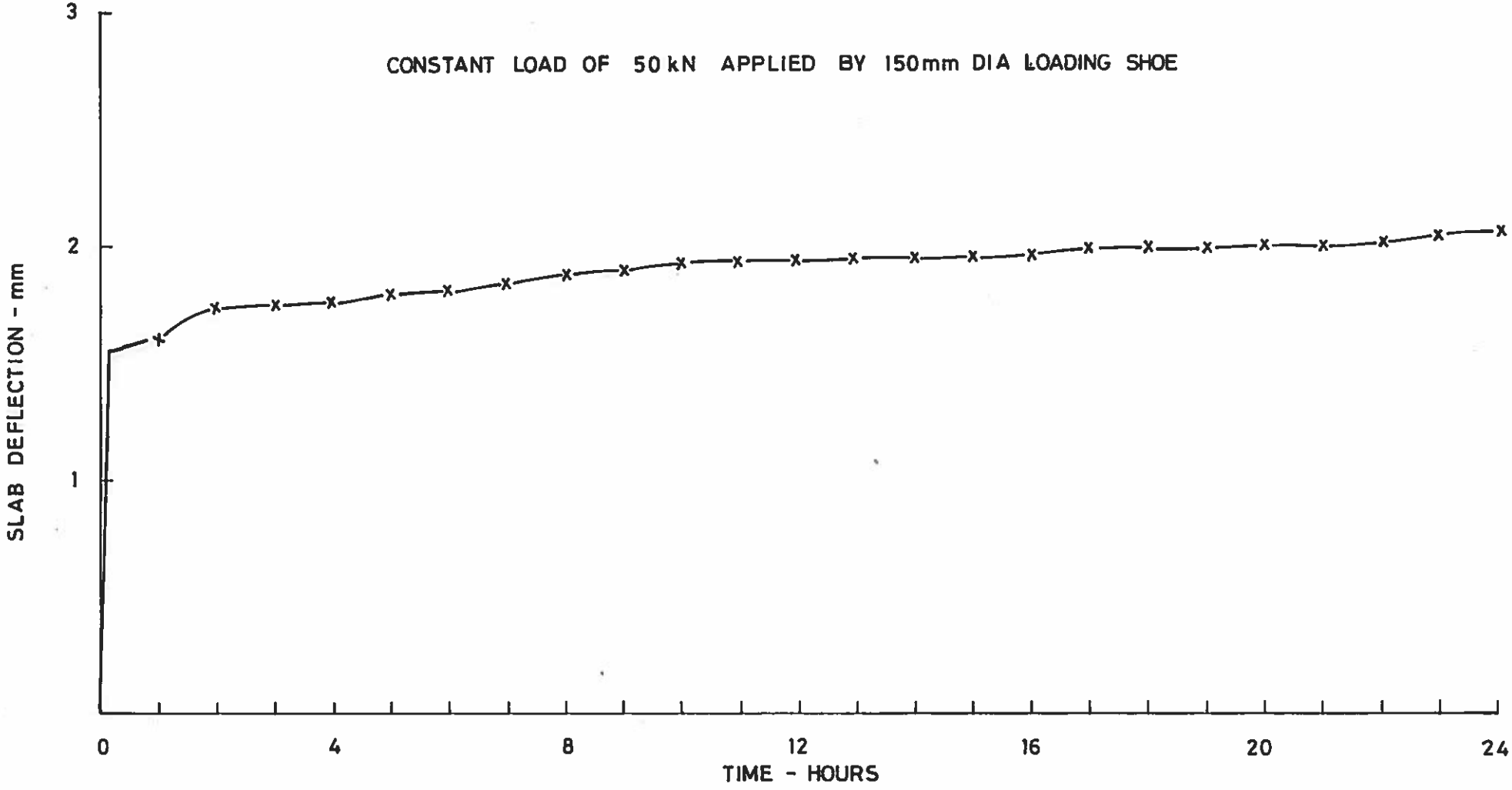

Fig 8.19 Slab Deflection - Time. Creep Test On Slab D2

Fig 8.19

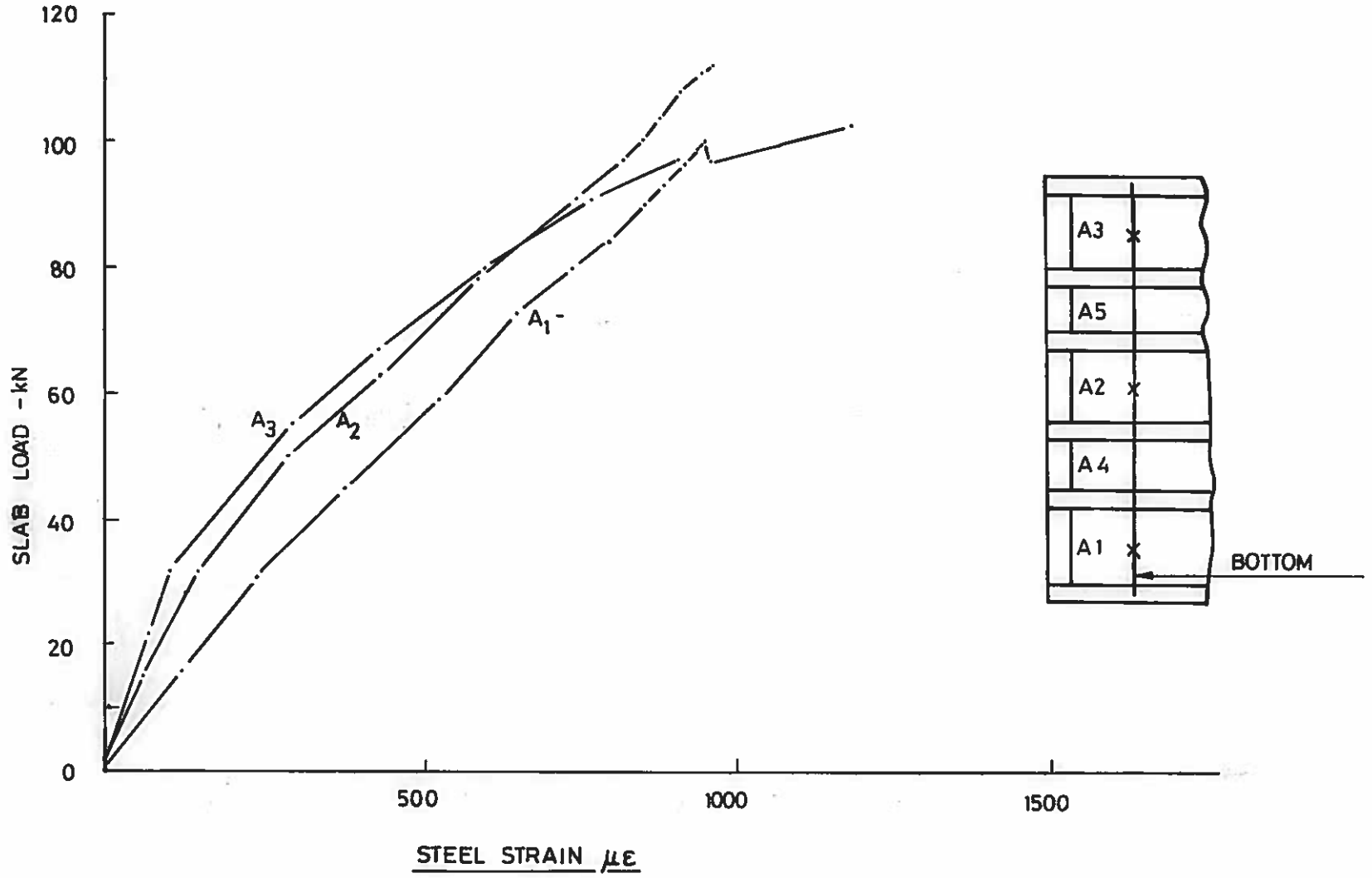

Fig 8.20 Variation of Steel Strain with Applied Load - Panel A

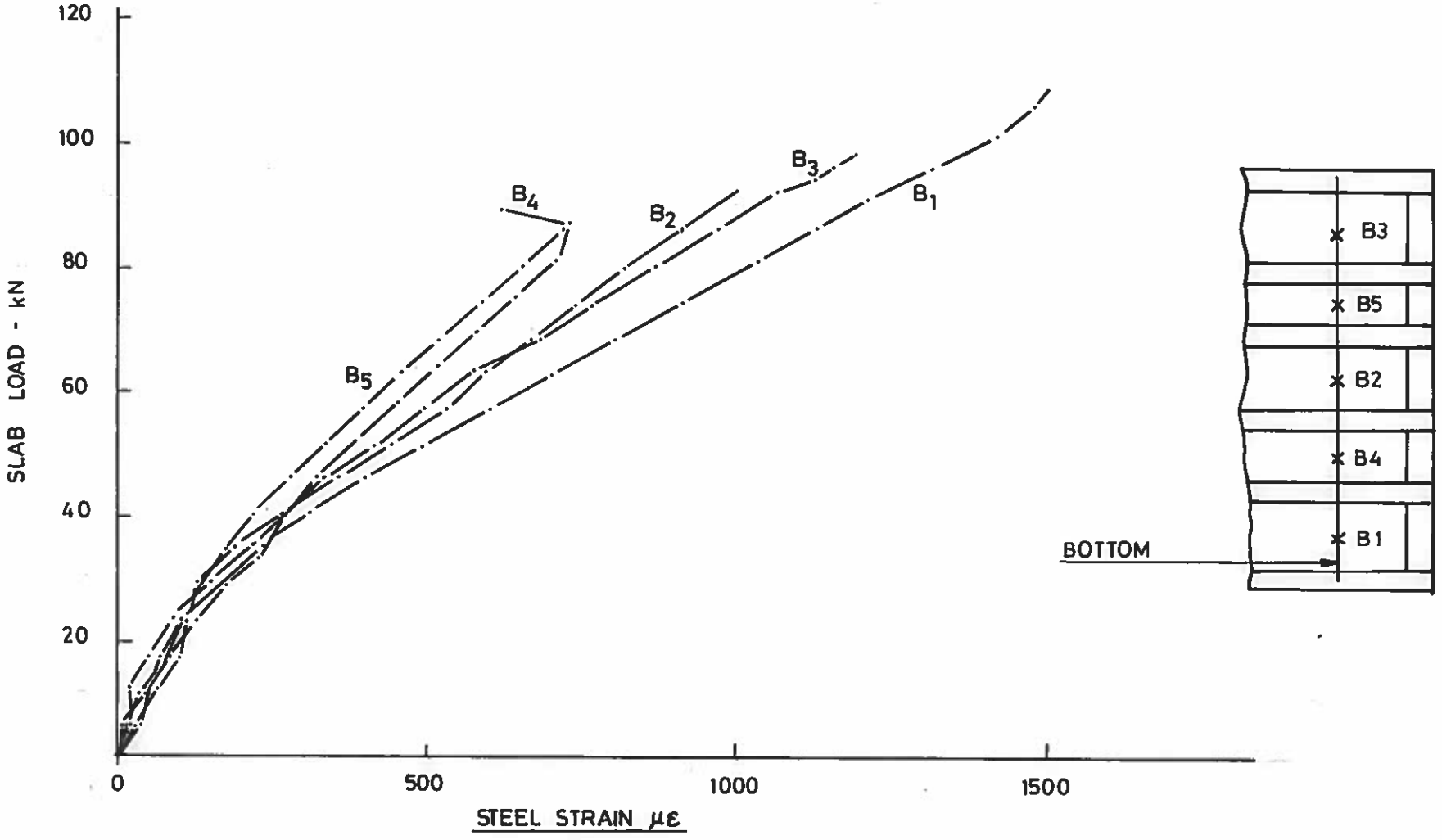

Fig. 8.21 Variation of Steel Strain with Applied Load - Panel B

Fig.8.21

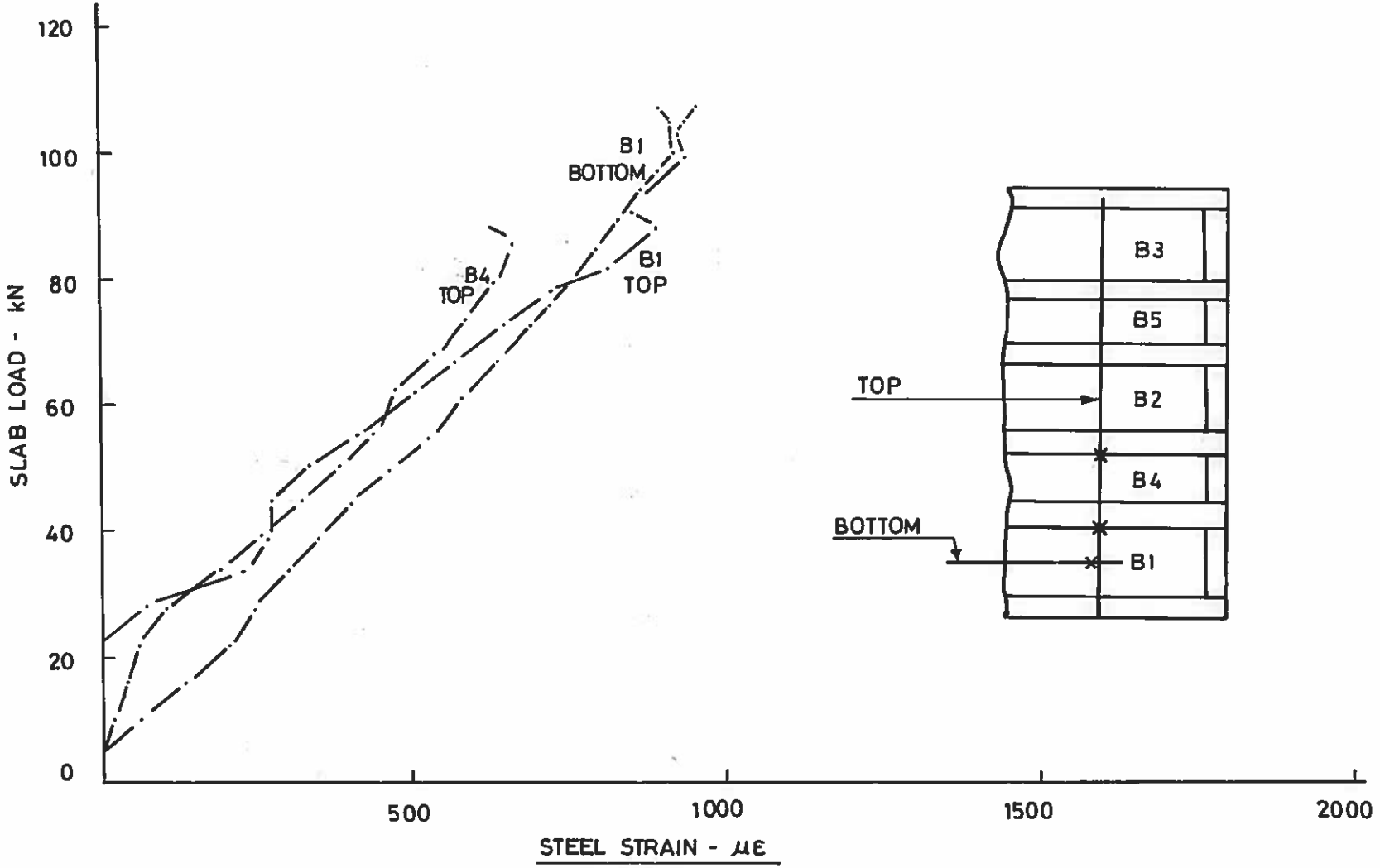

Fig. 8.22 Variation of Steel Strain with Applied Load - Panel B

Fig.8.22

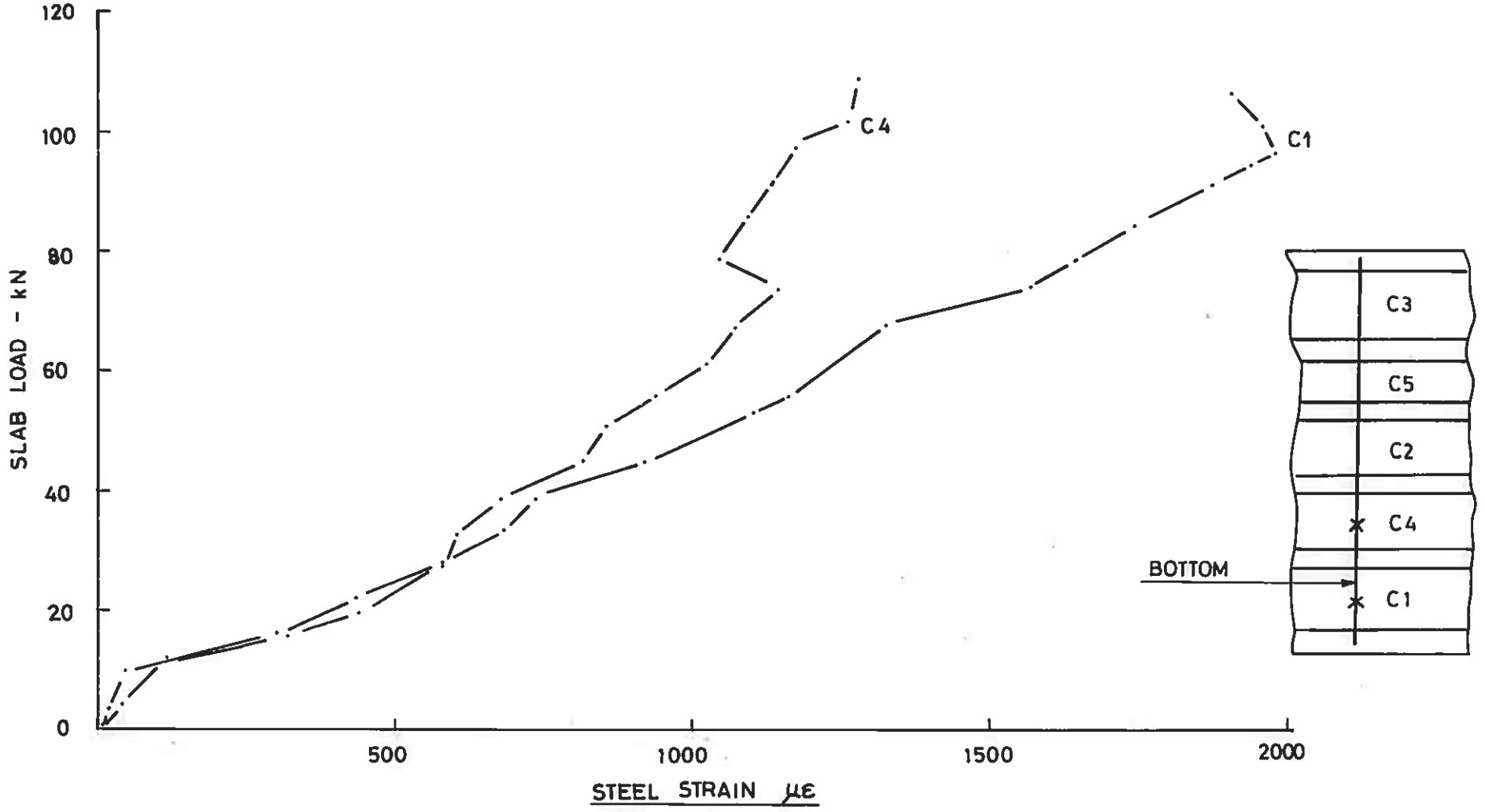

Fig. 8. 23 Variation of Steel Strain with Applied Load - Panel C

Fig.8.23

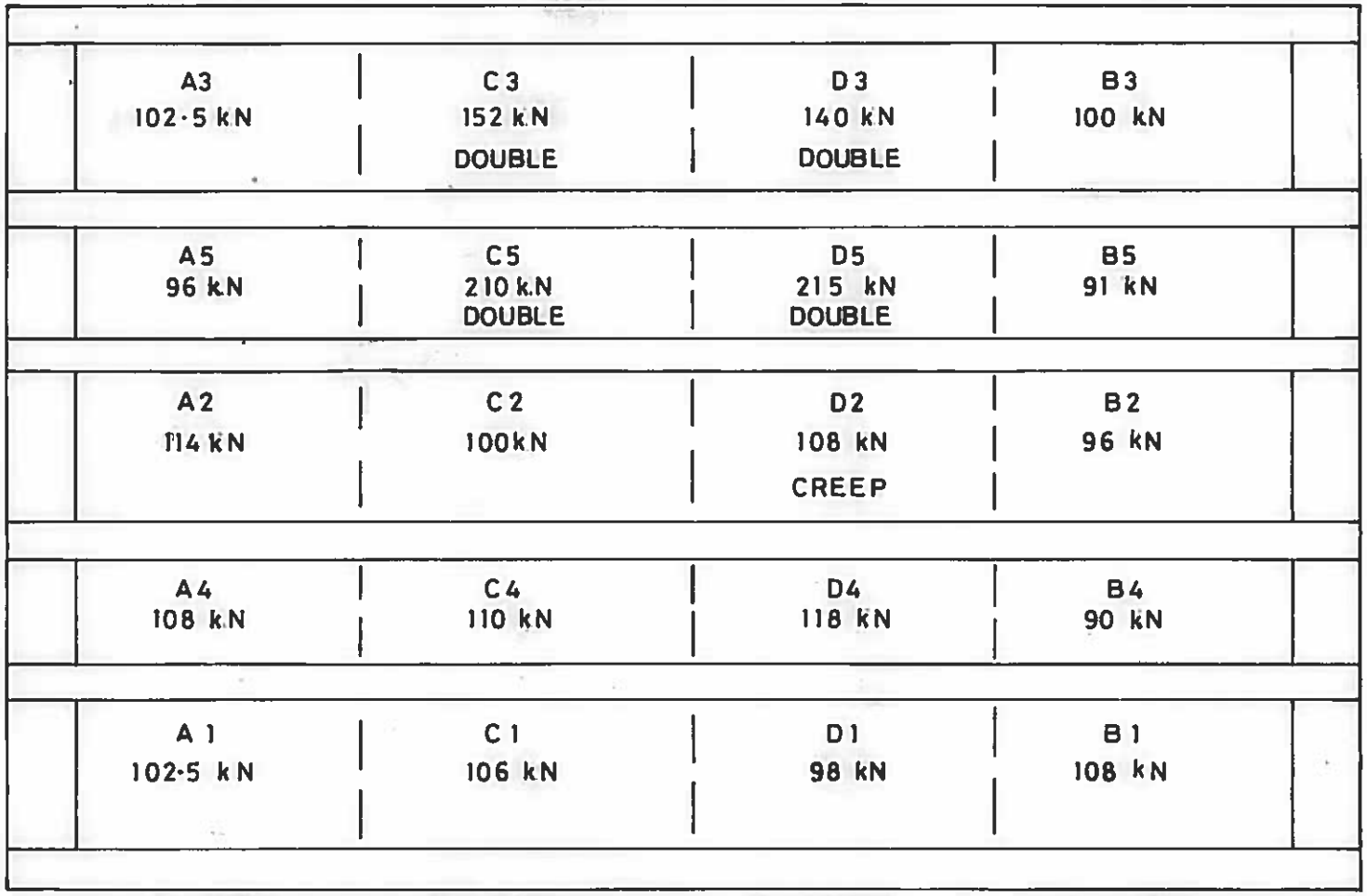

PROTOTYPE WHEEL LOAD OF 112·5kN IS EQUIVALENT TO 12·5kN MODEL LOAD

Fig. 8.24

Fig. 8.24 1/3 Scale Model - Failure Loads

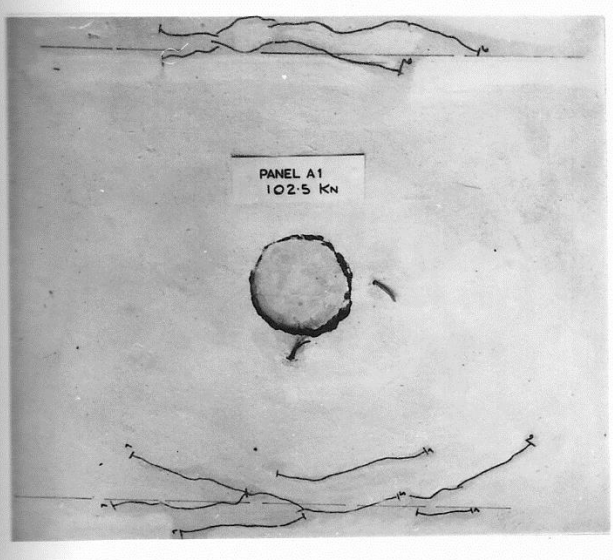

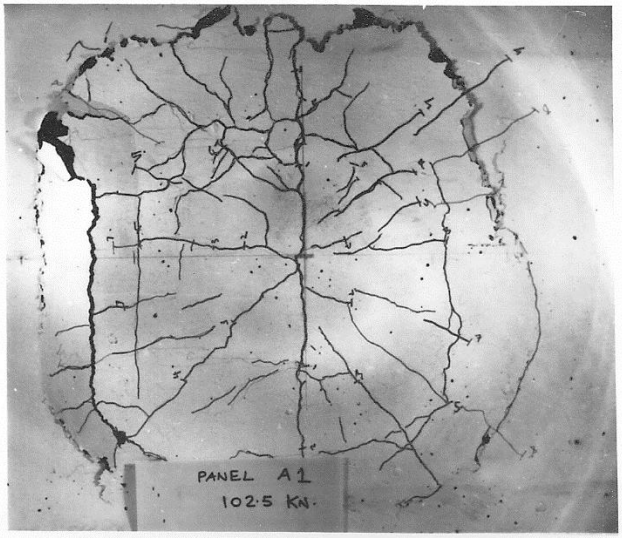

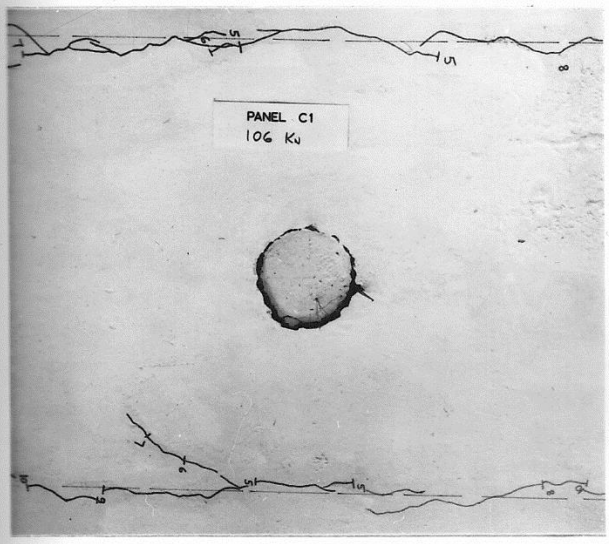

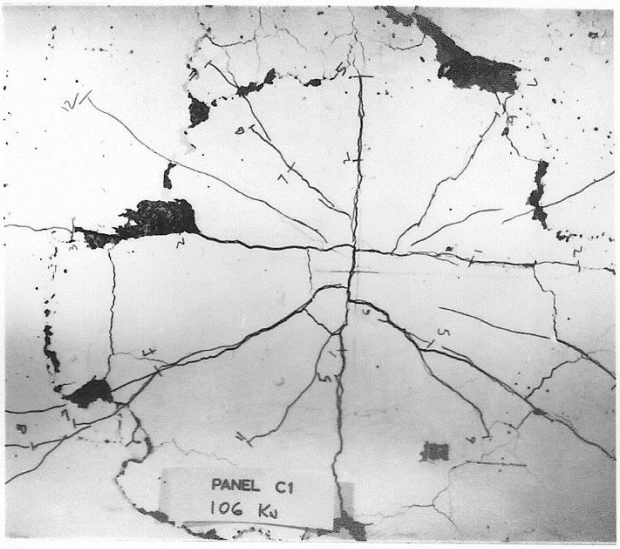

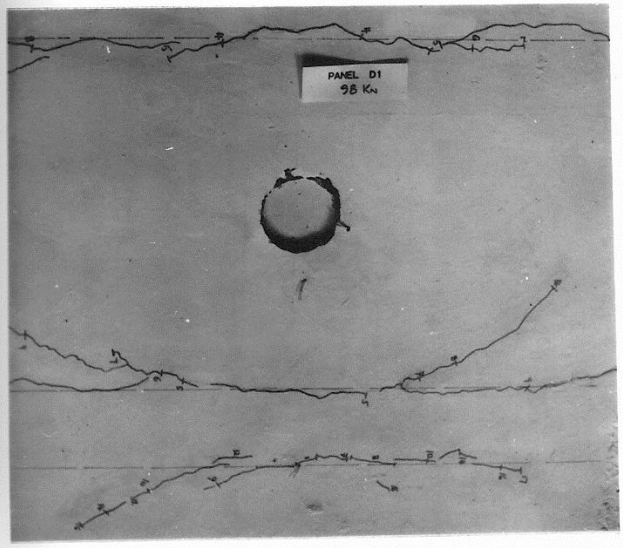

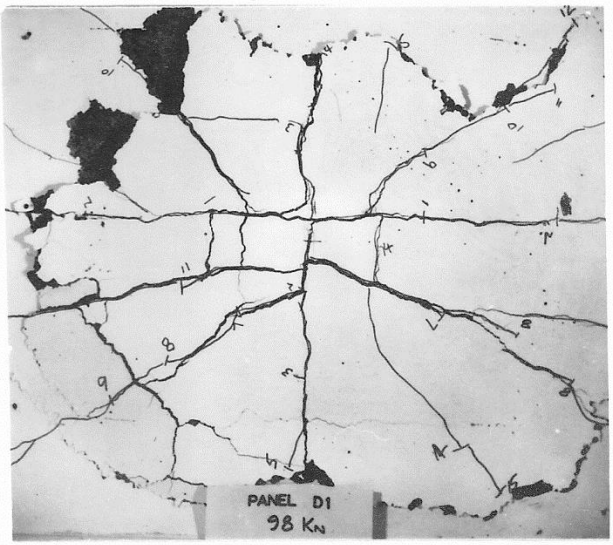

Plate 8.1 Typical Crack Patterns for Large Panels

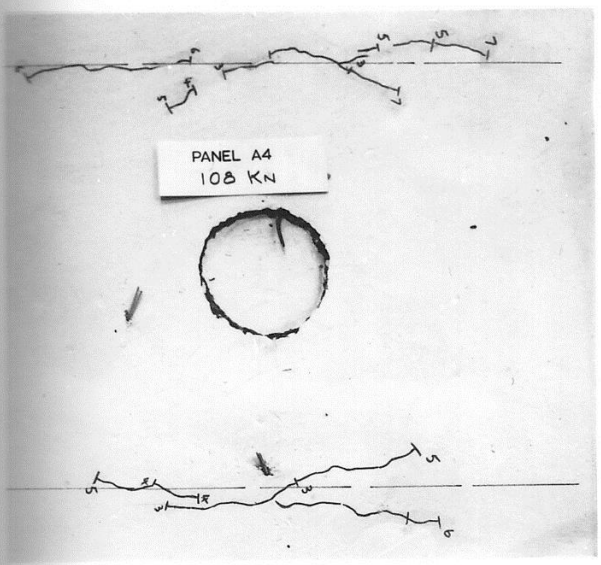

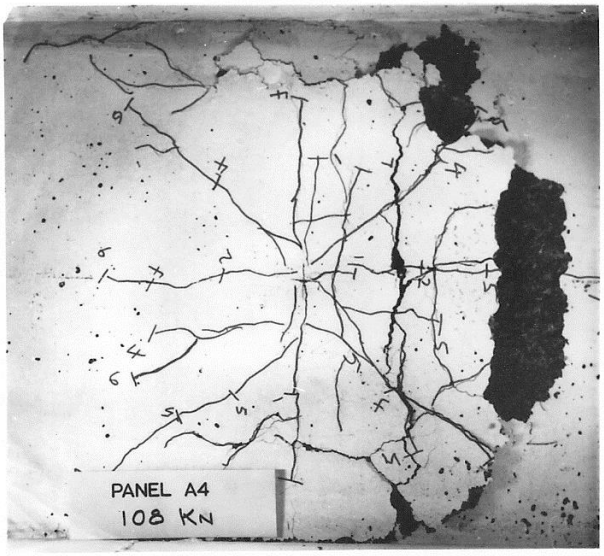

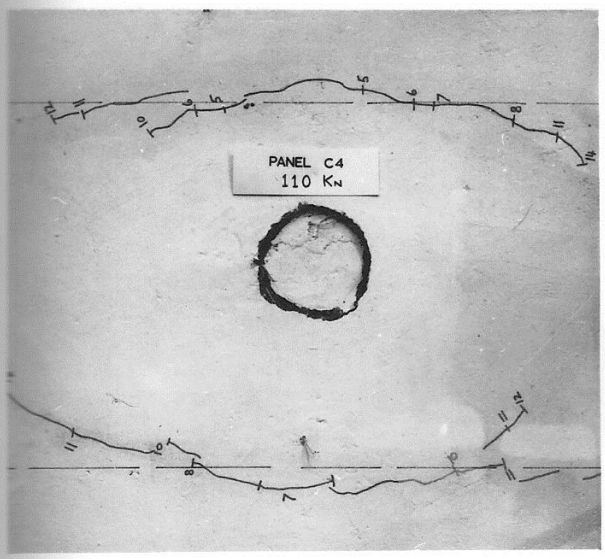

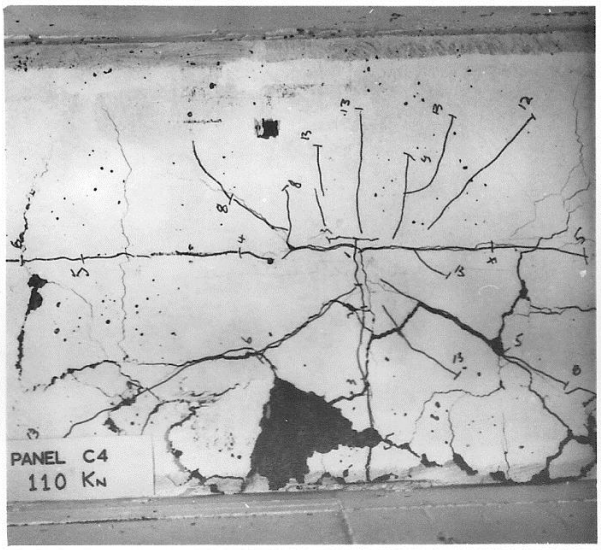

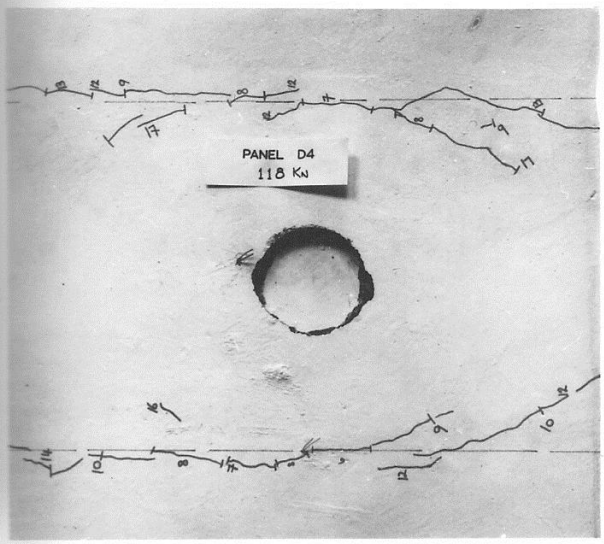

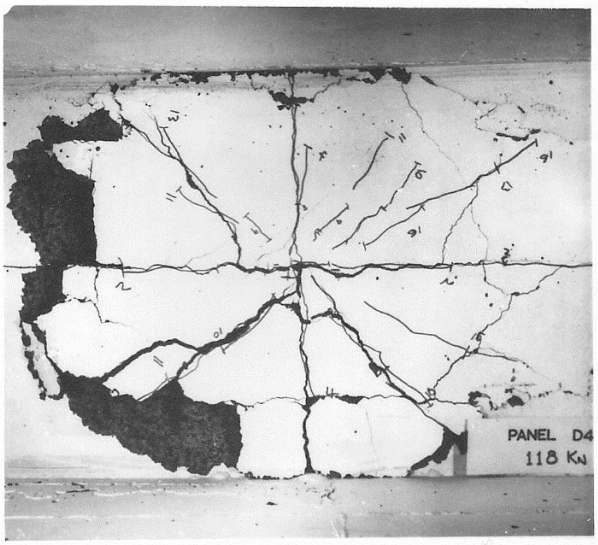

Plate 8.2 Typical Crack Patterns for Small Panels

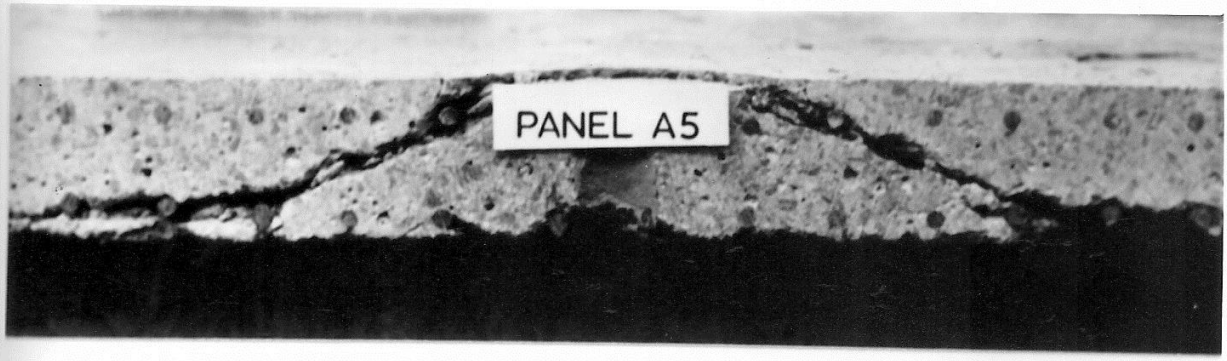

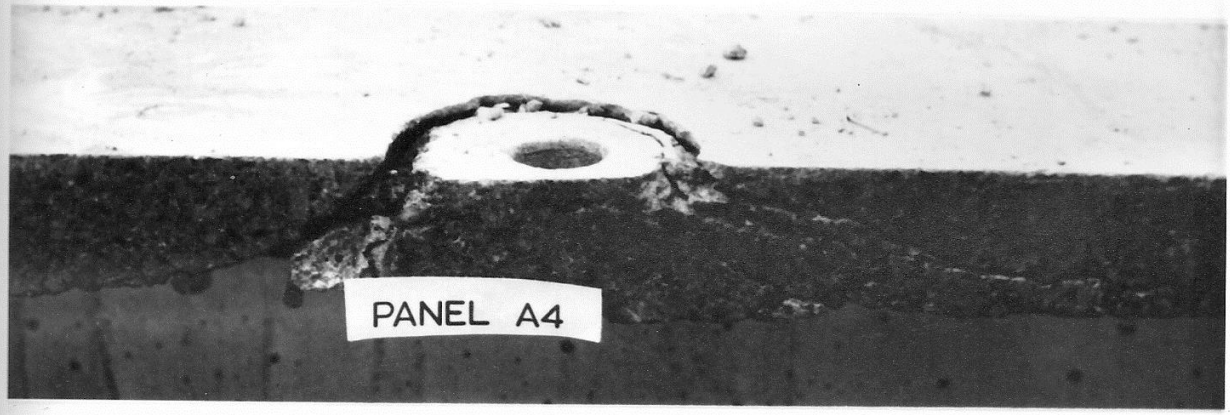

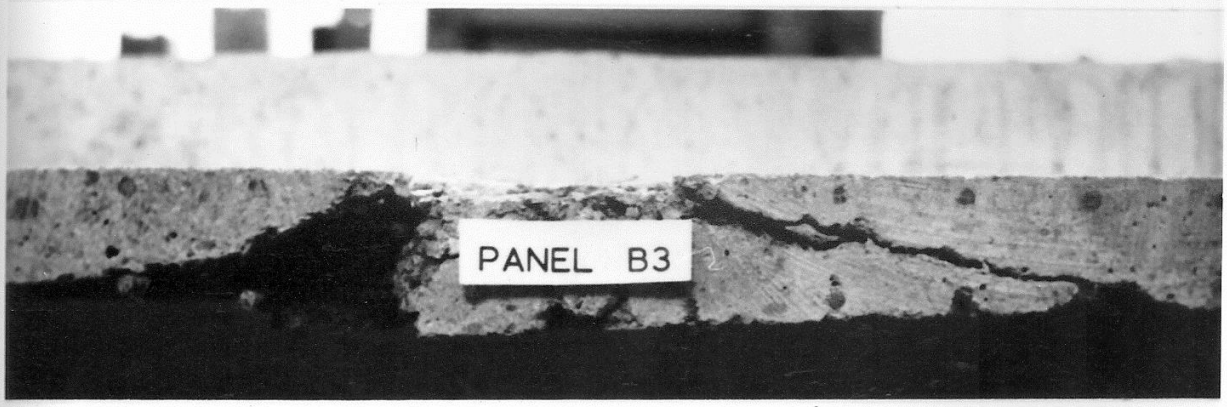

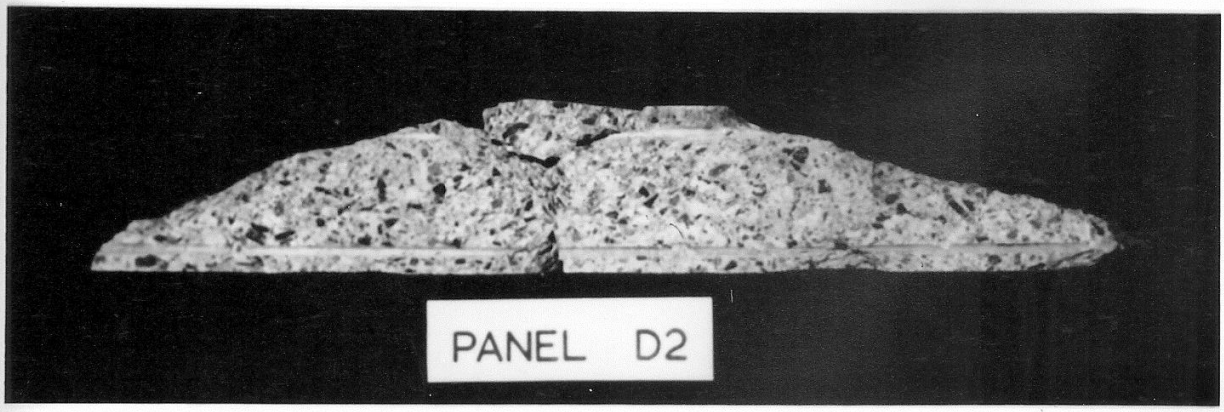

Plate 8.3 Typical Section Through Failure Cones

Plate 8.4 Typical Sections Through Diaphragms and Slab

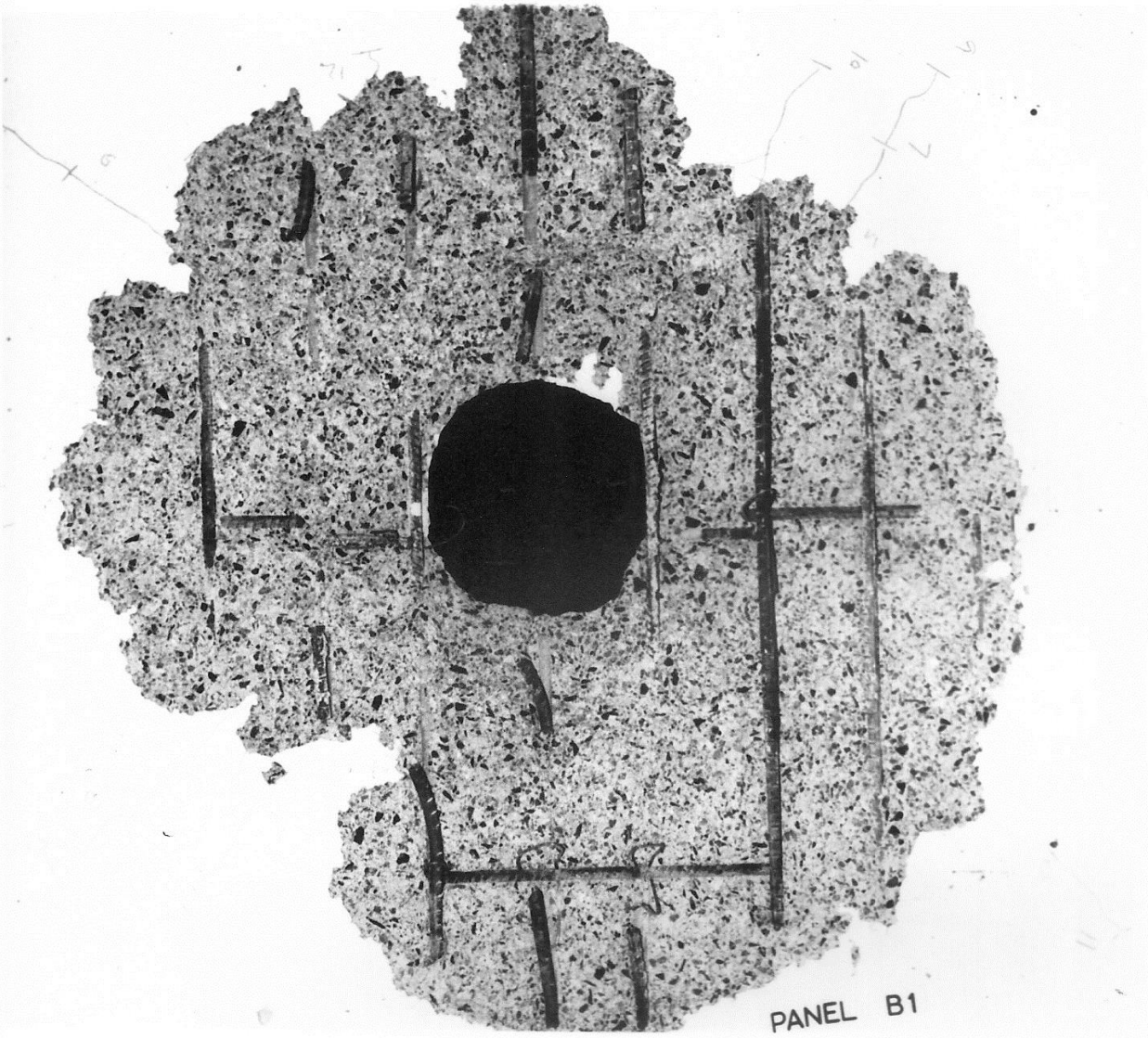

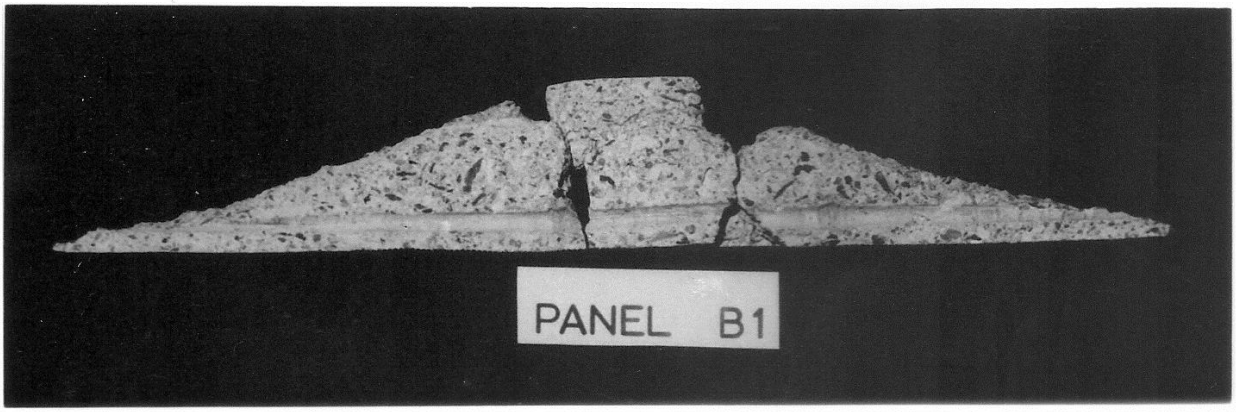

Plate 8.5 Soffit Failure Area and Cone B1

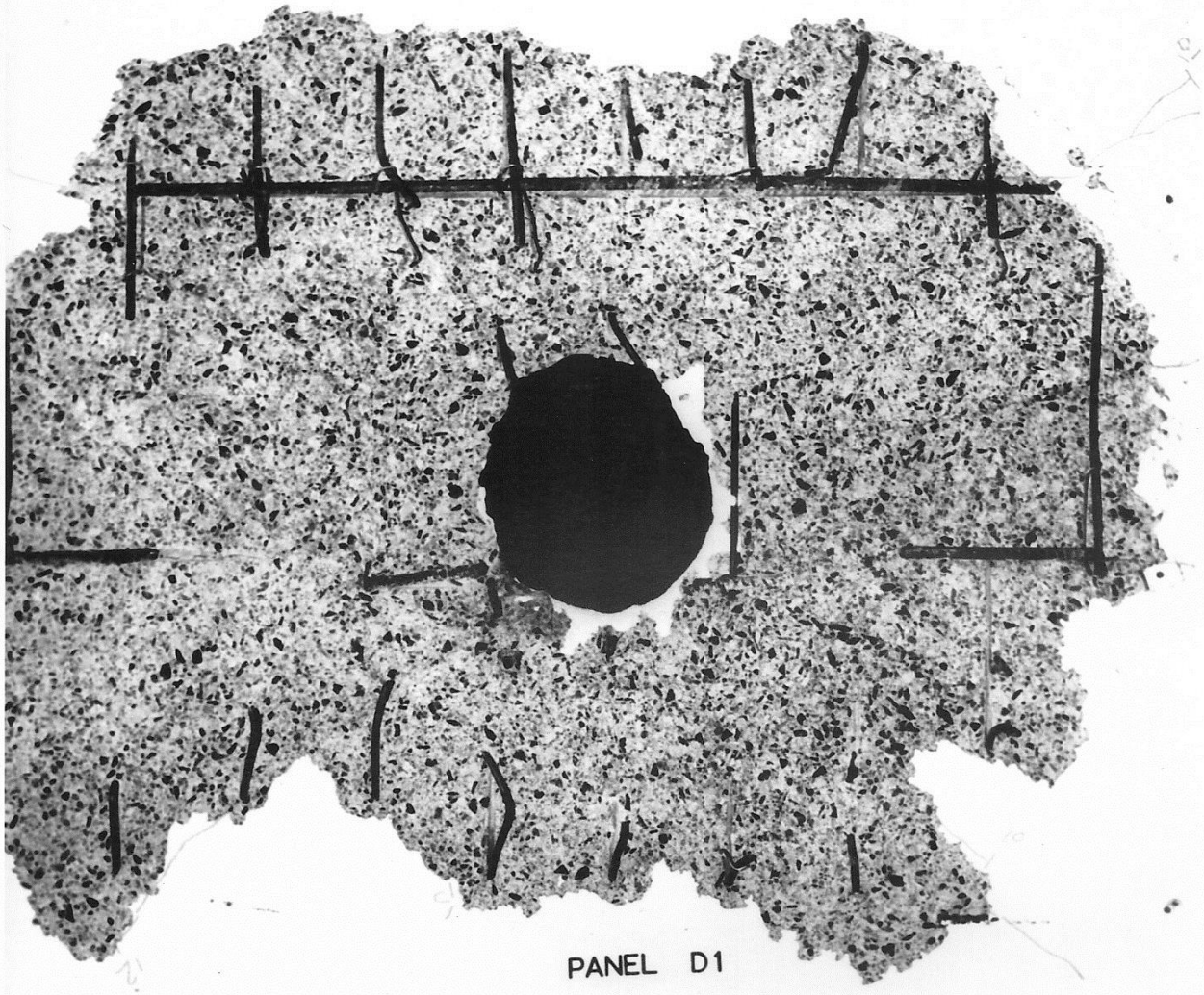

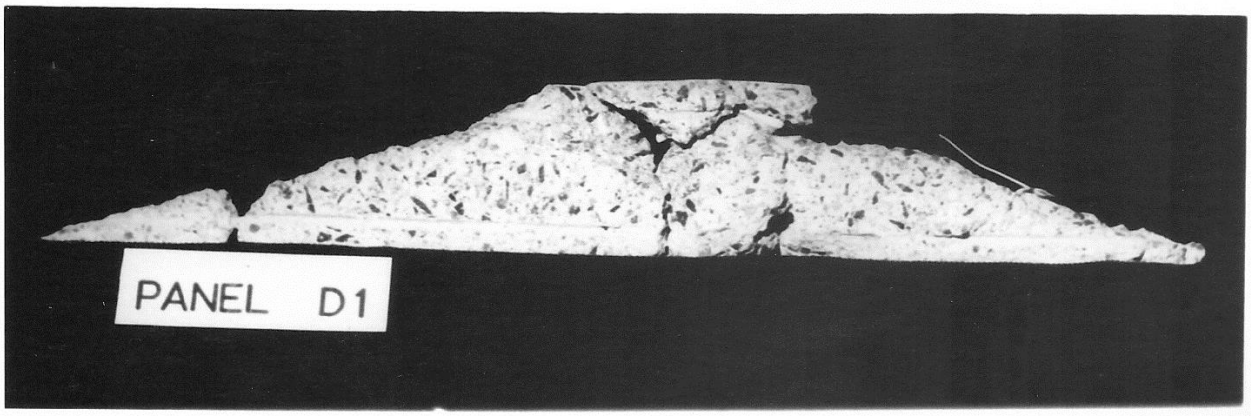

Plate 8.6 Soffit Failure Area and Cone D1

CHAPTER NINE

DESIGN OF RIGIDLY RESTRAINED BRIDGE SLABS

9.1 INTRODUCTION

The results of the tests on the $\frac{1}{3}$ scale model have shown a considerable enhancement to the design capacity of the standard slab with the M-beams spaced at up to 2 m apart. This enhancement has been attributed to the considerable in-plane restraint that is inherent in bridge slabs.

Although commonly designed by flexural methods all the panels, including those with low % steel, failed in a punching shear mode. Whilst the bridge design codes of both the United Kingdom and North America have punching shear requirements, these approaches, which have been reviewed in Chapter 2, differ greatly. Thus, to check their validity, the strengths predicted were compared with the actual failure loads and this highlighted their serious shortcomings. As a consequence a more appropriate method is proposed for estimating the ultimate load capacity of these slabs. This recognises the importance of arching action and its influence on the punching mode of failure.

The results of the model tests also showed that the amount of steel reinforcement in the slab had very little effect on the load capacity which indicates that for fully restrained bridge slabs the influence of arching action is a major contributing factor to the very high punching strength. Therefore with this in mind the proposed method for predicting the punching strengths of the model slabs used a punching shear equation which has been modified to allow for the compressive membrane forces generated by the arching of the slab. The proposed method has also been used to predict the load capacities of other relevant tests on bridge slab models. Design curves have also been generated which will predict the ultimate capacity of standard M-beam slabs for any given concrete strength and span to depth ratio.

Due to the large factor of safety which has been achieved against punching shear failure it is virtually impossible to generate a group of wheel loads of the magnitude required for failure of the slab without serious distress or collapse of the overall structure. Therefore, punching is not an important design parameter but the tests revealed that serviceability and, in particular, cracking is. As the prototype has not, as yet, been tested, recommendations have been made based on measurements and observations of the performance of the models at service load.

9.2 COMPARISON OF TEST RESULTS WITH DESIGN CODES

It was observed that all the test panels failed by punching shear and it was therefore relevant to compare the results of the model tests with the capacities predicted by both United Kingdom and North American bridge design codes, the details of which have been considered in Chapter 2.

The comparison between the predicted punching shear strengths using the above codes and the average failure loads for both large and small panels is shown in Fig. 9.1. The predicted values are based on average concrete strengths, slab depths and percentage steel reinforcement for each group of test panels. It is clear that the codes do not give a satisfactory prediction of the punching shear capacity of typical bridge slabs and a more appropriate method which allows for in-plane restraint will now be considered.

9.3 LOAD CAPACITY OF RIGIDLY RESTRAINED BRIDGE SLABS

9.3.1 General

From the tests on the $\frac{1}{3}$ scale model of Clinghans Bridge it was observed that all the panels failed in a punching shear mode which initiated

around the circular loading pad simulating the wheel load. The punching shear requirements of both the United Kingdom and North America bridge codes have not given an accurate estimate of the failure load and in order to improve the prediction of the failure load for bridge slabs an empirical shear formula modified to include the effect of compressive membrane action is proposed.

9.3.2 Basis of Method

The equation is derived from the 2 phase approach to punching by Long (1975) where:-

$$P_p = 4(c + d)\, d.0.42\, \sqrt{f'_c}\, (100\rho)^{0.25} \text{ (SI Units)}$$

The ACI notation has been used and this will be retained for application to restrained bridge slabs as material and load factors are not included at this stage. This equation has been calibrated for tests in which the yield strength of the reinforcement remained almost constant at approximately 320 N/mm^2. The critical section was taken as d/2 from the perimeter of the loaded area and although it was formulated for use with building slabs and square columns it was considered suitable, with modification, for predicting the punching strength of restrained bridge slabs.

It is generally accepted that a wheel load applied to a bridge slab is approximately circular in shape and when the perimeter of the square column is replaced by the perimeter of a circular wheel load the equation then becomes:-

$$P_p = \pi(\phi + d)d.\ 0.42\, \sqrt{f'_c}\, (100\rho)^{0.25}$$

It is further recognised that a circular column, relative to a square or rectangular column, is free of stress concentrations with a subsequent

increase of about 15% in the punching shear capacity. Allowing for this increase the above equation now becomes:-

$$P_p = 1.52(\phi + d)d \sqrt{f'_c} (100\rho)^{0.25}$$

This 15% improvement which allows for a reduction in the stress concentration around the perimeter of the column was based on a review of various tests by Regan (1981), in which the columns were assumed monolithic with the slab and hence the column load was applied by a hard circular surface. Wheel loads are of course applied to bridge slabs by rubber pneumatic tyres and this has been simulated in model tests by a rubber pad. The use of a rubber pad in the interface between loading shoe and deck slab will provide a better distribution of load and this should result in a higher load capacity for the slab. However, this additional and probably small enhancement has not been included in the above equation as this will provide a conservative prediction of the punching shear capacity of the slab.

9.3.3 Influence of Compressive Membrane Action

If it is accepted that the $(100\rho)^{0.25}$ term in the equation is a measure of the influence of the flexural strength on the shear capacity by its effect on the compression zone around the loaded area, it is this parameter which may be used to represent the influence of compressive membrane action by introducing an effective reinforcement ratio and the flexural term then becomes $(100\ \rho_e)^{0.25}$.

For rigidly restrained slabs, it is recognised that the effect of reinforcement upon the ultimate capacity is small and this was confirmed by the results of the model test. The relationship between slab capacity, reinforcement level and restraint has been investigated by other researchers and the following comments have been made.

1. Brotchie and Holley (1971) have suggested that, for a slab with a span to depth ratio of 20, the effect of arching was found to be equivalent in load capacity to approximately 2% of conventional reinforcement.
2. They also suggested that for a span to depth ratio of 5 arching action was equivalent in load capacity to over 3% of conventional reinforcement.
3. Brotchie and Holley (1971) concluded that unreinforced slabs when fully restrained laterally are stronger than conventionally reinforced but unrestrained slabs with normal ratios of steel.
4. Taylor and Hayes (1965) found that increasing the reinforcement from 1.57 to 3.14% had very little effect on the load capacity of a restrained slab.
5. Snowdon (1973) has shown that restrained unreinforced slabs had a load capacity of about 95% of the restrained slab with 2% reinforcement.

Therefore, it is suggested that an estimate of the strength of a slab section can be made by neglecting bending action and considering only arching action which for a bridge slab is shown in 9.2. Referring to Fig. 9.3 the maximum arching capacity of a section may be calculated as follows:-

$$\text{Moment of Resistance} = C_c \times \text{lever arm}$$

The lever arm is a function of the deflection of the section and for maximum possible arching the deflection = 0.

From Fig. 9.4

$$M_{ar(max)} = 0.85\, f'_c\, (h/2)^2 = 0.21\, f'_c h^2$$

This equation has been proposed by Christiansen (1963) for calculating membrane enhancement in one-way slabs.

$M_{ar(max)}$ can only occur however, for a section composed of perfectly rigid/plastic material, i.e. a material which becomes plastic under a very small magnitude of strain. The idealised stress/strain curve for such a material is shown in Fig. 9.5.

As concrete does not obey a rigid/plastic criterion $M_{ar(max)} = 0.21\ f'_c h^2$ cannot be attained because of a reduction in the lever arm under deformation. This can however be taken into account by deriving the arching moment (M_{ar}) as a function of the stress/strain properties of an elastic/plastic material and the span to depth ratio. The idealised stress/strain curve for an elastic/plastic concrete is shown in Fig. 9.6 and the variation of arching moment (M_{ar}) with deflection for a material of this nature is shown in Fig. 9.7.

Based on the deformation approach of McDowell, McKee and Sevin (1956) a relationship between the maximum arching moment $M_{ar(max)}$ and the span to depth ratio has been derived by Rankin (1982) for an idealised elastic/plastic type of concrete. Details of this method are given in Appendix F.

From this, the maximum arching moment of resistance can be calculated for any combination of L/h and f'_c in terms of:-

$$M_{ar} = k\ f'_c\ h^2$$

where k is a reduction coefficient and equals 0.21 for a perfectly rigid/plastic material.

This equation has been evaluated and presented in graphical form so that for any given L/h and f'_c the maximum arching moment can be read by interpolation as a function of $f'_c\ h^2$. These curves are presented in Fig 9.8 and are used as follows:-

$$\text{for } f'_c = 40 \quad L/h = 14 \quad M_{ar} = 0.145\, f'_c\, h^2$$

When the maximum arching moment has been calculated it can then be related to an effective steel reinforcement percentage ρ_e, assuming a yield stress equal to that used for the tests on which the shear equation by Long (1975) was derived.

Therefore:

$$\rho_e = \frac{k\ f'_c\ h^2}{320.0.75\ d^2} \qquad \text{(Appendix F)}$$

and the punching capacity of the fully restrained slab may then be predicted from the modified equation:-

$$P_p = 1.52(\phi + d)d\ \sqrt{f'_c}\ (100\rho_e)^{0.25}$$

9.3.4 Summary

The use of this equation to predict the punching shear capacity of fully restrained bridge slabs is based on the following assumptions.

1. In line with the experimental findings, existing flexural reinforcement has no influence on the load capacity of the slab.
2. The arching enhancement can be represented by an equivalent percentage flexural reinforcement.
3. The critical section is at d/2 from the perimeter of the loaded area.

With a proposed method for the prediction of the punching shear for restrained bridge slabs now established, the predicted strengths using the data from the model will now be compared with the test results.

9.4 COMPARISON OF PROPOSED METHOD WITH TEST RESULTS

9.4.1 General

The proposed method of predicting the punching shear strength of reinforced concrete bridge slabs has been compared with the test results from the $\frac{1}{3}$ scale model of Clinghans Bridge. The work of other researchers has also been considered; where appropriate results are available. For concrete beams the span has been taken as the clear distance between beams and for steel beams the actual beam spacing has been used. Full details of most of these additional models has been given in Chapter 6.

9.4.2 $\frac{1}{3}$ Scale Model of Clinghans Bridge

A comparison of the proposed method with the test results of the model is given in Table 9.1. These results take into account the variation of concrete strength and the thickness of the individual test panels. It will be seen from Table 9.1 that all the test panels had a ratio of P_t/P_p greater than unity with a mean of 1.19 and a standard deviation of 0.068. The proposed method showed a good correlation with this model which had a relatively constant concrete strength of about 40 N/mm^2 and steel reinforcement which varied from 0.24% to 1.76%.

9.4.3 Model Tests at the University of Illinois

An important series of tests which have been analysed are from the University of Illinois Experiment Testing Station and they form part of an extensive investigation into bridge decks of steel beams and concrete slabs using $\frac{1}{4}$ scale models. A description of the models and test programme was given in Chapter 6 and the comparison of results are given in Table 9.2. The first 2 series are from the tests of Newmark, Siess and Penman (1946) and are from models of right decks. The punching tests considered represent the average of about five tests on each model.

The third series of results are from the work of Newmark, Siess and Peckham (1948) and are similar to the previous models except that skews of 30^{o} and 60^{o} have been introduced. Again the results represent the average of about five tests on each model.

The final set of results shown in Table 9.2 are by Siess and Viest (1953) and are similar to the first group except that they are 2-span continuous over a central support and the results are the average of about 8 tests near the centres of the 2-spans.

In all groups of models both composite and non-composite slabs were tested and the results for these 2 forms of construction are statistically examined separately. The skew and continuity of the deck should not affect the punching shear strength of the slab and the main variables were composite or non-composite action with the steel beams and the strength of the slab at the time of test in which the cube strength varied from 18.8 to 37.3 N/mm^2. The bottom transverse slab reinforcement varied only from 0.87 to 1.09%.

From Table 9.2 it may be seen that apart from model 60N15 there was, as expected, a marked improvement in the punching shear capacity of the slabs which acted compositely with beams. The mean P_t/P_p was 1.04 for the non-composite decks and 1.32 for those which were composite. The results also showed standard deviations of 0.094 and 0.184 respectively which would seem to suggest that some composite action may have been developed.

Although these tests were carried out about 30 years ago, an artifically graded aggregate and standard portland cement was used for the model concrete. However, an important parameter in the design of a microconcrete mix is that the ratio of compressive to tensile strength

should be the same as for the prototype. For this particular mix there is evidence from the control cylinders that the concrete exhibited a rather high tensile strength which introduced scale effects and would account for the rather high ratios of P_t/P_p achieved for both the composite and non-composite models.

It must be stated however, that there is insufficient data available to make an accurate correction to each individual set of results, nevertheless, as assessment of the data available would suggest an increase in the predicted capacities of around 10%. Thus for the composite slabs the mean will be comparable with that for the author's tests.

9.4.4 Model Tests at the University of Manchester

This series of tests by Taylor and Hayes (1965) consisted of testing twenty two plain and reinforced slabs 383 mm square and 76.2 mm in depth with reinforcement of zero, 1.57 and 3.14%. The reinforced slabs were cast and tested in pairs, one simply supported and one restrained, using loading shoes 50.8, 101.6 and 152.4 mm square. The results of the restrained slabs only are compared with the proposed method which has been suitably modified for a square loading shoe.

The comparison of results is given in Table 9.3 and shows a mean P_t/P_p of 1.19, which is the same as the author's tests, and a standard deviation of 0.105. It should be noted that six of the panels were unreinforced and this group had a mean P_t/P_p of 1.15. Although a scaled aggregate was used no details of the tensile strength of the concrete are available. As may be seen from Table 9.3 a good correlation of test and predicted results has been achieved.

9.4.5 Tests at the Building Research Station

A further set of results considered are from unpublished tests by

Snowdon (1973) for the proposed floating airport at Maplin. Some details of these tests have been discussed in Chapters 2 and 6 and as may be seen from Table 9.4 a good correlation with the proposed method has been achieved. The mean P_t/P_p was 1.01 with a standard deviation of 0.0799. It should be noted that this series of tests related to high strength concrete with a wide variation of cube strengths at the time of test which ranged from 44.4 to 78.5 N/mm^2.

It is of interest that Snowdon (1973) concludes that the punching strength of restrained slabs depends almost entirely on the strength of the concrete being proportional to the square root of the cube strength. He also found that tension reinforcement increases the punching shear strength only marginally, a 14% increase was achieved for an increase in steel from zero to 2%.

9.4.6 Ontario MTC Tests

The results of these tests by Holowka, Dorton and Csagoly (1979) are also of interest. Some details of these tests are given in Chapters 2 and 6 and a comparison with the proposed method is presented in Table 9.5. This shows a mean P_t/P_p of 1.06 with a standard deviation of 0.101. These models were restrained circular slabs with most of the concrete having a cube strength of around 34 N/mm^2 at the time of test. Three different slab thicknesses were tested and there was a variation in the steel reinforcement which ranged from 0.2 to 1.0% and this was present only in the bottom of the slab. As may be seen from Table 9.5 good correlation of test and predicted results was achieved.

9.4.7 Model Tests at the Queens University, Kingston, Ontario

These tests by Hewitt (1972) and Batchelor, Hewitt, Csagoly and Holowka (1978) were an important contribution to the development of the

Ontario HBDC (1979) and are typical of a small scale ($\frac{1}{8}$) model of a complete bridge deck details of which are given in Chapter 6. The first series of 31 panels tested had orthotropic reinforcement of 1.0% and the comparison of the proposed method with these results is given in Table 9.6. An excellent correlation has been achieved with a mean P_t/P_p of 1.106 and a standard deviation of 0.1075, the concrete cube strength ranging from 43 to 47 N/mm^2.

The second series of 25 panels had isotropic reinforcement of 0.6, 0.4, 0.2 and zero % and a comparison with the proposed method is given in Table 9.7. It may be seen that the panels with 0.6% reinforcement show a similar correlation to the results in Table 9.6 with a mean P_t/P_p of 1.07. However, the panels with 0.4, 0.2 and zero % reinforcement have mean P_t/P_p of 0.98, 0.81 and 0.72 respectively and shows a trend with reducing levels of reinforcement. It should be noted that the above ratios do not include the panels which failed in flexure and also panel 7(C-1) which exhibited a large deflection and low failure load.

The relatively low ratio of P_t/P_p for the 0.2% and zero reinforcement levels would seem to suggest a loss of slab in-plane restraint at a high level of loading with a subsequent interaction of a flexural mode of failure which occurred in some of these panels. These results may be compared with the MTC circular slab tests where panels with 0.2% reinforcement had a mean P_t/P_p of 1.03, the Clinghan model with 0.25% reinforcement had a mean P_t/P_p of 1.16, the Manchester University unreinforced panels which had a P_t/P_p of 1.15 and the 2 unreinforced Maplin panels (45 and 46) which had a mean P_t/P_p of 1.08.

For this type of bridge deck the diaphragms must provide the necessary restraint to prevent the transverse movement of the beams

particularly in lightly reinforced slabs which will exhibit a high degree of cracking. It has been observed that both the end and intermediate diaphragms used in Hewitt's (1972) models were of a relatively light section and were also non-composite with the slab. Therefore, it is suggested that these diaphragms may have been inadequate to provide the high level of in-plane restraint required for the slabs with the low levels of transverse reinforcement. It must also be noted that there is no indication of lower failure loads in the panels adjacent to the end diaphragms and it must therefore be concluded that the 1.0% transverse reinforcement in the orthotropic slabs, which gave good correlation, compensated for the lack of slab in-plane restraint due to the light diaphragms.

Some additional tests were carried out on panels with mid-depth reinforcement and 3 beam models with reinforcement ranging from 0.6% to zero. As these were considered to be unrepresentative of beam and slab bridge decks they have not been included in this assessment.

9.4.7 Summary

In conclusion, the comparison of the proposed method for assessing the strength of fully restrained bridge slabs with experimental evidence from various sources has shown that it provides a satisfactory whilst conservative prediction of the punching shear strength of the slab. The models considered had span to depth ratios typical of bridge decks and the wide range of both concrete strengths and percentage steel reinforcement covered have all resulted in good correlation.

The method in its present form is still somewhat cumbersome for design hence it has been suitably translated into a more convenient form and this is discussed in the next section.

9.5 THE DESIGN OF M-BEAM BRIDGE SLABS

9.5.1 General

In a research programme of this type it is important that the results can be translated into a form that is suitable for use in the context of bridge design. With this in mind the following recommendations have been made in relation to the ultimate load capacity and serviceability of the slab having regard to the current design requirements.

9.5.2 Ultimate Load Capacity

For design purposes the proposed method for predicting the ultimate load capacity of restrained bridge slabs has been presented in graphical form (Fig. 9.9) in terms of the 28-day concrete cube strength and the span to depth ratio of the slab. The use of the graph shown in Fig. 9.9 with the standard 160 mm M-beam slab and the 2 m beam spacing with a concrete strength of 40 N/mm^2 will ensure a factor of safety, without load or material factors, of about 6. However, with this large reserve of strength against failure at ultimate, the important criterion from the design point of view is one of serviceability.

9.5.3 Serviceability Requirements

At an early stage of the project it was accepted that the prototype of Clinghans Bridge would be more suitable than the $\frac{1}{3}$ scale model to establish a level of reinforcement that would provide a satisfactory limit to cracking. However, as the results of the prototype tests will not be available for some time an assessment will be made based on the observations and results of the tests on the $\frac{1}{3}$ scale model.

It is appreciated that a considerable amount of research has been undertaken into the cracking similitude of model and prototype structures,

however, much still needs to be done to establish a better understanding of the problem, especially the bond characteristics of the various types of reinforcing bars. Nevertheless, it has been suggested by Clark (1973, 1974) that for large models, the type of concrete has little influence on the scaling of crack widths, but the reinforcement does, as it has been found that the bar deformations do not scale. He also suggests that plain wire model reinforcement tends to simulate prototype unbonded bars, deformed model reinforcement tends to simulate plain prototype bars and to simulate deformed prototype bars threaded model reinforcement is required. The proceedings of the International Conference on Micro-concrete Models edited by Garas and Armer (1980), provides an up to date assessment of the problem of bond and crack similitude in models.

Therefore, in view of the above findings, the use of a $\frac{1}{3}$ scale microconcrete model to predict the cracking characteristics of the prototype slab will result in a conservative estimate, however, this is considered to be an interim measure until the tests on the prototype of Clinghans Bridge are completed.

The behaviour of the model during the initial stages of loading has been discussed in Chapter 8 and the load at which each panel initially cracked and a crack width of 0.1 mm developed are recorded in Tables 8.1 and 8.2.

The data recorded in these tables has been used to predict the cracking characteristics of the prototype slab with loads being factored by 9 and the widths by 3. Referring to Fig. 9.10 the predicted initial cracking and 0.3 mm crack width lines have been drawn using average loads and reinforcement levels from Table 8.1 and 8.2 with average bar spacings from Fig. 7.5 to give the upper and lower line in each case.

It should be noted that the different bond strengths of the plain and deformed bars has not been taken into account.

From consideration of Fig. 9.10 it is proposed that an isotropic mesh of 0.6% reinforcement using 12 mm diameter deformed bars at 150 mm spacing will provide a satisfactory slab for serviceability. It may be observed from Fig. 9.10 that this proposed steel arrangement will provide an uncracked slab soffit under service load and a slab load of about 235 kN would be required to produce a crack 0.3 mm wide. The service load from both BE1/77 (1977) and BS5400 (1978) have also been shown in FIg. 9.10. The prototype Clinghans Bridge (Fig. 7.2) will have test panels with this arrangement of steel which will, in due course, allow the serviceability characteristics to be more satisfactorily monitored.

9.5.4 Influence on Costs

The use of 0.6% reinforcement (12 mm dia at 150 mm spacing) should provide a considerable saving in steel reinforcement as current design methods require about 1.5 to 2.0%. The cost of a current design using 1.75% (20 ø @ 150) transversely and 0.8% (16 ø @ 200) longitudinally is about £8/m^2. The cost of the proposed arrangement of steel using 0.6% isotropically (12 ø @ 150) is £2/m^2 which represents a saving of £6/m^2 or 75%. The effect of this reduction on the overall cost of M-beam decks is shown in Fig. 9.11 and varies from 4% to 7% depending on the beam spacing. It is also suggested that a prefabricated welded mesh of reinforcement would provide additional economy. Although there are certain reservations regarding the fatigue life of welded reinforcement, Batchelor, Hewitt and Csagoly (1978) have shown that, in general,

composite beam and slab bridge decks are satisfactory in this respect.

9.6 DESIGN REQUIREMENTS

9.6.1 General

The current design standard for reinforced concrete bridges is the Department of Transport Technical Memorandum (Bridges) No BE1/73 (1973) and it requires that bridge slabs are designed flexurally, the moments derived from the global and local analyses being added to give the total design moment. This is also the recommendation from the new bridge code BS 5400 (1978).

It is evident from the results of the model tests and the experimental work by other researchers, which has been reviewed, that the failure mode of the typical restrained bridge slab is one of punching shear and not flexure. The traditional approach was based on the solution of the equations for an elastic plate and, based on a flexural mode of failure, it was logical to add the moments from the global and local deformations. However, when considering failure in a punching shear mode the local wheel load need only be considered as the results from the various tests have shown the failure to be very localised. It is of interest that it is the practice in North America to consider only the local effects from the wheel load as the AASHTO (1977) requirements are based on a flexural design and the usual steel requirement is about 1%. It should also be noted that the Ontario HBDC takes full advantage of the compressive membrane forces available in bridge slabs and has adopted a standard reinforcement, with certain restrictions, of 0.3% isotropically.

9.6.2 Recommendations for the Design of Beam and Slab Bridge Decks

Proposals have been made for a more realistic approach to the design

of M-beam bridge decks and it is suggested that the same principles could be applied generally to beam and slab decks. The main recommendations are listed below and to ensure a satisfactory performance regarding the development of compressive membrane forces some restrictions regarding the design of the deck are considered.

1. An isotropic mesh of 12 mm diameter deformed bars at 150 mm spacing in both top and bottom of the slab will provide satisfactory strength and serviceability. For economy this mesh could be prefabricated welded panels.
2. For the in situ slab a concrete with a 28-day cube strength of 40 N/mm^2 should be used as a high strength concrete will improve punching, restrict cracking and provide a high level of durability.
3. These recommendations apply only to simply supported composite beam and slab bridge decks with end diaphragms and parapet edge beams. However, tests in Canada have indicated that the method is applicable to continuous beam and slab systems in the negative moment regions. This has also been verified by the tests carried out at the University of Illinois.
4. The span to depth ratio of the slab should be limited to 15. This is in line with the Ontario HBDC (1979) and although the proposed method is suitable for higher ratios there is insufficient experimental evidence at present to justify this, even though the Ontario circular slabs and the Maplin tests showed a satisfactory performance with a span to depth ratio of 18.
5. For concrete beams, end diaphragms only are required, however, for steel beams full width intermediate diaphragms spaced at

not more than 5 m should be provided. It is also suggested that for steel beams, concrete end diaphragms composite with the deck slab will provide better in-plane restraint than diaphragms constructed of steel sections.

Test Panel	f_{cu} N/mm^2	ρ %	h mm	d mm	k	ρ_e %	P_p kN	P_t kN	P_t/P_p
A1	39.8	1.67	57.3	48.3	0.176	3.26	85.5	102.5	1.19
A2	40.4	1.59	59.6	50.6	0.177	3.28	92.3	114.0	1.23
A3	44.7	1.76	54.8	45.8	0.170	3.59	86.0	102.5	1.19
A4	40.6	1.67	57.2	48.2	0.188	3.56	88.1	108.0	1.23
A5	44.7	1.72	56.1	47.1	0.188	3.94	92.2	96.0	1.04
B1	41.3	1.14	55.5	46.5	0.173	3.36	83.5	108.0	1.29
B2	43.5	1.21	53.3	44.3	0.170	3.55	81.7	96.0	1.17
B3	41.5	1.20	53.3	44.3	0.171	3.28	79.0	100.0	1.26
B4	43.5	1.16	53.9	45.9	0.187	3.72	86.8	90.0	1.04
B5	41.5	1.23	52.1	43.1	0.186	3.60	77.6	91.0	1.17
C1	37.6	0.48	57.1	49.6	0.179	2.96	84.2	106.0	1.26
C2	38.9	0.50	54.4	46.9	0.175	3.03	80.1	100.0	1.24
C3	41.3	0.47	52.7	45.2	0.172	3.19	79.9	102.0	1.27
C4	38.9	0.48	57.0	49.2	0.191	3.33	88.0	110.0	1.25
C5	41.3	0.52	56.3	48.8	0.188	3.42	89.6	105.0	1.17
D1	44.0	0.24	53.6	46.1	0.171	3.36	85.3	98.0	1.15
D2	45.6	0.25	55.1	47.6	0.170	3.44	91.2	108.0	1.18
D4	45.6	0.25	58.6	51.1	0.188	3.73	102.3	118.0	1.15
D5	44.0	0.25	54.7	47.2	0.188	3.68	90.5	107.5	1.18

Mean P_t/P_p = 1.19

Standard Deviation = 0.068

Variance = 0.0044

TABLE 9.1 - Comparison of Proposed Method with Model Test Results

Test Panel	f_{cu}+ N/mm^2	ρ %	h mm	d mm	k	ρ_e %	P_p kN	P_t kN	P_t/P_p
Series 1									
W5a*	19.0	0.87	44.5	36.5	0.205	1.92	33.3	33.0	0.99*
W5b*	23.6	0.87	44.5	36.5	0.194	2.25	38.8	34.5	0.89*
N5a*	19.9	0.87	44.5	36.5	0.200	1.96	34.3	35.9	1.04*
N5b*	18.8	0.87	44.5	36.5	0.205	1.89	33.0	34.9	1.06*
S5a	23.2	0.87	44.5	36.5	0.195	2.22	38.4	55.6	1.45
S5b	25.2	0.87	44.5	36.5	0.192	2.39	40.8	49.9	1.22
Series 2									
N15a*	27.7	1.09	44.5	36.4	0.188	2.58	43.5	46.6	1.07*
N15b*	24.8	1.09	44.5	36.4	0.192	2.35	40.0	45.3	1.13*
S15a	28.2	1.09	44.5	36.4	0.189	2.62	43.9	63.4	1.44
S15b	27.7	1.09	44.5	36.4	0.190	2.52	42.6	62.9	1.47
C15a	26.8	0.87	44.5	36.5	0.190	2.50	42.6	57.6	1.35
C15b	20.1	0.87	44.5	36.5	0.200	1.98	34.3	51.9	1.51
Series 3									
30N15*	35.0	1.09	44.5	36.4	0.180	3.11	50.9	55.6	1.09*
30C15	36.0	0.87	44.5	36.5	0.179	3.22	52.8	61.8	1.17
30S15	26.3	1.09	44.5	36.4	0.190	2.45	41.8	66.4	1.58
60N15*	28.5	1.09	44.5	36.4	0.189	2.66	44.4	53.4	1.20*
60C15	34.8	0.87	44.5	36.5	0.180	3.09	50.7	61.3	1.20
Series 4									
N30*	27.7	1.09	44.5	36.4	0.189	2.83	44.4	42.1	0.95*
C30	26.2	0.87	44.5	36.5	0.190	2.68	42.8	50.8	1.18
X30	37.3	0.87	44.5	36.5	0.175	3.52	54.8	53.4	0.98

+ Equivalent Cube Strength

Composite			*Non-Composite		
Mean P_t/P_p	=	1.32	Mean P_t/P_p	=	1.04
Standard Deviation	=	0.184	Standard Deviation	=	0.094
Variance	=	0.031	Variance	=	0.0078

TABLE 9.2 - Comparison of Proposed Method with University of Illinois Model Bridges

Test Panel	f_{cu} N/mm^2	ρ %	h mm	d mm	k	ρ_e %	P_p kN	P_t kN	P_t/P_p
IR2(a)	36.8	Zero	76.2	61.0	0.170	3.23	83.2	85.0	1.02
IR2(b)	32.5	Zero	76.2	61.0	0.176	2.96	76.6	89.0	1.16
IR3	35.6	Zero	76.2	61.0	0.170	3.12	99.9	130.0	1.30
IR4	35.6	Zero	76.2	61.0	0.170	3.12	118.3	150.0	1.26
IR5	27.3	Zero	76.2	61.0	0.187	2.63	114.3	119.5	1.04
IR6	27.3	Zero	76.2	61.0	0.187	2.63	129.7	114.0	1.11
2R2	32.5	1.57	76.2	63.5	0.176	2.73	79.6	83.8	1.05
2R3	30.7	1.57	76.2	63.5	0.179	2.62	93.9	115.0	1.22
2R4	29.0	1.57	76.2	63.5	0.180	2.49	107.0	139.5	1.30
2R5	27.6	1.57	76.2	63.5	0.182	2.39	118.4	145.0	1.22
2R6	23.0	1.57	76.2	63.5	0.192	2.10	118.6	157.5	1.32
3R2	28.5	3.14	76.2	63.5	0.181	2.46	70.5	80.0	1.13
3R4	28.4	3.14	76.2	63.5	0.181	2.45	104.8	135.0	1.28
3R6	27.1	3.14	76.2	63.5	0.183	2.37	138.1	172.5	1.29

Mean P_t/P_p = 1.19

Standard Deviation = 0.106

Variance = 0.0105

Note: The last number of the test panel reference is the size of the square loading shoe in inches.

TABLE 9.3 - Comparison of Proposed Method with Manchester University Model Tests

Test Panel	f_{cu} N/mm^2	ρ %	h mm	d mm	k	ρ_e %	P_p kN	P_t kN	P_t/P_p
1	54.0	0.61	100	82	0.120	3.19	309.1	349	1.13
2	54.2	0.61	100	82	0.120	3.20	309.5	331	1.07
7	71.0	0.61	100	82	0.112	3.90	373.1	359	0.96
8	70.0	0.61	100	82	0.110	3.78	364.9	389	1.07
10	70.0	2.64	100	76	0.110	3.78	331.0	359	1.08
11	62.9	2.64	100	76	0.115	3.55	309.3	359	1.16
12	64.0	2.64	100	76	0.112	3.52	311.9	357	1.14
13	50.0	0.47	125	107	0.146	3.28	425.4	408	0.96
14	51.0	0.47	125	107	0.145	3.34	430.2	418	0.97
15	64.0	2.00	125	107	0.140	4.03	507.6	537	1.06
16	65.0	2.00	125	107	0.140	4.09	510.5	537	1.05
17	53.0	2.00	125	107	0.144	3.43	441.5	453	1.03
18	53.0	2.00	125	101	0.144	3.87	420.6	431	1.02
19	55.0	0.85	125	101	0.145	3.74	447.9	429	0.96
20	55.0	0.85	125	101	0.145	3.74	447.9	424	0.95
21	66.0	0.85	125	101	0.139	4.28	504.7	508	1.01
22	67.0	0.85	125	101	0.139	4.35	512.9	498	0.97
23	64.0	0.47	125	101	0.140	4.05	506.9	478	0.94
24	65.0	0.47	125	101	0.140	4.10	510.5	418	0.82
29	51.5	2.00	125	101	0.145	3.78	411.8	446	1.08
30	52.0	2.00	125	101	0.145	3.82	416.6	419	1.01
31	78.0	2.00	125	101	0.138	5.46	554.1	478	0.86
32	78.5	2.00	125	101	0.138	5.49	559.0	536	0.96
33	55.0	0.47	125	107	0.142	3.54	452.9	424	0.94
34	56.0	0.47	125	107	0.142	3.60	460.4	478	1.04
35	66.5	0.47	125	107	0.139	4.19	519.8	508	0.98
36	67.5	0.47	125	107	0.139	4.25	527.7	508	0.96
45	45.2	Zero	125	100	0.149	2.23	372.7	428	1.14
46	46.2	Zero	125	100	0.149	2.27	378.7	389	1.03
47	45.0	0.47	125	107	0.150	3.04	523.6	538	1.03
48	45.0	0.47	125	107	0.150	3.04	523.1	508	0.97
49	44.4	0.47	125	107	0.150	3.00	262.5	289	1.10
50	44.9	0.47	125	107	0.149	3.01	265.8	292	1.10
51	57.0	0.47	125	107	0.143	3.67	464.5	438	0.94
52	61.0	0.47	125	107	0.143	3.85	488.0	437	0.90

Mean P_t/P_p = 1.01

Standard Deviation = 0.0799

Variance = 0.0062

Note: The loading shoe used for these tests was 200 mm diameter except panels No 47 and 48 which were 300 mm diameter and 49 and 50 which were 100 mm diameter.

TABLE 9.4 - Comparison of Proposed Method with BRS Maplin Tests

Test Panel	f_{cu}^{+} N/mm^2	ρ %	h mm	d mm	k	ρ_e %	P_p kN	P_t kN	P_t/P_p
A1	34.9	0.2	44.5	38.10	0.164	2.58	39.4	42.2	1.07
A2	34.0	0.2	44.5	38.10	0.166	2.55	38.6	46.7	1.20
A3	33.5	0.2	44.5	38.10	0.169	2.55	38.3	37.8	0.99
B1	35.1	0.2	38.1	31.75	0.156	2.61	37.1	37.8	1.02
B2	33.9	0.2	38.1	31.75	0.158	2.55	36.2	35.6	0.98
C1	33.8	0.2	31.75	25.40	0.147	2.56	22.4	22.2	0.99
C2	36.5	0.2	31.75	25.40	0.141	2.66	23.5	24.5	1.04
C3	35.9	0.2	31.75	25.40	0.142	2.63	23.3	22.2	0.95
D2	33.3	0.3	44.5	38.1	0.168	2.52	37.9	44.5	1.17
D3	33.8	0.3	44.5	38.1	0.165	2.51	38.2	48.9	1.28
E1	32.1	0.3	38.1	31.75	0.160	2.45	34.9	33.4	0.96
E2	35.3	0.3	38.1	31.75	0.156	2.62	37.1	35.6	0.96
E3	33.3	0.3	38.1	31.75	0.158	2.50	35.5	35.6	1.00
F1	33.7	0.3	31.75	25.4	0.148	2.57	22.2	22.2	1.00
F2	34.1	0.3	31.75	25.4	0.147	2.59	22.7	26.7	1.17
F3	33.3	0.3	31.75	25.4	0.148	2.54	22.3	22.2	1.00
G1	35.1	0.8	44.5	38.1	0.162	2.56	39.2	44.5	1.14
H1	35.2	0.8	38.1	31.75	0.155	2.61	37.4	37.8	1.01
I1	34.6	1.0	44.5	38.1	0.162	2.52	38.6	44.5	1.15
I2	35.8	1.0	44.5	38.1	0.161	2.59	39.9	48.9	1.22
I3	34.6	1.0	44.5	38.1	0.165	2.56	38.9	48.0	1.23
J1	36.2	1.0	38.1	31.75	0.155	2.67	37.9	36.9	0.97
J2	33.0	1.0	38.1	31.75	0.159	2.50	37.5	37.4	1.00
K1	34.9	1.0	31.75	25.4	0.144	2.59	23.0	26.7	1.16
K2	34.6	1.0	31.75	25.4	0.144	2.57	22.9	23.6	1.03

$^{+}$ Equivalent Cube Strength

Mean P_t/P_p = 1.06

Standard Deviation = 0.101

Variance = 0.0098

TABLE 9.5 - Comparison of Proposed Method with MTC Circular Slab Tests

Test Panel	f_{cu} + N/mm^2	ρ %	h mm	d mm	k	ρ_e %	P_p kN	P_t kN	P_t/P_p
1(B-1)	46.2	1.0	21.25	17.45	0.146	3.33	20.79	21.83	1.05
1(A-4)	46.2	1.0	23.20	19.02	0.152	3.48	23.29	24.24	1.04
1(B-3)	46.2	1.0	20.62	16.64	0.144	3.40	19.64	22.20	1.13
1(C-2)	46.2	1.0	21.51	17.81	0.148	3.32	21.28	21.97	1.03
2(B-1)	44.7	1.0	22.70	18.80	0.152	3.29	22.16	22.82	1.03
2(A-4)	44.7	1.0	23.95	19.86	0.156	3.28	23.79	26.48	1.11
2(B-3)	44.7	1.0	22.65	18.77	0.151	3.22	22.11	26.26	1.19
2(C-2)	44.7	1.0	23.70	19.69	0.155	3.33	28.62	24.39	1.03
2(B-2)	44.7	1.0	23.22	19.41	0.153	3.25	23.09	29.37	1.27
2(A-2.5)	44.7	1.0	25.25	21.59	0.157	3.19	26.11	30.71	1.18
2(A-1.75)	44.7	1.0	23.60	19.83	0.154	3.23	23.65	24.48	1.03
2(A-1)	44.7	1.0	23.19	19.30	0.153	3.28	23.97	22.16	0.96
2(C-1)	44.7	1.0	22.99	18.72	0.153	3.43	22.39	22.16	0.99
2(C-2.75)	44.7	1.0	23.72	19.30	0.155	3.48	23.20	25.72	1.11
2(C-2.25)	44.7	1.0	26.01	21.72	0.159	3.39	26.71	27.59	1.03
2(C-3.5)	44.7	1.0	22.50	18.72	0.150	3.22	22.03	25.94	1.18
2(B-4)	44.7	1.0	22.17	18.62	0.149	3.14	21.76	25.14	1.16
2(C-4.25)	44.7	1.0	22.63	18.82	0.151	3.24	22.23	22.47	1.01
3(B-1)	43.2	1.0	21.33	17.14	0.146	3.25	19.56	22.24	1.14
2(A-2)	43.2	1.0	21.03	16.81	0.149	3.35	19.27	23.35	1.21
3(B-4)	43.2	1.0	21.81	17.31	0.148	3.37	19.71	19.92	1.01
3(C-3)	43.2	1.0	20.62	16.61	0.148	3.28	18.89	25.35	1.34
3(A-3)	43.2	1.0	21.00	16.79	0.149	3.35	19.24	24.06	1.25
3(B-3)	43.2	1.0	21.13	16.90	0.149	3.35	19.34	24.24	1.25
3(C-1)	43.2	1.0	21.73	17.55	0.150	3.30	20.19	20.59	1.02
3(A-1)	43.2	1.0	21.46	17.24	0.150	3.30	19.66	21.48	1.09
4(C-4)	47.0	1.0	20.67	17.02	0.143	3.31	20.35	20.42	1.00
4(A-4)	47.0	1.0	20.78	17.09	0.143	3.31	20.45	20.01	0.98
5(C-1)	47.7	1.0	23.85	20.17	0.154	3.42	25.29	30.24	1.20
5(A-1)	47.7	1.0	23.54	20.04	0.154	3.37	25.00	24.46	0.98
5(B-1)	47.7	1.0	22.56	18.87	0.150	3.40	23.30	23.57	1.01

+ Equivalent Cube Strength

Mean P_t/P_p = 1.106

Standard Deviation = 0.1075

Variance = 0.0111

TABLE 9.6 - Comparison of Proposed Method with Queen's University Kingston, Ontario - Model Bridges Orthotropic Reinforcement

Test Panel	f_{cu} + N/mm^2	ρ %	h mm	d mm	k	ρ_e %	P_p kN	P_t kN	P_t/P_p
6(A-1)	44.7	0.6	23.6	18.30	0.155	3.81	22.38	24.91	1.11
6(B-1)	44.7	0.6	22.9	17.73	0.153	3.78	21.51	23.66	1.10
6(C-1)	44.7	0.6	22.6	17.39	0.151	3.67	20.80	24.02	1.15
6(A-3)	44.7	0.6	24.1	18.50	0.156	3.91	22.82	22.24	0.97
6(B-3)	44.7	0.6	23.4	17.95	0.154	3.87	21.95	23.30	1.06
6(C-3)	44.7	0.6	23.7	18.37	0.155	3.81	22.48	25.35	1.12
7(A-4)	41.7	0.6	23.9	18.59	0.157	3.57	21.68	22.24	1.03
								mean	1.07
5(A-3)	47.8	0.4	23.6	17.46	0.152	4.38	22.65	22.24	0.98
5(B-3)	47.8	0.4	24.6	19.76	0.155	3.79	25.31	25.09	0.99
5(C-3)	47.8	0.4	24.6	19.90	0.155	3.73	25.44	25.35	1.00
7(C-1)	41.7	0.4	24.2	18.97	0.158	3.54	22.17	17.34	0.78
8(C-1)	39.1	0.4	22.1	16.93	0.155	3.41	18.61	17.79	0.96
								mean	0.98
5(A-4)	47.8	0.2	24.1	19.08	0.154	3.87	24.41	21.79	0.89
5(B-4)	47.8	0.2	23.6	18.16	0.153	4.07	23.30	19.04	0.82
5(C-4)	47.8	0.2	23.0	17.96	0.151	3.91	22.67	16.90	0.75
6(A-2)	44.7	0.2	22.6	17.71	0.152	3.65	21.30	18.50	0.87
6(B-2)	44.7	0.2	22.5	17.86	0.152	3.57	21.38	18.68	0.87
6(C-2)	44.7	0.2	22.1	17.48	0.150	3.54	21.74	15.57	0.75
7(C-2)	41.7	0.2	23.0	18.13	0.156	3.45	20.87	15.57	0.75
8(A-4)##	39.1	0.2	21.9	16.92	0.154	3.33	18.44	13.92	0.75##
								mean	0.81
5(A-2)	47.8	0	22.6	18.08	0.150	3.71	22.58	15.57	0.69
5(B-2)##	47.8	0	21.4	17.12	0.145	3.58	21.03	15.39	0.73##
5(C-2)	47.8	0	24.7	19.76	0.158	3.89	25.49	20.91	0.83
7(C-3)	41.7	0	22.8	18.24	0.150	3.23	20.67	13.08	0.63
8(A-2)##	39.1	0	21.4	17.12	0.146	2.94	18.12	11.56	0.63##
								mean	0.72

+ Equivalent Cube Strength

Flexural Failure

TABLE 9.7 - Comparison of Proposed Method with Queen's University, Kingston, Ontario, Model Bridges Isotropic Reinforcement

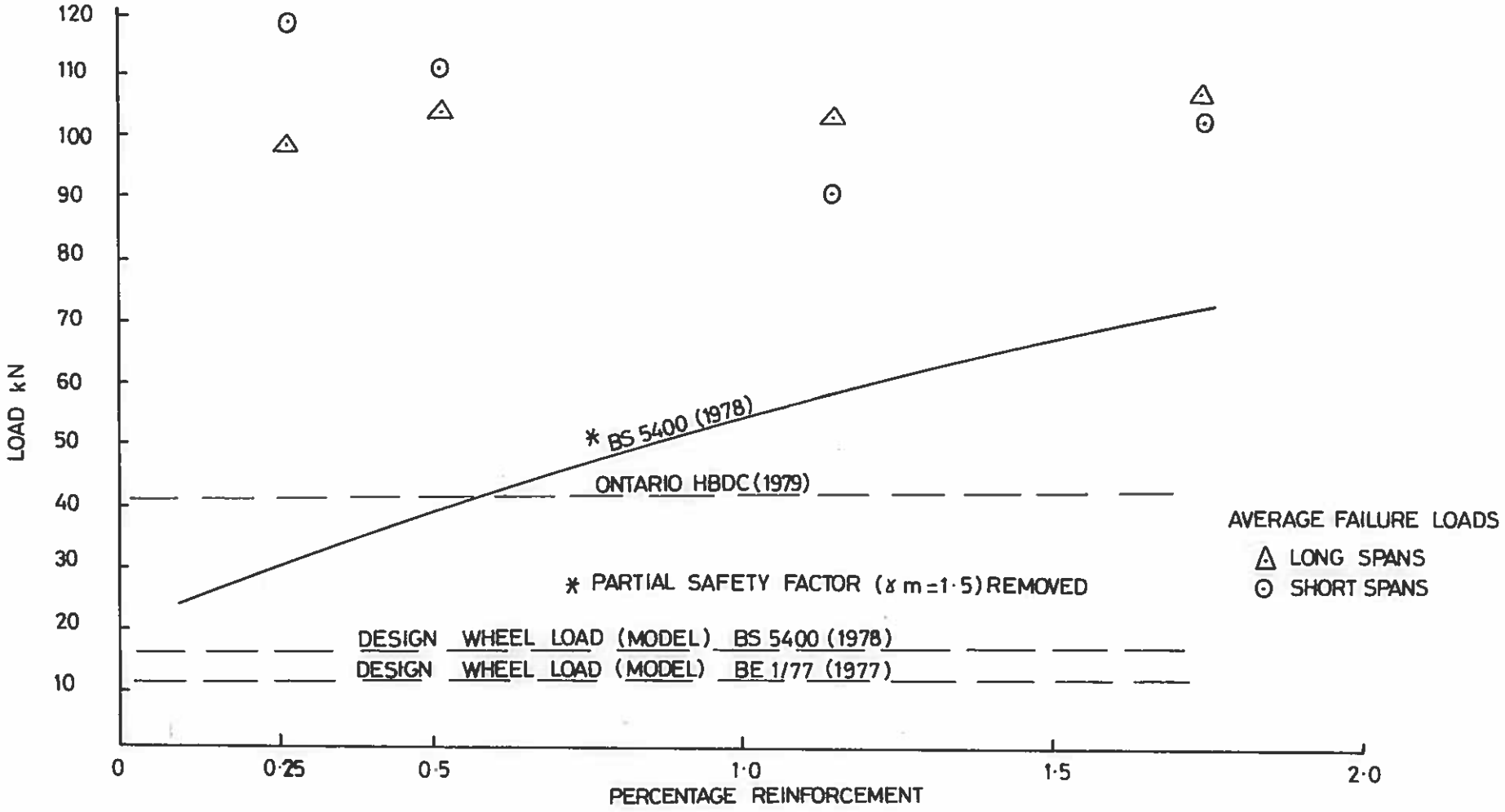

Fig. 9.1 Test Results of Bridge Deck

Fig. 9.1

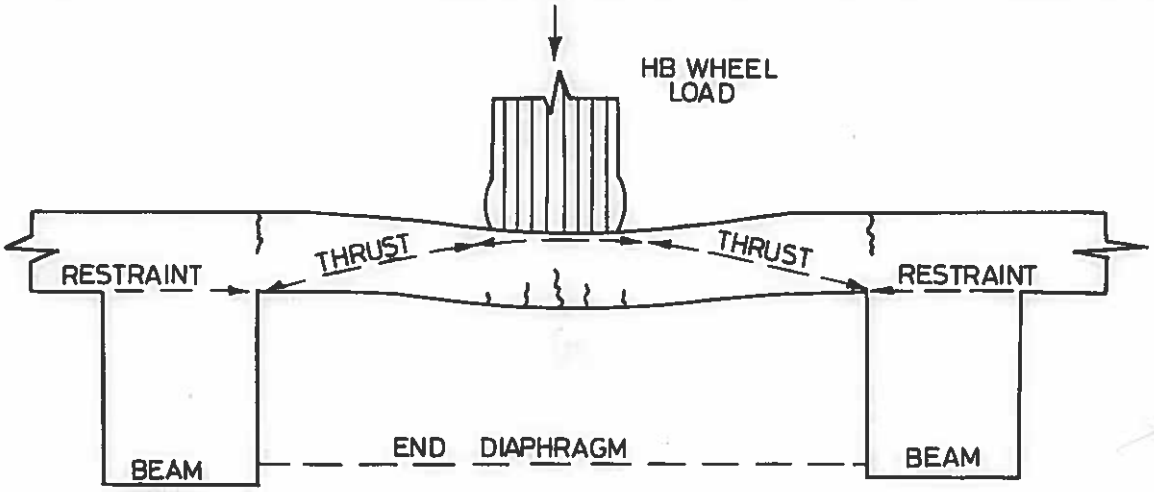

Fig. 9.2 Compressive Membrane Action in Bridge Deck

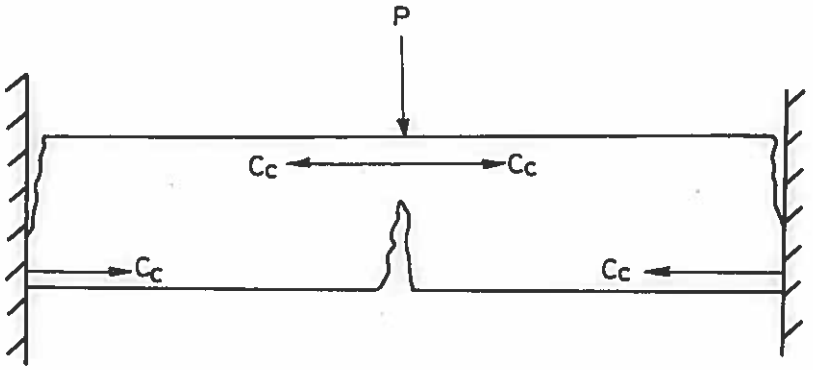

Fig. 9.3 Maximum Arching Capacity of a Slab

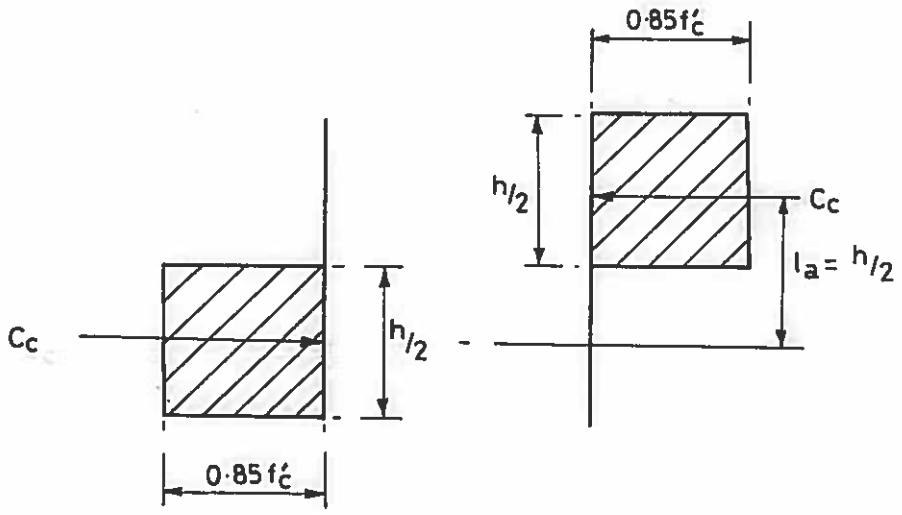

Fig. 9.4 Forces Causing Maximum Possible Arching

Fig.9.2
Fig.9.3
Fig.9.4

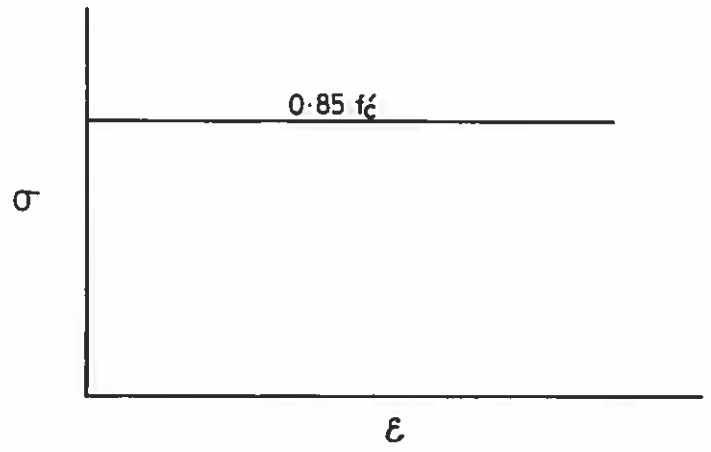

Fig. 9.5 Idealised Stress-Strain Curve For Rigid/Plastic Material

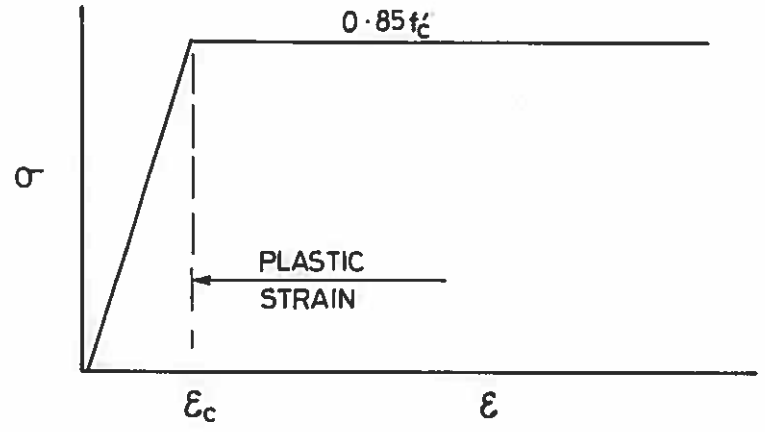

Fig. 9.6 Idealised Stress-Strain Curve For Elastic/Plastic Material

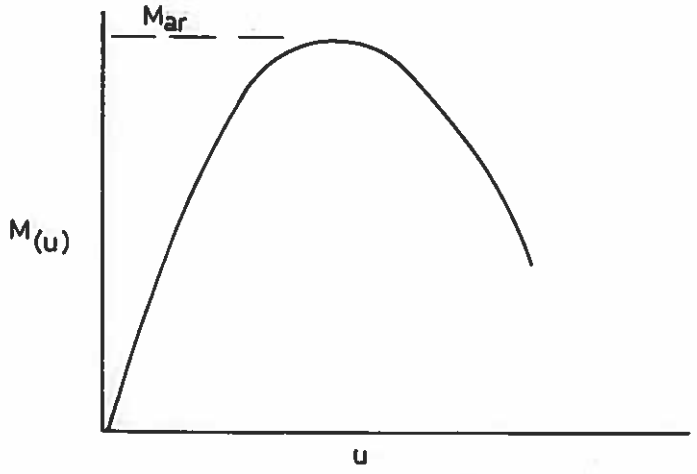

Fig. 9.7 Variation in Arching Moment With Deflection

Fig.9.5
Fig.9.6
Fig.9.7

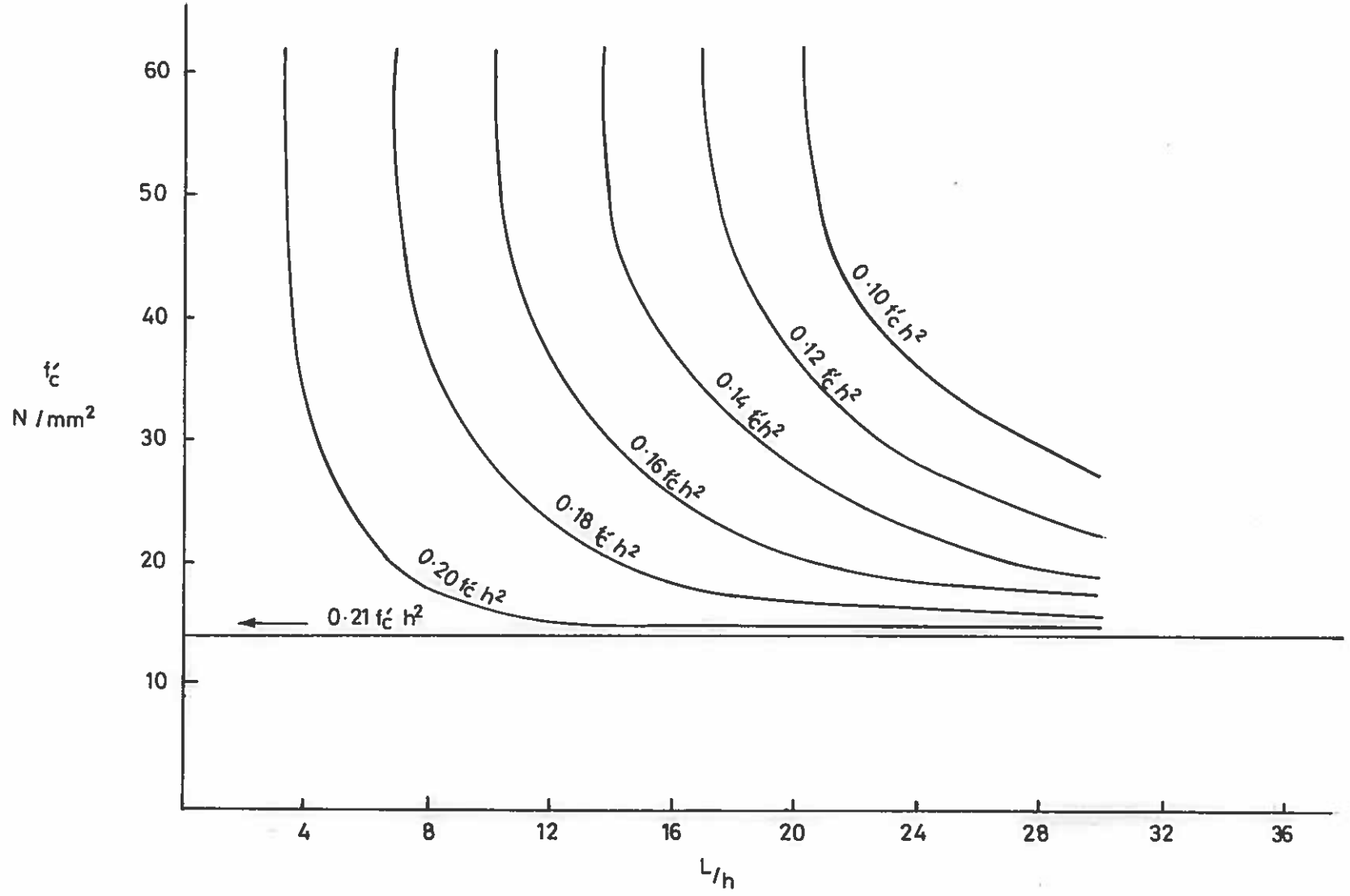

Fig. 9.8

Fig. 9.8 Maximum Arching Moment Curves

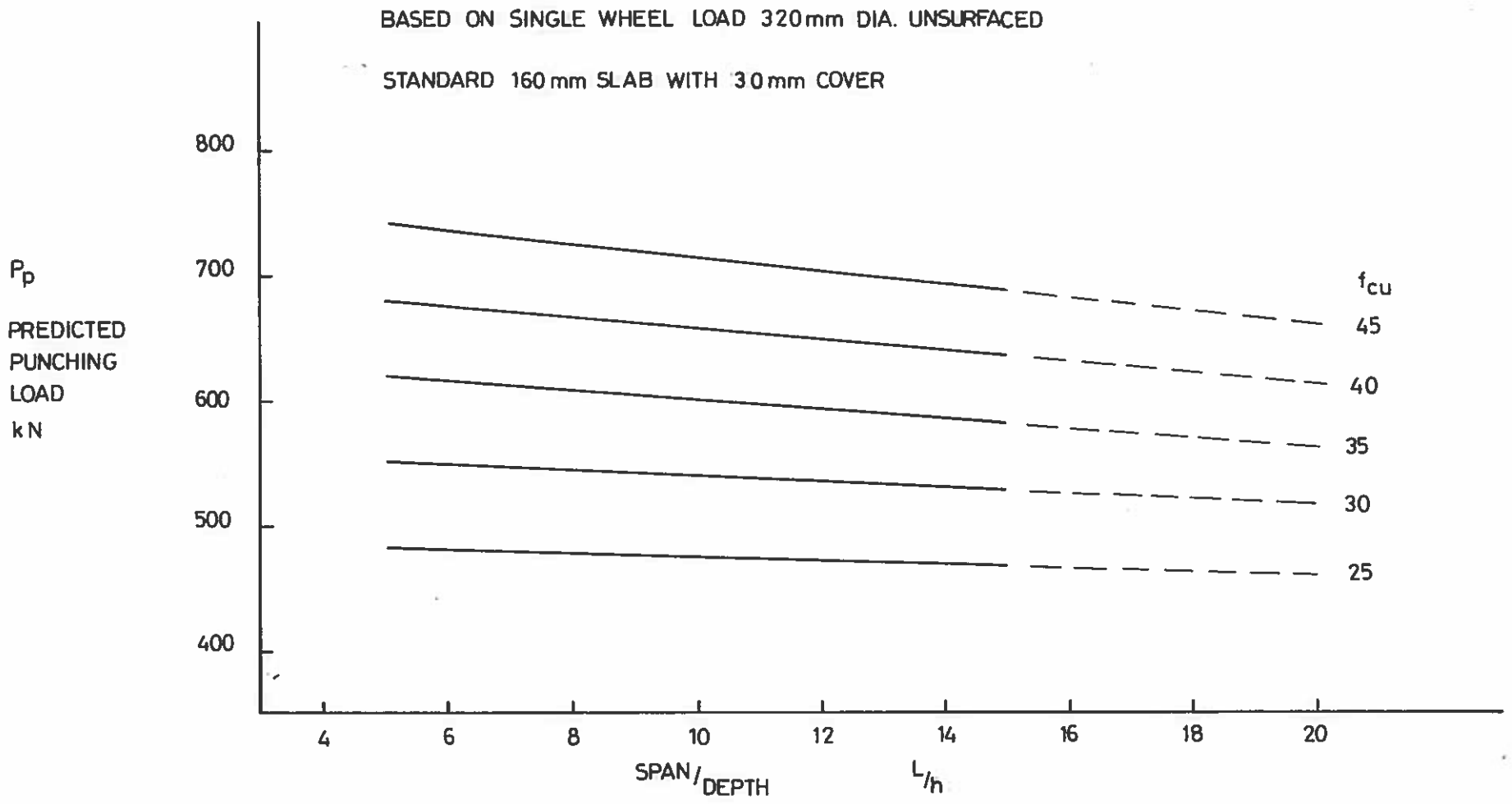

Fig. 9.9

Predicted Load Capacity For Standard M-Beam Slab

Fig.9.9

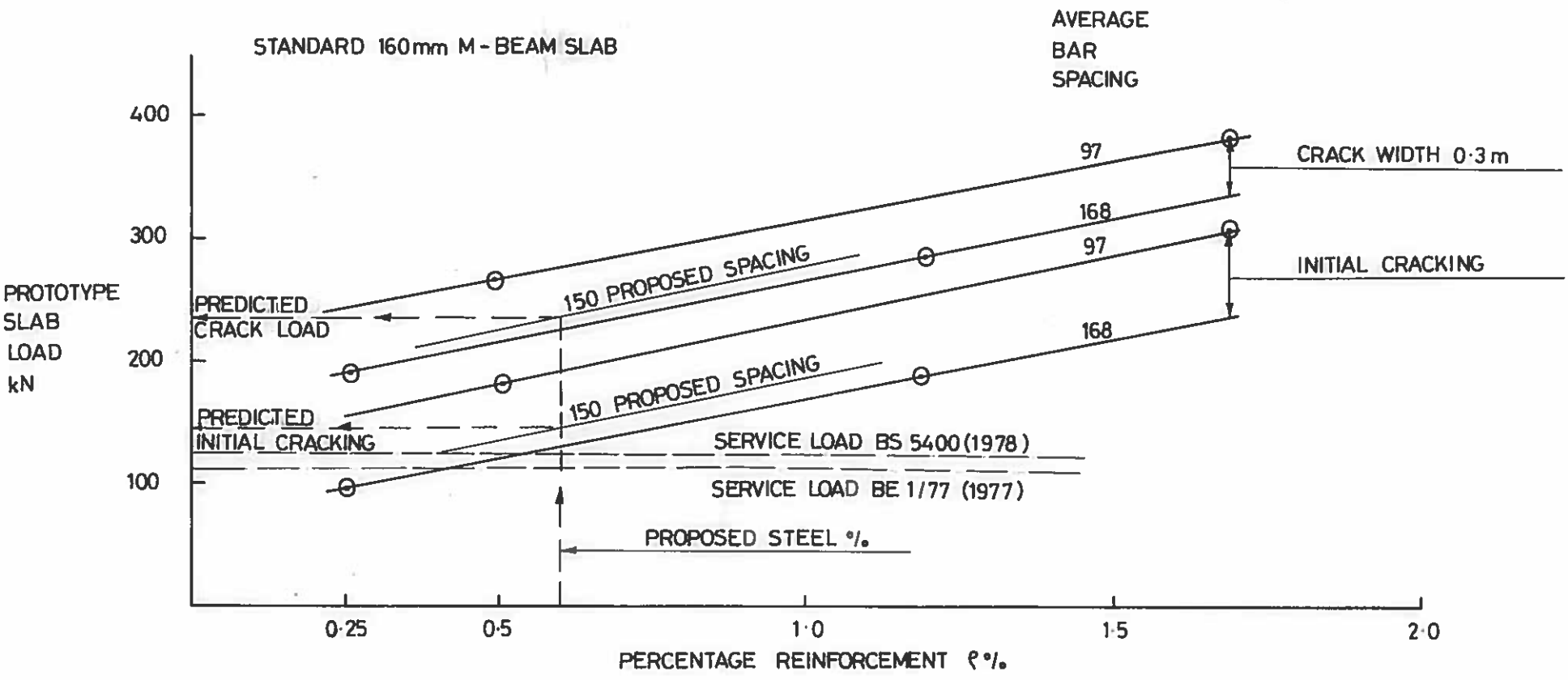

Fig. 9.10 Predicted Prototype Loads For Initial and Serviceability Cracking

Fig 9.10

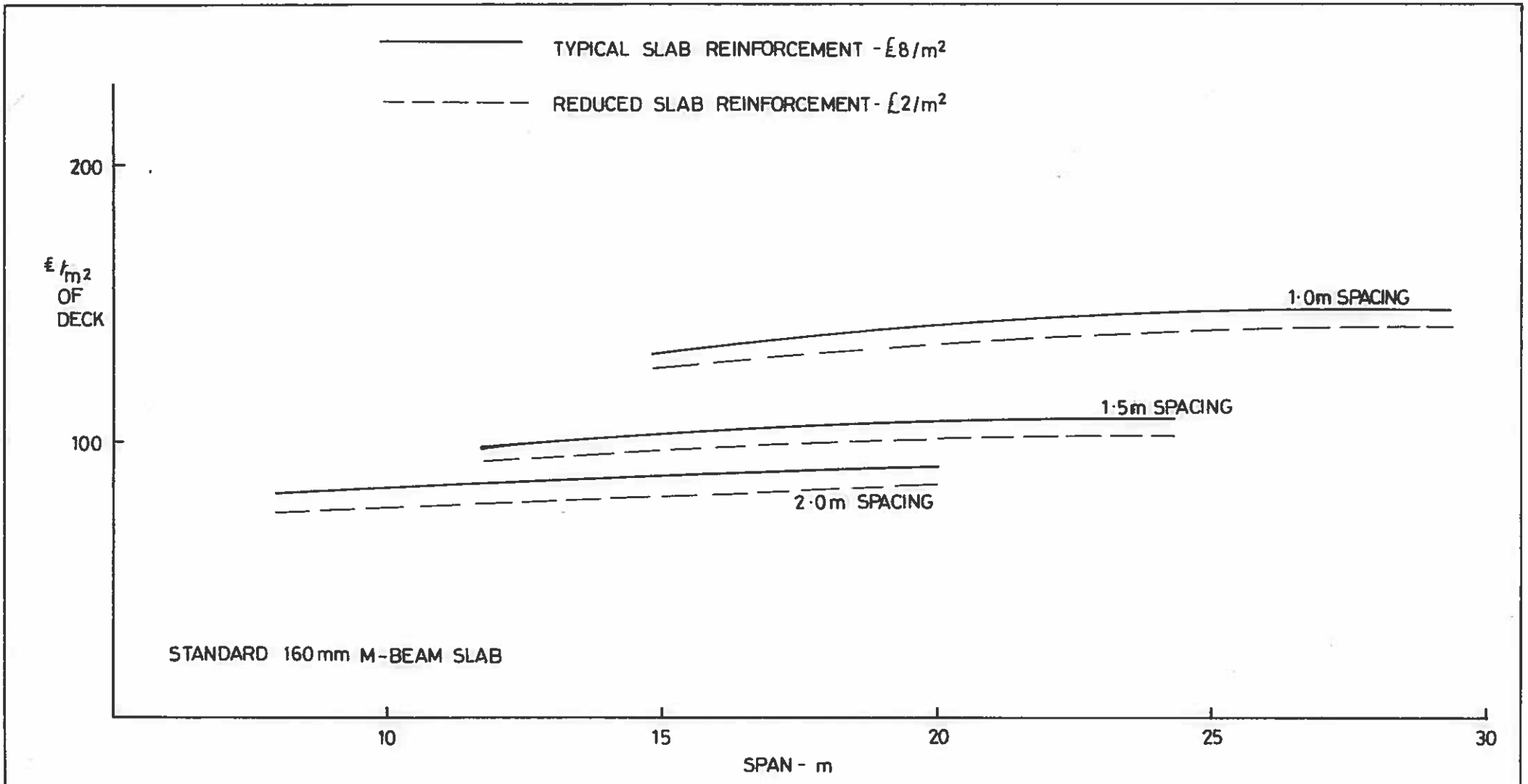

Fig. 9.11 Deck Costs Using Proposed Slab Reinforcement

Fig.911

CHAPTER TEN

CONCLUSIONS AND SUGGESTIONS FOR FURTHER RESEARCH

10.1 INTRODUCTION

10.2 SUMMARY OF CONCLUSIONS

10.3 SUGGESTIONS FOR FURTHER RESEARCH

10.1 INTRODUCTION

An analytical, field and model study of M-beam bridge decks is presented in this thesis. A series of load distribution tests on M-beam bridge decks has been used as the basis for a simplified design approach using charts and programs for the Hewlett Packard 1930A desk top computer. This study was aimed at improving the economics of design and construction of this type of bridge deck. A further development involved a study of the slab characteristics using a $\frac{1}{3}$ scale model and a more appropriate theoretical basis has been derived to predict the capacity of this type of bridge slab. The proposed method is compared with the test results from the model and other relevant research. From this programme of research, conclusions have been reached and in this chapter these are summarised and recommendations are made for further research.

10.2 SUMMARY OF CONCLUSIONS

1. Loading tests carried out on bridges immediately after construction provide an inexpensive and effective means of assessing the behaviour of bridge deck systems.
2. For tee beam decks, the use of a grillage analysis with a relatively coarse mesh gave a good agreement for both decks tested. Although the test results did show local peaks under the wheels, it was found that the grillage predictions were adequate for design purposes.
3. For pseudo-box decks measured beam soffit stresses were about 20% less than those predicted by the grillage analysis. However, by increasing the torsional inertia of the transverse grillage beams

by a factor of 7 a good correlation of all pseudo-box test results has been achieved. The calculation of the torsional inertia of the transverse grillage beam has not been resolved in a satisfactory manner and until this problem is fully explained this simple empirical approach may be adopted.

4. For both forms of construction the effect of edge stiffening associated with the standard edge feature need not be considered and the analysis can be based on the stiffness of the composite beams only. This will provide a conservative estimate of beam moments in the region of the edge beam.

5. The proposed design charts with the computer programs will provide a streamlined approach to the design and checking of M-beam decks which will result in considerable savings of design time.

6. The use of M-beams spaced at up to 2 m apart will allow this type of deck to be economically competitive for spans from 8 to 29 m. Although this means an increase in the span to depth ratio from 20 at 1 m spacing to 16 at 1.5 and 11 at 2 m it is similar to other forms of construction and in the remote rural situation this parameter is not usually important. By using these beams at up to 2 m spacing a saving of up to 35% in the cost of the deck may be achieved.

7. The quantity of steel reinforcement has very little effect on the ultimate load capacity of the slab. It does however, influence the serviceability limits of cracking and deflection.

8. Considering the transient nature of bridge live loads creep effects do not have any adverse effect on the ultimate load

capacity of the standard M-beam slab.

9. All the test panels failed by punching shear even though the current design methods are based on a flexural analysis.

10. Existing bridge codes do not provide an accurate prediction of the serviceability and ultimate load capacity of an M-beam deck slab as no account is taken of the considerable enhancement due to the in-plane restraint inherent in this type of deck.

11. A more appropriate method for the prediction of the ultimate load capacity of the slab of composite beam and slab bridge decks is proposed. The method applies to fully restrained slabs and in order to provide this restraint edge beams and diaphragms fully composite with the slab are required. The method uses a punching shear formula which has been modified to allow for compressive membrane forces by the introduction of an equivalent percentage of flexural reinforcement which is based on the arching characteristics of the slab.

12. For satisfactory serviceability it is proposed that a standard isotropic mesh of 12 mm diameter deformed bars at 150 mm spacing be used. This will result in a saving of about 75% in the cost of the steel which represents a saving of 4 to 7% in the overall cost of the superstructure.

13. For the in situ slab a 28-day cube strength of 40 N/mm^2 is recommended as this will improve the punching, cracking and durability characteristics.

14. Full depth reinforced concrete end diaphragms composite with the slab should be provided with both concrete and steel beams. For steel beam decks additional intermediate diaphragms not more than 5 m apart are required.

15. These recommendations apply only to simply supported composite beam and slab bridge decks and the transverse span to depth ratio of the slab should not exceed 15.

16. Although the above proposals have been made with the existing design criteria in mind, the implications of the proposed bridge code BS5400 (1978) must also be considered. The existing loading requirements are similar to the nominal loads given in Part 2 of BS5400 (1978) with a maximum HB vehicle wheel load of 112.5 kN. Although there is a small change to the geometry of the abnormal vehicle which now has a variable distance between bogies, for simply supported spans the minimum spacing of 6 m will be critical. Therefore the proposals for both beam and slab design will be suitable for use with BS5400 (1978).

10.3 SUGGESTIONS FOR FURTHER RESEARCH

1. For the pseudo-box construction the calculation of the torsional inertia of the transverse grillage beam has not been resolved satisfactorily and further research is required. Consideration is therefore being given to testing these bridges again after they have been in service for over 2 years, to determine whether cracking influences their performance.

2. An important aspect of the current project was the testing of Clinghans Bridge to verify the recommendations regarding serviceability of the standard M-beam slab. It is hoped that work will start soon on the construction and testing of this bridge which will complete the investigation of the strength of the M-beam slab.

3. The importance of providing adequate diaphragms has already been discussed and there is a need for further experimental information on the use of both steel and concrete diaphragms. This could be achieved by a programme of tests on $\frac{1}{6}$ scale model bridges using steel beams and a lightly reinforced slab. The performance of the slab at serviceability and ultimate loads could be assessed using composite and non-composite steel diaphragms. The use of concrete diaphragms with steel beams could also be investigated.

4. The use of the design charts to provide the necessary data for the design of M-beam bridge decks has proved to be a most successful application of the grillage analysis. In view of this, it is proposed that a similar exercise should be carried out for other forms of construction that are used in N. Ireland. It is envisaged that this approach could be applied to solid slab bridge decks, which would include the inverted tee beam with solid infill, for spans up to 16 m and steel beam and concrete slab decks up to about 35 m. The grillage properties required for solid slab decks have been well documented and for steel beams a grillage with zero torsional stiffness would provide an acceptable level of accuracy.

5. At an early stage of the project an attempt was made to measure the deflections of the elastomeric bearings used in the bridges that were tested. However, the results obtained were inconclusive due mainly to the lack of suitable instrumentation. There is very little information available on the performance of elastomeric bearings and in view of the current problems regarding the dura-

bility of buried joints it is suggested that a programme of tests be initiated to monitor the in-service deflections of these bearings.

6. It has been shown that when reinforced concrete slabs are provided with suitable edge restraint the punching strength is greatly increased and it is suggested that the advantages of this form of construction could be utilized in the design of off-shore structures. A slab restrained to allow the development of arching could provide a suitable working platform which has to withstand heavy concentrated loads and as these are generally of a transient nature they are similar to those experienced by bridge slabs. As regards the main structural members, this type of slab could also provide high resistance to impact from vessels. Current practice is to use prestressed concrete for some of these applications and although there are advantages regarding crack control, construction costs are high and a reinforced concrete solution may result in a more economic design. Epoxy coated reinforcement at relatively close spacings could be used to control cracking and reduce the possibility of corrosion.

7. A further application of restrained slabs which develop arching action is suggested for the design of nuclear pressure vessels. In particular, the high resistance to impact from concentrated loads would be suitable for the containment chamber which is designed to withstand a possible blow-out of part of the pressure vessel.

APPENDIX A

COMPARISON OF COSTS FOR SHORT SPAN BRIDGE DECKS

This appendix compares the relative cost of various types of simply supported bridge decks for spans from 8 to 29 m. Unit costs are given in Table A1 and are based on tenders submitted by N. Ireland contractors during the period October to December 1981. The comparison of the various types of construction is shown in Fig. A1 and the cost per m^2 of deck has been plotted against span. Fig. 5.4 was used to establish the size of the M-beam to be used for the various spans and beam spacings considered.

It will be seen from Fig. A1 that the M-beam deck, when used at up to 2 m spacing, provides an economically competitive design over the range of spans considered. It should also be noted that the use of M-beams will result in a lighter deck when compared with a solid slab or inverted tee beam deck and this should be reflected in the cost of the sub-structure.

Type of Construction	Beams/ tonne	Reinforcement/ tonne	Formwork m^2	Concrete/ m^3
M-Beam	105	320	12	45
Steel Beam	800	320	15	45
Solid Slab	N/A	340	30	45
Inverted Tee Beam with solid infill	105	320	12	45

TABLE A1 - Unit Costs for Final Quarter 1981 - £

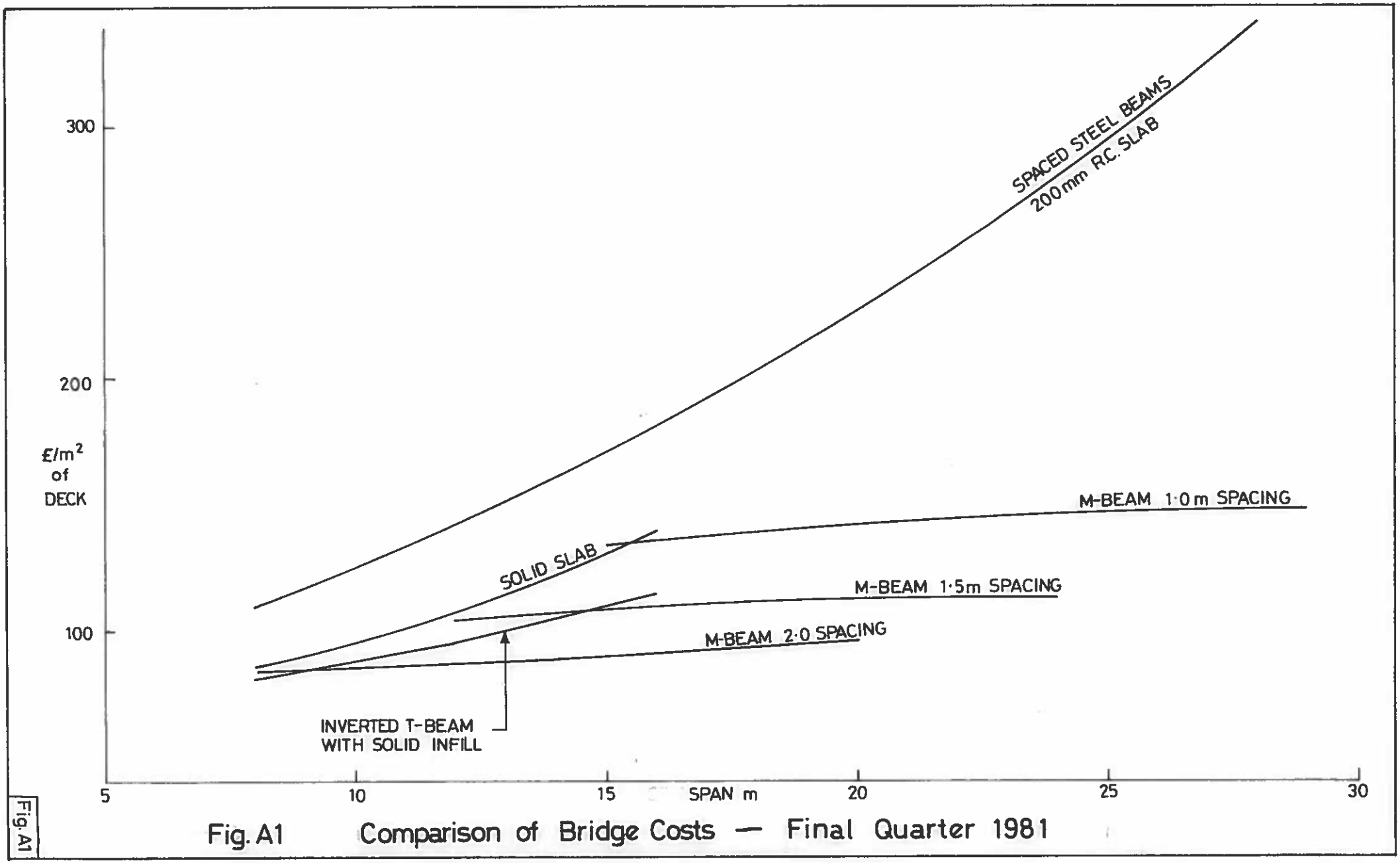

Fig. A1

Fig. A1 Comparison of Bridge Costs — Final Quarter 1981

APPENDIX B

POLYSTYRENE MODEL TESTS

INTRODUCTION

The calculation of the torsional inertia of a transverse grillage beam for a pseudo box-deck was considered in Chapter 2 and the Department of Transport has recommended the use of the method described in the C & CA publication by West (1973). However, when the test results were compared with the recommended method there was a difference of about 20% in the peak values and in the shape of the curve of midspan beam soffit stresses. Therefore, this appendix gives details of a short series of tests aimed at assessing the torsional inertia of the pseudo-box transverse grillage beam.

BASIS OF INVESTIGATION

If the transverse grillage beam was a solid rectangular section the torsional inertia could be calculated by the standard method of St. Venant. Therefore, by comparing the torsional stiffness of a solid rectangular beam with one which included the longitudinal voids the torsional inertia could be estimated by direct comparison with the calculated value for the solid section.

DETAILS OF MODELS

Three $\frac{1}{7}$ scale polystyrene models were constructed representing a 1 m transverse strip of a pseudo-box deck. To cover the range of beam sizes an M2, M5 and M8 beam section was selected, each with 4 voids and a solid end to mount in the torsion machine. A further 3 beams of solid cross-section were made, each pair being cut from adjacent sections of a polystyrene block to ensure similar material properties. The voids were cut from the beams using a template and hot wire.

The polystyrene models were fitted with wooden end plates which had steel centre rods to suit the jaws of the torsion testing machine. As the torque was increased the twist was measured and graphs of torque against twist for both solid and box sections plotted. A model being tested is shown in Plate B1.

RESULTS

Graphs showing a linear relationship between torque and twist are shown in Figure B1, the pseudo-box section being shown as a percentage of the solid section. These values are plotted in Figure B2 as reduction factors to be applied to the torsional inertia of the solid section to give the appropriate value for the pseudo-box section. By assuming a transverse grillage beam width to depth ratio of about 3 the actual torsional inertia of both the solid beam and the pseudo-box beam may be calculated and these are shown in Figure B3. This shows that the transverse torsional inertia of the pseudo-box deck increasing from 43×10^6 mm^4/m for the M1 beam to 160 mm^4/m for the M10. As discussed in Chapter 2 it is usual practice to use only one half of this value due to the complimentary twisting of the 2 dimensional plate. These values show only a marginal increase on those calculated by the recommended method.

CONCLUSION

The results of the test on the polystyrene models indicate that there is justification for an increase of about 50% in the torsional inertia of the transverse grillage beam. However in order to model the test results an increase of about 7 would be required. It is obvious therefore that a comprehensive investigation into this aspect of M-beam bridge deck design is required to successfully resolve this problem.

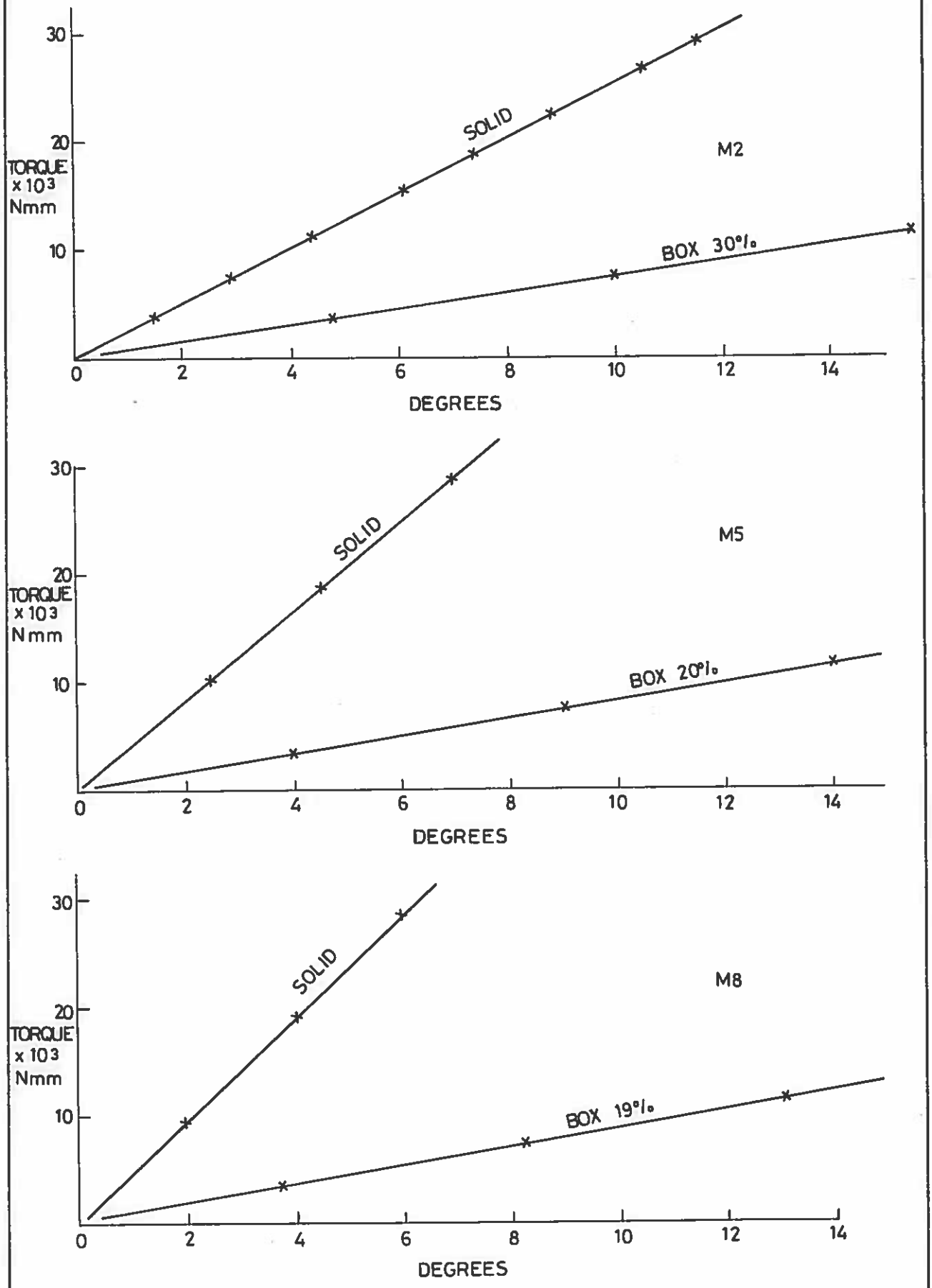

Fig. B1 Torsional Stiffness of Polystyrene Models

Fig. B1

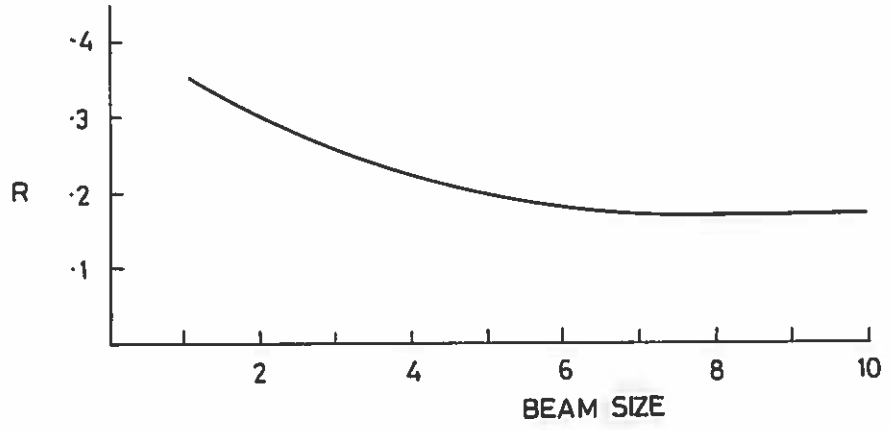

Fig. B2 Reduction Factor For Solid / Pseudo - Box Transverse Torsional Inertia

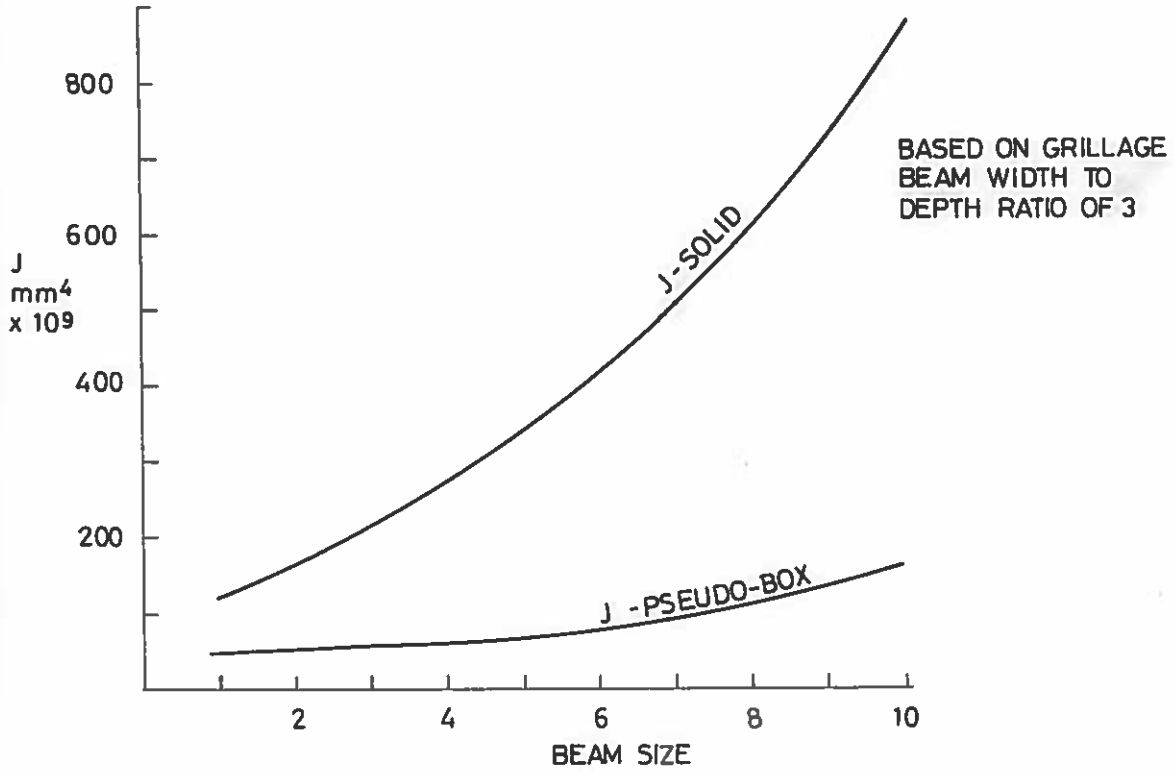

Fig. B3 Transverse Torsional Inertia For 1m Strip Pseudo-Box Deck

Fig B2
Fig B3

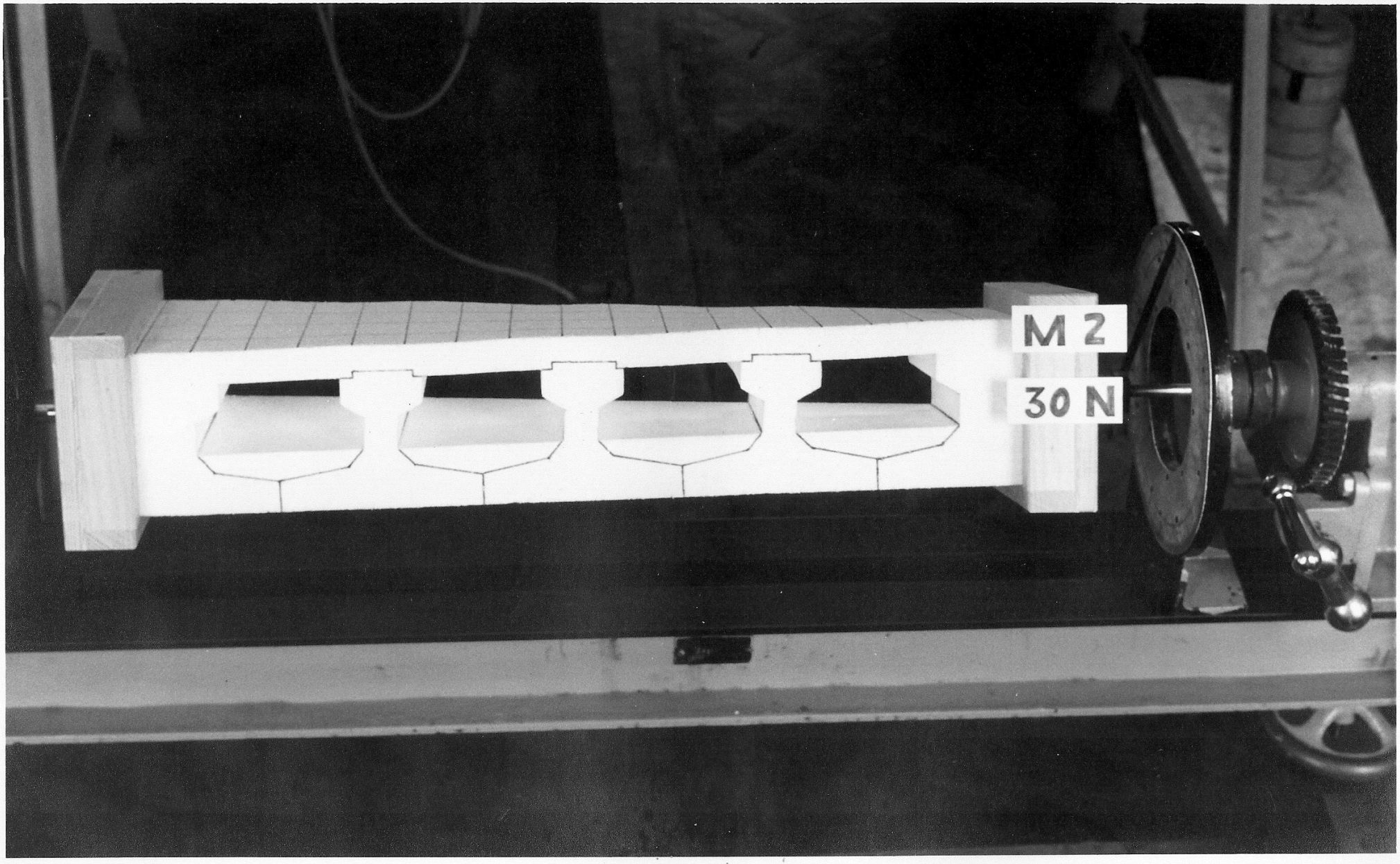

Plate B1

Polystyrene Test Model

APPENDIX C

COMPUTER PROGRAMS FOR M-BEAM BRIDGE DECKS

An important aspect of the streamlined design procedure discussed in Chapters 2 and 5 was the set of programs for the Hewlett Packard desk top computer. The use of these programs was mentioned briefly in the text and this appendix provides complete details of the flow charts, lists of variables and data files for each program. Actual operating instructions for the Hewlett Packard 9830 series computer are available in the handbook on M-beam design by Kirkpatrick (1979). It should be noted that M3-D and M6-D beams have been specified as the standard M4 and M7 beams have poor section moduli relative to the top flange and are therefore not recommended. These programs comply with the current DTp requirements for bridge design.

LIST OF PROGRAMS

1. Prestressed M-Beam
Section Properties For Use With Grillage Analysis
Preliminary Design Parameters

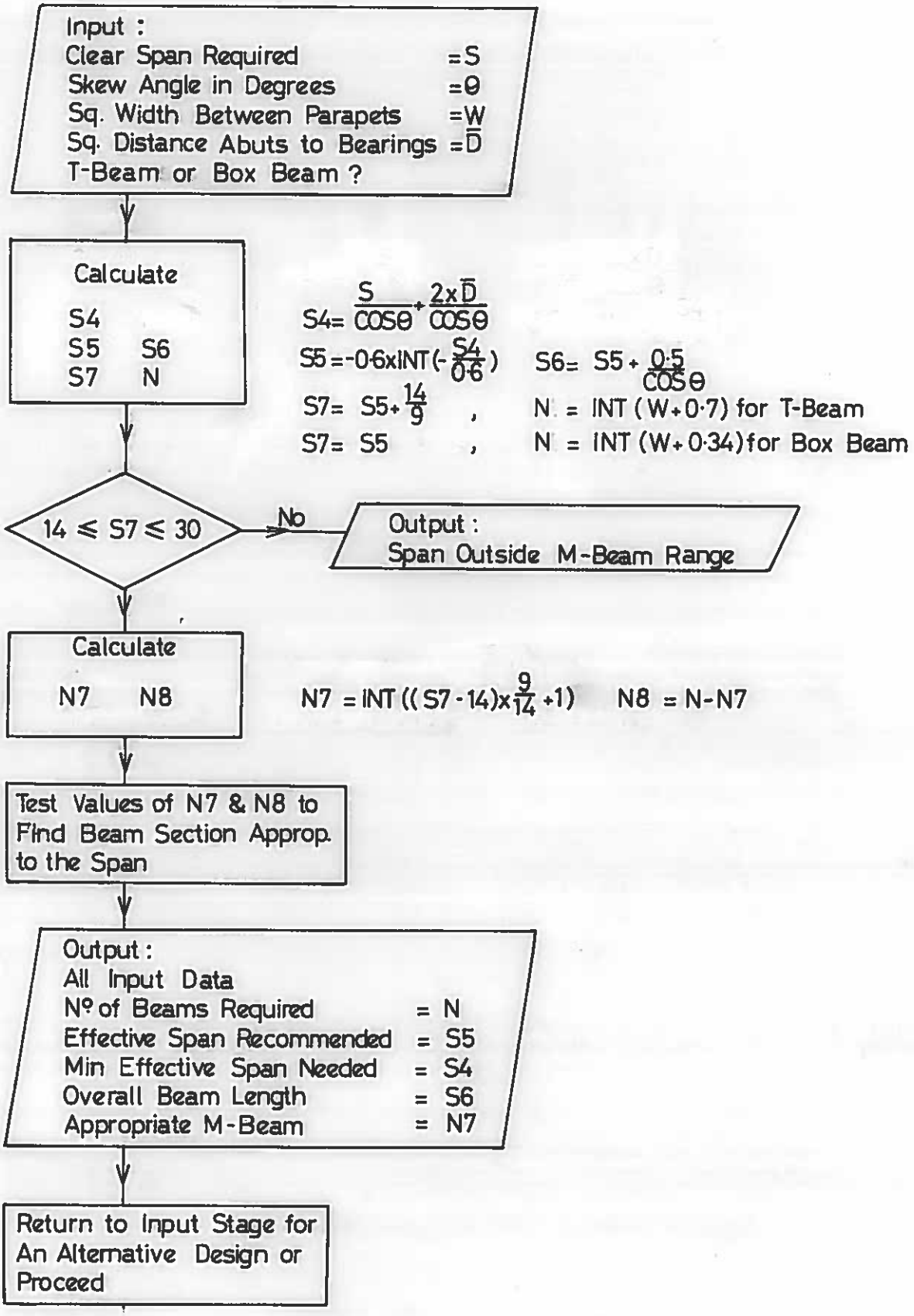

Section Properties For Inverted T-Beams

Input :
Width of Deck Between Parapet = W1
Effective Skew Span = L1
Size of Beam = B
Nº of Physical Beams = N1

Read From Data Files 1,2&3 :
1. Section Properties of Longitudinal Composite Grillage Beam
2. J2
3. Section Properties of Precast Beam

Calculate
W2 W3
N2 K1
J1 J3
N3 N5
N6 L2
I1 K2
J4 N4

$W2 = N1 - 1$ $\qquad W3 = \frac{W2}{N2 - 1}$

$N2 = N1$ if $N1 \leq 9$
$= 9$ if $9 < N1 \leq 18$
$= \frac{N1}{2}$ if $N1 > 18$ (to Next Higher Odd Integer)

$K1 = \frac{1}{3}\left(1 - \frac{100{\cdot}8}{10^3 \times W3} \times \left(1 - \frac{54{\cdot}613 \times 10^6}{(10^3 \times W3)^4}\right)\right.$

$J1 = K1 \times 160 \times 10 \times W3$ $\qquad J3 = \frac{J1}{2} + J2 \times \frac{N1}{N2}$

$N3 = \frac{N2}{1{\cdot}5}$ to Next Odd Integer

$N5 = N2 \times N3$ $\qquad N6 = N2(N3-1) + N3(N2-1)$

$L2 = \frac{L1 \times \cos\theta}{(N3 - 1)}$ $\qquad I1 = \frac{10^3 \times L2 \times 160^3 \times 0{\cdot}8}{12}$

$K2 = \frac{1}{3}\left(1 - \frac{100{\cdot}8}{10^3 \times L2} \times \left(1 - \frac{54{\cdot}6 \times 10^6}{(10^3 \times L2)^4}\right)\right)$

$J4 = \frac{K2 \times 160^3 \times 10^3 \times L2}{2}$ $\qquad N4 = \frac{N1}{N2}$

Plot Grid
Plot M-Beams

Calculate
K5 K6
A J5
J6 J7
I5 A5
I6 A6
Y6 Y7
I7

$K5 = \frac{1}{3}\left(1 - \frac{0{\cdot}63 \times 160}{\left(\frac{10^3 \times L2}{2} + 250\right)} \times \left(1 - \frac{160^4}{12\left(\frac{10^3 \times L2}{2} + 250\right)^4}\right)\right)$

$K6 = \frac{1}{3}\left(1 - \frac{0{\cdot}63 \times 500}{[D] - 160} \times \left(1 - \frac{500^4}{12(D-160)}\right)\right)$
[D] read from store

$A = ([A2] + 151000) \times N4$ [A2] read from store $\qquad J5 = K5 \times 160^3 \times \left(\frac{10^3 \times L2 + 250}{2}\right)$

$J6 = K6 \times 500 \times (D - 160)$ $\qquad J7 = \frac{J5}{2} + J6$

$I5 = \left(\frac{10^3 \times L2}{2} + 250\right) \times \frac{160^3}{12}$ $\qquad A5 = \left(\frac{10^3 \times L2}{2} + 250\right) \times 160$

$I6 = \frac{500(D-160)^3}{12}$ $\qquad A6 = 500(D - 160)$

$Y6 = 160 + \frac{(D-160)}{2}$ $\qquad Y7 = \frac{A5 \times 80 + A6 \times Y6}{A5 + A6}$

$I7 = (15 + A5 + (Y7-80)^2 + I6 + A6(Y7-Y6)^2) \times 0{\cdot}8$

Output :

Nº of Nodes = N5

Nº of Members = N6

Co-ordinates of Grid Points

Width of Deck = W1

Effective Skew Span = L1

Angle of Skew = θ

Nº of Physical Beams = N1

Nº of Longitudinal Grillage Beams = N2

Nº of Transverse Grillage Beams = N3

Nº of Physical Beams per Grillage Beam = N4

Section Properties of Precast Beam (cf Data File 3)

Precast Section No

Depth

Area

Height of Centroid Above Bottom Fibre

Second Moment of Area

Second Moduli : Top Fibre

Bottom Fibre

Self-Weight

Section Properties of Longitudinal Composite Grillage Beam

Precast Section No (cf Data File 1)

Total Depth

Height of Centroid Above Bottom Fibre

2nd Moment of Area x N4

Section Moduli

Top Fibre of Composite Section
Top Fibre of Precast Section
Bott. Fibre of Top Slab Section
Bott. Fibre of Precast Section
} x N4

Gross Area of Composite Section (mm^2) = A

Torsional Inertia of Grid Beam in Longit. Dit. (mm^4) = J3

Section Properties of Transverse Grillage Beam

Second Moment of Area of Transverse Beam (mm^4) = I1

Torsional Inertia of Transverse Beam (mm^4) = J4

Section Properties of End Diaphragm

Second Moment of Area of End Diaph. (mm^4) = I7

Torsional Inertia of End Diaph. (mm^4) = J7

Return to Start for Another Grillage or Finish

Section Properties For Pseudo-Box Beams

Input:

Width of Deck Between Parapets	=	W1
Effective Skew Span	=	L1
Size of Beam	=	B
Nº of Physical Beams	=	N1

Read From Data Files 3 & 4:

3. Section Properties of Precast Beam
4. Section Properties of Longitudinal Composite Grillage Beam

Calculate

W2 W3
N2 N3
N4 N5
N6 L2

$W2 = N1 - 1$ $\qquad W3 = \frac{W2}{N2-1}$

$N2 = N1$ if $N1 \leq 9$
$= 9$ if $9 < N1 \leq 18$
$= \frac{N1}{2}$ if $N1 > 18$ (to Next Higher Odd Integer)

$N3 = \frac{N2}{1.5}$ (to Next Odd Integer)

$N4 = \frac{N1}{N2}$ $\qquad N5 = N2 \times N3$

$N6 = N2(N3-1) + N3(N2-1)$ $\qquad L2 = \frac{L1}{N3-1} \times \cos\theta$

Plot Grid
Plot M-Beam

Calculate

I2 I3
I4 A3
T1 S1
C2 C3
R1 C4
Q1 C5
C6 C7
Y1 I8
I9 I5
A5 I6
A6 Y6
Y7 A4
I7 S2
G2 G4
Q2 G5
G6 G7

$I2 = 341333\,L2 \times 10^3$ $\qquad I3 = 183083\,L2 \times 10^3$

$I4 = [F4] \times L2 \times 10^9$ (read from store) $\qquad A3 = [D1] \times (10^3 \times L2 - T1)$ (read from store)

$T1 = \frac{2 \cdot 333}{\frac{10^3 \times D1^2}{I2 \times I4} + \frac{10^6 \times D1}{48} \times (\frac{1}{I2} + \frac{1}{I3})}$ $\qquad S1 = \frac{2\,D1}{T1} \times (10^3 \times L2 - T1)(\frac{1}{160} + \frac{1}{130})$

$C2 = \frac{4\,A3^2}{S1}$ $\qquad C3 = [C1] \times N4 \times 10^9$ (read from store) $\qquad R1 = L2 / W3$

$C4 = \frac{C2}{R1}$ $\qquad Q1 = \frac{C3}{C4}$ $\qquad C5 = \frac{C3}{1+Q1}$

$C6 = \frac{Q1 \times C3}{1+Q1}$ $\qquad C7 = C6 \times R1$ $\qquad Y1 = \frac{768000 + 5113\,(D1 - 56{\cdot}75)}{10113}$

$I8 = 206{\cdot}16 \times 10^6 + 96000\,(Y1 - 80)^2 + 5113\,(D1 - 56{\cdot}75 - Y1)^2$

$I9 = \frac{I8 \times L2 \times 0{\cdot}8}{0{\cdot}6}$ $\qquad I5 = (\frac{10^3 \times L2}{2} + 250) \times \frac{160^3}{12}$

$A5 = (\frac{10^3 \times L2}{2} + 250) \times 160$ (read from store) $\qquad I6 = \frac{500\,(D - 160)^3}{12}$

$A6 = 500([D] - 160)$ $\qquad Y6 = 160 + \frac{(D - 160)}{2}$ $\qquad Y7 = \frac{A5 \times 80 + A6 \times Y6}{A5 + A6}$

$A4 = D1\,(10^3 \times L2 - T1 - 125)$ $\qquad I7 = 0{\cdot}8(I5 + A5(Y7 - 80)^2 + I6 + A6(Y7 - Y6)^2)$

$S2 = \frac{D1}{T1} + \frac{D1}{T1 + 250} + (10^3 \times L2 - T1 - 125)(\frac{1}{160} + \frac{1}{130})$

$G2 = \frac{4\,A4^2}{S2}$ $\qquad G4 = \frac{G2}{R1}$ $\qquad Q2 = \frac{C3}{G4}$

$G5 = \frac{C3}{1+Q2}$ $\qquad G6 = \frac{Q2 \times C3}{1+Q2}$ $\qquad G7 = G6 \times R1$

Output :

Nº of Nodes = N5

Nº of Member = N6

Co.-ordinates of Grid Points

Width of Deck = W1

Effective Skew Span = L1

Angle of Skew = θ

Nº of Physical Beams = N1

Nº of Longitudinal Grillage Beams = N2

Nº of Transverse Grillage Beams = N3

Nº of Physical Beams Per Grillage Beam = N4

Section Properties of Precast Beam (cf Data File 3)

Precast Section No

Depth

Area

Height of Centroid Above Bottom Fibre

Second Moment of Area

Section Moduli
- Top Fibre
- Bottom Fibre

Self-Weight

Section Properties of Longitudinal Composite Grillage Beam (cf Data File 4)

Precast Section No

Total Depth

Second Moment of Area (mm^4) x N4

Cross-Area of Composite Grillage Beam (mm^2) x N4

Torsional Inertia of Grid Beam in Longit. Dir. (mm^4) = C5

Torsional Inertia of Grid Beam in Longit. Dir. (mm^4) = G5
Local to End Diaph.

Section Properties of Transverse Grillage Beam

Second Moment of Area of Transverse Beam (mm^4) = I 9

Torsional Inertia of Transverse Beam (mm^4) = C7

Section Properties of End Diaphragm

Second Moment of Area of End Diaph. (mm^4) = I 7

Torsional Inertia of End Diaph. (mm^4) = G7

Return to Start for Another Grillage or Finish

LIST OF VARIABLES FOR PROGRAM 1

W1	=	Width of deck between parapets	m
L1	=	Effective skew span	m
O	=	Angle of skew	degrees
N1	=	Number of M-beams required	
N2	=	Number of grid beams required (longitudinal)	
W2	=	Width of grid	m
W3	=	Spacing of longitudinal grid beams	m
J1	=	Torsional inertia of W3 width of slab	mm^4
K1	=	Torsional constant for W3	
J2	=	Torsional inertia of standard M-beam	mm^4
J3	=	Torsional inertia of longitudinal grid beam	mm^4
N3	=	Number of transverse grillage beams	
L2	=	Spacing of transverse grillage beams	m
A1	=	Area of transverse beam (L2 x 160)	mm^2
I1	=	2nd moment of area of transverse beam	mm^4
J4	=	Torsional inertia of transverse beam	mm^4
K2	=	Torsional constant J4	
N4	=	Number of physical beams to grillage beam	
A	=	CSA of composite grillage beam	mm^2
N5	=	Number of nodes	
N6	=	Number of members	
B	=	Size of beam	
K5	=	Torsional constant for slab local to diaphragm	
J5	=	Torsional inertia of slab local to diaphragm	mm^4
K6	=	Torsional constant for diaphragm	
J6	=	Torsional inertia of diaphragm	mm^4

J7 = Torsional inertia of diaphragm + slab mm^4

I5 = 2nd moment of area of slab local to diaphragm mm^4

A5 = Area of slab local to diaphragm mm^2

I6 = 2nd moment of area of diaphragm mm^4

A6 = Area of diaphragm mm^2

Y6 = Centroid of diaphragm from top of slab mm

Y7 = Centroid of combined slab + diaphragm from top of slab mm

I7 = 2nd moment of area of diaphragm + slab mm^4

I2 = I of top slab (transverse) Is1 (West (1973)) mm^4

I3 = I of bottom slab (transverse) Is2 (West (1973)) mm^4

I4 = Ibz (West 1973)

F4 = Constant for calculating I4 = F4 x L2

D1 = Distance between centroids of top and bottom slabs mm

T1 = Thickness of equivalent continuous side wall mm

A3 = Enclosed area of transverse pseudo-box mm^2

S1 = ds/t of transverse pseudo-box

A2 = C.S. area of precast grillage beam mm^2

C1 = Longit. torsional inertia of single box beam mm^4

C2 = Transverse torsional inertia of single equiv. box mm^4

C3 = Torsional inertia of longitudinal grillage beam mm^4

R1 = Spacing of transverse grid beams/spacing of long. grid beams

C4 = Torsional inertion of transverse grid beam mm^4

Y1 = Centroid of transverse pseudo-box beam from top slab mm

I8 = 2nd moment of area of 0.6 m of transverse grid pseudo-box mm^4

I9 = 2nd moment of area of transverse grid beam mm^4

A4 = Enclosed area of end diaphragm pseudo-box mm^2

S2 = ds/dt of transverse diaphragm pseudo-box

D	=	Depth of longitudinal composite beam	mm
C5	=	Final C_L for grid analysis	mm^4
C6	=	Unit C_T inertia	mm^4
C7	=	Final C_T for grid analysis	mm^4
G2	=	C2 for end diaphragm	mm^4
G4	=	C4 for end diaphragm	mm^4
Q1	=	Proportioning factor for unit torsional inertias	
Q2	=	Q1 for diaphragm	
G5	=	C5 for diaphragm	mm^4
G6	=	C6 for diaphragm	mm^4
G7	=	C7 for diaphragm	mm^4
S	=	Clear span	m
W	=	Square width between parapets	m
$\overline{D}$	=	Square distance from face of abutments to centre line of bearings	m
S4	=	Minimum effective span needed	m
S5	=	Effective span recommended	m
S6	=	Overall beam length	m
S7	=	Length of beam required	m
N	=	No of beams required	
N7	=	Appropriate size of M-beam	

2. Design of Prestressed M-Beams - Part 1

Input :

Beam Size	=	B
Bending Moments (kNm)		
Beam Self-Weight Moment	=	M1
Insitu Concrete Moment	=	M2
Superimposed Dead Load Moment	=	M3
Live Load Moment	=	M4
Eccentricity Control Factor	=	K3
28-Day Cube Strength (N/mm)	=	C1
Transfer Cube Strength (N/mm)	=	C2
Initial Prestressing Force in Each Tendon (kN)	=	S1
Cross Sectional Area of Each Tendon (mm)	=	AΘ
Differential Temperature Stresses		
For Heating Cycle — Stress in Top of Insitu Slab	=	H1
For Heating Cycle — Stress in Bottom of Insitu Slab	=	H2
For Heating Cycle — Stress in Top of Precast Beam	=	H3
For Heating Cycle — Stress in Bottom of Precast Beam	=	HΘ
For Cooling Cycle — Stress in Top of Insitu Slab	=	C6
For Cooling Cycle — Stress in Bottom of Insitu Slab	=	C7
For Cooling Cycle — Stress in Top of Precast Beam	=	C8
For Cooling Cycle — Stress in Bottom of Precast Beam	=	C9

Read From Data Files 5,6,7 & 8 :

5 : $\bar{Y}$, A, ZT, ZB, D,

6 : Z1, Z2, Z3, Z4, E6

7 : D1, D2, D3, D4

8 : $\bar{X}1$, $\bar{X}2$, $\bar{X}3$, $\bar{X}4$

Calculate

F1 G1
F2 G2
F3 G3
F4 G4
F5 G5
F6 G6
R1 R3
R2 R4

$$F1 = \frac{M1 \times 10^6}{ZT} \qquad G1 = \frac{M1 \times 10^6}{ZB}$$

$$F2 = \frac{M2 \times 10^6}{ZT} \qquad G2 = \frac{M2 \times 10^6}{ZB}$$

$$F3 = \frac{M3 \times 10^6}{Z2} \qquad G3 = \frac{M3 \times 10^6}{Z4}$$

$$F4 = \frac{M3 \times 10^6 \times 0{\cdot}8}{Z1} \qquad G4 = \frac{M3 \times 10^6 \times 0{\cdot}8}{Z3}$$

$$F5 = \frac{M4 \times 10^6}{Z2} \qquad G5 = \frac{M4 \times 10^6}{Z4}$$

$$F6 = \frac{M4 \times 10^6 \times 0{\cdot}8}{Z1} \qquad G6 = \frac{M4 \times 10^6 \times 0{\cdot}8}{Z3}$$

$$R1 = F1 + F2 + F3 + 2(D3) + F5 + C8 \qquad R3 = F4 + 2(D1) + F6 + H1$$

$$R2 = G1 + G2 + G3 + 2(D4) + G5 + C9 \qquad R4 = G4 + 2(D2) + G6 + C7$$

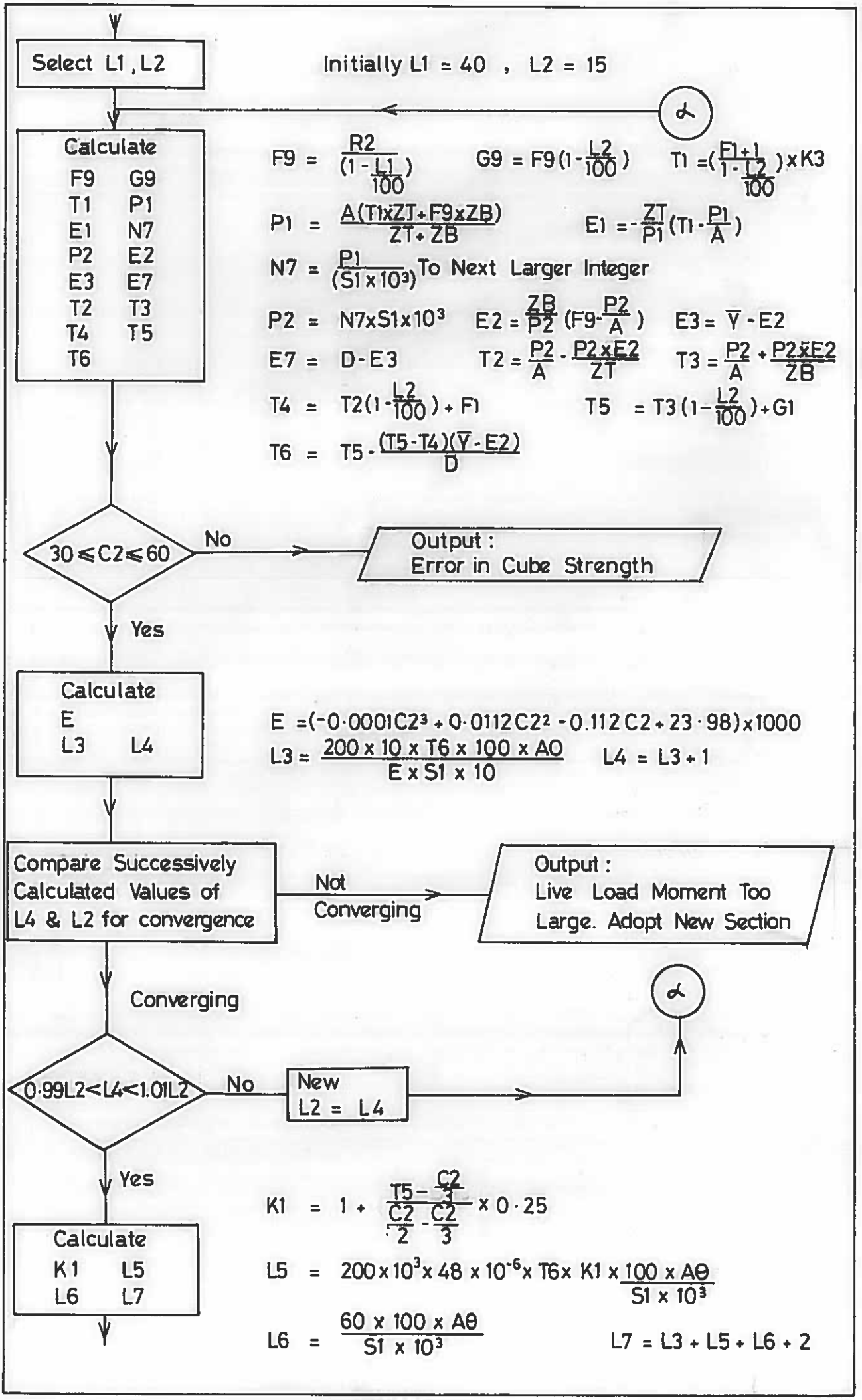
Select L1 , L2
Initially L1 = 40 , L2 = 15
Calculate
F9 G9
T1 P1
E1 N7
P2 E2
E3 E7
T2 T3
T4 T5
T6
F9 = R2 / (1 - L1/100)
G9 = F9 (1 - L2/100)
T1 = ((F1+1) / (1 - L2/100)) x K3
P1 = A(T1xZT + F9xZB) / (ZT + ZB)
E1 = - (ZT/P1) (T1 - P1/A)
N7 = P1 / (S1 x 10³) To Next Larger Integer
P2 = N7xS1x10³
E2 = (ZB/P2) (F9 - P2/A)
E3 = Y - E2
E7 = D - E3
T2 = P2/A - P2xE2/ZT
T3 = P2/A + P2xE2/ZB
T4 = T2 (1 - L2/100) + F1
T5 = T3 (1 - L2/100) + G1
T6 = T5 - (T5 - T4)(Y - E2) / D
30 ≤ C2 ≤ 60
No
Output : Error in Cube Strength
Yes
Calculate
E
L3 L4
E = (-0·0001C2³ + 0·0112C2² - 0.112 C2 + 23·98) x 1000
L3 = 200 x 10 x T6 x 100 x AO / E x S1 x 10
L4 = L3 + 1
Compare Successively Calculated Values of L4 & L2 for convergence
Not Converging
Output : Live Load Moment Too Large. Adopt New Section
Converging
0·99L2 < L4 < 1.01L2
No
New L2 = L4
Yes
Calculate
K1 L5
L6 L7
K1 = 1 + ((T5 - C2/3) / (C2/2 - C2/3)) x 0·25
L5 = 200 x 10³ x 48 x 10⁻⁶ x T6 x K1 x 100 x AΘ / S1 x 10³
L6 = 60 x 100 x AΘ / S1 x 10³
L7 = L3 + L5 + L6 + 2

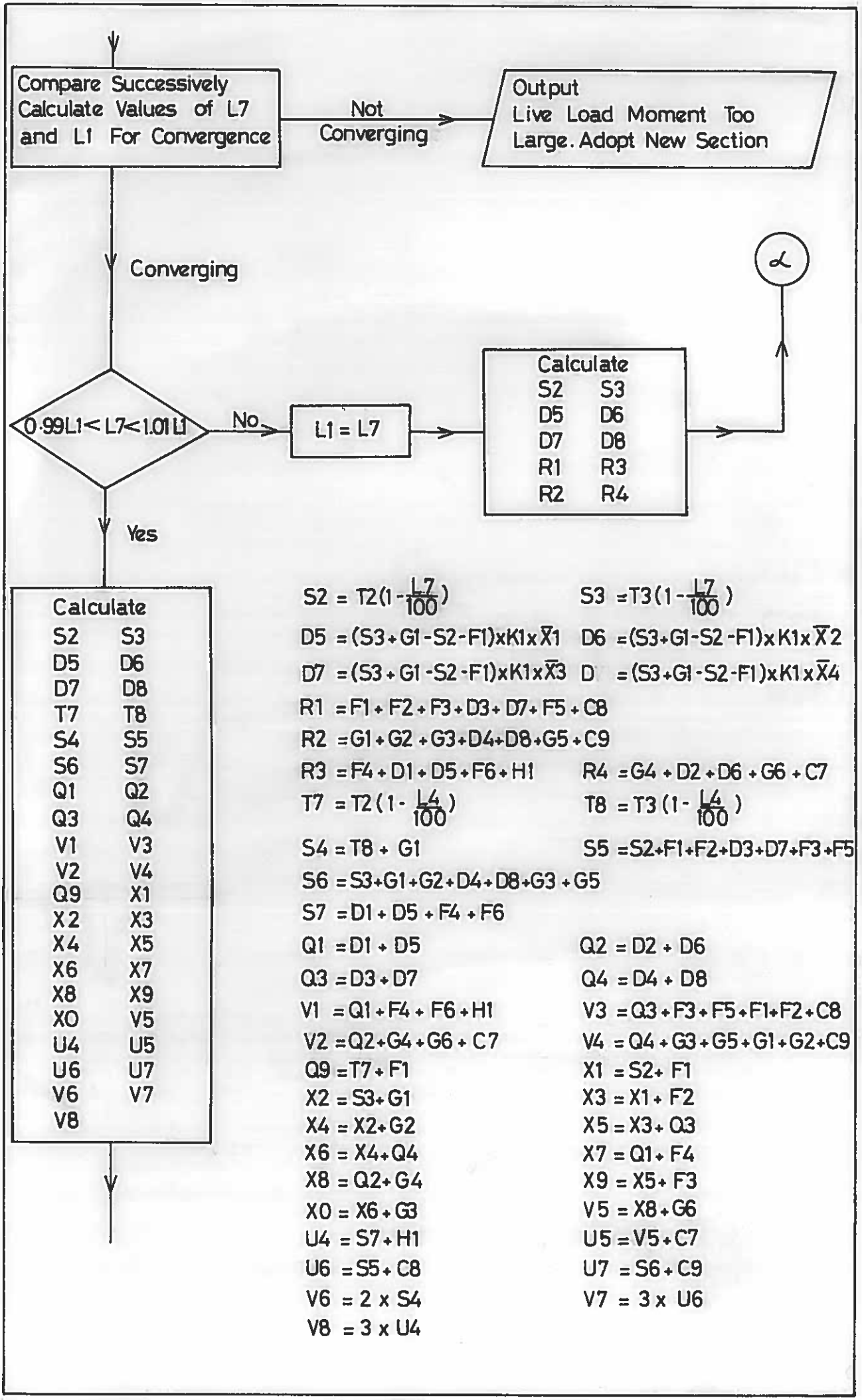

$S2 = T2(1-\frac{L7}{100})$ $S3 = T3(1-\frac{L7}{100})$

$D5 = (S3+G1-S2-F1)\times K1\times \bar{X}1$ $D6 = (S3+G1-S2-F1)\times K1\times \bar{X}2$

$D7 = (S3+G1-S2-F1)\times K1\times \bar{X}3$ $D = (S3+G1-S2-F1)\times K1\times \bar{X}4$

$R1 = F1+F2+F3+D3+D7+F5+C8$

$R2 = G1+G2+G3+D4+D8+G5+C9$

$R3 = F4+D1+D5+F6+H1$ $R4 = G4+D2+D6+G6+C7$

$T7 = T2(1-\frac{L4}{100})$ $T8 = T3(1-\frac{L4}{100})$

$S4 = T8+G1$ $S5 = S2+F1+F2+D3+D7+F3+F5$

$S6 = S3+G1+G2+D4+D8+G3+G5$

$S7 = D1+D5+F4+F6$

$Q1 = D1+D5$ $Q2 = D2+D6$

$Q3 = D3+D7$ $Q4 = D4+D8$

$V1 = Q1+F4+F6+H1$ $V3 = Q3+F3+F5+F1+F2+C8$

$V2 = Q2+G4+G6+C7$ $V4 = Q4+G3+G5+G1+G2+C9$

$Q9 = T7+F1$ $X1 = S2+F1$

$X2 = S3+G1$ $X3 = X1+F2$

$X4 = X2+G2$ $X5 = X3+Q3$

$X6 = X4+Q4$ $X7 = Q1+F4$

$X8 = Q2+G4$ $X9 = X5+F3$

$XO = X6+G3$ $V5 = X8+G6$

$U4 = S7+H1$ $U5 = V5+C7$

$U6 = S5+C8$ $U7 = S6+C9$

$V6 = 2 \times S4$ $V7 = 3 \times U6$

$V8 = 3 \times U4$

Output :

Program for the Design of Prestressed M-Beam

Results

All Part 1 Input Data

Youngs Modulus (N/mm^2) = E

Dead & Live Load Stresses N/mm^2

	Top of Insitu	Bottom of Insitu	Top of Precast	Bottom of Precast
Precast Beam			F1	G1
Insitu Concrete			F2	G2
Differential Shrinkage	Q1	Q2	Q3	Q4
Superimposed Dead Load	F4	G4	F3	G3
Live Load	F6	G6	F5	G5
Temperature	H1	C7	C8	C9
Total	V1	V2	V3	V4

Prestressing Details

Initial Prestressing Force (N) = P2

Nº of Prestressing Strands Required = N7

Initial Force in Each Strand (kN) = S1

Eccentricity (mm) = E3 Above Beam Soffit

Cross-Section Area of Strand (mm^2) = AΘ

Loss of Prestress at Transfer = L4 %

Final Loss of Prestress = L7 %

Eccentricity Control Factor = K3

Centroid of Tendons to Top Fibre (mm) = E7

If Nº of Strands (N7) and Eccentricity (E) are acceptable proceed. Otherwise Input New Values of N7 and/or E, Recalculate Values of P2, E2 ($= \bar{Y} - E3$), E7, T2, T3, T4, T5, T6, L3, L4, K1, L5, L6, L7, S2, S3, D5, D6, D7, D8, T7, T8, S4, S5, S6, S7, Q1, Q2, Q3, Q4, V1, V2, V3, V4, Q9, X1, X2, X3, X4, X5, X6, X7, X8, X9, XΘ, V5, U4, U5, U6, U7, V6, V7, V8 and Output New Results in Similar Format as Before

Output :

Final Stresses (N/mm^2)

	Top of Insitu	Bottom of Insitu	Top of Precast	Bottom of Precast
Initial Prestress			T2	T3
Prestress at Transfer			T7	T8
Prestress at Transfer & Self-Weight			Q9	S4
Final Prestress			S2	S3
Final Prestress & Self-Weight			X1	X2
Final Prestress & Self-Weight & Insitu Concrete			X3	X4
Final Prestress & Self-Weight & Insitu Concrete & Differential Shrinkage	Q1	Q2	X5	X6
Final Prestress & Self-Weight & Insitu Concrete & Differential Shrinkage & Superimposed Dead Load	X7	X8	X9	X0
Final Prestress & Self-Weight & Insitu Concrete & Differential Shrinkage & Superimposed Dead Load & Live Load	S7	V5	S5	S6
Final Prestress & Self-Weight & Insitu Concrete & Differential Shrinkage & Superimposed Dead Load & Live Load & Temperature	U4	U5	U6	U7

Minimum Precast Cube Strength Required at Transfer = V6
" " " " " " 28 Days = V7
" Insitu " " " " " " = V8

** NB. No Allowance has been made for Overstress **

If S6 is - VE : Btm. of P'Cast Beam is in Tension

If S7 is - VE : Top of Insitu is in Tension

If Q9 $\geq$ -1 Transfer Tension Stress at Top of P'Cast Beam Exceeds 1·0 N/mm^2

If Another Section With a New Prestress Force is to be Analysed Return to Start of Part 1, Otherwise Proceed to Part 2 of Program or Finish

LIST OF VARIABLES FOR PROGRAM 2

M1	=	BM from self-weight of precast beam	kNm
M2	=	BM from in situ concrete	kNm
M3	=	BM from superimposed dead load	kNm
M4	=	BM from live load	kNm
F1	=	Stress at top of precast section due to M1	N/mm^2
G1	=	Stress at bottom of precast section due to M1	N/mm^2
F2	=	Stress at top of precast section due to M2	N/mm^2
F3	=	Stress at top of precast section due to M3	N/mm^2
G3	=	Stress at bottom of precast section due to M3	N/mm^2
F4	=	Stress at top of in situ slab due to M3	N/mm^2
G4	=	Stress at bottom of in situ slab due to M3	N/mm^2
F5	=	Stress at top of precast section due to M4	N/mm^2
G5	=	Stress at bottom of precase section due to M4	N/mm^2
F6	=	Stress at top of in situ slab due to M4	N/mm^2
G6	=	Stress at bottom of in situ slab due to M4	N/mm^2
D1	=	Differential shrinkage stress at top of in situ slab	N/mm^2
D2	=	Differential shrinkage stress at bottom of in situ slab	N/mm^2
D3	=	Differential shrinkage stress at top of precast beam	N/mm^2
D4	=	Differential shrinkage stress at bottom of precast beam	N/mm^2
D5	=	Differential creep stress at top of in situ slab	N/mm^2
D6	=	Differential creep stress at bottom of in situ slab	N/mm^2
D7	=	Differential creep stress at top of precast beam	N/mm^2
D8	=	Differential creep stress at bottom of precast beam	N/mm^2
R1	=	Resultant stress at top of precast beam = F1 + F2 + F3 + 2D3 + F5 + C8	N/mm^2
G2	=	Stress at bottom of precast section due to M2.	N/mm^2

R2	=	Resultant stress at bottom of precast beam = G1 + G2 + G3 + 2D4 + G5 + C9	N/mm^2
R3	=	Resultant stress at top of in situ slab = F4 + 2D1 + F6 + H1	N/mm^2
R4	=	Resultant stress at bottom of in situ slab = G4 + 2D2 + G6 + C7	N/mm^2
B	=	Beam size	
K3	=	Eccentricity control factor	
C1	=	28-day cube strength of precast beam	N/mm^2
C2	=	Transfer cube strength	N/mm^2
S1	=	Initial prestressing force in each tendon	kN
A0	=	Cross-sectional area of each tendon	mm^2
L1	=	Percentage loss of prestress at 28 days	%
L2	=	Percentage loss of prestress at transfer	%
F9	=	Initial prestress required in bottom fibre allowing for L1 losses at 28 day	N/mm^2
G9	=	Initial prestress required in bottom fibre allowing for L2 losses at transfer	N/mm^2
T1	=	Top fibre tension stress due to prestress only at transfer	N/mm^2
P1	=	Initial prestress force required to give stresses F1 and T1	N/mm^2
E1	=	Eccentricity of P1 from beam centroid	mm
N7	=	No of tendons required	
P2	=	Initial prestressing force	kN
E2	=	Eccentricity of P2 from beam centroid	mm
E3	=	Centroid of P2 above soffit	mm
T2	=	Top fibre stress due to initial prestress P2	N/mm^2
T3	=	Bottom fibre stress due to initial prestress P2	N/mm^2

T4	=	Top fibre stress due to prestress + self-weight after L2 losses	N/mm^2
T5	=	Bottom fibre stress due to prestress + self-weight after L2 losses	N/mm^2
T6	=	Stress at centroid of tendons from fibre stresses T4 and T5	N/mm^2
L3	=	Loss of prestress due to elastic deformation	%
L4	=	Total loss of prestress at transfer	%
K1	=	Creep factor (ref. BE2/73 para 5.4)	
L5	=	Loss due to creep of concrete	%
L6	=	Loss due to shrinkage of concrete	%
L7	=	Total losses	%
T7	=	Top fibre stress at transfer due to prestress only	N/mm^2
T8	=	Bottom fibre stress at transfer due to prestress only	N/mm^2
S2	=	Top fibre stress due to prestress after L1 losses	N/mm^2
S3	=	Bottom fibre stress due to prestress after L1 losses	N/mm^2
S4	=	Stress in bottom of precast beam due to self-weight + prestress at transfer	N/mm^2
S5	=	Final stress at top of precast beam	N/mm^2
S6	=	Final stress at bottom of precast beam	N/mm^2
E7	=	Centroid of tendons to top fibre of composite beam	mm
S7	=	Final stress at top of in situ concrete	N/mm^2
Q1	=	D1 + D5	
Q2	=	D2 + D6	
Q3	=	D3 + D7	
Q4	=	D4 + D8	
V1	=	Q1 + F4 + F6 + H1	

V2 = Q2 + G4 + G6 + C7

V3 = Q3 + F3 + F5 + F1 + F2 + C8

V4 = Q4 + G3 + G5 + G1 + G2 + C9

Q9 = T7 + F1

X1 = S2 + F1

X2 = S3 + G1

X3 = S2 + F1 + F2

X4 = S3 + G1 + G2

X5 = X3 + Q3

X6 = X4 + Q4

X7 = Q1 + F4

X8 = Q2 + G4

X9 = X5 + F3

XO = X6 + G3

V5 = X8 + G6

V6 = 2 x S4

V7 = 3 x U6

V8 = 3 x U4

H1 = Differential temperature stress in top of in situ slab (heating cycle) N/mm^2

H2 = Differential temperature stress in bottom of in situ slab (heating cycle) N/mm^2

H3 = Differential temperature stress in top of precast beam (heating cycle) N/mm^2

HO = Differential temperature stress in bottom of precast beam (heating cycle) N/mm^2

C6 = Differential temperature stress in top of in situ slab (cooling cycle) N/mm^2

C7 = Differential temperature stress in bottom of in situ slab (cooling cycle) N/mm^2

C8 = Differential temperature stress in top of precast beam (cooling cycle) N/mm^2

C9 = Differential temperature stress in bottom of precast beam (cooling cycle) N/mm^2

E = Young's Modulus N/mm^2

U4 = S7 + H1

U5 = V5 + C7

U6 = S5 + C8

U7 = S6 + C9

Z1 = Section modulus - top fibre of composite section mm^3

Z2 = Section modulus - top fibre of precast section mm^3

Z3 = Section modulus - bottom fibre of top slab mm^3

Z4 = Section modulus - bottom fibre of precast section mm^3

$\overline{X}1$ = Shrinkage coefficient

$\overline{X}2$ = Shrinkage coefficient

$\overline{X}3$ = Shrinkage coefficient

$\overline{X}4$ = Shrinkage coefficient

E6 = Depth of composite section mm

$\overline{Y}$ = Height of centroid above bottom fibre mm

A = C.S. area mm^2

D = Depth of precast section mm

ZT = Section modulus of precast section - top fibre mm^3

ZB = Section modulus of precast section - bottom fibre mm^3

3. Design of Prestressed M-Beams - Part 2

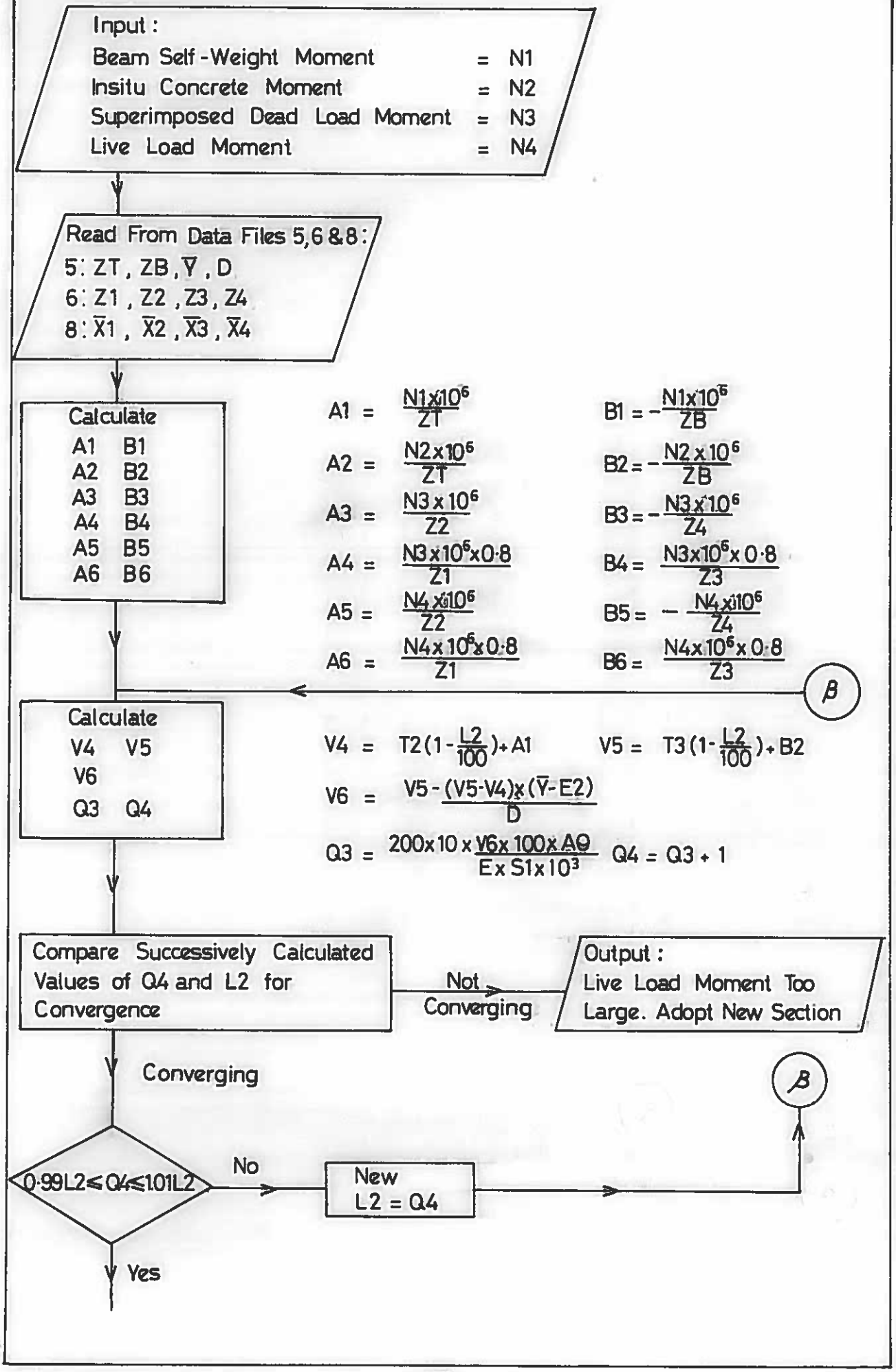

Calculate

P2	Q7
K2	Q5
W1	W2
W3	W4
J5	J6
J7	J8
H4	H5
H6	H7
K1	K2
K3	K4
V1	V2
V3	V4
X1	X2
X3	X4
X5	X6
X7	X8
X9	XΘ
K9	V5
Z5	Z6
Z7	Z8

$P2 = N7 \times S1 \times 10^3$ $\quad Q7 = Q3 + Q5 + L6 + 2$

$K2 = 1 + 0{\cdot}25\left(\frac{V5 - \frac{C2}{3}}{\frac{C2}{2} - \frac{C2}{3}}\right)$

$Q5 = 200 \times 48 \times 10^{-6} \times V6 \times K2 \times \frac{100 \times A\Theta}{S1}$

$W1 = T2\left(1 - \frac{L2}{100}\right)$ $\quad W2 = T3\left(1 - \frac{L2}{100}\right)$

$W3 = T2\left(1 - \frac{Q7}{100}\right)$ $\quad W4 = T3\left(1 - \frac{Q7}{100}\right)$

$J5 = (W4 + B1 - W3 - A1) \times K2 \times \bar{X}1$ $\quad J6 = (W4 + B1 - W3 - A1) \times K2 \times \bar{X}2$

$J7 = (W4 + B1 - W3 - A1) \times K2 \times \bar{X}3$ $\quad J8 = (W4 + B1 - W3 - A1) \times K2 \times \bar{X}4$

$H4 = W2 + B1$ $\quad H5 = W3 + A1 + A2 + D3 + J7 + A3 + A5$

$H6 = W4 + B1 + B2 + D4 + J8 + B3 + B5$ $\quad H7 = D1 + J5 + A4 + A6$

$K1 = D1 + J5$ $\quad K2 = D2 + J6$

$K3 = D3 + J7$ $\quad K4 = D4 + J8$

$V1 = K1 + A4 + A6 + H1$ $\quad V2 = K2 + B4 + B6 + C7$

$V3 = A1 + A2 + K3 + A3 + A5 + C8$ $\quad V4 = B1 + B2 + K4 + B3 + B5 + C9$

$X1 = W3 + A1$ $\quad X2 = W4 + B1$

$X3 = X1 + A2$ $\quad X4 = X2 + B2$

$X5 = X3 + K3$ $\quad X6 = X4 + K4$

$X7 = K1 + A4$ $\quad X8 = K2 + B4$

$X9 = X5 + A3$ $\quad X\Theta = X6 + B3$

$K9 = W1 + A1$ $\quad V5 = B6 + X8$

$Z5 = H7 + H1$ $\quad Z6 = V5 + C7$

$Z7 = H5 + C8$ $\quad Z8 = H6 + C9$

Output :
Results

Precast Beam Section M (B)
All Part 2 Input Data
Assumed Concrete Strength (N/mm^2)
Precast Cube Strength at Transfer = C1
" " " 28 Days = C2
Dead and Live Load Stresses (N/mm^2)

	Top of In Situ	Bottom of In Situ	Top of Precast	Bottom of Precast
Precast Beam			A1	B1
In Situ Concrete			A2	B2
Differential Shrinkage	K1	K2	K3	K4
Superimposed Dead Load	A4	B4	A3	B3
Live Load	A6	B6	A5	B5
Temperature	H1	C7	C8	C9
Total	V1	V2	V3	V4

Output Continued :

Prestressing Details

Initial Prestressing Force (N)	= P2	
Nº of Prestressing Strands Required	= N7	
Initial Force in Each Strand (kN)	= S1	
Eccentricity (mm)	= E3	Above Soffit
Cross Section Area of Strand (mm^2)	= AΘ	
Loss of Prestress at Transfer	= Q4 %	
Final Loss of Prestress	= Q7 %	
Eccentricity Control Factor	= K6	

	Top of In Situ	Bottom of In Situ	Top of Precast	Bottom of Precast
Initial Prestress			T2	T3
Prestress at Transfer			W1	W2
Prestress at Transfer and Self-Weight			K9	H4
Final Prestress			W3	W4
Final Prestress and Self-Weight			X1	X2
Final Prestress and Self-Weight and Insitu Concrete			X3	X4
Final Prestress and Self-Weight and In Situ Concrete and Differential Shrinkage	K1	K2	X5	X6
Final Prestress and Self-Weight and In Situ Concrete and Different Shrinkage and Superimposed Dead Load	X7	X8	X9	X0
Final Prestress and Self-Weight and In Situ Concrete and Differential Shrinkage and Superimposed Dead Load and Live Load	H7	V5	H5	H6
Final Prestress and Self-Weight and In Situ Concrete and Differential Shrinkage and Superimposed Dead Load and Live Load and Temperature	Z5	Z6	Z7	Z8

If Another Section With a New Prestress Force is to be Analysed Return To Start of Pt.1 Otherwise Return to Start of Pt.2 of Program or Finish.

LIST OF VARIABLES FOR PROGRAM 3

N1	=	BM from self-weight of precast beam	kNm
N2	=	BM from in situ concrete	kNm
N3	=	BM from superimposed dead load	kNm
N4	=	BM from live load	kNm
A1	=	Stress at top of precast section due to N1	N/mm^2
B1	=	Stress at bottom of precast section due to N1	N/mm^2
A2	=	Stress at top of precast section due to N2	N/mm^2
B2	=	Stress at bottom of precast section due to N2	N/mm^2
A3	=	Stress at top of precast section due to N3	N/mm^2
B3	=	Stress at bottom of precast section due to N3	N/mm^2
A4	=	Stress at top of in situ slab due to N3	N/mm^2
B4	=	Stress at bottom of precast section due to N3	N/mm^2
A5	=	Stress at top of precast beam due to N4	N/mm^2
B5	=	Stress at bottom of precast beam due to N4	N/mm^2
A6	=	Stress at top of in situ slab due to N4	N/mm^2
B6	=	Stress at bottom of in situ slab due to N4	N/mm^2
V4	=	Top fibre stress due to prestress + self-weight after L2 losses	N/mm^2
V5	=	Bottom fibre stress due to prestress + self-weight after L2 losses	N/mm^2
V6	=	Stress at centroid of tendons from fibre stresses V4 and V5	N/mm^2
Q3	=	Loss of prestress due to elastic deformation	%
Q4	=	Loss of prestress at transfer	%
Q5	=	Loss of prestress due to creep of concrete	%
Q7	=	Total loss of prestress	%
K2	=	Creep factor (ref BE2/73 para 5.4)	
W1	=	Top fibre stress at transfer due to prestress only	N/mm^2

W2 = Bottom fibre stress at transfer due to prestress only N/mm^2

W3 = Top fibre stress due to prestress after Q7 losses N/mm^2

W4 = Bottom fibre stress due to prestress after Q7 losses N/mm^2

H4 = Stress in bottom of precast beam due to prestress at transfer + self-weight N/mm^2

H5 = Final stress at top of precast beam N/mm^2

H6 = Final stress at bottom of precast beam N/mm^2

H7 = Final stress at top of in situ concrete N/mm^2

J5 = Differential creep stress - top of in situ N/mm^2

J6 = Differential creep stress - bottom of in situ N/mm^2

J7 = Differential creep stress - top of precast beam N/mm^2

J8 = Differential creep stress - bottom of precast beam N/mm^2

K1 = D1 + J5

K2 = D2 + J6

K3 = D3 + J7

K4 = D4 + J8

V1 = K1 + A4 + A6 + H1

V2 = K2 + B4 + B6 + C7

V3 = A1 + A2 + K3 + A3 + A5 + C8

V4 = B1 + B2 + K4 + B3 + B5 + C9

K9 = W1 + A1

X1 = W3 + A1

X2 = W4 + B1

X3 = X1 + A2

X4 = X2 + B2

X5 = X3 + K3

X6 = X4 + K4

X7 = K1 + A4

X8 = K2 + B4

X9 = X5 + A3

XO = X6 + B3

V5 = B6 + X8

Z5 = H1 + H7

Z6 = V5 + C7

Z7 = H5 + C8

Z8 = H6 + C9

L2 = Percentage loss of prestress at transfer %

P2 = Initial prestressing force N

$\overline{X}1$ = Shrinkage coefficient

$\overline{X}2$ = Shrinkage coefficient

$\overline{X}3$ = Shrinkage coefficient

$\overline{X}4$ = Shrinkage coefficient

Z1 = Section modulus - top fibre of composite section mm^3

Z2 = Section modulus - top fibre of precast section mm^3

Z3 = Section modulus - bottom fibre of top slab section mm^3

Z4 = Section modulus - bottom fibre of precast section mm^3

ZT = Section modulus of precast section - top fibre mm^3

ZB = Section modulus of precast section - bottom fibre mm^3

$\overline{Y}$ = Height of centroid above bottom fibre mm

D = Depth of precast section mm

C1 = Precast cube strength at transfer N/mm^2

C2 = Precast cube strength at 28 days N/mm^2

N7 = No of tendons required

E3 = Eccentricity (distance above soffit) mm

AO = C.S. area of strand mm^2

T2 = Top fibre stress due to initial prestress P2 N/mm^2

T3 = Bottom fibre stress due to initial prestress P2 N/mm^2

4. Composite Prestressed M-Beam Shear Reinforcement

Input :

Beam Size	= B
Nº of HA Cases	= C1
Nº of HB Cases	= C2
Shear Forces & Bending Moments (kN & kNm) Due to :-	
(a) Beam Self-Weight & Insitu Concrete	= S1 & M1
(b) Superimposed Dead Load	= S9 & M9
(c) HA Live Load Including K.E.L.	= S2 & M2 : C1 Times
(d) HB Live Load or 2·112 kN Wheels of HA or Accidental Wheel on F.Way or Verge	= S3 & M3 : C2 Times
28-Day Cube Strength (N/mm^2)	= U1
Distance From Centroid of Tendons to Top Fibre of Composite Beam (mm)	= D3
Bottom Fibre Compressive Stress Due Solely to Prestress After All Losses (N/mm^2)	= F9
Top Fibre Beam Stress Due to Self-Weight + Insitu Concrete + Prestress After All Losses (N/mm^2)	= F3
Bottom Fibre Beam Stress Due to Self-Weight + Insitu Concrete + Prestress After All Losses (N/mm^2)	= F4

Read From Data Files 9 & 10 :
9 : Y1 , I1 , Y2 , I2 , Y8 , D2 , A1 , D1 , A2 , Y3 , Y9 , A4 , Y4 , A3 , Y5
10 : A5, Y6

Calculate

S4	M4
S5	M5
S6	M6
Q9	Q5
M7	Q6
Q7	Z9
Q	Q8

$S4 = 1{\cdot}5\,(S1+S9)+2{\cdot}5\,S2$, $M4 = 1{\cdot}5\,(M1+M9)+2{\cdot}5M2$ } C1 Times

$S5 = 2\,((S1+S9)+S2)$, $M5 = 2\,((M1+M9)+M2)$ } C1 Times

$S6 = 1{\cdot}5(S1+S9)+2S3$, $M6 = 1{\cdot}5(M1+M9)+2M3$ } C2 Times

Q9 = Greater of (Lesser of S4 or S5) or S6

$$Q5 = \frac{0{\cdot}045 \times 160 \times D3\sqrt{U1}}{10^3}$$

$$M7 = \left(0{\cdot}45 \times \sqrt{U1} - M1 \times \frac{Y8}{I1} \times 10^6 + F9\right) \times \frac{I2}{(Y2 \times 10^6)}$$

$$Q6 = \left(\frac{Q - S1}{M - M1}\right) \times M7 \qquad Q7 = Q5 + S1 + Q6 \text{ (if } M1 = 0, Q7 = 0)$$

$$Q8 = \frac{0{\cdot}92 \times 160 \times D2}{10^3}\sqrt{U1} \qquad Z9 = \text{Greater of } \begin{matrix}(S4 - 0{\cdot}8Q7)\\(S5 - 0{\cdot}8Q7)\\(S6 - 0{\cdot}8Q7)\end{matrix} \begin{matrix}\}\text{C1 Times}\\ \\ \}\text{C2 Times}\end{matrix}$$

Q Becomes S4, S5 or S6 For Which Z9 is a Maximum

Q9 < Q8

No

Output :
Shear Resistance of Concrete is inadequate - Adopt a New Section
Design Ultimate Shear Force (kN) = Q9
Shear Resistance of Beam (kN) = Q8

γ

Yes

Calculate
F1 F2
P1 P2

$$F1 = \frac{S1 \times A5 \times Y6 \times 10^3}{160 \times I1}$$

$$F2 = \frac{(F4 - F3) \times (D1 - Y8)}{D1} + F3$$

$$P1 = \frac{F2}{2} - \sqrt{\left(\frac{F2}{2}\right)^2 + F1^2}$$

$$P2 = 0{\cdot}294\sqrt{U1}$$

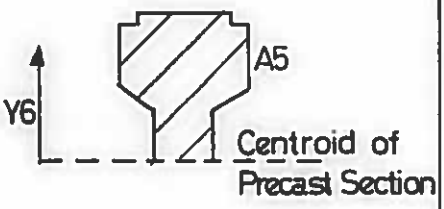

P1 + ve or ABS P1 ≤ ABS P2

No

Output :
Principal Tensile Stress Exceeds Permissible at Centroid of Composite Beam. Adopt a New Section
Principal Tensile Stress (N/mm²) = P1
Permissible Tensile Stress (N/mm²) = P2
(Positive Numeric Values)

γ

Yes

Calculate
F5 F6
P3

$$F5 = \frac{S1 \times A2 \times Y3 \times 10^3}{160 \times I1}$$

$$F6 = \frac{(F4 - F3) \times (D1 - Y9)}{D1} + F3$$

$$P3 = \frac{F6}{2} - \sqrt{\left(\frac{F6}{2}\right)^2 + F5^2}$$

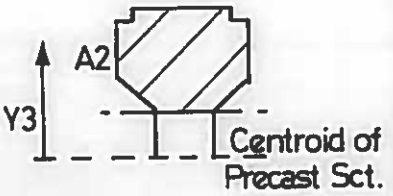

P3 + ve or ABS P3 ≤ ABS P2

No

Output :
Principal Tensile Stress Exceeds Permissible at Junction of Web & Top Flange. Adopt a New Section
Principal Tensile Stress (N/mm²) = P3
Permissible Tensile Stress (N/mm²) = P2
(Positive Numeric Values)

γ

Yes

Calculate
F7 F8
P4

$$F7 = \frac{S1 \times 250350 \times (Y8 - 115{\cdot}5) \times 10^3}{160 \times I1}$$

$$F8 = \frac{(F4 - F3) \times (D1 - 115{\cdot}5)}{D1} + F3$$

$$P4 = \frac{F8}{2} - \sqrt{\left(\frac{F8}{2}\right)^2 + F7^2}$$

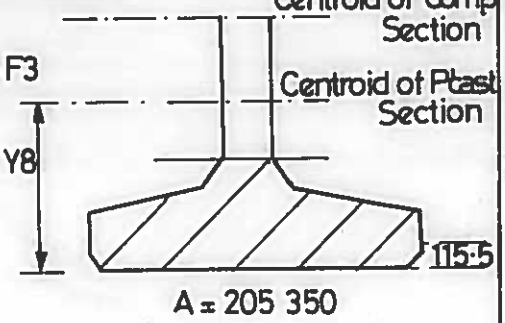

A = 205 350

P4 + ve or ABS P4 ≤ ABS P2

No

Output :
Principal Tensile Stress Exceeds Permissible at Junction of Web & Btm. Flange. Adopt a New Section
Principal Tensile Stress (N/mm²) = P4 } (Positive Numeric Values)
Permissible Tensile Stress (N/mm²) = P2 }

→ γ

Yes

Calculate
FΘ PΘ
P5

$$F\Theta = \frac{S1 \times A1 \times Y1 \times 10^3}{160 \times I1}$$

$$P\Theta = \frac{(F4 - F3) \times (D1 - Y2)}{D1} + F3$$

$$P5 = \frac{P\Theta}{2} - \sqrt{\left(\frac{P\Theta}{2}\right)^2 + F\Theta^2}$$

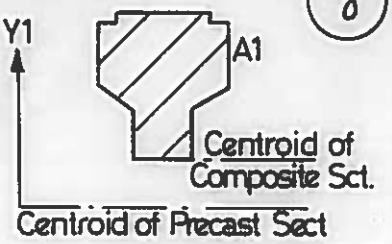

P5 + ve or ABS P5 ≤ ABS P2

No

Output :
Principal Tensile Stress Exceeds Permissible at Centroid of Precast Beam. Adopt a New Section
Principal Tensile Stress (N/mm²) = P5 } Positive Numeric Values
Permissible Tensile Stress (N/mm²) = P2 }

→ γ

Yes

Calculate
Q2 Q3
Q4 QΘ
R2 R1

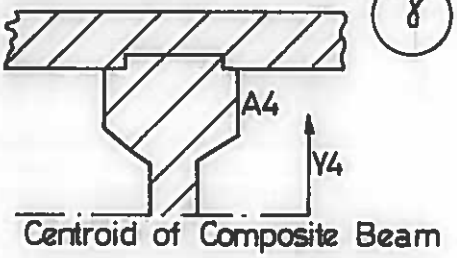

$$Q2 = \frac{I2 \times 160}{A4 \times Y4} \times \left(\sqrt{P2 \times (P2 - P\Theta)} - F\Theta\right) \times \frac{1}{10^3}$$

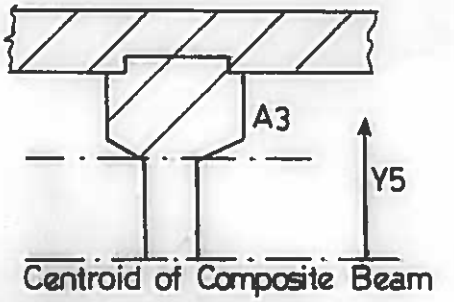

$$Q3 = \frac{I2 \times 160}{A3 \times Y5} \times \left(\sqrt{P2 \times (P2 - F6)} - F5\right) \times \frac{1}{10^3}$$

$$Q4 = (S1) + (\text{Lesser of } Q2, Q\Theta \text{ or } Q3)$$

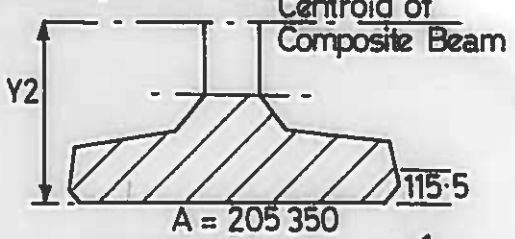

$$Q\Theta = \frac{I2 \times 160}{205\,350 \times (Y2 - 115{\cdot}5)} \times \left(\sqrt{P2 \times (P2 - F8)} - F7\right) \times \frac{1}{10^3}$$

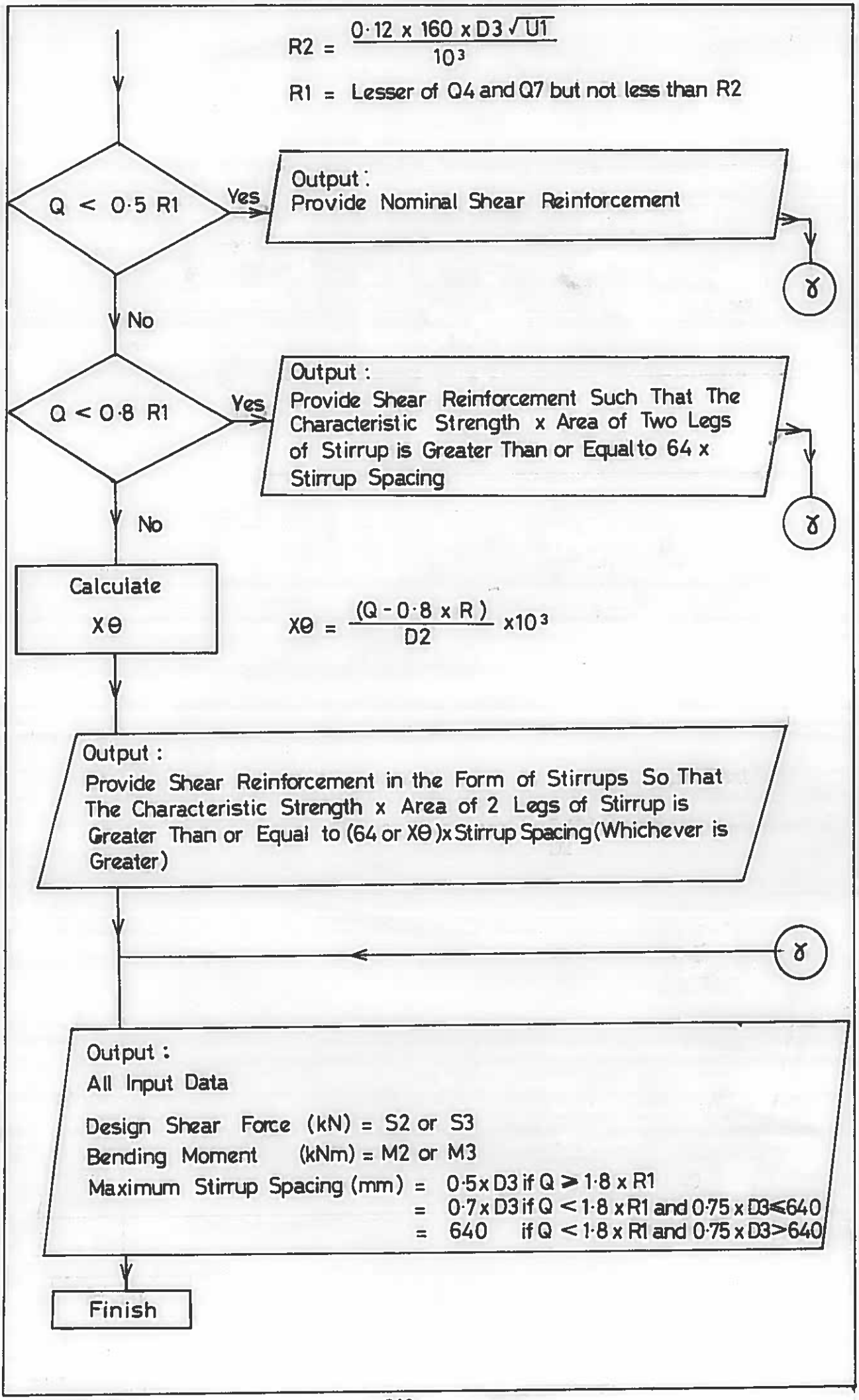
$R2 = \frac{0{\cdot}12 \times 160 \times D3\sqrt{U1}}{10^3}$
R1 = Lesser of Q4 and Q7 but not less than R2
Q < 0·5 R1
Yes
Output :
Provide Nominal Shear Reinforcement
γ
No
Q < 0·8 R1
Yes
Output :
Provide Shear Reinforcement Such That The Characteristic Strength x Area of Two Legs of Stirrup is Greater Than or Equal to 64 x Stirrup Spacing
γ
No
Calculate
XΘ
$X\Theta = \frac{(Q - 0{\cdot}8 \times R)}{D2} \times 10^3$
Output :
Provide Shear Reinforcement in the Form of Stirrups So That The Characteristic Strength x Area of 2 Legs of Stirrup is Greater Than or Equal to (64 or XΘ) x Stirrup Spacing (Whichever is Greater)
γ
Output :
All Input Data
Design Shear Force (kN) = S2 or S3
Bending Moment (kNm) = M2 or M3
Maximum Stirrup Spacing (mm) = 0·5 x D3 if Q ≥ 1·8 x R1
= 0·7 x D3 if Q < 1·8 x R1 and 0·75 x D3 ≤ 640
= 640 if Q < 1·8 x R1 and 0·75 x D3 > 640
Finish

LIST OF VARIABLES FOR PROGRAM 4

S1	=	Dead load shear force (self-weight + in situ concrete)	kN
S2	=	Live load shear force due to HA (including KE)	kN
S3	=	Live load shear force due to HB or two 112 kN wheels of HA or accidental wheel on footway or verge	kN
M1	=	Bending moment associated with S1	kNm
M2	=	Bending moment associated with S2	kNm
M3	=	Bending moment associated with S3	kNm
U1	=	28-day cube strength for precast beam	N/mm^2
Q9	=	The maximum shear force due to the loads prescribed in Clause 7 of BE1/73	kN
D2	=	Depth from the extreme compression fibre to the centroid of the bottom row of tendons	mm
Q8	=	$0.92 \times 160 \times D2 \times \sqrt{U1}/10^3$	kN
F2	=	Longitudinal stress at the centroid of the composite section due to loads supported solely by precast beam and prestressing force	N/mm^2
F1	=	Shear stress in the precast beam at the centroid of the precast section due to S1	N/mm^2
P1	=	Principal tensile stress at centroid of precast section due to F1 and F2	N/mm^2
P2	=	$0.294 \sqrt{U1}$	N/mm^2
F5	=	Shear stress in the precast beam at the junction of the web and top flange due to S1	N/mm^2
F6	=	Longitudinal stress in precast beam at the junction of the web and top flange due to loads supported solely by precast beam and prestressing force	N/mm^2

P3 = Principal stress at junction of web and top flange due to F5 and F6 N/mm^2

Q2 = Q2 (from BE2/73) kN

Q3 = Shear capacity of composite beam based on principal tensile stress at junction of web and top flange kN

Q4 = Qcw (from BE2/73) kN

D3 = The distance from the extreme compression fibre of the composite section to the centroid of all tendons (printed on output from beam design program) mm

Q5 = $0.045 \times 160 \times D3 \sqrt{U1}/10^3$ kN

M4 = 1.5 M1 + 2.5 M2 kNm

M5 = 2(M1 + M2) kNm

M6 = 1.5 M1 + 2 M3 kNm

S4 = 1.5 S1 + 2.5 S2 kN

S5 = 2(S1 + S2) kN

S6 = 1.5 S1 + 2 S3 kN

F9 = Bottom fibre compressive stress due solely to prestress after all losses (printed on output of beam design program) N/mm^2

Q6 = $\left[\frac{Q - S1}{M - M1}\right] M7$ kN

Q7 = Qcm (defined in BE1/73) kN

R2 = $0.12 \times 160 \times D3 \sqrt{U1}/10^3$ kN

R1 = Lesser of Q4 and Q7 and $\frac{1}{2}$ R2 kN

M7 = $(0.45\sqrt{U1} - M1 \times Y8 \times 10^6/I1 + F9) \times I2/Y2 \times 10^{-6}$ kNm

F3 = Top fibre beam stress due to self-weight + in situ concrete + prestress after all losses. (printed on output of beam design program) N/mm^2

F4 = Bottom fibre beam stress due to self-weight + in situ concrete + prestress after all losses (printed on output of beam design program) N/mm^2

Y9	=	Distance from soffit to junction of web and top flange	mm
F7	=	Shear stress in the precast beam at the junction of web and bottom flange due to S1	N/mm^2
F8	=	Longitudinal stress in precast beam at the junction of the web and bottom flange due to loads supported solely by precast beam and prestressing force	N/mm^2
P4	=	Principal stress due to F7 and F8	N/mm^2
Q0	=	Shear capacity of composite beam based on principal stress at junction of web and bottom flange	kN
F0	=	Shear stress at centroid of composite beam due to S1	N/mm^2
P0	=	Longitudinal stress at the centroid of the composite beam due to loads supported solely by precast beam and prestressing force	N/mm^2
P5	=	Principal stress at centroid of precast beam due to F0 and P0	N/mm^2
S9	=	Shear force due to superimposed dead load	kN
M9	=	Bending moment due to superimposed dead load	kN
B	=	Beam Size	
C1	=	Number of HA Cases	
C2	=	Number of HB Cases	
Z9	=	Greater of (S - 0.8 Q7) where S has values S4, S5 and S6	kN
Q	=	S4, S5 or S6 for which Z9 is a maximum	kN
X0	=	$(Q - 0.8\ R1)/D2 \times 10^3$	
I1	=	Second moment of area of precast beam	mm^4
I2	=	Second moment of area of composite beam	mm^4
A1	=	See flow chart	mm^2
A2	=	See flow chart	mm^2

A3	=	See flow chart	mm^2
A4	=	See flow chart	mm^2
A5	=	See flow chart	mm^2
D1	=	Centroid of precast beam from soffit	mm
Y1	=	See flow chart	mm
Y2	=	See flow chart	mm
Y3	=	See flow chart	mm
Y4	=	See flow chart	mm
Y6	=	See flow chart	mm
Y8	=	See flow chart	mm

5. Ultimate Moment of Resistance of Composite Section

Input :

Beam Size	= B
Bending Moments (kNm) due to	
(a) Beam Self-Weight	= A1
(b) Insitu Concrete	= A2
(c) Superimposed Dead Load	= A3
(d) HA Live Load Including K.E.L.	= A4
(e) HB Live Load or 2·112kN Wheels of H.A. or Accidental Wheel on Footway or Verge	= A5
Final Loss of Prestress	= L1%
Cross Sectional Area of Tendon (mm^2)	= AΘ
Initial Prestressing Force in each Tendon (kN)	= PΘ
28-Day Cube Strength of Precast Beam (N/mm^2)	= C1
28-Day Cube Strength of Insitu Slab (N/mm^2)	= C2
Nº of Layers of Tendons (Max 6)	= NΘ
Nº of Tendons in Each Layer	= N1, N2, ..., N6
Distance of Each Layer Above Soffit	= Y1, Y2, ..., Y6
Nº of Layers of H.Y.S. Compression Reinf. (Max. 2)	= N9
Nº of Bars in Each Layer	= N7, N8
Distance of Each Layer From Top Fibre	= Y7, Y8
Diameter of H.Y.S. Reinforcing Bar	= D9
Type of Strand (1 to 11)	= WΘ

↓

Read From Data Files 11 & 12 :
11: D , D2 , D1 , D4
12: EΘ

↓

Calculate
A6 A7
A8 A9
DΘ

$A6 = 1{\cdot}5(A1+A2+A3)+2{\cdot}5\times A4$ $\quad A7 = 2(A1+A2+A3+A4)$

$A8 = 1{\cdot}5(A1+A2+A3)+2\times A5$ $\quad A9 =$ Greater of A6, A7 or A8

$D\Theta = \frac{D}{2}$

↓

Calculate
F SΘ
S1 to S6
S7 to S8
E1 to E8

$F = \frac{P\Theta}{A\Theta} \times (1 - \frac{L1}{100}) \times 10^3$ $\quad S\Theta = \frac{F}{E\Theta}$

$S\eta = (D - Y\eta - D\Theta) \times 0{\cdot}0035 / (D\Theta + S\Theta)$ for η = 1 to 6

$S\eta = (D\Theta - Y\eta) \times 0{\cdot}0035 / D\Theta$ for η = 7 to 8

$E\eta$ the Prestressing Force, is Obtained From the Equation Representing the Idealised Load / Strain Curve for the Appropriate Tendon.

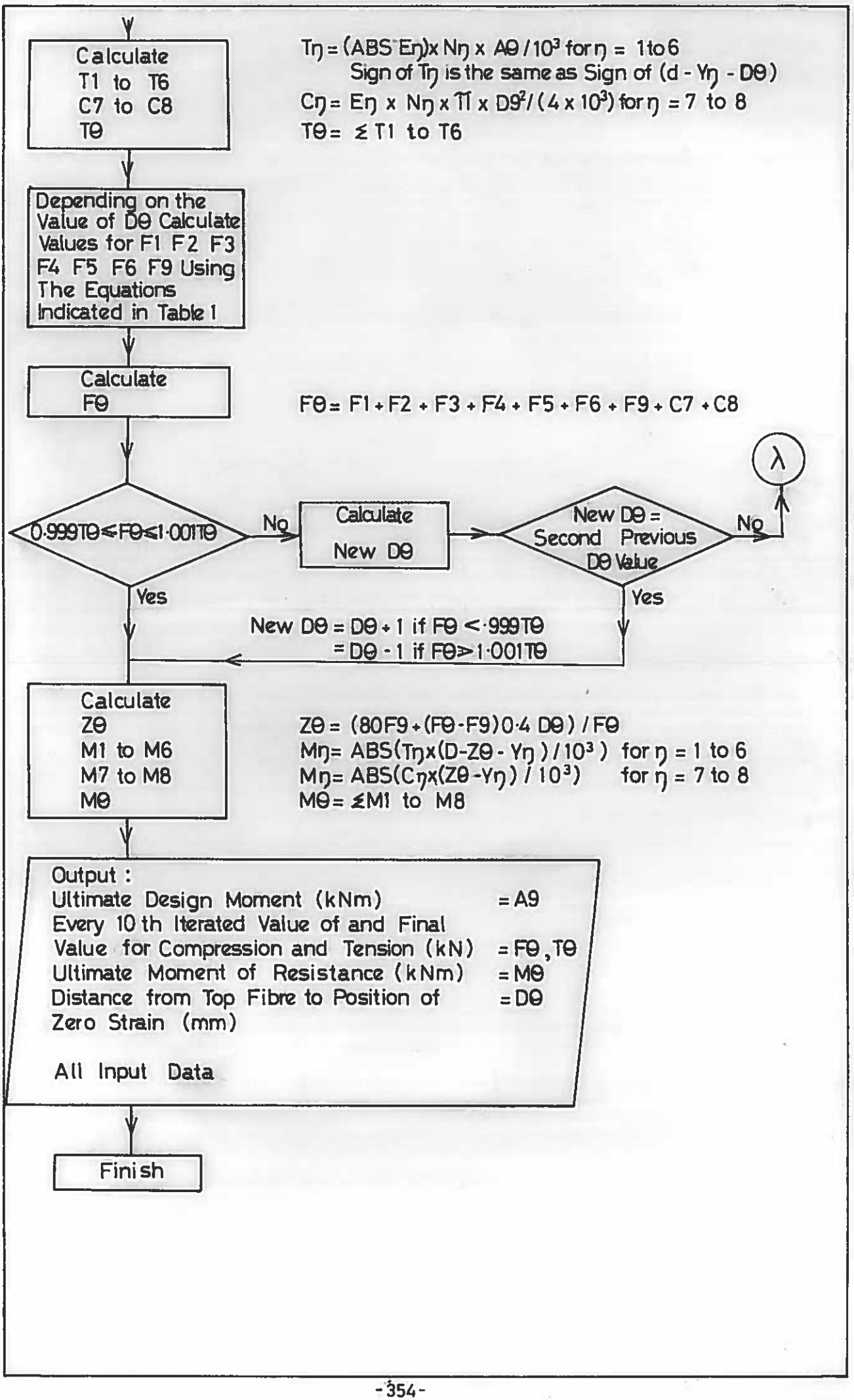
Calculate
T1 to T6
C7 to C8
TΘ
Tη = (ABS Eη)x Nη x AΘ / 10³ for η = 1 to 6
Sign of Tη is the same as Sign of (d - Yη - DΘ)
Cη = Eη x Nη x π x D9²/ (4 x 10³) for η = 7 to 8
TΘ = ≤ T1 to T6
Depending on the Value of DΘ Calculate Values for F1 F2 F3 F4 F5 F6 F9 Using The Equations Indicated in Table 1
Calculate
FΘ
FΘ = F1 + F2 + F3 + F4 + F5 + F6 + F9 + C7 + C8
λ
0·999TΘ≤FΘ≤1·001TΘ
No
Calculate
New DΘ
New DΘ = Second Previous DΘ Value
No
Yes
Yes
New DΘ = DΘ + 1 if FΘ < ·999TΘ
= DΘ - 1 if FΘ≥1·001TΘ
Calculate
ZΘ
M1 to M6
M7 to M8
MΘ
ZΘ = (80F9 + (FΘ - F9)0·4 DΘ) / FΘ
Mη = ABS(Tηx(D-ZΘ - Yη)/10³) for η = 1 to 6
Mη = ABS(Cηx(ZΘ -Yη) / 10³) for η = 7 to 8
MΘ = ≤M1 to M8
Output :
Ultimate Design Moment (kNm) = A9
Every 10 th Iterated Value of and Final Value for Compression and Tension (kN) = FΘ , TΘ
Ultimate Moment of Resistance (kNm) = MΘ
Distance from Top Fibre to Position of Zero Strain (mm) = DΘ
All Input Data
Finish

TABLE 1

	Value of DΘ										
	<130	130	B'ween 130 & 160	160	B'ween 160 & 175	175	B'ween 175 & D2	D2	B'ween D2 & D1	D1	>D1
F1=	1a	1b	1b	1b	1b	1b	1b	1b	1b	1b	1b
F2=	0	0	0	0	0	0	0	0	0	0	2a
F3=	0	0	0	0	0	0	0	0	3a	3b	3b
F4=	0	0	0	0	0	0	4a	4b	4b	4b	4b
F5=	0	0	5a	5b	5b	5b	5b	5b	5b	5b	5b
F6=	0	0	0	0	6a	6b	6b	6b	6b	6b	6b
F9=	9a	9a	9a	9b	9b	9b	9b	9b	9b	9b	9b

Equations Referred To –

1a = $300 \times D\Theta \times 0{\cdot}4 \times C2/10^3$
1b = $300 \times 130 \times 0{\cdot}4 \times C2/10^3$
2a = $160 \times (D\Theta - D1) \times 0{\cdot}4 \times C1/10^3$
3a = $(16800 - 160(D1 - D\Theta) - 2(D1 - D\Theta)^2) \times 0{\cdot}4 \times C1/10^3$
3b = $16800 \times 0{\cdot}4 \times C1/10^3$
4a = $400 \times (D\Theta - 175) \times 0{\cdot}4 \times C1/10^3$
4b = $400 \times D4 \times 0{\cdot}4 \times C1/10^3$
5a = $300 \times (D\Theta - 130) \times 0{\cdot}4 \times C1/10^3$
5b = $300 \times 30 \times 0{\cdot}4 \times C1/10^3$
6a = $300 \times (D\Theta - 160) \times 0{\cdot}4 \times C1/10^3$
6b = $300 \times 15 \times 0{\cdot}4 \times C1/10^3$
9a = $700 \times D\Theta \times 0{\cdot}4 \times C2/10^3$
9b = $700 \times 160 \times 0{\cdot}4 \times C2/10^3$

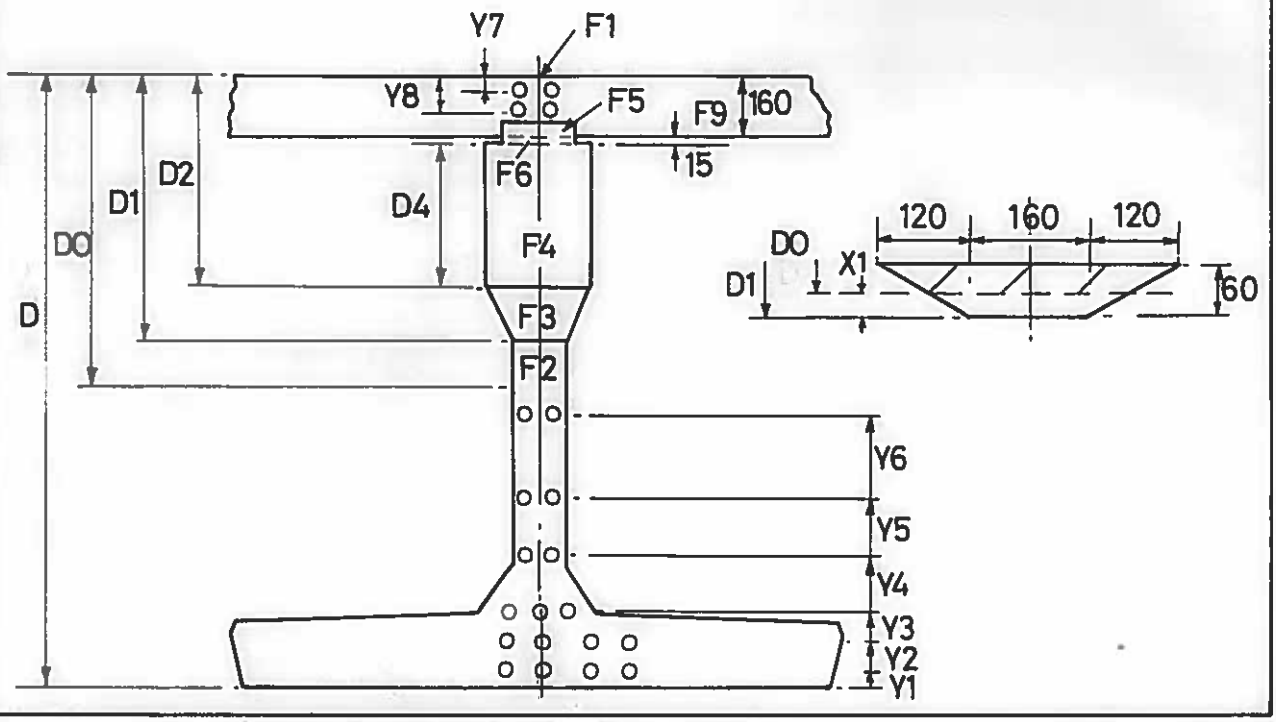

LIST OF VARIABLES FOR PROGRAM 5

B	= Beam size	
A1	= BM due to beam self-weight	kNm
A2	= BM due to in situ concrete	kNm
A3	= BM due to superimposed deadload	kNm
A4	= BM due to HA live load including KEL	kNm
A5	= BM due to HB live load or two 112 kN wheels of HA or accidental wheel on footway or verge	kNm
L1	= Final loss of prestress	%
A0	= Cross sectional area of tendon	mm^2
P0	= Initial prestressing force in each tension	kN
C1	= 28-day cube strength of precast beam	N/mm^2
C2	= 28-day cube strength of in situ slab	N/mm^2
N0	= Number of layers of tendons (max 6)	
Y1 to Y6	= Distance of each layer above beam soffit	mm
N1 to N6	= No of tendons in each layer	
N9	= No of layers of HYS compression reinforcement (max 2)	
N7 & N8	= No of bars in each layer	
Y7 & Y8	= Distance of each layer from top fibre	mm
D9	= Diameter of HYS reinforcing bars	mm
Wo	= Type of Strand (1 to 11) See handbook by Kirkpatrick (1979)	
A6	= 1.5 (A1 + A2 + A3) + 2.5 x A4	kNm
A7	= 2(A1 + A2 + A3 + A4)	kNm
A8	= 1.5 (A1 + A2 + A3) + 2 x A5	kNm
A9	= Greater of A6, A7 or A8	kNm
D	= Depth of composite beam	mm
D0	= Distance of line of zero strain from top fibre	mm

F	=	Final prestressing force in each tendon	kN
S0	=	Final strain in each tendon after prestress	
S1 to S6	=	Final strain in each tendon after prestress + bending	
S7 & S8	=	Final strain in each reinforcing bar due to bending	
E1 to E6	=	Factor to convert strain to stress for given strand type	
E7 & E8	=	Factor to convert strain to stress for given bar compression reinforcement	
T1 to T6	=	Final tension force in each layer of tendons	kN
C7 & C8	=	Final compression force in each layer of compression reinforcement	kN
T0	=	Total tension end load in beam	kN
F9	=	Compression force in area A9	kN
F1	=	Compression force in area A1	kN
F5	=	Compression force in area A5	kN
F6	=	Compression force in area A6	kN
F2	=	Compression force in area A2	kN
F3	=	Compression force in area A3	kN
F4	=	Compression force in area A4	kN
F0	=	Total compression end load in beam	kN
E0	=	Strain coefficient for prestressing strand	
Z0	=	Centroid of compression load from top fibre	mm
M1	=	Moment of T1 from Z0	kNm
M2	=	Moment of T2 from Z0	kNm
M3	=	Moment of T3 from Z0	kNm
M4	=	Moment of T4 from Z0	kNm
M5	=	Moment of T5 from Z0	kNm
M6	=	Moment of T6 from Z0	kNm

M7	=	Moment of C7 from Z0	kNm
M8	=	Moment of C8 from Z0	kNm
M0	=	Ultimate moment of resistance ΣM1 to M8	kNm
D1	=	See flow chart	mm
D2	=	See flow chart	mm
D4	=	See flow chart	mm

6. Test Loads For M-Beams-1

Input :

Beam Size	= B
Loss of Prestress at Time of Test	= L1 %
Cross Sectional Area of Tendon (mm^2)	= AΘ
Initial Prestressing Force in Each Tendon (kN)	= PΘ
28-Day Cube Strength of Precast Beam (N/mm)	= C1
Nº of Layers of Tendons (Max. 6)	= NΘ
Nº of Tendons in each Layer	= N1, N2, ..., N6
Distance Above Soffit of Each Layer (mm)	= Y1, Y2, ..., Y6
Type of Prestressing Strand	= WΘ
Effective Span	= L2

Read From Data Files 13 & 15 :
13: D, D1, D2, $\bar{Y}$, D4, D5, D6, D7, W9, ZB, A, I, ZT,
15: EΘ

Calculate VΘ DΘ

$$V\Theta = \frac{N1xY1 + N2xY2 + N3xY3 + N4xY4 + N5xY5 + N6xY6}{N1 + N2 + N3 + N4 + N5 + N6}$$

$$D\Theta = 0{\cdot}75\,D$$

Ψ

F SΘ
S1 to S6
E1 to E6
T1 to T6
TΘ

$$F\Theta = \frac{P\Theta}{A\Theta} \times \left(1 - \frac{L1}{100}\right) \times 10^3 \qquad S\Theta = \frac{F\Theta}{E\Theta}$$

$$S\eta = (D - Y\eta - D\Theta) \times \frac{0{\cdot}0035}{D\Theta} + S\Theta \text{ for } \eta = 1 \text{ to } 6$$

Eη, the prestressing force is obtained from the equation representing the idealised load / strain curve for the appropriate tendon

$$T\eta = (ABS\ E\eta) \times N\eta \times \frac{A\Theta}{10^3} \text{ for } \eta = 1 \text{ to } 6$$

$$T\Theta = \Sigma\, T1 \text{ to } T6$$

Depending on the Value of DΘ Calculate Values for F2, F3, F4, F5, F6, F7, F8 Using the Equations Indicated in Table 2

Calculate FΘ

$$F\Theta = F2 + F3 + F4 + F5 + F6 + F7 + F8$$

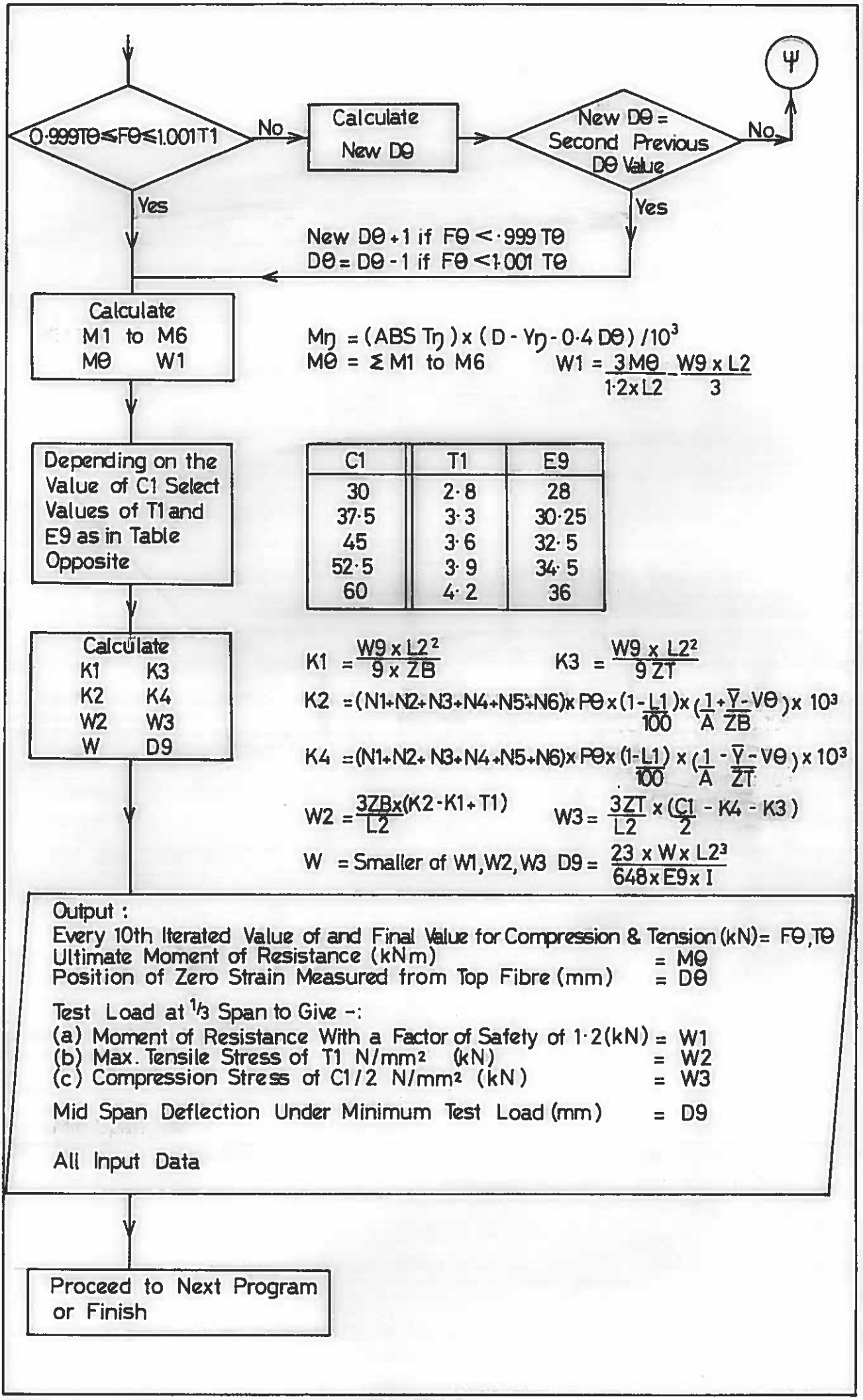
Ψ
0·999TΘ≤FΘ≤1.001T1
No
Calculate New DΘ
New DΘ = Second Previous DΘ Value
No
Yes
Yes
New DΘ + 1 if FΘ < ·999 TΘ
DΘ = DΘ - 1 if FΘ < 1·001 TΘ
Calculate M1 to M6 MΘ W1
Mη = (ABS Tη) x (D - Yη - 0·4 DΘ) /10³
MΘ = Σ M1 to M6
W1 = 3MΘ / 1·2xL2 - W9 x L2 / 3
Depending on the Value of C1 Select Values of T1 and E9 as in Table Opposite
C1 | T1 | E9
30 | 2·8 | 28
37·5 | 3·3 | 30·25
45 | 3·6 | 32·5
52·5 | 3·9 | 34·5
60 | 4·2 | 36
Calculate K1 K3 K2 K4 W2 W3 W D9
K1 = W9 x L2² / 9 x ZB
K3 = W9 x L2² / 9 ZT
K2 = (N1+N2+N3+N4+N5+N6) x PΘ x (1 - L1/100) x (1/A + Y̅ - VΘ / ZB) x 10³
K4 = (N1+N2+N3+N4+N5+N6) x PΘ x (1 - L1/100) x (1/A - Y̅ - VΘ / ZT) x 10³
W2 = 3ZB x (K2 - K1 + T1) / L2
W3 = 3ZT / L2 x (C1/2 - K4 - K3)
W = Smaller of W1, W2, W3
D9 = 23 x W x L2³ / 648 x E9 x I
Output :
Every 10th Iterated Value of and Final Value for Compression & Tension (kN) = FΘ, TΘ
Ultimate Moment of Resistance (kNm) = MΘ
Position of Zero Strain Measured from Top Fibre (mm) = DΘ
Test Load at 1/3 Span to Give -:
(a) Moment of Resistance With a Factor of Safety of 1·2 (kN) = W1
(b) Max. Tensile Stress of T1 N/mm² (kN) = W2
(c) Compression Stress of C1/2 N/mm² (kN) = W3
Mid Span Deflection Under Minimum Test Load (mm) = D9
All Input Data
Proceed to Next Program or Finish

TABLE 2

	Value of DΘ													
	B'ween 0 & 45	45	B'ween 45 & D2	D2	B'ween D2 & D1	D1	B'ween D1 & D5	D5	B'ween D5 & D6	D6	B'ween D6 & D7	D7	B'ween D7 & D	≥D
F2 =	0	0	0	0	0	0	2a	2b	2b	2b	2b	2b	2b	2b
F3 =	0	0	0	0	3a	3b	3b	3b	3b	3b	3b	3b	3b	3b
F4 =	0	0	4a	4b	4b	4b	4b	4b	4b	4b	4b	4b	4b	4b
F5 =	5a	5b	5b	5b	5b	5b	5b	5b	5b	5b	5b	5b	5b	5b
F6 =	0	0	0	0	0	0	0	0	6a	6b	6b	6b	6b	6b
F7 =	0	0	0	0	0	0	0	0	0	0	7a	7b	7b	7b
F8 =	0	0	0	0	0	0	0	0	0	0	0	0	8a	8b

Equations Referred To

$2a = 160 \times (D\Theta - D1) \times 0{\cdot}4 \times C1 / 10^3$
$2b = 160 \times (D5 - D1) \times 0{\cdot}4 \times C1 / 10^3$
$3a = (16800 - 160 \times (D1 - D\Theta) - 2 \times (D1 - D\Theta)^2) \times 0{\cdot}4 \times C1 / 10^3$
$3b = 16800 \times 0{\cdot}4 \times C1 / 10^3$
$4a = 400 \times (D\Theta - 45) \times 0{\cdot}4 \times C1 / 10^3$
$4b = 400 \times D4 \times 0{\cdot}4 \times C1 / 10^3$
$5a = 300 \times D\Theta \times 0{\cdot}4 \times C1 / 10^3$
$5b = 300 \times 45 \times 0{\cdot}4 \times C1 / 10^3$
$6a = (320 + 2 \times (D\Theta - D5)) \times (D\Theta - D5) \times 0{\cdot}4 \times C1 / (2 \times 10^3)$
$6b = 19200 \times 0{\cdot}4 \times C1 / 10^3$
$7a = (640 + 12{\cdot}6 \times (D\Theta - D6)) \times (D\Theta - D6) \times 0{\cdot}4 \times C1 / (2 \times 10^3)$
$7b = 31750 \times 0{\cdot}4 \times C1 / 10^3$
$8a = 960 \times (D\Theta - D7) \times 0{\cdot}4 \times C1 / 10^3$
$8b = 960 \times 160 \times 0{\cdot}4 \times C1 / 10^3$

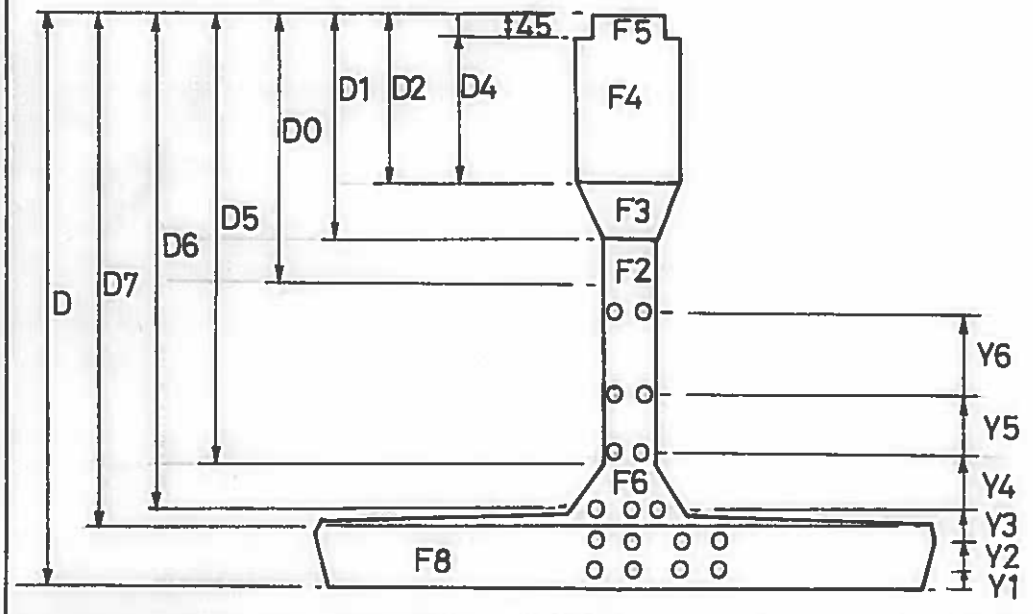

LIST OF VARIABLES FOR PROGRAM 6

B = Beam size		
L1 = Loss of prestress at time of test	%	
A0 = CSA of tendon	mm^2	
P0 = Initial prestressing force in each tendon	kN	
C1 = 28-day cube strength of precast beam	N/mm^2	
N0 = No of layers of tendons (max 6)		
N1 to N6 = No of tendons in each layer		
Y1 to Y6 = Distance of each layer above soffit	mm	
W0 = Type of prestressing strand 1 to 11 see handbook by Kirkpatrick (1979)		
L2 = Effective span	m	
V0 = Centroid of prestressing force above soffit	mm	
D0 = Plane of zero strain from top fibre	mm	
F = Stress in each tendon after losses	N/mm^2	
S0 = Strain in each tendon after losses		
S1 to S6 = Final strain in each layer of tendons due to bending + prestress at time of test		
E1 to E6 = Conversion factor for stress to give strain for a given type of strand W0		
T1 to T6 = Tension load in each layer of tendons	kN	
T0 = Total tension load in precast beam	kN	
F2 = Compression force in area A2	kN	
F3 = Compression force in area A3	kN	
F4 = Compression force in area A4	kN	
F5 = Compression force in area F5	kN	
F6 = Compression force in area F6	kN	

F7 = Compression force in area F7 kN

F8 = Compression force in area F8 kN

FO = Total compression force in precast beam kN

M1 to M6 = BM of each layer about centroid of compression forces (0.4 DO)

MO = Moment of resistance of precast beam kNm

W1 = Test loads at $\frac{1}{3}$ span to give MO with a FOS of 1.2 kN

K1 = Bottom fibre stress at $\frac{1}{3}$ span due to self-weight N/mm^2

K2 = Bottom fibre stress at $\frac{1}{3}$ span due to prestress after losses at time of test N/mm^2

W2 = Test loads at $\frac{1}{3}$ span to give tension stress T1 at bottom fibre kN

K3 = Top fibre stress at $\frac{1}{3}$ span due to self-weight N/mm^2

K4 = Top fibre stress at $\frac{1}{3}$ span due to prestress after losses at time of test N/mm^2

W3 = Test loads at $\frac{1}{3}$ span to give compression stress of C1/2 at top fibre kN

D9 = Deflection at midspan due to application of the smaller of W1, W2 or W3 mm

T1 = Permissible tensile stress in bottom fibre for given 28-day cube strength N/mm^2

W = Smaller of W1, W2 and W3 kN

E9 = Young's modulus N/mm^2

D = Depth of precast section mm

D1 = See flow chart mm

D2 = See flow chart mm

$\overline{Y}$ = Height of centroid above bottom fibre mm

D4 = See flow chart mm

D5	=	See flow chart	mm
D6	=	See flow chart	mm
D7	=	See flow chart	mm
W9	=	Self-weight	kN/m
A	=	C.S. area of precast section	mm^2
I	=	Second moment of area	mm^4
ZT	=	Section modulus - top fibre	mm^3
ZB	=	Section modulus - bottom fibre	mm^3
Eθ	=	Strain coefficient for prestressing strand	

7. Test Loads For M-Beams · 2

Shear Strength of Beams Under Test Loads

Input :

Beam Size	= B
Shear Force & Bending Moment (kN & kNm) Due to :	
(a) Self-Weight	= S1, M1
(b) Test Load	= S2, M2
Loss of Prestress at Time of Test	= L1 %
Initial Prestressing Force in Each Tendon	= PΘ
Nº of Effective Tendons	= N
Centroid of Tendons Above Beam Soffit (mm)	= EΘ
28-Day Cube Strength of Precast Beam (N/mm^2)	= C1

↓

Read From Data File 16 :
16 : D , A , ZB , $\bar{Y}$, I , ZT

↓

Calculate
S4 M4
S5 M5
S6 M6
Q9 Q5
F9 M7
T1 T2
T3 X

$S4 = 1{\cdot}5S1 \times 2{\cdot}5S2$ $\quad M4 = 1{\cdot}5\,M1 + 2{\cdot}5\,M2$

$S5 = 2x(S1 + S2)$ $\quad M5 = 2x(M1 + M2)$

$S6 = 1{\cdot}5\,S1 \times 2S2$ $\quad M6 = 1{\cdot}5\,M1 + 2M2$

Q9 = Greater of (Lesser of S4 or S5) or S6

$Q5 = 0{\cdot}045 \times 160 \times (D - E\Theta)\sqrt{C1}/10^3$

$F9 = 10^3 \times P\Theta \times N \times (1 - \frac{L1}{100}) \times (\frac{1}{A} + \frac{\bar{Y} - E\Theta}{ZB})$

$M7 = (0{\cdot}45\sqrt{C1} + F9) \times I/(\bar{Y} \times 10^6)$

$T1 = Q5 + S4 \times M7/M4$ $\quad T2 = Q5 + S5 \times M7/M5$

$T3 = Q5 + S6 \times M7/M6$ $\quad X = 0{\cdot}12 \times 160 \times (D - E\Theta)\sqrt{C1}/10^3$

↓

Compare Values of T1, T2, T3 With X ; Those Less than X Reset Equal To X

T1 = T1 or X Whichever is Greater
T2 = T2 or X Whichever is Greater
T3 = T3 or X Whichever is Greater

↓

Calculate
Z1 Z2
Z3

$Z1 = S4 - 0{\cdot}8T1$ $\quad Z2 = S5 - 0{\cdot}8T2$

$Z3 = S6 - 0{\cdot}8\,T3$

↓

Compare Values of Z1, Z2, Z3 and Select Q & Q7 Accordingly

Z1 Greatest : Q = S4 , Q7 = T1
Z2 Greatest : Q = S5 , Q7 = T2
Z3 Greatest : Q = S6 , Q7 = T3

↓

Calculate
Q8

$Q8 = 0{\cdot}92 \times 160 \times (D - 60)\sqrt{C1}/10^3$

↓

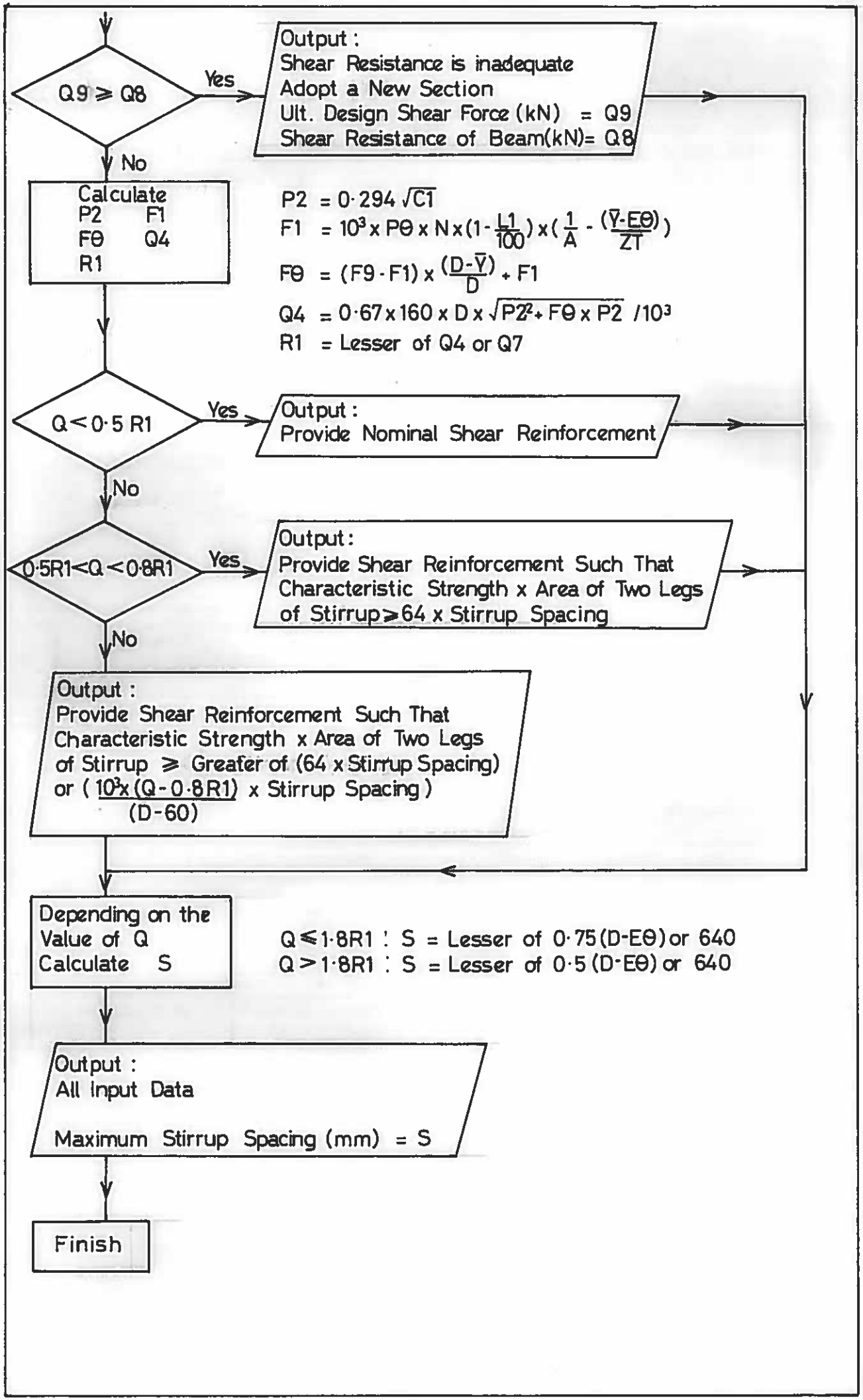
Q9 ≥ Q8
Yes
Output :
Shear Resistance is inadequate
Adopt a New Section
Ult. Design Shear Force (kN) = Q9
Shear Resistance of Beam(kN)= Q8
No
Calculate
P2 F1
FΘ Q4
R1
P2 = 0·294 √C1
F1 = 10³ x PΘ x N x (1 - L1/100) x (1/A - (Ȳ-EΘ)/ZT)
FΘ = (F9 - F1) x (D-Ȳ)/D + F1
Q4 = 0·67 x 160 x D x √(P2² + FΘ x P2) /10³
R1 = Lesser of Q4 or Q7
Q < 0·5 R1
Yes
Output :
Provide Nominal Shear Reinforcement
No
0·5R1 < Q < 0·8R1
Yes
Output :
Provide Shear Reinforcement Such That
Characteristic Strength x Area of Two Legs
of Stirrup ≥ 64 x Stirrup Spacing
No
Output :
Provide Shear Reinforcement Such That
Characteristic Strength x Area of Two Legs
of Stirrup ≥ Greater of (64 x Stirrup Spacing)
or (10³x (Q - 0·8R1) / (D-60) x Stirrup Spacing)
Depending on the
Value of Q
Calculate S
Q ≤ 1·8R1 : S = Lesser of 0·75 (D-EΘ) or 640
Q > 1·8R1 : S = Lesser of 0·5 (D-EΘ) or 640
Output :
All Input Data
Maximum Stirrup Spacing (mm) = S
Finish

LIST OF VARIABLES FOR PROGRAM 7

B	=	Beam size	
S1	=	Shear force due to self-weight	kN
M1	=	Bending moment due to self-weight	kNm
S2	=	Shear force due to test load	kN
M2	=	Bending moment due to test load	kNm
L1	=	Loss of prestress at time of test	%
PO	=	Initial prestressing force in each tendon	kN
N	=	No of effective tendons	
EO	=	Centroid of tendons above beam soffit	mm
C1	=	28-day cube strength of precast beam	N/mm^2
S4	=	1.5 x S1 + 2.5 x S2	kN
S5	=	2(S1 + S2)	kN
S6	=	1.5 x S1 + 2S2	kN
M4	=	1.5 x M1 + 2.5 M2	kNm
M5	=	2(M1 + M2)	kNm
M6	=	1.5 M1 + 2 M2	kNm
Q9	=	Greater of (lesser of S4 or S5) or S6	kN
Q5	=	$0.045 \times 160 (D-EO) \sqrt{C1} \times 10^{-3}$	kN
F9	=	Bottom fibre beam stress due to prestress after L1 losses	N/mm^2
M7	=	$(0.45 \sqrt{C1} + F9) I/\bar{Y} \times 10^{-6}$	kNm
D	=	Depth of precast section	mm
Q7	=	Q5 + Q6 (Qcm from BE2/73)	kN
A	=	C.S. area of precast section	mm^2
Q	=	S4, S5 or S6 for which ZO is a maximum	kN
Q8	=	$0.92 \times 160 (D-60) \sqrt{C1} \times 10^{-3}$	kN
P2	=	$0.294 \sqrt{C1}$	N/mm^2

F1	=	Top fibre beam stress due to prestress after L1 losses	N/mm^2
F0	=	Stress at centroid of beam due to prestress after L1 losses	N/mm^2
Q4	=	Q_{cm} (from BE2/73)	kN
R1	=	Lesser of Q4 and Q7	kN
S	=	Spacing of stirrups	mm
X	=	$0.12 \times 160 \times (D-E0) \sqrt{C1} \times 10^{-3}$	kN
T1	=	Q5 + S4 x M7/M4 or X whichever is greater	kN
T2	=	Q5 + S5 x M7/M5 or X whichever is greater	kN
T3	=	Q5 + S6 x M7/M6 or X whichever is greater	kN
Z1	=	S4 - 0.8 T1	kN
Z2	=	S5 - 0.8 T2	kN
Z3	=	S6 - 0.8 T3	kN
$\bar{Y}$	=	Height of centroid above bottom fibre	mm
I	=	Second moment of area	mm^4
ZT	=	Section modulus - top fibre	mm^3
ZB	=	Section modulus - bottom fibre	mm^3

DATA FILE 1

Beam Size	Depth D	Bot Fibre To Centroid	2nd Mom of area	Section Moduli ($x10^6$)			
				Top Fibre Composite	Top Fibre Precast	Bot Fibre Top Slab	Bot Fibre Precast
1	770	361	29.66	72.56	106.31	119.12	82.11
2	850	406	39.05	87.91	124.36	137.50	96.22
3	930	450	49.82	103.75	142.35	155.69	110.77
3-D	1010	493	62.06	120.13	160.53	174.03	125.76
5	1090	524	74.95	132.35	171.90	184.60	143.11
6	1170	572	90.96	152.12	194.36	207.67	159.01
6-D	1250	619	108.56	172.12	216.81	230.63	175.29
8	1330	642	124.55	181.02	223.21	235.89	194.02
9	1410	694	146.72	204.92	250.37	263.88	211.41
10	1490	745	170.49	228.77	277.23	291.44	228.93

DATA FILE 2

Beam Size	J2 ($x10^6$)
1	2159.38
2	2555.50
3	3344.74
3-D	4517.45
5	2883.58
6	3672.82
6-D	4844.80
8	3211.00
9	4000.24
10	5278.38

DATA FILE 3

Beam Size	Depth	Area A2	Bot Fibre To Centroid	2nd Mom of Area	Section Moduli		Self Wt.
					Top Fibre	Bot Fibre	
1	640	284650	220	10.38	24.72	47.17	7.11
2	720	316650	265	16.20	35.64	61.04	7.90
3	800	348650	310	23.02	46.96	74.31	8.70
3-D	880	380650	354	30.94	58.77	87.49	9.51
5	960	355050	357	35.81	59.39	100.33	8.87
6	1040	387050	409	47.56	75.39	116.23	9.66
6-D	1120	419050	459	60.45	91.51	131.59	10.48
8	1200	393450	454	65.19	87.39	143.57	9.82
9	1280	425450	512	82.98	108.09	161.96	10.61
10	1360	457450	568	101.88	128.65	179.36	11.42

DATA FILE 4

Beam Size	F4	D1	C1	2nd Mom of Area	C.S.A. Comp Grillage Beam	D
1	0.4387	465	30.186	30.525	514700	770
2	0.5761	545	40.427	40.648	546700	850
3	0.6678	625	46.996	52.365	578700	930
3-D	0.3242	705	58.152	63.514	553100	1010
5	0.4244	785	68.583	79.559	585100	1090
6	0.5017	865	75.831	97.278	617100	1170
6-D	0.2774	945	86.988	110.753	591500	1250
8	0.3547	1025	98.225	133.788	623500	1330
9	0.4187	1105	105.877	158.554	655500	1410
10	0.4731	1185	121.950	185.193	687500	1490

DATA FILE 5

Beam Size	D	A	$\bar{Y}$	2nd Mom of Area	ZT ($x10^4$)	ZB ($x10^4$)	Self Wt.
1	640	284650	220	1038	2472	4717	7.11
2	720	316650	265	1620	3564	6104	7.90
3	800	348650	310	2302	4696	7431	8.70
3-D	880	380650	354	3094	5877	8749	9.51
5	960	355050	357	3581	5939	10033	8.87
6	1040	387050	409	4756	7539	11623	9.66
6-D	1120	419050	459	6045	9151	13159	10.48
8	1200	393450	454	6519	8739	14357	9.82
9	1280	425450	512	8298	10809	16196	10.61
10	1360	457450	568	10188	12865	17936	11.42

DATA FILE 6

Beam Size	E6	Bot Fibre To Centroid	2nd Mom of Area	Z1 ($x10^4$)	Z2 ($x10^4$)	Z3 ($x10^4$)	Z4 ($x10^4$)
1	770	361	29.66	7256	10631	11912	8211
2	850	406	39.05	8791	12436	13750	9622
3	930	450	49.82	10375	14235	15569	11077
3-D	1010	493	62.06	12013	16053	17403	12576
5	1090	524	74.95	13235	17190	18460	14311
6	1170	572	90.96	15212	19436	20767	15901
6-D	1250	619	108.56	17212	21681	23063	17529
8	1330	642	124.56	18102	22321	23589	19402
9	1410	694	146.72	20492	25037	26388	21141
10	1490	745	170.49	22877	27723	29144	22893

DATA FILE 7

Beam Size	D1	D2	D3	D4
1	-0.185	-0.444	0.950	-0.28
2	-0.275	-0.488	0.894	-0.26
3	-0.334	-0.519	0.886	-0.27
3-D	-0.385	-0.550	0.817	-0.27
5	-0.371	-0.519	0.856	-0.22
6	-0.423	-0.557	0.808	-0.23
6-D	-0.471	-0.588	0.770	-0.24
8	-0.426	-0.540	0.830	-0.23
9	-0.495	-0.595	0.761	-0.21
10	-0.543	-0.629	0.718	-0.19

DATA FILE 8

Beam Size	$\overline{X}1$	$\overline{X}2$	$\overline{X}3$	$\overline{X}4$
1	-0.064	-0.039	0.185	-0.052
2	-0.073	-0.047	0.166	-0.048
3	-0.079	-0.053	0.152	-0.047
3-D	-0.083	-0,058	0.141	-0.044
5	-0.080	-0.058	0.152	-0.039
6	-0.086	-0.063	0.138	-0.036
6-D	-0.089	-0.067	0.127	-0.036
8	-0.091	-0.069	0.134	-0.029
9	-0.090	-0.070	0.126	-0.033
10	-0.093	-0.073	0.116	-0.032

DATA FILE 9

Beam Size	A1	A2	A3	A4	Y1	Y3
1	68940	48300	167300	187940	306	348
2	93740	80300	199300	212740	320	343
3	118700	112300	231300	237700	329	338
3-D	144300	144300	263300	263300	336	334
5	113260	80300	199300	232260	427	491
6	137580	112300	231300	256580	435	479
6-D	162060	144300	263300	281060	442	334
8	132780	80300	199300	251780	523	634
9	156460	112300	231300	275460	533	616
10	182700	148300	267300	301700	537	605

DATA FILE 9 (contd)

Beam Size	Y4	Y5	I1 ($x10^7$)	I2 ($x10^7$)	Y2	D2
1	272	297	1038	2966	361	710
2	285	302	1620	3905	406	790
3	297	305	2302	4982	450	870
3-D	307	310	3094	6206	493	950
5	378	424	3581	7495	524	1030
6	389	423	4756	9096	572	1110
6-D	398	421	6045	10855	619	1190
8	466	546	6519	12455	642	1270
9	476	541	8298	14672	694	1350
10	482	540	10188	17049	745	1430

Beam Size	D1	Y9	Y8
1	640	490	220
2	720	490	265
3	800	490	310
3-D	880	490	354
5	960	730	357
6	1040	730	409
6-D	1120	730	459
8	1200	970	454
9	1280	970	512
10	1360	970	568

DATA FILE 10

Beam Size	Y6	A5
1	248	91500
2	272	116300
3	288	141100
3-D	334	116780
5	361	139980
6	379	163660
6-D	415	140620
8	444	162860
9	466	185580
10	475	211020

DATA FILE 11

Beam Size	D	D1	D4	D2
1	770	280	45	220
2	850	360	125	300
3	930	440	205	380
3-D	1010	520	285	460
5	1090	360	125	300
6	1170	440	205	380
6-D	1250	520	285	460
8	1330	360	125	300
9	1410	440	205	380
10	1490	520	285	460

DATA FILE 12

Strand Type	Eθ
1	210325
2	202000
3	206248
4	203934
5	194597
6	193906
7	203066
8	196404
9	189521
10	185529
11	179598

DATA FILE 13

Beam Size	D	A	$\bar{Y}$	I ($\times 10^9$)	ZT ($\times 10^6$)	ZB ($\times 10^6$)
1	640	284650	220	10.38	24.72	47.17
2	720	316650	265	16.20	35.64	61.04
3	800	348650	310	23.02	46.96	74.31
3-D	880	380650	354	30.94	58.77	87.49
5	960	355050	357	35.81	59.39	100.33
6	1040	387050	409	47.56	75.39	116.23
6-D	1120	419050	459	60.45	91.51	131.58
8	1200	393450	454	65.19	87.39	143.57
9	1280	425450	512	82.98	108.09	161.96
10	1360	457450	568	101.88	128.65	179.36

DATA FILE 13 (Contd)

Beam Size	W9	D1	D4	D2	D5	D6	D7
1	7.11	150	45	90	350	430	480
2	7.90	230	125	170	430	510	560
3	8.69	310	205	250	510	570	640
3-D	9.52	390	285	330	590	670	720
5	8.87	230	125	170	670	750	800
6	9.66	310	205	250	750	830	880
6-D	10.48	390	285	330	830	910	960
8	9.82	230	125	170	910	990	1040
9	10.61	310	205	250	990	1070	1120
10	11.42	390	285	330	1070	1150	1200

DATA FILE 14

1	30.0	2.8	28.00
2	37.5	3.3	30.25
3	45.0	3.6	32.50
4	52.5	3.9	34.50
5	60.0	4.2	36.00

DATA FILE 15

Strand Type	Eθ
1	210325
2	202000
3	206248
4	203934
5	194597
6	193906
7	203066
8	196404
9	189521
10	185529
11	179598

DATA FILE 16

Beam Size	D	A	$\bar{Y}$	I ($\times 10^9$)	ZT ($\times 10^6$)	ZB ($\times 10^6$)
1	640	284650	220	10.38	24.72	47.17
2	720	316650	265	16.20	35.64	61.04
3	800	348650	310	23.02	46.96	74.31
3-D	880	380650	354	30.94	58.77	87.49
5	960	355050	357	35.81	59.39	100.33
6	1040	387050	409	47.56	75.39	116.23
6-D	1120	419050	459	60.45	91.51	131.58
8	1200	393450	454	65.19	87.39	143.57
9	1280	425450	512	82.98	108.09	161.96
10	1360	457450	568	101.88	128.65	179.36

APPENDIX D

CALCULATION OF PROTOTYPE SLAB REINFORCEMENT

For HA loading consider the 2 No 112.5 kN wheel loads at 0.9 m centres. (Fig. D1).

For the Westergaard Eqns:-

Contact Pressure = $1.4\ N/mm^2$

Area = $\frac{112.5 \times 10^3}{1.4}$

= $80 \times 10^3\ mm^2$

Equivalent diameter = $\sqrt{\frac{4 \times 80 \times 10^3}{\pi}}$

= 320 mm

Equivalent diameter = 320 + 2t

With 100 mm of surfacing

(Fig. D1) = 320 + 200

= 520 mm

Ref. Fig. D2

Maximum moment occurs under P_1 when $v = \frac{a}{4}$

$$Mx = Mox + 0.21072\ P_1 \log \left[\frac{\text{Cot } \frac{\pi a}{4S}}{2}\right]$$

and $$Mox = 0.21072\ P\ (\log \frac{S}{Cl} + 0.48253)$$

$$Cl = 2 \left[\sqrt{0.4C^2 + h^2} - 0.675\ h\right]$$

where h = 160

and C is the lesser of 3.45 h or 520.

$\therefore$ C = 520

$$Cl = 2 \left[\sqrt{0.4 \times 520^2 + 160^2} - 0.675\ h\right]$$

Cl = 514 mm

$$\therefore \text{Mox} = 0.21072\ P\ \left(\log \frac{2000}{514} + 0.48253\right)$$

$$= 0.21072\ P\ (\log 3.89 + 0.48253)$$

$$= 0.21072\ P\ (0.5899 + 0.48253)$$

$$= 0.2259\ P$$

Consider the second part of the equation for Mx.

$$= 0.21072\ P \log \left[\frac{\text{Cot } \frac{\pi a}{4S}}{2}\right]$$

$$= 0.21072\ P \log \left[\frac{\text{Cot } \frac{\pi \times 900}{4 \times 2000}}{2}\right]$$

$$= 0.21072\ P \log \left[\frac{1}{2\ \text{Tan } 0.3534}\right]$$

$$= 0.21072\ P \log 1.355$$

$$= 0.0278\ P$$

Correction for built-in support

$$= -0.0699\ P$$

$$\therefore M_x = (0.2259 + 0.0278 - 0.0699)\ P$$

$$= 0.1838\ P$$

With P = 112.5 kN

M_x = 20.58 kNm

Steel reinforcement with 30 mm cover

$$R = \frac{M}{bd_1^2}$$

$$= \frac{20.58 \times 10^6}{1000 \times 120^2}$$

$$= 1.43$$

f_s = 230 N/mm^2

r = 0.007 (from design chart)

A_s = 0.007 x 1000 x 120

= 840 mm^2/m

Use 20 mm dia. bars at 150 mm pitch.

$\therefore A_s = 2090$

$$\text{actual } r = \frac{2090}{1000 \times 120}$$

$$= 0.174$$

From the design chart

$f_c = 6.8 \text{ N/mm}^2$

$f_s = 100 \text{ N/mm}^2$

Check crack width.

$$\frac{d_1}{d_2} = \frac{120}{40}$$

$$= 3.0$$

Reduction factor

$$= 0.6$$

From tables the steel stress to give a crack width of 0.25 mm

$$= 0.6 \times 200$$

$$= 120 \text{ N/mm}^2$$

Applied steel stress

$$= 100 \text{ N/mm}^2$$

The following steel arrangements will be incorporated into the bridge deck for test purposes.

20 mm dia. at 150 mm pitch

16 mm dia. at 150 mm pitch

12 mm dia. at 150 mm pitch

8 mm dia. at 150 mm pitch

This will give approximate steel ratios of 1.7%, 1.10%, 0.60% and 0.25% which is comparable with that provided in the model.

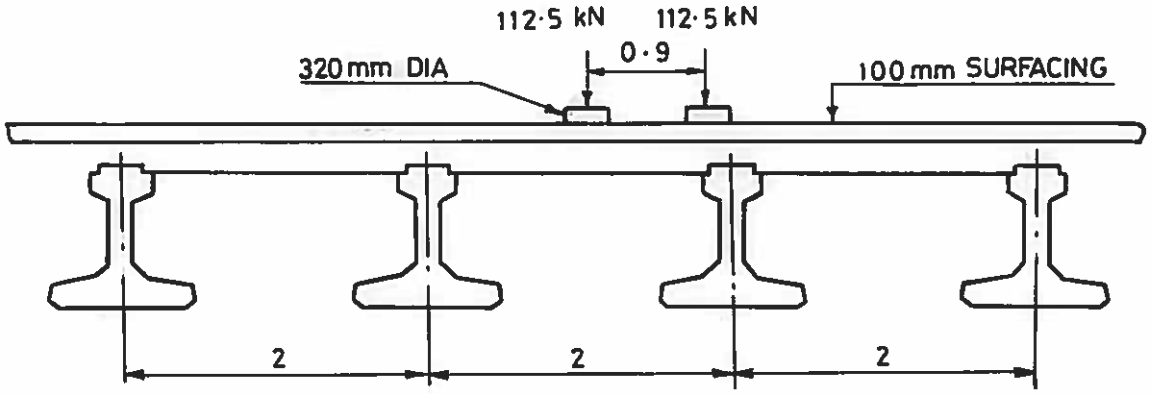

Fig. D1 2 Nº 112·5kN H.A. Wheel Loads

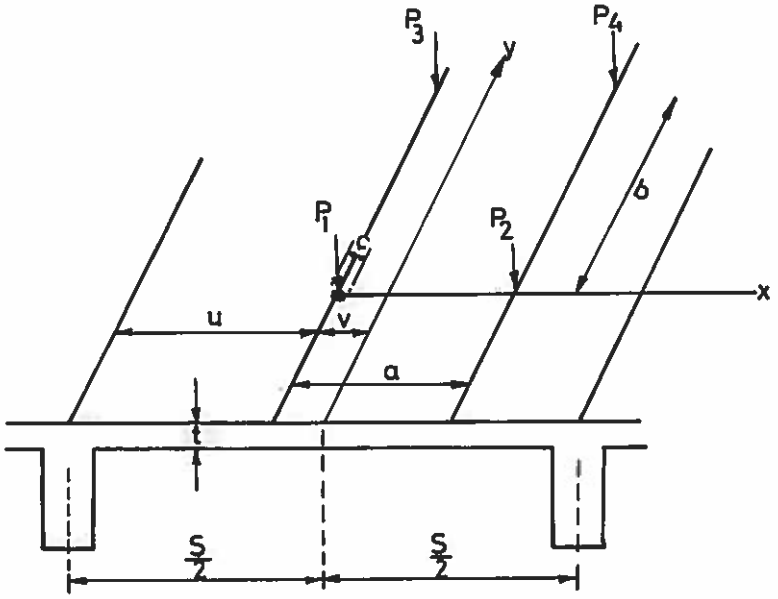

Fig. D2 Westergaard's Notation

Fig. D1
Fig. D2

APPENDIX E

DESIGN OF MODEL BEAMS

REQUIREMENTS

1. Should have a stiffness of approximately $\frac{1}{27}$ of the prototype.
2. Capable of carrying a live load of 50 kN at midspan.
3. Top flange should be $\frac{400}{3}$ = 133 mm

   I of M3 beam = 23×10^9 mm^4

LIST OF SYMBOLS

A_{st} = Area of tensile reinforcement

p_{st} = Permissible tensile stress in the reinforcement

p_{cb} = Permissible compressive stress in the concrete in bending

b_r = breadth of the beam

d_1 = the effective depth to the tensile reinforcement

d_s = depth of the slab

d = depth of the beam

I = Second moment of area of beam

b_1 = effective width of slab

l_a = lever arm to centre of slab

M = applied bending moment

M_r = moment of resistance

γ = moment of resistance factor

C = second moment of area factor

D = overall depth of beam and slab

$$\text{Required I of model} = \frac{23 \times 10^9}{27}$$

$$= 0.85 \times 10^9 \text{ mm}^4$$

$$I = \frac{bd^3}{12}$$

$$\therefore \text{ depth of beam d required} = \sqrt{\frac{12 \times 0.85 \times 10^9}{133}}$$

$$d = 425 \text{ mm}$$

Design Bending Moments

Self-Wt $w = (0.425 \times 0.133 + 0.583 \times 0.053) \frac{25}{10^6}$

$= 2.19$ kN/m

$M = \frac{2.19 \times 4.67^2}{8}$

$= 5.97$ kNm

Live Load $M = \frac{50 \times 4.67}{4}$

$= 58.4$ kNm

Total BM $= 5.97 + 58.4$

$=$ approx. 65 kNm

The 133 x 425 mm beam will be composite with the slab and designed as a reinforced concrete tee beam to CP114 using the load factor method.

Effective width of slab (Fig. E1)

the lesser of:-

a. Centres of beams = 583 mm

b. Effective span /3 = 1560 mm

c. $b + 12\, d_s$ $= 133 + 12 \times 53$

$= 769$ mm

$\therefore b_1 = 583$ mm

Ref. Fig. E1

$l_a = 425 + \frac{53}{2} - 30$

$= 421.5$ mm

$M = A_{st} \cdot l_a \cdot p_{st}$

$\therefore A_{st} = \frac{65 \times 10^6}{421.5 \times 230}$

$= 670$ mm^2

2 No bars 20 mm dia = 628 mm^2

2 No bars 25 mm dia = 982 mm^2

$\therefore$ Use 2 No 25 dia. bars.

Moment of resistance

a. Based on concrete strength of tee beam

$$M_r = \gamma \cdot p_{cb} \cdot b \cdot d_1^2$$

$$\frac{b_1}{b} = \frac{583}{133} = 4.38$$

$$\frac{d_1}{d_s} = \frac{421.5}{53} = 7.95$$

$$\therefore \quad \gamma = 0.11$$

$$M_r = 0.11 \times 13 \times 583 \times 421.5^2 \times 10^{-6}$$

$$= 148 \text{ kNm}$$

b. Beam alone based on concrete strength (Fig. E2)

$$M_r = \frac{p_{cb} \cdot b \cdot d_1^2}{4}$$

$$= \frac{13 \times 133 \times 395^2}{4}$$

$$= 67.5 \text{ kNm}$$

c. Beam alone based on the strength of the steel

$$M_r = A_{st} \cdot p_{st} \cdot l_a$$

$$l_a = d_1 - \frac{3 A_{st} \cdot p_{st}}{4b \cdot p_{cb}}$$

$$= 395 - \frac{3 \times 982 \times 230}{4 \times 133 \times 13}$$

$$= 395 - 98$$

$$= 297 \text{ mm}$$

$$M_r = \frac{982 \times 230 \times 297}{106}$$

$$= 67 \text{ kNm}$$

Second moment of area of tee beam

$$I = C\, b_r\, D^3$$

$$\frac{b_r}{b} = \frac{133}{583} = 0.228$$

$$\frac{d_s}{D} = \frac{53}{478} = 0.11$$

$\therefore$ C = 0.137

$$I = 0.137 \times 133 \times 478^3$$

$$= 1.99 \times 10^9 \text{ mm}^4$$

For the M3 beam composite with 1.75 m of slab

$$I = 64 \times 10^9 \text{ mm}^4$$

$\therefore$ I required for model

$$= \frac{64 \times 10^9}{27}$$

$$= 2.3 \times 10^9 \text{ mm}^4$$

This is a reasonable representation.

The various second moment of areas are summarised in Table E1.

	I_p	$I_p/27$	I_m
Beam	23×10^9	0.85×10^9	0.85×10^9
Beam and slab	23×10^9	2.37×10^9	1.99×10^9

Table E1. - Summary of Second Moments of Area - mm^4

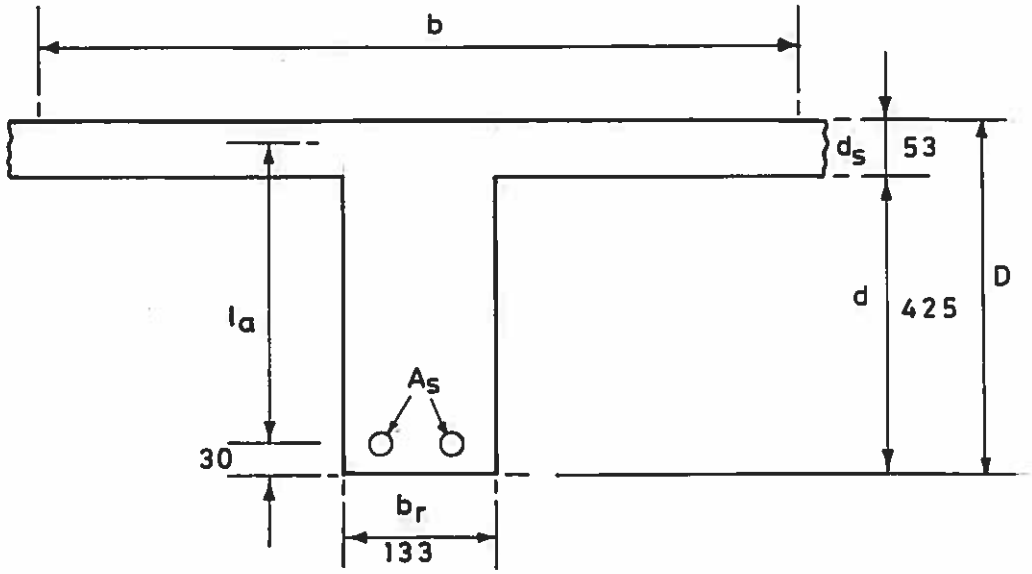

Fig. E1 Design Of Tee Beam

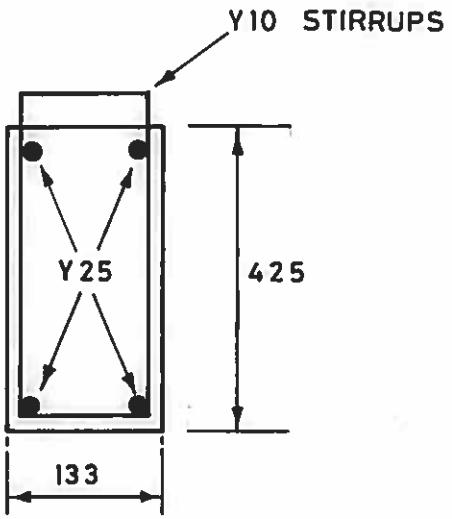

Fig. E2 Final Beam Design

Fig.E1
FigE2

APPENDIX F

COMPRESSIVE MEMBRANE ACTION IN RESTRAINED BRIDGE SLABS

This appendix provides details of the method proposed by Rankin (1982) to establish the relationship between the maximum arching moment M_{ar}, the span to depth ratio and the concrete strength. The geometry of deformation of a laterally restrained, unreinforced strip has been considered by McDowell, McKee and Sevin (1956) in relation to the arching behaviour of masonary walls. This idealised two-dimensional mode of action is shown in Fig. F.1.

Having eatablished the mode of deformation, some knowledge of the material characteristics was required and this was assumed to be of the classical elastic-plastic form as shown in Fig. F.2. The relationship between ε_c and f'_c was based on the ACI equivalent stress block coefficients. A curve of this form is shown in Fig. F.3 and may be expressed analytically as:-

$$\varepsilon_c = (-1188 + 96f'_c - 0.796f'^2_c)10^{-6} \qquad \text{(Eqn.1)}$$

From a knowledge of the slab deformation and the material stress-strain relationship the maximum arching moment of resistance was found in terms of the midspan deflection and the non-dimensional parameters R and M_r.

where

$$R = \frac{\varepsilon_c L^2}{4h^2} \qquad \text{(Eqn.2)}$$

and

$$M_r = \frac{4M_{ar}}{0.85f'_c(h/2)^2} \qquad \text{(Eqn.3)}$$

For bridge slabs R is usually less than 0.25 which represents a state of plastic strain. The relationship between R and M_r which results in the maximum arching resistance is shown in Fig. F.4 and may be expressed analytically as:-

$$M_r = 4.3 - 16.1\sqrt{(0.00033 + 0.1243R)} \qquad \text{(Eqn.4)}$$

The maximum arching moment M_{ar} is therefore:-

$$M_{ar} = M_r \frac{0.85f'_c(h/2)^2}{4}$$

$$= k\, f'_c\, h^2$$

$$\text{where } k = \frac{0.21}{4} M_r \qquad \text{(Eqn.5)}$$

For a rigid/plastic material R = 0 and $M_r = 4$. Therefore

$$M_{ar(max)} = 0.21 f'_c h^2 \qquad \text{(Eqn.6)}$$

Figure 9.8 shows curves of $k\, f'_c\, h^2$ plotted against f'_c and L/h and was derived by taking constant values of k and calculating M_r from equation (5). The value of R was then evaluated from equation (4), ε_c from equation (1) and L/h from equation (2).

Having established M_{ar} the equivalent reinforcement ρ_e was calculated as follows:-

$$M_{ar} = A_s.f_y.\text{lever arm}$$

$$A_s = \rho_e.d/\text{unit width of slab}$$

$$\text{lever arm} = 0.75d \text{ (approximately)}$$

$$\therefore \quad k f'_c h^2 = \rho_e.d.f_y.0.75d$$

$$\text{and} \quad \rho_e = \frac{k f'_c h^2}{f_y.0.75d^2}$$

as the original equation proposed by Long (1975) was based on tests having a fairly narrow range of yield strengths, f_y can be assumed to be 320 N/mm^2.

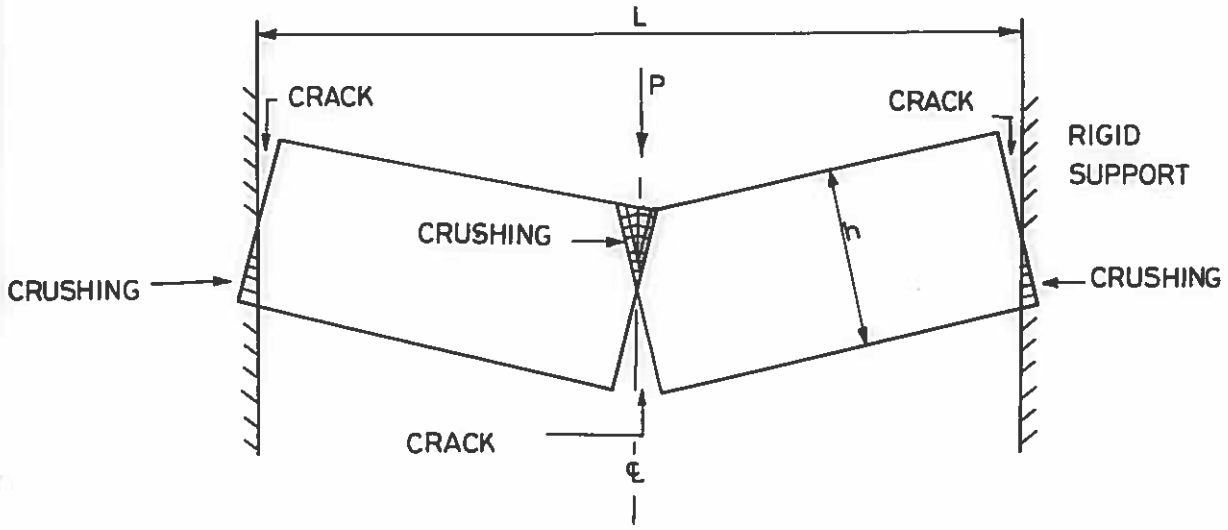

Fig. F1 Idealised Mode of Action

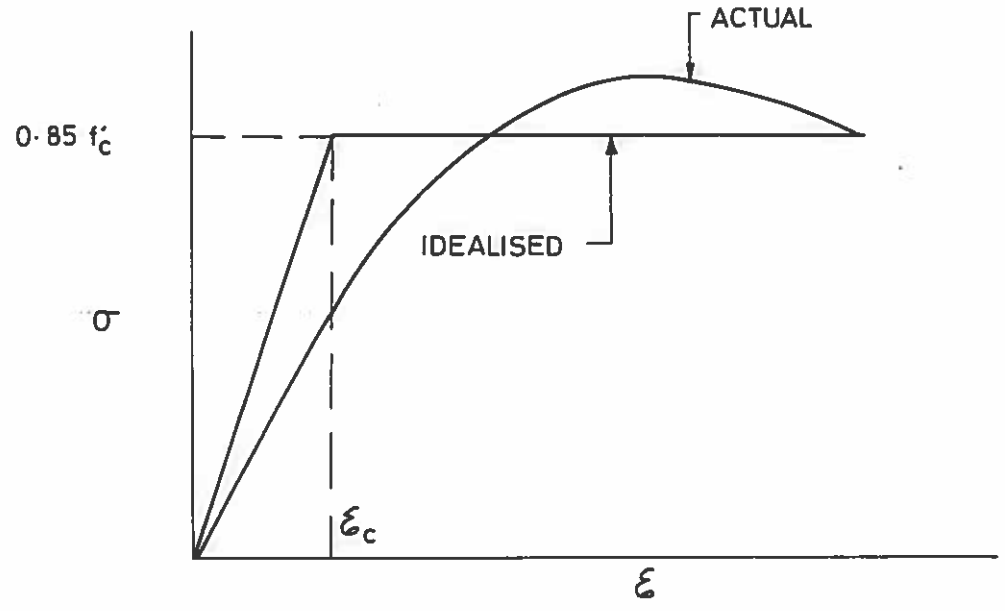

Fig. F2 Idealised Stress - Strain Relationship

Fig. F1
Fig. F2

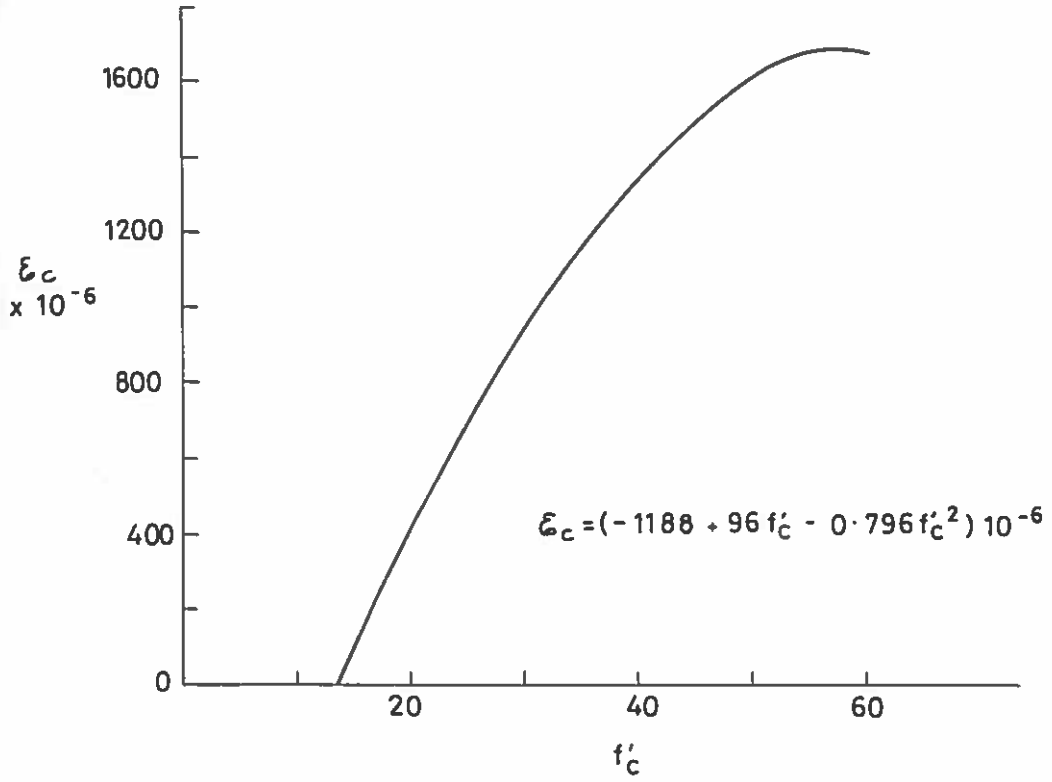

Fig. F3 Idealised Plastic Strain Relationship

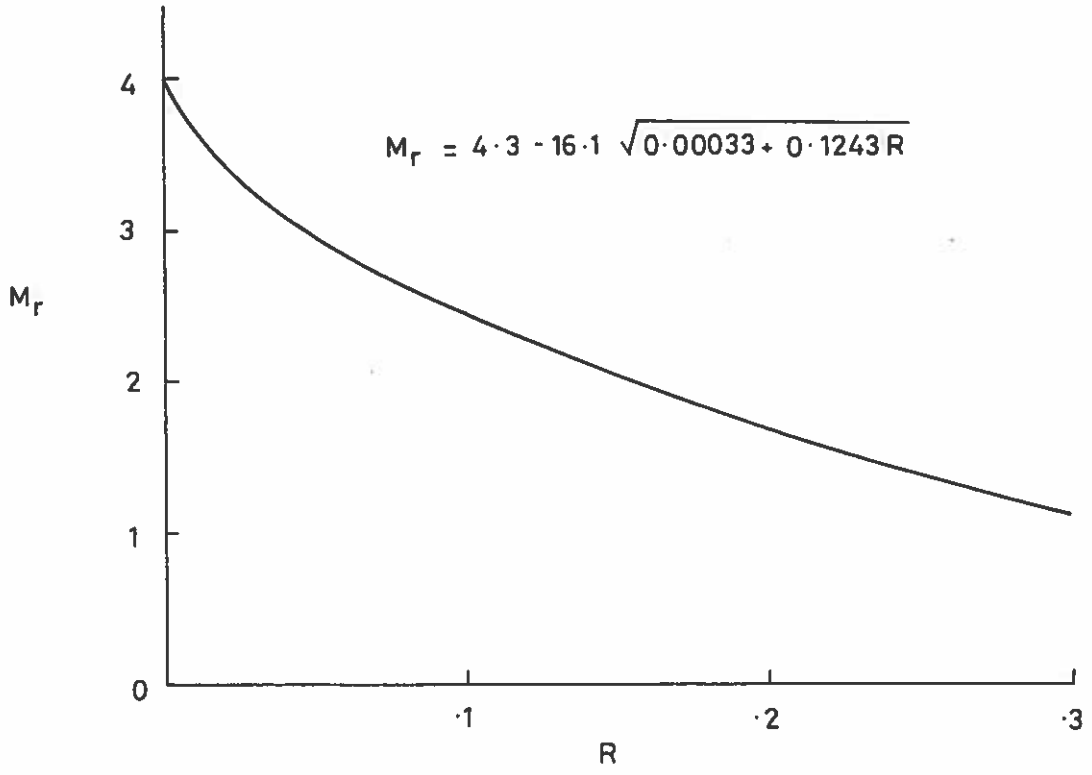

Fig. F4 Variation of Arching Moment Ratio

Fig F3
Fig F4

BIBLIOGRAPHY

ACI COMMITTEE 318 (1977), "Building Code Requirements for Structural Concrete", American Concrete Institute, Detroit, 1977, 102 pp.

AMERICAN ASSOCIATION OF STATE HIGHWAY AND TRANSPORTATION OFFICIALS, (1973), "Standard Specification for Highway Bridges", Eleventh Edition, Washington, D.C., 1973.

AMERICAN ASSOCIATION OF STATE HIGHWAY AND TRANSPORTATION OFFICIALS, (1977), "Standard Specifications for Highway Bridges", Twelth Edition, Washington, D.C., 1977.

AOKI, Y., and SEKI, H., (1971), "Shearing Strength and Flexural Cracking and Capacity of Two-way Slabs Subjected to Concentrated Load", American Concrete Institute, Publication SP-30, 1971, pp 103-126.

BAKHT, B., and CSAGOLY, P., (1977), "Testing of Perley Bridge", Ministry of Transportation and Communications, Ontario, Research Report, RR207, 1977, pp 64.

BAREŠ, R., and MASSONNET, C., (1968), "Analysis of Beam Grids and Orthotropic Plates by the Guyon-Massonnet-Bares method", Crosby Lockwood, London 1968, pp. 459.

BATCHELOR, B. de V., HEWITT, B.E., CSAGOLY, P., and HOLOWKA, M., (1978), "Investigation of the Ultimate Strength of Deck Slabs of Composite Steel/Concrete Bridges", Transportation Research Record 664, National Academy of Sciences, Washington D.C. (1978), pp 161-170.

BATCHELOR, B. deV., HEWITT, B.E., and CSAGOLY, P., (1978), "An Investigation of the Fatigue Strength of Deck Slabs of Composite Steel/Concrete Bridges", Transportation Research Record 664, National Academy of Sciences, Washington, D.C., 1978, pp 153-161.

BATCHELOR, B. deV., and TISSINGTON, I.R., (1976), "Shear Strength of Two-Way Bridge Slabs", Journal of the Structural Division, ASCE, Dec. 1976, ST12, pp 2315-2331.

BEEBY, A.W., (1979), "The Prediction of Crack Widths in Hardened Concrete", The Structural Engineer, 57A, No. 1, January 1979, pp 9-17.

BEST, B.C., and ROWE, R.E., (1959), "Abnormal Loading on Composite Slab Bridges", Cement and Concrete Association, London, Research Report No. 7, October 1959, pp 28.

BROTCHIE, J.F., and HOLLEY, M.J. (1971), "Membrane Action in Slabs", American Concrete Institute, Publication SP-30, 1971, pp 345-377.

BS 5400 (1978), "Steel, Concrete and Composite Bridges", British Standards Institution, London, 1978.

C.S.A. STANDARD S6, (1974), "Specification for the Design of Highway Bridges", Canadian Standards Association, Ontario, 1974.

CEMENT AND CONCRETE ASSOCIATION, (1971), "An Interim Report of Tests on a Quarter Scale Model of a Composite Precast Concrete Bridge Deck", Cement and Concrete Association, London 1971, (Unpublished).

CHRISTIANSEN, K.P.,(1963), "The Effect of Membrane Stresses on the Ultimate Strength of the Interior Panel in a Reinforced Concrete Slab", The Structural Engineer, London, V. 41, No. 8, Aug. 1963, pp 261-265.

CLARK, L.A., and WEST, R., (1973), "Bibliography of Experimental Work on Slabs and Pseudo-Slab Bridges", Cement and Concrete Association, London, 1973, pp 57.

CLARK, L.A., (1973), "Flexural Cracking in Slab Bridges", Technical Report 42.479, Cement and Concrete Association, London, May 1973, pp 12.

CLARK, L.A., (1974), "Flexural Crack Simulate in Slabs Spanning One Way", Technical Report 42.496, Cement and Concrete Association, London, October 1974, pp 25.

CLARK, L.A., (1975), "Comparisons of Various Methods of Calculating the Torsional Inertia of Right Voided Slab Bridges", The Cement and Concrete Association, London, 1975, Technical Report 508, pp 34.

CLARK, L.A., and ELLIOT, G., (1981), "Crack Control in Concrete Bridges", The Structural Engineer, 58A, No. 5, May 1980, pp 157-162.

COUSINS, W.T.E., (1978), "Load Test on Shaw's Bridge", Department of the Environment (NI) Roads Service, Internal Report, 1978.

CP 114,(1969), "The Structural Use of Reinforced Concrete in Buildings", British Standards Institution, London, 1969.

CP115,(1969), "The Structural Use of Prestressed Concrete in Buildings", British Standards Institution, London, 1969.

CP116,(1969), "The Structural Use of Precast Concrete", British Standards Institution, London, 1969.

CRAEMER, H., (1954), "Load Distributing Effect of a Plate Upon Beams", Civil Eng., and Public Works Review, Vol. 49, No. 575, 1954, pp 510-513.

CSAGOLY, P., HOLOWKA, M., and DORTON, R.,(1978), "The True Behaviour of Thin Concrete Bridge Slabs", Transportation Research Record 664, National Academy of Sciences, Washington, D.C. (1978), pp 171-179.

CSAGOLY, P., (1979), "Design of Thin Concrete Deck Slabs by the Ontario Highway Bridge Design Code", Ministry of Transportation and Communications, Ontario, SRR-79-11. 1979, pp 26 + Figs.

CUSENS, A.R., and PAMA, R.P., (1969), "Distribution of Concentrated Loads on Orthotropic Bridge Decks", The Structural Engineer, Vol. 47, No. 9, Sept. 1969, pp 377-385.

CUSENS, A.R., (1974), "Load Distribution in Concrete Bridge Deck", CIRIA Report No. 53, London 1974, pp 38.

CUSENS, A.R., and PAMA, R.P., (1975), "Bridge Deck Analysis", John Wiley and Sons London 1975, pp 278.

DEPARTMENT OF TRANSPORT, (1976), "Specification for Road and Bridge Works", London, 1976, pp 194.

DEPARTMENT OF TRANSPORT, (1978), "The Standard Bridge Manual Part 1", London, 1978, pp 15 + Figs.

DORTON, R.A.,(1976), "The Conestogo River Bridge Design and Testing", Canadian Structural Engineering Conference, 1976. pp 39.

DORTON, R.A.,and CSAGOLY, P.F., (1977). "The Development of the Ontario Bridge Code", Ministry of Transportation and Communications, Ontario. Paper prepared for the 1977 National Lecture Tour, CSCE Struct. Division, pp 67.

ELLIOT, G., CLARK, L.A., and SYMMONS, R.M., (1979), "Tests on a ¼ Scale Model of a Voided-Slab Bridge Deck", Cement and Concrete Association, London, Technical Report No. 527 Publication 42.527, 1979, pp. 40.

EWELL, W.W., OKUBO, S., and ABRAMS, J.I., (1952), "Deflections in Gridworks and Slabs", Trans. A.S.C.E., Vol. 117, 1952, pp 869-912.

GARAS, F.K., and ARMER, G.S.T., (1980), "Reinforced and Prestressed Micro-Concrete Models", The Construction Press, 1980, 387 pp.

GOODALL, J.K., (1971), "The Torsional Stiffness of Multicellular Rectangular Box Sections", Proceedings of the International Conference on Developments in Bridge Design and Construction, Cardiff, 1971, pp 347-355.

GUYON, Y., (1946), "Calcul des Ponts Langes à Poutres Multiples Soledarisées par des Entretoises", Annales des Ponts et Chaussées. No. 24, Sept-Oct. 1946, pp 552-612.

GUYON, Y., (1949), "Calcul des Ponts Dalles", Annales des Ponts et Chaussées. Vol. 119, 1949, No. 29, pp 555-589 and No. 36, pp 683-716.

HAMBLY, E.C., (1974), "Concrete Box Girder Bridges", discussion on paper by Maisel, B.L., Rowe, R.E., and Swann, R.A., The Structural Engineer, Vol. 52, Number 7, July 1974, pp 257-272.

HAMBLY, E.C., (1976), "Bridge Deck Behaviour", Chapman and Hall, London, 1976, pp 272.

HENDRY, A.W., and JAEGER, L.S., (1958), "The Analysis of Grid Frameworks and Related Structures", London Chatto and Windus, 1958, pp 308.

HETÉNYI, M., (1938), "A Method for Calculating Grillage Beams", S. Timoshenko, 60th Anniversary Volume, New York, 1938, pp 60-72.

HEWITT, B.E., (1972), "An Investigation of the Punching Strength of Restrained Slabs with Particular Reference to the Deck Slabs of Composite I-Beam Bridges", Ph.D. Thesis, The Queens University of Kingston, Ontario, Canada, 1972.

HEWITT, B.E., and BATCHELOR, B. de V., (1975), "Punching Shear Strength of Restrained Slabs", Journal of the Structural Division, ASCE, Sept 1975, Vol. 101, ST9, pp 1839-1853.

HIGHWAY ENGINEERING COMPUTER BRANCH, (1975), "HECB/B/19 GRIDS, Program for the Grillage Analysis of Slab and Pseudo-Slab Bridge Decks", Department of Transport, London, 1975.

HIGHWAY ENGINEERING COMPUTER BRANCH, (1977), "HECB/B/20 PREBEM, Pretensioned Prestressed Beam Design and Analysis Program", Department of Transport, London, 1977.

HIGHWAY ENGINEERING COMPUTER BRANCH, (1978), "HECB/B1/7, User Guide for Slab and Pseudo-Slab Bridge Decks", Department of Transport, London, 1978.

HILL, R., (1950), "The Mathematical Theory of Plasticity", Oxford University Press, 1950, pp 354.

HOGNESTAD, E., (1953), "Yield-Line Theory for the Ultimate Strength of Reinforced Concrete Slabs", ACI Journal, Proceedings V. 49, 1953, p. 637-656.

HOLOWKA, M., DORTON, R., and CSAGOLY, P., (1979), "Punching Shear Strength of Restrained Circular Slabs", Ministry of Transportation and Communications Toronto, Ontario, Unpublished Research Report, 1979.

HOLOWKA, M., and CSAGOLY, P., (1980), "Testing of a Composite Prestressed Concrete AASHTO Girder Bridge", Ministry of Transportation and Communications, Toronto, Ontario, Research Report, RR.222, 1980, pp 14.

HOPKINS, D.C., and PARK, R., (1971), "Tests on a Reinforced Concrete Slab and Beam Floor Designed with allowance for Membrane Action", American Concrete Institute, Publication SP-30, 1971, pp 223-250.

JENSEN, V.P., (1939), "Moments in Simple Span Bridge Slabs with Stiffened Edges", University of Illinois Engineering Experiment Station, Bulletin Series, No. 315, August 1939, pp 35 + Figs.

JOHANSEN, K.W., (1962), "Yield Line Theory", Cement and Concrete Association, London 1962, pp 181.

JOHNSON, R.P., and ARNAOUTI, C., (1980), "Punching Shear Strength of Concrete Slabs Subjected to In-Plane Biaxial Tension", Magazine of Concrete Research, Vol. 32, No. 110, March 1980, pp 45-50.

KELLEY, E.F., (1926), "Effective Width of Concrete Bridge Slabs Supporting Concentrated Loads", Public Works, March 1926, pp 7-17.

KIRKPATRICK, J.,(1977), "Load Distribution Tests on Ballymacoss Railway Bridge", The Department of the Environment for N.Ireland, Roads Service, Internal Report, 1977, pp 23.

KIRKPATRICK, J., (1979), "M-Beam Bridge Decks", The Department of the Environment for N. Ireland, Roads Service, 1979, pp 63.

KIRKPATRICK, J., (1982), "Test Results for a 1/3 Scale Model Concrete Bridge Deck", The Queens University of Belfast, Department of Civil Engineering, Supplementary Report, 1982, pp 57.

KOLLBRUNNER, C.F., and BASLER, K., (1969), "Torsion in Structures", Translated by E.C. Glauser, Berlin, Springer Verlag, 1969, pp 280.

LAZARIDES, T.O., (1952), "The Design and Analysis of Openwork Prestressed Concrete Beam Grillages", Civil Engineering and Public Works Review, Vol. 47, June 1952, p 471, et seq.

LEONHARDT, F., and ANDRA, W., (1950), "Die Vereinfachte Tragerrostberechnung", Julius Hoffman Press, Stuttgart, 1950.

LIGHTFOOT, E., and SAWKO, F., (1959), "Structural Frame Analysis by Electronic Computer. Grid Frameworks Resolved by Generalised Slope Deflection", Engineering, Vol. 187 No. 4843, Jan 1959, pp 18-20.

LITTLE, G., (1954), "The Distribution of Load in a Box Section Bridge from Tests on a Xylonite Model", Magazine of Concrete Research, Vol. 6, No. 18, Dec. 1954, pp 121-132.

LITTLE, G., (1955), "Tests for Load Distribution in a Model Prestressed Concrete Bridge", Civil Engineering and Public Works Review, Vol. 50, Part 1, No. 585, March 1955, pp 285-287, Part 2, No. 586, April 1955, pp 421-422.

LONG, A.E.,(1975), "A Two Phase Approach to the Prediction of the Punching Strength of Slabs", Journal of the American Concrete Institute, Proceedings, Vol. 72, No. 2, Feb 1975, pp 37-45.

LOO, Y.C., and CUSENS, A.R., (1978). "The Finite Strip Method in Bridge Engineering", Cement and Concrete Association Viewpoint Publication 1978, pp 220.

McDOWELL, E.L., McKEE, K.E., and SEVIN, E., (1956), "Arching Action Theory of Masonary Walls", Proceedings of the American Society of Civil Engineering, Struct. Div., March 1956, pp 915-17.

MANTON, B.H., and WILSON, C.B., (1971), "MoT/C & CA Standard Bridge Beams", London, Cement and Concrete Association, 1971, Publication 46.012, pp. 36.

MASSONNET, C., (1950), "Méthods de Calcul des Ponts à Poutres Multiples Tenent Compte de Leur Résistance à la Torsion", International Association for Bridge and Structural Engineering, Zurich, Publication Vol. 10. 1950, pp 147-182.

MORICE, P.B., and LITTLE, G., (1954), "Load Tests on a Small Prestressed Concrete Highway Bridge", Cement and Concrete Association, London, Technical Report TRA 153, 1954, pp. 21.

MORICE, P.B., and LITTLE, G., (1956), "The Analysis of Right Bridge Decks Subjected to Abnormal Loading", Cement and Concrete Association, London, 1956, publication 46.002, pp. 43.

MORICE, P.B., LITTLE, G., and ROWE, R.E., (1956), "Design Curves for the Effects of Concentrated Loads on Concrete Bridge Decks", Cement and Concrete Association, London, 1956, Publication 46.009, pp. 24.

NÁDAI, A., (1925), "Die Elastischen Platten", Berlin, Verlag Springer, 1925.

NEWMARK, N.M., (1938), "A Distribution Procedure for the Analysis of Slabs Continuous Over Flexible Beams", University of Illinois, Engineering Experiment Station Bulletin No. 84, June, 1938, pp. 120.

NEWMARK, N.M., SIESS, C.P., (1942), "Moments in I Beam Bridges", University of Illinois Engineering Experiment Station, Bulletin Series No. 336, June 1942, pp. 149.

NEWMARK, N.M., and SIESS, C.P., (1943), "Design of Slab and Stringer Highway Bridges", Public Roads, V. 23, No. 7, Jan-Feb-Mar., 1943, pp. 157 et seq.

NEWMARK, N.M., SIESS, C.P., and PENMAN, R.R., (1946), "Studies of Slab and Beam Highway Bridges, Part I Tests of Simple Span Right I Beam Bridges", University of Illinois, Engineering Experiment Station, Bulletin Series No. 363, March 1946, pp. 132.

NEWMARK, N.M., SIESS, C.P., and PECKHAM, W.M., (1948), "Studies of Slab and Beam Highway Bridges, Part II Tests of Simple-Span Skew I Beam Bridges", University of Illinois, Engineering Experiment Station, Bulletin Series No. 375, January, 1949, pp. 60.

NEWMARK, N.M., (1949), "Design of I-Beam Bridges", Symposium on Highway Bridge Floors", Trans., ASCE. Vol. 114, 1949, pp. 997-1032.

OCKLESTON, A.J., (1955), "Load Tests on a Three-Storey Reinforced Concrete Building in Johannesburg", The Structural Engineer, Vol. 33, October 1955 pp. 304-322.

ONTARIO MINISTRY OF TRANSPORTATION AND COMMUNICATIONS, (1979), "The Ontario Highway Bridge Design Code", Toronto, Ontario, 1979.

PARK, R., (1964), "Ultimate Strength of Rectangular Concrete Slabs Under Short Term Uniform Loading with Edges Restrained Against Lateral Movement", Proceedings, Institution of Civil Engineers, London, V. 28, June 1964, pp. 125-150.

PARK, R., (1965), "The Lateral Stiffness and Strength Required to Ensure Membrane Action at the Ultimate Load of a Reinforced Concrete Slab and Beam Floor", Magazine of Concrete Research London, V. 17, No. 50, Mar. 1965, pp. 29-38.

PIPPARD, A.J.S., and DE WAELE, J.P.A., (1938), "The Loading of Interconnected Bridge Girders", Journ. Inst. C.E., Vol. 10, No. 1, 1938, pp. 97-114.

PIPPARD, A.J.S., (1952), "Studies in Elastic Structures", Arnold, London, 1952, pp. 361.

POWELL, D.S., (1956), "The Ultimate Strength of Concrete Panels Subjected to Uniformly Distributed Loads", M.Sc. Thesis, Cambridge University 1956.

PRAGER, W., and HODGE, P.G., (1951), "Theory of Perfectly Plastic Solids", Wiley, 1951, pp. 264.

PUCHER, A., (1964), "Influence Surfaces of Elastic Plates", Wien, New York, Springer Verlag, 1964, pp. 33 ch. 93.

RANKIN, G.I.B., (1982), "Punching Failure and Compressive Membrane Action in Reinforced Concrete Slabs", Ph.D. Thesis to be submitted, 1982, Department of Civil Engineering, The Queen's University of Belfast.

REGAN, P.E., and YU, C.W., (1973), "Limit State Design of Structural Concrete", Chatto and Wandus, London, 1973, pp. 325.

REGAN, P.E., (1981), "Behaviour of Reinforced Concrete Flat Slabs", CIRIA Report No. 89, 1981, pp. 90.

RICHART, F.E., NEWMARK, N.M., and SIESS, C.P., (1949), "Highway Bridge Floors", University of Illinois Engineering Experiment Station Bulletin, Vol. 47, No. 25.

ROWE, R.E., (1958), "The Analysis and Testing of a Type of Bridge Suitable for Medium Right Spans Subjected to Abnormal Loading", Cement and Concrete Association, London, Reserach Report No. 6, Nov. 1958, pp. 28.

ROWE, R.E., (1959), "Loading Tests on Two Prestressed Concrete Bridges", Proceedings of the Institution of Civil Engineers, Vol. 13, Aug. 1959, pp. 477-498.

ROWE, R.E., (1962), "Concrete Bridges Design", CR Books Ltd., 1962, pp. 336.

SAWKO, F., (1960), "Analysis of Grid Framework and Related Structures", Thesis submitted to the University of Leeds for the degree of M.Sc., 1960.

SAWKO, F., (1964), "Analysis of Grillages in the Elasto-Plastic Range", Civil Engineering and Public Works Review. Vol. 59, No. 6, June 1964, pp. 866-869.

SAWKO, F., (1965), "Electronic Computers Versus Distribution Methods", Civil Engineering and Public Works Review, Vol. 60, No. 4, April 1965, pp. 534-538. Discussion No. 6, June 1965, pp. 807-809.

SAWKO, F., (1967), "Computer Analysis of Grillages Curved in Plan", International Association for Bridges and Structural Engineering, Publications Vol. 27, 1967, pp. 151-170.

SIESS, C.P.,(1949), "Composite Construction for I-Beam Bridges", Symposium on Highway Bridge Floors, Trans. A.S.C.E., Vol. 114, 1949, pp. 1023-1045.

SIESS, C.P., VIEST, I.M., and NEWMARK, N.M.,(1952), "Studies of Slab and Beam Highway Bridges, Part III Small Scale Tests of Shear Connections and Composite T-Beams", University of Illinois, Engineering Experiment Station, Bulletin Series No. 396, Feb. 1952, pp. 135.

SIESS, C.P., and VIEST, I.M., (1953), "Studies of Slab and Beam Highway Bridges, Part V Tests of Continuous Right I-Beam Bridges", University of Illinois, Engineering Experiment Station, Bulletin Series No. 436, Oct 1953, pp. 91.

SNAITH, M.S., (1978), "A Digital Portable Weighbridge", The Journal of the Institution of Highway Engineers, July 1978, pp. 9-12.

SNOWDON, L.C., (1973), "Some Tests on the Strength in Punching Shear of Reinforced Concrete Slabs", Building Research Station, Watford, 1973, (Unpublished).

SOMERVILLE, G., and TILLER, R.M., (1970), "Standard Bridge Beams for Spans from 7 m to 36 m", London, Cement and Concrete Association, 1970, Publication 46.005, pp. 31.

SOMERVILLE, G., (1969), "Load Tests on Smallbrook Ringway Bridge , Birmingham," Cement and Concrete Association, London, Technical Report TRA 422, 1969, pp. 9.

TAYLOR, R., and HAYES, B., (1965), "Some Tests on the Effect of Edge Restraint on Punching Shear in Reinforced Concrete Slabs", Magazine of Concrete Research, Vol. 17, 1965, pp. 39-44.

TECHNICAL MEMORANDUM (BRIDGES) No. BE1/73, (1973), "Reinforced Concrete for Highway Structures", Department of Transport, London, 1973.

TECHNICAL MEMORANDUM (BRIDGES) No. BE2/73, (1973), "Prestressed Concrete for Highway Structures", Department of Transport, London, 1973.

TECHNICAL MEMORANDUM (BRIDGES) No. BE1/77, (1977), "Standard Highway Loadings", Department of Transport, London, 1977.

THOMAS, F.G., (1939), "Studies in Reinforced Concrete VIII. The Strength and Deformation of Some Reinforced Concrete Slabs Subjected to Concentrated Loading", Technical Report No. 25, HMSO, London, 1939, pp. 51.

THOMAS, F.G., and SHORT, A., (1952), "A Laboratory Investigation of Some Bridge Deck Systems", Proc. Inst. C.E., Part 1, Vol. 1, 1952, pp. 125-187.

THOMPSON, D.M., (1981), "Loading Tests on Highway Bridges : A Review", Transport and Road Research Laboratory Report 1032, 1981, pp. 27.

THOMSON, W., and TAIT, P.G., (1867), "A Treatise on Natural Philosophy", Vol. 1, Oxford University Press, 1867.

TONG, P.Y., and BATCHELOR, B., deV., (1971), "Compressive Membrane Action in Two-Way Bridge Slabs", American Concrete Institute, Publication No. SP-30, 1971, pp. 271-286.

WEST, R., (1973), "Recommendations on the Use of Grillage Analysis for Slab and Pseudo-Slab Bridge Decks", Cement and Concrete Association/ CIRIA, 1973, Technical Report No. 46.017, pp. 24.

WEST, R., (1973), "The Use of a Grillage Analogy for the Analysis of Slab and Pseudo-Slab Bridge Decks", Cement and Concrete Association, London, 1973, Research Report 21, 41.021, pp. 104.

WEST. R., (1970), "A Discussion of Some Experimental Results for the Bending of Cantilever Slabs", Cement and Concrete Association, London, 1970, D/N 7002. pp. 6 + Figs.

WESTERGAARD, H.M., and SLATER, W.A., (1921), "Moments and Stresses in Slabs", ACI Journal, Proceedings V. 17, 1921, pp. 415-538.

WESTERGAARD, H.M. (1930), "Computation of Stresses in Bridge Slabs Due to Wheel Loads", Public Roads, Vol. 11, No. 1, March 1930, pp. 1-23.

WHITTAKER, E.T., and WATSON, G.N., (1915), "A Course of Modern Analysis", Cambridge University Press, 1915 , pp. 560.

WOOD, R.H., (1961), "Plastic and Elastic Design of Slabs and Plates, With Particular Reference to Reinforced Concrete Floor Slabs", Ronald Press Co., New York, 1961, pp. 334.

WOODRING, R.E., and SIESS, C.P., (1968), "Influence Surfaces for Continuous Plates", Journal of the Structural Division, ASCE, V. 94, No. ST1, January, 1968, pp. 211-226.

VIEST, I.M., SIESS, C.P., APPLETON, J.H., and NEWMARK, N.M., (1952), "Studies of Slab and Beam Highway Bridges, Part IV Full Scale Tests of Channel Shear Connectors and Composite T-Beams", University of Illinois Engineering Experiment Station, Bulletin Series No. 405, Dec. 1952, pp. 147.